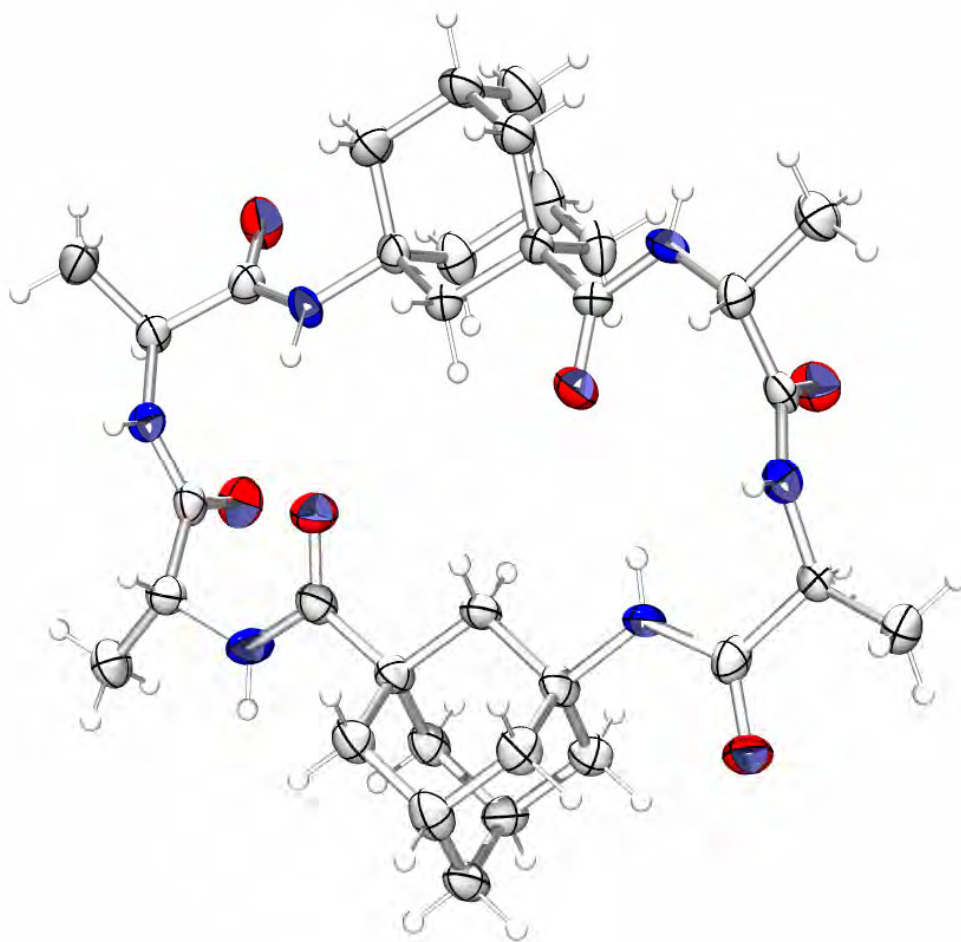


γ -Aminoadamantane Carboxylic Acids: Orientating Building Blocks in Peptide Chemistry



Inaugural-Dissertation zur Erlangung des Doktorgrades
der Naturwissenschaftlichen Fachbereiche
(Fachbereich 08 – Biologie und Chemie)
der Justus-Liebig-Universität Giessen

Vorgelegt von
Lukas Wanka
aus Wöllstadt
Giessen 2007

Die vorliegende Arbeit wurde am Institut für Organische Chemie der Justus-Liebig Universität Giessen von Juli 2002 bis Juni 2007 unter der Anleitung von Herrn Prof. Dr. Peter. R. Schreiner, Ph.D. angefertigt. Ihm gebührt mein Respekt und Dank für die außergewöhnliche Freiheit bei der Durchführung der hier beschriebenen Arbeiten und das immanente „forward-thinking“ sowie seine Unterstützung, die über die Promotion in seinem Arbeitskreis weit hinaus reicht.

sometimes is seen a strange spot in the sky
a human being that was given to fly

Für Christina

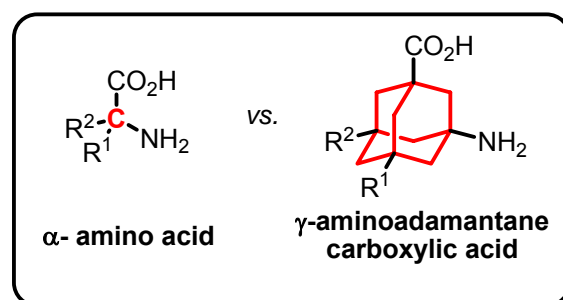
Contents

1. Abstract	1
2. Zusammenfassung	4
3. Introduction	8
3.1. Natural products incorporating the adamantane motif	8
3.2. Medicinal chemistry of adamantane derivatives	10
4. Project	44
5. Direct Functionalization of Adamantanes	47
5.1. ^A Xaas through bromine-free C–H to C–N bond amidations	47
5.2. ^A Xaas through PTC-halogenation and subsequent conversions.	55
6. Peptide chemistry	59
6.1. Protective groups and strategy	59
6.2. Peptide synthesis in solution	60
6.3. Solid phase peptide synthesis (SPPS)	64
6.4. Cyclizations	67
6.5. Summary	72
7. Biological Properties	73
7.1. Anti <i>Influenza A</i> activity	73
7.2. ^A Xaas as analogues of GABA	75

8. Peptidic Organocatalysts	78
8.1. Peptidic catalysts incorporating ^A Gly	78
8.2. Peptidic thioureas and organocatalytic Morita-Baylis-Hillman reactions.....	81
9. Structural Features	90
9.1. Computational methods and strategy	90
9.2. Infrared spectroscopy	95
9.3. NMR spectroscopy	95
9.4. Minimum requirements for an ^A Gly induced turn motif	96
9.5. Homooligomeric ^A Gly	112
9.6. Alternating peptides: Fmoc-Gly- ^A Gly-Gly- ^A Gly-O ^t Bu	118
9.7. Conformational analysis of ^A Xaa based organocatalysts incorporating His residues.....	118
9.8. Conformational analysis of ^A Xaa based thiourea organocatalysts.....	125
10. Summary & Outlook	131
11. Acknowledgement	136
12. Experimental Part	139
12.1. General remarks.....	139
12.2. General procedures.....	139
12.3. Direct C–H to C–N acetamidations.....	141
12.4. Synthesis of γ -aminoadamantane-1-carboxylic acids	148
12.5. Direct C–H to C–N- amidations using amides as the nucleophiles.....	151
12.6. Oxyfunctionalizations	153
12.7. PTC halogenations and subsequent conversions	155
12.8. Protective group chemistry	161
12.9. Peptide chemistry.....	167
12.10. Solid phase peptide synthesis of ^A Gly homooligomers.....	179

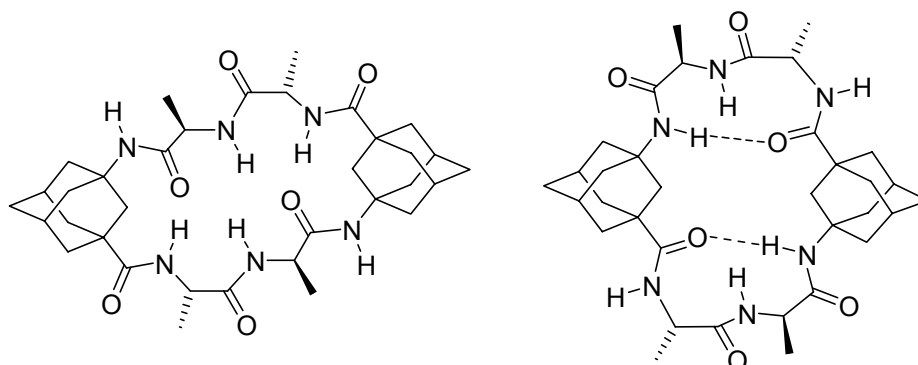
12.11. Solid phase synthesis of cyclization precursors	182
12.12. Cyclization experiments: Synthesis of cyclo-(D-Ala- ^Δ Gly-L-Ala) ₂	182
12.13. Biological tests	183
12.14. ^Δ Gly-based peptidic organocatalysts incorporating His residues.....	184
12.15. Synthesis of peptidic thiourea organocatalysts incorporating ^Δ Gly	192
12.16. Catalyst screening of peptidic thioureas in the Morita-Baylis-Hillman reaction.....	203
12.17. Solid phase peptide synthesis of model peptides.....	204
12.18. Miscellaneous: Synthesis of compound 266	206
13. Abbreviations	296
14. References.....	299
15. Bibliography	311

A number of syntheses for pharmaceutically relevant aminoadamantanes have been reported in the literature. Likewise, γ -aminoadamantane carboxylic acids (A Xaas) have been synthesized decades ago, but have had only very low impact to medicinal chemistry, presumably due to inefficient syntheses of the free γ amino acids and almost non-existent protective group chemistry.



Therefore, in a first project of this thesis two alternative routes towards the synthesis of monomeric A Xaas have been worked out, making available six A Xaas as building blocks in peptide chemistry. The syntheses developed herein include an improved, bromine-free acetamidation protocol (Ritter-type reaction) of tertiary adamantane C–H bonds as well as the development of a novel, direct, bromine-free formamidation. Both of these reactions can be utilized in large scale and they are also well-suited for the amidation of 1,3-dimethyladamantane in an improved technical synthesis of Memantine. An alternative route utilizes the PTC halogenation protocol that has been developed in our group to direct carboxy- and amido- functionalities into the desired tertiary positions of the adamantane framework. This approach holds the potential of making available a broad range of A Xaas from one common precursor; and attempts for a stereoselective bromination utilizing chiral PT catalysts are also described herein. The second project of the thesis is the establishment of protective group chemistry and peptide assembly in solution as well as via solid phase peptide chemistry (SPPS). The focus lies on the Fmoc- / $-\text{O}^t\text{Bu}$ protective group strategy as it is applicable without serious problems in solution and on solid phase. A multitude of various peptides are reported that have been synthesized for different purposes. One potential application of peptides incorporating A Xaas are cyclopeptides that could serve as monomers for the assembly of synthetic ion channels, utilizing the pronounced lipophilicity of the adamantane nucleus. The results of the cyclization

studies are disillusioning as only one cyclohexapeptide (**213**) could be obtained and analyzed via X-ray single crystal structure analysis.



Cyclohexapeptide **213**

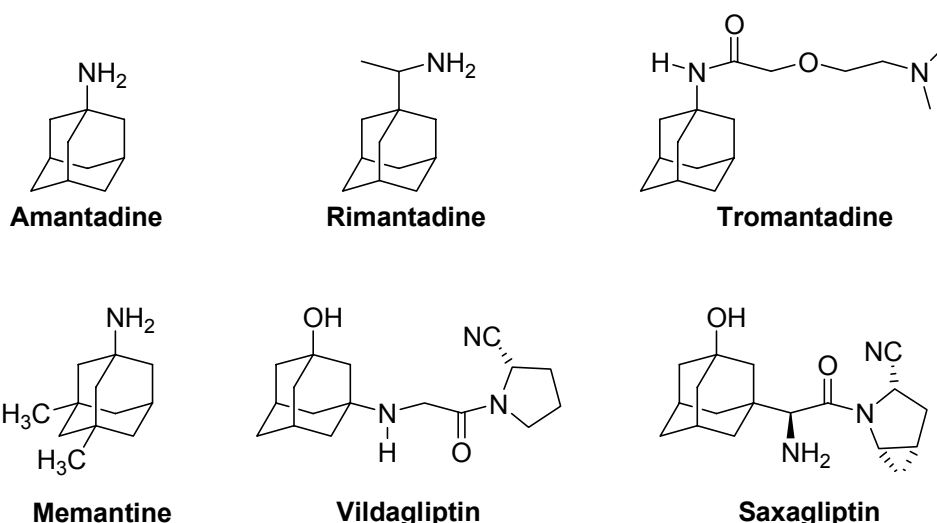
Only very few A Xaa derivatives reported herein could be tested with respect to their Pharmaceutical activities, but both anti-*Influenza A* activities and a blockade of the GABA transporter system testify the prospective value of the A Xaas in medicinal chemistry.

A third part of the thesis describes applications of peptides based upon orientating A Xaa building blocks as organocatalysts. Histidine based peptides were successfully applied in stereoselective organocatalytic acylation reactions, and peptides incorporating a thiourea motif catalyze the Morita-Baylis-Hillman reaction, albeit at low stereoselectivity only.

The tendency of cyclization, pharmaceutical activity, and the stereoselectivity observed in organocatalysis can be attributed to the orientating effect of the A Xaa building block when incorporated into a peptide chain. Therefore, in the final part of this thesis, studies on the structure of A Xaa based peptides were performed utilizing computational methods as well as IR- and NMR-techniques. Obviously, a relatively stable, intramolecularly hydrogen bonded turn motif is only favoured when the A Xaa residue is surrounded by at least two α -Xaa residues at preferably the *N*-terminus. While the structure analyses via NOESY NMR are tedious, in particular for homooligomers of A Gly, conclusions can be drawn that, at least in part, support the observations made in the organocatalysis experiments and the cyclizations.

2. Zusammenfassung

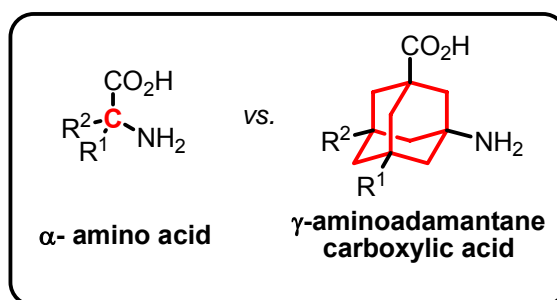
Im Jahre 1964 wurde gefunden, daß 1-Aminoadamantan (Amantadine) gut geeignet zur Behandlung und Prophylaxe von *Influenza A* Infektionen ist. In frühen Arbeiten danach haben mehrere Gruppen diverse Studien zur Modifikation des Aminoadamantan-Pharmakophors durchgeführt, ohne das Target, den M2-Ionenkanal des Virus, zu kennen. In der Tat fand man wirksamere Aminoadamantane, zum Beispiel Rimantadine, die auch zur Bekämpfung anderer Viren geeignet waren und ein günstigeres Nebenwirkungsprofil aufwiesen. Tromantadine konnte zur Bekämpfung von Herpes simplex (HSV) auf den Markt gebracht werden. Wichtiger als diese mehr oder minder geplante Forschung war jedoch die zufällige Erkenntnis, daß einfache Aminoadamantane ausgesprochen wirksam bei der Behandlung von Erkrankungen des Zentralnervensystems (ZNS) sind. So wurde gefunden, daß Amantadine die Symptome der Parkinson Krankheit günstig beeinflusst. Auch wurde gefunden, daß Memantine (1-Amino-3,5-dimethyladamantan hydrochlorid) ein milder, nicht-kompetitiver Antagonist des NMDA Rezeptors ist. Memantine ist heute das einzige Medikament, das bei mittleren und schweren Graden der Alzheimer Demenz eingesetzt wird.



Als Einführung in das Themengebiet der vorliegenden Dissertation wird zunächst die Historie der Anwendung von Derivaten des Adamantans in der medizinischen Chemie

dargestellt. Wir werden sehen, daß die Komplexität der untersuchten Verbindungen zunimmt. Aus den einfachen Aminoadamantanen wurden funktionellere Gerüste wie die Dipeptidyl-Peptidase Inhibitoren Vildagliptin und Saxagliptin, die unmittelbar vor Markteintritt in den Milliardenmarkt der Diabetes-Medikamente stehen.

Zur Synthese von pharmazeutisch interessanten Aminoadamantanen stehen in der Literatur eine Vielzahl von Prozeduren bereit. Ebenso ist die Klasse der in dieser Arbeit behandelten γ -Aminoadamantan Carbonsäuren (A Xaas) schon seit Jahrzehnten bekannt. Bemerkenswerterweise haben diese Bausteine bis heute jedoch keinen nennenswerten Einzug in die medizinische Chemie gehalten, wahrscheinlich in Ermangelung generell anwendbarer Synthesestrategien für die Monomere sowie deren Schützung und Kupplung zu Peptiden.

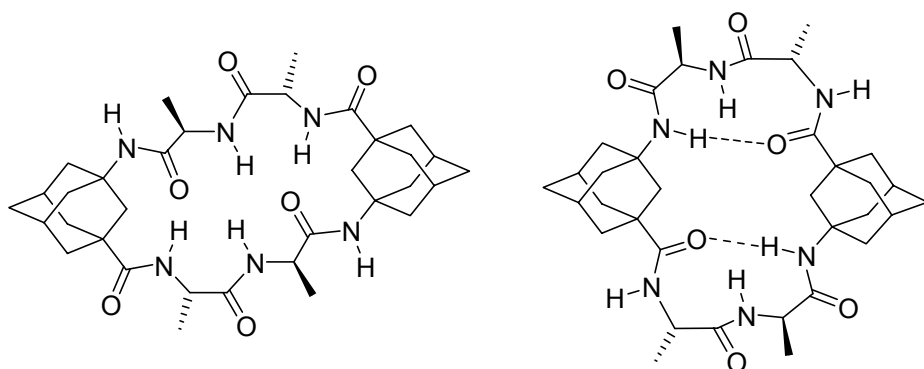


Im ersten Teil der vorliegenden Dissertation werden daher zwei alternative Synthesestrategien der monomeren A Xaas beschrieben. Damit werden zunächst sechs A Xaas als Bausteine für die Peptidchemie verfügbar. Die Darstellung der Monomere beinhaltet eine verbesserte Ritter-Typ-Reaktion, bei der die tertiäre Position im Adamantangerüst bromfrei acetamidiert wird. Darüber hinaus wurde eine neuartige, direkte und ebenfalls bromfreie Formamidierung entwickelt. Diese beiden Amidierungsreaktionen können in großem Maßstab eingesetzt werden; sie sind ferner auch geeignet zur Amidierung von 1,3-Dimethyladamantan, wodurch verbesserte, insbesondere *bromfreie* Synthesen des Wirkstoffes Memantine möglich werden. Eine alternative Route benutzt das phasentransferkatalytische Halogenierungsprotokoll, das in unserer Arbeitsgruppe ausgearbeitet worden ist. Dabei werden die gewünschten Carboxy- und Amidofunktionalitäten durch eine davor durchgeführte Halogenierung in die gewünschten tertiären Positionen des Adamantans eingeführt. Dieser Ansatz macht potentiell eine Vielzahl von A Xaas aus einem gemeinsamen

Vorläufer zugänglich. Einige Versuche zu einer stereoselektiven PTK-Bromierung mit chiralen Phasentransferkatalysatoren sind ebenso beschrieben.

Der zweite Schwerpunkt dieser Dissertation ist die Ausarbeitung der Schutzgruppenchemie der α Xaas und von Protokollen zu deren Peptidkupplung, sowohl in Lösung als auch an der festen Phase (SPPS). Der Focus liegt klar auf der Fmoc- / O^t Bu Strategie, da diese problemlos in Lösung und an der festen Phase anwendbar ist. Eine Vielzahl von Peptiden, die auf α Xaas basieren, wird für verschiedenste Anwendungen zur Verfügung gestellt.

Eine potentielle Anwendung der neuen Bausteine sind cyclische Peptide, die zum Design synthetischer Ionenkanäle benutzt werden können, wobei die ausgesprochen lipophilen Eigenschaften der α Xaas sehr nützlich sind. Die Resultate der hier beschriebenen ersten Cyclisierungsstudie sind jedoch ernüchternd, da nur ein cyclisches Peptid dargestellt und mit Röntgenstrukturanalyse untersucht werden konnte.



Nur wenige der in der vorliegenden Arbeit beschriebenen Substanzen konnten hinsichtlich ihrer pharmakologischen Eigenschaften untersucht werden, die erfolgreichen Tests dieser wenigen Substanzen als anti-*Influenza A* Agenzien und als Blocker des GABA Transporters mGAT1 sind jedoch ausgesprochen ermutigend. Weitere solcher Tests mit den nun zur Verfügung stehenden Substanzbibliotheken bieten sich an, auch und insbesondere an anderen Targets des ZNS.

Ein dritter Teil dieser Dissertation beschreibt Anwendungen von Peptiden, die auf α Xaas basieren, als peptidische Organokatalysatoren, bei denen die orientierende Wirkung der α Xaas ausgenutzt werden kann. α Xaa-Peptide mit einem modifizierten His-Rest wurden erfolgreich in der stereoselektiven, organokatalytischen Acylierung

von Alkoholen eingesetzt; A Gly-basierende Peptide, die eine Thioharnstoff-Einheit beinhalten, wirken als Organokatalysatoren in der Morita-Baylis-Hillman-Reaktion, wenn auch (bisher) mit nur geringer Enantioselektivität.

Die beobachteten Tendenzen bei der Cyclisierung und die Stereoselektivitäten, die bei den organokatalytischen Experimenten beobachtet wurden, können zumindest größtenteils mit den strukturellen Eigenschaften der A Xaa-basierenden Peptide erklärt werden. Dazu wurden im letzten Teil dieser Dissertation Untersuchungen mit Kraftfeld- und DFT-Rechnungen sowie IR- und NMR-Messungen durchgeführt. Offensichtlich benötigt man zumindest eine tetramere Peptidkette mit einem A Gly Rest bevorzugt in Position 3, um relativ stabile, durch eine intramolekulare Wasserstoffbrücke stabilisierte Turns zu designen. Die Strukturuntersuchungen mit NOESY NMR sind nicht trivial, insbesondere bei homooligomeren des A Gly, die strukturellen Vorlieben, die gefunden wurden, erklären jedoch zufriedenstellend die meisten der experimentellen Befunde.

3. Introduction

3.1. Natural products incorporating the adamantane motif

The pharmaceutical activity of organic compounds is essentially determined by the functional group(s) comprised in the molecule (in this context, decisive functional groups are regarded *pharmacophors*) and their three-dimensional adjustment in space, which determines affinity to the respective targets. In addition to the interaction of a drug with its target, pharmacodynamics and pharmacokinetics govern its action. Obviously, the sheer *activity* of a drug, historically described by the “key-lock” principle by Fischer can be regarded dominated by the three-dimensional assembly of pharmacophoric groups. The paradigm shift to a more dynamic view at the processes of docking of a drug to its target led to the more precise model of an “induced fit”, but the defined spatial array of pharmacophors in the drug’s active conformer remains a vital prerequisite for its activity.

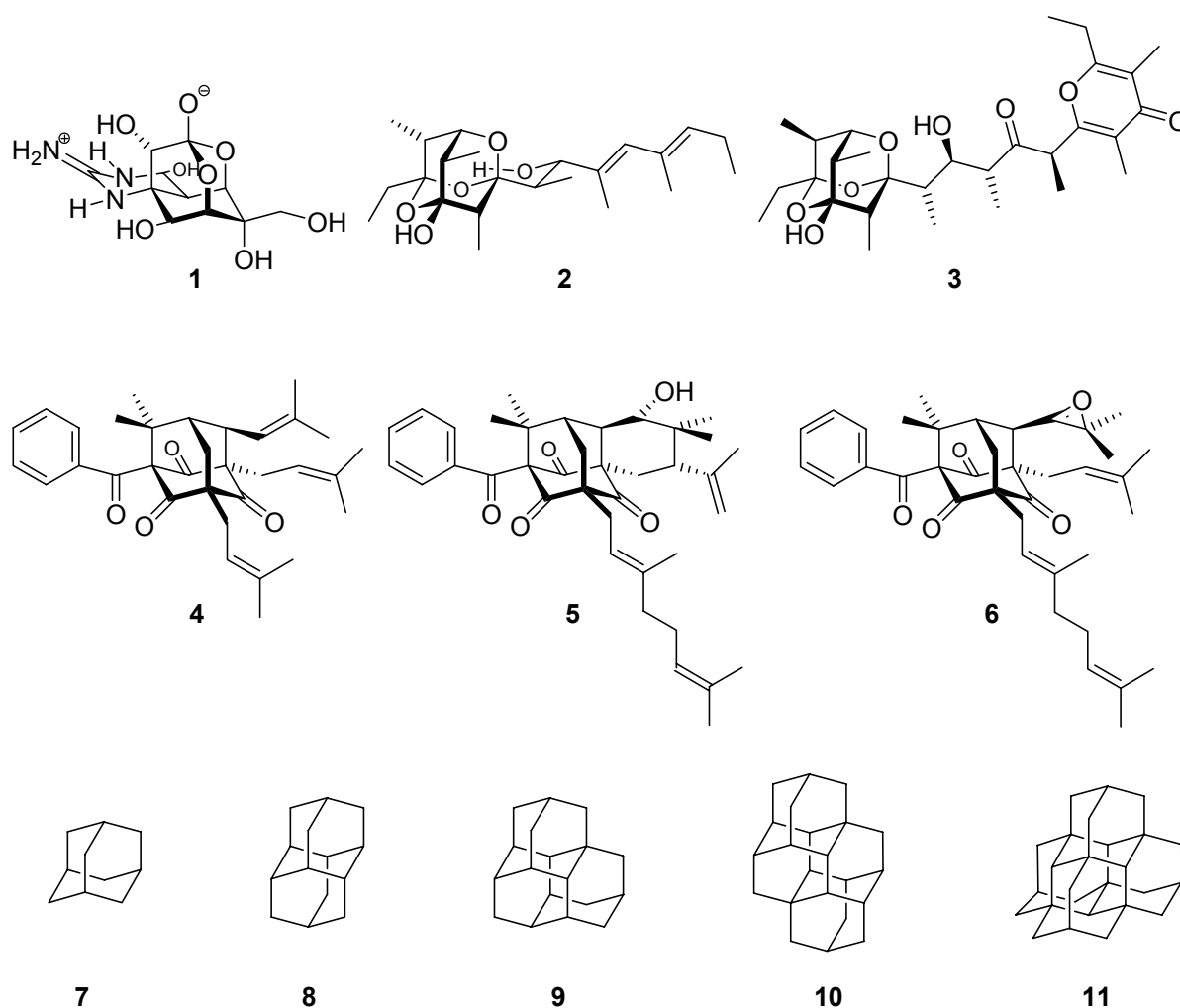
Somewhat more intriguing is the relationship between a drug’s three-dimensional structure and its ADME characteristics. Both a drug’s *absorption*, e. g., when crossing the Blood-Brain-Barrier, and its *distribution* to the target tissue again depend (among others, e. g., lipophilicity) on its structure. In prodrug concepts, carrier moieties designed for a guided distribution of the drug are being used. A drug’s *metabolism* and *excretion* are the most significant organic-chemical processes of drug action and, therefore, highly structure dependent.

Nature as the oldest source of pharmacologically active substances has designed substances to specifically and fast display the favored effect. One of “Nature’s marvels”^[1] is the toxic principal of puffer fish (*Tora fugu*) ovaries, tetrodotoxin **1**. Its unique structure consists of multiple hydroxy groups, an orthoacid and a guanidine arranged by the dioxadamantane core. Tetrodotoxin (TTX) is both a synthetic challenge^[1-4] and a prototype tool for the elucidation of structure and functionality of its target, voltage-gated Na⁺ ion channels.^[5] Muamvatin **2**, isolated from the mollusc *Siphonaria normalis*^[6, 7] and Caloundrin B **4** from *Siphonaria zelandica*^[8] both incorporate a densely substituted trioxadamantane nucleus.

Hypericum sampsonii (Guttiferae) are being used in traditional chinese medicine for centuries to treat a multitude of disorders including snakebites, swellings, backache

and diarrhoea.^[9] While the active ingredients are not (yet) known specifically, some of them, the sampsoniones, were isolated and their structure was elucidated. In addition to substituted homoadamantanes (Sampsoniones A–H),^[9–11] Plukentione A (**4**), Sampsonione I (**5**) and Sampsonione J (**6**) were isolated.^[12, 13] These incorporate an adamantane moiety as the central scaffold and **5** displays cytotoxicity against P388 cancer cell lines.^[12, 14]

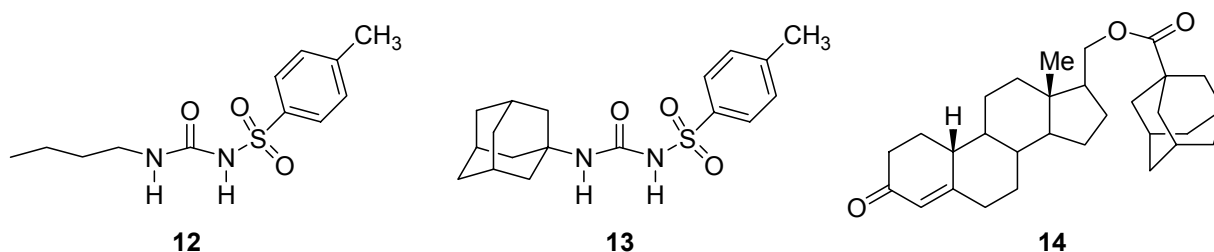
While the natural products hitherto mentioned stem from natural sources, one must not forget that adamantane **7**^[15] and the higher diamondoids^[16] up to at least undecamantane are found in trace amounts in most raw petroleum and are, therefore, natural products as well. Diamondoids like diamantane **8**, triamantane **9**, [121]tetramantane **10** and [1(2,3)4]pentamantane **11** are a current focus of interest due to their ready accessibility; selective functionalizations yield building blocks of interest for, e. g., nanotechnology and electronics.^[17]



Scheme 1. Natural products incorporating an adamantane motif.

3.2. Medicinal chemistry of adamantane derivatives

Early attempts to exploit adamantane's beneficial properties were hampered by its limited availability. Shell had patented hexa- and dodecachloroadamantane as synthetic insecticides,^[18] but no actual use has been reported. Schleyer's seminal synthesis of adamantane by lewis-acid catalyzed rearrangements^[19] made **7** readily available in large quantities and hallmarked the starting point for the usage of adamantane and its derivatives in medicinal chemistry. In a series of papers, Gerzon et al. reported the effect of the attachment of adamantane moieties to compounds already known as being biologically active. This "add-on" concept was first exemplified by replacing the n-butyl sidechain of the first-generation hypoglycemic agent tolbutamide **12** with a 1-adamantyl moiety. **13** was reported 15.5 times more active than **12** in rats and dogs with minor toxic side effects.^[20] A clinical study in 30 humans was also performed, resulting in a five times increased activity of **13** with respect to **12**. While the *N*-alkyl group in *N*-alkyl-*N'*-sulfonylureas can widely be varied while maintaining efficacy, *N*-adamantylureas showed an enhanced long-term activity. Minor changes in the adamantyl moiety, e. g., bridgehead-methylation, caused a significant drop in activity, indicating a role of the adamantyl substituent as secondary pharmacophore. Notably, until recently (see 3.2.5.3) no follow-up work on this field has been disclosed.

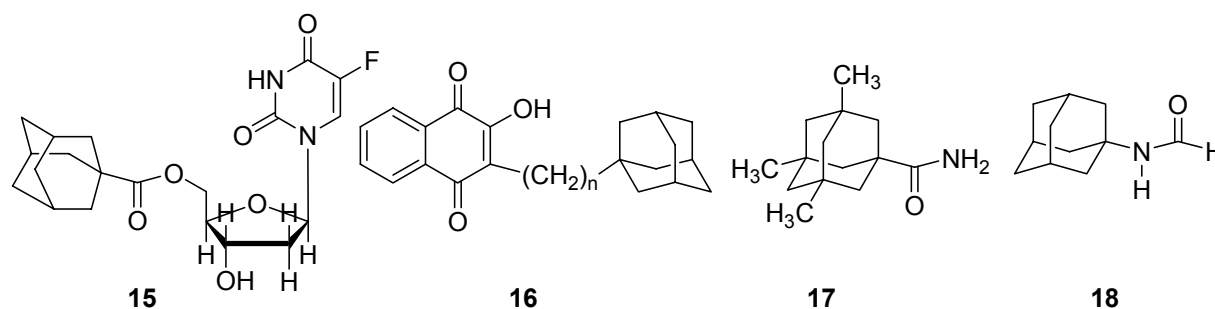


Scheme 2. Early examples of the adamantane moiety used as an "add-on".

Attaching an adamantane moiety to anabolic steroids effects enhanced muscle growing properties in rats. Steroid adamantanoates like nortestosterone adamantanoate 17 β (**14**) proved more highly active with a longer duration with respect

to non-adamantanoylated analogues.^[21] Again, methylation of the adamantane add-on led to a sharp decrease in efficacy.

When modified by adding an adamantane carboxylic acid ester moiety, nucleosides like **15** display an enhanced lipid solubility that is crucial for medicinal applications. A series of adamantanoylated nucleosides was prepared and their efficacy against numerous disorders (e. g., suppression of antibody formation, antitumor activity, cytotoxicity, antiviral properties, and inhibition of adenosine deaminase) was evaluated in animal experiments^[22] to search for an application of an easily accessible class of compounds. While the addition of the adamantane moiety resulted in better distribution of the compound in the host and enhanced metabolic stability, it also triggers the precision of fit into the respective receptor binding pocket, acting as a secondary pharmacophore. Again, only minor changes in the adamantane moiety yielded dramatic changes in the efficacy of the compounds; the precision of fit of the molecules in their respective target's binding pockets are strongly influenced by the adamantane moiety.



Scheme 3. Experimental adamantane containing pharmaceuticals

Naphthoquinones were a well-known class of antimalarials in the 1960's, and because of encouraging results using cyclohexyl substituted derivatives, 1-adamantyl substituted analogs **16** ($n = 1-5$) were prepared and tested in *Plasmodium berghei* infected mice – without success due to significant toxicity.^[23] Again Gerzon and coworkers at Eli Lilly reported the sedative action of adamantyl carboxamides (e. g., **17**) and some adamantanols in mice, cats, and dogs. Interestingly, adamantyl amides like **18** act as stimulants causing convulsions and tremors.^[24] These early contributions to the medicinal chemistry of adamantane derivatives were mainly driven by an “add-on” concept of replacing (cyclo)alkyl sidechains by an (methylated) adamantane sidechain, thereby providing pronounced lipophilicity to already known

pharmacophors. Two main conclusions, however, were drawn: efficacy of compounds incorporating an adamantane moiety is highly sensitive to alkylation (in other words, the shape of the “lipophilic bullet” navigates the fit into any at that time unknown target protein binding pocket) and adamantane triggers neurochemical activity for reasons of, e. g., enhanced crossing of the blood-brain-barrier.^[24]

3.2.1. Adamantane antivirals, antimicrobials and antifungals

The first striking application of an adamantane derivative in medicinal chemistry originated in 1964, when the activity of 1-aminoadamantane hydrochloride **19** in combating infections with *Influenza A*, *Influenza A'*, *Influenza A-2*, and *Influenza C* strains was found.^[25] *Influenza B* strains and other viruses were found to be resistant. **19** was approved by the FDA in 1966 and is still being used today (amantadine, symmetrel) as an *Influenza* prophylaxis. These findings led to a marked increase of the number of publications on medicinal chemistry applications of adamantane and its derivatives. Many aminoadamantane (and structurally related) derivatives were prepared and their antiviral activity was investigated. These efforts shed light on the management of *Influenza* and other virus diseases including Hepatitis C and HIV, and branches of this research led to compounds with potential as antimicrobials, antifungals, and antimalarials.

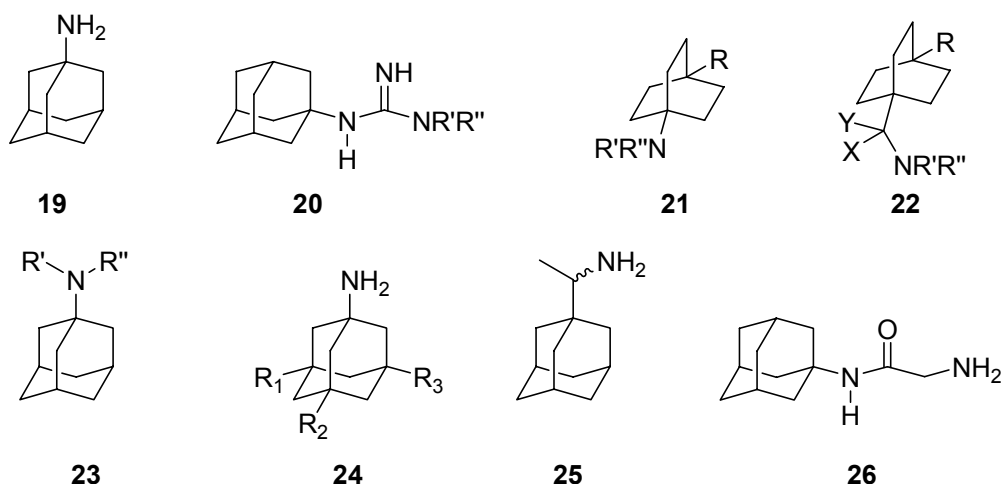
3.2.1.1. *Influenza A* – the amantadine & rimantadine story

Not knowing the exact target, it was found that the virus' penetration of the host cell is blocked by amantadine (**19**), thereby remaining susceptible to antibody inactivation for a prolonged period of time.^[25] The antiviral action of **19** was found dose-dependent, the toxicity was low ($LD_{50} = 1080$ mg / kg in mice upon oral application). Having one antiviral “hit” at hand, research mainly followed the “lipophilic, spheric cage hydrocarbon amine” path.

(a) A survey of the modifications performed with the aminoadamantane lead.

Adamantyl guanidines **20** were considered attractive due to their higher basicity – however, out of eight derivatives tested (R' and $R'' = H$ or alkyl/cycloalkyl), only the non-alkylated guanidine significantly inhibited two strains of *Influenza A* viruses *in vitro*

as well as in mice, but not to a higher degree than amantadine.^[26] Likewise, bicyclo[2.2.2]octane amine as well as Bicyclo[2.2.2]oct-2-enamines (**21** and **22**) did not meet aminoadamantane's efficacy.^[27] The chase continued, and in a screen of another 91 cage amines including N- and C-alkylated adamantanamines (**23** and **24**), 1-adamantanemethylamines and homoadamantanamines, some consistent structure-activity-relationships (SAR) were concluded with the antiviral dose₅₀ (AVI₅₀) as a quantitative measure of activity of the screened compounds in virus-infected mice.^[28] None of the N-substituted compounds **23** (40 were screened) was significantly more active than **19**. With increasing size of the N-substituents the activity diminishes; the same holds true when functional groups are incorporated into the N-substituents. Substitution of the tertiary positions of the adamantane nucleus in amantadine was found being detrimental to activity. Inserting a bridge of one or more carbons between the 1-adamantyl- and the amino group led to compounds with generally high antiviral activity, with Rimantadine (**25**), α -methyl-1-adamantanemethylamine, outperforming amantadine in terms of activity as already had been reported before.^[29] **25** incorporates a stereogenic center at the carbon bridge. Resolution and screening of the enantiomers yielded identical activity for both enantiomers. Furthermore, incorporation of a homoadamantane skeleton instead of the adamantane did not lead to enhanced activity. Glycinate **26** displayed an AVI₅₀ comparable to that of amantadine (5.6 and 4.6 mg/kg, respectively). Replacing the amino group in **19** by –H, –OH, –SH, –CN, –CO₂H, –Cl or –Br gave inactive compounds.



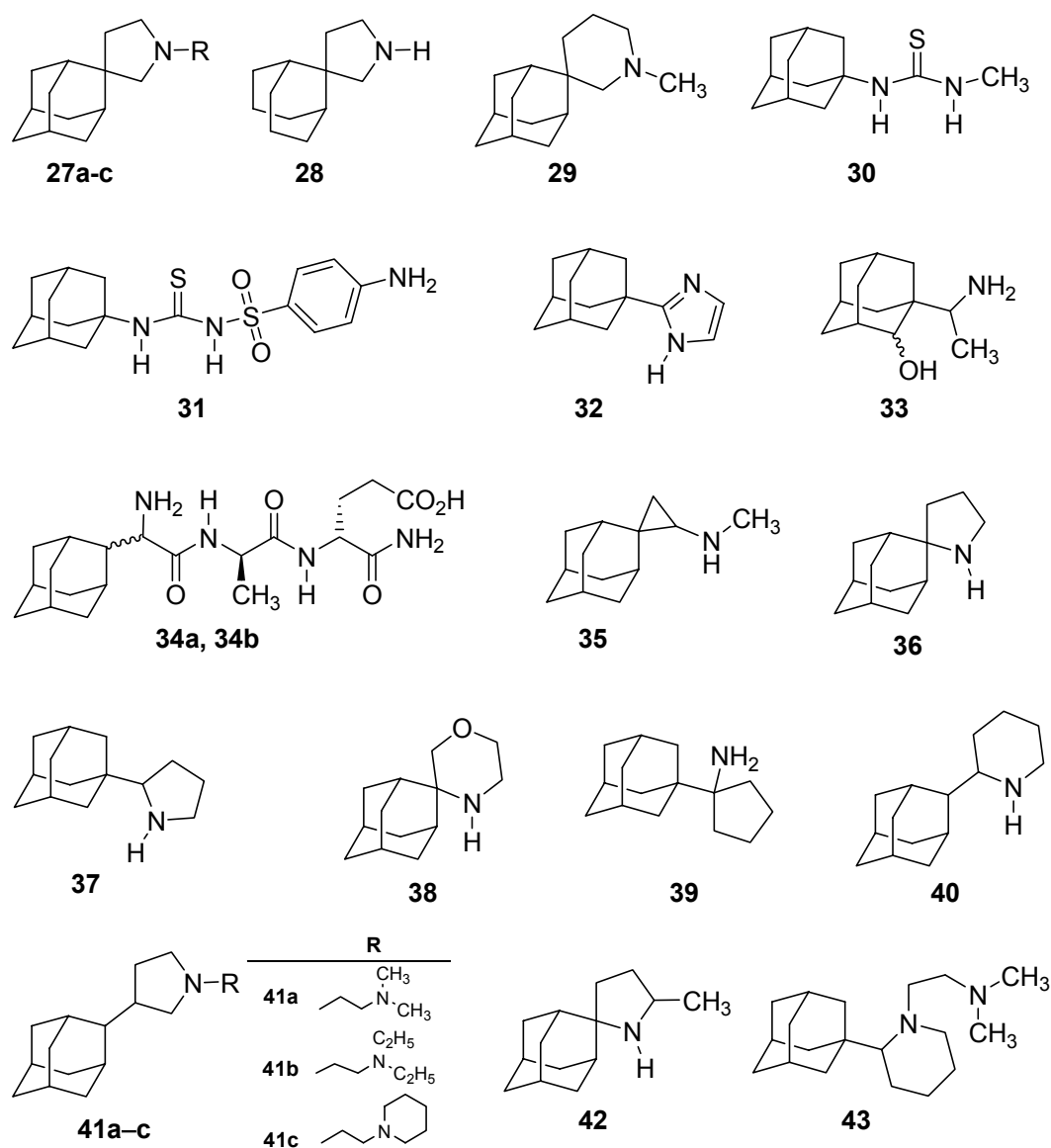
Scheme 4. Structural variations alongside the amantadine lead

Taken together, these findings supported the concept of the amino group as a primary pharmacophore that is assisted by an (unsubstituted) adamantane moiety in the

appropriate distance as a secondary pharmacophore, both leading to pronounced activity in a synergistic manner. It is noteworthy that the target protein was still not known at that time.

Ever since these days, newly synthesized (amino)adamantane derivatives were tested with respect to their antiviral activities. Having adamantane easily at hand in large scale, adamantane spiro-3'-pyrrolidines **27** were synthesized. **27a** (R=H) and **27c** (R=C₂H₅) displayed similar or better *in vivo* anti-*Influenza A* activity than amantadine, while **27b** (R=CH₃) was reported to be three times more active.^[30] It also proved to be active against other viruses, e. g., the *Rhino* virus. These authors also varied the hydrocarbon moiety; while **28** has also strong anti-*Influenza* activity, these properties vanish when the 3'-pyrrolidine pharmacophore is attached to other hydrocarbons like, e. g., 2-bornane or cyclohexane moieties. Since problems with toxicity were encountered with the pyrrolidines, piperidines have also been examined.^[31] **29** displayed anti-*Influenza A* properties comparable to those of amantadine. A number of N-adamantylthioureas (e.g., **30**) were also prepared and screened against *Influenza A* viruses.^[32, 33] Since they have proven active *in vivo* at low toxicity, derivatives have been screened and **31** has been identified to compare favorably with amantadine with respect to both efficacy and toxicity.^[34] Furthermore, **31** showed a reduced level of CNS related side effects producing mild tremors and ataxia in mice only at high doses (>600 mg/kg ip.). Imidazoles^[35] (**32**) and metabolites from rimantadine isolable from human urine (e.g., **33**)^[36] have also been tested in cell culture experiments yielding slightly (**32**) and significantly (**33**) lower inhibition of *Influenza A* virus reproduction with respect to amantadine and rimantadine. Combining peptidic fragments with immunomodulatory activity and adamantane derivatives with well-known antiviral properties yielded "adamantylpeptides" **34a** and **34b** that were both having comparable minimum inhibitory concentrations (MIC) to amantadine.^[37] Notably, **34a** (incorporating the D-Gly(2-Ada) residue) showed the same MIC to the *Influenza A* H₁N₁ subtype as does amantadine (MIC = 12.5 µg/200µL), while **34b** (incorporating the L-Gly(2-Ada) residue) had an eight times higher MIC. Testing the same compounds against the H₃N₂ subtype showed **34a** four times less active than **34b**, and both of them significantly less than amantadine. Cyclopropylidene amine **35**,^[38] **36**, and the structurally closely related pyrrolidine **37** as well as structural variations **38**, **39**,^[39] and **40**^[40] were screened against a multitude of viruses including *Influenza A*

and B, Herpes-, Polio- and HI- viruses. **35** displayed an MIC₅₀ of 1.2 $\mu\text{g/mL}$, **36** of even lower 0.56 $\mu\text{g/mL}$. **36** produced no observable toxicity in the host cells up to 400



Scheme 5. More recent developments of anti-*Influenza* aminoadamantanes

$\mu\text{g/mL}$. The MIC₅₀ values of **37** (0.6 $\mu\text{g/mL}$), **38** (1.7 $\mu\text{g/mL}$), and **39** (2.5 $\mu\text{g/mL}$) as measured *in vitro* against *Influenza A* (H_3N_2) in MDCK cells compare relatively well to both amantadine and rimantadine (MIC₅₀ = 0.8 and 0.14 $\mu\text{g/mL}$, respectively).^[39]

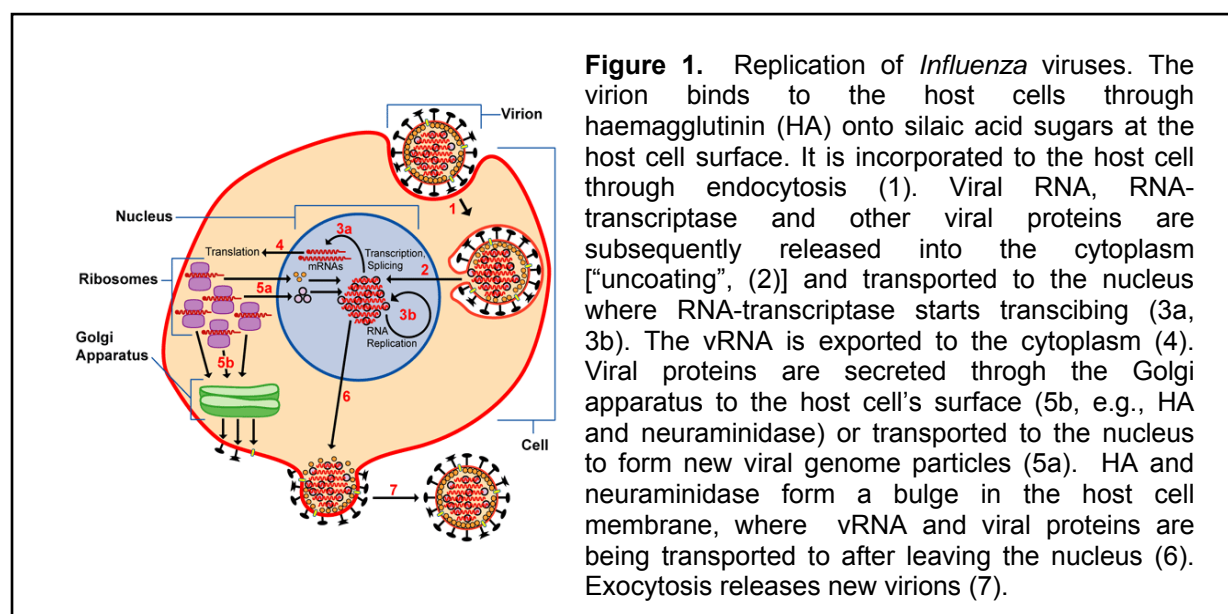
Piperidine **40** was reported to possess 3–4 times higher activity against *Influenza A* H_2N_2 virus strain than amantadine or rimantadine^[40] at low cytotoxicity. N-substituted derivatives **41** were the first diamino adamantane derivatives reported to date that possess anti-*Influenza A* activity.^[41]

The MIC₅₀ values of **41a** (0.38 μM) and **41c** (1.7 μM) are significantly lower than with amantadine (2.6 μM) when used in the same *in vitro* test environment. In this case, *Influenza A* (H₂N₂) infected MDCK cells have been used. Since these compounds have a somewhat larger molecular volume and two instead of one amino group, the authors proposed an appropriate binding site in the M2 pore that provides H-bond interactions for both functional groups. Methylation of **36** did not increase its efficacy and **42** did not fare well against the “gold standard”, amantadine.^[42] The latest structural variation of aminoadamantane derivatives as compounds to combat *Influenza A* virus is represented by **43**.^[43] This piperidine also bears two amino groups along with the adamantane moiety; besides an (albeit comparatively low) anti-*Influenza A* activity, it also shows low micromolar EC₅₀ against HIV-1 and has been proposed as a lead structure for anti-HIV drugs. After decades of structural variations along the aminoadamantane motif and marketing amantadine **19** and rimantadine **25**, amantadine and rimantadine were the only antivirals to combat *Influenza* epidemics prophylactically as well as therapeutically (in addition to vaccination) until neuraminidase inhibitors came up; rimantadine is slightly more active while displaying less CNS related side effects.^[44] The adamantane derivatives are efficient, cheap, and can be stored for decades as a safety measure for the threat of pandemics^[45] while neuraminidase inhibitors are not (yet) available for this purpose at appropriate cost.^[46] In recent years even more powerful antivirals alongside the aminoadamantane lead were identified; novel variations of the aminoadamantane motif and a combination therapy approach^[47] could be advantageous in the future. While this seems encouraging, all these compounds share the same fate: A lack of efficacy against *Influenza B* and a rapid development of so-called “adamantane resistant” strains. The avian flu (H₅N₁) *Influenza* strains, which are a possible origin of a new pandemic, are mostly amantadine- and rimantadine- resistant.^[48]

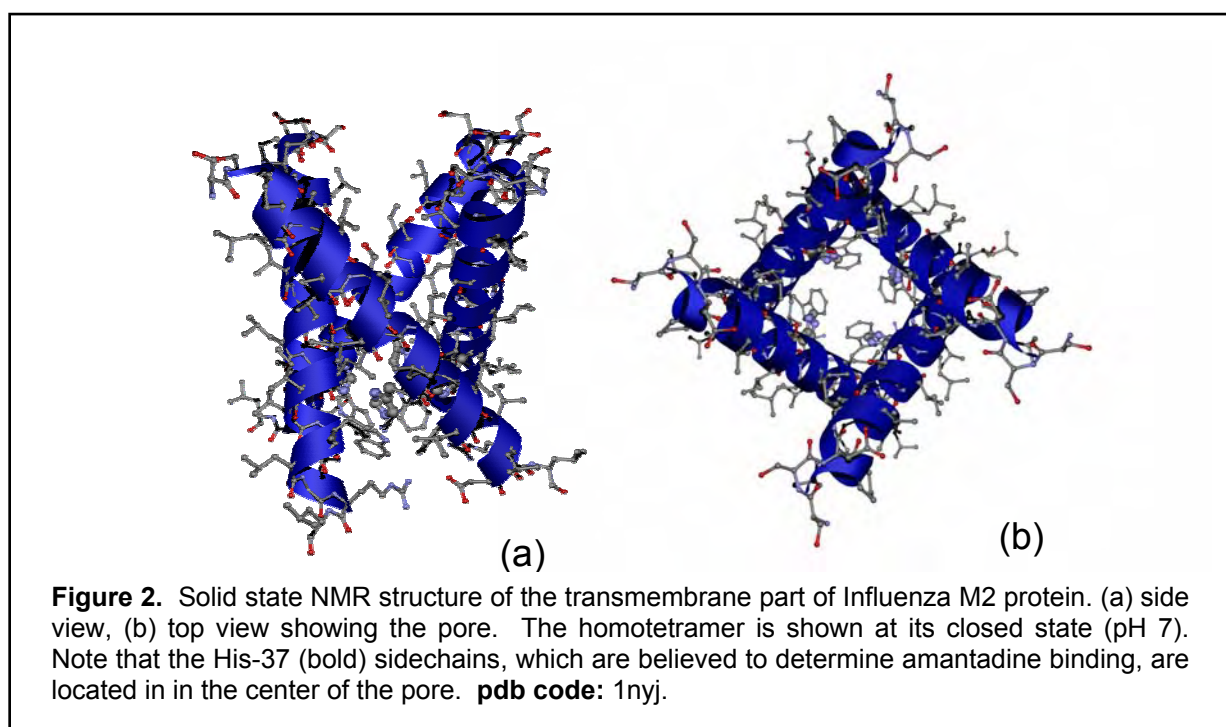
(b) Mechanism of action: Blocking the M2 ion channel

In the early years, the structure modifications of the aminoadamantane lead were made without knowing the target. It was known then that the aminoadamantanes inhibit virus replication at the early steps of the infection, namely the penetration of the host cell by the virus particle. The development of resistance of H₃N₂ and H₂N₂ *Influenza* strains towards Rimantadine was ascribed to a single change in the gene coding for the M2 protein.^[49] Shortly thereafter, wild-type and mutant M2 surface

proteins were expressed in *Xenopus laevis* oocytes and it was found that the M2 protein, a 97 residue protein that minimally forms a homotetramer (type III integral protein) has ion channel activity.^[50] When treated with amantadine, the proton conductivity of the wild-type M2 protein was abrogated as shown by electrophysiological measurements. M2 isolates from amantadine resistant virus strains showed that in these channels the proton conductivity was higher than in the wild-type forms, and conductivity was not significantly attenuated by amantadine (in reverse, in some cases membrane currents were increased by application of the drug). pH regulation plays a pivotal role in the maturation of the *Influenza* haemagglutinin (HA) surface protein, which is triggered by the M2 channel.^[51] The M2 channel functions during uncoating of the virus and its maturation, as it modifies the pH inside the virions as well as in the trans-Golgi vesicles (see Figure 1).^[52] From comparison of the M2 blocking capabilities of amphiphilic amines including amantadine and rimantadine with that of polyamines (the latter being two to three magnitudes smaller), it has been concluded that two alternative binding sites exist in the M2 channel, one for the alkylamines, and another one for polyamines. This assumption is supported by the finding that diamino substituted adamantanes like **43** show anti-*Influenza* activities smaller than amantadine and rimantadine do.^[43] From molecular modeling, the binding site for the amino adamantane derivatives is believed to be associated with the His-37 residue of M2.^[53] In conclusion, the aminoadamantanes stop *Influenza* virus multiplication by inhibiting the virion uncoating (Figure 1, step 2).



This step is highly pH sensitive, and consequently dependent on the pH regulatory capabilities of the M2 channel. Therefore, blocking M2 stops viral reproduction *within* the host cell. Structure determination of the M2 protein is still a vital field of research; utilizing solid-state NMR techniques, the structure of the transmembrane part of *Influenza A* M2-protein (M2-TMP) providing a molecular look at its pore has been measured in hydrated dimyrisitylphosphatidylcholine bilayers (Figure 2).^[54]

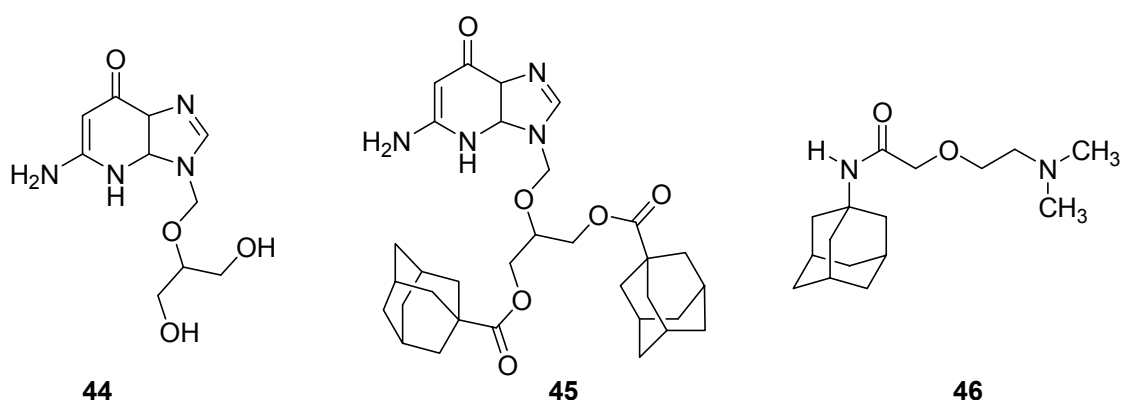


3.2.1.2. Herpes simplex – the tromantadine story

In the course of synthesizing and screening new aminoadamantane derivatives as antivirals, one of the earliest target viruses along with the *Influenza* viruses was *Herpes simplex* (HSV). One strategy was to synthesize a nucleobase analog that is being included into the viral DNA within the DNA replication through the Herpes viral DNA-polymerase, thereby stopping chain elongation of the newly synthesized vDNA. Another concept is the inhibition of the viral DNA-polymerase.^[55] Adamantoylation triggered ganciclovir **44**, an anti *Herpes simplex* drug, more lipophilic while increasing its stability towards cleavage by esterases. The adamantate is being cleaved by

esterases within the skin tissue, where acute HSV infection takes place. Therefore, bis-adamantanoate **45** is regarded a prodrug.^[56]

A different approach was chosen in the case of tromantadine **46**, which was found to display anti-HSV activity in 1971.^[57] It is still being used today and marketed as Viru-Merz[®]. Tromantadine is assumed to inhibit the synthesis of a protein required for fusion, it is believed to block the processing of the carbohydrate portion of the viral glycoproteins. Such inhibitors of glycoprotein synthesis can stop HSV-1 induced fusion and virus production.^[58] While the identification of tromantadine as an anti-HSV-1 agent may have been accomplished upon the search for amantadine analogues, it remains remarkable that it represents the third drug out of the aminoadamantane class identified within seven years after adamantane itself has become readily available, all of these drugs are being marketed until today.



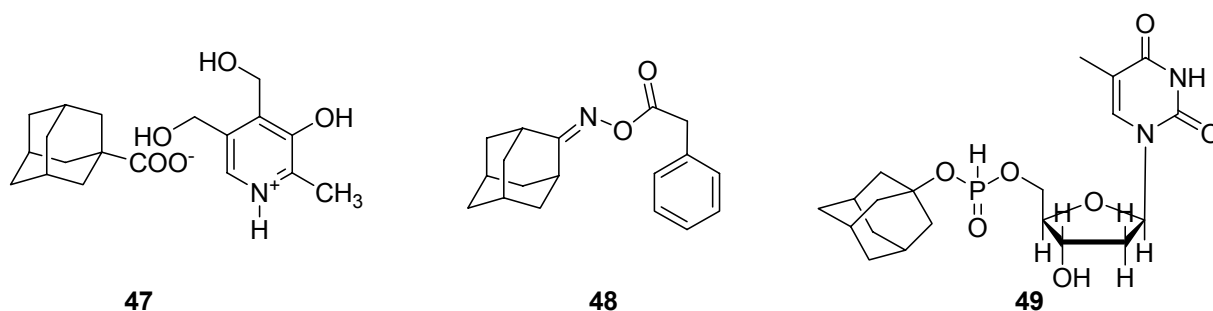
Scheme 6. Anti-HSV-1 agents

3.2.1.3. Hepatitis C, HIV, and SARS viruses

The antiviral activity of amantadine **19** against chronic *Hepatitis C* has not been verified yet, but a comparative study of combined amantadine with the antiviral drugs IFN- α -2a and ribavirin compared to a combination where amantadine was replaced by placebo was performed in 400 humans with chronic *Hepatitis C*.^[59] In 52% of the amantadine group the serum HCV concentration was undetectable after the study, compared to 43.5% of the placebo group.

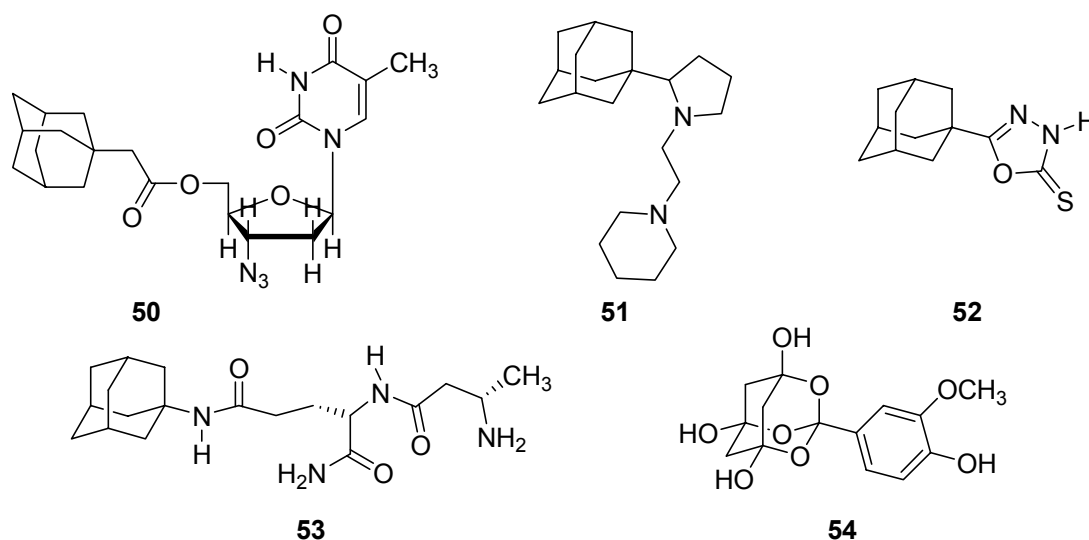
But not only aminoadamantanes were tested as agents to combat Hepatitis C. Early reports of anti-HCV activity of pyridoxin adamantanoates (e. g., **47**) showed *in vitro* activity of these salts.^[60] Another class of substances tested *in vitro* were the O-

acyloximes of 2-adamantanone (48).^[61] The lipophilicity of adamantane derivatives has also been used in a prodrug-approach utilizing adamantyl nucleoside-5'-hydrogenphosphates (e.g., 49) as depot forms of the respective nucleosides which, after being released and incorporated in the HCV genome, inhibits the virus reproduction in cell cultures. Other adamantane derivatives were patented as an "add-on" to (mostly macrocyclic) HCV-polymerase inhibitors.



Scheme 7. Some adamantanes tested against *Hepatitis C* viruses.

A prodrug approach has also been reported in the early chemotherapy of human immunodeficiency virus (HIV). Azidothymine prodrugs like 50 were synthesized to match the requirement of high lipophilicity.^[62] Variations of the aminoadamantane motif were of course also tested (e. g., 51). These proved to be effective against HIV-1 but not HIV-2 *in vitro* up to micromolar dose.^[63] Another target is represented by the HIV-1 fusion cofactor Gb₃. Adamantane substituted analogues provide high affinity to gp 120, an HIV-1 surface glycoprotein, thereby possibly inhibiting viral fusion.^[64] Adamantane substituted vancomycin derivatives also showed antiretroviral (e.g., HIV-1 and HIV-2) properties.^[65, 66] The adamantane substituted aminomethyl-1,3,4-oxadiazoline-2-thione 52 was reported to display dose-dependent, micromolar activity against HIV-1 *in vitro*, but cytotoxicity of this class of compounds usually exceeded their antiviral activity.^[67] The immunoadjuvant adamantylamide dipeptide (Ad-DP, 53) and some of its analogues also show some effectivity against a number of infections, amongst others HIV and *Haemophilus influenzae*.^[68, 69] However, to date no clinical trials or even anti HIV drugs incorporating an adamantane motif have been reported. The trioxa-adamantane-triols (TAT's or bananins) represent an emerging class of anti-retroviral substances.^[70] Molecules like, e. g., VANBA (54) inhibit SARS corona virus NSP10 protein ATPase which seems to be essential for SARS replication and therefore represents a valuable target to this virus lacking M2 surface protein.



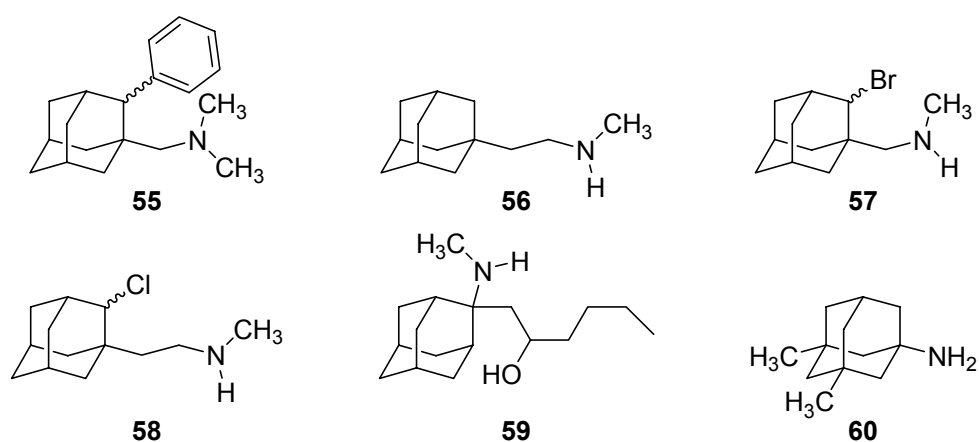
Scheme 8. Adamantane derivatives studied for the combat of HIV and SARS corona viruses.

3.2.2. Adamantane in neurochemistry and related fields: Blocking Channels

3.2.2.1. The dopaminergic system and Parkinson's disease – another amantadine story

The discovery of symptomatic benefit of Parkinson's disease (PD) upon treatment with amantadine was made fortuitously by Schwab et al. while examining amantadine's anti-*Influenza* activity in a clinical study.^[71] Research on this field largely paralleled the search for anti-*Influenza* adamantane derivatives. In early screenings, 89 aminoadamantanes were screened in an animal model (reserpine induced catalepsy).^[72-74] Most of the compounds tested did not compete well with the standard (nortriptyline) when administered subcutaneously, but on the other hand, activity was similar when administered orally. The adamantanes also displayed reduced toxicities. Best results were achieved with **55–59**. At about the same time amongst other bridgehead alkylated compounds, 3,5-dimethylaminoadamantane **60** was patented as an antiparkinson agent.^[75] This substance has later attracted eminent attention in another indication (see 3.2.2.6). Alkylation of the bridgehead positions in aminoadamantanes plays a pivotal role in the substance's glutamergic properties, as found out by comparison of a series of six alkylated congeners and aminoadamantane in different Parkinson models in mice.^[76] **60** proved to be the most effective compound in this model system. The authors reasoned that metabolic stability, low toxicity, molecular shape, and high propensity to cross the blood-brain-barrier (that is,

lipophilicity) are essential for the aminoadamantanes to display the favorable properties of an indirect release of neurotransmitter from intact dopaminergic neurons, thereby equilibrating the imbalanced dopamin-acetylcholin ratio that results from a degeneration of dopaminergic neurons in the *substantia nigra*, which is the origin of the symptoms associated with Parkinson's disease.



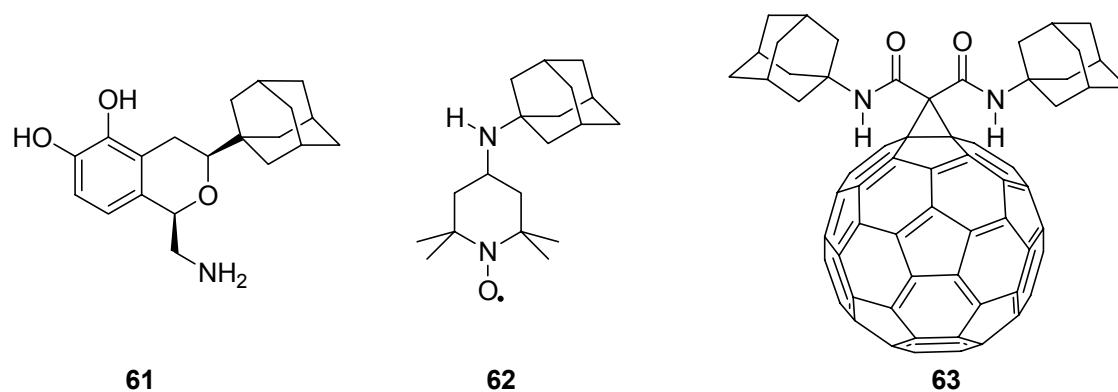
Scheme 9. Adamantanes screened for anti-Parkinson activity.

In humans taking L-Dopa, combined administration of **60** resulted in a marked improvement of the parkinsonian symptoms, which was attributed to the mode of action of **60** as an NMDA receptor antagonist, resulting in reduction of glutamate concentrations that can be pathological (see below).^[77] **60** and **19** were examined in *post mortem* human frontal cortex homogenates.^[78] While **60** seems to interact selectively with the phencyclidine (PCP) binding site of the NMDA receptor, **19** binds to both the σ - and NMDA- receptors. **19** and **60** were found to protect cerebellar and cortical neuronal cell cultures against glutamate toxicity (with **60** being consistently more effective), but they did not work in dopaminergic neuronal cultures.^[79] Therefore, the aminoadamantanes would fail in the neuroprotection of the nigrostriatal neurons of the *substantia nigra*. This stresses the role of aminoadamantanes in Parkinson's disease: They obviously do not expand the lifespan of the decisive type of neurons under the pathogenic conditions of PD, but do provide support of a balanced dopamine/acetylcholin neurotransmitter system. By microdialysis experiments it was demonstrated in rats that **60** does increase dopamine release up to 50% over the basal level *in vivo*.^[80] These authors highlighted that there is an interaction between non-competitive NMDA receptor antagonists and dopaminergic systems and attributed

the benefits of the aminoadamantanes in Parkinson's disease to changes in the balance between the excitatory amino acids and dopamine. In a study to determine the effect of short- and long-term treatments with amantadine on the activity of the neuronal dopamine transporter, it has been shown that long-term amantadine treatment increases the activity of the dopamine transporter.^[81] This probably represents a compensatory mechanism to enhanced dopamine release upon treatment with amantadine.

Two other strategies to combat parkinsonism are represented by selective dopamine receptor agonists and compounds used to catch reactive oxygen species that cause oxidative stress, thereby causing neuronal cell loss. A-77636 (**61**), an adamantane derivative also bearing structural motifs resembling catecholamines, has been found to be a long-acting, selective dopamine D₁ receptor agonist at nanomolar affinity. These D₁ receptor subtypes occur in high concentrations within the *substantia nigra* that is predominantly affected by neuronal death in PD. A-77636 has proven effective in the reduction of Parkinson-like symptoms in rats and monkeys, whereas its enantiomer lacks anti-Parkinson activity in this test.^[82] From these findings it was concluded that the D-1 dopamine receptor may be involved in the expression of symptoms of PD. In more recent reports it has been stated that A-77636 also interacts with the D-2 receptors, making the anti-Parkinson activity of D-1 receptor agonists more puzzling.^[83]

Oxidative stress is regarded another crucial factor causing neuronal cell death. Reactive oxygen species are being generated in excess as compared to the antioxidant capacity of neural cells upon, e.g., prolonged treatment with the anti-Parkinson drug Levedopa. Consequently, amantadine **19** was modified with a nitroxyl moiety displaying antioxidant properties to give **62**, which was designed to reduce oxidative stress by ROS.^[84] Upon deep oxidative stress generated by a neurotoxin in rats it was shown that the nitroxyl moiety is essential to display anti-Parkinson activity.



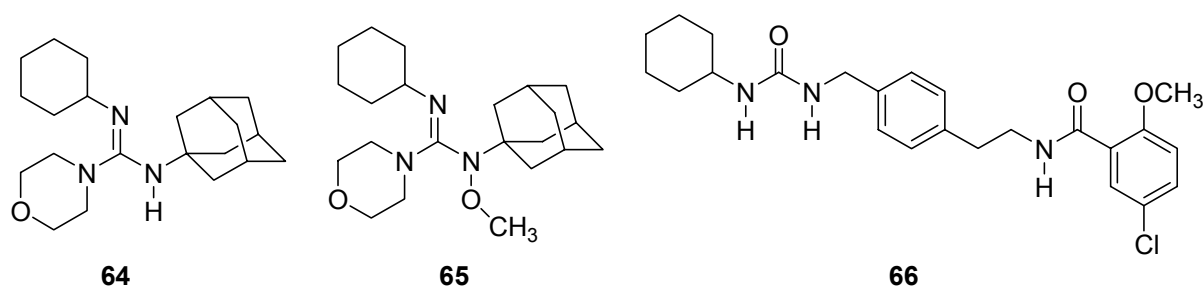
Scheme 10. Recently published anti-Parkinson pharmaceuticals incorporating an adamantane motif.

In summary, amantadine's mechanism(s) of action are not solely dopaminergic; it also displays noradrenergic and serotonergic as well as neuroprotective properties. Its precise mechanism of action in terms of PD remains to be elucidated as do the actual molecular biologic disorders that initiate PD. However, amantadine **19**, memantine **60**, and other aminoadamantanes have proven valuable in the examination of the different aspects in several neurotransmitter systems involved in PD. Combination of the aminoadamantane pharmacophor with other pharmacophors in principle is possible as shown in, e. g., **62**. As an additional benefit, these types of structures display enhanced lipophilicity and therefore a higher propensity to cross the blood-brain-barrier (BBB). Such a combination of different functional entities in one molecule is also being used in **63**. The lipophilic fullerene and adamantane moieties are advantageous in crossing the BBB, The effect of amantadine has been observed (increased dopamin release in rat striatum tissue) and the fullerene moiety displays an additional antioxidant activity.^[85] Whether such "exotics" are druggable remains to be elucidated.

3.2.2.2. K_{ATP} channels, glutamate- and AMPA- receptors

Potassium channels play an important role in the regulation of blood pressure, their modulation therefore is a promising target for pharmaceuticals. ATP sensitive potassium channels are controlled by the intracellular content of ATP and open upon lowering the intracellular ATP concentration. Control of pancreatic K_{ATP} channels through, e. g., sulfonylureas like tolbutamide results in an increase of insuline excretion. U-37883-A **64**, a K_{ATP} antagonist, is the first nonsulfonylurea that

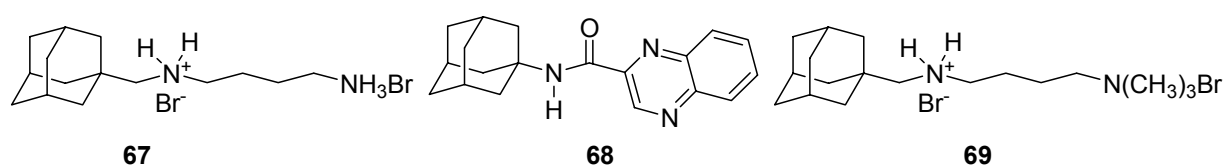
consistently blocks pharmacological responses to various potassium channel openers *in vitro* and *in vivo*.^[86] Furthermore, it displays a tissue selectivity, the sulfonylurea drug glyburide **65** being selective in favor of pancreatic K_{ATP} channels while U-37883-A selectively blocks K_{ATP} channels in vascular smooth muscle. While some analogues like U-52090 (**66**, it displaces U-37883-A from its binding site with similar potencies) have also been reported,^[87] none of these compounds has reached market, although the indication (type 2 diabetes) is promising (see 3.2.5.3).



Scheme 11. K_{ATP} channel blockers

Glutamate receptors (GluRs) are involved in CNS functions such as long-term potentiation and long-term depression, processes crucial for learning, and have therefore attracted attention as targets in a range of CNS disorders like Alzheimer's disease. They are subdivided in three subtypes according to their predominant agonists: NMDA, AMPA, and kainate. Adamantane derivatives used for selective blocking of the NMDA receptor are discussed below (see 3.2.2.4).

While cage amines like Memantine (**60**) and IEM-1754 (**67**) were of interest in structure elucidation and the localization of specific binding sites of glutamate receptors subtypes through analysis of their pharmacological and electrophysiological properties,^[88] NPS2390 (**68**) played a role in the identification of a common binding site shared by different antagonists of mGlu1 receptors.^[89] **68** also has been used in the elucidation of a distribution profile of mGluR1 in rat brain.^[90]



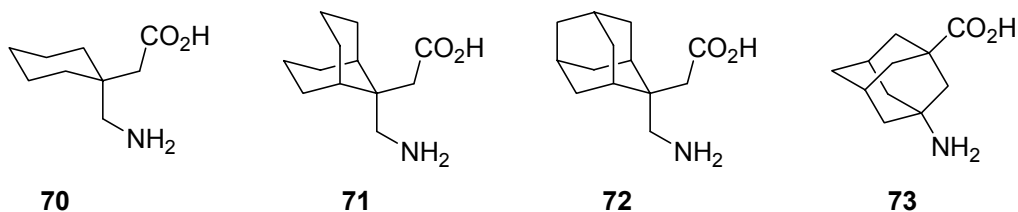
Scheme 12. Adamantane derivatives used as GluR ligands.

IEM-1460 (**69**) and **67** were utilized to shed light on the block of AMPA receptors as expressed in *Xenopus* oocytes and in fresh rat hippocampal slices.^[91] Using these (and other) dicationic antagonists, a topographical model of the channel binding site in AMPA and NMDA receptors was proposed.^[92]

3.2.2.3. The GABAergic system

γ -Amino butyric acid (GABA), the main inhibitory neurotransmitter in CNS, plays a decisive role in signal transmission and, from a medicinal point of view, in CNS related diseases like, e. g., epilepsy. GABA mediates its action via different subtypes of GABA receptors^[93, 94] and transporters.^[95] Given the well-known propensity of many adamantane derivatives to display activity towards CNS through their ability to cross the blood-brain-barrier, one could reason that adamantanes, in particular amino acids thereof, should have promise to serve as hits in the medicinal chemistry of the GABAergic system as well. The actual situation is, however, more intriguing.

Gabapentin (**70**), today one of Pfizer's best selling drugs (marketed as Neurontin[®]), was originally designed as a lipophilic structural analogue of GABA,^[96] but it has later been shown that its primary target neither are GABA receptors and pumps, nor enzymes on the GABA metabolic pathway.^[97] Today's consensus is that gabapentin interacts with the α_2 - δ subunit of voltage-gated Ca^{2+} channels. Modulation of the α_2 - δ subunit results in an attenuation of Ca^{2+} flux into the neurons, which inhibits the release of neurotransmitters into the synaptic cleft. Amongst others, the release of excitatory neurotransmitter glutamate is reduced, leading towards control of, e. g., epileptic seizures.^[98, 99] Several alkylated analogs of gabapentin have been disclosed, including **71** and **72**.^[100]



Scheme 13. Lipophilic analogues of GABA

Some alkylated derivatives of gabapentin, including **71**, have been reported to have greater binding affinity to the gabapentin binding site than gabapentin itself,^[100] with a comparable anticonvulsant activity in an animal model. The adamantane derived γ -amino acid **72** was shown to bind to the same target and to reduce neuronal Ca^{2+} current as measured electrophysiologically.^[99] In addition to its anticonvulsive properties, it also displayed analgesic properties in mice. Notably, derivatives like the γ -aminoadamantane-1-carboxylic acid **73** have not been considered as GABA analogues in the literature.

3.2.2.4. Alzheimer's disease, the NMDA receptor and more – the memantine story

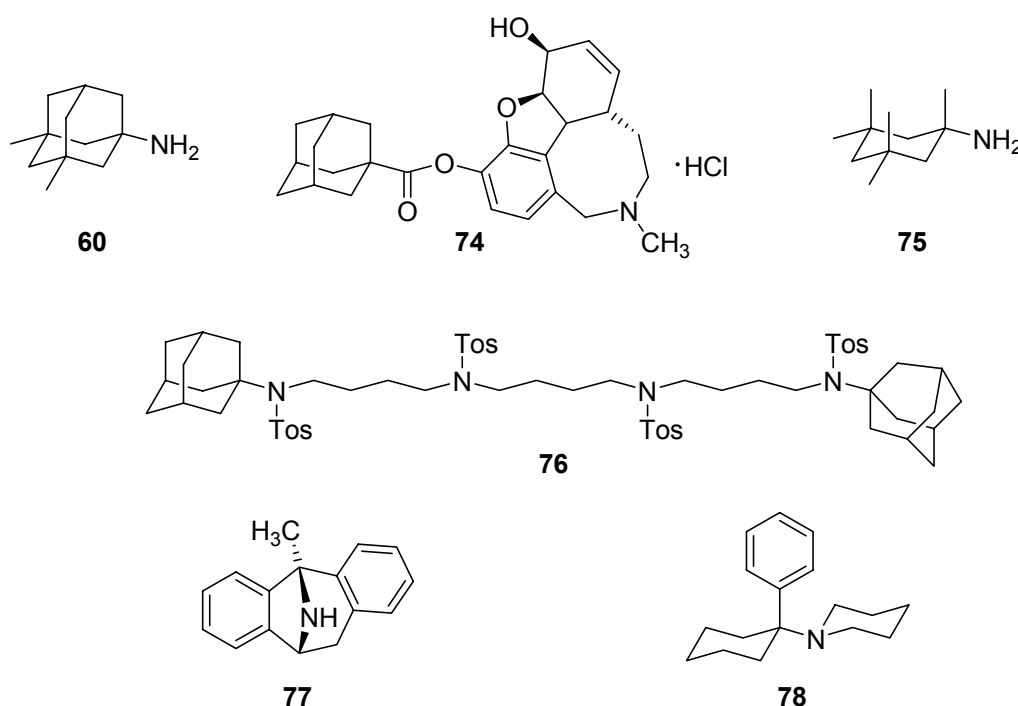
Dementia and Alzheimer's disease are emerging threats for the aging population in industrialized countries. Today, AD is ten times more frequent than AIDS. Therefore, research and (pharmaceutical) therapies are urgently needed. The precise molecular coherence causing AD is still not finally understood, but an understanding for its development, pathological features and several drug targets has been elaborated out in recent years.

AD begins with loss of cholinergic neurons in the hippocampus.^[101] This causes a further decline in neurons, loss of memory, loss of any capacity to communicate, and death. From a neuropathological point of view, AD affected brain develops neurofibrillary tangles and amyloid plaques in regions of the brain that are involved in learning and memory. Neurofibrillary tangles consist of fibres inside the brain cells formed by tau protein. The amyloid plaques are being formed by deposition of the 40–42 residue peptide amyloid β (βA). Much attention of neurochemists towards AD is driven through the formation of amyloid plaques.^[102, 103] The amyloid plaques are being formed by fragments of the so-called amyloid precursor protein APP upon its degradation by α -, β -, and γ -secretases whose interplay is crucial.

Current chemotherapies include inhibitors of acetylcholinesterase and antagonists of the NMDA receptor. Cholinesterase inhibitors are being prescribed in early stages of AD; they combat the effect of the loss of cholinergic neurons by inhibiting acetylcholin's degradation through esterases, thereby maintaining an appropriate concentration of acetylcholin. One experimental candidate for such an

acetylcholinesterase inhibitor is the galanthamine derived adamantane derivative

74.^[104]

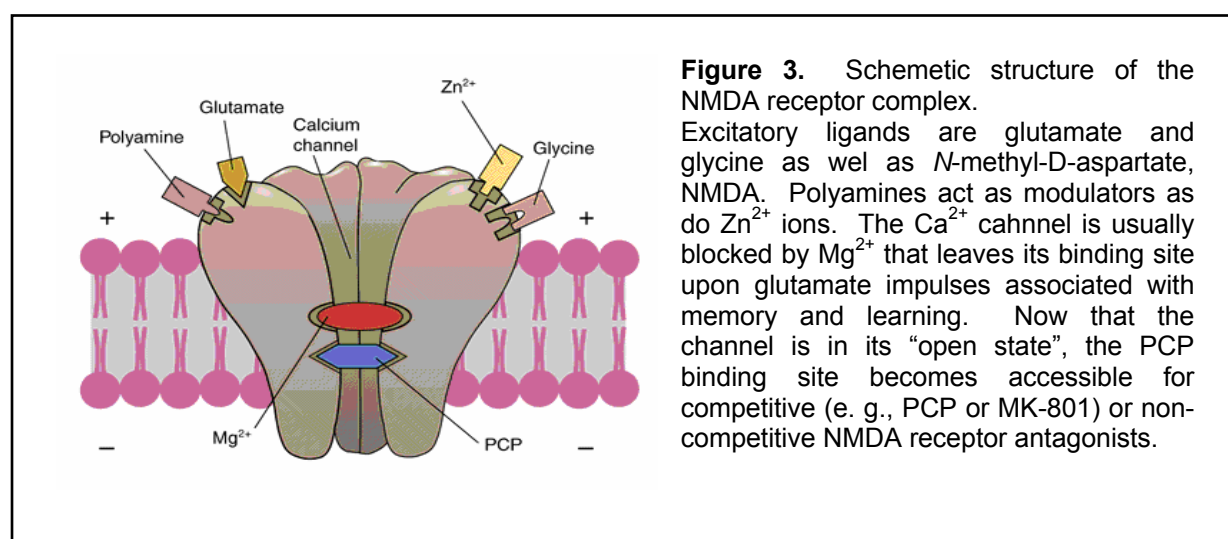


Scheme 14. NMDA receptor ligands and an adamantane-derived acetylcholin esterase inhibitor

NMDA receptor antagonists are currently the only medication for intermediate to severe cases of AD. Memantine (**60**) and related aminoadamantanes were patented for the treatment of dementia in 1990^[105]. Memantine's efficacy has early been attributed to its effect on NMDA receptors. These receptors are subtypes of the GluRs. They are being overactivated by excess glutamate associated with neuronal cell loss caused AD; NMDA receptor overactivation leads to an increased influx of Ca²⁺ into the postsynaptic neuron. This process causes reduced sensitivity for glutamate mediated signals associated with memory and learning due to increased "noise", finally leading to catabolic processes and, ultimately, cell death.

Memantine was found to display an open channel block of the NMDA receptor's calcium channel.^[106] Micromolar levels of memantine were found to display neuroprotective properties in rats. Polyamines like the adamantylated spermine derivative **75** have been shown to modulate the NMDA receptor in an allosteric fashion,^[107] being antagonists of [³H]MK-801 at higher concentrations while enhancing MK-801 binding at lower concentrations. This requires a distinct binding site at the NMDA receptor complex. By labelling one of the two methyl groups in memantine

utilizing ^{18}F , the drug was shown to bind at the phencyclidine (PCP) binding site of the NMDA receptor complex, which is located inside the ion channel (Figure 3).^[108] The kinetics of the channel blockade plays a decisive role in the clinical tolerability of aminoadamantanes like **60**: Being a moderate-affinity channel blocker, it does not cause side effects like, e. g., PCP (“Angel Dust”), but due to its rapid association rate, it does efficiently block Ca^{2+} influx into the neuron.^[109, 110] Today’s consensus is that the moderate affinity towards the PCP binding site of the NMDA receptor complex, the rapid association (and dissociation) kinetics, dose-dependence and favorably low side effects render memantine druggable.^[111, 112] It has been approved in Europe (2002) and the US (US-FDA approval: October, 2003; brand names include Axura[®], Ebixa[®], Namenda[®] and Akatinol[®]) and is at the cusp of becoming a blockbuster. Detailed studies of affinity and kinetics of the blocking of NMDA receptor ion channels, mostly utilizing electrophysiological measurements under a broad variety of pharmaceutical conditions (for this purpose, amongst others, a multitude of adamantane amines were studied)^[92, 109, 113, 114] led to an understanding of structure and functionality of this glutamate receptor subtype that is shown schematically in Fig. 3.^[115] The pentamethyl-aminocyclohexane derivative **75** is currently in clinical trials and planned as a follow-up for memantine. Its molecular shape and, therefore, its mechanism of action compares to that of memantine.^[116, 117]



3.2.3. Adamantanes in neurochemistry 2: neuropeptides and serotonin analogues

Given the lipophilic properties utilized for a number of applications in CNS related diseases as mentioned several times above, and being aware of the fact that aminoadamantanes display activity to a number of targets while being readily available, it almost seems mandatory that scientists tried to modify neuropeptides utilizing the (amino)adamantane motif. Seven families of neuropeptides will be briefly treated in the following.

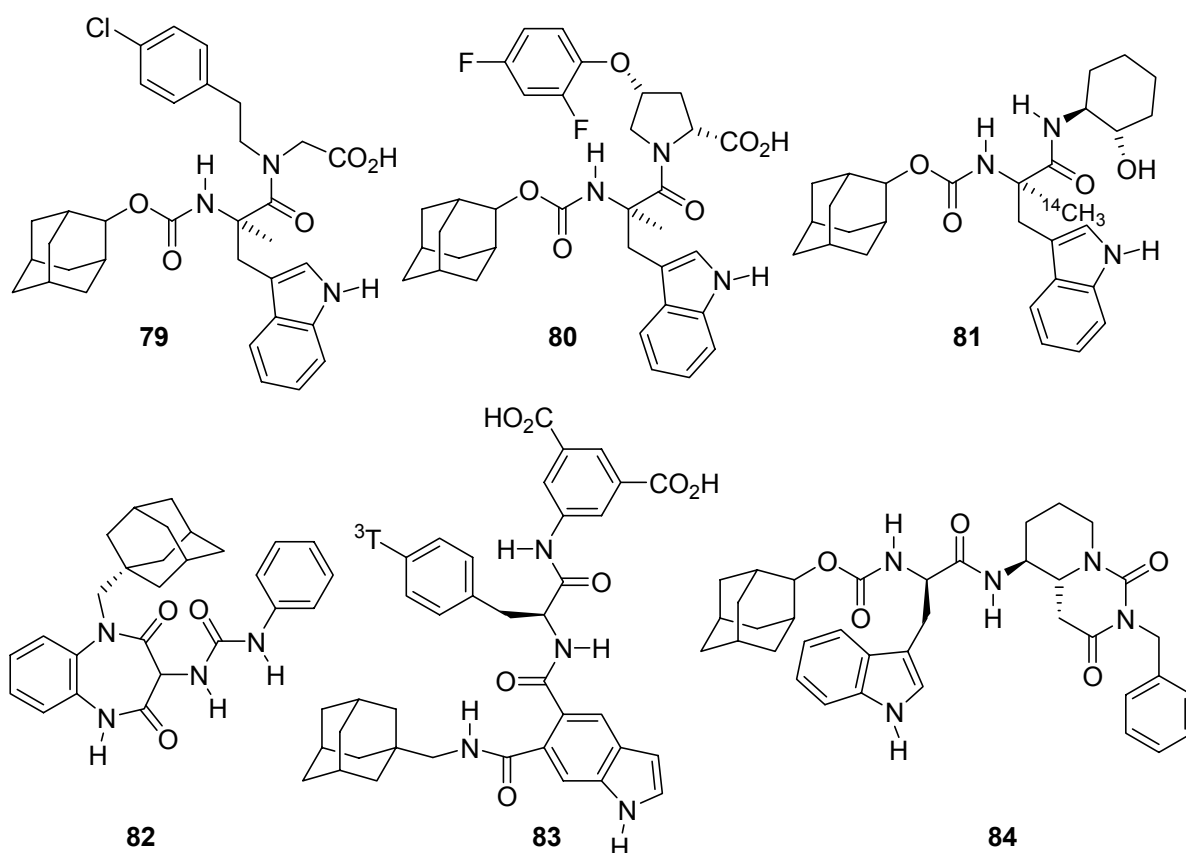
3.2.3.1. Cholecystokinin

The cholecystokinins (CCK) are a family of six neuropeptides varying in length from eight to 83 residues. However, CCK-8 (H-Asp-Tyr(SO₃⁻)-Met-Gly-Trp-Met-Asp-Phe-NH₂) has the sequence of the C-terminus of all members of the CCK family. CCK mediates satiety by acting on CCK receptors that are distributed widely in the CNS. CCK receptors in the brain are also involved in memory and anxiety and, therefore, a target of pharmaceutical chemists.

By replacing an *N*-terminal Boc protective group with the 2-Adoc protective group, CCK₈ mimetic analog peptide **79** was identified.^[118] It is a selective antagonist of CCK_B receptors that are of role in neurochemistry to block panic attacks. Introduction of conformational constraint through cyclization yielded **80**, that preserved the CCK_B affinity of **79** but improved its antagonist activity.

Its enhanced bioavailability was ascribed to reduced enzymatic degradation upon enhanced lipophilicity.^[119] The radiolabelled derivative **81** has been used to characterize CCK_B receptor binding.^[120] **82** also displays a remarkable selectivity for CCK_B receptors: It binds to CCK_B receptors with $K_i = 3.0$ nM while $K_i = 2900$ nM for CCK_A receptors.^[121] Metabolites of **82** in rat, dog, and human liver microsomes^[122] identifying hydroxylation of tertiary adamantane C–H bonds as a main biodegradation (as has been known from the literature^[36]) have been detected. Another radiolabelled CCK_B antagonist, **83**, provided additional evidence to the assumption that there are two binding sites of this receptor in rat cortex.^[123] Unifying the urea motif from **82** and the 2-Adoc-indol moiety from **79** and **80** was accomplished in **84**. The significance of

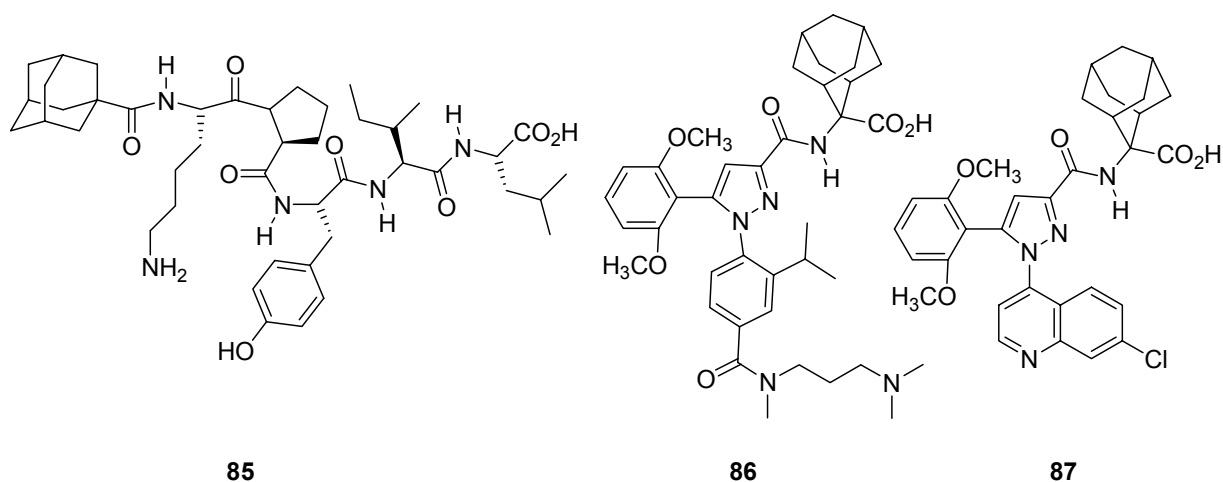
the adamantane moiety is illustrated by the fact that upon substitution of 2-Adoc with Boc, the affinity to CCK_B drops by one order of magnitude.^[124]



Scheme 15. Peptidomimetic CCK_B receptor antagonists incorporating an adamantane moiety.

3.2.3.2. Neurotensin

Neurotensin, an endogenous tridecapeptide, plays a dual role as (a) a peptidic hormone in the periphery and (b) neuromodulator or neurotransmitter in dopamine transmission in the CNS. It exhibits hypothermic, psychotropic, and analgesic properties while only the C-terminal pentapeptide [(NT(8-13))] is necessary for the analgesic effects.



Scheme 16. Some neurotensin receptor antagonists incorporating an adamantane motif.

Modulating this C-terminal pentamer led to the discovery of adamantanecarbonyl-NT(9-13) **85**, which had a longer duration of action compared with NT(8-13).^[125] Leaving the path of modifications at a peptidic backbone, **86** incorporating 2-aminoadamantane-2-carboxylic acid, was identified. It acts as a neurotensin receptor antagonist at nanomolar affinity *in vitro*, compared with **85**, it also displays increased bioavailability.^[126] ³H radiolabelled **86** has also been utilized for elucidation of its binding properties at the neurotensin receptors NTR₁ and NTR₂ in rat brain.^[127] It has found utilization in the development of antipsychotic drugs as well.^[128] Closely related **87** was useful in molecular modeling studies to identify the binding sites of antagonists and agonists at NTR₁.^[129] Blockade of NTRs with **87** attenuates initiation and expression of amphetamine-induced locomotor sensitisation. Therefore, antagonists of this type are discussed as drugs of clinical usefulness in the treatment of neuropsychiatric disorders.^[130]

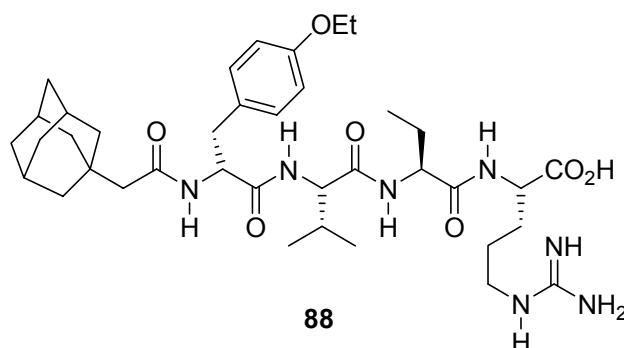
3.2.3.3. Bradykinin

Bradykinin (H-Arg-Pro-Pro-Gly-Phe-Ser-Pro-Phe-Arg-OH) functions as a vasodilator as well as playing a role in the mechanism of pain. Acylating bradykinins with, e. g., adamantane-1-carboxylic acid resulted in a bradykinin receptor antagonist with at least the 33-fold activity.^[131] Adamantane derivatives of different substructures of the bradykinin sequence were utilized to gain insight into the pharmacology of bradykinin and its receptor, e. g., in the characterization of bradykinin receptors in the human nasal airway^[132], elucidation of the thrombin-bradykinin interplay in inflammatory

response,^[133] and in studies dealing with the stimulation of the production of a vasodilator through bradykinin.^[134]

3.2.3.4. Vasopressins and Oxytocin

The vasopressins are nonapeptidic hormones that act at three receptor systems, one of which, the so-called AVPR1B is located in the brain and plays a role in hormone secretion through stress. A concept reminiscent of the modification of a neurotensin C-terminal fragment to yield **85** was also utilized here: an adamantaneacetylated derivative of arginine-vasopressin fragment 4-9 (**88**), acting as an V_2 receptor selective antagonist, has been utilized in studies for the elucidation of the functionality of arginine-vasopressin fragment 4–9 in the cholinergic system involved in learning. AVP₄₋₉ supposedly stimulates acetylcholin release in rat hippocampus and thereby facilitates learning and memory in rodents.^[135] **88** as an antagonist of the vasopressin receptor also played a significant role in, e. g., the localization of intravascular vasopressin receptors playing an important role in blood pressure regulation.^[136]



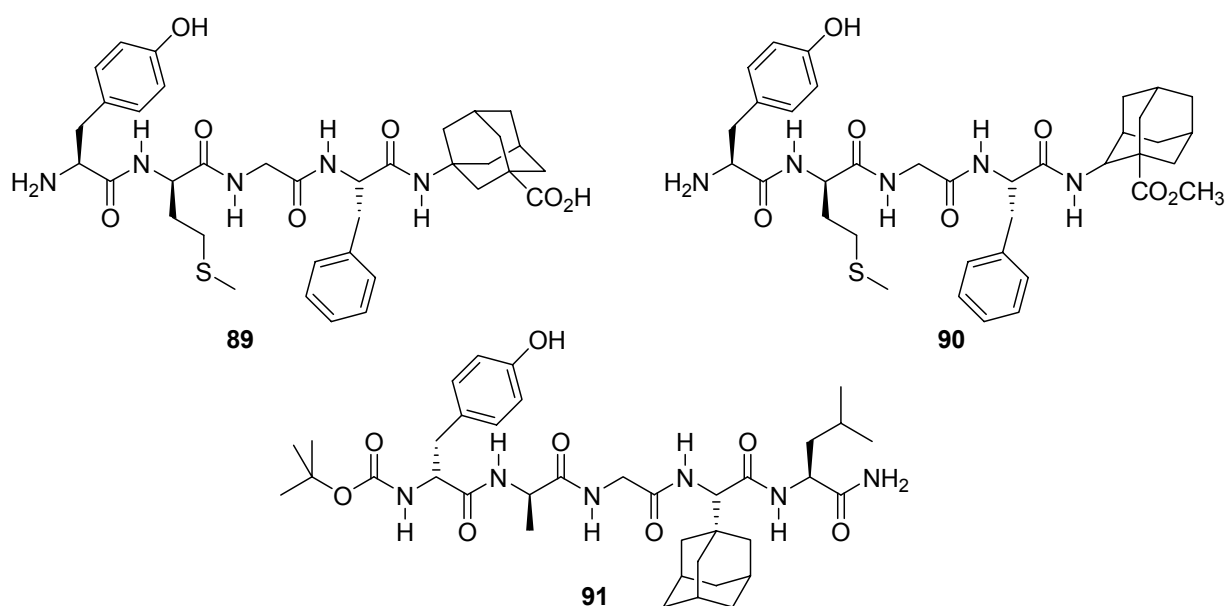
Scheme 17. Adamantaneacetyl-D-Tyr(OEt)-Val-Abu-Arg, utilized as vasopressin receptor antagonist.

There are also reports on the modification of the mammalian peptide hormone and neurotransmitter oxytocin generated by, amongst other modifications, incorporation of an adamantane moiety.^[137]

3.2.3.5 Enkephalins

The enkephalins are two pentapeptides that act as the ligands for the opiate receptor in the brain. They differ in the C-terminal amino acid only: [Met]enkephalin has the

sequence H-Tyr-Gly-Gly-Phe-Met-OH, [Leu]enkephalin has H-Tyr-Gly-Gly-Phe-Leu-OH. The enkephalins act as neurotransmitters and neuromodulators. Many analogues have been synthesized to develop more potent and less addictive anodynes.^[138-140] These include peptides incorporating γ -aminoadamantane-1-carboxylic acid and other adamantane derivatives in position 5 as exemplified by **89** and **90**.^[139] Another way of incorporating the adamantane moiety is the use of “adamantylglycine”, which also has been realized in, e. g., **91**.^[141] This peptide was about three-times as potent as the analogue with a leucine residue instead of the adamantylglycine (Ada) residue. The adamantane containing enkephalin analogues also displayed resistance towards hydrolysis through different enzymes. Such a type of modification with the highly lipophilic adamantane residue is in this context regarded a tool for drug delivery to the CNS.^[142]



Scheme 18. Adamantylated enkephalin analogues

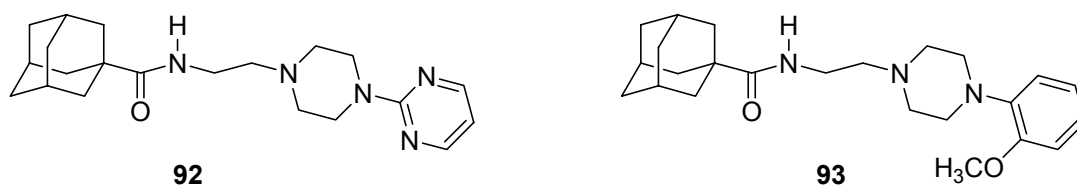
A number of enkephalin analogues incorporating adamantane have been examined as tumor-cell targeted entities (cf. 3.2.6).^[143]

3.2.3.6 Serotonin

Next to its role in the regulation of blood pressure, serotonin is also a neurotransmitter in the CNS involved in depression and anxiety. A total of 14 serotonin receptors have

been found. Therefore, selective agonists/antagonists are needed to use different receptors as drug targets.

In a screening of 74 compounds incorporating adamantane, 3-methyladamantane or noradamantane moieties, **92** and **93** were identified to have acceptable affinities and selectivities in *in vivo* models. These two compounds derived from anxiolytic pharmaceuticals, were found to be potent 5-HT_{1A} partial agonists while being 5-HT₂ antagonists.^[144] Therefore, **92** entered clinical trials as adatsanserin as an anxiolytic agents also useful against depression. Libraries of novel arylpiperazines, including adamantane amides, have subsequently been synthesized on solid phase.^[145] In a screening towards 5-HT_{1A}/5-HT_{2A} selectivity, it was figured out that obviously the terminal amide part decisively influences the selectivity.



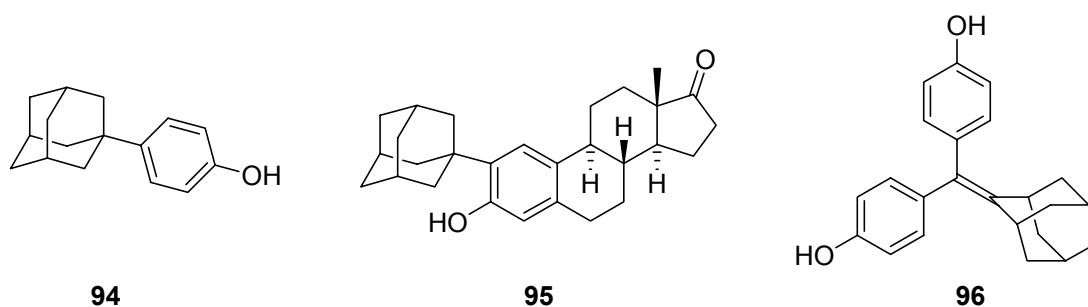
Scheme 19. Serotonin receptor ligands

3.2.4. Estrogenic, opioid, and σ receptors

Estrogen, a steroid hormone, influences growth, differentiation and functioning of many target tissues. Estrogen receptors α and β (ER α and ER β) are activated by hormonal ligands, and after a conformational change the receptors dimerize; the receptor then binds to chromatin to modulate transcription of target genes.^[146] Because of the fact that estrogens show tissue selectivity, differentiation between an action as agonist or antagonist is in many cases delicate. Therefore, the term selective estrogen receptor modulator (SERM) has been coined. ER α knockout mice have reduced fertility, reflecting the fact that ER α is primarily to be found in breast and uterine tissue. By contrast, ER β knockout mice show impairment of cognitive function due to ER β being located mainly in the brain, bone and vascular epithelium.

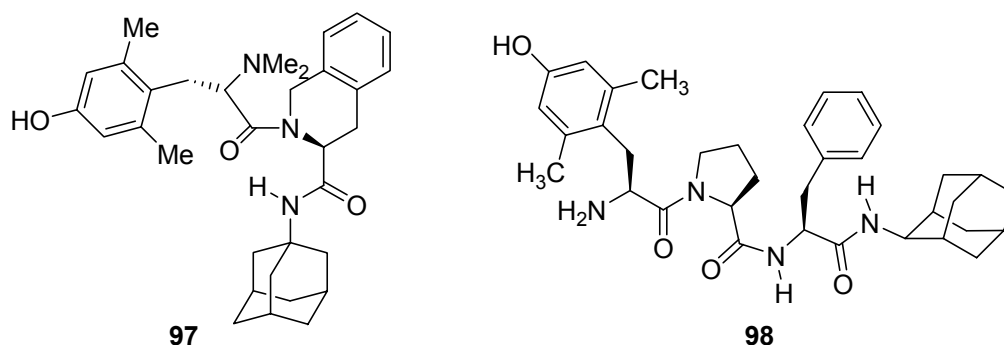
The health risk of estrogenic compounds from the environment or from industrial sources is debated. Compounds displaying estrogen receptor binding at high micromolar concentrations are, amongst others, phenols substituted with a lipophilic entity such as adamantane in **94**.^[147] The adamantylated estratriol derivative **95** is a

non-receptor binding estrogen analogue that has found to display neuroprotective properties. It decreases glutamate toxicity, which is of interest where androgen effects are not wanted.^[148] The same neuroprotective and non-feminizing effect has also been observed in glutamate-induced neurotoxicity in rat RGC-5 cells from the retinal ganglion.^[149] Since it does not bind to an estrogen receptor, it is obvious that the neuroprotection must be ascribed to other characteristics, e. g., antioxidant properties.^[150] Biphenol **96** is an example for an experimental estrogen receptor ligand that failed to be subtype specific; a norbornane moiety instead of the adamantane yielded far better selectivity.^[151]



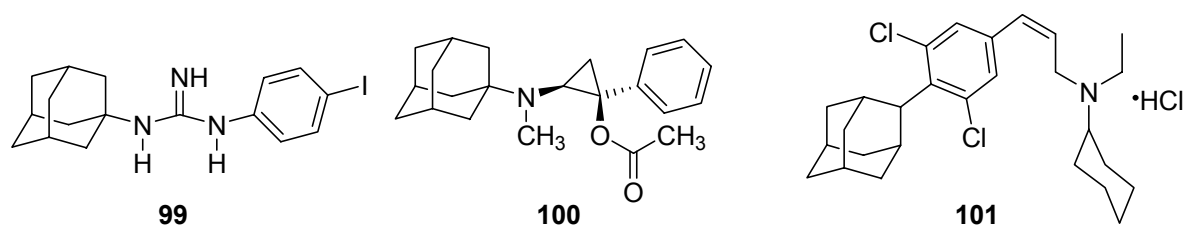
Scheme 20. Experimental estrogenic adamantane derivatives

Opioid receptors are a G-protein coupled transmembrane proteins that have been characterized into three main subtypes: δ , κ and μ . Through adamantoylation, it was attempted to improve the affinity of a peptide ligand as shown in compound **97**. It displayed μ -opioid receptor affinity ($K_i = 6.59$ nM), but that is three-times less than the affinity of the parent endomorphin analogue tripeptide.^[152] There is, however, interest in the structure elucidation of opioid receptors and their receptor-ligand interactions to guide future agonist/antagonist design. Therefore, the X-ray structures of a number of ligands incorporating the so-called Dmt-Tic pharmacophore and, in part, an adamantane motif (**98**), has been examined.^[153]



Scheme 21. Opioid receptor ligands incorporating adamantane.

The molecular processes underlying the functionality of σ receptors are poorly understood; however, antagonists are under investigation as antipsychotics. Agonists display hallucinogenic effects. Adamantanylated ditolylguanidine analogues like **99** have early been examined in this context to gain insight in the distribution and pharmacology of this receptor family.^[154, 155] When added to the rigid cyclopropane derivative in **100**, the adamantane moiety caused higher affinity and selectivity for σ sites than for opioid and dopamine receptors.^[156] This selectivity prompted the synthesis of more derivatives alongside this “lead” and the proposal of a first SAR model.^[157] Pharmacological research concerning rheumatoid arthritis in a mouse model led to the discovery of SSR125329A (**101**), which also is a high-affinity σ receptor ligand.^[158]



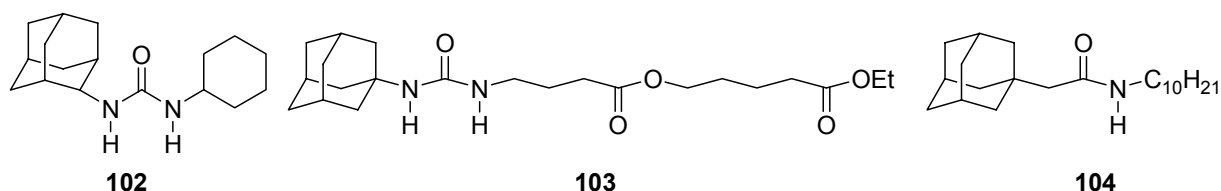
Scheme 22. σ receptor ligands.

3.2.5. Enzyme inhibition

The specific inhibition of enzymes hallmarks one ultimate goal in medicinal chemistry. Of the different approaches to utilize adamantane derivatives in this classical field of pharmacology, three examples are treated here.

3.2.5.1. Epoxide hydrolases

Epoxide hydrolases play a decisive role in, e. g., drug metabolism. One such hydrolase, the soluble epoxide hydrolase is involved in the metabolism of endogenous chemical mediators which are involved in the regulation of blood pressure and inflammatory processes.^[159] Ureas are an important class of inhibitors of soluble epoxide hydrolase (sEH), and an N-adamantylsubstituted derivative gave the best results.^[160] **102** inhibited human sEH *in vitro* with an IC₅₀ of 0.12 μM, whereas the dicyclohexylurea, the initial hit in pharmacophor scan, had an IC₅₀ of 0.16. Both were also active *in vivo* in mice. While this small improvement cannot be regarded as a breakthrough, it prompted additional work on this lead structure. One obstacle was low solubility of the dialkyl ureas, that has been tackled by the introduction of polar groups in one of the alkyl substituents as exemplified by **103** [IC₅₀ (human sEH) = 0.10 μM]. These authors stated in their SAR that the adamantyl urea serves as the primary pharmacophor, a polar carbonyl group in about 7.5 Å distance to the urea carbonyl represents the secondary pharmacophor, and an alkyl ester represents the tertiary pharmacophor.^[161] This model was further refined and the primary pharmacophor was altered, finding that amides like **104** exhibited identical activities in comparison to the ureas [IC₅₀(human sEH) = 0.10 μM].^[162] One of these adamantane substituted sEH inhibitors were found to be helpful in the attenuation of tobacco-smoke induced inflammation of the airways in mice,^[163] but in a combinatorial approach it was recently found out that the adamantane moiety is not essential and can be replaced by, e. g., nonrigid carbocycles or para/meta substituted phenyl groups.^[164]



Scheme 23. Adamantyl urea inhibitors of epoxide hydrolases

3.2.5.2. Dipeptidyl peptidases and type 2 diabetes: vildagliptin and saxagliptin

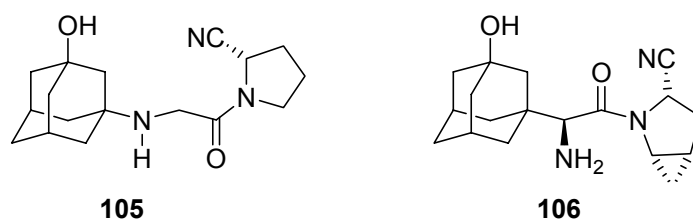
While the adamantane moiety “only” plays the role of a lipophilic “add-on” in the aforementioned case of sEH inhibition, two cases of adamantane derivatives that are

currently in late clinical trials and are about to make it to the market – which is the treatment of diabetes and, therefore, a multi billion dollar market.

While it has been known that some adamantane derivatives displayed hypoglycemic properties^[20], in recent years an emerging class of hypoglycemics, the dipeptidyl peptidase inhibitors, created a furor. This enzyme's role in diabetes is crucial; the current consensus^[165, 166] is that it cleaves the two N-terminal amino acids of incretin hormones which, upon this modification, lose their prandial insulinotropic effect. Inhibition of DPP-IV therefore restores the incretin hormone's activity which makes clinically tolerable inhibitors interesting for the treatment of type 2 diabetes.

Novartis has identified **106** as one such inhibitor drug candidate that, like others, resembles the dipeptidyl substrate cleavage product.^[167] The hydroxyadamantane moiety provided the steric bulk that is needed adjacent to the P-2 site. This drug, named vildagliptin, has been submitted for approval to FDA and EMEA in 2006 and is expected to enter the market soon as "Galvus".^[168]

Another "big-pharma" player has independently identified **106** as an DPP-IV inhibitor.^[169] It shares the structural features of **105** and is currently in phase III clinical trials. The mechanism of action of these two drugs is the same, although sometimes **105** is referred to as a reversible inhibitor while **106** is regarded a covalently bonded inhibitor. **106** also has higher affinity ($IC_{50} = 0.45$ nM) than **105** ($IC_{50} = 3.5$ nM).^[168]



Scheme 24. Vildagliptin and Saxagliptin, dipeptidyl-peptidase IV inhibitors.

3.2.5.3. I_2^{PP2A} – another memantine story?

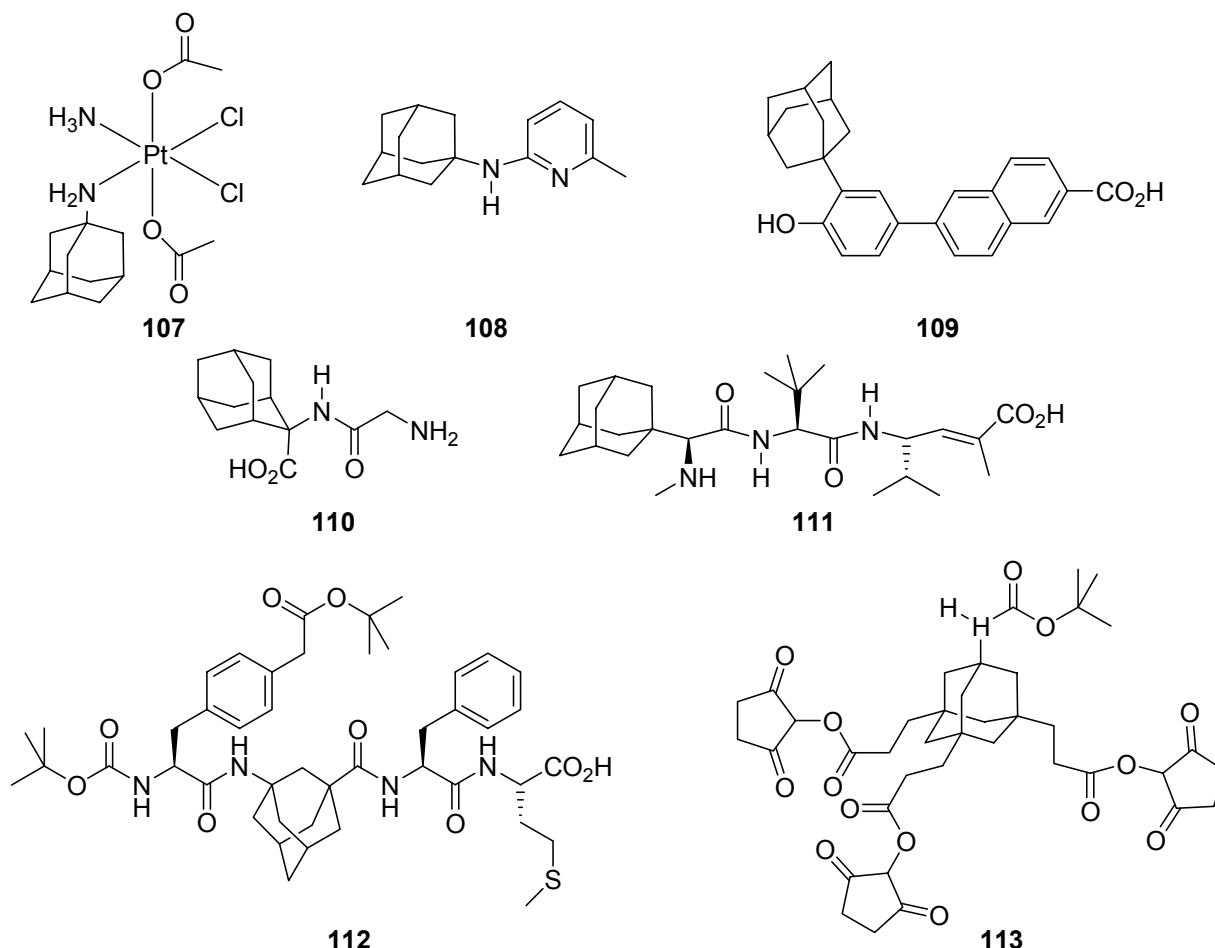
Another finding one must not forget in the context of enzyme modulation utilizing adamantane derivatives is the finding of Iqbal et al. that memantine **60**, in addition to its well-known and clinically useful NMDA-receptor antagonism (see 3.2.2.4), obviously has another target involved in Alzheimer's disease. They have found that

memantine inhibits and reverses hyperphosphorylation of tau protein, which is in this hyperphosphorylated form the major protein subunit of the neurofibrillary tangles found in AD.^[170] The enzyme responsible for the dephosphorylation of tau is termed protein phosphatase-2A (PP-2A), and there are inhibitor proteins for this enzyme called I_1^{PP2A} and I_2^{PP2A} . By up-regulation of these inhibitors, hyperphosphorylation of tau protein was observed, which is assumed to be a consequence of the inhibition of the dephosphorylation activity of PP-2A and an increase in the phosphorylation of tau protein by kinases that are regulated by PP-2A.^[171] While memantine had no effect on PP-2A activity, it obviously interacts with I_2^{PP2A} within the cell, thereby reducing tau phosphorylation.^[172, 173]

3.2.6. Adamantane derivatives in cancer research

With cancer research making up a large part of today's efforts in pharmaceutical research, it is obvious that adamantane derivatives have also been utilized here. A few of them (with no claim of being exhaustive) are given here. The cisplatin analogue **107** was planned to be of help in cisplatin resistant cancer cell lines.^[174, 175] **108** has been subjected to testing with respect to its potential as an adjuvant augmenting the efficacy of cancer vaccine-based therapies or in the local treatment of certain tumors.^[176] **109** has been found to be a retinoid, which are promising agents for the prevention and treatment of several human malignancies including lung cancer.^[177, 178] The peptide **110** incorporating an amino acid based upon the adamantane nucleus,^[179] was tested with respect to its anti tumor properties *in vitro*.^[180] It also proved to be highly resistant towards degradation through proteases – it was in turn an inhibitor of leucine aminopeptidase. Another peptidic entity equipped with an adamantane moiety is **111**, which is an analogue of hemiasterlin. The hemiasterlins, natural-compound derived antitumor agents display antitumor properties, and so does **111**.^[181] We already encountered enkephalin analogues incorporating an adamantane moiety above (see 3.2.3.5), and a further development is represented by **112**. This tetrapeptide analogue of [Met]enkephalin is one very recent example of the incorporation of γ -aminoadamantane carboxylic acids in peptides. It has been shown to display anti tumor activity (albeit comparatively

low).^[143] In compound **113** the adamantane core is used as a directing scaffold for the assembly of ligand/marker conjugates for multivalent ligand receptor interactions, e. g. in prostate cancer studies.^[182]

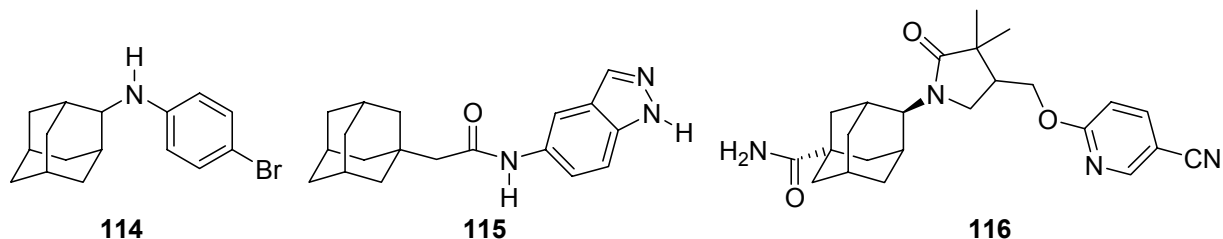


Scheme 25. Adamantane derivatives in cancer research.

3.2.7. Miscellaneous and some exotics

Even more applications of the adamantane nucleus in medicinal chemistry could be reported. One such derivative worth mentioning in this context is **114** (dubbed bromantan) having neurostimulatory properties.^[183] It also was used as an athletic performance enhancer,^[184] e. g., during the 1996 summer olympics. Indazolyl derivative **115** is a lead structure identified during a screening of combinatorial libraries of P2X₇ receptor antagonist.^[185] Finally, **116** is another example where the adamantane moiety is used to direct functional groups into the position needed to

precisely interact with a target molecule or protein. In this example, the adamantane (and other rigid bi- and tricycloalkane scaffolds) was used in a study to find inhibitors of 11 β -hydroxysteroid dehydrogenase 1.^[186-189]



Scheme 26. Adamantane derivatives as used as stimulants, P2X₇ antagonists, and 11 β -HSD1

3.2.8. Summary

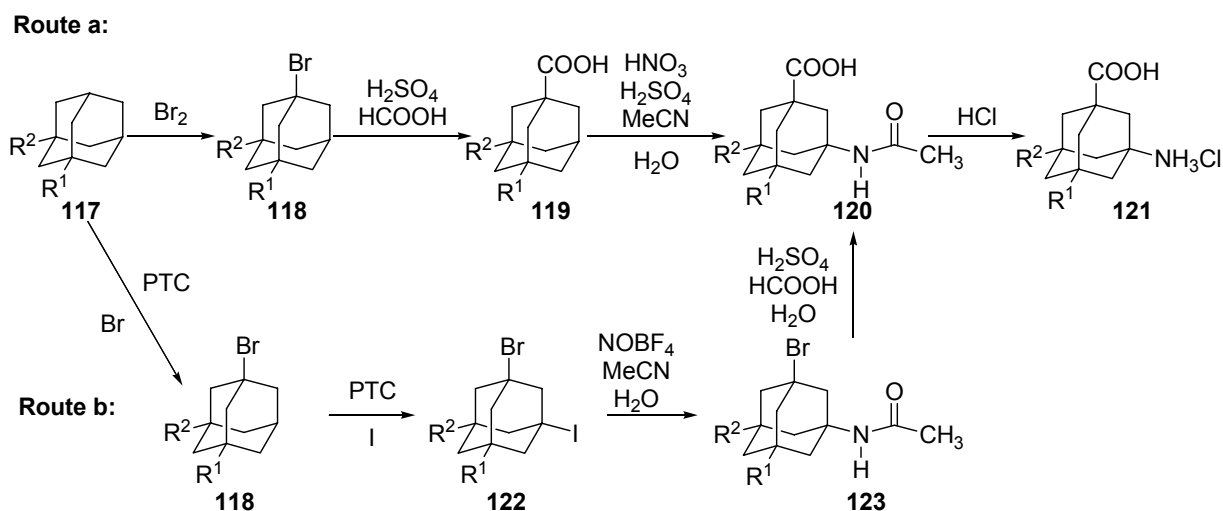
What can be concluded from this survey on medicinal applications of adamantane derivatives? Four “hits” (Amantadine, Rimantadine, Memantine, Tromantadine) almost “instantly” made it to market just from the group of aminoadamantanes only several years after Schleyer’s seminal synthesis of the core hydrocarbon itself. In other words, apart from being a “paraffine” the adamantane nucleus obviously in several cases can be regarded as a pharmacophore itself, in particular when equipped with one (or more) other functional group(s). Since these early years at the beginning of the 1960s, the adamantane moiety was utilized as an “add-on” to increase lipophilicity of already known pharmaceutically active compounds in a multitude of cases, e. g. to enhance the penetration of the blood-brain-barrier. In more recent years, the complexity of the adamantane derivatives examined has increased. The DPP-IV inhibitors **105** and **106** incorporate adamantane bearing two functional groups directly attached to it. Since these substances are inhibitors of an enzyme and given an “induced fit” mechanism, the spatial arrangement of these functional groups is essential. This concept, best to be characterized as an “orienting scaffold” is also being used in **116** and **113**, exploiting the overall pseudo-tetrahedral symmetry and the orientating effect of a functionalized adamantane derivative. Notably, 3-aminoadamantane-1-carboxylic acids like **73** have only found application in two cases (enkephalin analogues and tumor-directed agents), despite the fact that these amino acids have been known for decades.^[190] Such γ -aminoadamantane carboxylic acids,

especially given today's powerful methods of combinatorial synthesis and high-throughput screening, would hallmark novel building blocks in the toolkits of peptide- and medicinal chemists. To truly make available these building blocks, routine methods for their preparation, protective group chemistry and their coupling to model peptides need to be worked out systematically. Furthermore, the impact of the incorporation of γ -aminoadamantane carboxylic acids into peptidic structures has to be elucidated. The present thesis provides a contribution to this chemistry.

4. Project

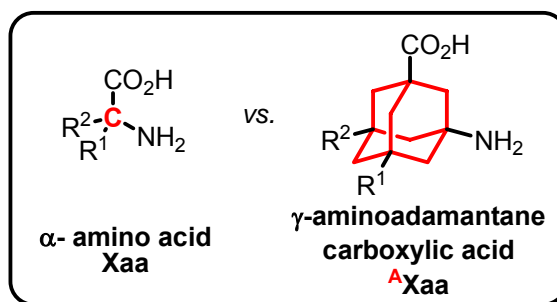
The objectives of the proposed research are the synthesis of a number of γ -aminoadamantane-1-carboxylic acids, elaboration of contemporary tractable peptide chemistry using these γ -amino acids as building blocks, and structural examination of the novel peptides. If possible, putative biological activities shall also be examined.

In recent years, the selective halogenation of alkanes under phase-transfer catalytic conditions has been elaborated out in this group.^[191-193] Substitution of at least two of the tertiary positions of adamantane with different halogens was realized in a number of examples.^[194] As C–Hal to C–CO₂H and C–Hal to C–NH₂ transformations are available, access to γ -aminoadamantane carboxylic acids is viable (Scheme 27, route b).



Scheme 27. Routes to γ -aminoadamantane-1-carboxylic acids

A different approach towards **121** relies on procedures reported in the literature^[190, 195, 196] (Scheme 27, route a). This concept utilizes the carboxylation of appropriately substituted precursors **117** through electrophilic bromination using elemental bromine and subsequent Koch-Haaf reaction. Direct amidation under strongly acidic conditions can then be utilized to directly attach the nitrogen to the adamantane core yielding acetamides **120**. The final step in both routes is the acidic hydrolysis of the amides, whereupon the γ -aminoadamantane-1-carboxylic acids are obtained as their respective hydrochlorides.

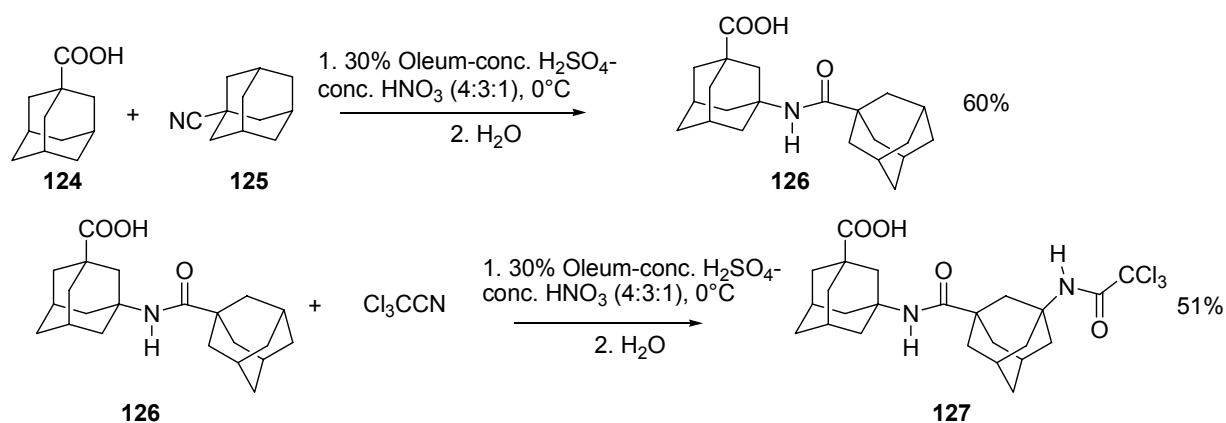


Scheme 28. α -amino acids (left) and γ -aminoadamantane-1-carboxylic acids (right).

Adamantane derived γ -amino acids are “upscaled” analogues of α -amino acids with the highly lipophilic and rigid adamantane replacing the α carbon (Scheme 28). In this thesis, the γ -aminoadamantane-1-carboxylic acids will be named with the three-letter code known from peptide chemistry, the superscript $^{\text{A}}$ Xaa indicating the adamantane-based γ -amino acids. The overall functional group arrangement stays the same – but on a larger scale. From the literature, only the three simplest $^{\text{A}}$ Xaas were known: $^{\text{A}}$ Gly ($\text{R}^1 = \text{R}^2 = \text{H}$), $^{\text{A}}$ Ala ($\text{R}^1 = \text{CH}_3$, $\text{R}^2 = \text{H}$) and $^{\text{A}}$ Aib ($\text{R}^1 = \text{R}^2 = \text{CH}_3$).^[190] Therefore, the primary goal of the present work is to synthesize and fully characterize a larger set of $^{\text{A}}$ Xaas to provide a toolbox for peptide synthesis. Protective group chemistry of the $^{\text{A}}$ Xaas was almost non-existent at the beginning of this research. Only $^{\text{A}}$ Gly-OMe has been reported and incorporated as C-terminal residue into a number of peptides (see 3.2.3.5.).^[139] After our first publication of parts of the present work,^[197] Boc- $^{\text{A}}$ Gly was also reported from another group (see 3.2.6.).^[143]

Preliminary work on the field of $^{\text{A}}$ Gly peptides has been accomplished in our group by Derek Wolfe who has synthesized small peptidic structures by direct C–H to C–N functionalization utilizing a modified Ritter-type protocol^[195, 198] yielding dimeric $^{\text{A}}$ Gly **127** (Scheme 29).

Clearly, the strongly acidic conditions in these reactions are not desirable in routine peptide synthesis. Therefore, protective group chemistry and routine peptide synthesis in solution as well as on solid phase utilizing $^{\text{A}}$ Xaas as novel building blocks had to be established. Representative homooligomers and hybrid peptides incorporating both $^{\text{A}}$ Xaas and α -amino acids, including – if possible – small cyclic peptides, should be synthesized.



Scheme 29. Peptidic structures incorporating the ^AGly motif.

Elucidation of the structural propensities of the novel peptides by means of molecular mechanics- and DFT-computations is supplemented by NMR-, IR-, and X-ray studies. Given the pharmaceutical activities of a multitude of adamantane derivatives that have been presented in Chapter three, an examination of biological properties like, e. g., antiviral activity or the use of ^AXaa derivatives as analogues of GABA has also been targeted whenever possible in cooperation with medicinal or biochemical groups.

5. Direct Functionalization of Adamantanes

5.1. γ -AAs through bromine-free C–H to C–N bond amidations

To attach carboxy- and amino groups to adamantane's tertiary positions, a number of methods are available. The introduction of a carboxy group is generally performed by Koch-Haaf reaction.^[199, 200] Usually, bromo- or hydroxyadamantanes are used as the precursors.^[201] There are, however, also reports where unfunctionalized adamantane is used.^[202] For the introduction of nitrogen functionalities, a multitude of reactions have been reported. Generally, all of them share the same concept: generation of a (radical) cation that is nucleophilically attacked by a nitrile quenching the reaction mixture with water yields acetamides. These are features known from the Ritter reaction for the synthesis of acetamides from alcohols or olefins under strongly acidic conditions.^[198] Acetamidation of adamantane derivatives is the key step in the synthesis of pharmaceutically active compounds **19** and **60**; therefore, several protocols have been worked out that can be distinguished by the way the intermediate 1-adamantyl (radical)cation^[203] is generated. Since bromination of the tertiary positions of adamantane derivatives proceeds with excellent yields and selectivities, one usually uses halogenations to direct the newly introduced nitrogen functionalities into these positions.^[190] Furthermore, adamantyl halides such as bromides and iodides naturally are more reactive than the unhalogenated precursors – in other words, halogenation *activates* the adamantane derivatives for subsequent conversions, may it be Koch-Haaf-, Ritter-type- or other reactions. Bromination has, however, several significant drawbacks. Since the molecularity of the electrophilic bromination of adamantane is about 7,^[204] one has to use a large excess of bromine (usually ten equivalents) that has to be distilled off or removed via reduction after the reaction. Furthermore, bromine has to be distilled prior to use because of traces of metals contained in technical bromine that form Lewis acids which cause selectivity problems (over-bromination).^[201, 204, 205] Haaf has introduced the acetamido group by replacing carboxylic acid- or ester groups with amides in concentrated H₂SO₄.^[206] A typical Ritter-type acetamidation protocol was used by Gerzon et al. who dissolved

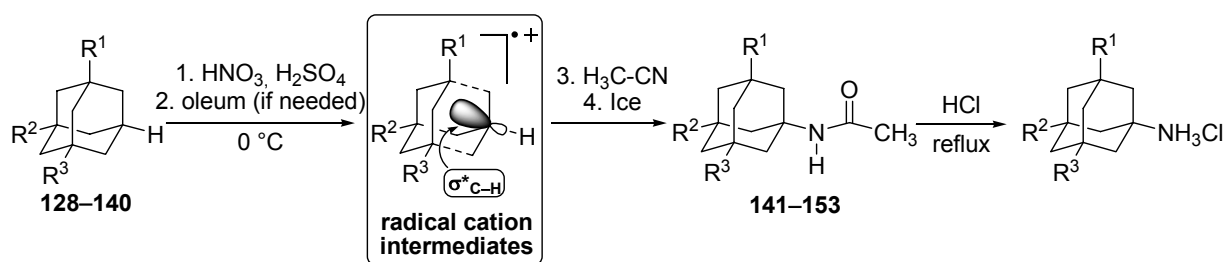
brominated precursors in acetonitrile and started the reaction by dropwise addition of H_2SO_4 .^[20] A radical-induced acetamidation of adamantane derivatives was described by Jones et al.^[207] These authors utilized $\text{Pb}(\text{OAc})_4$ as an oxidizer in acetonitrile as the solvent. Another variant has been disclosed by Olah.^[208] NOPF_6 , a single-electron transfer (SET) acceptor, was utilized to generate the reactive radical cationic intermediate that was, as usually, attacked nucleophilically by the solvent (acetonitrile) and quenched with water to give the acetamide.

A practical method to synthesize γ -acetamidoadamantane-3-carboxylic acid ($\text{Ac}^{\text{A}}\text{Gly}$) was published by Butenko et al.^[195] By treating adamantane-1-carboxylic acid with a mixture of concentrated nitric acid, concentrated sulfuric acid and oleum at 10 – 15 °C the corresponding (radical)cation was generated that was reacted with acetonitrile and quenched with ice. Adamantanols in hot trifluoroacetic acid can also be reacted with nitriles to give the corresponding amides.^[209] The requirements for a standard method of amidation to synthesize $\text{A}^{\text{X}}\text{aas}$ via the acetamides alongside route a (Scheme 27) should be practical on large scale, avoid poisonous reagents like $\text{Pb}(\text{OAc})_4$, expensive and unstable SET initiators like NOPF_6 and NO_2BF_4 ^[210] and, most importantly, should be bromine-free, that is, a direct C–H to C–N bond amidation is desirable. Under these premises, Butenko's method seems to be best suited. Butenko, however, used a mixture of conc. HNO_3 , conc. H_2SO_4 and 20% oleum (1 : 3 : 4) which also appeared to be unhandy. Derek Wolfe has re-examined the acetamidation of adamantane-1-carboxylic acid and found that the oleum can be omitted when the reaction is conducted at 0 °C upon dropwise addition of the acetonitrile. This procedure was further optimized by the author. The pool of substrates was also broadened. For the synthesis of the $\text{A}^{\text{X}}\text{aas}$, several precursors were prepared and subjected to the modified acetamidation protocol, the results are given in Table 1. What must be pointed out are significant differences in the reactivities of the substances studied. Therefore, different reaction conditions have been applied that have been worked out individually for all the starting compounds tested. **128** reacted smoothly with very high yield. It readily dissolves in a mixture of 65% HNO_3 / 95% H_2SO_4 (1 : 7.5), while oleum had to be used for the alkylated precursors **129** – **131**. The significant drop in the yield of **144** was due to the fact that **131** did not dissolve completely in the acid mixture to form the "(radical)cation solution" needed for a smooth reaction upon addition of acetonitrile.

Table 1. Acetamidations performed by modified Ritter-type reaction.^[a]

entry	starting compound		product		yield [%] ^[b]
1		128		141	84
2		129		(±)-142^[c]	93
3		130		143	92
4		131		(±)-144^[c]	39
5		132		(±)-145^[c]	77
6		133		(±)-146^[c]	37
7		134		147¹	56
8		135		148	90
9		136		149	42
10		137		150	15
11		138		151	-
12		139		152	-
13		140		153	-

^[a] For the preparation of the respective precursors, see experimental part. Experimental procedures and workup vary; please also refer to the experimental part for details. ^[b] Yields of isolated product after recrystallization or silica gel chromatography. ^[c] For racemic compounds, only one enantiomer is shown.



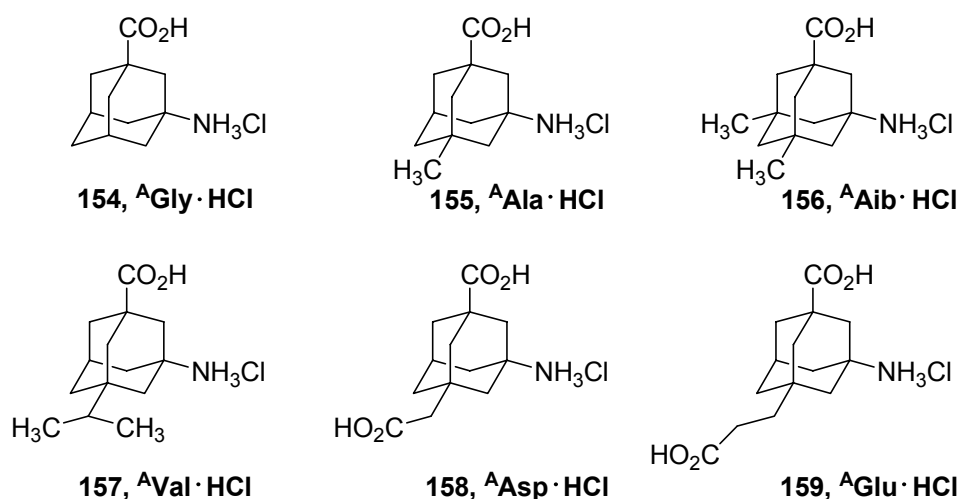
Scheme 30. Differences in reactivity of the precursors due to hyperconjugative effects

Acetamidation of **135** succeeds without the need to use oleum, applying comparable reaction conditions to **136** resulted in a significant drop in yield, while **137** requires oleum to react. Bicyclo [3.3.1]nonane **138** as well as cis- and trans- decalin could not be amidated even when adding oleum and at extended reaction times.

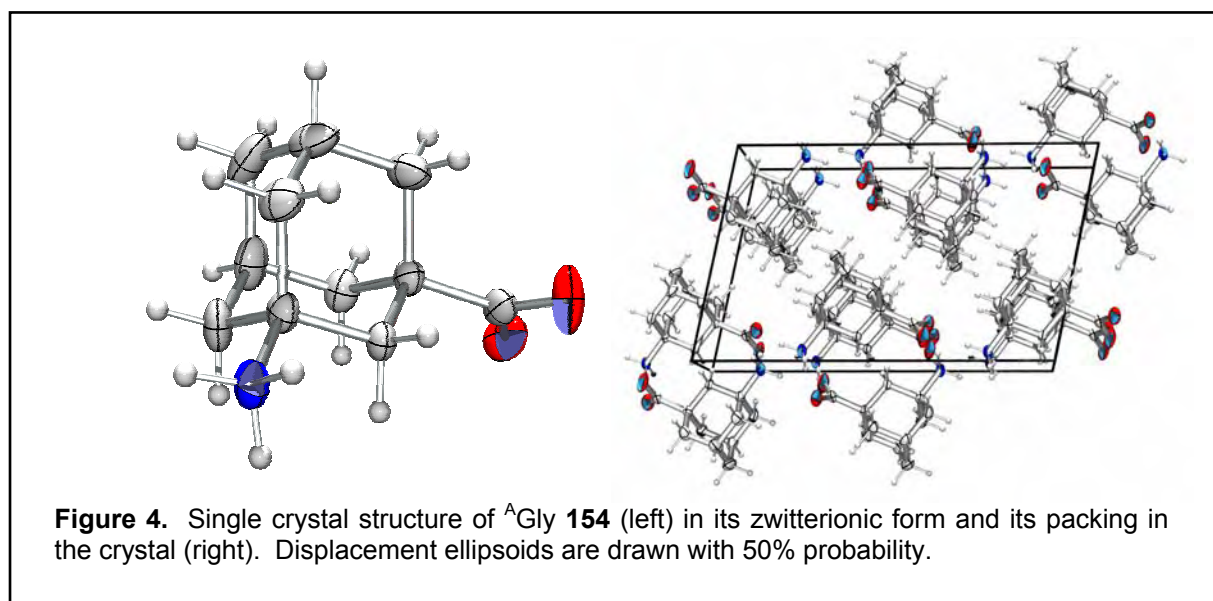
These findings can best be rationalized by two factors that interact here: *reactivity* and *solubility*. Reactivity parallels the stability of intermediate radical cations^[203] that are probable intermediates here (generated by the SET-acceptor NO_2^+ present in the nitrating acid) which are stabilized through hyperconjugation of adamantane C–C- σ bonds (Scheme 30). This hyperconjugation is intensified in electron-rich alkylated precursors such as **130** or **135**, while it is reduced when electron-withdrawing carboxylic acid groups are directly attached to the adamantane nucleus (**128–133**). Such carboxylate groups in turn enhance solubility in aqueous acidic media.

138–140 lack σ -bonds that could stabilize radical cations and did not significantly dissolve in the nitrating acid mixtures tested. Furthermore, yields of amides **149** and **150** are reduced due to their pronounced volatilities. The reduced yields of **144** and **146** can be explained by possible side reactions such as cage rearrangements or the formation of anhydrides.

The desired ^AXaas are easily obtained in large scale and good yields by acid hydrolysis of the corresponding acetamides (Scheme 30, last step) as their respective hydrochlorides. Six ^AXaas were obtained utilizing this direct acetamidation pathway (Scheme 31). Neutralization of the hydrochlorides and crystallization from water is advantageous for analysis, but not necessary for peptide synthesis. After neutralization to pH = 5, which corresponds to the isoelectric point of glycine, crystals of zwitterionic **154** were obtained suitable for single crystal X-ray structure determination. This represents the first ^AXaa crystal structure reported to date (Figure 4).



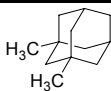
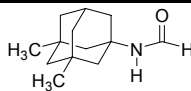
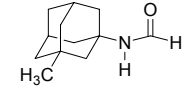
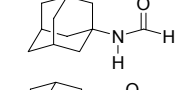
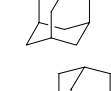
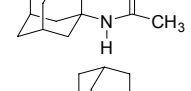
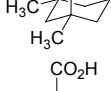
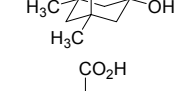
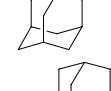
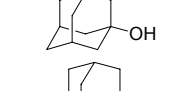
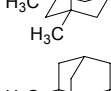
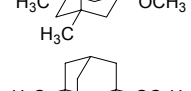
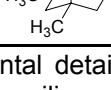
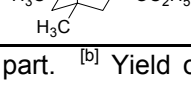
Scheme 31. ^AXaas obtained through direct C–H to C–N acetamidation



When using 1,3-dimethyladamantane **135**, hydrolysis of the respective amide with hydrochloric acid directly yields 1-amino-3,5-dimethyladamantane **60** (Memantine, see Chapter 3) as the hydrochloride. Likewise, hydrolysis of **137** yields amantadine **19**. Acid hydrolysis in these two cases gives, however, only low yields. The hydrolysis of formamides is advantageous as it proceeds much more smoothly at lower concentration of acid, which is important for the large-scale synthesis of these two marketed pharmaceuticals. Therefore, a *bromine-free* method for the preparation of these formamides would be most welcome.

Hence, we set out to develop such a reaction. Literature procedures for the synthesis of adamantane formamides in most cases require brominated precursors. Haaf has prepared formamidoadamantane from adamantane using HCN as the nucleophile under strongly acidic conditions with *tert* butanol as a cosolvent.^[211] Radical induced formamidation of adamantane using Pb(OAc)₄ and NaCN has also been reported.^[207] The most practical method for formamidation reported to date works by heating brominated adamantanes with excess formamide for a longer period of time.^[105] This procedure is in fact currently being used in the industrial synthesis of memantine **60**. Again, the available protocols share the drawbacks of either the need for poisonous reagents, tedious experimental procedures and / or the requirement of already activated starting compounds – in most cases, the latter is achieved by bromination. We reasoned that quenching of the “radical cation solution” of 1,3-dimethyladamantane, prepared as described above for the acetamidation, with an amide (here: formamide) instead of acetonitrile, would possibly give the desired product.

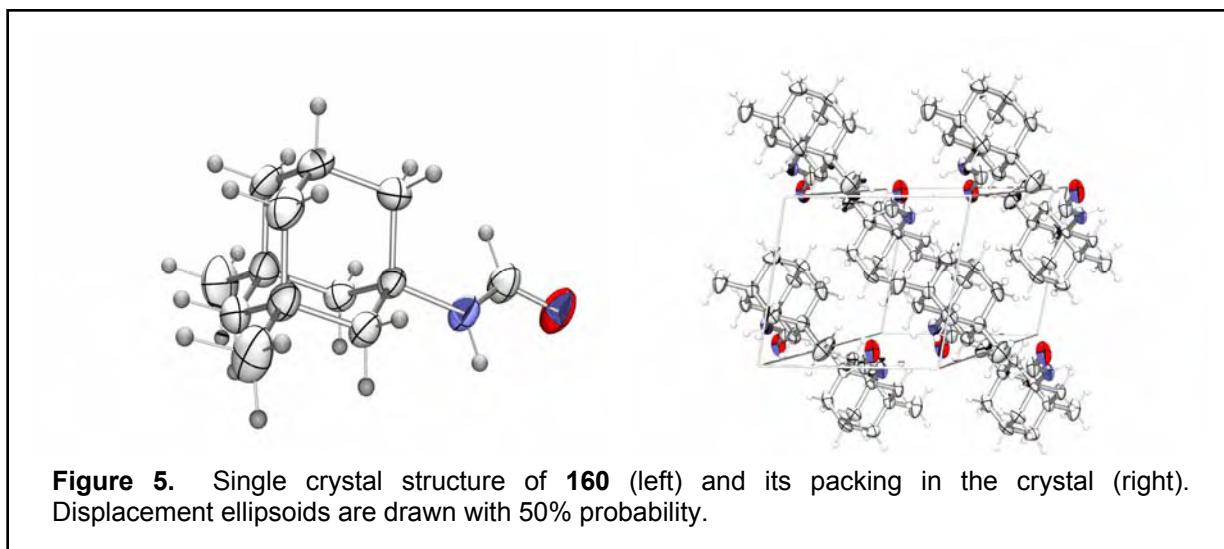
Table 2. Direct functionalization of adamantane derivatives using amides, water and alcohols as the nucleophiles.^[a]

entry	starting compound	nucleophile	product	yield [%] ^[b]
1		<chem>H2N-C(=O)-H</chem>		89
2		<chem>H2N-C(=O)-H</chem>		45
3		<chem>H2N-C(=O)-H</chem>		13
4		<chem>H2N-C(=O)-CH3</chem>		38
5		<chem>H2O</chem>		81
6		<chem>H2O</chem>		70
7		<chem>CH3OH</chem>		38
8		<chem>C2H5OH</chem>		8

^[a] For experimental details, please refer to the experimental part. ^[b] Yield of isolated product after recrystallization or silica gel column chromatography.

Dropwise addition of formamide to the acid solution of 1,3-dimethyladamantane under the same conditions as described for the acetamidation resulted in a sluggish, highly exothermic reaction. Nitrous gases formed and, upon addition of more formamide, a broth of ammonium sulfate emerged. Workup of this reaction mixture and GC-MS analysis showed, besides 1-Hydroxy-1,3-dimethyladamantane, starting compound and several side products, a signal of 1-formamido-3,5-dimethyladamantane in about 24% GC-yield. By dropwise addition of the radical cation solution to a large excess of ice-cooled formamide (in marked contrast to the acetamidation protocol) upon vigorous stirring in a dry apparatus under argon, clean conversion of 1,3-dimethyladamantane to 1-formamido-3,5-dimethylaminoadamantane could be accomplished. After the addition of the radical cation solution to formamide, the reaction mixture had to be stirred at rt, whereupon careful aqueous workup and silica gel column chromatography yielded the desired formamide in excellent yield (Table 2).

Crystals of **160** were grown by slow evaporation of a solution in n-hexane (Figure 5). This direct amidation protocol using amides as the nucleophiles was also applied to some other adamantane derivatives. The yields of the amides obtained by this protocol generally paralleled the ones obtained by the acetamidations using acetonitrile as the nucleophile. The approach of quenching an adamantane (radical)cation solution is expandable to other nucleophiles as well, as exemplified by entries 5–8. Quenching the (radical)cation solution with water yields hydroxy adamantanes; using alcohols as the nucleophile yields ethers, albeit in moderate to low yield only due to the extremely pronounced volatility of the ethers. This method also appears to be an operationally simpler synthesis of adamantyl alcohols than procedures reported in the literature.^[212-214]

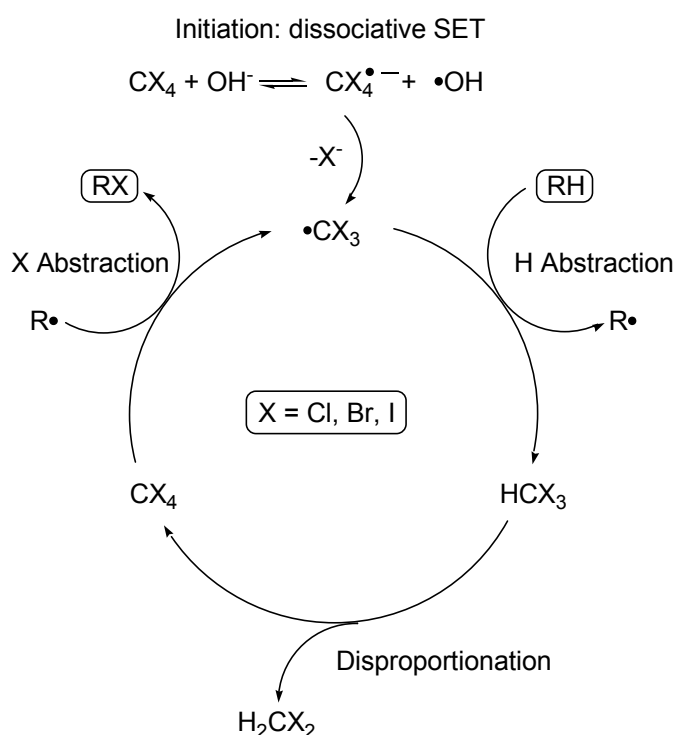


Hydrolysis of the formamide **160** was accomplished by heating it in 2 N HCl, directly yielding 1-amino-3,5-dimethyladamantane (memantine, **60**) as its hydrochloride in >99% purity (GC) after one simple reprecipitation step.

The acetamidations of a broad range of substrates completely omit a bromination step, solely require technical grade reagents and are operationally simple. Therefore, they are of interest for large-scale production of pharmaceutically active aminoadamantanes. The same holds true for the formamidation of 1,3-dimethyladamantane. Patent applications covering these novel methods have been filed,^[215, 216] studies dealing with the scalability of the preparation of **160** in technical scale are currently underway and the patent application describing the novel synthesis of **160** has recently been sold to Merz pharmaceuticals, Frankfurt (Germany). Further α -Xaas should become available through this route given, e. g., the availability of adamantane-1-propionic and butanoic acid^[217] or a multitude of other adamantane derivatives. The strongly acidic reaction conditions used in the amidation procedures limit, however, the general applicability of this pathway.

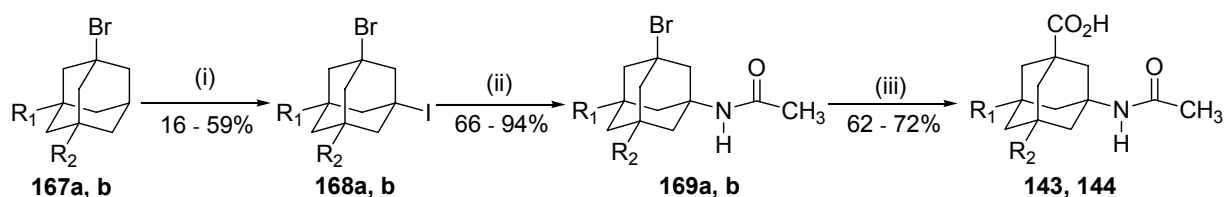
5.2. A Xaas through PTC-halogenation and subsequent conversions.

An alternative strategy to A Xaas utilizes phase-transfer catalyzed halogenations developed in this group (Scheme 32).^[191, 192, 194] A proposed model of the PTC halogenation of alkanes is shown in Scheme 32. The hydroxide ion is extracted into the organic phase; upon desolvation it acts as an SET donor and initiates the radical reaction. Convenient phase-transfer catalysts are quaternary ammonium salts. The standard PT catalyst utilized in this research is tetra n-butyl ammonium bromide (TBABr). Chain carriers are $\cdot CX_3$ radicals; CX_4 is regenerated by disproportionation of haloform to give CH_2X_2 and CX_4 . Application of phase-transfer catalysis constricts reactive species to a small interphase zone or extracts them into the organic phase at the PT catalyst, thereby avoiding unselective over-functionalization.



Scheme 32. Proposed catalytic cycle of the PTC halogenation protocol

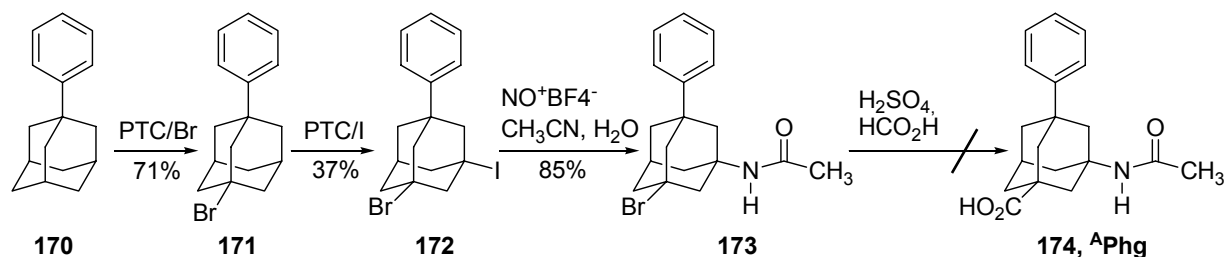
Due to the functional group tolerance of this method, this allows for a larger variety of R^1 and R^2 (Scheme 27) than the direct amidation protocol described above, particularly with regard to future applications. The strategy is outlined in Scheme 33 for the synthesis of A Aib and A Val.



Scheme 33. PTC strategy towards acetamido precursors of ^AAib and ^AVal. See text for details.

The iodination of 1-bromo-3,5-dimethyladamantane (**167a**, easily available by elemental bromine halogenation) with CH_3I and solid NaOH in fluorobenzene suspension with ultrasound acceleration^[218] yielded 1-iodo-3-bromo-5,7-dimethyladamantane (**168a**, $\text{R}^1 = \text{R}^2 = \text{CH}_3$) in 59% yield after silica gel column chromatography. This bromoiodoadamantane was subjected to nitrosonium ion induced Ritter-type reaction^[208] to selectively substitute the iodine with an acetamido functionality while leaving the bromine unreacted. The bromoacetamide **169a** ($\text{R}^1 = \text{R}^2 = \text{CH}_3$) was then subjected to Koch-Haaf carboxylation (62%) to yield Ac-^AAib **143** in an overall yield of 34% starting from **167a**. While this PTC approach clearly is more laborious, relies on brominated precursors, and the chromatographical workup is time-consuming, it broadens the pool of substrates to be converted to ^AXaas due to the functional group tolerance of the PTC halogenation protocol and the avoidance of nitrating acid media. We then set to test this approach with an isopropyl adamantane. Because **144** could be obtained in only 39% yield when using the direct acetamidation protocol, this derivative appeared to be an attractive test substrate.

After synthesizing precursor **167b** ($\text{R}^1 = 2\text{-propyl}$, $\text{R}^2 = \text{H}$), PTC-iodination yielded **168b** in 16% yield only, mainly because of very small R_f and problems with overlapping fractions during the tedious chromatographic workup. The subsequent acetamidation (66%) and the final Koch-Haaf carboxylation (72%) worked satisfactorily. The challenging synthesis of ^APhg starting from 1-phenyladamantane was also attempted (Scheme 34).

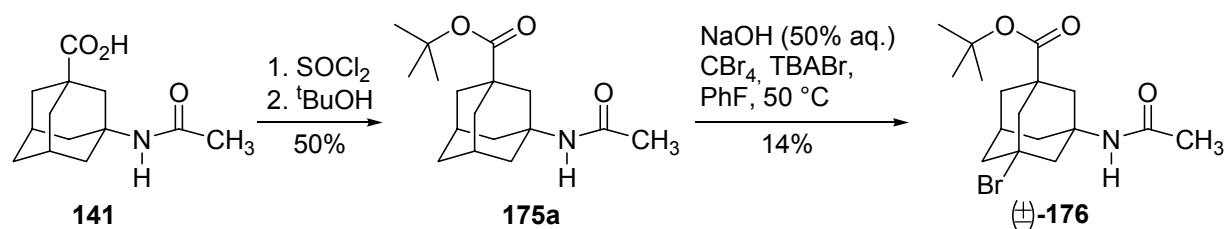


Scheme 34. Attempted synthesis of ^APhg

While the yield of PTC bromination of **170** to **171** could be improved by a modification of the protocol^[194] (room temperature, extending the reaction time to 11.5 days), the subsequent PTC iodination did not give satisfying yields of **172** due to partial hydrolysis of **172** on the silica gel column as proven by the identification of the corresponding alcohol via GC-MS. As above, iodine-selective nitrosonium ion induced Ritter-type reaction could be realized in good yield to give bromo acetamido adamantane **173**. Carboxylation of this derivative did not succeed, presumably due to sulfonylation of the activated phenyl group yielding a sulfonic acid derivative that could not be isolated from the aqueous reaction mixture.

Given the facile large-scale access to acetamidated ^AXaas like, e. g., **141**, the (stereo)selective introduction of residues attached to the tertiary positions of such a compound is a challenging, but rewarding goal – successful adoption of this scheme would provide numerous ^AXaas from one common precursor. Best suited for the introduction of multiple sidechains would again be halogenation as the first step.

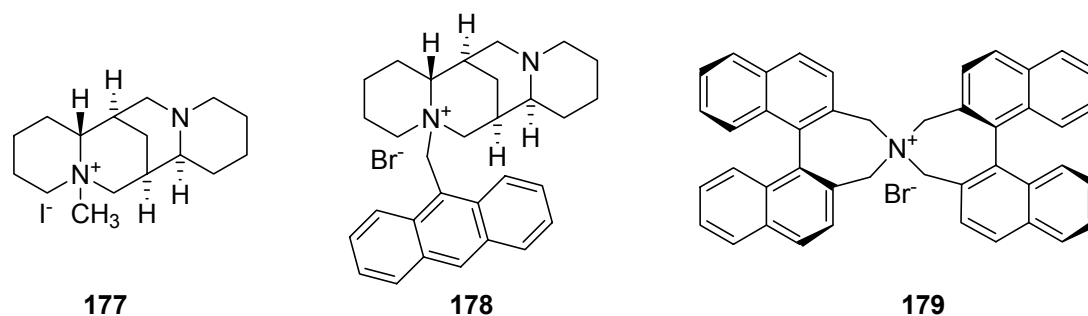
To tackle this plan, the carboxylic acid group in **141** was protected as the *tert* butyl ester, whose base stability is also advantageous in the strongly basic conditions of the PTC halogenation procedures. Indeed, PTC bromination of **175a** did yield monobrominated **176**, albeit in low yield only (whereas Ac-^AGly-OMe **175b** could not be PTC halogenated as expected). While this reaction cannot be regarded optimized as of today, it still is an example for a highly remarkable functional group tolerance in a direct C–H functionalization. The range of accessible ^AXaas by substituting the bromine using, e. g., TMS-substituted reagents following Sasaki's procedures^[219, 220] and cleavage of the protective groups is appealing.



Scheme 35. “Post-functionalization” of Ac-^AGly-O-*t*Bu via PTC-bromination

Ac-^AGly-O^tBu **175a** is a prochiral molecule. To test whether stereoselective bromination of this substrate would be feasible, chiral PT catalysts have also been

tested (Scheme 36). Spartein methyl iodide **177** and spartein anthracenylmethyl bromide **178** were prepared by Dipl. Chem. Torsten Weil; **179** was a gift from Prof. Dr. Andrey A. Fokin. Test reactions were run in 1 mmol scale using 20 mol% of the respective catalyst and 5 equivalents of the bromine source CBr_4 . They were intensively stirred for 14 days at room temperature. **177–179** were suitable as PT catalysts in this reaction system but the yield was low ($\sim 10\%$). The products obtained after silica gel column chromatography were subjected to chiral HPLC (Astec cyclobond 1 2000 column, 4.6 x 250 mm, eluent: n-hexane / acetonitrile / water (35 : 63 : 2). From the integration of the chromatograms small enantiomeric excess (e. r. up to $\sim 52 : 48$ when using **177** as the catalyst), but no clean baseline separation of the enantiomers of **176** could be realized so that no significant stereoselectivity was achieved here.



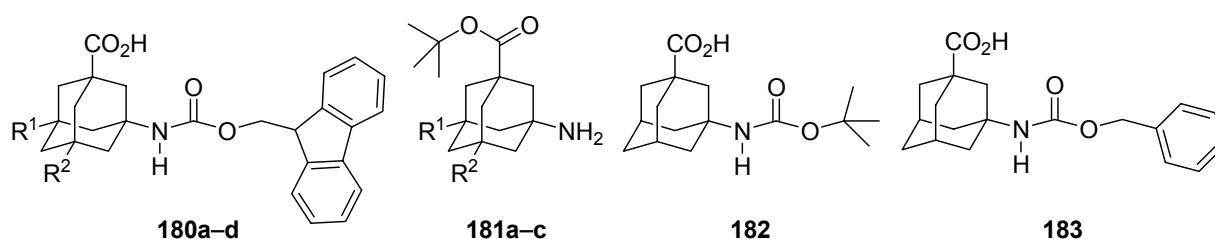
Scheme 36. Chiral PT catalysts tested in the PTC bromination of **175**.

Enantiomer separation of chiral ^AXaa derivatives (particularly in view of peptide chemistry) in principle is possible. We have also resolved $\text{Ac-}^A\text{Ala-O}^t\text{Bu}$ analytically via chiral HPLC (Macherey-Nagel Nucleodex[®] β -PM column). Preparative scale resolution of free acids (e. g., (\pm) -**144**) by co-crystallization with quinine as reported in the literature for closely related adamantane carboxylic acids^[221] appears to be a viable (albeit laborious) route.

6. Peptide chemistry

6.1. Protective groups and strategy

Protective groups can easily be introduced to either carboxy- or amino functionalities using standard methods (Scheme 37).



Scheme 37. Protected A Xaa derivatives. (a): $R^1 = R^2 = H$ (A Gly); (b): $R^1 = H, R^2 = CH_3$ (A Ala); (c): $R^1 = R^2 = CH_3$ (A Aib); (d): $R^1 = H, R^2 = CH_2CO_2H$ (A Asp)

Carpino's original protocol for the introduction of N-terminal 9-fluorenylmethoxycarbonyl (Fmoc) protection^[222] using Fmoc-Cl led to the Fmoc- A Xaas in satisfying yields. Problems with solubility encountered during this conversion can in part be ascribed to dipeptide formation that is usual for lipophilic amino acids. Using Fmoc-OSu as the reagent and a modified procedure, this could be circumvented and solution volumes were reduced.^[223] Due to relatively low solubility of the Fmoc- A Xaas itself in the extraction step (EtOAc), yields remained rather low.

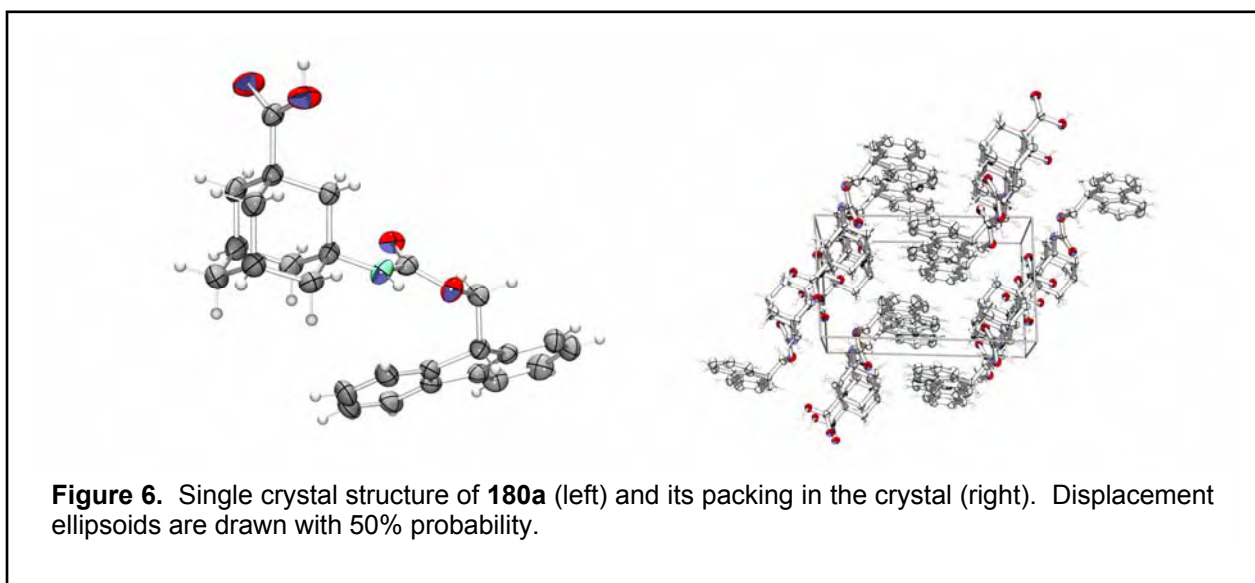


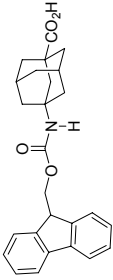
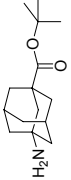
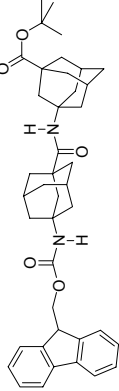
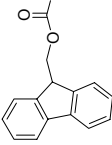
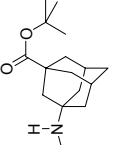
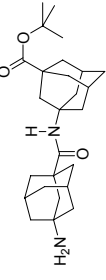
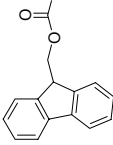
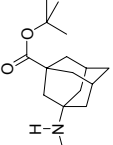
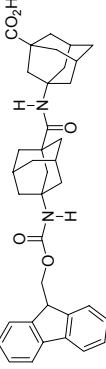
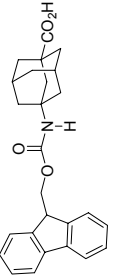
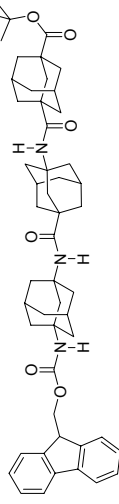
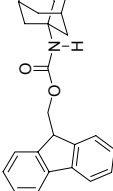
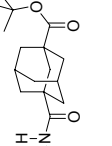
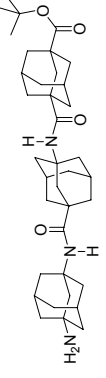
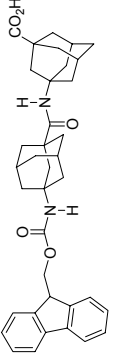
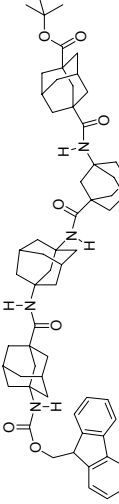
Figure 6. Single crystal structure of **180a** (left) and its packing in the crystal (right). Displacement ellipsoids are drawn with 50% probability.

Complementing Fmoc-protection, *tert* butyl esters **181a–c** have been prepared which allows for an Fmoc-*tert* butyl strategy in solution phase peptide assembly and the standard Fmoc tactics in SPPS. *N*-Boc- and *N*-Cbz-protection is also feasible (**182**, **183**).

6.2. Peptide synthesis in solution

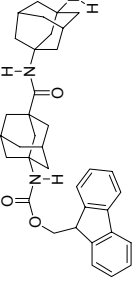
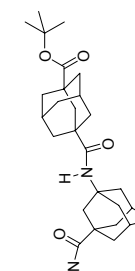
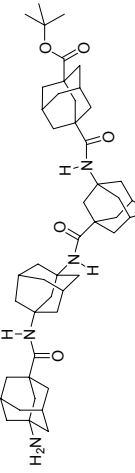
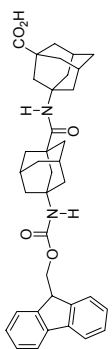
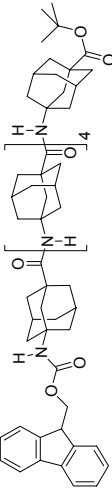
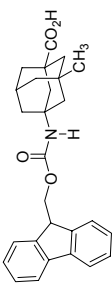
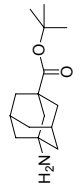
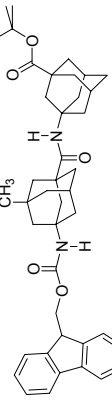
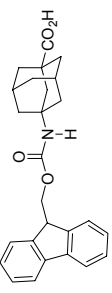
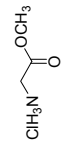
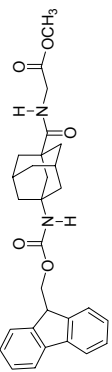
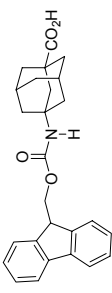
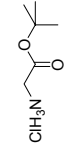
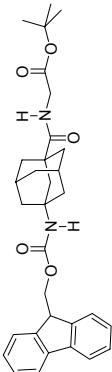
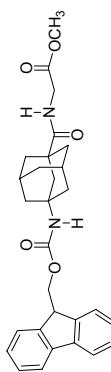
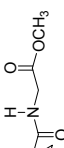
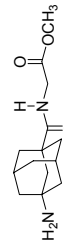
The formation of an amide bond connecting two ^AXaas can be regarded a “difficult sequence” due to steric hindrance. This reflected in the initial efforts to perform peptide couplings in solution using DIC/HOBt methodology yielding unsatisfactory results in terms of yield and reaction time. Therefore, the uronium-salt coupling reagent HBTU was tested.^[224, 225] Utilizing this peptide assembly protocol, homooligomers of ^AXaas as well as hybrid ^AXaa / α -Xaa peptides can routinely be prepared in solution and isolated in high yields after silica gel column chromatography. Cleavage of the *tert* butyl ester group and the Fmoc group was accomplished by using standard protocols taken from the literature.^[226] The solution phase synthesis of several peptides incorporating ^AXaas is summarized in Table 3.

Table 3. Peptides incorporating ^AXaas as synthesized via solution phase methodology

acid component	amine component	meth- od ^[a]	product	yield [%] ^[b]
		A		184 92
		C		185 93
		D		186 80
		B		187 73
		C		188 87
		A		189 93

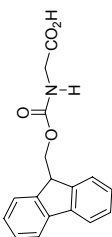
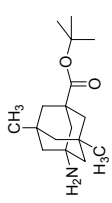
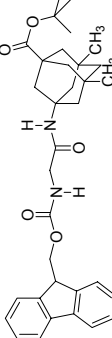
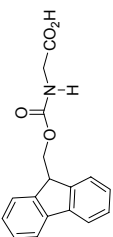
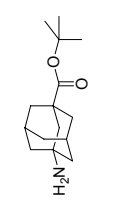
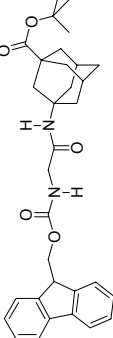
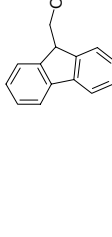
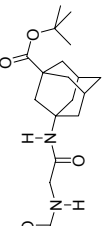
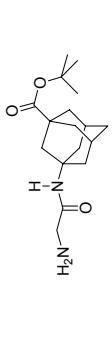
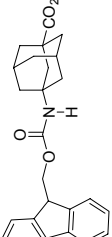
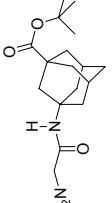
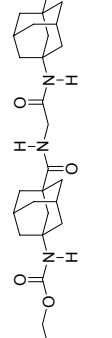
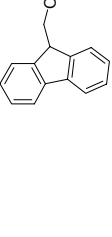
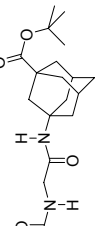
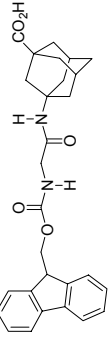
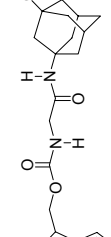
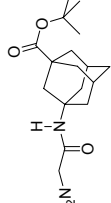
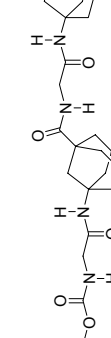
(continued)

Table 3 (continued)

acid component	amine component	meth- od ^[a]	product	yield [%] ^[b]
		C		190 74
	190	A		191 68
		A		192 57
		A		194 88
		A		196 86
		C		197 98

(continued)

Table 3 (continued)

acid component	amine component	meth- od ^[a]	product	yield [%] ^[b]
		A		198 69
		A		199 56
		C		200 80
		A		201 82
		D		202 77
		A		203 63

^[a] Method A: HBTU and DIPEA in THF or MeCN, rt over night; Method B: DIC and HOBT in THF, 3 days; Method C: Diethylamine in MeCN or THF, rt, Method D: trifluoroacetic acid in dichloromethane, rt. Please refer to the experimental part for details. ^[b] Yield of isolated product after silica gel column chromatography or recrystallization.

6.3. Solid phase peptide synthesis (SPPS)

Are peptides incorporating A Xaas also amenable through routine solid phase peptide synthesis?^[227-229] A first proof-of-principle study was conducted by Dr. Chiara Cabrele, who monitored the purity of homooligomeric A Gly as synthesized on 2-chloro trityl resin by cleavage of the respective Fmoc-oligomer formed on resin upon chain elongation from a small amount of beads and analyzing it by means of RP-HPLC. Results are summarized in Table 4 and Figure 7.

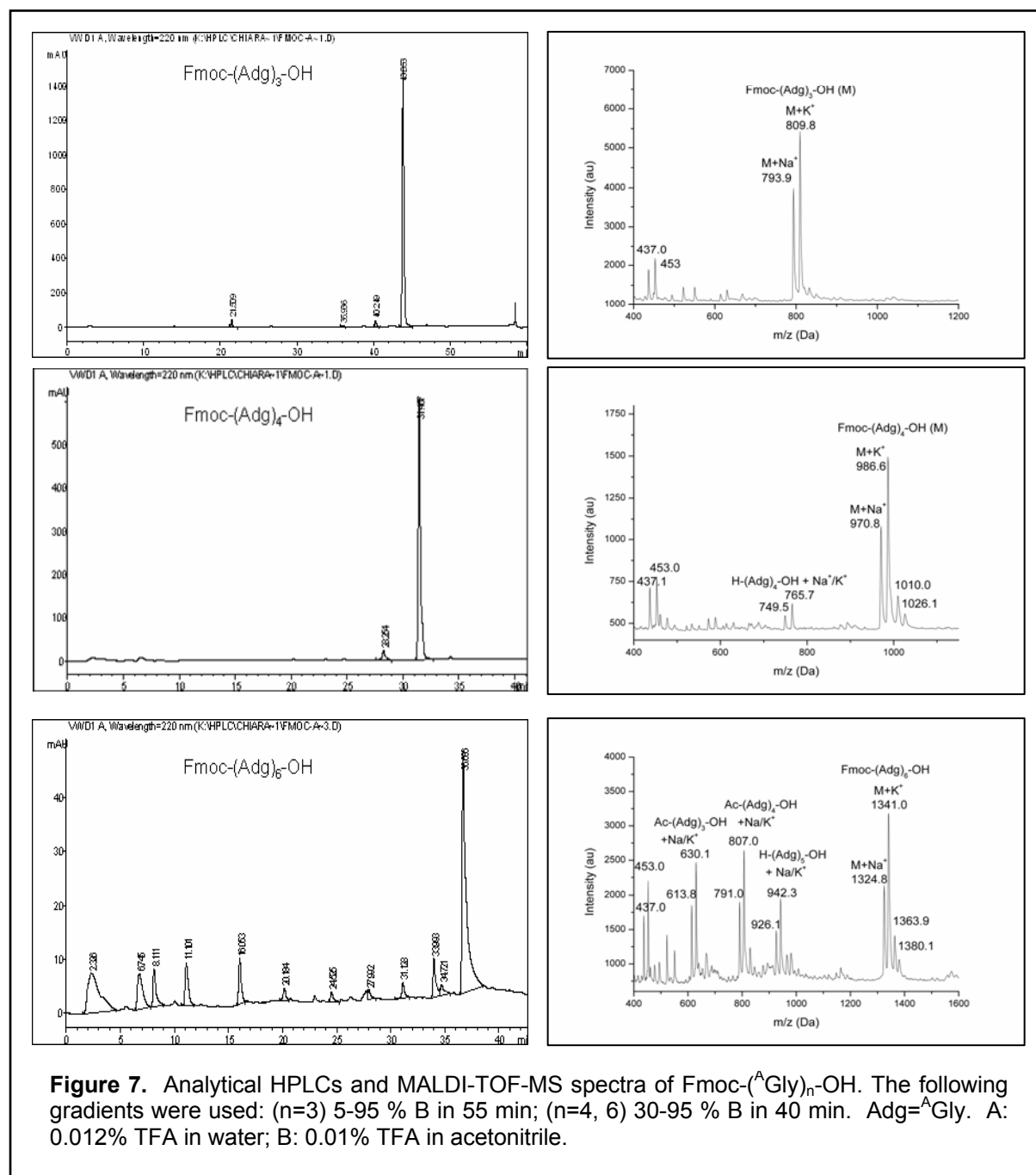
Table 4. Analytical data of Fmoc-protected A Gly trimer, tetramer, and hexamer

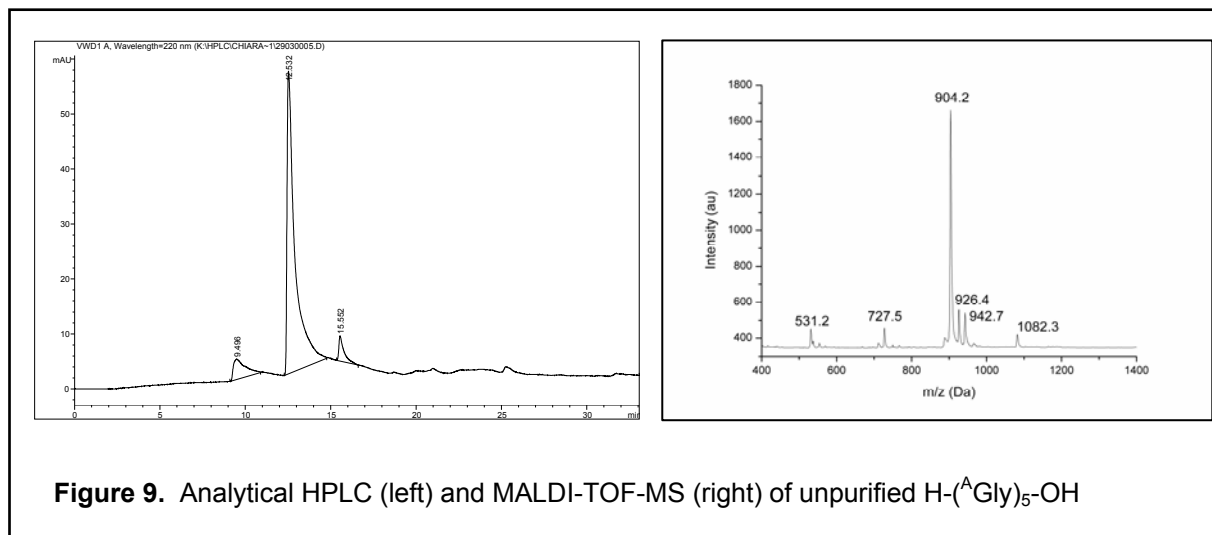
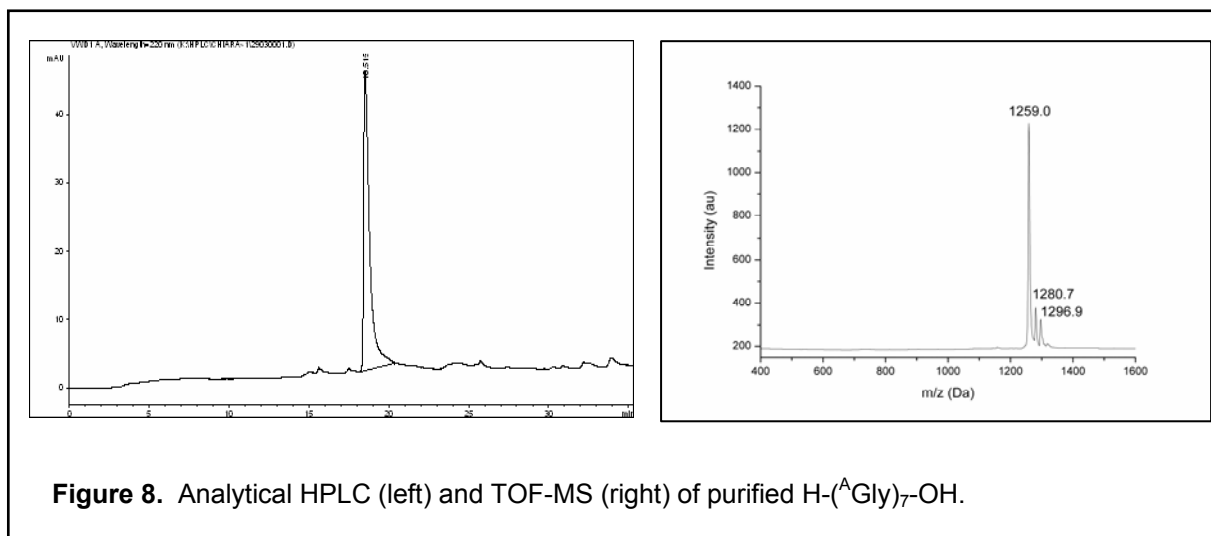
product	HPLC-gradient	t _R (min)	% CH ₃ CN	MW _{calc} (Da)	MW _{found} (Da)
Fmoc-(A Gly) ₃ -OH	5-95% B in 55 min	43.85	76.75	771.42	793.9 (M+Na ⁺)
Fmoc-(A Gly) ₄ -OH	30-95% B in 40 min	31.46	81.12	948.54	970.8 (M+Na ⁺) 1324.8 (M+Na ⁺);
Fmoc-(A Gly) ₆ -OH	30-95% B in 40 min	36.69	89.62	1302.77	926.1 (pentamer+Na ⁺); 791.0 (Ac-tetramer+Na ⁺); 613.8 (Ac-trimer+Na ⁺)

After a final Fmoc-cleavage the A Gly heptamer was cleaved from the resin and purified by reversed-phase HPLC (Figure 8). The conclusion that can be drawn from this synthesis is that, starting from the tetramer, chain elongation couplings become increasingly difficult requiring double coupling procedures to warrant sufficient yields of the respective chain assembly reaction. This was checked in the synthesis of pentameric A Gly employing double couplings for the fourth and fifth chain elongation step. Figure 9 shows the analytical RP-HPLC chromatogram and MALDI-TOF MS of the pentamer after cleavage from the resin, showing satisfying purity.

These findings demonstrate that, when using the appropriate chain elongation procedures, peptides incorporating A Xaas can indeed be prepared via SPPS, while no severe problems are encountered even in the case of homooligomeric A Gly. After these encouraging results, a multitude of peptides for different applications have been routinely synthesized in our group utilizing different SPPS resins and techniques, so that protected A Xaas now are established as building blocks “ready to use” in solution-

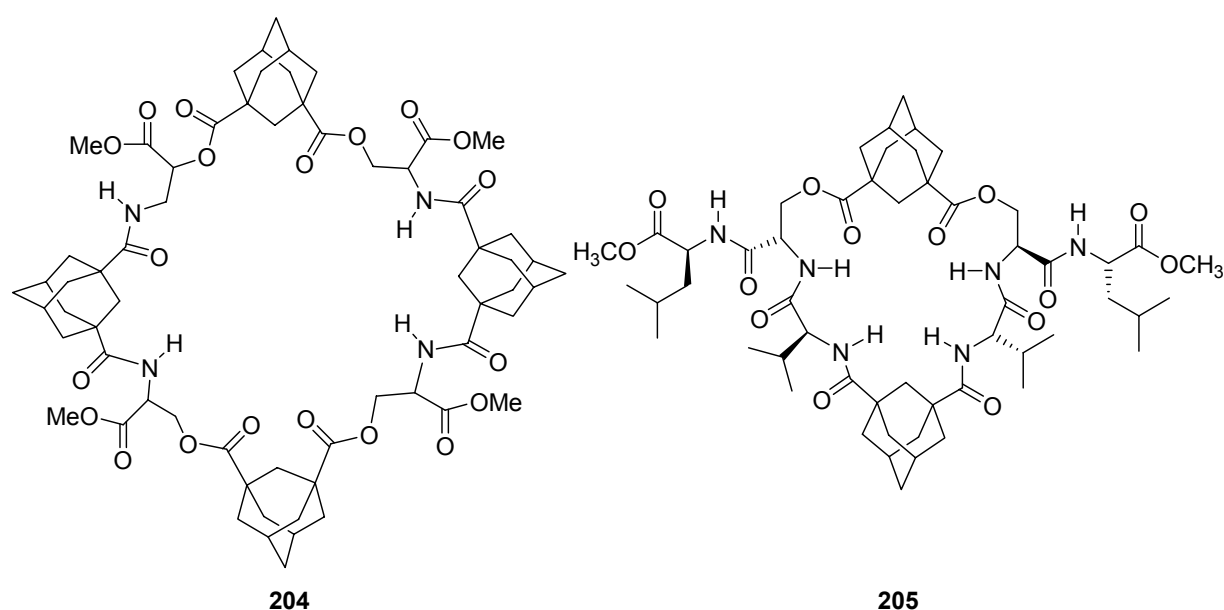
as well as solid-phase-peptide synthesis. This also holds true for the use of automated synthesizers, making available large libraries of different peptidic oligomers for various applications (vide infra).





6.4. Cyclizations

Many natural products isolated from marine sources, fungi or microorganisms are cyclic peptidic structures, displaying important biological properties like, e. g., toxicity, antiviral, antifungal or antibiotic properties.^[230-232] These can, at least in part, be attributed to their limited flexibility as a consequence of being cyclic, thereby orientating decisive pharmacophoric groups in an arrangement required for enhanced (when compared with their open-chain analogues) receptor–ligand interactions.^[233] Other striking characteristics of some cyclopeptides or cyclodepsipeptides include their reduced degradation through proteolytic enzymes,^[228] ion carrier capacity (as demonstrated by valinomycin, which transports potassium ions through cell membranes^[234]) and their propensity to assemble to columnar stacks through self-association^[235, 236] that could be utilized in the design of synthetic ion channels.^[237-240] Ranganathan has synthesized a large variety of adamantane-containing cyclodepsipeptides with the key feature of acting as ion transporters (Scheme 38).^[241-245] Best transport capabilities were shown by 24-membered macrocycles that incorporate two adamantane nuclei as well as six carbonyl oxygens for the complexation of the cation. **205** paralleled the potassium cation transport capabilities of valinomycin.



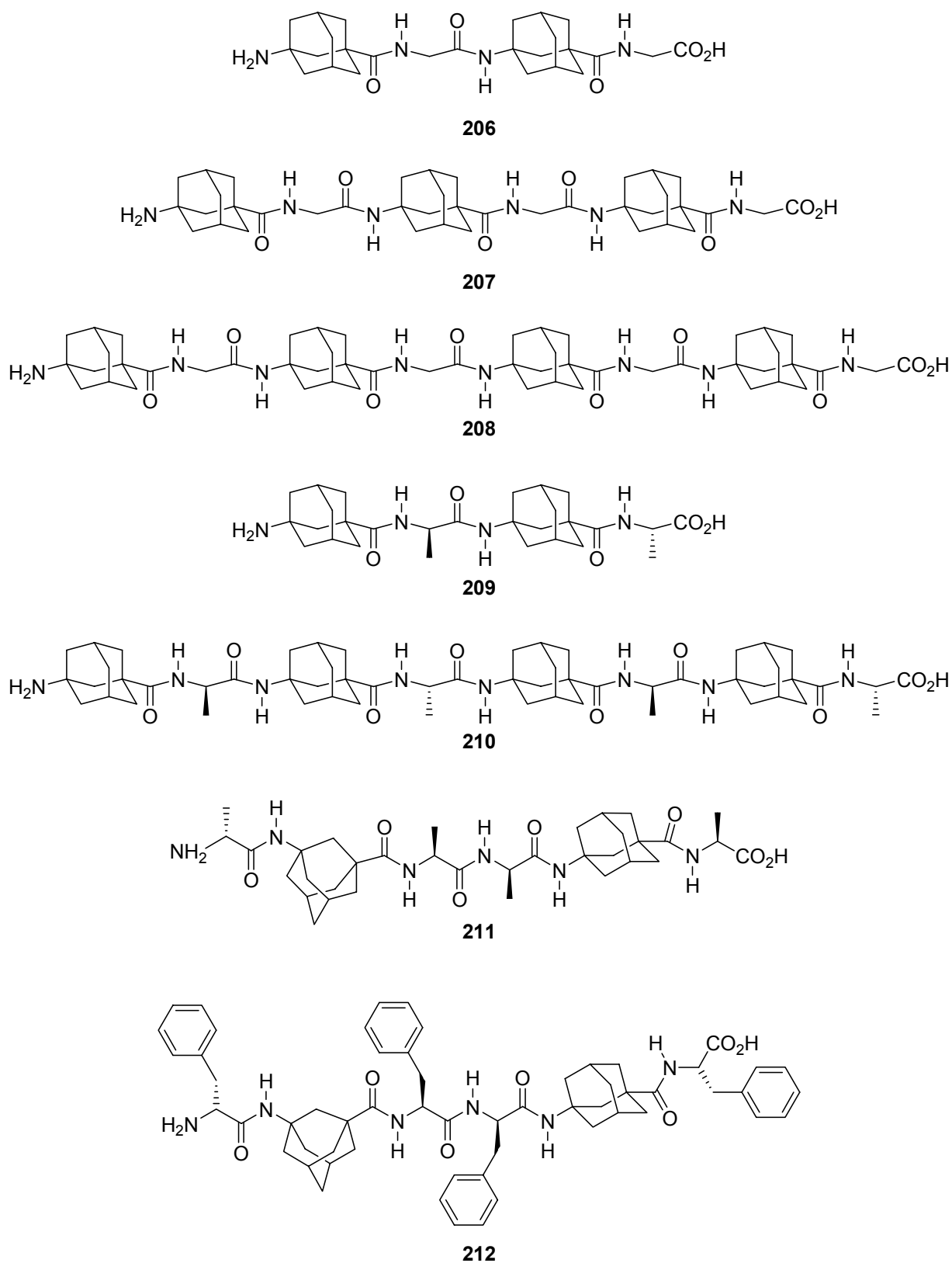
Scheme 38. Ranganathan's cyclodepsipeptides incorporating adamantane moieties

The reasons underlying these findings are clear: the adamantane provides lipophilicity to the outside of the macrocycle, functional groups suitable for ion complexation are pointing inwards. This research did, however, not provide the cyclic, adamantane containing structures in a straightforward manner. For example, **204** and **205** were prepared through sequential condensation of 1,3-adamantane dicarbonyl dichloride with the appropriate Ser derivative. The adamantane building block did provide orientation to the peptidic “arms”, thereby facilitating the cyclization. **204** and **205** are, however, no cyclopeptides and the synthesis of such structures is therefore limited. With the ^AXaas and the well-crafted peptide chemistry thereof at hand, a number of precursors for cyclization studies of peptides incorporating ^AGly were prepared (Scheme 39). Enhanced propensity for head-to-tail cyclization would indicate a turn-like structure of the linear precursors, thereby bringing the end groups in proximity, facilitating cyclization.^[246] Additionally, alternating α -Xaa / ^AGly cyclopeptides incorporating ^AGly residues with alternating stereochemistry should display an overall planar structure as do Ghadiri’s cyclopeptides, thereby possibly enhancing their stacking to tubular structures with pronounced lipophilicity. This would enhance their propensity to interact with lipid bilayers in the design of artificial channels.

The precursors for the cyclization study were prepared via SPPS using commercially available Wang resin preloaded with the appropriate Fmoc- α -Xaa. Double coupling procedures were employed for every chain elongation to warrant successful coupling. After the final chain assembly step, the *N*-terminal Fmoc protective group was removed with piperidine and the peptide was cleaved from the resin using TFA. The precursors were analyzed with ESI-MS (Table 5) and subjected to the cyclization conditions without further purification.

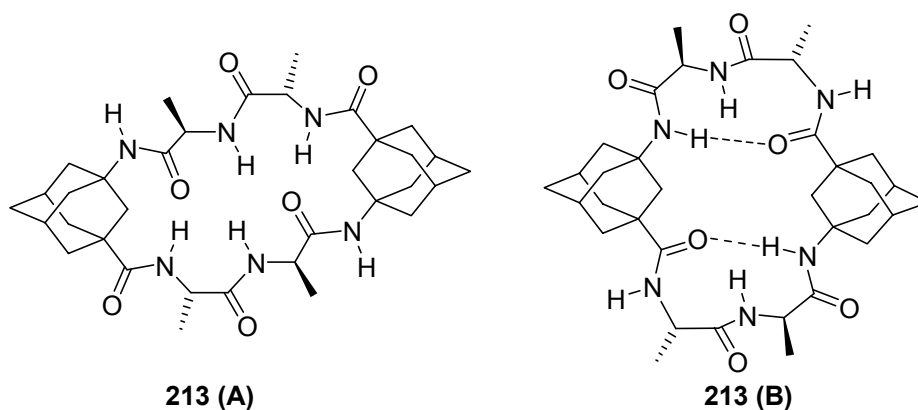
Table 5. Sequences and ESI-MS data of the cyclization precursors

no.	sequence	M _{abs.} [Da] (calcd.)	M _{abs.} [Da] (found)
206	H- ^A Gly-Gly- ^A Gly-Gly-OH	486.3	487.3
207	H- ^A Gly-Gly- ^A Gly-Gly- ^A Gly-Gly-OH	720.4	721.5
208	H- ^A Gly-Gly- ^A Gly-Gly- ^A Gly-Gly- ^A Gly-Gly-OH	954.6	955.7
209	H- ^A Gly-D-Ala- ^A Gly-L-Ala-OH	514.3	515.3
210	H- ^A Gly-D-Ala- ^A Gly-L-Ala- ^A Gly-D-Ala- ^A Gly-L-Ala-OH	1010.6	1011.7
211	H-D-Ala- ^A Gly-L-Ala-D-Ala- ^A Gly-L-Ala-OH	656.4	657.4
212	H-D-Phe- ^A Gly-L-Phe-D-Phe- ^A Gly-L-Phe-OH	960.5	961.5



Scheme 39. Linear precursor peptides tested in cyclization reactions

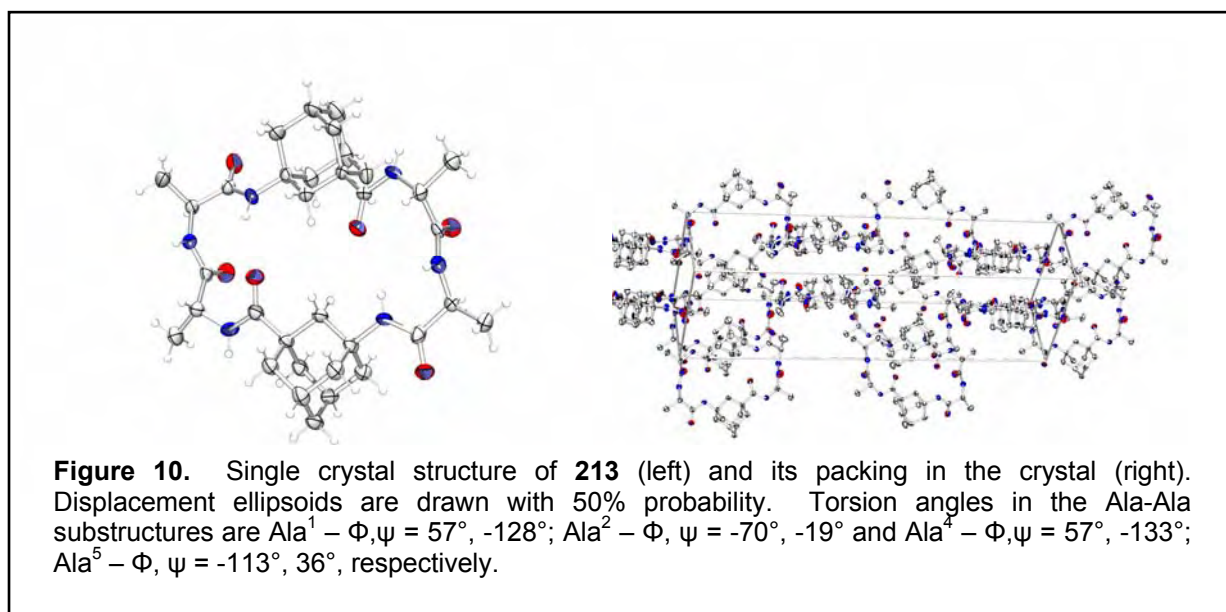
Because the peptide couplings in solution utilizing HBTU worked reliably and in good yields, the coupling reagent of choice was HATU.^[247] Its (in comparison to HBTU) additional nitrogen was reported to facilitate such cyclizations by acting as a hydrogen bond acceptor. The cyclization reactions were run at rt for 14 days in highly diluted (1.4 mM) acetonitrile solutions. After workup, the crude reaction mixtures were analyzed by ESI-MS. With the exception of precursor **211** no cyclization products could be detected. The crude product from cyclization of **211** was purified by HPLC (isolated product: 19 mg = 21% of **213** as calculated from the initial loading of the resin). ESI-MS from the pure product showed a prominent signal of *dimeric* cyclopeptide **213** ($M_{\text{abs.}} = 1299.5$, $[2M+Na]^+$) and an almost invisible signal for the monomer, which indicates the propensity of **213** to form di- or oligomeric aggregates.



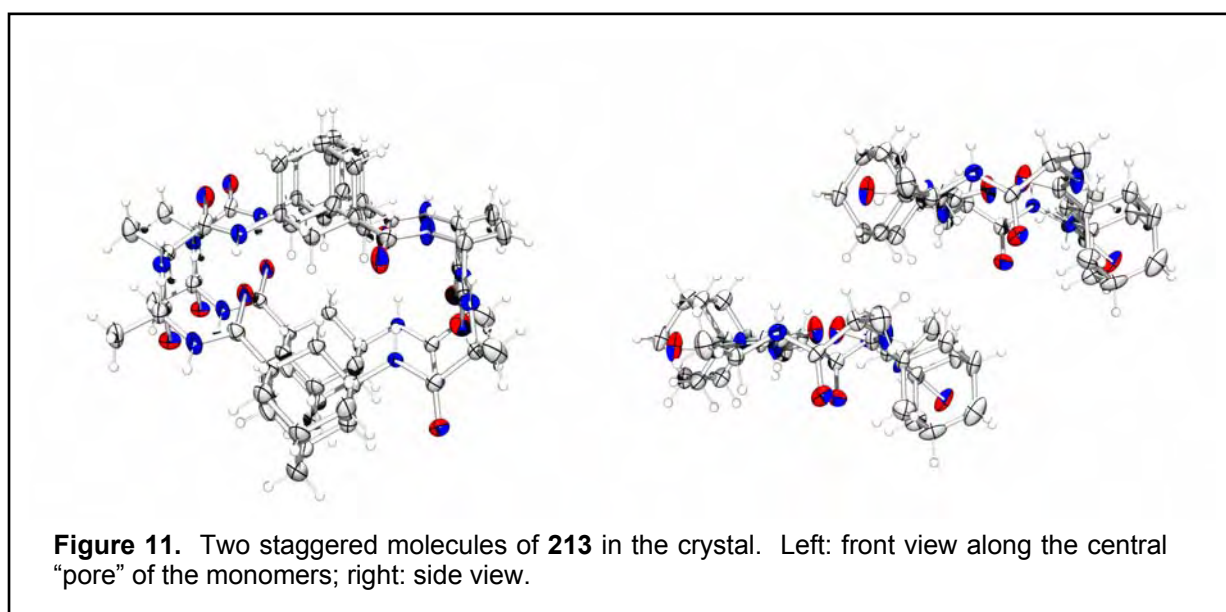
Scheme 40. Cyclic peptide based upon α Gly and Ala residues of alternating stereochemistry (A). (B) shows its preferred conformation in the solid state as derived from X-ray structural analysis.

From the initial design considerations it was envisioned that **213** would give simple NMR spectra due to an overall C_2 symmetry. Assuming this point group one would, e. g., expect only 13 signals in the ^{13}C NMR and one signal for the alanine $-\text{CH}_3$ groups. ^1H and ^{13}C NMR spectra are, however, much more complex and not interpretable. This also supports the assumption that **213** forms oligomeric aggregates that complicate the NMR spectra. To proof this assumption, NMR titrations would be needed that could not be performed due to the small amount of **213** available and its low solubility. Fortunately, crystals suitable for X-ray structure analysis could be grown from $\text{CHCl}_3/\text{MeOH}$ solution (Figure 10). Decisive for this structure are two different β -turns as indicated in Scheme 40 (B). This finding can, at least in part, explain the results of the cyclization experiments: **206–210** do not incorporate a α -Xaa- α -Xaa substructure that, upon formation of a β -turn, could facilitate cyclization of

the respective precursor. **212**, however, should display similar conformational features. The reason for failure of its cyclization still needs to be determined.



Remarkably, the cyclic monomers of **213** do not stack to form channels as was initially expected. In fact, at least in the crystal, the monomeric rings are staggered with the stacks held together through “inter-stack” hydrogen bonding of the D-Ala–L-Ala amide moieties that are orientated approximately perpendicular to the plane being formed by the cyclopeptide backbone (Figures 10 and 11). An adamantane from one monomer is located over the center of another monomer, leaving only a narrow channel.



6.5. Summary

The A Xaas can easily be equipped with protective groups at either the N- or C-terminus. Peptide couplings in solution generally work in high yields with only minor problems associated with the higher oligomer's low solubility in organic solvents typically used for the synthesis and chromatographic workup. Application of standard SPPS techniques allows for the rapid preparation of libraries of oligomers that can be used for different purposes (vide infra). The cyclizations that were attempted in an initial test showed, however, that one structural prerequisite enabling cyclization is obviously the presence of a α -Xaa– α -Xaa sequence that forms a β -turn, thereby facilitating the ring closure reaction.

7. Biological Properties

An organic chemist is not only interested in the synthesis of new compounds, but also in the elucidation of their capabilities. One field of eminent interest, not only in the framework of this thesis, is the biological activity of the compounds prepared. In cooperation with Dr. S. Pleschka, Institute of Medicinal Virology, University of Giessen, initial *in vitro* antiviral studies of three ^AXaas were performed. Uptake of ^AXaa derivatives through the GABA transporter mGAT1 was studied in the group of Prof. W. Schwarz, Max-Planck-Institute for Biophysics, Frankfurt. Both tests are at the very beginning of a systematic survey and are by no means complete but, however, clearly indicate the activity of at least one compound (a "hit") in both test systems. Now that a multitude of ^AXaa derivatives has become easily available, the results of the biological activities that are described in brief in the following part encourage more detailed studies with a bigger repertory of test compounds.

7.1. Anti *Influenza A* activity

Given the well-known antiviral activity of a number of aminoadamantanes (see Chapter 3), it was self-evident to test some of the ^AXaa derivatives with respect to their activities against *Influenza A* viruses. Tests were conducted in cell cultures of MDCK cells that were infected with *Influenza A* / WSN HK and *Influenza A* / FPV Bratislava (H₇N₇) viruses, respectively in the presence of ^AGly (**154**), ^AAla (**155**) and ^AAib (**156**) as their respective hydrochlorides. For comparison, amantadine **19** was also included. Virus titers are shown relative to a control without amantadine or the ^AXaas. The results are presented in Figures 12 and 13.

The rapid development of resistance of *Influenza A* viruses against antiviral agents (see 3.2.1.1.) is reflected in the increase of WSN-HK virus concentration when amantadine is present (2). Starting from the second run, the ^AXaas (3 – 5) consistently display antiviral activity greater than amantadine, with ^AAla · HCl giving the lowest virus titer in the test against this *Influenza* subtype (Figure 12).

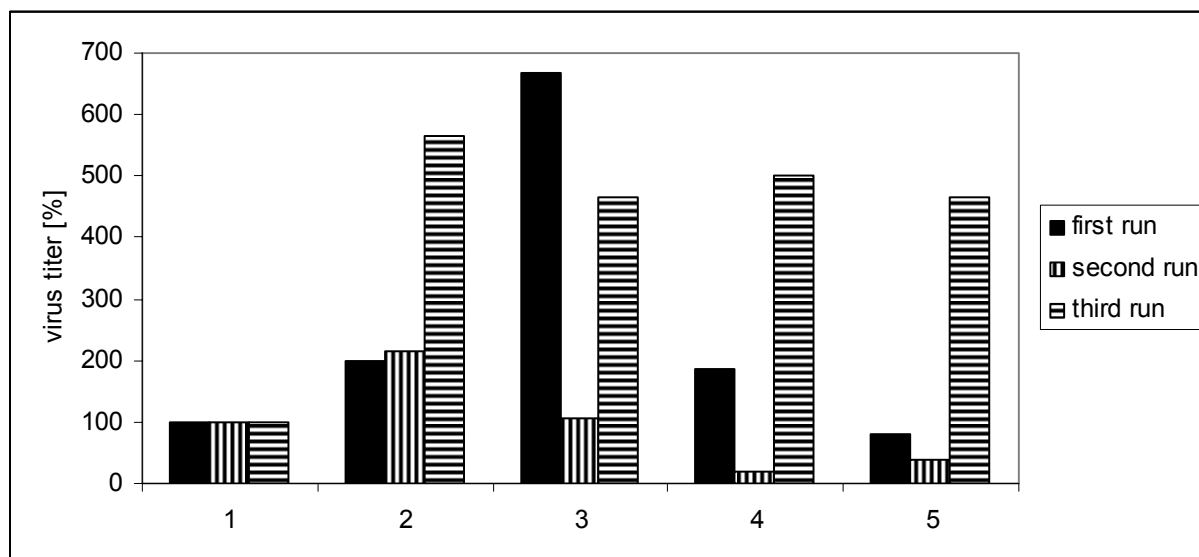


Figure 12. Antiviral activity of (2) amantadine (**19**) 5 μM, (3) ^AGly · HCl (**154**) 5 μM, (4) ^AAla · HCl (**155**) 20 mM, and (5) ^AAib · HCl (**156**) (5 μM) against *Influenza A / WSN HK*. Virus titer is shown relative to a control experiment (1) where no antiviral agent was used.

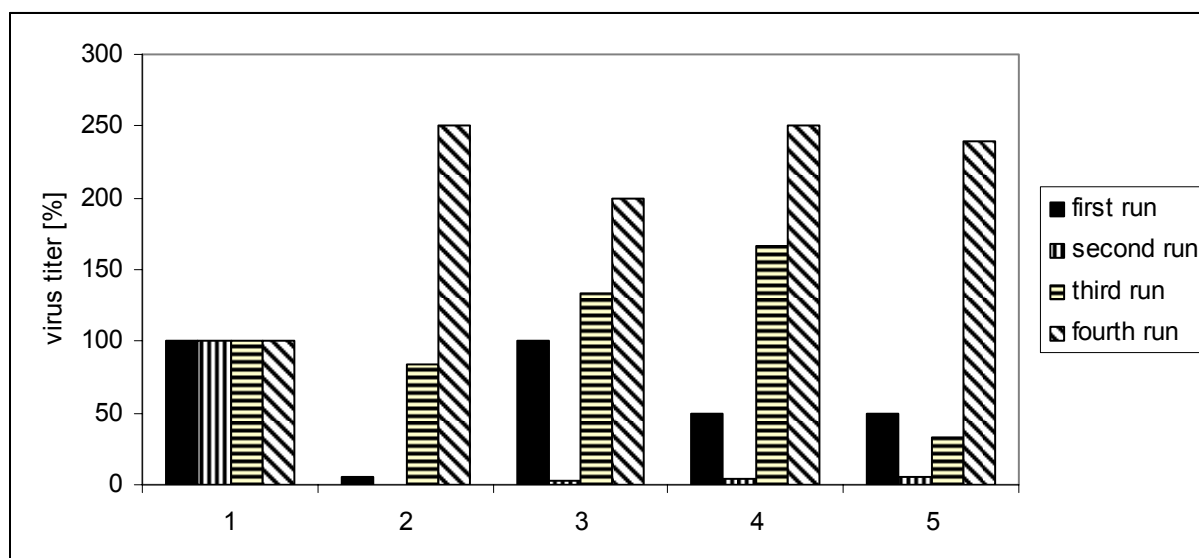


Figure 13. Antiviral activity of (2) amantadine (**19**) 5 μM, (3) ^AGly · HCl (**154**) 1 μM, (4) ^AAla · HCl (**155**) 5 μM, and (5) ^AAib · HCl (**156**) 5 μM. against *Influenza A / FPV/Bratislava/79*. Virus titer is shown relative to a control experiment (1) where no antiviral agent was used.

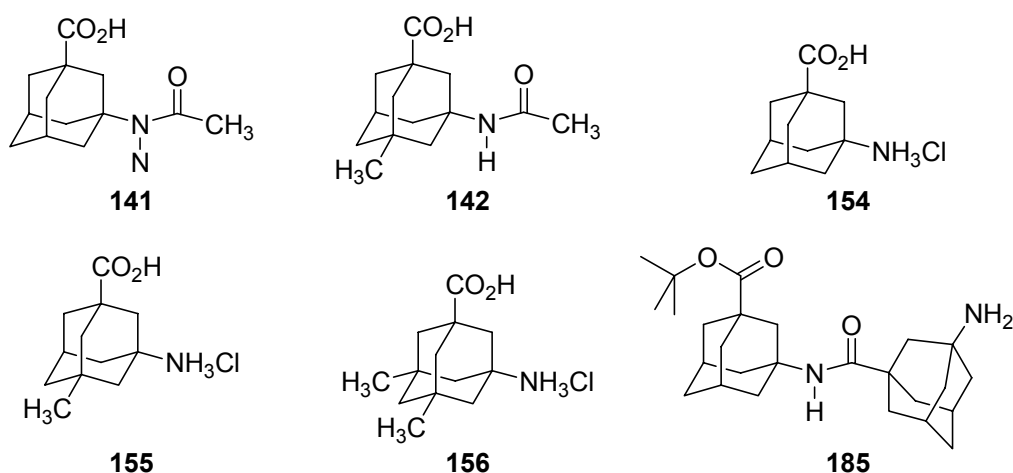
The abovementioned is in principle also observed with the FPV virus (Figure 13). As with the WSN subtype, the FPV titers are reduced significantly in the second and third run when compared to amantadine. ^AAib · HCl in this case appears to be the most active substance.

What can be concluded from these preliminary findings with only three ^AXaa derivatives tested is that they do inhibit virus multiplication in cell culture experiments to an extent comparable to amantadine. The slowed development of resistances (one

test run ~ three days) could make Δ Xaa derivatives interesting for a combination therapy.^[47]

7.2. Δ Xaas as analogues of GABA

In Chapter 3.2.2.3., some lipophilic analogues of GABA were presented. These were found to not interact with the GABA receptor(s), but presumably with voltage gated Ca^{2+} channels. We have prepared and tested several Δ Xaa derivatives (Scheme 41) as analogues of GABA in preliminary uptake experiments through the GABA transporter mGAT1 as expressed in oocytes of *Xenopus laevis*. The mGAT transporters function as a regulatory system in the GABAergic system by “pumping” GABA, the inhibitory neurotransmitter, back into the neurons. Thereby the concentration of GABA in the synaptic cleft is reduced, which can be disadvantageous in diseases like, e. g., epilepsy where an appropriate concentration of inhibitory neurotransmitters is needed to combat convulsion attacks.^[96] Selective blockade of the transporter system furthermore provides information to its precise physiological function.^[248] The uptake of GABA in the presence of the Δ Xaa derivatives shown in Scheme 41 is given in Figure 14 against a control experiment where no mGAT1 was injected to the oocytes.



Scheme 41. Δ Xaa derivatives tested as mGAT1 inhibitors.

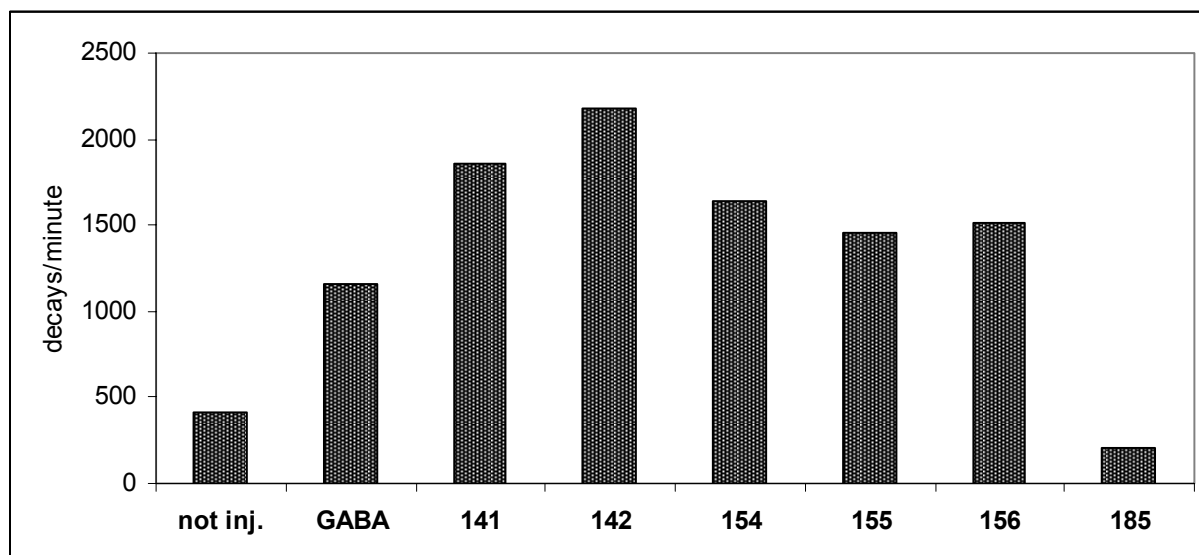


Figure 14. Uptake of GABA into *Xenopus laevis* oocytes through mGAT1 in the presence of GABA and A Xaa derivatives. Concentration of GABA and **141–185** was 1 mM. not inj.: no mGAT1 expressed in the oocytes. See experimental part for details.

GABA uptake was greater than with GABA alone when acetamides **141** and **142** as well as the hydrochlorides **154–156** were present. One simple explanation could be the a high concentration of cell-membrane disturbing DMSO used for the preparation of the stock solutions from the tested candidates. The hydrochlorides **154 – 156** did not significantly alter their efficacies upon bridgehead alkylation. Dipeptide **185** displayed good, concentration-dependent (Figure 15) blocking of the mGAT1 transporter although DMSO also was used in this experiment.

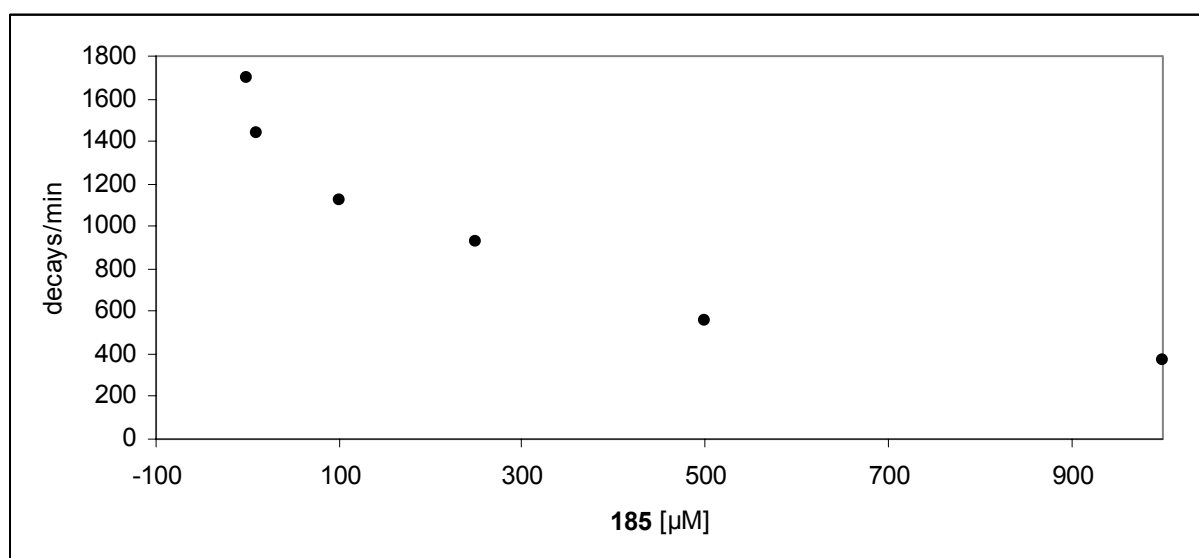


Figure 15. Concentration dependence of GABA uptake through mGAT1 in oocytes of *Xenopus laevis* upon variation of the concentration of dimer **185**. Please refer to the experimental part for details.

It is clear that from these preliminary tests no consistent structure-activity relationship (SAR) can be deduced. There is, however, activity of the test substances, and dipeptide **185** represents a “hit” that displays the desired mGAT1 blocking properties in a dose-dependent manner. One “hit” out of six substances tested appears a not too bad ratio.

It is clear that several other promising properties of Δ Xaa derivatives, in particular of the peptides incorporating the novel building blocks, are yet to be examined systematically. The expected resistance of such peptides towards proteolytic cleavage^[249] is just one field holding promise for future research.

8. Peptidic Organocatalysts

Elements of secondary structure play a pivotal role in protein folding as well as protein-protein interactions. This can be utilized in the design of peptidic and peptidomimetic structures as tailored pharmaceuticals with the goal of a selective fit into the binding pocket of the desired target protein. Such target proteins in many cases are enzymes that are inhibited by (small) molecules that mimic the structures of the enzyme's substrates but display a higher affinity to the enzyme.

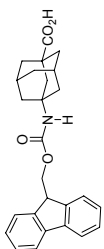
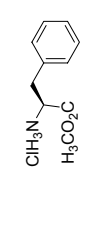
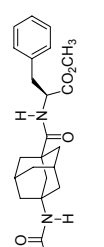
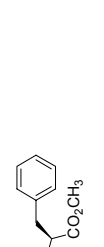
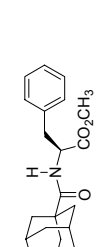
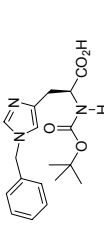
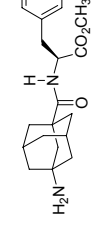
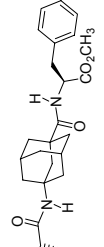
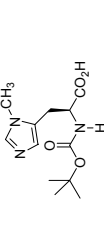
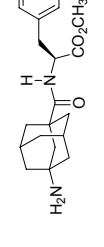
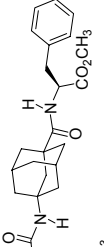
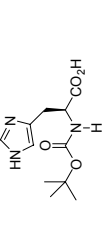
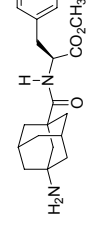
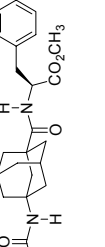
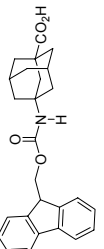
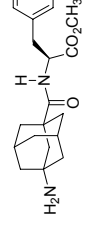
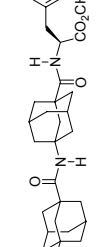
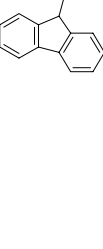
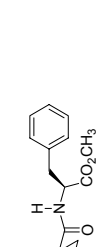
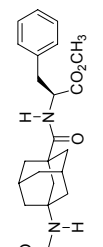
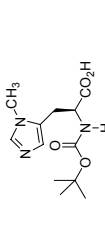
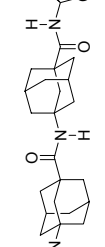
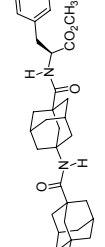
8.1. Peptidic catalysts incorporating α Gly

Is it, in turn, possible to design enzyme-like effects for a given task? In organocatalysis, this is the ultimate goal. By far most enzymes –in this context better depicted as biocatalysts– are proteins, and one highly popular and fruitful field of organocatalysis^[250] is dealing with the mimicry of enzymatic catalysis through designed peptides.^[251] The seminal works of Miller^[252] shed light on peptide catalyzed transformations such as acylations,^[253] azidations,^[254-256] phosphorylations,^[257-259] Morita-Baylis-Hillman reactions,^[260] and Rauhut-Currier reactions.^[261] Some of these stereoselective catalytic transformations made it to total synthesis which outlines the maturity of the concept.^[262] Miller and others have attributed the stereoselectivity of (amongst other transformations) peptide catalyzed acylations to the secondary structure of the backbone of the catalyst,^[253, 263, 264] stable turn structures yielding higher stereoselectivities.

Incorporation of α Xaas into peptides was envisaged to result in the formation of rigid turns; therefore, preparation and testing of the catalytic activity of a number of representative peptides incorporating α Xaas as the orientating tether was accomplished. One common motif of Miller's organocatalysts is (at least) one His residue acting as nucleophile; acylations are the reactions most frequently studied and appeared easy to analyze. Therefore, His-peptide catalyzed acylations appeared to be a good starting point for our project.

The first peptidic catalysts incorporating α Gly we synthesized via solution synthesis following the route depicted in Table 6. Fmoc- α Gly-Phe-OMe was prepared by the

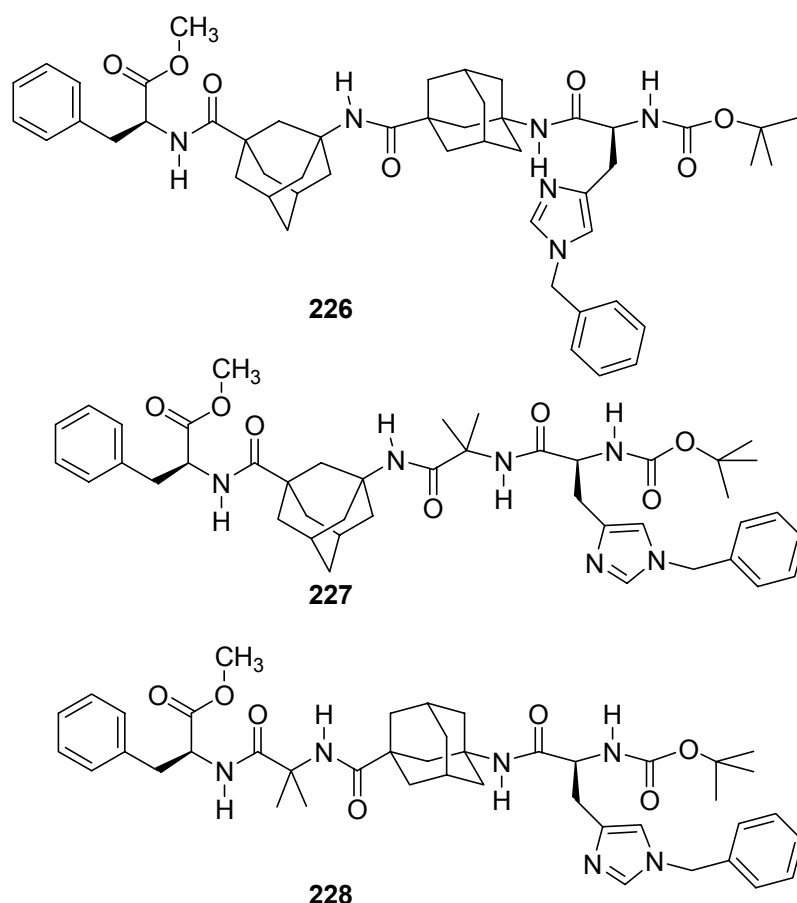
Table 6. Solution phase synthesis of Δ^1 Gly based His organocatalysts.

acid component	amine component	meth- od ^[a]	product	yield [%] ^[b]
		A		215 90
		C		216 94
		A		218 88
		A		220 66
		A		222 77
		A		223 60
		C		224 77
		A		225 64

^[a] Method A: HBTU/DIPEA in THF or MeCN; ^[b] isolated product after silica gel column chromatography; ^[c] contained impurities after chromatography.

HBTU mediated standard procedure mentioned above, and the Fmoc group was cleaved with diethyl amine. Another Fmoc-amino acid was, if necessary, introduced by repeating the coupling- and Fmoc-cleavage step. The catalytic entity, His residues with different sidechain protection, was attached at the N-terminus. For reasons of comparability, we only have chosen C-terminal –OMe- and N-terminal –Boc- protection.

Peptides **218** and **220** were also examined for their conformational propensities (see Chapter 9). Solution phase synthesis may have its well-known advantages –usually high purity of the final product– it is, however, time consuming. SPPS seemed to be advantageous in the synthesis of these (and other) peptidic catalysts. Therefore, the catalysts **218**, **220**, **222**, and **225** have also been prepared using commercially available Wang resin preloaded with Fmoc-Phe and endcapped.



Scheme 42. Peptidic organocatalysts for stereoselective transacylations.^[265]

After swelling, the Fmoc-cleavage was accomplished with piperidine (25% in DMF, 2 × 40 min), double coupling procedures were carried out with the Fmoc- and Boc-

protected amino acids used for the individual chain elongation step (two times 1 h with each 2 eq. Fmoc amino acid, 2 eq. HBTU, 2 eq. HOBt·H₂O, 4 eq. DIPEA¹). Cleavage from the resin was accomplished by shaking for four days in methanol / triethylamine / THF (9 : 1 : 1).^[266]

In addition to the abovementioned peptides, Boc-His(τ -Bn)-^AGly-^AGly-Phe-OMe (**226**), Boc-His(τ -Bn)-^AGly-Aib-Phe-OMe (**227**), and Boc-His(τ -Bn)-Aib-^AGly-Phe-OMe (**228**) were prepared via SPPS (Scheme 42). Evaporation of the solvents yielded the crude peptidic catalysts that were, along with samples of the catalysts obtained from solution phase synthesis, provided to Christian Müller, who conducted further purification and test reactions with these and other peptide catalysts. Stereoselective transacylations and desymmetrizations of *meso*-diols with e.r. values up to 91 : 9 could be achieved with this methodology. For details, please refer to Christian Müller's diploma thesis and the recently submitted publication dealing with this topic.^[265]

8.2. Peptidic thioureas and organocatalytic Morita-Baylis-Hillman reactions

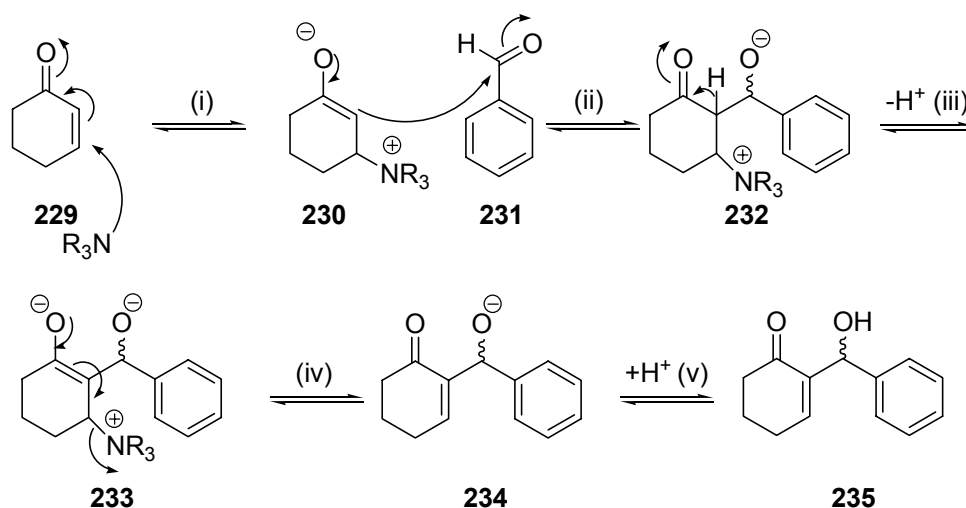
8.2.1. Catalyst design

Nature provides us with enzymes whose activity as well as chemo- and stereoselectivity in a number of reactions is unrivaled. This is despite the fact that Nature's toolkit consists essentially only of 20 (22) amino acids. As a result, peptidic organocatalysis quite frequently employs unnatural amino acids as key building blocks to govern predictable orientation of the catalytically active entities in space. Miller and others frequently use D-Pro and a number of α -alkylated amino acids like Aib in key positions of the catalyst's sequences.^[267] Another principle of variation in peptidic organocatalysis is the introduction of functional groups *beyond* proteinogenic amino acids that have been reported to act as organocatalysts for themselves. Assembling several organocatalytically active groups with the power and versatility of peptide chemistry providing the scaffold easily makes available multi-functional designed organocatalysts with reactivities beyond that of enzymes.

¹ To neutralize hydrochlorides (e.g. in case of Boc-His(τ -Bn)-OH·HCl), one extra equivalent of DIPEA was used.

One such catalytic entity is the *N*-3,5-trifluoromethylphenyl thiourea motif that has been established by our group^[192, 268, 269] and others.^[270-273] A multitude of organic transformations were successfully catalyzed by thiourea based organocatalysts. The main (but not exclusive)^[274, 275] mode of action is the activation of carbonyl groups through explicit hydrogen bonding provided by the (acidic) N–H functionalities of the thiourea motif.

A challenging task for organocatalysis is represented by the Morita-Baylis-Hillman reaction.^[276-278] Mechanistically, the reaction is believed to commence with a nucleophilic Michael addition of a tertiary amine (typically DABCO is used) at the β -position of an activated enone **229** forming an zwitterionic enolate **230**. This reacts with an aldehyde **231** (ii) to give another zwitterion **232** which is then deprotonated (iii) to **233** as the catalyst is released leaving **234** (iv). Proton transfer (v) affords the final product **235** (Scheme 43).^[279]

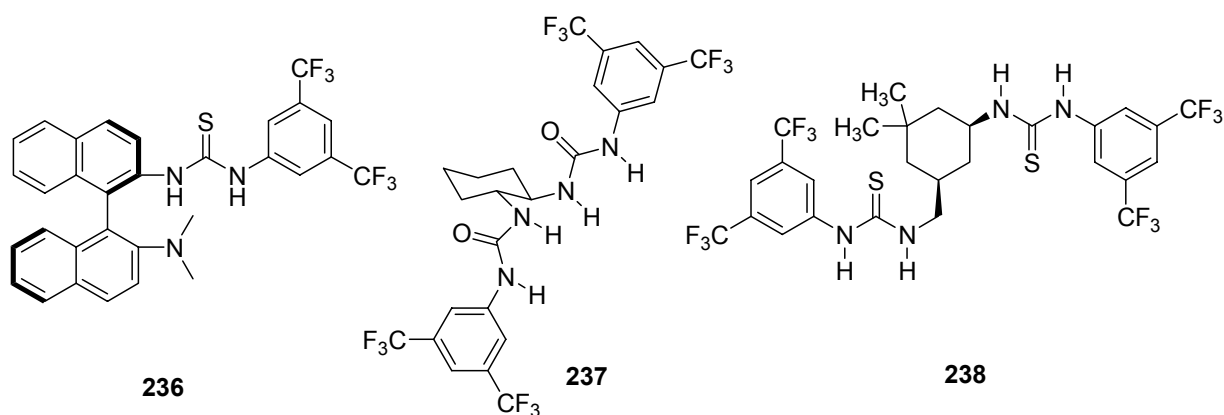


Scheme 43. Mechanistic model for the Morita-Baylis-Hillman reaction

Organocatalytic variants include the use of His containing peptides as introduced as organocatalysts by Miller^[260, 280] and bifunctional thiourea derivatives.^[281, 282] Best results to date (in terms of yields and stereoselectivities) were obtained by the use of bis-thiourea derivatives (Scheme 44).^[283, 284]

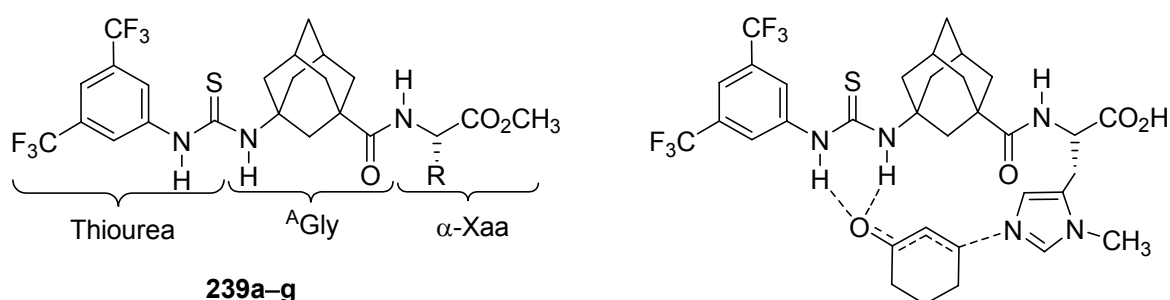
In Miller's His-peptide approach, proline or pipercolic acid have to be used as a separate cocatalyst; Nagasawa and Berkessel need to add a nucleophile (DABCO) to the reaction mixture. With the bifunctional strategy (**236**), no co-catalyst is needed.

How can one tether a thiourea motif with a peptide fragment incorporating a nucleophile while “folding” into a stable turn structure?



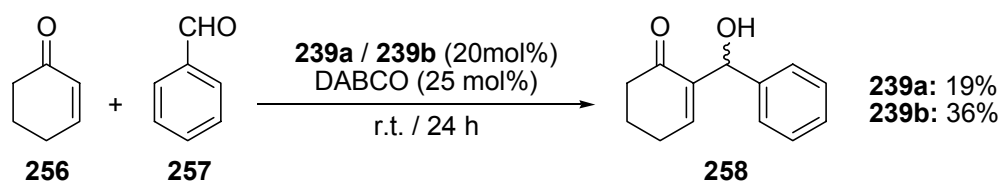
Scheme 44. Thiourea organocatalysts successfully applied in Morita-Baylis-Hillman reactions.

Installation of a thiourea motif in a peptide is not a trivial task, because usually α -peptides are being degraded upon acidification of the intermediate thioureas. The thiohydantoin formation via cyclization through nucleophilic attack of the thiourea sulfur is routinely used in Edman degradation with phenyl isothiocyanate and in automated peptide sequencing.^[285, 286] We used the addition of 3,5-bis(trifluoromethyl)isothiocyanate^[275] to the unprotected N-terminus of the peptide chain for thiourea synthesis. When incorporating an A Xaa residue at the N-terminus of the peptide chain, formation of a five-membered ring from the thioureas (**239a–g**) to form thiohydantoin is no longer possible. This renders peptidic thioureas incorporating A Xaas bench-top stable. Of the multitude of peptidic thioureas amenable through this approach, a small library of seven peptidic thioureas was synthesized (Scheme 45, Table 7) and screened as organocatalysts in the Morita-Baylis-Hillman reaction.



Scheme 45. Peptidic thiourea catalysts prepared and proposed synergistic activation of an enone.

As proof-of-principle experiment, MBH reaction of cyclohexenone with benzaldehyde was chosen (Scheme 46). These reactions were performed in 0.5 mmol scale as has been described in the literature.^[283] Silica gel column chromatography of the crude reaction mixture was performed eluting with n-hexane / ethyl acetate (1 : 1), R_f (**258**) = 0.28.

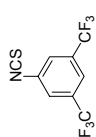
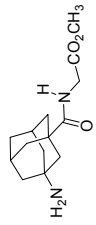
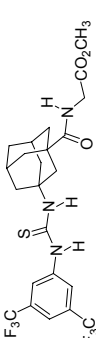
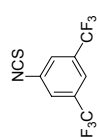
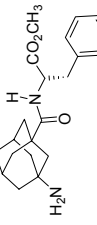
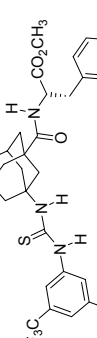
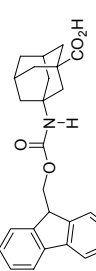
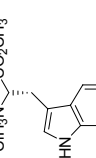
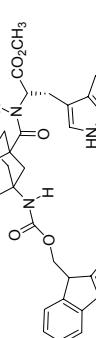
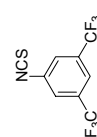
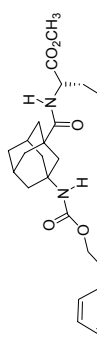
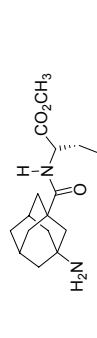
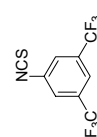
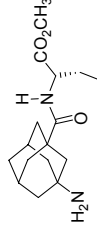
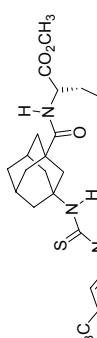
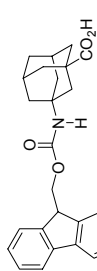
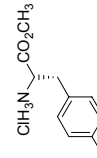
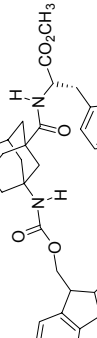


Scheme 46. Proof-of-principle MBH reaction catalyzed by **239a** and **239b**.

GC-MS analysis of the product fraction gave one product peak only; NMR spectra were in agreement with expected spectra. A blind reaction using DABCO, but no catalyst, gave no MBH product **258** (as analyzed by TLC and GC-MS). In this test reaction, the peptidic organocatalysts indeed showed activity: **239a** yielded **258** in 19% yield of isolated product after column chromatography; **239b** gave 36% yield. With both catalysts, however, no enantiomeric excess could be achieved (chiral stationary phase GC). For reasons of comparability with Katharina Lippert's work,² the peptidic thiourea organocatalysts **239a–g** were then screened in the Morita-Baylis-Hillman reaction of cyclohexenone with cyclohexane carbaldehyde. This test reaction has been reported to deliver high enantiomeric excess in the literature.^[284] The results are summarized in Table 8. Reactions were run in parallel in 0.25 mmol scale and monitored by GC-MS. Monitoring of the reaction was, however, not reproducible since the relative concentrations of the product did not increase steadily. Therefore, reaction times could not be optimized and were arbitrarily chosen. After workup, the crude reaction mixture was purified by silica gel column chromatography (eluent: n-hexane / ethyl acetate (3 : 1), R_f (**260**) = 0.13) and analyzed by GC-MS. One clean product peak ($M^+ = 208$) was observed in each product fraction. There was significant decomposition of the product upon standing in solution; therefore, no NMR data could be collected.

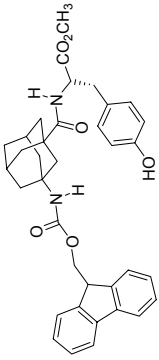
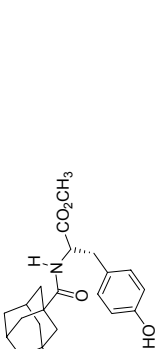
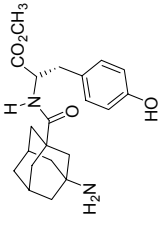
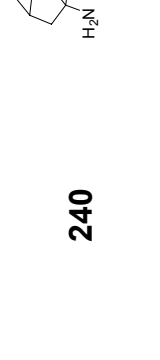
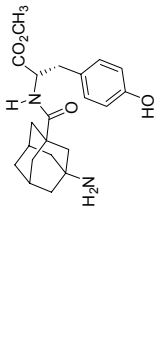
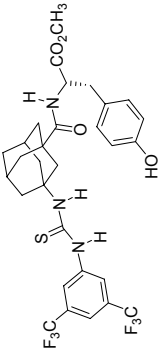
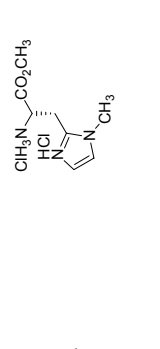
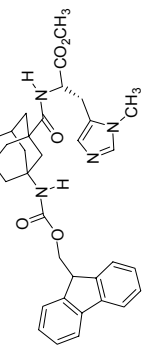
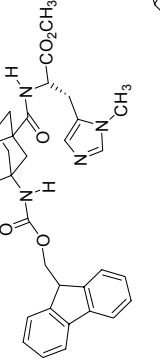
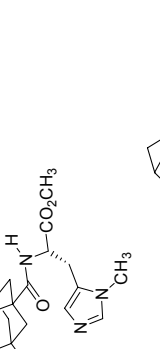
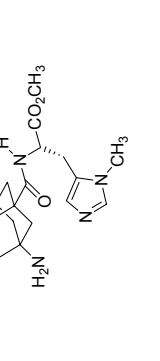
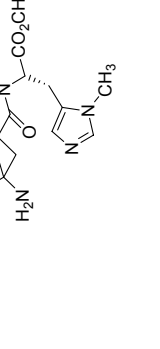
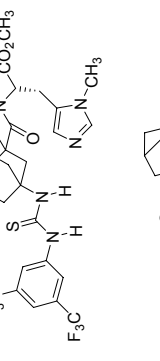
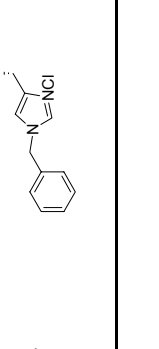
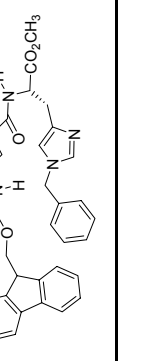
² Katharina M. Lippert, Diploma thesis, University of Giessen, 2007.

Table 7. Synthesis of the peptidic thiourea derivatives.

Acid component	Amine component	meth -od ^[a]	Product	Yield [%] ^[b]
		E		239a 81
		E		239b 91
		A		242 87
		C		243 94
		E		239c 81
		A		245 62

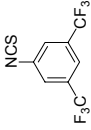
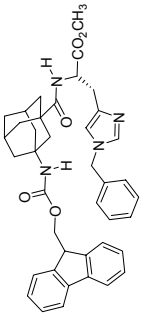
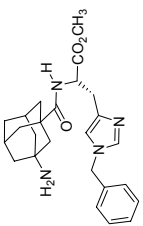
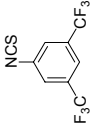
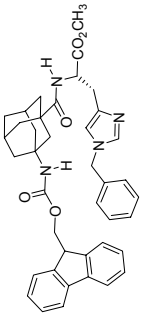
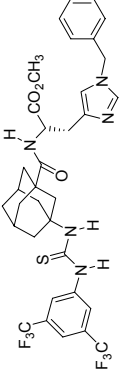
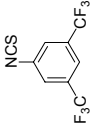
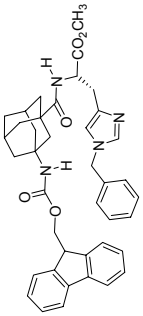
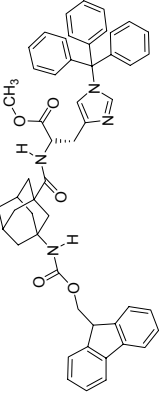
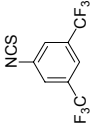
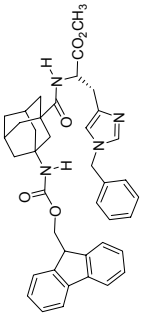
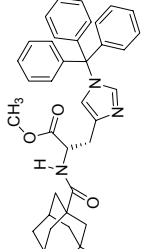
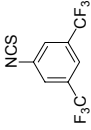
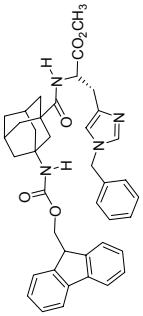
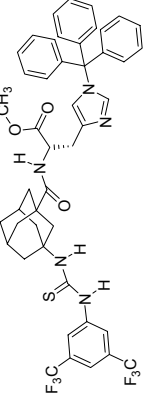
(continued)

Table 7 (continued)

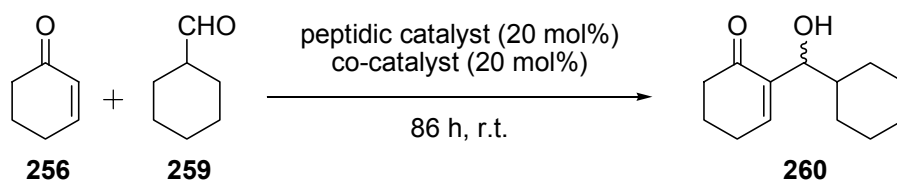
Acid component	Amine component	meth- od ^[a]	Product	Yield [%] ^[b]
		C		246 89
		E		239d 91
		A		248 82
		C		249 93
		E		239e 95
		A		251 81

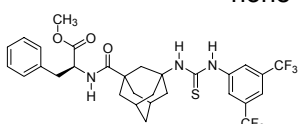
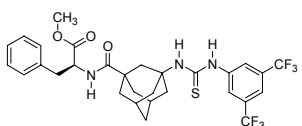
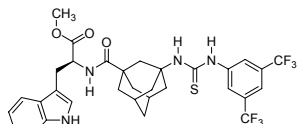
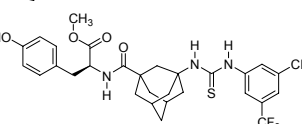
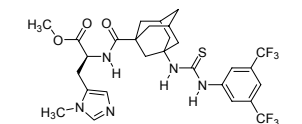
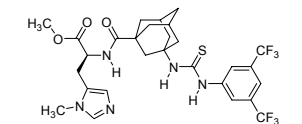
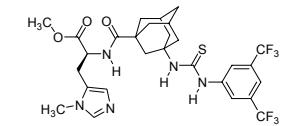
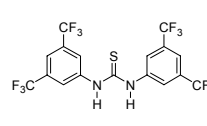
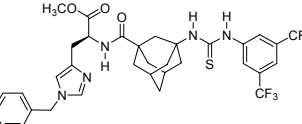
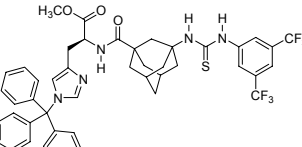
(continued)

Table 7 (continued)

Acid component	Amine component	meth- od ^[a]	Product	Yield [%] ^[b]
		251		252 84
		240		239f 76
		180a		254 -[^{c]}
		254		255 90 ^[d]
		255		239g 29

^[a] Method A: HBTU/DIPEA in THF or MeCN, rt; Method C: HNEt₂ in MeCN, rt; Method E: stirring at rt in THF solution. ^[b] yield of isolated product after reprecipitation or silica gel column chromatography. ^[c] compound was used without purification; ^[d] over two steps.

Table 8. Initial catalyst screen in an organocatalytic Morita-Baylis-Hillman reaction.

entry	peptidic catalyst (20 mol%)	co-catalyst (20 mol%)	yield [%] ^[a]	e.r. ^[b]
2	none	DABCO	- ^[c]	-
3	 239b	DABCO	20	50:50
4	 239b	1-methylimidazole	0	-
5	 239c	DABCO	52	50:50
6	 239d	DABCO	20	49:51
7	 239e	DABCO	11	49:51
8	 239e	none	5	52:48
9	 239e		26	47:53
10	 239f	none	10	50:50
11	 239g	none	traces	-

^[a] Yield of isolated product after silica gel column chromatography; ^[b] detected by chiral stationary phase GC using a Hydrodex β -6-TBDM column

Conclusions that could be drawn from these results are hampered by the fact that the test reaction chosen is not suitable for the elaboration of ideal reaction conditions (like, e. g., an end point), in particular, since the MBH adduct from cyclohexenone and cyclohexyl carbaldehyde does readily eliminate under basic conditions. However, low enantiomeric excesses were detected in some cases. Therefore, after a re-examination of the reaction utilizing more stable test substrates (e.g., **258**), further studies of the organocatalytic MBH reaction utilizing peptidic thiourea organocatalysts incorporating ^AXaas do hold promise. Notably, the minimum enantiomer in entry eight becomes the majority enantiomer in entry nine, which can be regarded as a hint towards alternative reaction paths.

9. Structural features

What are the structural consequences of the incorporation of an α Xaa-residue into peptides? Besides the importance of functional group adjustment in medicinal applications (as has been outlined above), interest in this problem is also driven by other fundamental considerations. For the design of peptidic catalysts, rigid turn structures are required (see Chapter 8). Interaction between the substrate (cyclohexenone) and the organocatalyst's (**239e**) "binding site" is a crucial concept in catalyst design for the MBH reaction and, therefore, also covered in this chapter. Head-to-tail cyclization of peptides is also facilitated by an arrangement of the peptide chain termini that brings close the (activated) C-terminus and the N-terminal amino functionality. Several of these aspects were treated by computational studies; whenever appropriate, experimental data (solution-phase IR, nOe NMR, etc.) were also collected to support computational results.

9.1. Computational methods and strategy

Peptides, even the short sequences to be treated here, give a large number of conformers that need to be considered in conformational analysis. Frequently a protein displays its bioactivity in one conformation only which is selected upon protein folding, which governs unique selectivity of, e. g., enzymes. Misfolding can have drastic consequences, as exemplified by prion diseases. Therefore, meaningful conformers that are populated in solution need to be identified. Computing all of them using high-level HF or DFT methods is not possible due to limits in computing power; hence, a pre-selection had to be made.

All conformer distribution analyses discussed herein were performed following the same strategy: A conformer distribution analysis using the MMFF-94 force field as implemented in Spartan '02^[287] was performed as a first step with no conformational constraints. The MMFF-94 conformers lowest in energy were then geometry optimized using B3LYP/6-31+G(d,p) model chemistry using the Gaussian03 program suite.^[288]

9.1.1. Computation of Conformer Distributions^[289]

As mentioned, Spartan '02 implemented conformational grid search was used to generate conformer starting geometries which subsequently were optimized utilizing the MMFF-94 force field as implemented in Spartan. Force fields can be regarded as a set of equations which together describe the potential energy surface (PES) of a molecule, typically by a sum of energy terms:

$$E_{\text{total}} = E_{\text{bond}} + E_{\text{bend}} + E_{\text{torsion}} + E_{\text{vdW}} + E_{\text{elec}} + E_{\text{cross}} \quad (1)$$

Each term represents a summation of energy functions for bonds, bond angles, dihedral angles, etc. in a molecule and reflects the physics of an interaction of the atoms in a molecule or between the atoms of different molecules. Each individual part of the right-hand side of eq. (1) is implemented into a force field by a function of somewhat arbitrary complexity, but usually the polynoms are truncated so that, e. g., E_{bond} in its simplest form is given by

$$E_{\text{bond}} = \frac{1}{2} k_{\text{AB}} (r_{\text{AB}} - r_{\text{AB,eq}})^2 \quad (2)$$

which is Hooke's law for a spring, k representing the force constant of the spring – or, in the case of a molecule, the bond, and r_{AB} the actual bond length upon elongation of the A–B bond within the molecule while $r_{\text{AB,eq}}$ is the equilibrium bond length. In practical force fields, the truncated Taylor expansion in eq. (2) is substituted by a more realistic function that includes additional cubic and quartic terms to account for a more realistic bond potential function.

$$E_{\text{bond}} = \frac{1}{2} [k_{\text{AB}} + k_{\text{AB}}^{(3)} (r_{\text{AB}} - r_{\text{AB,eq}}) + k_{\text{AB}}^{(4)} (r_{\text{AB}} - r_{\text{AB,eq}})^2] (r_{\text{AB}} - r_{\text{AB,eq}})^2 \quad (3)$$

Such a function is found in force fields like MM3, while others use quadratic terms only because of the greater computational simplicity. E_{bend} , the term for valence angle bending, can be formulated in an analogous manner as a polynomial expansion:

$$E_{\text{bend}} = \frac{1}{2} \left[k_{\text{ABC}} + k_{\text{ABC}}^{(3)} (\theta_{\text{ABC}} - \theta_{\text{ABC,eq}}) + k_{\text{ABC}}^{(4)} (\theta_{\text{ABC}} - \theta_{\text{ABC,eq}})^2 + \dots \right] (\theta_{\text{ABC}} - \theta_{\text{ABC,eq}})^2 \quad (3)$$

In the molecule, θ_{ABC} represents the valence angle between bonds A–B and B–C. Until which term the expansion is utilized in the respective force field is again determined by the balance of computational cost and accuracy. The term for molecular torsions can be written as

$$E_{\text{torsion}} = \frac{1}{2} \sum_{\{j\}_{\text{ABCD}}} V_{j,\text{ABCD}} \left[1 + (-1)^{j+1} \cos(j\omega_{\text{ABCD}} + \psi_{j,\text{ABCD}}) \right] \quad (4)$$

Since the torsion is periodic, the torsional energy equation (4) also has to be in a periodic form which is typically implemented as a Fourier series.

The van-der-Waals term E_{vdw} is usually given by a function derived from a Lennard-Jones-, Morse- or Hill-potential, while electrostatic interactions in E_{elec} are described in the simplest way by assigning to each van der Waals atom a partial charge yielding

$$E_{\text{elec}} = \frac{q_A q_B}{\epsilon_{\text{AB}} r_{\text{AB}}} \quad (5)$$

E_{cross} accounts for the fact that bonds, bond angles and torsions are not isolated in a molecule but couple with one another. Different parametrization and complexity of the mathematical functions that describe the different molecular interactions account for the multitude of existing force fields, most of which have been designed for specific tasks (e.g., highest possible accuracy or convenient speed when treating macromolecules).

The Merck Molecular Force Field 1994 (MMFF-94)^[290-294] is considered widely suitable for the computational treatment of organics and biomolecules. It has been parametrized using high-level correlated Møller-Plesset optimized structures and covers an unusually broad range of chemical structures. Therefore, this force field has been chosen for all computations of conformer distribution within this work.

The MMFF-94 conformers (usually, the ten lowest MMFF-94 conformers were selected) were subsequently used as the starting geometries for DFT geometry optimizations.

9.1.2. Selection of DFT Model Chemistry

To provide precise information of the energetics and structures of the rather large molecules treated herein, the method of choice was density functional theory (DFT).^[295] In this approach to electronic structure computation, the classical wavefunction is substituted with the electron density to describe an electronic system mathematically. By separating the total energy into different elements, it can be described as

$$E = E^T + E^V + E^J + E^X + E^C \quad (6)$$

E^T represents the kinetic energy of the electrons and the nuclei; E^V results from the attraction of the electrons through the nuclei; E^J the energy from the interaction of the electrons with the magnetic field that is generated by the electron's motion, E^X is the so-called exchange energy that finally results from Pauli's principle (two electrons with the same spin can not be located at the same position) and is also referred to as Fermi-Correlation. Lastly, E^C is the correlation of electrons with opposite spins, an attractive interaction.

Quantum chemical calculations differ in the treatment of these last three terms, the electron correlation. Because they are a multi-body problem, they can not be treated consistently. Within density functional theory (DFT), these last three terms are substituted with a functional of electron density that can be computed much easier than the multi-electron wavefunctions known from Hartree-Fock theory. Today, most DFT computations are based upon Kohn-Sham theory^[296] that combines HF- and density functional theories. Most widely applied today is the BLYP-method (**B**ecke, **L**ee, **Y**ang, **P**arr)^[297, 298] because it delivers molecular geometries of high accuracy and reasonable molecular energies at modest computational cost. The kinetic term E^T (eq. 6) is described by the Hartree-Kinetics-Functional^[299] which treats E^T as the sum of the individual kinetic energies of the single electrons independently from one another.

The so-called exchange energy E^X is defined by Becke's DFT-functional.^[298] The correlation energy E^C is given by Lee, Yang and Parr's functional.^[300] These two functionals also account for gradients of the electron density. Another very popular approach is the combination of various functionals in a parametrized fashion; the coefficients of these parameters were necessary to fit the results from DFT computations to experimental values. Therefore, such DFT computations can not be recognized as "clean" *ab initio* methods. Today's most popular method is B3LYP^[298], which uses three constants for parametrization. In addition to the relatively good accuracies at modest computational cost, the DFT computations also give smaller basis set superimposition error (BSSE).^[301] Also, DFT methods are generally not as dependent from the selection of a basis set than other computational methods are.

A basis set describes the set of functions used for the actual computations, these functions are composed of a finite number of atomic orbitals centered at the nucleus of each atom of the molecule. The functions are combined (linear combination of atomic orbitals, LCAO ansatz). In the early days, Slater-type orbitals (STO's) were used which correspond to a set of functions that decay exponentially with increasing distance from the atom. Gaussian orbitals are much better suited for the calculation of overlap- and other integrals, and they can also be used to approximate STO's, thereby saving computational cost.

The minimal basis sets are typically composed of the minimum number of basis functions required for all electrons of the respective atom. For an atom from the first row of the periodic table (Li–Ne), a minimal basis set would consist of five functions (1s, 2s, 2p_x, 2p_y, and 2p_z). One such minimal basis set is the STO-3G^[302] basis set, in which every Slater-type orbital is replaced by three Gaussians.

Minimal basis sets often give poor results only; several improvements are typically used. The so-called split valence basis sets (for instance, 3-21G or 6-31G) use two (three, four,...) basis functions (zeta functions) for each valence orbital and are also referred to as double (triple, quadruple,...) zeta basis sets. Examples for double-zeta basis sets are the commonly used 6-31G basis sets that have exclusively been used in the present research. Additional flexibility to basis sets is provided by polarization functions as in, e. g., 6-31G(d), where a d-function is used for heavy atoms (in computational chemistry, heavy atoms are all atoms but hydrogen). The 6-31G(d,p) basis set used in the geometry optimization of the present study also adds polarization functions (p orbitals) to the hydrogens, which is essential for the correct reproduction

of long-range interactions like, e. g., hydrogen bonding. Addition of diffuse functions is used to account for the “tail” portion of an atomic orbital. In 6-31+G(d,p), diffuse functions (with smaller coefficients) are added for the heavy atoms, in 6-31++G(d,p), diffuse functions are also used for the description of hydrogen atoms. Since in the present study only the relative energies of conformers (i.e., minima on the PES) were computed, no computation of the frequencies was performed. In this work, all DFT computations were performed using the Gaussian 03 package. Unless otherwise noted, all geometry optimizations were performed using the B3LYP/6-31+G(d,p) level of theory.

9.2. Infrared spectroscopy

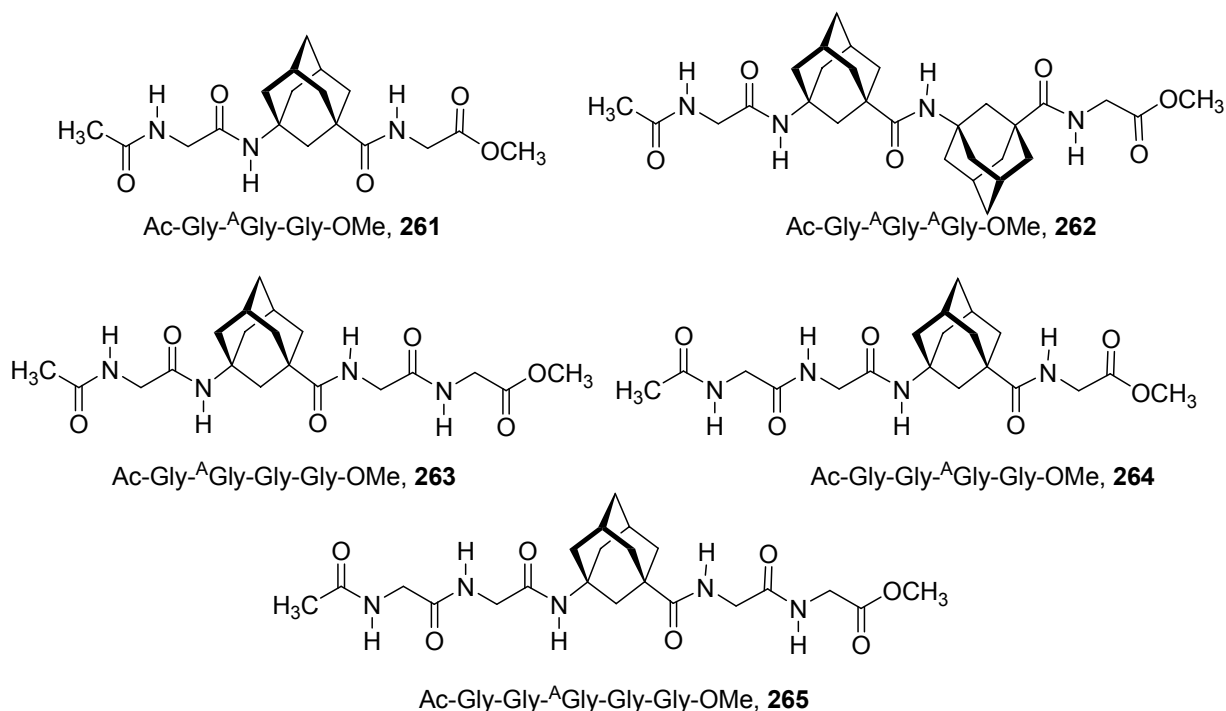
Gellman has established IR spectroscopy as a tool for the determination of intramolecular amide-amide hydrogen bond.^[303] He has examined model substrates in dilute (1 mM) dichloromethane solutions. Sharp bands in the N–H stretch region at 3450 – 3460 cm^{-1} were assigned to non-hydrogen bonded N–H, broad bands at 3300 – 3330 cm^{-1} were assigned to internally hydrogen bonded N–H. This method has been utilized by Gellman^[304, 305] and others^[306, 307] to probe the intramolecular hydrogen bonding propensities of amides and ureas. In this work, 10 mM and 1 mM solutions of the respective peptides and peptidic thioureas were prepared and studied IR spectroscopically in the non-hydrogen bonding solvents CH_2Cl_2 and CDCl_3 , respectively. Any turn-like structure should display intramolecular hydrogen bonding and should, therefore, be detectable by IR spectroscopy.

9.3. NMR spectroscopy

Whenever possible, NMR spectroscopy has also been used for solution phase structure confirmation. After complete signal assignment via ^1H - and ^{13}C -NMR along with COSY-, HSQC-, DEPT¹³⁵ / APT-, and HMBC- spectra, nOe spectroscopy was performed to confirm assumed turn motifs via interresidual nOe crosspeaks.

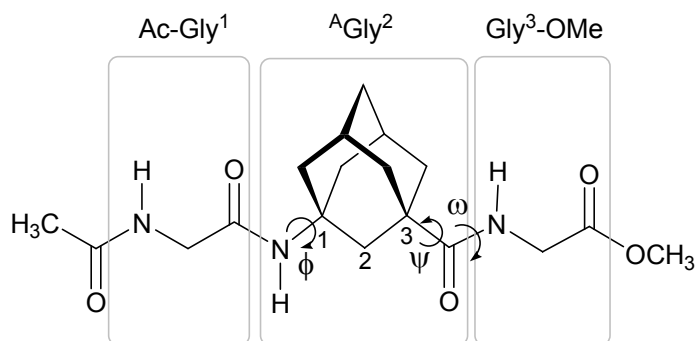
9.4. Minimum requirements for an ^AGly induced turn motif

As a first test system to probe the influence of one or two ^AXaa residues on the folding propensities of short peptides, five model sequences were prepared by SPPS methods (Scheme 47).



Scheme 47. “Minimum sequences” incorporating ^AGly for conformational analysis.

To provide geometry parameters for the computed structures, the classical torsional angles known from peptide chemistry (Φ , ψ , ω) were used. For the ^AGly residue, these angles had to be modified as depicted in Scheme 48. The concepts of an “upscaled” or “inflated” α -carbon becomes obvious here; all torsional angles are directly comparable to those of α -peptides.



Scheme 47. Peptidic dihedral angles of an A Gly residue in trimer **261** as used in this thesis.

The geometrical parameters used to classify conformers throughout this study are defined as follows:

- *Acylated N-terminal Gly¹ residue:*
 $\Phi = \text{C}=\text{O}(\text{Acetyl}) - \text{N}(\text{Gly}^1) - \text{C}_\alpha(\text{Gly}^1) - \text{C}=\text{O}(\text{Gly}^1)$;
 $\psi = \text{N}(\text{Gly}^1) - \text{C}_\alpha(\text{Gly}^1) - \text{C}=\text{O}(\text{Gly}^1) - \text{N}(\text{Gly}^2)$;
 $\omega = \text{C}_\alpha(\text{Gly}^1) - \text{C}=\text{O}(\text{Gly}^1) - \text{N}(\text{Gly}^2) - \text{C}^1(\text{Gly}^2)$.
- *A Gly² residue:*
 $\Phi = \text{C}=\text{O}(\text{Gly}^1) - \text{N}(\text{Gly}^2) - \text{C}_1(\text{Gly}^2) - \text{C}_2(\text{Gly}^2)$;
 $\psi = \text{C}_2(\text{Gly}^2) - \text{C}_3(\text{Gly}^2) - \text{C}=\text{O}(\text{Gly}^2) - \text{N}(\text{Gly}^3)$;
 $\omega = \text{C}_3(\text{Gly}^2) - \text{C}=\text{O}(\text{Gly}^2) - \text{N}(\text{Gly}^3) - \text{C}_\alpha(\text{Gly}^3)$.
- *C-terminal Gly residue:*
 $\Phi = \text{C}=\text{O}(\text{Gly}^2) - \text{N}(\text{Gly}^3) - \text{C}_\alpha(\text{Gly}^3) - \text{C}=\text{O}(\text{Gly}^3)$;
 $\psi = \text{N}(\text{Gly}^3) - \text{C}_\alpha(\text{Gly}^3) - \text{C}=\text{O}(\text{Gly}^3) - \text{OCH}_3$
 $\omega = \text{not to be defined in an ester.}$

9.4.1. Structural analysis of tripeptide 261

Visual inspection of the 100 conformers lowest in energy of an MMFF-94 conformer equilibrium search using Spartan '02 did not show any conformer displaying Gly¹ – Gly³ hydrogen bonding motifs. The 15 conformers lowest in energy after MMFF-94 optimization were subsequently taken as starting geometries for further optimizations using the B3LYP/6-31+G(d,p) level of theory as described above. Table 9 gives their relative energies as computed by MMFF-94 or DFT, respectively. In Table 10, geometry parameters of the conformers are listed. Both MMFF-94 and DFT computations yield local minima that were very similar in energy. Because of the very

similar relative energies of a series of at least eight conformations, no meaningful conclusion can be drawn for a preferred conformation of **261**. Obviously a number of conformations will be populated at rt – all of them showing no interresidual hydrogen bonding, that is, no stabilized turn motif. Furthermore, conformers 1 and 2 from the MMFF-94 analysis are enantiomers to structures 3 – 5. The global minimum (6) and its enantiomer (7) could not be identified with the force field method. Several other structurally closely related conformers lie within 0.4 kcal/mol at B3LYP/6-31+G(d,p). Some of the conformers computed are shown in Figure 16.

Table 9. relative energies of the conformers of trimer **261**. Values given in kcal/mole relative to the global minimum.

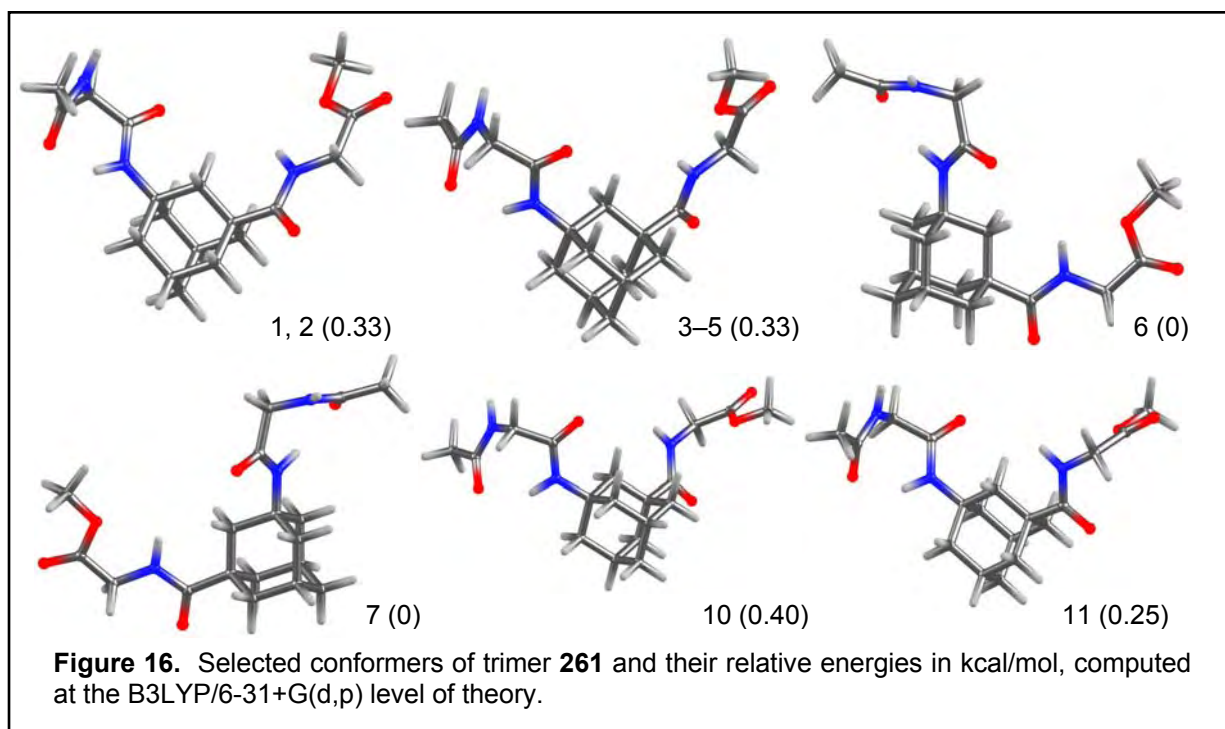
no.	E_{rel} [kcal/mol] DFT ^[a]	R_{rel} [kcal/mol] MMFF-94 ^[b]	Comment
1	0.33	0.00	
2	0.33	0.00	same conformer
3	0.33	0.00	
4	0.33	0.00	same conformer, enantiomer to 1 and 2
5	0.33	0.00	
6	0.00	0.07	global minimum
7	0.00	0.07	enantiomer of 6
8	0.00	0.07	
9	0.00	0.07	same conformer
10	0.40	0.52	
11	0.25	0.52	
12	0.07	0.56	
13	0.07	0.56	enantiomer to 12
14	0.14	0.57	
15	0.14	0.57	same conformer

^[a] Computed using B3LYP/6-31+G(d,p) level of theory; ^[b] computed using MMFF-94 as implemented in Spartan '02.

Table 10. Geometry parameters from minimum conformers of trimer **261**.^[a]

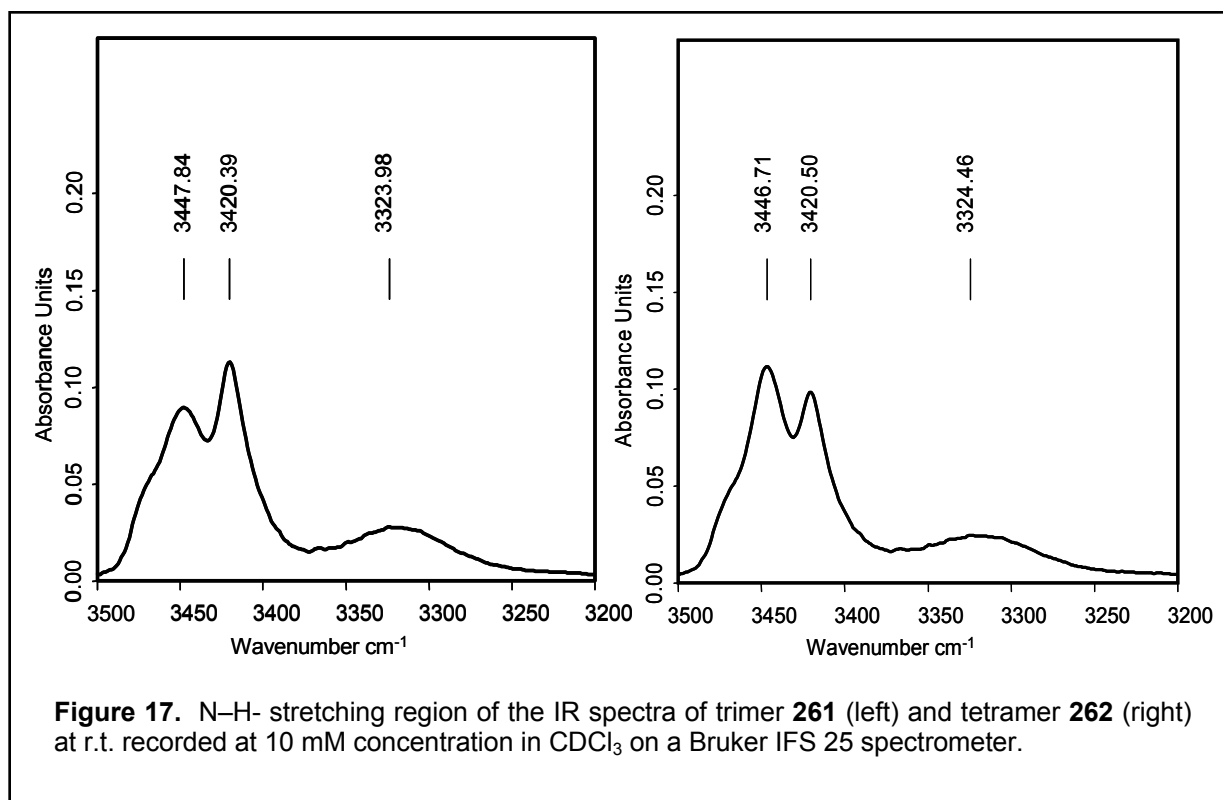
no.	Gly ¹			Gly ²			Gly ³	
	Φ	Ψ	ω	Φ	Ψ	ω	Φ	Ψ
1	-83.5	68.3	-179.0	59.5	-54.3	-178.1	176.4	-0.4
2	-83.6	68.4	-179.0	59.5	-54.1	-178.1	176.1	-0.4
3	83.6	-68.4	179.0	-59.5	54.3	178.1	-176.4	0.5
4	83.5	-68.3	179.0	-59.5	54.3	178.1	-176.4	0.4
5	83.5	-68.4	179.0	-59.5	54.3	178.1	-176.4	0.4
6	-83.7	69.9	-175.4	-59.9	8.5	177.6	-174.7	0.7
7	83.7	-69.9	175.4	59.9	-8.4	-177.7	174.8	-0.8
8	-83.7	69.8	-175.4	-59.9	8.5	177.6	-174.2	0.4
9	-83.7	69.9	-175.4	-59.9	8.4	177.6	-174.3	0.5
10	83.7	-67.6	-179.7	-58.2	30.6	172.6	-92.5	4.2
11	-83.6	67.3	178.9	58.3	-8.8	-174.5	88.9	1.0
12	83.6	-68.8	176.7	60.3	-6.2	-173.5	98.3	-3.0
13	-83.6	68.8	-176.8	-60.3	6.2	173.5	-98.3	2.9
14	-83.6	68.8	-176.8	-59.9	10.6	-178.2	96.4	-2.3
15	-83.6	68.9	-176.8	-59.9	10.5	-178.2	96.3	-3.4

^[a] Computed at the B3LYP/6-31+G(d,p) level of theory



Intramolecular hydrogen bonding is not possible in **261** due to the rigid γ amino acid A Gly that renders Gly¹ and Gly³ too distant from one another – the peptidic “arms” attached to the A Xaa being too short to reach one another. This also reflects in the IR spectrum of a 10 mM solution of **261** in CDCl₃ (Figure 17) that does not show an intense band indicative of hydrogen bonding. The weak band at $\sim 3320\text{ cm}^{-1}$ can be attributed to intermolecular hydrogen bonding present to some extent at this comparably high concentration of 10 mM.

Analysis of the NMR spectra confirms the findings above: No nOe crosspeaks indicating interresidual hydrogen bonding could be observed. Therefore, it seems reasonable to conclude that there *can not be* backbone hydrogen bonding in a tripeptide of α -Xaa- A Gly- α -Xaa sequence. To design a turn motif that is stabilized through intramolecular backbone hydrogen bonding, at least a tetramer is required.



9.4.2. Structural analysis of tetrapeptide **262**

Introduction of a second ^AGly residue gives such a tetramer, Ac-Gly-^AGly-^AGly-Gly-OMe (**262**). Performing the MMFF conformational analysis as described above yields the conformers whose relative energies are compiled in Table 11; structural parameters are summarized in Table 12. Out of the ten lowest conformers that were computed with MMF-94, none displayed a hydrogen-bond stabilized turn structure. There were, however, hydrogen-bonding minima present on this PES, albeit at significantly higher relative energy. Two of those minima were selected and, along with the ten minima lowest in energy, optimized with the B3LYP/6-31+G(d,p) model chemistry. The relative energies of these local minima (11, 12) were 2.4 kcal/mol above the local minimum when computed with DFT, while they were significantly higher at the MM method. Two explanations are possible: One could be that either the force field does not adequately account for elongated hydrogen bonds (as present in 11 and 12, see also Figure 18) or, in turn, the DFT method overestimates the stabilizing effect of such a hydrogen bond. The other, more probable explanation is an inadequate parametrization of the force field for the ^AGly-^AGly motif, resulting in an

overestimation of its rigidity. This latter inconvenience of the theoretical method chosen is also supported by the fact that even the popular DFT methods used in the computations presented herein generally underestimate hydrogen bonding due to the missing van der Waals term.^[308, 309]

Table 11. Energetics of the conformers of **262**

no.	E_{rel} [kcal/mol] DFT ^[a]	R_{rel} [kcal/mol] MMFF-94 ^[b]	Comment
1	0.54	0.00	very similar conformer
2	0.55	0.00	
3	0.36	0.15	
4	0.00	0.15	global minimum (DFT)
5	0.88	0.52	enantiomeric conformers
6	0.88	0.52	
7	0.63	0.54	enantiomer of 9
8 ^[c]	-	0.68	
9	0.63	0.70	enantiomer of 7
10 ^[c]	-	0.70	
11	2.40	6.90	hydrogen bonded conformer
12	2.40	8.17	hydrogen bonded conformer

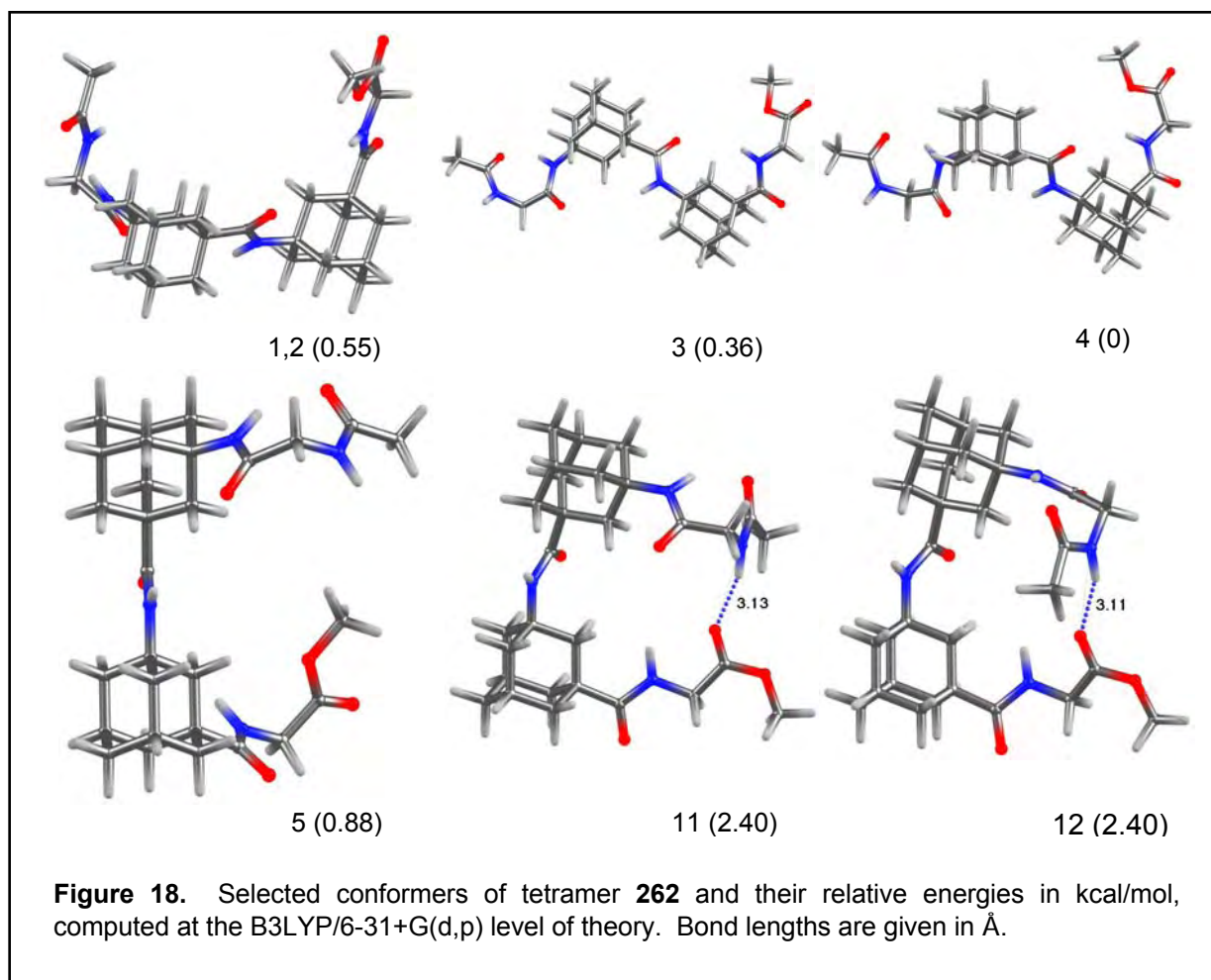
^[a] Computed using B3LYP/6-31+G(d,p) level of theory; ^[b] computed using MMFF-94 as implemented in Spartan '02. ^[c] No minimum could be found within the accessible computing time.

Table 12 Torsional angles [°] from minimum conformers of tetramer **262**^[a]

no.	Gly ¹			Gly ²			Gly ³			Gly ⁴	
	Φ	Ψ	ω	Φ	Ψ	ω	Φ	Ψ	ω	Φ	Ψ
1	-83.3	68.5	-178.5	59.0	-58.4	-179.0	-60.8	48.2	177.5	179.0	2.8
2	-83.2	68.8	-178.4	58.9	-58.4	-178.9	-60.8	47.2	177.3	178.8	2.7
3	83.5	-69.0	177.4	60.5	-49.3	-179.5	58.9	-14.0	-173.2	137.7	5.7
4	83.3	-68.0	177.4	59.6	-17.4	-175.9	-61.5	3.6	178.6	-175.8	1.9
5	83.4	-68.1	179.8	-59.4	57.2	179.5	61.2	-58.8	176.8	-102.8	1.9
6	-83.5	68.1	-179.8	59.4	-57.2	-179.5	-61.2	58.5	-176.9	103.0	-2.0
7	83.3	-69.2	178.3	-59.2	59.7	-178.8	59.8	-44.4	-173.5	96.2	-2.4
8 ^[b]											
9	-83.3	69.4	-178.2	59.3	-59.9	178.8	-59.9	44.7	173.5	-95.6	1.3
10 ^[c]	82.0	-68.9	176.9	61.1	-50.9	-174.5	-61.6	43.0	164.9	-95.9	177.9
11	85.3	-68.6	163.8	-54.8	92.6	-157.1	57.0	4.2	177.5	-174.3	178.6
12	-85.1	69.8	-165.0	-30.3	93.6	-156.5	56.9	0.8	177.9	-152.7	-179.9

^[a] Computed using B3LYP/6-31+G(d,p) level of theory; ^[b] No minimum could be found within the accessible computing time; ^[c] Computed at the B3LYP/6-31G(d) level of theory.

The IR spectrum (Figure 17, right) also confirms that there is no hydrogen bonding in CDCl₃ solution. As with the trimer **261**, analysis of the NMR spectra did not indicate any turn motif, so that, in compliance of computational conformer analysis, IR measurements and NMR spectroscopy, an intramolecularly hydrogen bonded structure can be ruled out for tetramer **262**.



9.4.3. Structural analysis of tetrapeptide **263**

The conformational analysis for the tetramer Ac-Gly-^AGly-Gly-Gly-OMe and its isomer sequence **264** were chosen to analyze which “peptidic arm” of an ^AXaa has to be elongated to enable intramolecular, interresidual hydrogen bonding that could be utilized in the design of stable turns useful in, e. g., organocatalysis. Following the same strategy as for **251** and **262**, MMFF-94 and DFT computations gave the conformers that are described in Tables 13 and 14. MMFF-94 conformational search gave non-hydrogen bonded structures for the 9 conformers that are minimal in energy. Conformer no. 10 however shows a N–H (Gly¹) – C=O (Gly⁴) interresidual hydrogen bond. This conformer is, however, not the global minimum (neither from the MMFF-94 conformational search nor from the DFT computations). Conformers no. 11 – 15 were selected for DFT geometry optimization after visual inspection of the 100 lowest energy MMFF-94 conformers because they appeared to display a turn-like structure

that could enable them to form such a hydrogen bond as well. Indeed, DFT optimized conformers 11 and 12/13 (a pair of enantiomers) were computed as hydrogen bonded as well, albeit with a relatively weak (bond length $\text{NH}\cdots\text{O}=\text{C} = 3.24 \text{ \AA}$) H-bond in conformer 11, while conformers 12 – 15 were computed $> 7 \text{ kcal/mol}$ above the global minimum and, therefore, can not be regarded as reasonably populated conformers. The MMFF/DFT conformational analysis for tetramer **263** gives a global minimum that does not show internal hydrogen bonding. Such turn-like structures are computed, but they are energetically not favorable, so that from the results of the conformational analyses no turn structure with an intramolecular hydrogen bond is expected.

Table 13 Energetics of the conformers of tetramer **263**

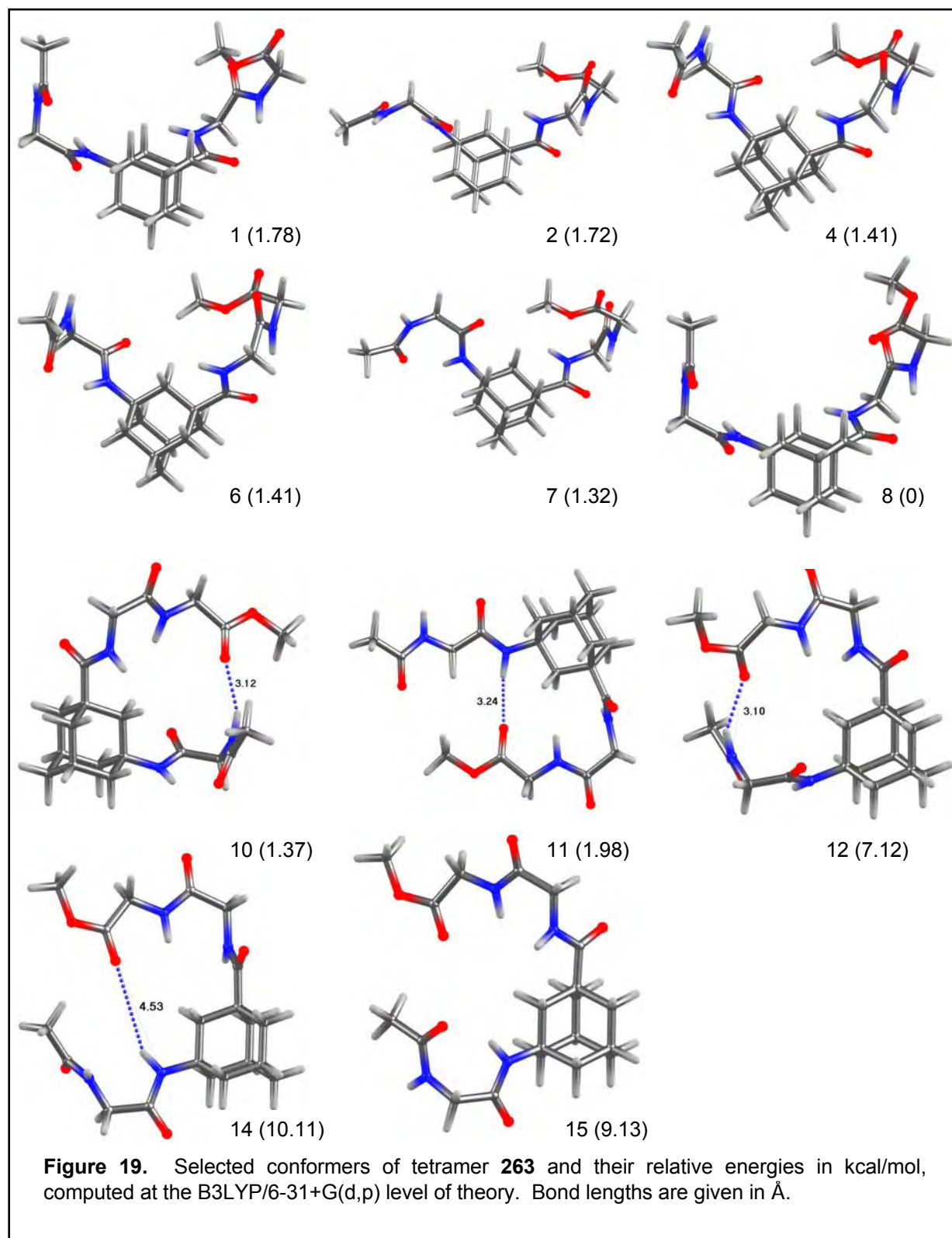
no.	E_{rel} [kcal/mol] DFT. ^[a]	E_{rel} [kcal/mol] MMFF-94 ^[b]	Comment
1	1.78	0.00	
2	1.72	0.43	
3	1.72	0.43	same conformer
4	1.41	0.52	very similar to conformer 6
5	_[c]	0.65	
6	1.41	0.71	very similar to conformer 4
7	1.32	0.79	enantiomer of 9
8	0.00	0.91	global minimum (DFT)
9	1.32	0.96	enantiomer of 7
10	1.37	0.98	hydrogen bonded conformer
11	1.98	3.33	hydrogen bonded conformers
12	7.12	7.65	hydrogen-bonded
13	7.12	7.65	conformers, enantiomers
14	10.11	9.89	
15	9.13	10.04	

^[a] Computed using B3LYP/6-31+G(d,p) level of theory; ^[b] computed using MMFF-94 as implemented in Spartan '02. ^[c] No minimum could be found within the accessible computing time.

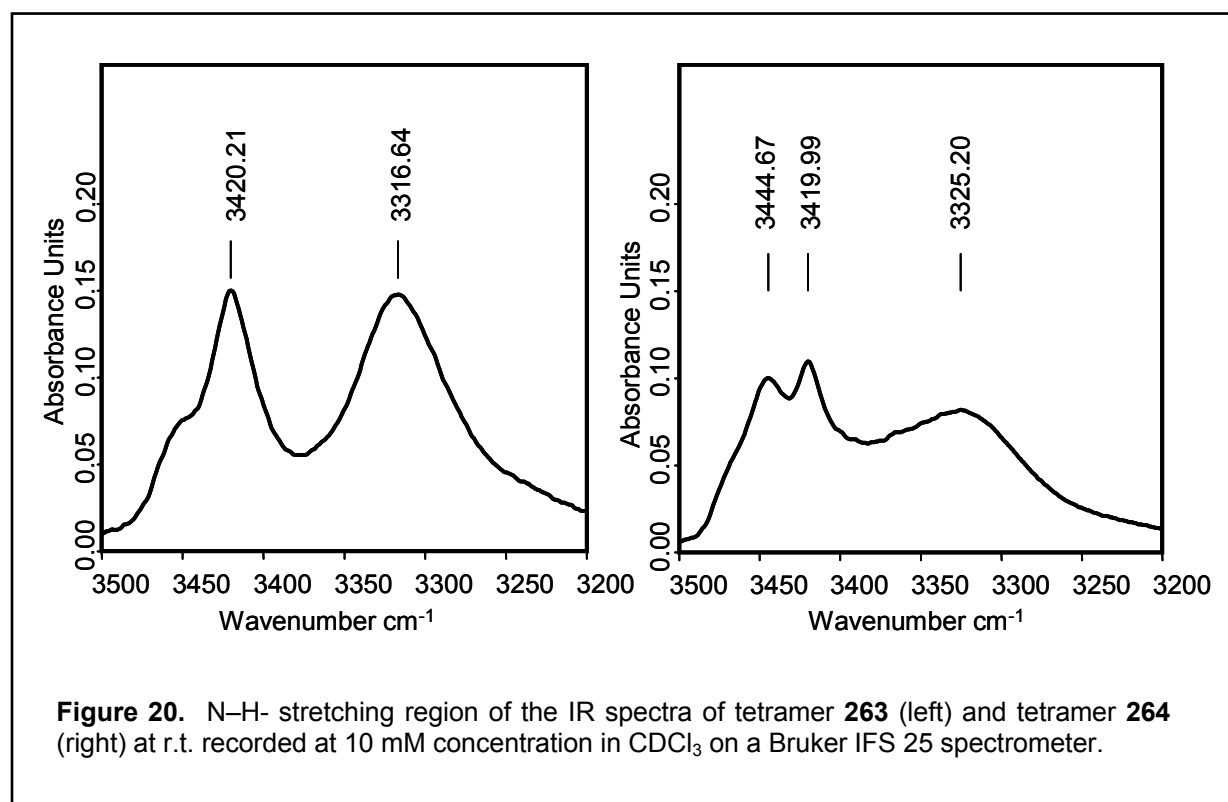
Table 14 Torsional angles [$^{\circ}$] from minimum conformers of tetramer **263**.^[a]

no.	Gly ¹			Gly ²			Gly ³			Gly ⁴	
	Φ	Ψ	ω	Φ	Ψ	ω	Φ	Ψ	ω	Φ	Ψ
1	-83.3	69.0	-179.2	58.3	-7.7	-176.1	-82.6	68.5	-177.7	93.3	-2.7
2	-83.1	67.8	-177.3	-60.1	8.1	174.5	82.6	-66.1	177.9	-96.2	9.2
3	-83.0	67.9	-177.3	-60.1	8.2	174.5	82.7	-66.0	177.9	-97.0	10.2
4	-83.2	67.2	179.2	59.3	43.9	178.5	82.9	-68.6	175.3	-95.5	5.9
5 ^[b]											
6	-83.2	67.7	179.6	59.3	45.5	178.5	82.9	-68.8	175.7	-98.1	8.1
7	-82.9	69.0	-176.8	-61.0	-23.3	178.7	-83.8	65.6	-171.4	87.2	-4.3
8	-83.2	67.7	-178.7	58.1	-13.4	-178.5	-81.8	68.9	-170.9	88.6	-179.6
9	82.9	-69.1	176.8	61.0	23.3	-178.7	83.8	-65.5	171.4	-87.3	4.5
10	86.4	-71.5	160.3	-53.1	-50.8	178.0	-109.7	14.4	176.1	134.1	178.7
11	-134.4	139.8	175.0	175.3	64.5	-166.2	102.9	-11.4	-178.5	-170.1	-177.9
12	86.0	-68.2	163.1	-53.5	-57.4	177.7	-107.4	10.9	179.3	140.9	-177.7
13	-86.0	68.2	-163.1	53.5	57.4	-177.7	107.3	-11.0	-179.3	-140.8	177.7
14	108.0	-11.6	-174.2	178.2	-85.5	-179.2	-97.8	8.2	175.5	-175.8	-179.9
15	-82.4	60.8	-173.0	171.8	7.8	178.4	120.1	-14.5	176.5	-156.6	176.9

^[a] Computed using B3LYP/6-31+G(d,p) level of theory; ^[b] No minimum could be found within the accessible computing time.



The N–H stretching region of the IR spectrum of tetramer **263** shows an intense, but sharp band at 3317 cm^{-1} that does question the results from the computational conformational analysis (Figure 20).



The nOe NMR spectrum of **263** shows two cross peaks of intermediate intensity between NH(^AGly²) and O-CH₃ and between H_α(Gly¹) and O-CH₃, as well as several weak cross peaks [NH(^AGly²) - H_α(Gly³), NH(Gly¹) - H_α(Gly³), NH(Gly³) - H_α(Gly¹)] that, taken together, hint towards a conformation that is best represented by conformer 11. Based upon the data from the computational analysis as well as from IR- and NMR results, respectively, a consistent assignment of the preferred conformation of tetramer **263** can not be done at this point.

9.4.4. Structural analysis of tetrapeptide **264**

The results of the conformational analysis for this sequence (Ac-Gly-Gly-^AGly-Gly-OMe) are collected in Tables 15 and 16; a selection of conformers is presented in Figure 21. Strikingly, the minimum conformer from DFT computations is hydrogen bonded in this tetramer. Furthermore, several other low-lying conformers also show interresidual hydrogen bonding (e.g., conformers no. 1, 4, 6, 8). The IR spectrum also shows a strong and broad band at 3325 cm⁻¹ indicative for intramolecular hydrogen bonds (Figure 20, right panel) that supports the computed findings.

Table 15 Energetics of the conformers of tetramer **264**

no.	E_{rel} [kcal/mol] DFT ^[a]	E_{rel} [kcal/mol] MMFF-94 ^[b]	Comment
1	1.25	0.00	
2	0.00	0.81	
3	0.00	1.23	same conformer
4	2.60	1.86	
5	3.68	1.95	no hydrogen bond
6	2.49	2.06	
7	5.44	2.57	
8	0.14	2.85	
9	3.82	3.55	no hydrogen bond
10	3.96	3.64	no hydrogen bond
11	2.53	4.72	
12	5.86	7.18	
13	5.79	7.41	
14	5.83	7.49	
15	3.88	8.40	

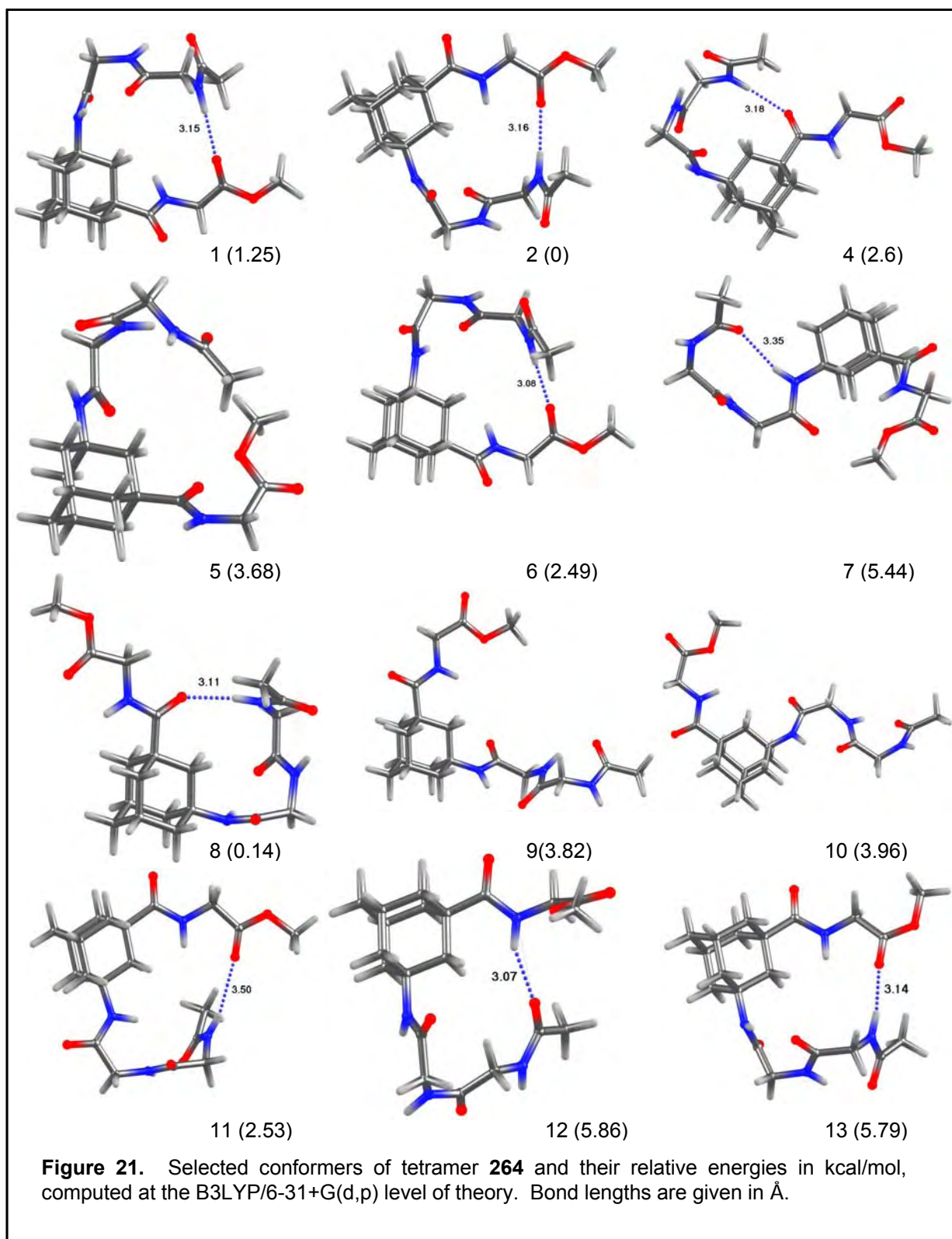
^[a] Computed using B3LYP/6-31+G(d,p) level of theory; ^[b] computed using MMFF-94 as implemented in Spartan '02.

Table 16 Torsional angles [°] from minimum conformers of tetramer **264**.^[a]

no.	Gly ¹			Gly ²			Gly ³			Gly ⁴	
	Φ	Ψ	ω	Φ	Ψ	ω	Φ	Ψ	Ψ	ω	Φ
1	82.4	-56.8	172.1	-73.5	92.3	-161.4	63.3	-53.6	174.2	-85.9	164.6
2	82.2	-58.4	174.8	-75.1	90.7	-164.7	64.6	6.2	174.8	-166.0	174.9
3	82.2	-58.0	175.0	-75.3	90.1	-164.7	64.4	7.0	174.5	-165.9	174.9
4	-84.1	61.0	-167.7	76.5	-82.9	149.5	-59.9	153.1	177.3	-176.4	-1.9
5	80.5	-83.0	176.6	-84.2	71.0	-164.1	57.4	-94.4	170.3	-94.6	19.5
6	-82.5	68.6	-177.1	81.1	-68.2	162.6	-111.1	-45.4	176.8	-102.7	174.9
7	62.1	-131.7	177.6	-103.7	14.5	-180.0	-60.0	6.0	178.7	179.8	1.8
8	84.1	-61.6	166.4	-76.0	84.8	-149.6	62.9	-165.1	-177.5	178.5	179.9
9	81.7	-62.5	174.9	84.0	-61.8	-178.3	-58.3	6.2	178.5	179.9	1.1
10	-81.7	63.8	-175.3	-83.8	66.2	-176.9	-59.4	8.7	177.7	-175.3	0.7
11	-84.6	60.0	-178.8	91.6	-6.9	-172.7	170.6	-1.4	-178.6	-179.6	-177.3
12	134.2	-167.4	-5.1	76.0	24.0	-171.4	63.8	14.9	-178.9	95.4	-7.5
13	-82.0	56.5	-177.3	76.0	-88.4	163.9	-63.3	-5.9	-173.8	163.7	-177.3
14	138.6	-164.4	-2.0	74.9	24.0	-170.0	64.1	8.3	177.9	-75.8	-15.2
15	141.1	-161.6	0.0	74.0	21.3	-169.6	63.0	8.6	173.7	-87.0	169.8

^[a] Computed using B3LYP/6-31+G(d,p) level of theory.

Within the NOESY spectrum of tetramer **264**, however, no crosspeak indicating such a turn structure could be found. The conclusion from this data is that there probably is a propensity of a peptidic backbone α -Xaa- α -Xaa-^AXaa- α -Xaa to form a hydrogen bonded turn motif.



9.4.5. Structural analysis of pentapeptide 265

Like with the other oligomers of this series, conformational analysis was performed computationally, the results of which are summarized in Tables 17 and 18 and in Figure 22, respectively. For this peptide with dimeric peptide “arms” attached at the central ^AGly, MMFF-94 and DFT both give the same conformer as the global minimum of the PES. Furthermore, all the computed conformers display intramolecular, interresidual hydrogen bonding. The IR spectrum of a 10 mM solution of **265** in CDCl₃ is shown in Figure 23, the broad, intense peak at 3322 cm⁻¹ supports this finding. One must, however, not forget that a concentration of 10 mM of the test substances is rather high in comparison to literature studies.^[303, 304, 310] Therefore, IR spectra of the N–H stretching regions of tetramer **264** and pentamer **265** were also recorded in 1 mM

Table 17 Energetics and torsional angles [°] of the conformers of pentamer **265**

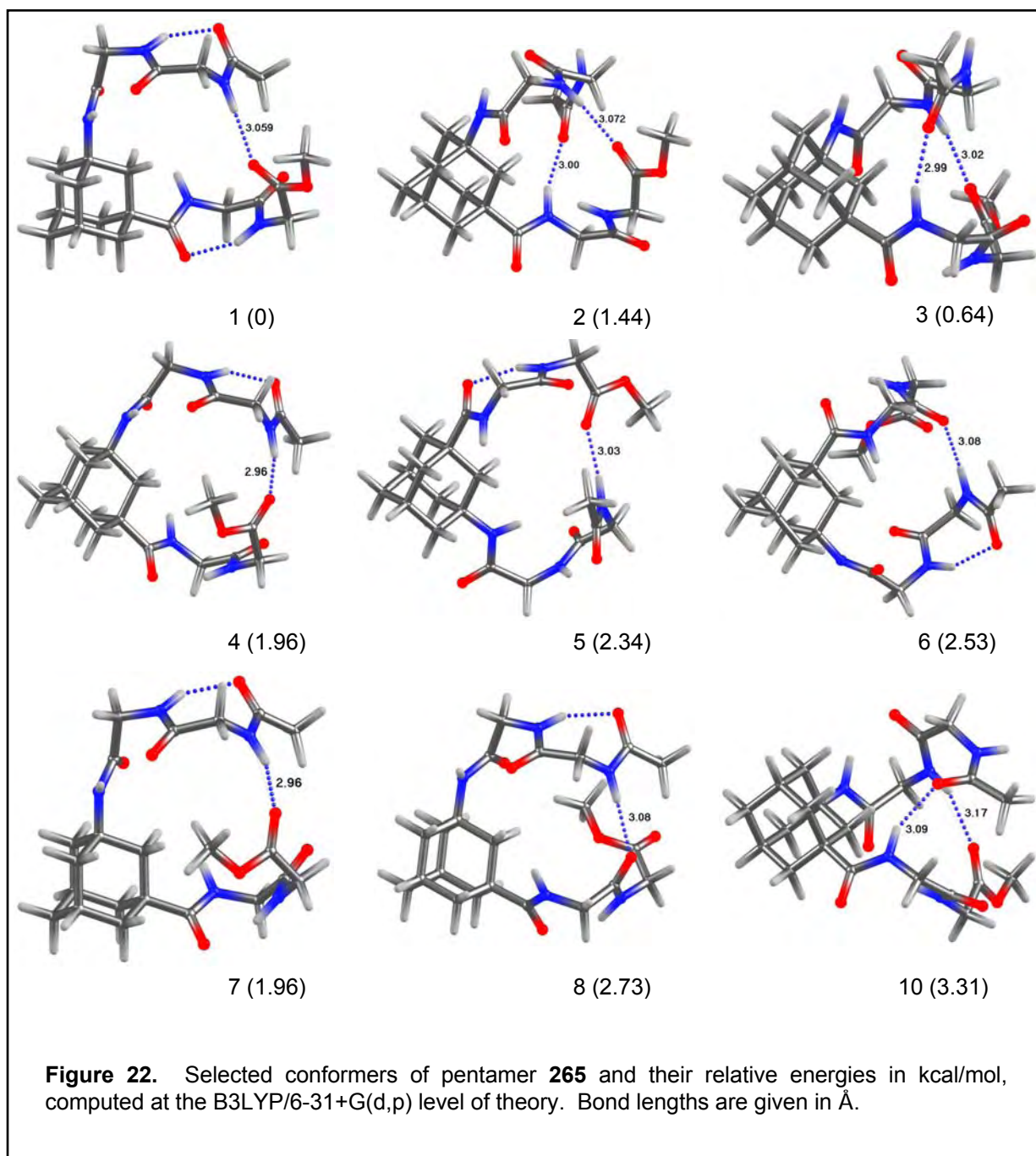
no.	E _{rel} [kcal/mol] DFT ^[a]	E _{rel} [kcal/mol] MMFF-94 ^[b]	comment	Φ	Gly ¹ ψ	ω
1	0.00	0.00	global minimum	82.2	-60.4	176.1
2	1.44	0.25	double hydrogen bonded	-82.2	161.5	-176.7
3	0.64	0.62	double hydrogen bonded	83.7	-171.8	173.1
4	1.96	0.64		81.4	-65.4	-179.7
5	2.34	0.76	enantiomer to 9	85.0	-60.2	178.7
6	2.53	0.83		81.7	-60.6	175.7
7	1.96	0.97		81.4	-65.8	-179.9
8	2.73	1.00		81.8	-57.0	179.4
9	2.34	1.51	enantiomer to 5	-85.1	60.2	-178.7
10	3.31	2.08	double hydrogen bonded	-93.6	-5.4	174.8

^[a] Computed using B3LYP/6-31+G(d,p) level of theory; ^[b] computed using MMFF-94 as implemented in Spartan '02. ^[b] Torsional angles in °. for further torsional angles, see Table 18.

Table 18 Torsional angles [°] from minimum conformers of pentamer **265** (continued)^[a]

no.	Gly ²			^A Gly ³			Gly ⁴			Gly ⁵	
	Φ	ψ	ω	Φ	ψ	ω	Φ	ψ	ψ	ω	Φ
1	-77.6	83.7	-164.1	60.0	-41.8	-178.1	-80.6	64.6	-178.2	81.3	176.0
2	86.5	-76.0	153.2	-54.5	-47.8	179.7	-104.6	9.6	175.9	135.4	177.7
3	-88.8	76.0	-148.2	55.8	69.4	-173.2	80.7	-59.2	177.2	-92.4	-157.7
4	-76.7	94.3	-168.8	62.9	-54.5	174.7	-80.4	68.5	-177.3	100.4	67.8
5	-97.4	10.4	176.2	-178.3	-72.4	179.3	-80.2	65.8	178.8	87.3	173.2
6	-73.1	101.3	-159.9	60.8	-50.6	168.9	-77.3	85.6	-178.9	86.5	40.6
7	-76.8	94.6	-168.2	62.7	-53.4	174.2	-80.2	69.4	-177.4	98.1	69.1
8	-72.2	98.6	-155.1	59.3	49.0	-172.3	77.3	-82.6	-179.8	-91.6	7.9
9	97.2	-10.2	-176.1	178.3	72.2	-179.3	80.2	-65.8	-178.8	-87.2	-173.4
10	-86.2	67.5	-152.8	47.7	41.8	-172.1	106.2	-19.1	-176.9	-116.8	-170.8
11	-77.6	83.7	-164.1	60.0	-41.8	-178.1	-80.6	64.6	-178.2	81.3	176.0
12	86.5	-76.0	153.2	-54.5	-47.8	179.7	-104.6	9.6	175.9	135.4	177.7
13	-88.8	76.0	-148.2	55.8	69.4	-173.2	80.7	-59.2	177.2	-92.4	-157.7
14	-76.7	94.3	-168.8	62.9	-54.5	174.7	-80.4	68.5	-177.3	100.4	67.8
15	-97.4	10.4	176.2	-178.3	-72.4	179.3	-80.2	65.8	178.8	87.3	173.2

^[a] Computed using B3LYP/6-31+G(d,p) level of theory.



concentration in dichloromethane, conditions routinely used in the literature (Figure 24). For the tetramer the band at ~ 3325 cm diminishes, whereas for the pentamer **265** still a significant absorbance is present at 1 mM concentration. In accordance with the computations, this supports that intramolecular hydrogen bonding should be present in **265**. Analysis of the NOESY NMR gives further support to this assumption: A cross peak indicating proximity between N-H(Gly³) (7.31 ppm) and one or both of the H $_{\alpha}$ of Gly¹ and / or Gly² (assignment not sure due to overlapping signals) is only possible in a turn where the peptidic “arms” attached to the ^AGly residue take part in a

hydrogen bond with one another. Such a scenario is best reproduced by conformers 2 or 3.

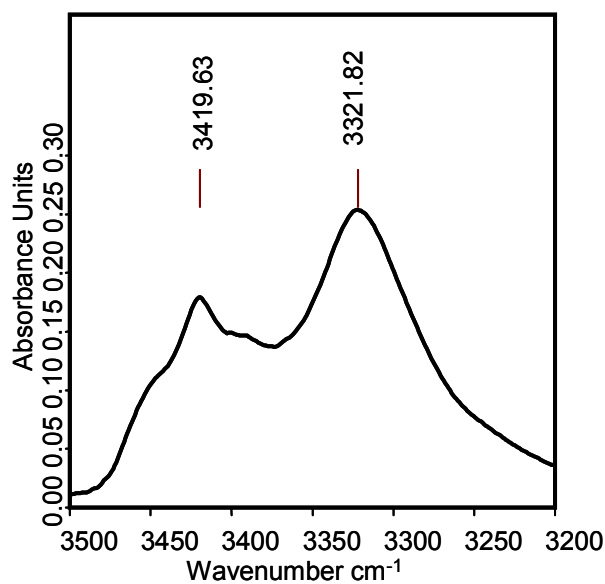


Figure 23. N–H- stretching region of the IR spectrum of pentamer **265** at r.t. recorded at 10 mM concentration in CDCl₃ on a Bruker IFS 25 spectrometer.

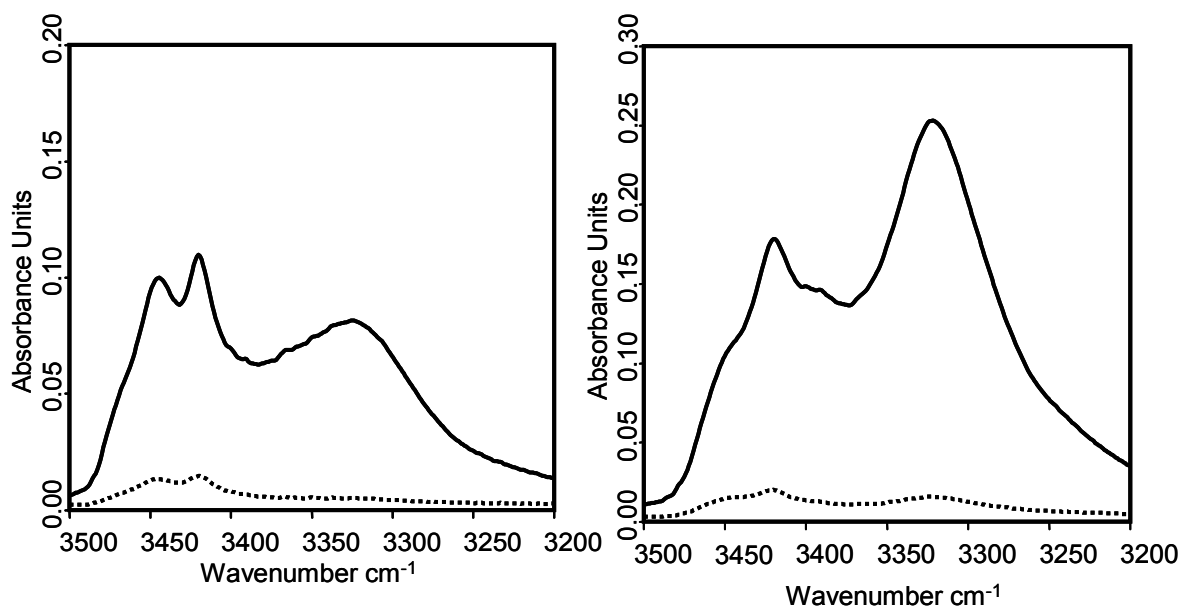


Figure 24. N–H- stretching region of the IR spectra of tetramer **264** (left) and pentamer **264** (right) at r.t. Solid line: 10 mM, dashed line: 1 mM in CDCl₃. Spectra were recorded at r.t. on a Bruker IFS 25 spectrometer.

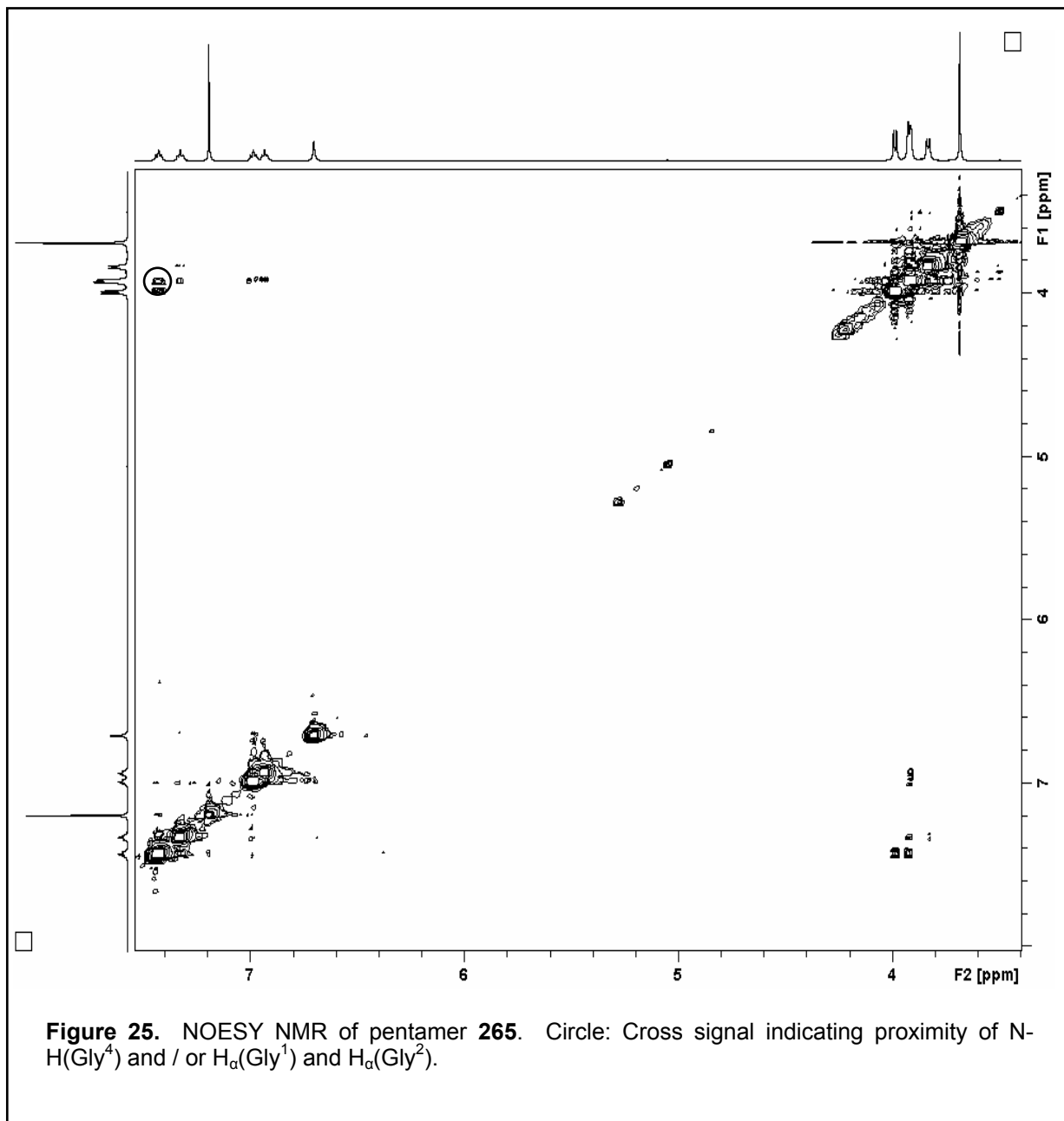


Figure 25. NOESY NMR of pentamer 265. Circle: Cross signal indicating proximity of N-H(Gly⁴) and / or H_α(Gly¹) and H_α(Gly²).

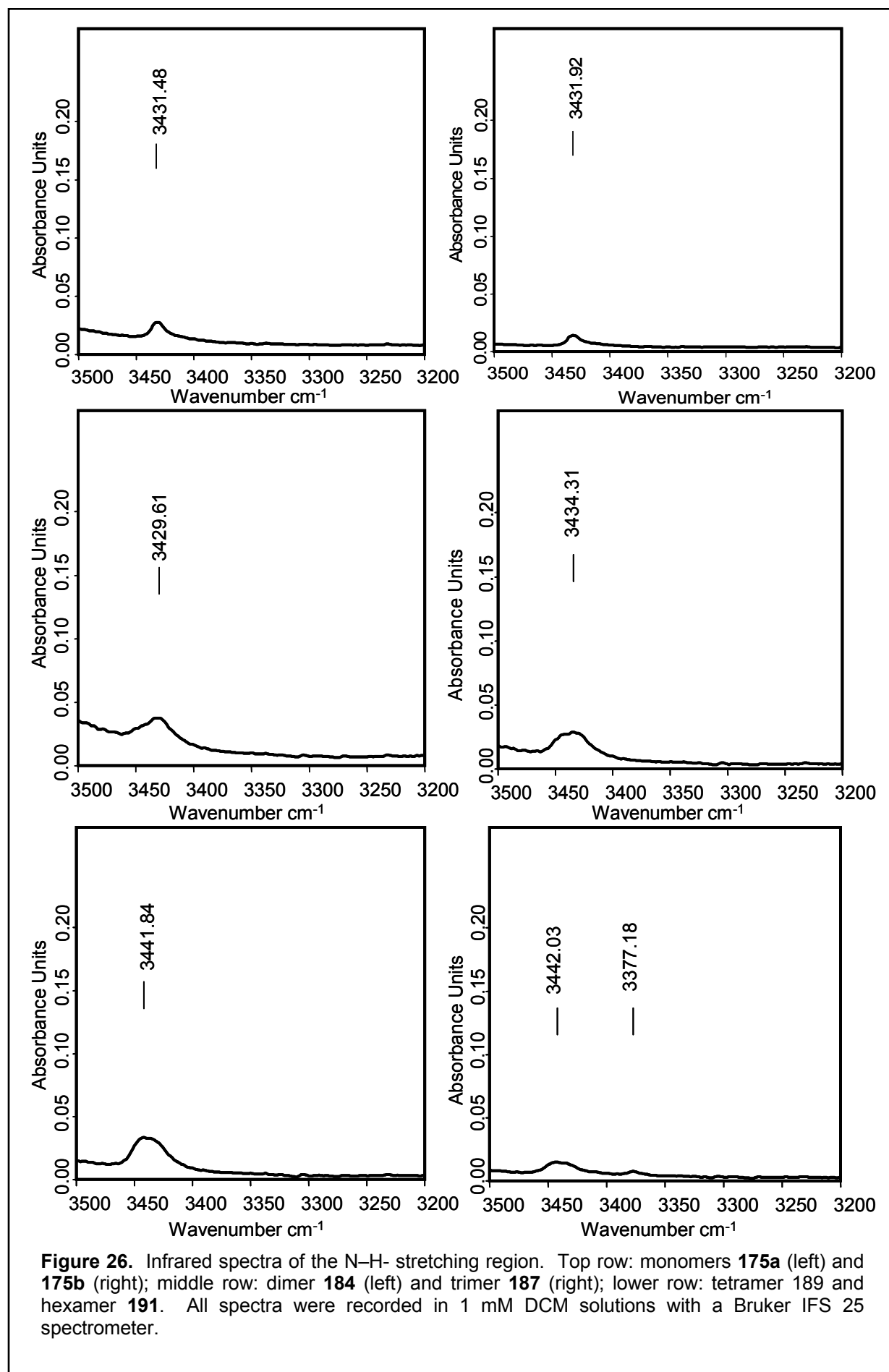
9.5. Homooligomeric A Gly

Next to the abovementioned considerations on the minimum length of a α -peptide chain (attached to one or two A Xaa residues) that is necessary to form turns that enable interresidual hydrogen bonding to stabilize the turn, the conformational propensities of homooligomers Fmoc- A Gly- A Gly-O t Bu **184**, Fmoc- A Gly- A Gly- A Gly-O t Bu **187**, and Fmoc- A Gly- A Gly- A Gly- A Gly-O t Bu **189** were also studied NMR-spectroscopically. Oligomers incorporating γ -aminobutyric acid (GABA) or analogues of GABA have been reported to fold to novel structures at relatively short sequences;^[311-313] therefore, we set out to analyze whether A Xaa oligomers also display characteristic folding propensities.

The N–H stretching regions of the IR spectra of **184**, **187**, **189** and **191** are shown in Figure 26. These spectra were recorded at 1 mM concentration in dichloromethane. None of the homooligomers displayed a broad band at $\sim 3320\text{ cm}^{-1}$ that usually is regarded indicative of intramolecular hydrogen bonds in this concentration range. As reference substrates, Ac- A Gly-O t Bu (**175a**) as well as Ac- A Gly-OMe (**175b**) were also examined under the same conditions.

175a and **175b** clearly showed no hydrogen bonding under these conditions, as no peak is present in the 3320 cm^{-1} region. Since these “mono-peptides” cannot form hydrogen bonds intramolecularly, by these findings also intermolecular hydrogen bonding can be ruled out for this class of compounds under the conditions of the IR experiment. Dimer **184**, Trimer **187**, and tetramer **189** display very similar IR spectra. Obviously, no hydrogen bonding is present also for these structures. Only the hexameric A Gly derivative **191** showed a clearly observable broad band at 3377 cm^{-1} , which is a remarkably high wavenumber for an N–H stretch involved in a hydrogen bond (the corresponding hydrogen bond, if present, could be described as “weak” from that wavenumber).

NMR structural analysis was massively hampered by the fact that with the 400 MHz NMR spectrometer the amide protons of the tetramer and hexamer could not be resolved. Therefore, unambiguous signal assignment is not possible, and as a result possible intramolecular hydrogen bonds via NOESY could not be analyzed with the available 400 MHz resolution.



Characteristic signal patterns in a TOCSY experiment are also not amenable due to the adamantane “blocks” between the individual amide motifs (in A Xaa homooligomers, there are no α -protons that could be utilized for the detection of a nOe between α -hydrogens of residue i and NH of residue $i + 1$ as in the TOCSY experiment).

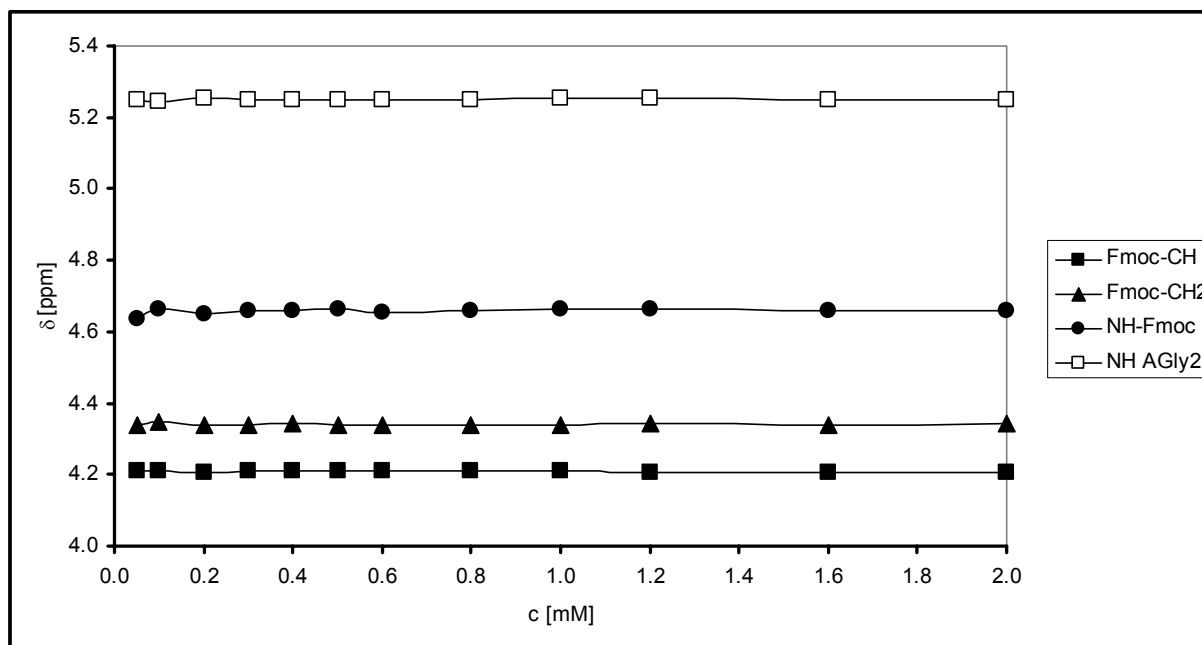
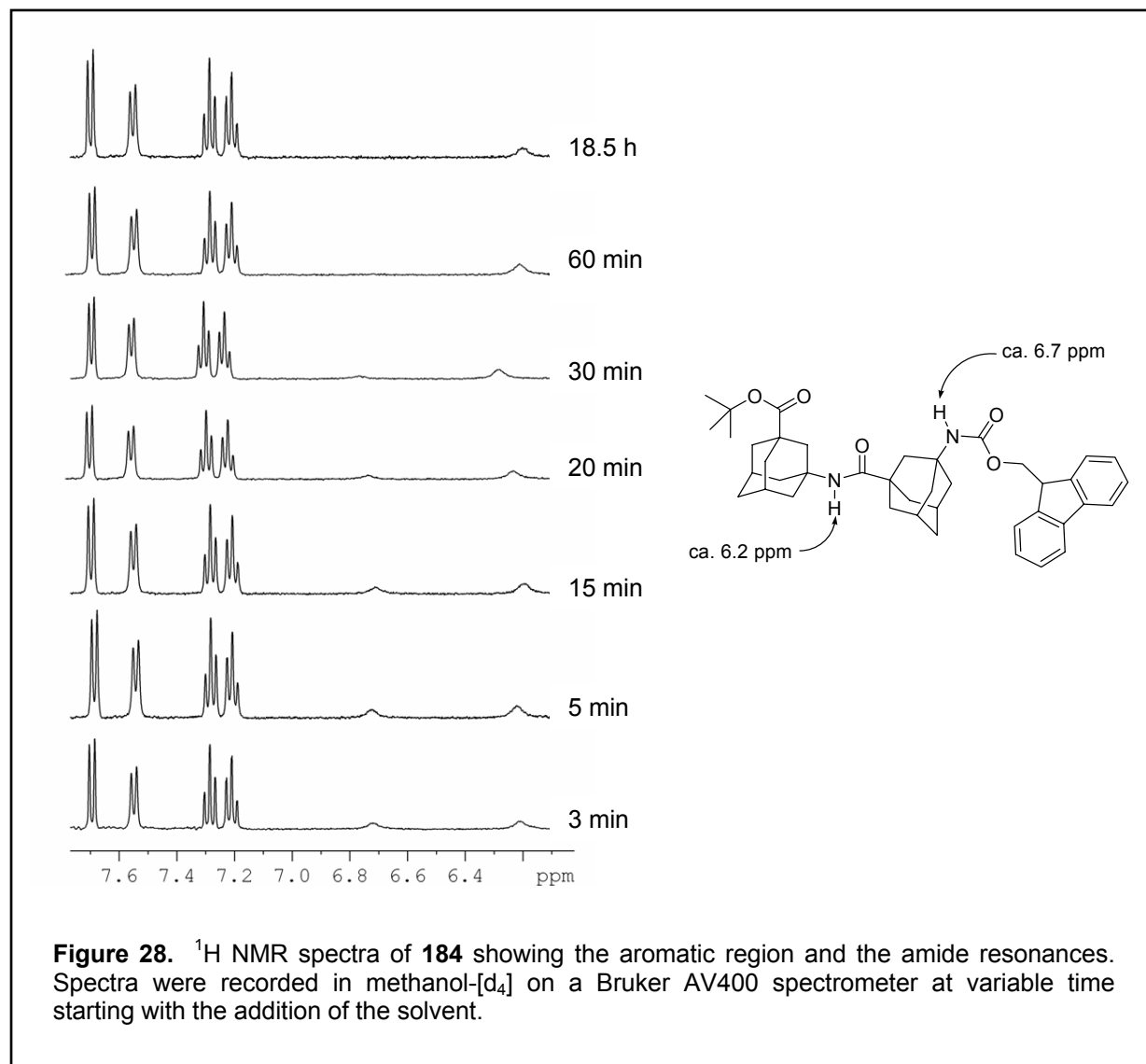


Figure 27. Dependence of selected ^1H chemical shifts in dimer **184** in CDCl_3 solution

Were intermolecular hydrogen bonds present, their chemical shift should be concentration dependent. However, for dimeric A Gly **184**, no such concentration dependence could be detected using CHCl_3 as the solvent (Figure 26). Two interpretations of these findings are possible: either no intermolecular hydrogen bonds or extremely strong hydrogen bonds. The latter case, however, would also yield in a downfield shift of the respective amide resonance that is not observed in the A Gly homooligomers.

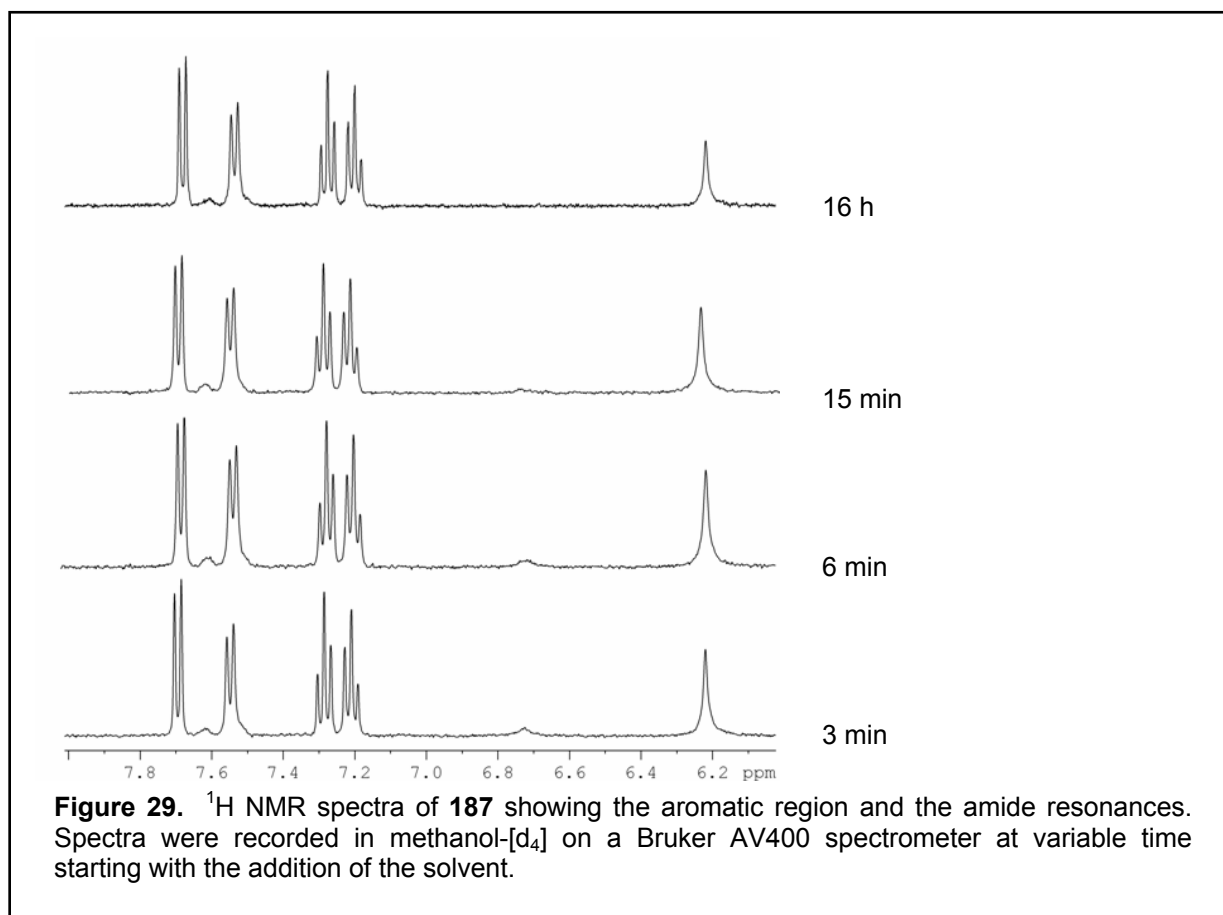
$^1\text{H} / ^2\text{D}$ exchange experiments would give further proof of the non-hydrogen bonded structure of the homooligomers studied. Free, solvent accessible amide protons should readily exchange with ^2D in, e. g., methanol- $[\text{d}_4]$ solution.^[314] Such exchange experiments were performed for dimer **184**, trimer **187**, and tetramer **189**, respectively, the results are outlined in Figures 28 – 30. It is important to note that in a hydrogen bond forming solvent like methanol- $[\text{d}_4]$, the amide signals of the Fmoc-NH groups are no more at $\delta \sim 4.7$ ppm as in non-hydrogen bonding solvents like CDCl_3 (*vide supra*) but at $\delta \sim 6.7$ ppm, thereby demonstrating the solvent accessibility^[315] of these N-

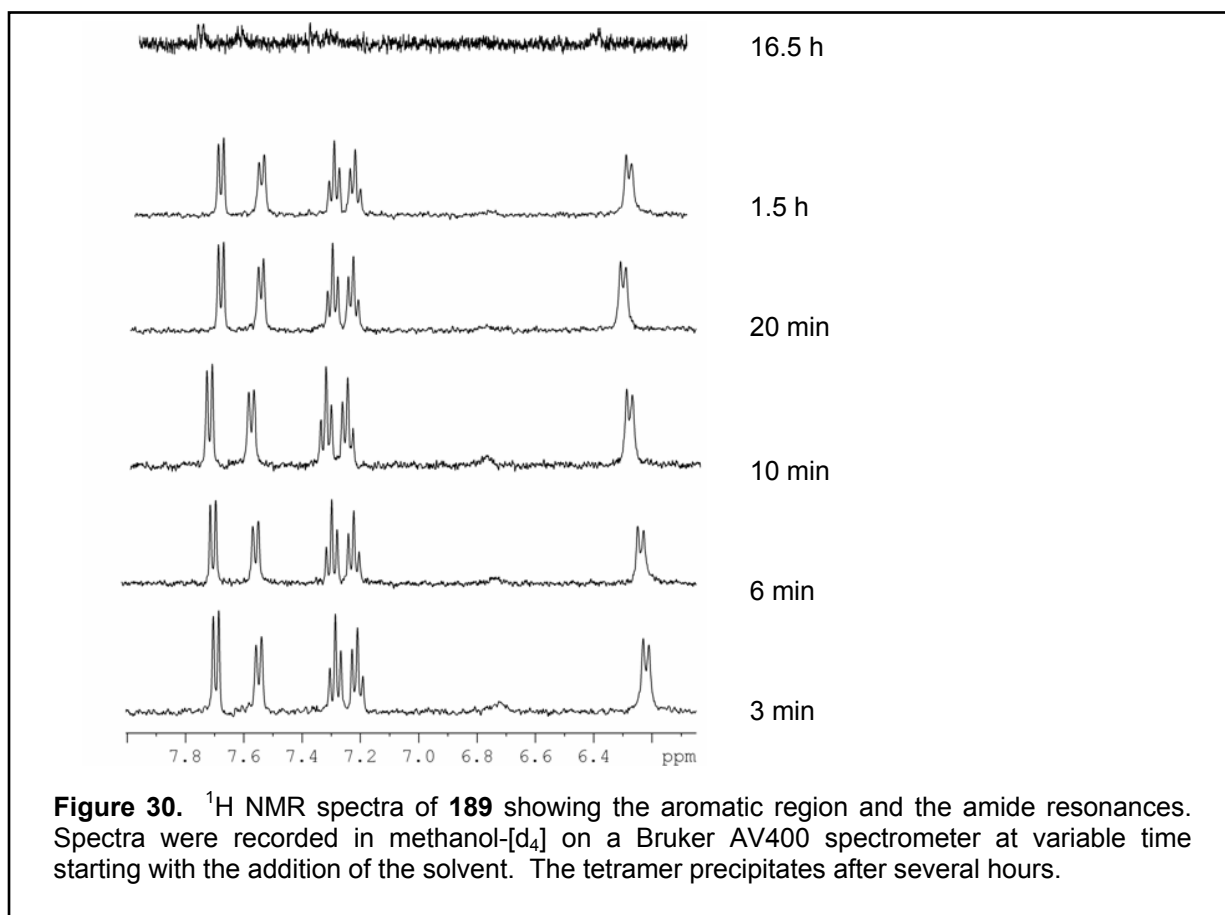
terminal amide protons. In contrast, the central amide protons corresponding to amide bonds “embedded” in adamantane moieties do not shift to a comparable extent in methanol- $[d_4]$ ($\delta \sim 6.3$ ppm) when compared with $CDCl_3$ ($\delta \sim 5.3$ ppm), reflecting a decrease in solvent accessibility.



The pH dependence of the H/D exchange rates were not considered here, but still a dramatic difference between the exchange kinetics of the two amide protons in **184** is present. While the Fmoc-amide proton completely exchanges with deuterium within one hour, the $^A\text{Gly}^2$ amide proton does not significantly exchange even after 18.5 h. Such a slow exchange rate can be attributed to an involvement of the respective amide proton in a hydrogen bond. While intramolecular hydrogen bonding can be ruled out for **184** due to steric considerations, stable intermolecular hydrogen bonding

appears improbable due to the invariability of the ^1H chemical shifts of the amide protons in **184** at variable concentrations. Therefore, structural effects^[316] modulating the acidity of the amide protons seem to account for their decelerated exchange kinetics, with the electron-rich adamantane nuclei on both sides of the central amide group in **184** additively reducing its acidity. This can best be exemplified by the ^1H chemical shifts of the respective amide protons in CDCl_3 , that is, in the absence of a hydrogen-bonding solvent. The ^1H chemical shift of the central amide proton of dimer **184** ($\delta_{\text{N-H}} = 5.24$ ppm) is almost identical to the amide resonance in the “mono-peptide” **175b** ($\delta_{\text{N-H}} = 5.23$ ppm) and compares well with the N–H signal of *N-tert*-Butyl-2,2-dimethylpropionamide ($\delta_{\text{N-H}} = 5.38$ ppm).^[317] Since the latter two monomers can by no means be regarded as prone to association to intermolecularly hydrogen bonded oligomers in solution (see also Figure 26), this can also be ruled out for homodimer **184**.





A very similar H / D exchange pattern is observed for the trimeric and tetrameric ^AGly with the amide protons embedded between the adamantane moieties exchanging only to a minor extent during the observation period, while the N-terminal Fmoc amine proton exchanges within one hour. Although the ^AGly - ^AGly amide signals cannot precisely be assigned at 400 MHz spectrometer resolution, two signals for the three central amide resonances are observed for the tetramer **189**. The exchange properties of the respective amide protons are obviously very similar, indicating no influence of hydrogen bonding on the exchange rate for any of the homooligomers studied. Due to the poor solubility of hexamer **191** in methanol at appreciable concentrations for NMR, this compound could not be studied here. As a result, no indication of secondary structure propensities of the homooligomeric ^AGly peptides could be found.

9.6. Alternating peptides: Fmoc-Gly-^AGly-Gly-^AGly-O^tBu

Structural information on a peptide of alternating ^AXaa / α -Xaa sequence would give an explanation for the failed cyclizations observed with peptides of that kind (Chapter 6.4.). As a model peptide, Fmoc-Gly-^AGly-Gly-^AGly-O^tBu **203** was synthesized in solution using HBTU mediated couplings and an Fmoc-/O^tBu protective group strategy as outlined in 6.2. Due to the incorporation of α -Xaas, this substance shows an improved differentiation of the amide resonances; in the 400 MHz ¹H NMR spectrum of **203**, four resolved amide resonances are observed that enable an assignment and, therefore, facilitate the extraction of structural information from NOESY experiments.

Table 19. NMR data of tetramer **203**.

Amino acid	NH <i>J</i> (NH,H _{α})	C=O	H _{α} C _{α}	5-H/7-H 5-C/7-C	2-H 2-C	9-H/10-H 9-C/10-C	4-H/8-H 4-C/8-C	6-H 6-C
Gly ¹	5.80 ~5 Hz	167.7	3.90 44.7	-	-	-	-	-
^A Gly ²	6.87 -	176.8	-	2.52 – 2.36 29.2	2.17 – 2.04 42.6	2.30 – 1.50 40.6	2.30 – 1.50 38.7	2.30 – 1.50 35.2
Gly ³	6.77 ~5 Hz	167.5	3.85 43.5	-	-	-	-	-
^A Gly ⁴	6.69 -	175.8	-	2.31 – 2.17 29.0	2.17 – 2.04 42.3	2.30 – 1.50 39.9	2.30 – 1.50 37.9	2.30 – 1.50 35.0
other: Fmoc: 7.75 (d), 7.57 (d), 7.38 (t), 7.28 (dt); O ^t Bu: 1.40								

Careful analysis of the NOESY cross peaks gave no indication of a head-to-tail proximity that could be beneficial in head-to-tail cyclizations. Alternating α -Xaa / ^AXaa peptides obviously do not significantly populate turn-like conformations.

9.7. Conformational analysis of ^AXaa based organocatalysts incorporating His residues

Miller and Formaggio attributed part of the stereoselectivity of their peptidic acylation catalysts to their propensity to form a stable turn.^[253, 263] From their studies, the sequence Pro-Aib has crystallized out as turn-inducing.^[318] We reasoned that an ^AXaa residue could fulfil a similar task – orientating the terminal amino acids in a rigid manner. Whether such types of peptidic catalysts incorporating both an ^AGly residue as the orientating tether and a nucleophilic His residue as the catalytically active entity

do prefer a turn motif will be discussed in this chapter. Boc-His(τ -Bn)-^AGly-Phe-OMe **218** and Boc-His(π -Me)-^AGly-Phe-OMe **220** were synthesized via the reliable HBTU activated coupling strategy (see Chapter 8.1.) in solution and analyzed NMR- and IR-spectral data along with a computational conformation analysis following the strategy outlined in Chapter 9.4.

The IR spectra of **218** and **220** were recorded at 1 mM concentration in dry dichloromethane (Figure 31). In the N–H stretching region of **218** three bands for the three different amides are visible, one of which (at 3337 cm⁻¹) indicating an intramolecular hydrogen bond. For **220**, no such broad band exists, hinting at a non-hydrogen bonded conformation. The results from the combined MMFF-94 / DFT conformational analysis of the benzylated organocatalyst **218** are summarized in Tables 20 and 21. MMFF-94 and DFT computations fail to give similar results with respect to the energetic sequence of the conformers; the DFT global minimum (conformer 5) is computed 4.58 kcal/mol higher in energy than the MMFF minimum. Important for efficacy in nucleophilic organocatalysis is the fact that the tertiary imidazol nitrogen is involved in a N(Imidazol¹)–HN(His) hydrogen bond in all of the computed conformers (Figure 32). This can, at least in part, explain the lower catalytic effect of organocatalysts incorporating the His(τ -Bn) residue when compared with the His (π -Me) residue (*vide infra*) in, e.g., transacylation reactions.^[265]

Table 20. Relative energies of the conformers of organocatalyst **218**. Values given in kcal/mole relative to the global minimum.

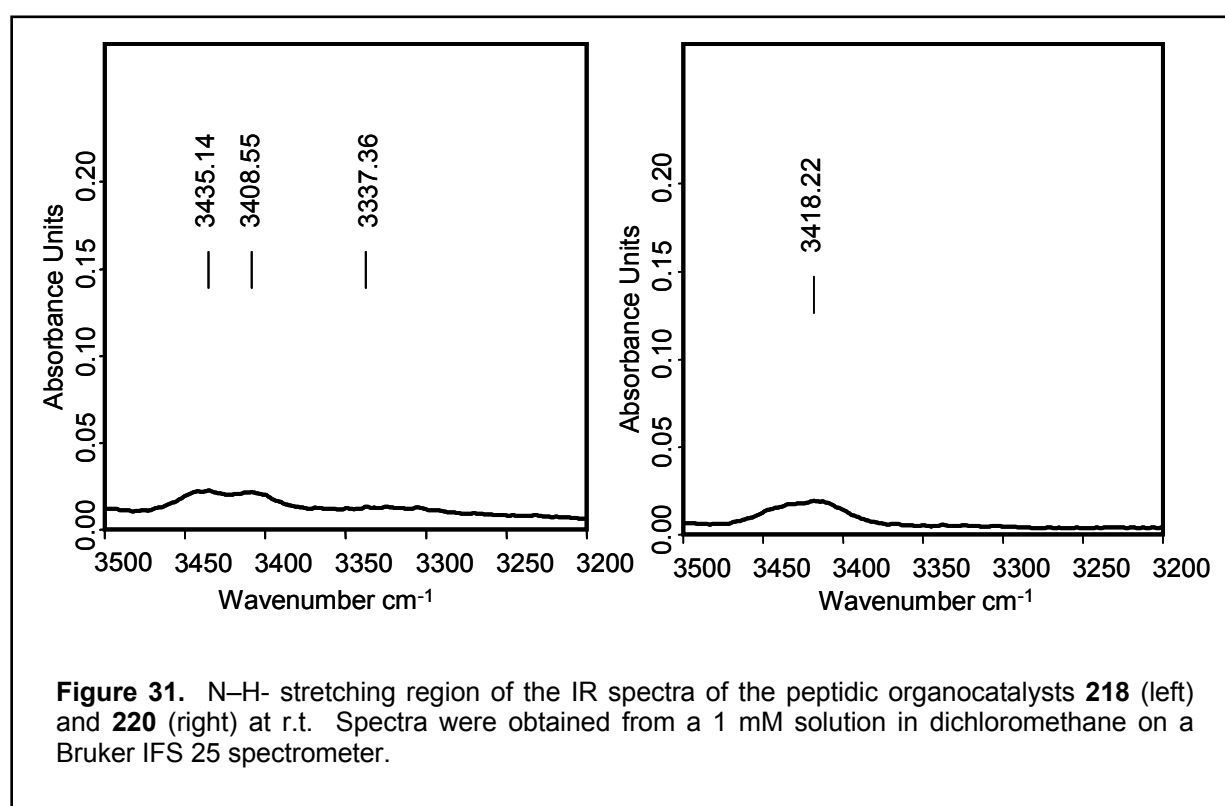
no.	E _{rel} [kcal/mol] DFT ^[a]	R _{rel} [kcal/mol] MMFF-94 ^[b]	Comment
1	1.71	0.00	
2	0.61	3.44	
3	_ ^[c]	4.11	
4	2.78	4.31	
5	0.00	4.58	
6	1.02	4.92	
7	2.13	5.10	
8	1.47	5.41	
9	0.81	5.57	
10	0.81	5.96	same conformer

^[a] Computed using B3LYP/6-31+G(d,p) level of theory; ^[b] computed using MMFF-94 as implemented in Spartan '02. ^[c] No minimum could be found at the B3LYP/6-31+G(d,p) level of theory within the available computing timeframe.

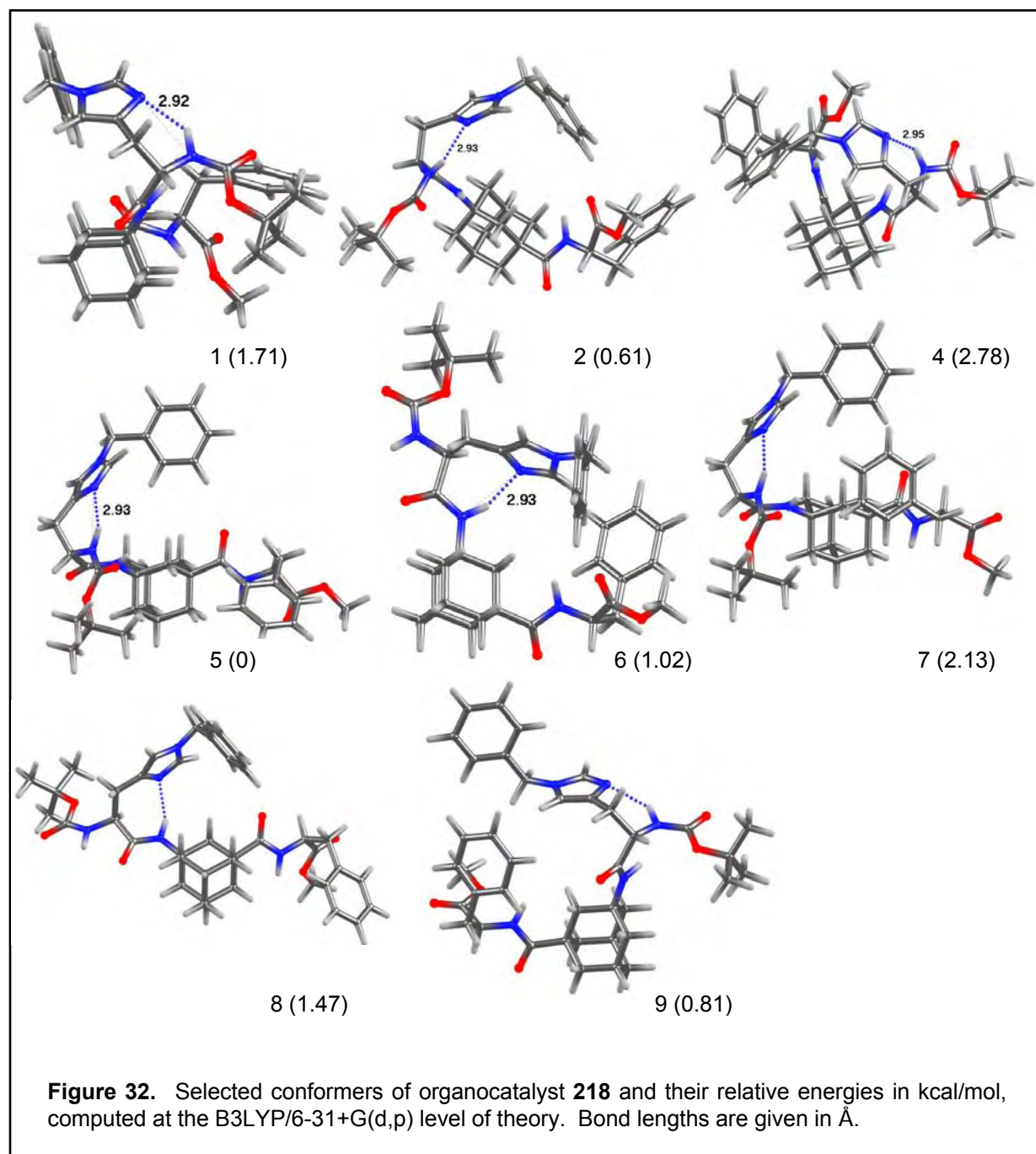
Table 21. Geometry parameters from minimum conformers of organocatalyst **218**.^[a]

no.	His(τ -Bn) ¹			^A Gly ²			Phe ³	
	Φ	Ψ	ω	Φ	Ψ	ω	Φ	Ψ
1	-84.71	-17.45	-179.97	172.39	91.01	-177.06	-153.14	-7.63
2	-92.07	-12.28	174.73	176.80	-65.62	172.35	-152.01	170.71
3 ^[b]	-87.99	-9.56	178.98	178.67	-2.63	177.26	-155.30	-2.79
4	-98.44	-3.20	174.91	178.75	-51.34	174.53	-136.12	-1.24
5	-88.93	-17.30	177.99	174.31	119.59	175.86	-155.18	172.65
6	-152.94	161.99	175.13	-175.80	36.57	171.77	-149.42	170.65
7	-86.01	-17.11	178.51	173.91	100.35	-172.64	-121.52	-25.42
8	-152.13	163.20	175.37	-172.97	-126.22	178.55	-145.97	-7.67
9	-99.39	-6.20	174.89	57.51	-8.45	-179.12	-98.94	6.73
10	-99.39	-6.20	174.89	57.51	-8.45	-179.12	-98.94	6.73

^[a] Computed at the B3LYP/6-31+G(d,p) level of theory; ^[b] computed using B3LYP/6-31G(d).

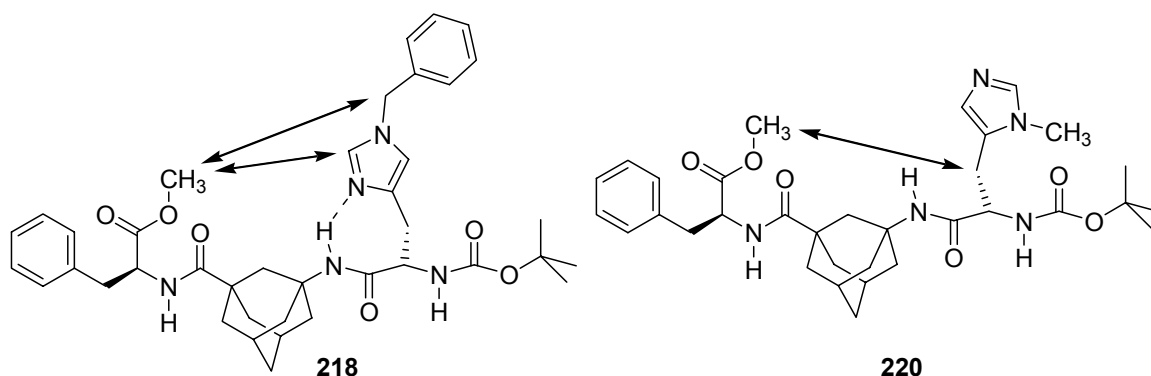


Analysis of the NOESY crosspeaks of **218** supports a conformational proposal where the terminal amino acids do not form a backbone-interresidual hydrogen bond motif as utilized to stabilize a turn in, e. g., Miller’s catalytic peptides. This is in line with the conformational propensities found for model peptide **261** (*vide supra*).



Weak crosspeaks between the His(τ -Bn) imidazole and the methyl ester show that, however, that the terminal amino acids are nevertheless orientated towards an “open-turn” through the nearly tetrahedral angle purported from the 1,3-disubstituted ^AGly tether (Scheme 48). The ¹³C NMR spectrum of **218** shows the adamantane methylene carbons (C⁴ / C⁸ and C⁹ / C¹⁰) having no longer the same chemical shift due to specific interactions with the (chiral) His residue. This can be attributed to the His imidazole being orientated towards the adamantane nucleus and, therefore,

towards the C-terminal Phe residue as best visualized in conformers 1 or 4 (Figure 32). Side-selective interactions between the N-benzyl imidazol sidechain and the adamantane leads to a decrease of its symmetry and, therefore, a split of its ^{13}C signals.



Scheme 48. Representation of interresidual nOe interactions observed in organocatalysts **218** and **220**.

Table 22. Relative energies of the conformers of organocatalyst **220**. Values given in kcal/mol relative to the global minimum.

no.	E_{rel} [kcal/mol] DFT ^[a]	R_{rel} [kcal/mol] MMFF-94 ^[b]
1	3.67	0.00
2	1.54	0.80
3	4.85	1.67
4	2.98	1.73
5	0.28	2.19
6	1.90	2.54
7	0.00	2.61
8	3.08	2.89
9	1.50	3.74
10	1.50	3.86
11	_[c]	3.90
12	3.07	4.14
13	4.50	4.16
14	1.20	4.20
15	1.26	4.32

^[a] Computed using B3LYP/6-31+G(d,p) level of theory; ^[b] computed using MMFF-94 as implemented in Spartan '02. ^[c] No minimum could be found at the B3LYP/6-31+G(d,p) level of theory within the available computing timeframe.

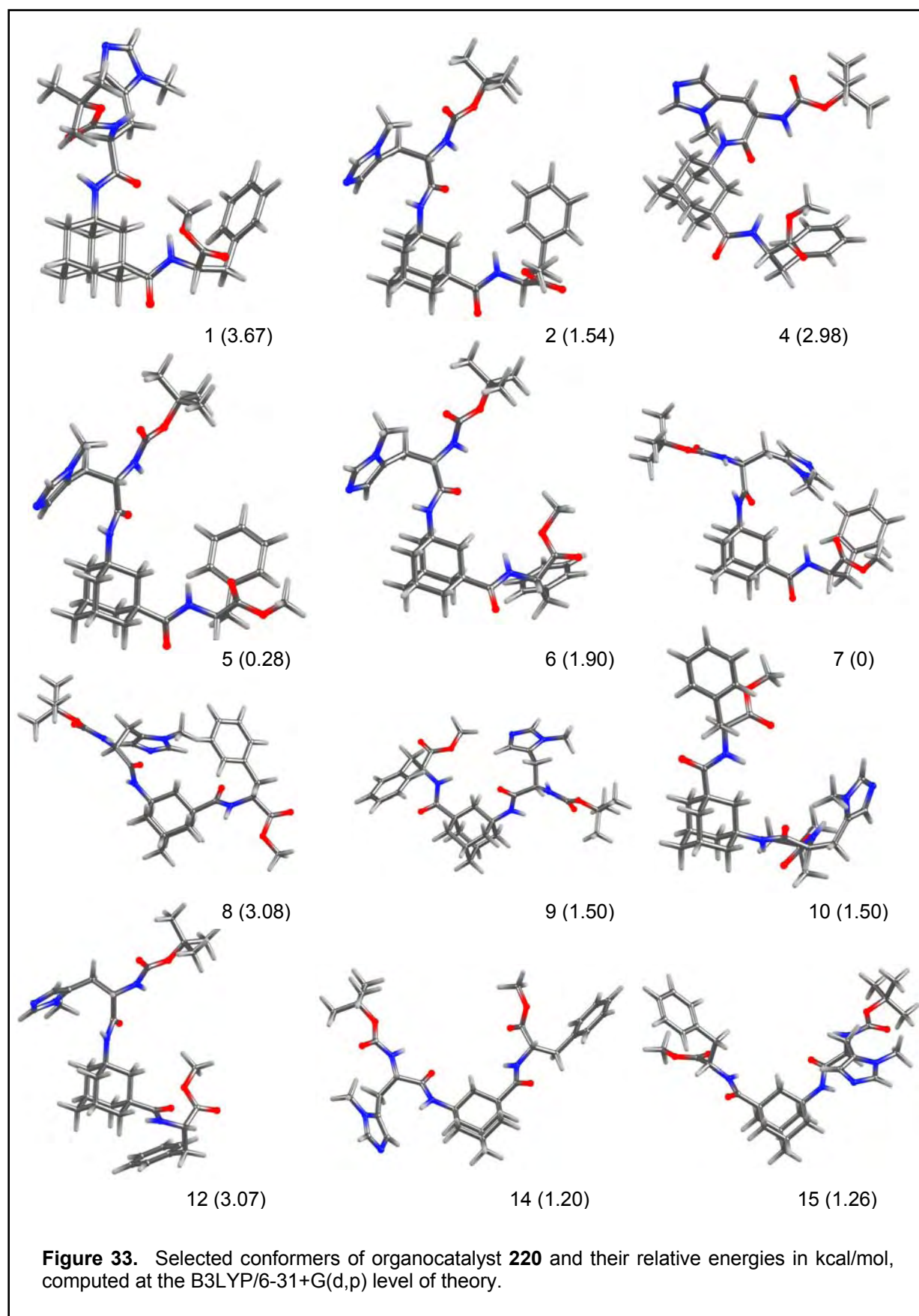
From the 1 mM IR spectrum in dichloromethane, we have deduced that His(π -Me) organocatalyst **220** does *not* display interresidual hydrogen bonding. The results from a computational conformational analysis confirm this finding as the minimum conformers computed with both MMFF-94 and DFT also do not possess such hydrogen bonds. The 12 conformers lowest in energy at the B3LYP/6-31+G(d,p) level of theory are compiled in Figure 33. From inspection of these it becomes clear that a

direct comparison of the ^AGly containing histidine catalysts presented herein and the ones utilized by Miller and Formaggio is not possible. While Miller's catalysts represent turns that are stabilized through intramolecular hydrogen bonding, the ^AGly residue in the central position acts as a template that orientates the terminal amino acids responsible for (a) catalytic activity and (b) generation of the chiral environment in catalytic stereoselective transformations by the fixed backbone scaffold present in the 1,3-disubstituted adamantane moiety. While NOESY-NMR data suggest proximity between the catalytically active His sidechain and the Phe-OMe methyl group, (Scheme 48), rotational flexibility in these trimers seems to be present still. Another α -amino acid residue at either side of the ^AXaa moiety in addition to the terminal residues would be welcome to further stabilize turn-like overall structure of the Peptide backbone by a "head-to-tail"-hydrogen bond as is apparently present in, e. g., tetramer **264**. This assumption is supported by recent findings in this group that indeed tetrameric peptide catalysts incorporating an ^AGly motif give markedly better stereoselectivity in catalytic transacylations than their trimeric analogues.^[265]

Table 23. Geometry parameters from minimum conformers of organocatalyst **220**.^[a]

no.	His(π Me) ¹			^A Gly ²			Phe ³	
	Φ	Ψ	ω	Φ	Ψ	ω	Φ	Ψ
1	-87.57	67.63	-179.41	60.62	-2.40	177.94	-123.34	0.17
2	-154.92	166.94	175.69	62.03	-6.80	178.79	-110.61	1.31
3	76.95	-52.97	179.80	61.17	-7.22	178.96	-99.56	2.88
4	-153.27	133.76	178.61	61.23	1.17	177.05	-135.09	-5.86
5	-153.99	162.71	177.10	61.15	8.92	174.19	-146.96	172.83
6	-154.34	164.29	176.09	60.76	-48.19	176.61	-145.86	-7.26
7	-102.68	115.11	-179.09	-62.08	1.84	175.34	-150.38	168.98
8	-157.29	148.16	171.44	-59.38	124.57	177.10	-115.47	-19.42
9	-127.25	14.85	177.13	58.34	-13.80	175.80	-120.51	-27.84
10	-85.36	51.69	176.73	57.86	-11.38	-178.45	-157.52	145.97
11 ^[b]	-	-	-	-	-	-	-	-
12	-149.418	130.383	-178.97	62.148	-119.725	173.41	-93.837	4.104
13	-88.43	68.99	-178.40	-65.22	111.92	178.00	-100.52	-11.98
14	-155.80	165.56	176.86	61.85	-62.87	179.40	-154.29	141.85
15	-156.20	168.80	177.44	-59.49	71.76	-177.02	-154.16	145.36

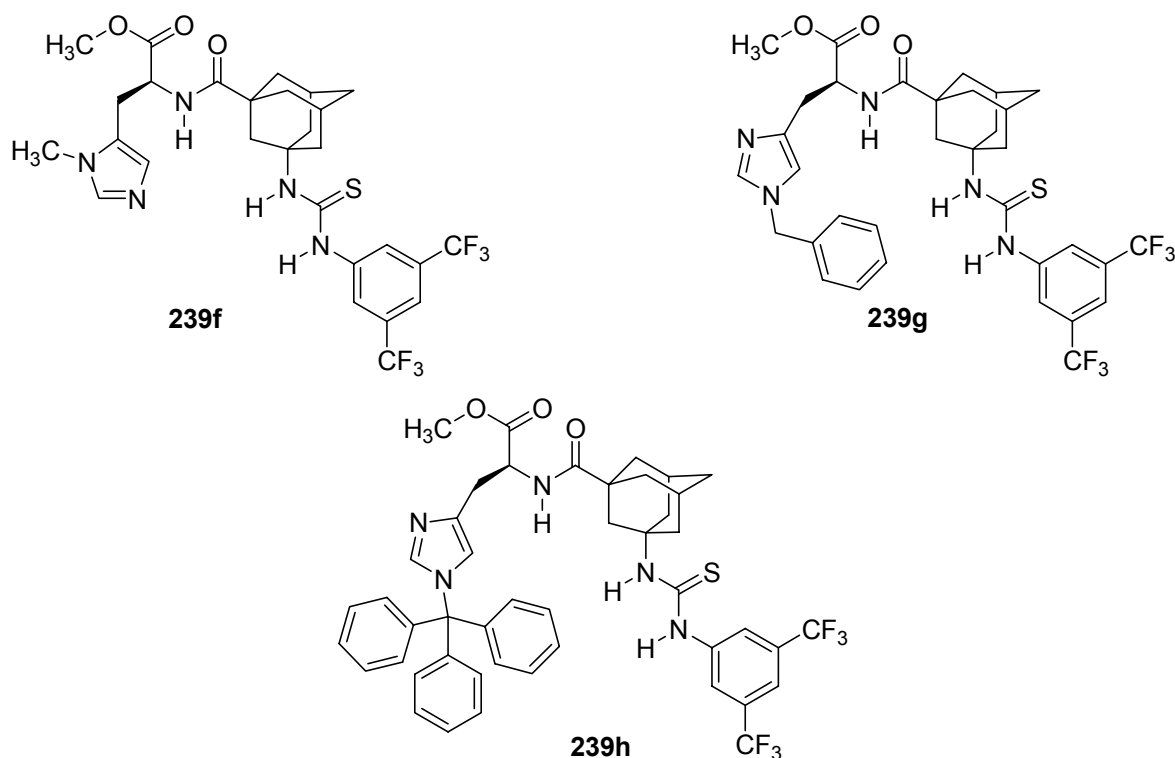
^[a] Computed at the B3LYP/6-31+G(d,p) level of theory; ^[b] no minimum could be found on the B3LYP/6-31+G(d,p) level of theory due to limited computing time.



9.8. Conformational analysis of ^AXaa based thiourea organocatalysts

The peptidic thioureas introduced in Chapter 8.2. incorporate, next to a thiourea motif that is well-known as a “privileged organocatalyst”^[319] in a multitude of organic reactions, an ^AXaa residue within a peptidic framework. Edman degradation is prevented through the ^AGly residue that not only blocks thiazolone formation but also induces a turn-like conformation due to its pseudo-tetrahedral symmetry. The N-terminal α -Xaa residue provides stereochemical information and, in case of His residues, the nucleophilic catalyst needed for the Morita-Baylis-Hillman reaction.

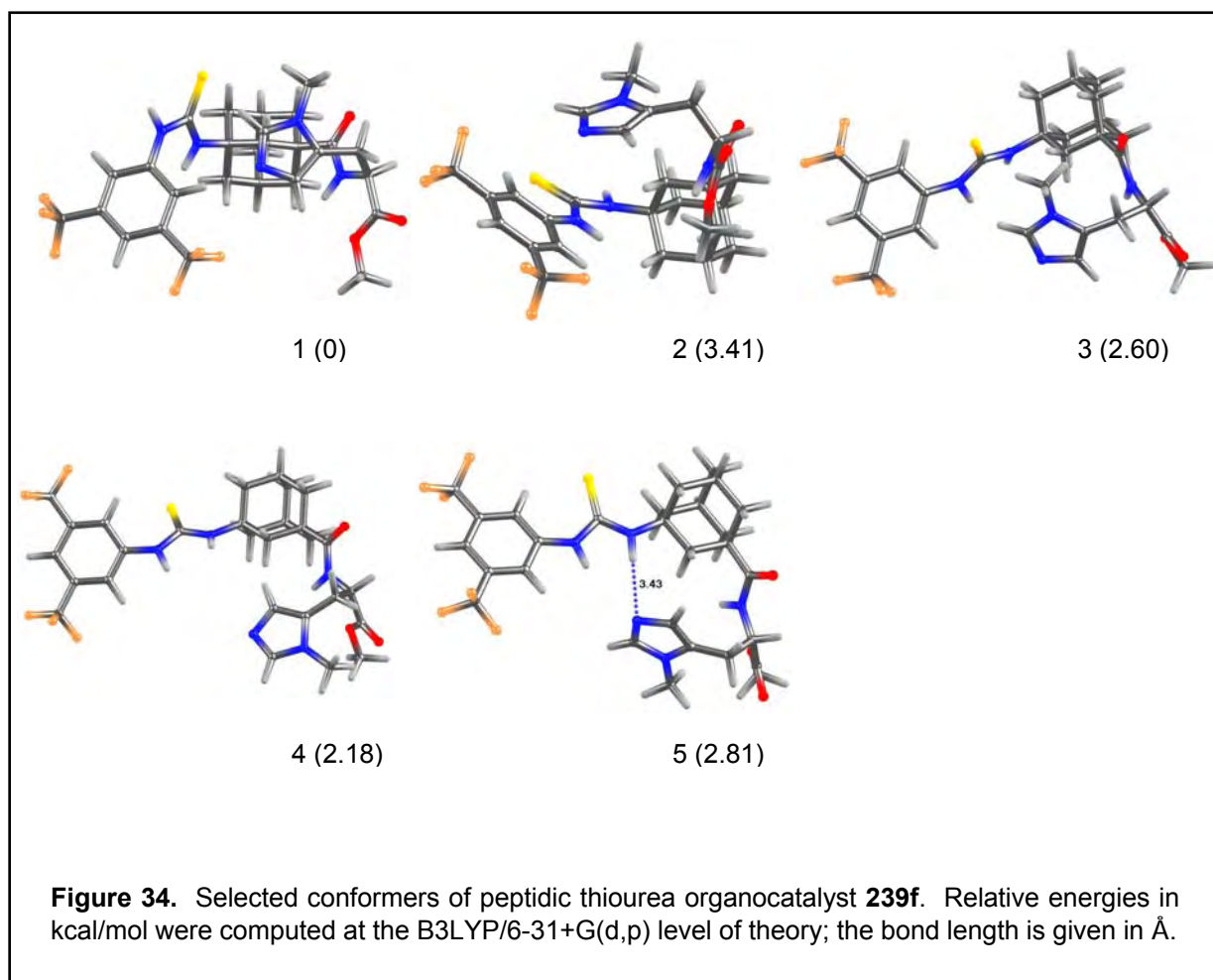
The analysis of NOESY-NMR for the peptidic thioureas **239e–g** (Scheme 50) gave in all cases NOESY cross peaks that hint towards a “folded” conformation, that is, the His sidechain obviously is in proximity to the thiourea moiety. Further support can be obtained from ¹³C NMR, where (as in **218** and **220**) the adamantane carbon signals split into two sets, which can be attributed to the “shielding” influence of the His imidazol ring and (for **239f** and **239g**) its aromatic protective groups.



Scheme 50. Bifunctional peptidic thiourea organocatalysts.

The NMR data can be found in the experimental part. The assignment of NOE interaction is, however, tedious and therefore, for **239g** a computational conformation analysis has also been performed. The MMFF-94 minima display transoid thiourea

moieties (conformers 1 and 2). These are not the preferred conformations when it comes to interactions with a carbonyl oxygen like, e. g., an enone that has to be activated in the Morita-Baylis-Hillman reaction. Hence, after inspection of the other MMFF-94 conformers, the three MMFF-94 conformers displaying cisoid thiourea moieties and are lowest in energy were also computed on DFT level (conformers 3–5). It is important to note that the turn-like conformation with the His sidechain in proximity with the thiourea motif is being computed for all of the five conformers that have been studied on the DFT level of theory. Furthermore, the cisoid conformers are not as unfavorable as predicted by the force field method so that one can conclude that such conformations do play a role in these molecules. The five conformers are shown in Figure 34, their energetics and geometry parameters can be found in Tables 24 and 25.



In the mechanistic proposal for the Morita-Baylis-Hillman reaction outlined in Scheme 43, the first step of the catalyst's action is the formation of an enolate by nucleophilic

attack of the tertiary amine forming an enolate; that would be stabilized by the “oxyanion hole” that is provided by the thiourea motif.^[275] This first step, the addition of organocatalyst **239f** to cyclohexenone was computed using the strategy outlined above.

Table 24. Relative energies of selected conformers of organocatalyst **239f**. Values given in kcal/mol relative to the global minimum.

no.	E_{rel} [kcal/mol] DFT ^[a]	R_{rel} [kcal/mol] MMFF-94 ^[b]	Comment
1	0.00	0.00	transoid thiourea motif
2	3.41	0.71	
3	2.60	8.59	
4	2.18	10.37	cisoid thiourea motif
5	2.81	10.44	

^[a] Computed using B3LYP/6-31+G(d,p) level of theory; ^[b] computed using MMFF-94 as implemented in Spartan '02.

Table 25. Geometry parameters from minimum conformers of organocatalyst **218**.^[a]

no.	thiourea			^A Gly ²			Pmh ³ -OMe	
	α ^[b]	β ^[c]	γ ^[d]	Φ	Ψ	ω	Φ	Ψ
1	-124.0	15.0	-166.3	60.0	78.0	-167.8	-171.3	-8.4
2	-10.9	173.9	-25.8	-46.8	75.5	176.4	-155.0	-0.2
3	46.5	-170.2	-167.5	57.6	71.6	-174.1	-163.6	-3.2
4	-42.4	174.2	174.1	-175.2	60.9	179.6	-149.0	3.0
5	7.0	-177.0	178.2	-179.4	67.6	-163.2	-150.1	5.4

^[a] Computed at the B3LYP/6-31+G(d,p) level of theory; ^[b] defined as $C^{\text{ortho}} - C^{\text{ipso}} - N^1 - \underline{C}=\text{S}$; ^[c] defined as $C^{\text{ipso}} - N^1 - \underline{C}=\text{S} - N^3$; ^[d] defined as $N^1 - \underline{C}=\text{S} - N^3 - C^1$ (adamantane).

The results of the combined MMFF-94 / DFT computations are summarized in Tables 26 and 27 (the geometry parameters of the catalyst's backbone are given) as well as in Figure 35.

Table 26. Relative energies of selected conformers of the complex of organocatalyst **239f** with cyclohex-2-en-1-one. Values given in kcal/mol relative to the global minimum.

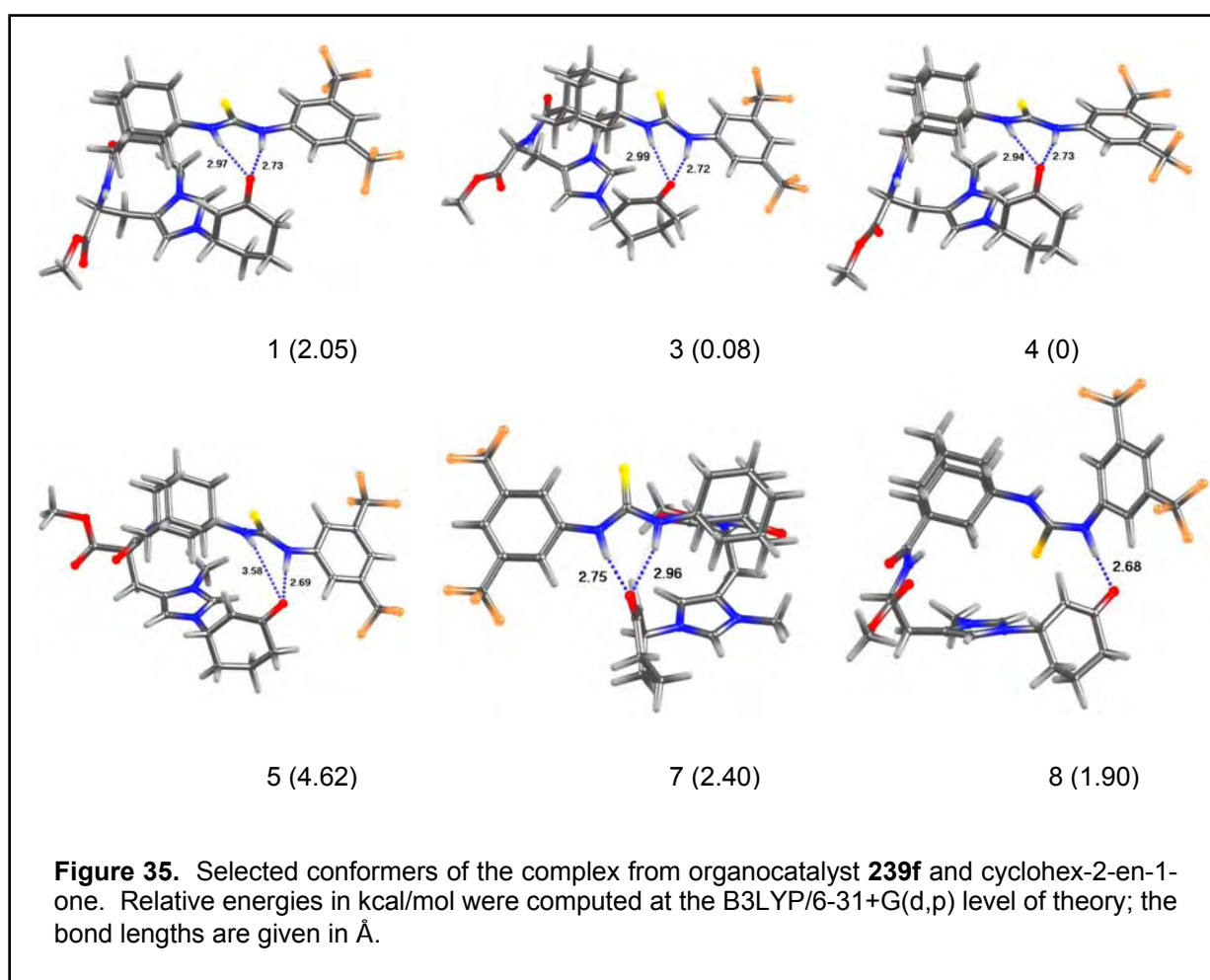
no.	E_{rel} [kcal/mol] DFT ^[a]	R_{rel} [kcal/mol] MMFF-94 ^[b]	Comment
1	2.05	0.00	same conformer
2	2.05	0.00	
3	0.08	0.36	
4	0.00	0.45	same conformer
5	4.62	2.18	
6	4.62	2.18	
7	2.40	3.56	
8	1.90	4.45	
9	1.92	4.46	
10	5.61	5.16	

^[a] Computed using B3LYP/6-31+G(d,p) level of theory; ^[b] computed using MMFF-94 as implemented in Spartan '02.

Table 27. Geometry parameters from minimum conformers of the complex of organocatalyst **239f** with cyclohex-2-en-1-one.^[a]

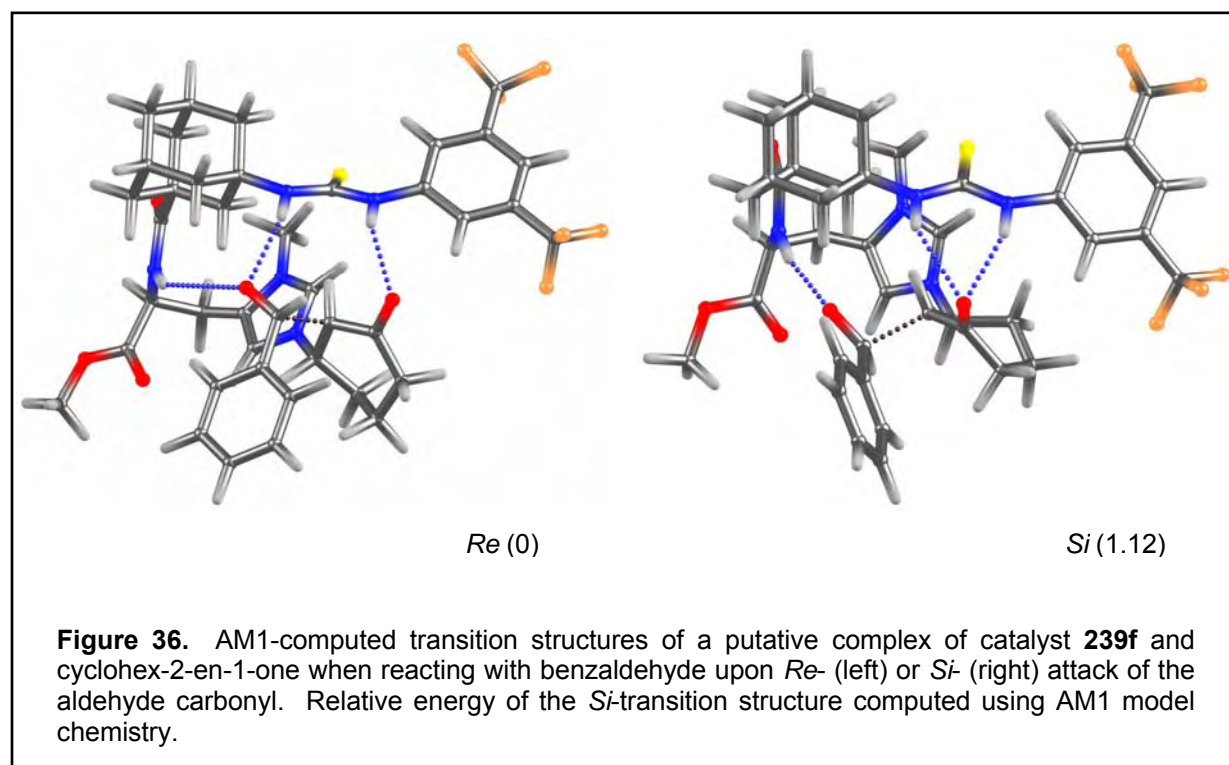
no.	thiourea			Φ	^A Gly ²		Pmh ³ -OMe	
	$\alpha^{[b]}$	$\beta^{[c]}$	$\gamma^{[d]}$		ψ	ω	Φ	ψ
1	-173.6	-169.9	-177.7	63.7	91.7	-171.5	-170.7	16.8
2	8.9	-169.9	-177.7	63.7	91.7	-171.5	-170.6	16.7
3	-1.3	-167.6	-176.4	63.1	95.5	-170.6	-173.2	163.5
4	-178.8	-170.3	-177.8	62.7	92.0	-170.2	-173.6	163.4
5	-156.1	-163.3	-167.9	54.3	-59.9	176.2	55.8	38.9
6	-156.1	-163.3	-167.9	54.3	-59.9	176.2	55.8	38.9
7	168.6	169.4	158.7	-57.8	22.9	-175.3	-175.1	159.2
8	147.2	-17.4	-175.4	57.1	66.8	-176.2	-167.1	168.8
9	147.2	-17.6	-175.2	56.9	66.8	-176.3	-167.1	168.9
10	-157.3	-162.9	-167.8	53.9	-59.6	177.0	65.8	-155.7

^[a]Computed at the B3LYP/6-31+G(d,p) level of theory; ^[b]defined as $C^{\text{ortho}} - C^{\text{ipso}} - N^1 - \underline{C}=\text{S}$; ^[c]defined as $C^{\text{ipso}} - N^1 - \underline{C}=\text{S} - N^3$; ^[d]defined as $N^1 - \underline{C}=\text{S} - N^3 - C^1$ (adamantane).



When activating the enone, the minimum conformers of this complex display cisoid orientation of the thiourea motif, both amide groups of the thiourea are involved in N–H...O hydrogen bonding, thereby stabilizing the enolate (for comparison, see Figure

34, conformers 1 and 2). The bond lengths of the respective hydrogen bonds reflect the higher acidity of the aryl substituted amide (more acidic – stronger hydrogen bond) when compared with the adamantane substituted part. For the next step in the Morita-Baylis-Hillman reaction, which is represented by the formation of the C–C-bond, the nucleophilic attack of the enolate (stabilized by the bifunctional catalyst **239f**) at the aldehyde is possible in a *Re*- or *Si*- fashion, respectively.



The corresponding transition structures of such a reaction could be localized with semiempirical computations (AM1) only; however, some basic conclusions for the course of the Morita-Baylis-Hillman reaction of cyclohex-2-en-1-one with benzaldehyde catalyzed by **239f** can be drawn:

- the difference in energy of the two transition states is small, hinting at low enantiodifferentiation (as is observed experimentally).
- upon *Re*- attack, the benzaldehyde pushes the enolate oxygen out of the thiourea's "oxyanion binding pocket".
- upon *Si*-attack, obviously a backbone amide has an assisting effect.

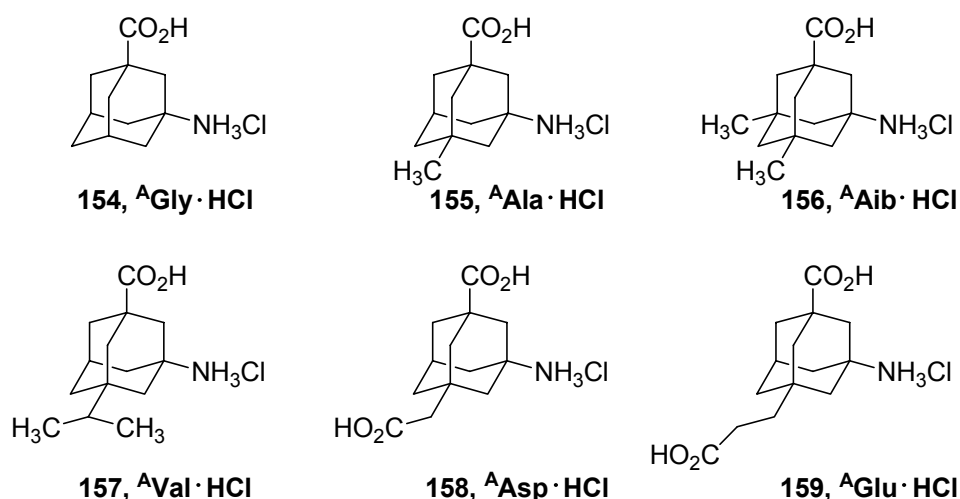
- best orientation and activation of both the enone and the aldehyde would be realized by a trifunctional bistiourea, which is in line with the findings of Nagasawa and Berkessel.^[283, 284]
- To increase stereochemical induction (that is, to increase energetic differences between the transition structures for the *Re*- and *Si*- attack, respectively), the introduction of bulkier histidine ester groups (*tert* butyl, adamantyl) and alkylated analogs of cyclohexenone would be best suited.

While the transition structures in Figure 36 represent at best preliminary results (computation of these preoptimized structures at the B3LYP/6-31+G(d,p) level of theory would give much more reliable energies and structures, but could not be finished within three months on four Opteron CPUs), they are in line with the unsatisfying experimental results (see Chapter 8.2., Table 8) in terms of stereochemical induction.

10. Summary & Outlook

With the results summarized in the present thesis, the synthesis of representative monomeric A Xaas, their protective group-, and peptide- chemistry can be regarded established.

The toolkit of available A Xaas has been expanded to six representative monomers, two fundamentally different routes of access have been worked out and utilized in a diversified manner. A Gly, A Ala, A Aib, A Val, A Asp, and A Glu are amenable using the classical pathway of direct amidation of an appropriate precursor and hydrolysis of the acetamides.



Scheme 51. A Xaas

Using this classical pathway employing a modified Ritter-type protocol that does *not* require brominated precursors, we also succeeded in the acetamidation of hydrocarbons like, e. g., 1,3-dimethyladamantane in very good yield.

Additionally, an unprecedented reaction of adamantane derivatives has been worked out: A direct, bromine-free formamidation using technical grade reagents only (Chapter 5.1., Table 2). A patent application dealing with the synthesis of 1-formamido-3,5-dimethyladamantane utilizing this novel reaction has been filed and sold to an industry partner, since it represents a key intermediate in the synthesis of the anti-Alzheimer drug Memantine[®] (see Chapter 3.2.2.4.).

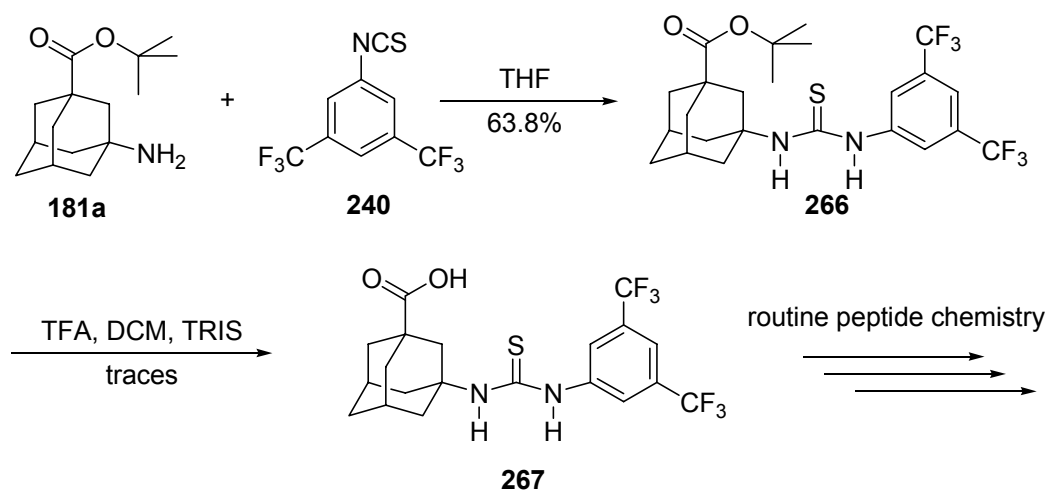
An alternative access to ^AXaas utilizing our group's PTC halogenation protocol and subsequent reactions has also been exemplified in the synthesis of ^AAib and ^AVal, but failed in the synthesis of ^APhg. The strength of this pathway lies in the functional group tolerance of the PTC halogenations which enables us to synthesize precursor **176**, that could serve as the starting compound for a multitude of further ^AXaa derivatives upon exchange of the bromine with various sidechains utilizing well-established functionalization protocols.^[219, 220]

Introduction of protective groups at either the carboxy or amino group has been accomplished by standard procedures, and reliable protocols for the synthesis of peptides incorporating ^AXaas have been worked out for peptide synthesis in solution and on solid phase. A multitude of such γ -peptides were described in the previous chapters; these peptides not only represent valuable targets for medicinal applications (as has probably been found for **185**, which seems to hold promise for the development of blockers for the GABA transporter system), but also interesting scaffolds for peptidic organocatalysts. The overall pseudo-tetrahedral symmetry of the adamantane nucleus of each ^AXaa orientates the peptidic sidechains to stable turn-like structures that have successfully been utilized in the organocatalysis of transacylation reactions and Morita-Baylis-Hillman reactions.

Utilization of peptides incorporating a His residue and an ^AGly residue as turn inducer in transacylation reactions has given encouraging results that have been submitted for publication. This field of application is currently being expanded by Dipl. Chem. Christian Müller.

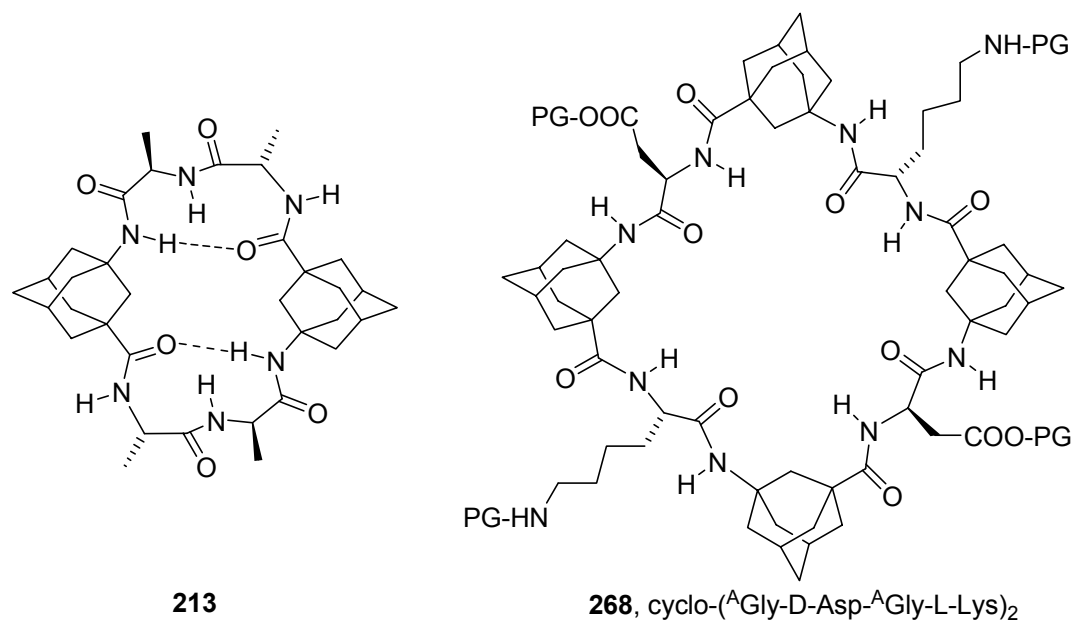
The organocatalysts utilized for the MBH reactions represent a novel class of *peptidic thiourea derivatives*. Given the well-known and widely utilized catalytic activity of thiourea derivatives like, e. g., **239a-g**, synthesis and screening of such types of structures in the catalysis of other reactions appears easily accessible while highly attractive. To use the "blocked" thiourea motif in routine peptide synthesis, preparation of **267** (which should be applicable as carboxylic acid for the N-terminus of almost any peptide) would be the next logic expansion to this chemistry. Synthesis of **266** was accomplished in large scale and good yield from **181a** and **240** (Scheme 52). Cleavage of the ^tBu ester protective group of **264** in principle is possible (as has been demonstrated by a coupling of the crude reaction mixture with Phe-OMe · HCl; the

product showing **239b** in the ESI-MS). Development of a reliable and scalable procedure for this conversion would highly be welcome.



Scheme 52. Attempted synthesis of building block **267**.

The cyclization of linear precursor sequences incorporating two or more ^AGly moieties has been studied with mixed results. While most of the cyclizations failed to give the target cyclopeptide, **213** could be isolated in satisfactory overall yield.



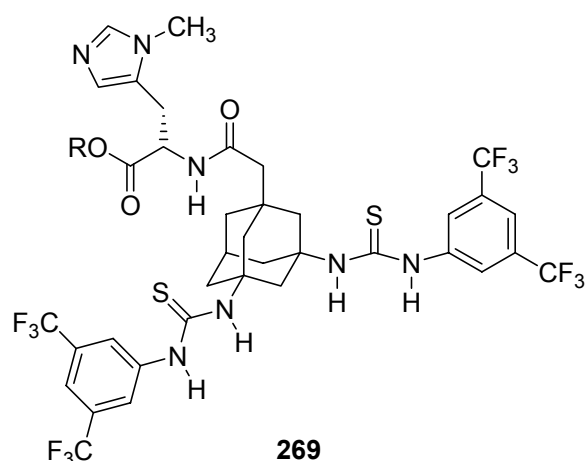
Scheme 53. Cyclopeptide **213** and proposed precursor cyclopeptide for designed ion channels **268**.

While **213** readily crystallizes, NMR spectra are puzzling and, considering the ESI MS, suggest a high propensity of such cyclic peptides to form aggregates. Synthesis of a

series of precursors, detailed studies on the cyclization step, and structural analysis of the resulting cyclopeptides remains a challenging, but rewarding goal. In view of designed artificial ion channels, such highly lipophilic cyclopeptides remain attractive (Scheme 53). Application of the appropriate protective group scheme and on-resin cyclizations could enable the synthesis of columnar structures of highly lipophilic exterior, variable in diameter and height, and stacked through selectively tied amide bonds.

Such cyclizations can also be regarded as a proof of turn structures of the respective precursor sequences. Computations of conformer distribution, IR- and NMR- studies have shed light on the conformational propensities of, e. g., peptides **261** – **265** (Chapter 9). The structural predictions that can be derived from the data compiled in Chapter 9 are mostly consistent; however, more reliable X-ray analyses of ^AXaa containing peptides are needed to finally confirm the assumptions made.

While this seems to hold promise in the long run, the synthesis of peptide libraries incorporating ^AXaa residues has become more easily feasible with the purchase of an automated peptide synthesizer. Screening of such libraries with respect to organocatalysis and medicinal applications will lead to an improved understanding of the structural requirements of these peptides for enantioselective organocatalysis on one hand and structure-activity relationships in medicinal screens on the other.



Scheme 54. Proposed trifunctional organocatalyst for the Morita-Baylis-Hillman reaction.

The two main routes of research pushing further ^AXaa chemistry both end up in peptidomimetic chemistry – from opposite directions: Design of peptidomimetic drugs can be regarded as optimization of the substrate for a given binding site of a protein

target, while the design of organocatalysts represents the opposite way, the optimization of an enzyme's active site for a given reaction.

One example for the latter is **269** (Scheme 54), a proposal for a trifunctional "Morita-Baylis-Hillmanase" that combines Nagasawa's and Berkessel's bis-thiourea motif and Miller's His peptide on an adamantane scaffold. 3,5-dibromoadamantane-1-acetic acid has already been prepared in our group, so that the synthesis of **269** lies within reach. Theoretical examination of such types of structures, e. g., by using a "docking" algorithm implemented in several molecular modeling packages,^[320] appears to be better suited for the design of organocatalysts than the very costly MMFF/DFT approach that was utilized within the present thesis.

11. Acknowledgement

I am obliged to thank a number of people who contributed to the becoming of this thesis, directly or indirectly.

At first, my supervisor, Prof. Dr. Peter R. Schreiner, Ph.D., who gave me a project for which I could work hard, and the liberty to look what lays off the path. Motivation and endurance to follow this research were greatly influenced by his notorious optimism. Most impressive, however, is his gift in letting a chemist feel significant.

I am equally obliged to Prof. Dr. Andrey A. Fokin, who taught me high-level and high-throughput preparative ukrainian chemistry as well as high-spin celluloid chemistry. He always had an open ear for any of my requests, concerns and complaints, and has been helpful in many more respects. благодаря его помощи я быстро справился с работой.

I thank the University of Giessen for financial support through a scholarship (HGFÖN).

Dr. Chiara Cabrele, University of Regensburg, not only pioneered SPPS of the Δ Xaas, but also introduced me to practical SPPS methods – thank you for that.

Thanks also to Dipl. Chem. Maksims Vanejews (Riga) for his participation in the project and to M. Sc. Derek Wolfe (Athens) for his excellent preliminary work.

Many thanks to the TransMit GmbH, in particular to Dr. Kerstin Lischka, Dr. Peter Stumpf and Dr. Carsten Bepler for their dedication concerning all “patent issues”.

Many coworkers at the Institute of Organic Chemistry have done more than just their jobs. Dr. Hans Peter Reisenauer has helped me a lot with the solution IR measurements, Dr. Heike Hausmann spent loads of time and effort with my two-dimensional NMR experiments, and Dr. Erwin Röcker with all kinds of problems associated with HPLC, LC/MS and ESI- as well as HRMS. Dr. Jörg Neudert has always dealt with any concerns associated with the “Praktikum” in an remarkably unagitated manner, thereby facilitating their solution. I wish to thank Antonie Pospiech

and Gertrud Stammeler for the NMR and IR measurements, Rainer Schmidt for the HPLC separations, and Roland Meurer for the elemental analyses.

If all else fails, you can always ask Dr. Jörg Glatthaar – he will know a workaround for almost any problem one can possibly come up with. Thank you, not only for the oxyhydrogen burner.

X-Ray crystal structure determination would not have been possible without the guidance and help of Dr. M. Serafin, Mr. Günther Koch and Dipl. Chem. Sven Kroker as well as Dipl. Chem. Christian Würtele.

Thanks to Steffen Wagner for his way of enthusiasm and teachableness, and to Anika Merz for measuring melting points.

Volker Erb, Jana Eggenstein, Jürgen Merte, and Beatrix Todt maintained a steady flow of glassware, chemicals, TLC cards, and compressed gases straight into my hood. Thank you.

Many students have also been working –voluntarily or not– on the ^AXaa field. Surprisingly, some of them were not as deterred as one could imagine and are groupmembers today: Dipl. Chem. Adelina Nemirowski, Dipl. Chem. Christian E. Müller, Dipl. Chem. Nicole Schichtel, Dipl. Chem. Yvonne Schober, Dipl. Chem. Sabine Günther, Cand. Chem. Katharina M. Lippert, Tobias Hoppe, Arton Berisha, Romy Mlinzk, Inna Fink, Christian Küchenthal, Christian Kanzler, Michael Schröder, Kerstin Sann, Jenny Friebe, and Michal Pietrowicz.

Dipl. Chem. Nihat Knispel (Acylation), Dipl. Chem. Christian Müller (Acylation and SPPS) and Cand. Chem. Katharina M. Lippert (peptidic thioureas and MBH-reactions) took parts of the chemistry presented herein from my five-year mission, explored strange new molecules, sought out new reactivity and mechanisms and boldly went where no man has gone before. Thank you for that – and good luck for further endeavors!

I thank the center for scientific computing (CSC), university of Frankfurt, for large amounts of computing walltime on their Opteron clusters. Dipl. Chem. Volker Lutz has been of help with all problems concerning my account – thank you.

A gift of 1,3-dimethyladamantane and other alkylated adamantanes from Merz pharmaceuticals, Frankfurt (Germany) is gratefully acknowledged.

To all the PRS groupmembers: Thank you for an (in every respect) instructional time.

I also am obliged to every single tax payer who ultimately keeps scientific research going. Hopefully I will be able to give it back some day.

Most importantly, two cowboys have shared this lonesome ride through the Giessen plains with myself and Clint straight from the start: The chemists Mike Kotke and Torsten Weil. These fine men obviously also took this one-way ticket to hell – and back!

In spite of the fact that the following people did not get to meet me much frequently during recent years, in fact it was them who kept me going in this grim period:
My parents Rosemarie and Willibald, my brothers Markus and Michael, my sister Ulrike, my grandmother Maritsch, Thorsten, Heidi, Antonia, Lilli, Christian, and Anna.

There *is* life beyond chemistry.

Throughout all these last five years, there was one person who has suffered most from my tempers and just refused to leave me alone with them. Thank you, Christina. Will you marry me?

12. Experimental Part

12.1. General remarks

Unless otherwise noted, chemicals were purchased from Acros Organics, Aldrich, Lancaster, Merck, Bachem or Fluka at the highest purity grade available and were used without further purifications. All solvents were distilled prior to use. Dry solvents were prepared using standard laboratory procedures and were stored under Argon over an appropriate drying agent until used. Column chromatography was conducted using J.T. Baker silica gel (0.063 – 0.200 mm) or, for flash column chromatography, Merck silica gel 60 (0.040 – 0.063 mm), respectively. Melting points (< 190 °C) were measured using a Büchi SMP 20 apparatus and are not corrected; melting points > 190 °C were measured using a Bunsen burner melting point apparatus and are also not corrected. ¹H and ¹³C NMR spectra were recorded on Bruker AV400 or AV200 spectrometers, respectively, using TMS or 3-Trimethylsilyl-(*d*₄)-propanoic acid sodium salt as the internal standard with chemical shifts given in ppm relative to TMS or the respective solvent residual peaks. Assignments have been made using DEPT 135 and / or APT spectra. Multiplets in ¹H-NMR spectra are designated s (singlet), d (doublet), t (triplet), q (quartet), quint. (quintet), sept. (septet), and m (multiplet), respectively. Infrared spectra were recorded on a Bruker IFS25 spectrometer. MS / HRMS were recorded on a Finnigan MAT95 sectorfield spectrometer; ESI mass spectra on a Finnigan LCQ Duo spectrometer using methanol / acetic acid solutions of the respective compounds. Elemental analyses were measured using a Carlo Erba 1106 CHN analyzer. GC-MS analyses were performed with a HP 5890 gas chromatograph equipped with a HP MSD 5971 detector.

12.2. General procedures

12. 2. 1. General procedure A: HBTU-mediated peptide coupling in solution

The C- and N-terminally protected amino acids or peptide fragments were dissolved in equimolar ratio in dry acetonitrile or THF under Argon using oven-dried glassware. The mixture was cooled to 0 °C using an ice bath and one equivalent on

Diisopropylethylamine (DIPEA) was added. When hydrochlorides were used as the amino components, two equivalents of DIPEA were used. Finally, one equivalent of HBTU was added and the mixture was stirred over night upon warming to room temperature. Brine was added and the mixture was thoroughly extracted with chloroform. The combined organics were washed with 1 N HCl, 5% NaHCO₃, water and brine and dried over Na₂SO₄. After filtration and evaporation of the solvents, the crude peptide mixtures were purified via silica gel column chromatography.

12. 2. 2. General procedure B: DIC/HOBt-mediated peptide coupling in solution

The peptide coupling using this method of activation was performed as described for (187).

12. 2. 3. General Procedure C: cleavage of Fmoc-protection in solution

Cleavage of N-terminal Fmoc-protective groups was accomplished by dissolving the peptide in dry acetonitrile and cooling the solution to 0 °C using an ice bath. Diethylamine was added and the mixture was stirred over night upon warming to room temperature. The solvents were then carefully removed *in vacuo* using a rotary evaporator, and the residue was purified via silica gel column chromatography.

12. 2. 4. General procedure D: cleavage of –O^tBu-protection in solution

The peptide was dissolved in dichloromethane and cooled to 0 °C with an ice bath. Trifluoroacetic acid was added and the mixture was stirred over night upon warming to room temperature. The solvents were carefully evaporated *in vacuo* using a rotary evaporator; residues of TFA were removed by repeatedly adding dichloromethane and evaporation *in vacuo*. The residue was purified by recrystallization.

12. 2. 5. General procedure E: synthesis of peptidic thiourea derivatives

The N-terminally deprotected peptides were dissolved in dry THF and cooled to 0 °C with an ice bath. A solution of an equimolar amount of 3,5-Bis(trifluoromethyl)phenyl isothiocyanate in dry THF was then added via an addition funnel over the course of 1 h at 0 °C. The mixture was stirred over night upon slowly warming to room temperature. The solvents were then carefully evaporated *in vacuo* using a rotary evaporator and the residue was purified by reprecipitation (266, 239a) or silica gel column chromatography (239b – 239g).

12.3. Direct C–H to C–N Acetamidations

3-Acetamidotricyclo[3.3.1.1^{3,7}]decane-1-carboxylic acid (141): 25.0 g (138.7 mmol) adamantane-1-carboxylic acid (**128**) were suspended in 20 mL nitric acid and cooled to 0 °C with an ice bath. Using an addition funnel, 150 mL sulfuric acid were added over the course of 90 min keeping the reaction mixture at 0 °C. The reaction mixture was stirred for another 2 h at 0 °C, whereupon 100 mL of technical grade acetonitrile were added via an addition funnel within 3 h at 0 °C. After another 3 h of stirring at 0 °C, the reaction mixture was poured over ice (~ 1 kg) with shaking. The colorless precipitate was collected via suction filtration, washed with water and recrystallized from a mixture of acetic acid / water / acetone (5 : 5 : 2) and dried over potassium hydroxide at 110 °C / 15 mbar overnight to give 27.58 g (116.23 mmol, 83.8%) of the acetamide **141** as colorless crystals, mp 251 °C (lit.^[190] 255 – 256 °C). **¹H NMR** (400 MHz, d₆-DMSO): δ /ppm = 10.29 (br s, 1 H, CO₂H); 7.38 (br s, 1 H, NH); 2.08 (m, 2 H); 1.99 (s, 2 H); 1.86 (m, 4 H); 1.74 (s, 3H, CH₃); 1.70 (d, J = 2.4 Hz, 4 H); 1.56 (br s, 2 H). **¹³C NMR** (100 MHz, d₆-DMSO): δ /ppm = 177.6 (C=O); 168.7 (C=O); 50.8 (C_q); 42.1, 41.4 (C_q), 40.1, 37.7, 35.0, 28.5, 23.7 (CH₃). **IR** (KBr): $\tilde{\nu}$ /cm⁻¹ = 3337, 2950, 2920, 2858, 1700, 1688, 1630, 1552, 1238. **MS** (EI, 70 eV): m/z = 237 (100%), 219 (14.9%), 191 (98.6%), 180 (47.5%), 162 (57.6%), 150 (40.6%), 136 (55.4%), 94 (69.7%). **HRMS** found, 237.1373, calc. 237.1365.

3-Acetamido-5-methyltricyclo[3.3.1.1^{3,7}]decane-1-carboxylic acid (142): 1-Methyladamantane was synthesized using a literature procedure,^[321] 3-brominated with excess bromine,^[20] and converted to 3-methyladamantane-1-carboxylic acid.^[190] 2.576 g 3-Methyladamantane-1-carboxylic acid (**129**, 13.3 mmol) were suspended in 10 mL nitric acid and cooled to 0 °C with an ice bath. After the addition of 13 mL sulfuric acid, the mixture was stirred at 0 °C for 10 min. 11 mL of oleum (20% SO₃) were then added and the mixture was stirred for 1 h at 0 °C and 3 h at rt. After cooling to 0 °C, 10 mL of technical grade acetonitrile were added, the mixture was stirred for 10 min at 0 °C and 3 h at rt. Finally, the mixture was poured over ~ 300 g of ice with shaking and left standing in the refrigerator over night. The colorless precipitate was collected via suction filtration and recrystallized from a mixture of acetic acid / water / acetone (5 : 5 : 3). After drying over potassium hydroxide at 110 °C / 15 mbar overnight, 2.8765 g (12.3 mmol, 92.6%) of acetamide **142** were isolated as colorless

crystals, mp 262 °C (lit.^[190] 265 – 266 °C). **¹H NMR** (400 MHz, d₆-DMSO): δ /ppm = 12.08 (br s, 1 H, CO₂H); 7.40 (br s, 1 H, NH); 2.11 (m, 1 H); 1.92 (m, 2 H); 1.85 – 1.68 (m, 2 H); 1.74 (s, 3 H, CH₃); 1.67 – 1.55 (m, 4 H); 1.44 (s, 2 H); 1.38 – 1.27 (m, 2 H); 0.83 (s, 3 H, CH₃). **¹³C NMR** (100 MHz, d₆-DMSO): δ /ppm = 177.5 (C=O), 168.6 (C=O), 51.6 (C_q), 46.9, 44.5, 42.07 (C_q), 42.04, 41.5, 39.3, 37.0, 31.3 (C_q), 29.9, 28.9, 23.6. **IR** (KBr): $\tilde{\nu}$ /cm⁻¹ = 3340, 2947, 2936, 2921, 2902, 2863, 1692, 1615, 1553, 1268, 1230. **MS** (EI, 70 eV): m/z = 251 (92.9%), 206 (100%), 194 (30.3%), 176 (27.5%), 164 (28.10%), 150 (76.8%), 108 (42.6%). **HRMS** found, 251.1527, calc. 251.1521.

3-Acetamido-5,7-dimethyltricyclo[3.3.1.1^{3,7}]decane-1-carboxylic acid (143): 1-Bromo-3,5-dimethyladamantane was converted to the corresponding 3,5-dimethyladamantane-1-carboxylic acid using a literature procedure.^[190] 20.66 g (99.2 mmol) of 3,5-dimethyladamantane-1-carboxylic acid (**130**) were suspended in 60 mL nitric acid and cooled to 0 °C with an ice bath. After the addition of 100 mL sulfuric acid, the mixture was stirred at 0 °C for 10 min. 35 mL of oleum (25% SO₃) were now added and the mixture was stirred for 30 min at 0 °C and 1 h at rt. After cooling to 0 °C, 60 mL of technical grade acetonitrile were added, the mixture was stirred for 10 min at 0 °C and 3 h at rt. Finally, the mixture was poured over ~ 2 kg of ice with shaking and left standing in the refrigerator over night. The colorless precipitate was collected via suction filtration and recrystallized from a mixture of acetic acid / water / acetone (5 : 5 : 4). After drying over potassium hydroxide at 110 °C / 15 mbar overnight, 24.2866 g (91.5 mmol, 92.3%) of acetamide **143** were isolated as colorless crystals, mp 306 °C (lit.^[190] 307 – 308 °C). **¹H NMR** (400 MHz, d₆-DMSO): δ /ppm = 12.09 (br s, 1 H, CO₂H); 7.35 (br s, 1 H, NH); 1.85 (m, 2 H); 1.73 (s, 3 H, CH₃); 1.60 – 1.46 (m, 4 H); 1.42 – 1.31 (m, 4 H); 1.12 – 1.03 (m, 2 H); 0.84 (s, 6 H, 2 × CH₃). **¹³C NMR** (100 MHz, d₆-DMSO): δ /ppm = 177.4 (C=O), 168.7 (C=O), 52.4 (C_q), 49.3, 46.2, 43.9, 42.7 (C_q), 40.9, 31.9 (C_q), 29.5 (2 × CH₃), 23.6 (CH₃). **IR** (KBr): $\tilde{\nu}$ /cm⁻¹ = 3340, 2942, 2898, 2860, 2848, 2477, 1687, 1611, 1553, 1271, 1261, 1225, 711. **MS** (EI, 70 eV): m/z = 265 (85.7%), 220 (78.6%), 207 (10.4%), 194 (20.2%), 176 (31.7%), 164 (100.0%), 150 (35.2%), 122 (31.1%), 107 (30.0%). **HRMS** found, 265.1670, calc. 265.1678. **Elem. Anal.:** C₁₅H₂₃NO₃ (265.35): calcd. C 67.90, H 8.74, N 5.28; found C 68.12, H 9.12, N 5.32.

3-Acetamido-5-isopropyltricyclo[3.3.1.1^{3,7}]decane-1-carboxylic acid (144): 3-Bromo-1-isopropyladamantane was synthesized according to literature procedures.^[322] It was then converted to 3-isopropyladamantane-1-carboxylic acid using the procedure described above.^[190] 3.7 g (16.64 mmol) of 3-isopropyladamantane-1-carboxylic acid (**131**) were suspended in 10 mL nitric acid and cooled to 0 °C with an ice bath. After the addition of 17 mL sulfuric acid, the mixture was stirred at 0 °C for 10 min. 6 mL of oleum (25% SO₃) were now added and the mixture was stirred for 1 h at 0 °C and 3 h at rt. After cooling to 0 °C, 10 mL of technical grade acetonitrile were added, the mixture was stirred for 10 min at 0 °C and 1.5 h at rt. Finally, the mixture was poured over ~ 400 g of ice with shaking and left standing in the refrigerator over night. The yellowish precipitate was extracted with ethyl acetate, the combined organics were dried (Na₂SO₄), and the solvent was evaporated under reduced pressure. The residual solid was dissolved with 5% aqueous NaOH, filtered and precipitated with concentrated hydrochloric acid. It was then collected via suction filtration and recrystallized from a mixture of acetic acid / water / acetone (5 : 5 : 2). After drying over potassium hydroxide at 110 °C / 15 mbar overnight, 1.815 g (6.5 mmol, 39.0%) of acetamide **144** were isolated as colorless crystals, mp 188 – 189 °C. **¹H NMR** (400 MHz, CDCl₃): δ /ppm = 12.14 (br s, 1 H, COOH); 7.42 (br s, 1 H, NH), 2.14 (m, 1 H, CH), 2.00 – 1.88 (m, 2 H); 1.88 – 1.70 (m, 2 H); 1.74 (s, 3 H, CH₃); 1.68 – 1.53 (m, 4 H); 1.45 (br s, 2 H); 1.40 – 1.31 (m, 2 H); 1.28 (sept, J = 6.8 Hz, 1 H, CH(CH₃)₂); 0.79 (d, J = 7.2 Hz, 6 H, CH(CH₃)₂). **¹³C NMR** (100 MHz, CDCl₃): δ /ppm = 181.6 (COOH), 170.3 (C=O), 53.4 (C_q), 42.9, 42.6, 41.9, 40.2, 39.6, 37.5 (2 signals), 37.05, 37.01, 29.2, 24.4 (CH₃), 16.4 (CH(CH₃)₂). **IR** (KBr): $\tilde{\nu}$ /cm⁻¹ = 3367, 2969, 2933, 2908, 2859, 1694, 1616, 1549, 1254, 1225. **MS** (EI, 70 eV): m/z = 279 (65.6%), 236 (87.2%), 194 (81.6%), 190 (100%), 178 (16.6%), 162 (9.7%), 138 (18.5%). **HRMS** found, 279.1830, calc. 279.1834. **Elem. Anal.:** C₁₆H₂₅NO₃ (314.26): calcd. C 68.79, H 9.02, N 5.01; found C 69.09, H 9.26, N 4.55.

3-Acetamido-5-carboxymethyltricyclo[3.3.1.1^{3,7}]decane-1-carboxylic acid (145): 3-Carboxymethyladamantane-1-carboxylic acid was prepared following literature procedures.^[323] 10.739 g (45.1 mmol) of 3-carboxymethyladamantane-1-carboxylic acid (**132**) were suspended in 36 mL nitric acid and cooled to 0 °C with an ice bath.

After the addition of 50 mL sulfuric acid, the mixture was stirred at 0 °C for 10 min. 30 mL of oleum (25% SO₃) were now added and the mixture was stirred for 1 h at 0 °C and 3 h at rt. After cooling to 0 °C, 35 mL of technical grade acetonitrile were added, the mixture was stirred for 10 min at 0 °C and 3 h at rt. Finally, the mixture was poured over ~ 1 kg of ice with shaking and left standing in the refrigerator over night. The colorless precipitate was collected via suction filtration and recrystallized from a mixture of acetic acid / water / acetone (5 : 5 : 2). After drying over potassium hydroxide at 110 °C / 15 mbar overnight, 10.2955 g (34.9 mmol, 77.4%) of acetamide **145** were isolated as colorless crystals, mp 148 – 150 °C. **¹H NMR** (400 MHz, d₆-DMSO): δ/ppm = 12.0 (br s, 2 H, 2 × CO₂H); 7.45 (br s, 1 H, NH); 2.16 – 2.09 (m, 1 H); 2.06 (s, 2 H); 1.98 – 1.87 (m, 2 H); 1.87 – 1.65 (m, 4 H); 1.74 (s, 3 H, CH₃); 1.65 – 1.53 (m, 4 H); 1.51 – 1.40 (m, 2 H). **¹³C NMR** (100 MHz, d₆-DMSO): δ/ppm = 177.4 (C=O), 172.2 (C=O), 168.8 (C=O), 51.4 (C_q), 47.0, 44.5, 42.2, 41.9 (C_q), 41.5, 39.9, 39.3, 37.0, 33.7 (C_q), 28.6, 23.6. **IR** (KBr): $\tilde{\nu}/\text{cm}^{-1}$ = 3495, 3437, 3396, 2948, 1727, 1628, 1609, 1544, 1234, 1184, 575. **MS** (EI, 70 eV): m/z = 295 (20%), 193 (8.5%), 149 (7.8%), 91 (11.0%); **HRMS** found, 295.1436, calc. 295.1420. **Elem. Anal.:** C₁₅H₂₁NO₅ (295.33): calcd. C 61.00, H 7.17, N 4.47; found C 61.43, H 7.35, N 4.45.

3-(3-Acetamido-5-carboxy-1-tricyclo[3.3.1.1^{3,7}]decane) propanoic acid (146): Adamantane-1-propanoic acid was synthesized by homologization of adamantane-1-acetic acid as described in the literature.^[217] The propanoic acid was then brominated using excess bromine and converted to the dicarboxylic acid **133** via Koch-Haaf reaction as described above. 2.311 g (9.2 mmol) of dicarboxylic acid **133** were suspended in 7.5 mL nitric acid and cooled to 0 °C with an ice bath. After the addition of 10.5 mL sulfuric acid, the mixture was stirred at 0 °C for 10 min. 7 mL of oleum (25% SO₃) were then added and the mixture was stirred for 1 h at 0 °C and 3 h at rt. After cooling to 0 °C, 8 mL of technical grade acetonitrile were added, the mixture was stirred for 10 min at 0 °C and 3 h at rt. Finally, the mixture was poured over ~ 250 g of ice with shaking and left standing in the refrigerator over night. The white precipitate was collected via suction filtration and recrystallized from a mixture of acetic acid / water / acetone (5 : 5 : 2). After drying over potassium hydroxide at 110 °C / 15 mbar overnight, 1.039 g (3.36 mmol, 36.7%) of acetamide **146** were isolated as colorless crystals, mp 222 – 223 °C. **¹H NMR** (400 MHz, d₆-DMSO): δ/ppm = 12.03 (br s, 2 H,

2 \times CO₂H); 7.40 (br s, 1 H, NH); 2.16 – 2.07 (m, 3 H); 1.93 (br s, 2 H); 1.87 – 1.70 (m, 2 H); 1.74 (s, 3 H, CH₃); 1.70 – 1.53 (m, 4 H); 1.45 – 1.34 (m, 2 H + 2 H), 1.32 (br s, 2 H). ¹³C NMR (100 MHz, d₆-DMSO): δ /ppm = 177.5 (C=O), 174.8 (C=O), 168.7 (C=O), 51.5 (C_q), 44.4, 42.1 (C_q), 41.9, 41.7, 39.5, 37.4, 37.2, 33.6 (C_q), 28.6, 27.6, 23.7. IR (KBr): $\tilde{\nu}$ /cm⁻¹ = 3396, 3122, 2935, 2861, 1742, 1726, 1591, 1554, 1227, 1162, 1134, 852, 580. MS (EI, 70 eV): m/z = 309 (17.5%), 291 (27.1%), 249 (50.1%), 192 (43.3%), 148 (100%), 105 (39.4%). HRMS found, 309.1569, calc. 309.1576. Elem. Anal.: C₁₆H₂₃NO₅ (309.36): calcd. C 62.12, H 7.49, N 4.53; found C 61.87, H 7.44, N 4.66.

2-(3-Acetamido-3,5-dimethyltricyclo[3.3.1.1^{3,7}]dec-1-yl) acetic acid (147): 3,5-dimethyladamantane-1-acetic acid (**134**) was prepared from 1-bromo-3,5-dimethyladamantane by a modified literature procedure.^[324] 6.670 g (30 mmol) of the carefully dried acetic acid **134** were suspended in 6 mL nitric acid and cooled to 0 °C with an ice bath. 33 mL sulfuric acid were then added with an addition funnel over the course of 3 h at 0 °C and stirring was continued for another 3 h at 0 °C. 33 mL of technical grade acetonitrile were then added with an addition funnel within 1 h. To complete the reaction, the mixture was stirred for another 3 h at 0 °C and the mixture was finally poured over ~ 250 g of crushed ice with shaking, whereupon a colorless precipitate formed. The mixture was placed in the refrigerator over night and the precipitate was collected via suction filtration. The crude product was recrystallized from a mixture of acetic acid / water / acetone (5 : 5 : 4). After drying over potassium hydroxide at 110 °C / 15 mbar overnight, 4.723 g (16.91 mmol, 56.4%) of acetamide **147** were isolated as colorless crystals, mp > 190 °C. ¹H NMR (400 MHz, CDCl₃): δ /ppm = 5.36 (br. s, 1 H, NH); 2.22 – 2.10 (m, 2 H); 1.95 – 1.82 (m, 4 H); 1.81 – 1.70 (m, 2 H); 1.65 – 1.50 (m, 4 H); 1.36 – 0.99 (m, 8 H); 0.88 (s, 6 H, 2 \times CH₃). ¹³C NMR (100 MHz, CDCl₃): δ /ppm = 176.2 (C=O), 170.0 (C=O), 54.0; 49.8, 47.6, 47.1, 46.7, 44.4, 35.4, 32.7, 29.6, 24.5. IR (KBr): $\tilde{\nu}$ /cm⁻¹ = 3357, 3289, 2960, 2909, 2864, 1702, 1646, 1612, 1570, 1562, 1235, 1147. MS (EI, 70 eV): m/z = 279, 221, 164 (100%), 150, 122, 107. HRMS found, 279.18348, calc. 279.18344.

1-Acetamido-3,5-dimethyltricyclo[3.3.1.1^{3,7}]decane (148): This acetamide is known from the literature.^[325] 6.572 g (40 mmol) 1,3-Dimethyladamantane (**135**) were

suspended in 8 mL nitric acid and cooled to 0 °C with an ice bath. 44 mL sulfuric acid were then added with an addition funnel over the course of 4 h at 0 °C and stirring was continued for another 2 h at 0 °C. 44 mL of technical grade acetonitrile were then added with an addition funnel within 90 min. To complete the reaction, the mixture was stirred 1 h at 0 °C and another 1 h at rt. Finally, the mixture was poured over ~ 250 g of crushed ice with shaking. The mixture was extracted with diethyl ether (3 × 100 mL), the combined organics were washed with water, 5% NaHCO₃, water and brine and dried (Na₂SO₄). After evaporation of the solvent, 7.99 g (36.11 mmol, 90.3%) of the acetamide **148** were obtained as a slightly yellowish powder, mp 109 °C (lit.^[325] 109 – 110 °C). **¹H NMR** (400 MHz, CDCl₃): δ/ppm = 5.27 (br s, 1 H, NH); 2.13 (quint, J = 3 Hz, 1 H); 1.90 (s, 3 H, CH₃); 1.83 (d, J = 3 Hz, 2 H); 1.68 – 1.58 (m, 4 H); 1.42 – 1.24 (m, 4 H); 1.21 – 1.08 (m, 2 H); 0.84 (s, 6 H, 2 × CH₃). **¹³C NMR** (100 MHz, CDCl₃): δ/ppm = 169.3 (C=O), 53.5 (C_q); 50.7, 47.6, 42.7, 40.2, 32.4, 30.2 (C_q), 30.1 (2 × CH₃), 24.7 (CH₃). **IR** (KBr): $\tilde{\nu}/\text{cm}^{-1}$ = 3294, 3259, 2945, 2904, 2862, 2843, 2834, 1653, 1632, 1556, 1455, 1359, 1310, 605. **MS** (EI, 70 eV): *m/z* = 221 (64.5%), 164 (100%), 150 (93.7%), 122 (15.6%), 107 (28.2%). **HRMS** found, 221.1773, calc. 222.1780.

1-Acetamido-3-methyltricyclo[3.3.1.1^{3,7}]decane (149): 0.751 g (5 mmol) 1-methyladamantane (**136**) were suspended in 1 mL nitric acid and cooled to 0 °C with an ice bath. 7 mL sulfuric acid were then added with an addition funnel over the course of 3 h at 0 °C and stirring was continued for another 3 h at 0 °C. 7 mL of technical grade acetonitrile were then added with an addition funnel within 1 h. To complete the reaction, the mixture was stirred 5 h at 0 °C. Finally, the mixture was poured over ~ 100 g of crushed ice with shaking. The mixture was extracted with diethyl ether (3 × 50 mL), the combined organics were washed with water, 5% NaHCO₃, water and brine and dried (Na₂SO₄). After evaporation of the solvent, the residue was purified by column chromatography eluting with diethyl ether (R_f = 0.30). 0.431 g (2.08 mmol, 41.6%) of the acetamide **149** were isolated as slightly yellowish powder, mp = 108 °C (lit.^[20] 108 – 109 °C). **¹H NMR** (400 MHz, CDCl₃): δ/ppm = 5.15 (br s, 1 H, NH); 2.13 – 2.08 (m, 2 H); 1.97 – 1.86 (m, 4 H); 1.90 (s, 3 H, CH₃); 1.70 (br s, 2 H); 1.66 – 1.49 (m, 2 H); 1.45 – 1.35 (m, 4 H); 0.83 (s, 3 H, CH₃). **¹³C NMR** (100 MHz, CDCl₃): δ/ppm = 169.3 (C=O), 52.7 (C_q), 48.4, 43.4, 41.0, 35.7, 31.9 (C_q), 30.4,

29.8 (CH₃), 24.7 (CH₃). **IR** (KBr): $\tilde{\nu}/\text{cm}^{-1}$ = 3286, 3078, 2944, 2910, 2862, 2841, 1639, 1559, 1456, 1371, 1306. **MS** (EI, 70 eV): m/z = 207 (35.9%), 150 (100%), 136 (13.5%), 108 (22.2%), 93 (11.3%). **HRMS** found, 207.1609, calc. 207.1623.

1-Acetamidotricyclo[3.3.1.1^{3,7}]decane (150) through Ritter-type reaction: 5.4492 g (40 mmol) adamantane (**137**) were suspended in 50 mL nitric acid and cooled to 0 °C with an ice bath. After the addition of 60 mL sulfuric acid, the mixture was stirred at 0 °C for 10 min. 40 mL of oleum (25% SO₃) were then added and the mixture was stirred for 1 h at 0 °C and 3 h at rt. After cooling to 0 °C, 40 mL of technical grade acetonitrile were added, the mixture was stirred for 10 min at 0 °C and 4 h at rt. Finally, the mixture was poured over ~ 600 g of ice with shaking. The mixture was extracted with diethyl ether (3 × 100 mL), the combined organics were washed with water, 5% NaHCO₃, water and brine and dried (Na₂SO₄). After evaporation of the solvent, the residue was purified by column chromatography eluting with diethyl ether (R_f = 0.29). 1.3301 g (6.88 mmol, 17.2%) of the acetamide **150** were isolated as slightly yellowish powder, mp = 142 °C (lit.^[28] 149 – 149.5 °C). **¹H NMR** (400 MHz, CDCl₃): δ/ppm = 5.18 (br s, 1 H, NH); 2.10 – 2.02 (m, 3 H); 2.02 – 1.94 (m, 6 H); 1.90 (s, 3 H, CH₃); 1.70 – 1.61 (m, 6 H). **¹³C NMR** (100 MHz, CDCl₃): δ/ppm = 169.4 (C=O), 52.0 (C_q), 41.7, 36.4, 29.5, 24.7. **IR** (KBr): $\tilde{\nu}/\text{cm}^{-1}$ = 3280, 3079, 2906, 2847, 1643, 1560, 1304. **MS** (EI, 70 eV): m/z = 193 (35.9%), 150 (6.9%), 136 (100%), 94 (46.6%). **HRMS** found, 193.1465, calc. 193,14666.

Attempted acetamidations of bicyclo[3.3.1]nonane (138), trans-decalin (139) and cis-decalin (140): The alkanes were suspended in technical nitric acid (65%) and the suspensions were cooled to 0 °C with an ice bath. Dropwise addition of technical sulfuric acid (95 – 98%) as described for the synthesis of **148** did in all cases not yield a homogeneous solution (two phases were observed). Increased stirring time and the addition of oleum according to the synthesis of **149** did not give significant changes. By the addition of technical grade acetonitrile and quenching with crushed ice with subsequent extraction (ethyl acetate) a mixture of the respective starting compounds **138** – **140** and a number of side products, but none of the compounds **151** – **153** could be detected by GC-MS analysis.

12.4. Synthesis of γ -Aminoadamantane-1-carboxylic Acids

General procedure: The respective precursors **141** – **146** were refluxed in concentrated hydrochloric acid (36 – 38%) / water as described below. After evaporation of the hydrochloric acid under reduced pressure to dryness, the crude products were treated with an organic solvent and collected via suction filtration. All compounds were dried in a desiccator over P₂O₅ and paraffine pellets at reduced pressure for 48 h.

3-aminotricyclo[3.3.1.1^{3,7}]decane-1-carboxylic acid hydrochloride (154): 12.396 g (52.2 mmol) **141**, 140 mL HCl, 60 mL water, 72 h reflux. Workup by treating the crude product with acetone. Yield: 10.58 g (45.7 mmol, 87.4%), mp 332 °C (lit.^[195] 338 – 340 °C). **(1) Hydrochloride:** ¹H NMR (400 MHz, d₆-DMSO): δ /ppm = 12.33 (br s, 1 H, CO₂H); 8.37 (br s, 3 H, NH₃Cl); 7.43 (t, J(¹⁵N-H) = 50.8 Hz); 2.23 – 2.14 (m, 2 H); 1.96 – 1.87 (m, 2 H); 1.86 – 1.70 (m, 6 H); 1.70 – 1.48 (m, 4 H). ¹³C NMR (100 MHz, CDCl₃): δ /ppm = 176.8 (C=O), 51.2 (C_q), 41.3, 41.0 (C_q), 38.9, 36.9, 34.1, 28.0. **IR** (KBr): $\tilde{\nu}$ /cm⁻¹ = 3391, 3144, 3103, 2924, 1700, 1601, 1510, 1227. ¹H NMR data are in accordance with the literature.^[143] The hydrochloride was neutralized by heating with an equimolar amount of NaOH in water. The zwitterion was then recrystallized from water and dried at 110 °C under reduced pressure over phosphorous pentaoxide. Mp > 355 °C (lit.^[326] > 300 °C) **(2) Zwitterion:** ¹H NMR (400 MHz, D₂O, 3-TMS-d₄-propanoic acid sodium salt): δ /ppm = 2.32 – 2.25 (m, 2 H); 1.96 – 1.91 (m, 2 H); 1.89 – 1.80 (m, 6 H); 1.75 – 1.60 (m, 4 H). ¹³C NMR (100 MHz, D₂O, 3-TMS-d₄-propanoic acid sodium salt): δ /ppm = 187.9 (C=O), 55.7 (C_q), 46.8 (C_q), 45.0, 42.0, 40.5, 36.8, 31.6. **IR** (KBr): $\tilde{\nu}$ /cm⁻¹ = 3438, 2929, 2898, 2858, 2634, 1620, 1547, 1511, 1391. **MS** (EI, 70 eV): m/z = 195 (46.7%), 150 (30.0%), 138 (63.5%), 108 (14.5%); 94 (100%). **HRMS** found, 195.1248, calc. 195.1259. **Elem. Anal.:** C₁₁H₁₇NO₂ (195.26): calcd. C 67.66, H 8.77, N 7.17; found C 67.57, H 8.94, N 7.21.

3-amino-5-methyltricyclo[3.3.1.1^{3,7}]decane-1-carboxylic acid hydrochloride (155): 3.015 g (12.9 mmol) of acetamide **142**, 100 mL HCl, 75 h reflux. Workup by treating the crude product with acetone. Yield: 2.545 g (10.4 mmol, 80.5%), mp 315 °C (lit.^[190] 320 – 322 °C). **(1) Hydrochloride:** ¹H NMR (400 MHz, d₆-DMSO): δ /ppm =

12.34 (br s, 1 H, CO₂H); 8.38 ppm (br s, 3 H, NH₃Cl); 7.39 (t, J(¹⁵N-H) = 50.8 Hz); 2.21 (br s, 1 H); 1.92 – 1.77 (m, 2 H); 1.77 – 1.56 (m, 4 H); 1.56 – 1.44 (m, 2 H); 1.44 – 1.24 (m, 4 H); 0.88 (s, 3 H, CH₃). ¹³C NMR (100 MHz, d₆-DMSO): δ /ppm = 176.7 (C=O), 51.8 (C_q), 45.6, 43.8, 42.0 (C_q), 41.2, 40.4, 38.2, 36.3, 31.4 (C_q), 29.3, 28.4. The hydrochloride was neutralized by heating with an equimolar amount of NaOH in water. The zwitterion was then recrystallized from water and dried at 110 °C under reduced pressure over phosphorous pentoxide. Mp 336 °C (lit.^[190] 338 – 339 °C). **(2) Zwitterion:** ¹H NMR (400 MHz, D₂O and d₆-DMSO): δ /ppm = 2.31 – 2.23 (m, 1 H); 1.88 – 1.76 (m, 2 H); 1.76 – 1.57 (m, 4 H); 1.57 – 1.46 (m, 2 H); 1.46 – 1.30 (m, 4 H); 0.92 (s, 3 H, CH₃). ¹³C NMR (100 MHz, D₂O and d₆-DMSO): δ /ppm = 184.3 (C=O), 54.8 (C_q), 47.3, 46.3, 45.7 (C_q), 43.2, 42.7, 39.7, 38.6, 33.4 (C_q), 30.9, 30.6. IR (KBr): $\tilde{\nu}$ /cm⁻¹ = 3416, 2942, 2912, 2860, 2153, 1635, 1558, 1530, 1389, 1350, 732. MS (EI, 70 eV): m/z = 209 (19.8%), 164 (40.1%), 152 (35.1%), 138 (14.2%), 122 (8.8%), 108 (100%), 94 (18.4%). HRMS found, 209.1409, calc. 209.1416. Elem. Anal.: C₁₂H₁₉NO₂ (209.28): calcd. C 68.87, H 9.15, N 6.69; found C 68.57, H 9.51, N 7.08.

3-amino-5,7-dimethyltricyclo[3.3.1.1^{3,7}]decane-1-carboxylic acid hydrochloride (156): 7.730 g (29.1 mmol) of acetamide **143**, 170 mL HCl, 80 h reflux. Workup by treating the crude product with ethyl acetate. Yield: 6.425 g (24.7 mmol, 84.9%), mp. 337 °C (lit.^[190] 346 – 347 °C). **(1) Hydrochloride:** ¹H NMR (400 MHz, d₆-DMSO): δ /ppm = 12.36 (br s, 1 H, CO₂H); 8.42 (br s, 3 H, NH₃Cl); 7.39 (t, J(¹⁵N-H) = 50.7 Hz); 1.79 (br s, 2 H); 1.53 – 1.32 (m, 8 H); 1.19 – 1.06 (m, 2 H); 0.89 (s, 6 H, 2 × CH₃). ¹³C NMR (100 MHz, d₆-DMSO): δ /ppm = 176.6 (C=O), 52.5 (C_q), 48.5, 44.9, 43.2, 42.6, 39.8 (C_q), 32.0 (C_q), 29.0 (2 × CH₃). The hydrochloride was neutralized by heating with an equimolar amount of NaOH in water. The zwitterion was then recrystallized from water and dried at 110 °C under reduced pressure over phosphorous pentoxide. Mp 337 °C (lit.^[190] 352 - 353 °C). **(2) Zwitterion:** ¹H NMR (400 MHz, D₂O, 3-TMS-d₄-propanoic acid sodium salt): δ /ppm = 1.80 (br s, 2 H); 1.55 – 1.40 (m, 8 H); 1.27 – 1.18 (m, 2 H); 0.90 (s, 6 H, 2 × CH₃). ¹³C NMR (100 MHz, D₂O 3-TMS-d₄-propanoic acid sodium salt): δ /ppm = 187.9 (C=O), 57.1 (C_q), 51.1, 48.3 (C_q), 48.0, 46.9, 44.0, 35.2 (C_q), 31.5 (2 × CH₃). IR (KBr): $\tilde{\nu}$ /cm⁻¹ = 3428, 2946, 2922, 2864, 2849, 2652, 2559, 2120, 1638, 1564, 1538, 1455, 1382, 1348, 726. MS (EI, 70 eV): m/z = 223 (9.7%), 178 (35.8%), 152 (34.6%), 134 (4.8%), 122 (100%), 108 (35.5%). HRMS

found, 223.1567, calc. 223.1572. **Elem. Anal.:** C₁₃H₂₁NO₂ (223.31): calcd. C 69.92, H 9.48, N 6.27; found C 69.72, H 9.67, N 6.34.

3-amino-5-(2-propyl)tricyclo[3.3.1.1^{3,7}]decane carboxylic acid hydrochloride (157): 1.276 g (4.57 mmol) of acetamide **144**, 20 mL HCl, 10 mL H₂O, 69 h reflux. Workup by treating the crude product with acetone. Yield: 657 mg (2.40 mmol, 52.5%), mp 274 °C. **¹H NMR** (400 MHz, d₆-DMSO): δ/ppm = 12.35 (br s, 1 H, CO₂H); 8.38 (br s, 3 H, NH₃⁺Cl); 7.41 (t, J(¹⁵N-H) = 43.6 Hz); 2.28 – 2.20 (m, 2 H); 1.91 – 1.27 (m, 11 H); 0.75 (d, J = 6.8 Hz, 6 H, 2 × CH₃). **¹³C NMR** (100 MHz, d₆-DMSO): δ/ppm = 176.9 (C=O), 52.1 (C_q), 41.8 (C_q), 40.8, 40.7, 38.9, 38.6, 36.7, 36.4 (C_q), 36.1, 36.0, 28.2, 16.2. **IR** (KBr): $\tilde{\nu}/\text{cm}^{-1}$ = 3442, 3006, 2945, 2860, 1734, 1702, 1472, 1200, 663. **MS** (EI, 70 eV): *m/z* = 237 (40.0%), 213 (27.9%), 194 (48.4%), 192 (81.1%), 180 (43.8%), 150 (33.6%), 136 (85.1%), 108 (14.0%), 94 (65.7%). **HRMS** found, 237.1732, calc. 237.1729 (M⁺ – HCl).

3-amino-5-carboxymethyltricyclo[3.3.1.1^{3,7}]decane-1-carboxylic acid hydrochloride (158): 1.846 g (6.24 mmol) of acetamide **145**, 70 mL HCl, 25 mL H₂O. Workup by treating the crude product with acetone. Yield: 1.662 g (5.74 mmol, 92%), mp 252 °C. **¹H NMR** (400 MHz, d₆-DMSO): δ/ppm = 12.28 (br s, 2 H, 2 × CO₂H); 8.33 (br s, 3 H, NH₃Cl); 2.27 – 2.19 (m, 1 H); 2.13 (s, 2 H, CH₂CO₂H); 1.94 – 1.78 (m, 2 H); 1.78 – 1.55 (m, 8 H); 1.53 – 1.42 (m, 2 H). **¹³C NMR** (100 MHz, d₆-DMSO): δ/ppm = 176.6 (C=O), 171.9 (C=O), 51.7 (C_q), 46.3, 43.1, 41.8, 41.6 (C_q), 40.4, 39.0, 38.3, 36.3, 33.7 (C_q), 28.2. **IR** (KBr): $\tilde{\nu}/\text{cm}^{-1}$ = 3427, 3020, 2938, 2863, 2598, 1726, 1709, 1368, 1200. **MS** (EI, 70 eV): *m/z* = 253 (37.6%), 208 (75.7%), 196 (30.8%), 166 (17.5%), 152 (70.2%), 138 (19.2%), 106 (43.1%). **HRMS** found, 253.1320, calc. 253.1314 (M⁺ – HCl). **Elem. Anal.:** C₁₃H₂₀ClNO₄ (289.60): calcd. C 53.89, H 6.96, N 4.83; found C 53.75, H 6.98, N 4.46.

3-amino-5-carboxytricyclo[3.3.1.1^{3,7}]decane-1-propanoic acid hydrochloride (159): 453 mg (1.47 mmol) of acetamide **146**, 10 mL HCl, 5 mL H₂O, 69 h reflux. Workup by treating the crude product with acetone. Yield: 375 mg (1.23 mmol, 83.9%), mp 265 °C. **¹H NMR** (400 MHz, d₆-DMSO): δ/ppm = 12.21 (br s, 2 H, 2 × CO₂H); 8.34 (br s, 3 H, NH₃Cl); 7.37 (t, J(¹⁵N-H) = 50.8 Hz); 2.28 – 2.19 (m, 1 H); 2.16

(t, $J = 8.0$ Hz, 2 H, $\text{CH}_2\text{CH}_2\text{CO}_2\text{H}$); 1.92 – 1.79 (m, 2 H); 1.78 – 1.22 (m, 10 H); 1.44 (t, $J = 8.2$ Hz, 2 H, $\text{CH}_2\text{CH}_2\text{CO}_2\text{H}$). ^{13}C NMR (100 MHz, d_6 -DMSO): $\delta/\text{ppm} = 176.7$ (C=O), 174.5 (C=O), 51.8 (C_q), 43.3, 42.0, 41.4, 40.6 (C_q), 38.6, 38.4, 36.8, 36.5, 33.8 (C_q), 28.2, 27.5. IR (KBr): $\tilde{\nu}/\text{cm}^{-1} = 3142, 2997, 2920, 2864, 2585, 1728, 1704, 1494, 1218, 1187, 1155, 667$. MS (EI, 70 eV): $m/z = 267$ (20.2%), 222 (44.0%), 204 (16.1%), 192 (22.3%), 180 (12.5%), 166 (39.0%), 148 (40.6%), 138 (16.7%), 120 (11.1%), 106 (16.5%). HRMS found, 267.1476, calc. 267.1471 ($\text{M}^+ - \text{HCl}$).

12.5. Direct C–H to C–N- amidations using amides as the nucleophiles

1-Formamido-3,5-dimethyltricyclo[3.3.1.1^{3,7}]decane (160): This compound is known from the literature.^[327] However, since it was neither isolated nor characterized and was prepared previously via a different route, its preparation and full characterization is reported here. 6.572 g (40 mmol) 1,3-dimethyladamantane (**135**) were suspended in 5 mL nitric acid and cooled to 0 °C with an ice bath. 50 mL sulfuric acid were then added with an addition funnel over the course of 1 h at 0 °C and stirring was continued for another 5 h at 0 °C. The mixture was then upon vigorous stirring and cooling with an ice bath poured into 100 mL of technical formamide. The resulting mixture was stirred under argon for 30 min at 0 °C and another 2 h at rt. After addition of 200 mL dichloromethane and 200 mL of water, the layers were separated. The aqueous phase was extracted twice with 100 mL of dichloromethane, the combined organics were washed with water (3 \times 200 mL) and brine (200 mL). After drying with Na_2SO_4 , the solvent was removed and the residual yellowish oil was purified via silica gel column chromatography eluting with ethyl acetate ($R_f = 0.42$) to yield 7.384 g (35.6 mmol, 89.0 %) of formamide **160** as a colorless powder, mp 69.5 °C. ^1H NMR (400 MHz, CDCl_3): $\delta/\text{ppm} = 8.14, 8.17, 7.98$ and 7.97 (4 \times s, 1 H, NHCHO); 6.72 – 6.31 and 5.51 – 5.23 (m / br s, 1 H, NHCHO); 2.24 – 2.10 (m, 1 H); 1.89 – 1.83 (m, 1 H); 1.72 – 1.63 (m, 3 H); 1.51 – 1.40 (m, 2 H); 1.39 – 1.30 (m, 4 H); 1.20 – 1.13 (m, 1 H); 0.83 and 0.81 (2 s, 6 H, CH_3). ^{13}C NMR (100 MHz, CDCl_3): $\delta/\text{ppm} = 162.3$ and 160.4 (C=O), 53.6 and 52.3 (C_q), 50.5 and 50.1, 47.7, 42.6 and 42.5, 40.3, 32.5 and 32.4 (C_q), 30.04 and 29.95. IR (KBr): $\tilde{\nu}/\text{cm}^{-1} = 3198, 3103, 2946, 2909, 2864, 2847, 1691, 1451, 1326, 795$. MS (EI, 70 eV): $m/z = 207$ (53.3%), 192 (6.6%), 162 (7.6%), 150 (100%), 136 (90.9%), 106 (9.9%). HRMS found,

207.1617, calc. 207.1623. **Elem. Anal.:** C₁₃H₂₁NO (207.31): calcd. C 75.32, H 10.21, N 6.76; found C 75.06, H 10.42, N 6.71.

1-Formamido-3-methyltricyclo[3.3.1.1^{3,7}]decane (161): 1.503 g (10 mmol) 1-methyladamantane (**136**) were suspended in 1 mL of nitric acid and cooled to 0 °C with an ice bath. 25 mL of sulfuric acid were then added with an addition funnel over the course of 3 h and stirring was continued at 0 °C for another 3 h. The mixture was then upon intensive stirring and cooling to 0 °C added to 50 mL technical formamide. The resulting mixture was stirred at 0 °C for 30 min and another 2 h at rt. The resulting mixture was extracted with dichloromethane (3 × 100 mL), the combined organics were washed with water and dried (Na₂SO₄). After evaporation of the solvent, the residue was purified by column chromatography eluting with ethyl acetate, R_f (**161**) = 0.37. 0.864 g (45%) 1-formamido-3-methyladamantane were isolated as a colorless solid, mp = 66 °C (sealed capillary). **¹H NMR** (200 MHz, CDCl₃): δ/ppm = 8.25 (d, J = 12.4 Hz) and 8.05 (d, J = 9.0 Hz), 1 H, NHCHO (2 isomers); 6.62 (bs) and 5.33 (bs), 1 H, NHCHO (2 isomers); 2.22 – 1.33 (m, 14 H, CH/CH₂ of adamantane); 0.87 (s) and 0.85 (s), 3 H, -CH₃ (2 isomers). **¹³C NMR** (50 MHz, CDCl₃): δ/ppm = 162.6 and 160.4 (C=O), 53.0 and 51.6, 50.7 and 48.4, 43.3 and 43.2, 42.9 and 41.1, 35.5 and 35.1, 32.0 and 31.9, 30.4 and 30.3, 29.7 and 29.6 (2 isomers). **IR** (KBr): $\tilde{\nu}$ /cm⁻¹ = 3439, 3211, 3083, 2902, 2849, 1696, 1675, 1536, 1456, 1313. **MS** (EI, 70 eV): m/z = 193 (66.5%), 178 (2.9%), 148 (5.7%), 136 (100%), 122 (18.4%), 108 (11.6%), 92 (19.8%). **HRMS** found, 193.14625, calc. 193.14666. **Elem. Anal.:** C₁₂H₁₉NO (193.29): calcd. C 74.57, H 9.91, N 7.25; found C 74.62, H 10.04, N 7.05.

1-Formamidotricyclo[3.3.1.1^{3,7}]decane (162): 2.725 g (20 mmol) adamantane **137** were suspended in 2 mL nitric acid and cooled to 0 °C with an ice bath. 25 mL sulfuric acid were added within 10 min and stirring at 0 °C was continued for another 10 min. 5 mL oleum (25% SO₃) were then added, the reaction vessel was closed and intensively stirred for 18 h at 0 °C. The resulting mixture was added to 50 mL of technical formamide under vigorous stirring within 30 min at 0 °C. Stirring was continued for 30 min at 0 °C and 90 min at rt, whereupon 100 mL of dichloromethane and 100 mL ice water were added. The layers were separated, the aqueous layer was extracted with dichloromethane, the combined organics were washed with water,

5% NaHCO₃ and brine (50 mL each) and dried (Na₂SO₄). The yellowish oil obtained after evaporation was purified by silica gel column chromatography eluting with ethyl acetate, R_f (**162**) = 0.33. 480 mg (13%) 1-formamidoadamantane were isolated as slightly yellowish powder, mp = 134 °C (lit.^[28] 139.4 – 141.5 °C). ¹H NMR (200 MHz, d₆-DMSO): δ /ppm = 8.28 (d, J = 12.5 Hz) and 8.03 (d, J = 1.9 Hz, 1 H, NHCHO, 2 isomers), 6.21 and 5.24 (br s, 1 H, NHCHO, 2 isomers), 2.24 – 1.44 ppm (m, 15 H, CH-/CH₂). ¹³C NMR (50 MHz, d₆-DMSO): δ /ppm = 162.4 and 160.33 (C_q, NHCHO); 52.2 and 50.8 (C_q, C-NHCHO), 44.1, 41.8, 36.2 and 35.9, 29.4 and 29.3. ¹H-NMR data are in accordance with the literature.^[328]

1-Acetamidotricyclo[3.3.1.1^{3,7}]decane (150) through direct amidation with acetamide: 2.725 g (20 mmol) adamantane (**137**) were suspended in 2 mL nitric acid and cooled to 0 °C with an ice bath. Within 10 min, 25 mL sulfuric acid were added and stirring was continued for 10 min at 0 °C. 10 mL oleum (25% SO₃) were added, the reaction vessel was closed and stirring at 0 °C was continued for 18 h. The resulting mixture was added within 30 min at 0 °C to 20 g of solid acetamide upon vigorous stirring. Stirring was continued for 30 min at 0 °C and 90 min at rt. 100 mL dichloromethane and 100 mL ice water were added, the layers were separated and the aqueous layer was extracted with dichloromethane (2 × 20 mL). The combined organics were washed with water, 5% NaHCO₃ and brine (50 mL each) and dried with Na₂SO₄. After evaporation of the solvent, the residual yellowish oil was purified by silica gel column chromatography eluting with diethyl ether, R_f (**150**) = 0.29. 1.448 g (38%) of **150** were isolated as slightly yellowish powder, mp 143.5 °C. The spectroscopic data are in accordance with those obtained for **150** obtained by method (a).

12.6. Oxyfunctionalizations

3,5-Dimethyltricyclo[3.3.1.1^{3,7}]decane-1-ol (163): 6.572 (40 mmol) 1,3-dimethyladamantane (**135**) were mixed with 8 mL of nitric acid and cooled to 0 °C with an ice bath. 44 mL sulfuric acid were added via an addition funnel within 2 h at and stirring at 0 °C was continued for 3h. The mixture was poured over ~800 g ice and the colorless precipitate was collected via suction filtration and dried over P₂O₅ under reduced pressure. 5.846 g (81%) of **163** were isolated as a colorless powder, mp. 94

°C (lit.^[329] 96.8 – 97.1 °C. ¹H NMR (400 MHz, CDCl₃): δ/ppm = 2.19 (sept., J = 3.2 Hz, 1 H, CH); 1.58 – 1.54 (m, 2 H, adamantane-CH₂); 1.53, br. s, 1 H, -OH; 1.42 – 1.18 (m, 8 H, 4 × adamantane-CH₂); 1.11 (s, 2 H, adamantane-CH₂); 0.87 (s, 6 H, 2 × CH₃). ¹³C NMR (100 MHz, CDCl₃): δ/ppm = 69.9 (C-OH), 51.5, 50.5, 43.8, 42.5, 33.8 (C_q), 31.1, 29.9. ¹³C NMR shifts are in accordance with literature values.^[330]

3-Hydroxytricyclo[3.3.1.1^{3,7}]decane-1-carboxylic acid (164): 7.210 g (40 mmol) **128** were suspended in 4 mL nitric acid at 0 °C. Upon stirring, 50 mL sulfuric acid were added within 2 h at 0 °C. Stirring at 0 °C was continued for another 3 h and the mixture was poured over ~100 g of ice. The colorless precipitate was collected via suction filtration, washed with water and dried over P₂O₅ in a desiccator at reduced pressure. 5.507 g (70%) **164** were isolated. ¹H NMR (200 MHz, d₆-DMSO): δ/ppm = 7.19 (br s, 3 H, CO₂H and OH); 2.19 – 2.01 (m, 2 H, adamantane-CH₂) 1.63 – 1.54 (m, 6 H, 3 × adamantane-CH₂); 1.54 – 1.40 (m, 6 H, adamantane-CH₂). ¹³C NMR (50 MHz, d₆-DMSO): δ/ppm = 177.7 (CO₂H), 66.3 (C-OH), 46.5 (C-CO₂H), 44.2, 42.8, 37.6, 34.8, 29.7. ¹H-NMR data are in accordance with the literature.^[331]

3,5-dimethyltricyclo[3.3.1.1^{3,7}]decane-1-yl-methyl ether (165): 1.643 g (10 mmol) **135** were mixed with 1 mL nitric acid at 0 °C. 12.5 mL sulfuric acid were added with an addition funnel over the course of 3 h upon stirring at 0 °C. Stirring was continued for another 3 h, whereupon the mixture was added to 25 mL of methanol upon cooling to 0 °C. The mixture was stirred at 0 °C for 30 min and at rt for 90 min. 50 mL dichloromethane and 50 mL water were added, the layers were separated and the aqueous layer was extracted with dichloromethane (3 × 20 mL). The combined organics were washed with water, 5% NaHCO₃ and brine (50 mL each) and dried (Na₂SO₄). The slightly yellowish oil obtained after evaporation of the solvent was purified by silica gel column chromatography eluting with *n*-pentane/diethyl ether (95:5), R_f (**165**) = 0.22. 0.735 g (38%) **165** were isolated as a colorless liquid. ¹H NMR (400 MHz, CDCl₃): δ/ppm = 3.23 (s, 3 H, OCH₃); 2.20 (sept., J = 3.0 Hz, adamantane-CH); 1.60 – 1.55 (m, 2 H, adamantane-CH₂); 1.43 – 1.24 (m, 8 H, adamantane-CH₂); 1.12 (br s, 2 H, adamantane-CH₂); 0.87 (s, 6 H, 2 × CH₃). ¹³C NMR (100 MHz, CDCl₃): δ/ppm = 73.6 (COCH₃), 50.8 (CH₂), 48.0 (OCH₃), 47.0 (CH₂), 42.8 (CH₂), 39.4 (CH₂), 33.4 (C-CH₃), 30.8 (CH₃), 30.1 (CH). IR (film): $\tilde{\nu}$ /cm⁻¹

= 2945, 2920, 2902, 2863, 2845, 1455, 1197, 10095, 1089. **MS** (EI, 70 eV): m/z = 194 (35.6%), 163 (41.8%), 137 (96.1%), 107 (28.6%). **HRMS** found, 194.16664, calc. 194.16707. **Elem. Anal.**: C₁₃H₂₂O (194.31): calcd. C 80.72, H 11.73; found C 80.42, H 11.72.

3,5-dimethyltricyclo[3.3.1.1^{3,7}]decane-1-yl-ethyl ether (166): 1.643 g (10 mmol) **135** were mixed with 1 mL nitric acid at 0 °C. 12.5 mL sulfuric acid were added with an addition funnel over the course of 3 h upon stirring at 0 °C. Stirring was continued for another 3 h, whereupon the mixture was added to 25 mL of absolute ethanol upon cooling to 0 °C. The mixture was stirred at 0 °C for 30 min and at rt for 90 min. 50 mL dichloromethane and 50 mL water were added, the layers were separated and the aqueous layer was extracted with dichloromethane (3 × 20 mL). The combined organics were washed with water, 5% NaHCO₃ and brine (50 mL each) and dried (Na₂SO₄). The slightly yellowish oil obtained after evaporation of the solvent was purified by silica gel column chromatography eluting with *n*-pentane/diethyl ether (95:5), R_f (**166**) = 0.24. 0.1724 g (8.3%) **166** were isolated as a colorless liquid. **¹H NMR** (200 MHz, CDCl₃): δ /ppm = 3.46 (q, J = 6.1 Hz, 2 H, OCH₂-CH₃); 2.19 (sept., J = 3.0 Hz, adamantane-CH); 1.60 – 1.55 (m, 2 H, adamantane-CH₂); 1.43 – 1.24 (m, 15 H, adamantane-CH₂ and -CH₂CH₃); 0.86 (s, 6 H, 2 × CH₃). **¹³C NMR** (50 MHz, CDCl₃): δ /ppm = 73.6 (COC₂H₅), 55.2, 50.8, 47.8, 42.9, 40.1, 33.4, 30.9, 30.2 (CH), 16.4 (-CH₂CH₃). **IR** (film): $\tilde{\nu}$ /cm⁻¹ = 2973, 2946, 2902, 2864, 2845, 1455, 1187, 1115, 1087. **MS** (EI, 70 eV): m/z = 208, 193, 163, 151 (100%), 137, 123, 109, 107. **HRMS** found, 208.18317, calc. 208.18272. **Elem. Anal.**: C₁₄H₂₄O (208.34): calcd. C 80.71, H 11.61; found C 80.98, H 11.90.

12.7. PTC halogenations and subsequent conversions

1-Iodo-3-bromo-5,7-dimethyltricyclo[3.3.1.1^{3,7}]decane (168a): 2.432 g (10 mmol) of 1-bromo-3,5-dimethyladamantane, 15.76 g (40 mmol) CHI₃, 10 g powdered NaOH and 484 mg (15 mol%) of tetra-*n*-butylammonium bromide were mixed with 80 mL of fluorobenzene in a 250 mL flask. The flask was equipped with a condenser, put into an ultrasonic cleaning bath (Bender & Hobein Laboson 200) and agitated at 45 °C. After 3, 4, 5, 6, 7 and 8 days the mixture was filtered through a glass frit and the solvent was evaporated under reduced pressure. The residue was then mixed with

the same amount of reagents as described above. After a total 9 days of agitation the mixture was worked up as described above and purified through silica gel column chromatography eluting with *n*-pentane, $R_f = 0.31$. After evaporation of the solvent, 2.192 g (5.94 mmol, 59.4%) of **168a** were isolated as a colorless powder, mp 98 – 99 °C. **¹H NMR** (400 MHz, CDCl₃): δ /ppm = 2.91 (br s, 2 H); 2.28 – 2.14 (m, 4 H); 2.03 (br s, 4 H); 1.38 – 1.19 (m, 2 H); 0.89 (s, 6 H, 2 × CH₃). **¹³C NMR** (100 MHz, CDCl₃): δ /ppm = 61.5 (C_q), 60.1, 56.0, 53.1, 48.0, 43.1 (C_q), 39.1 (2 × C_q), 28.8 (2 × CH₃). **IR** (KBr): ν /cm⁻¹ = 2951, 2924, 2863, 2841, 1452, 1442, 1315, 1167, 891, 828, 703. **MS** (EI, 70 eV): m/z = 289 (4.4%, M⁺ – Br), 243 / 241 (100%, M⁺ – I), 185 (15.6%), 161 (42.2%), 119 (20.0%). **Elem. Anal.**: C₁₂H₁₈BrI (369.08): calcd. C 39.05, H 4.91; found C 39.14, H 4.72.

1-Iodo-3-bromo-5-(1'-methyl)ethyltricyclo[3.3.1.1^{3,7}]decane (168b): 3.858 g (15 mmol) 1-bromo-3-(1'-methyl)ethyladamantane, 29.5 g (75 mmol) CHI₃, 730 mg (2.25 mmol) tetra-*n*-butylammonium bromide and 21 g powdered NaOH were suspended in 80 mL fluorobenzene, equipped with a condenser, put into an ultrasonic cleaning bath and agitated at 45 °C for 16 h. The mixture was filtered through a glass frit and the solvent was evaporated under reduced pressure. The reaction was restarted twice with the same amounts of solvent and reagent. The residue was then purified by silica gel column chromatography eluting with *n*-pentane, $R_f = 0.31$. After evaporation of the solvent, 0.93 g (2.42 mmol, 16.2 %) of **168b** were isolated as a colorless powder. NMR and GC/MS analyses proved the identity of the product that was used for further conversions without additional purification. **¹H NMR** (400 MHz, CDCl₃): δ /ppm = 3.09 – 2.95 (m, 2 H); 2.54 – 2.35 (m, 2 H); 2.34 – 2.18 (m, 4 H); 2.19 – 2.06 (m, 3 H); 1.61 – 1.50 (m, 2 H); 1.34 (sept, $J = 7.0$ Hz, 1 H, CH(CH₃)₂); 0.84 (d, $J = 7.0$ Hz, 6 H, CH(CH₃)₂). **¹³C NMR** (100 MHz, CDCl₃): δ /ppm = 62.9 (C_q), 61.5, 52.1, 49.6, 49.2, 46.8, 44.9 (C_q), 44.7 (C_q), 36.9, 35.5, 35.45, 16.4. **MS** (HP 5971): m/z = 303 (4%, M⁺ – Br), 257 / 255 (100%, M⁺ – I), 175 (56%), 91 (77%).

1-Bromo-3-acetamido-5,7-dimethyltricyclo[3.3.1.1^{3,7}]decane (169a): 58.4 mg (0.5 mmol) NOBF₄ were suspended in 3 mL of dry acetonitrile and cooled to –50 °C. 185 mg (0.5 mmol) **168a** in 15 mL dry acetonitrile were slowly added and the resulting mixture was stirred under argon upon warming to –15 °C within ~2 h. The mixture

was then quenched with 20 mL water and extracted three times with 20 mL diethyl ether. The combined organics were washed with saturated NaHSO₃ (2 × 20 mL) until the organic layer turned colorless. After washing with water (5 × 20 mL) and brine (20 mL), the solution was dried (Na₂SO₄). The solvents were then evaporated under reduced pressure and the residue was purified by silica gel column chromatography eluting with diethyl ether, R_f = 0.27. After evaporation of the solvent, 142 mg (0.47 mmol, 94.4%) of **169a** were collected as a colorless powder, mp. 178 – 179 °C. **¹H NMR** (400 MHz, CDCl₃): δ /ppm = 5.24 (br s, 1 H, NH); 2.49 – 2.42 (m, 2 H); 2.03 – 1.88 (m, 4 H); 1.91 (s, 3 H, COCH₃); 1.78 – 1.58 (m, 4 H); 1.25 – 1.14 (m, 2 H); 0.92 (s, 6 H, 2 × CH₃). **¹³C NMR** (100 MHz, CDCl₃): δ /ppm = 169.4 (C=O), 62.7 (C_q), 55.3 (C_q), 54.0, 50.8, 48.9, 46.0, 35.8 (2 × C_q), 29.0 (2 × CH₃), 24.5 (COCH₃). **IR** (KBr): $\tilde{\nu}$ /cm⁻¹ = 3295, 3081, 2947, 2928, 2902, 2865, 1676, 1655, 1639, 1558, 1370, 1323, 606. **MS** (EI, 70 eV): m/z = 301 (2.8%), 299 (2.6%), 220 (100%), 178 (19.5%), 164 (26.7%), 121 (25.9%), 105 (9.7%). **HRMS** found, 299.0906, calc. 299.0884. **Elem. Anal.**: C₁₄H₂₂BrNO (300.23): calcd. C 56.00, H 7.38, N 4.66; found C 55.84, H 7.35, N 4.59.

1-Bromo-3-acetamido-5-(1'methyl)ethyltricyclo[3.3.1.1^{3,7}]decane (169b): 230 mg (1.93 mmol) NOBF₄ were suspended in dry acetonitrile and cooled to –50 °C. A solution of 740 mg (1.93 mmol) **168b** was slowly added and the resulting mixture was stirred under argon upon warming to 0 °C within ~2 h. The mixture was then quenched with 20 mL water and extracted three times with 20 mL diethyl ether. The combined organics were washed with saturated NaHSO₃ (2 × 20 mL) until the organic layer turned colorless. After washing with water (5 × 20 mL) and brine (20 mL), the solution was dried (Na₂SO₄). The solvents were then evaporated under reduced pressure and the residue was purified by silica gel column chromatography eluting with ethyl acetate / *n*-hexane (1 : 1), R_f = 0.26. After evaporation of the eluent, 400 mg (1.27 mmol, 65.9%) of **169b** were obtained as a colorless powder, mp. 135 °C. **¹H NMR** (400 MHz, CDCl₃): δ /ppm = 5.27 (br s, 1 H, NH); 2.63 – 2.49 (m, 2 H); 2.30 – 2.13 (m, 3 H); 2.09 – 1.97 (m, 3 H); 1.92 (s, 3 H, COCH₃); 1.87 – 1.66 (m, 3 H); 1.45 (br s, 2 H); 1.37 (sept, J = 7.0 Hz, CH(CH₃)₂); 0.85 (d, J = 7.0 Hz, 6 H, CH(CH₃)₂). **¹³C NMR** (100 MHz, CDCl₃): δ /ppm = 169.3 (C=O), 64.1 (C_q), 55.0 (C_q), 52.0, 50.0, 47.6, 42.0, 41.1 (C_q), 39.5, 36.8, 36.3, 32.1, 24.6 (COCH₃), 16.6 (CH(CH₃)₂). **IR** (KBr):

$\tilde{\nu}/\text{cm}^{-1}$ = 3266, 3085, 2977, 2957, 2933, 2922, 2867, 1654, 1638, 1566, 1370, 606.

MS (EI, 70 eV): m/z = 315 (0.7%), 313 (0.7%), 234 (100%), 220 (8.3%), 192 (27.5%), 175 (16.7%), 150 (14.8%), 136 (12.0%), 119 (7.8%), 108 (8.5%), 93 (15.8%). **HRMS** found, 313.1040, calc. 313.1041 **Elem. Anal.:** C₁₅H₂₄BrNO (314.26): calcd. C 57.33, H 7.70, N 4.46; found C 57.39, H 7.68, N 4.80.

3-Acetamido-5,7-dimethyltricyclo[3.3.1.1^{3,7}]decane-1-carboxylic acid (143) via Koch-Haaf-reaction:^[199, 202] In a 250 mL round-bottomed flask, 600 mg (2 mmol) of the bromo acetamide **169a** were dissolved in 80 mL concentrated sulfuric acid (95 – 98%). The solution had an intense, red-brown color. 40 mL formic acid (100%) were then slowly added upon stirring at room temperature over the course of 4.5 h. The reaction mixture was then poured over ~ 500 g of crushed ice upon shaking. A colorless precipitate formed slowly, that was collected via suction filtration the next day. The crude product was dissolved in 5% NaOH, filtered, and precipitated through the addition of concentrated hydrochloric acid (pH ~ 4). This precipitate was again collected via suction filtration, dried in a desiccator over CaCl₂ over night under reduced pressure, and recrystallized from water / glacial acetic acid / acetone (5 : 5 : 4). After drying over KOH *in vacuo* at 90 °C, 329 mg (1.24 mmol, 62.1%) of the acetamide **143** were obtained as colorless crystals. Analytical data of the sample made using this procedure were in accordance with the data obtained from **143** prepared by acetamidation (*vide supra*).

3-Acetamido-5-isopropyltricyclo[3.3.1.1^{3,7}]decane-1-carboxylic acid (144) via Koch-Haaf-reaction: Using the same procedure as described above for **143**, bromo acetamide **169b** was converted to the acetyl amino acid **144** in 2.0 mmol scale and 72% yield. Analytical data of this sample were in accordance with **144** synthesized via the direct acetamidation protocol (*vide supra*).

1-Bromo-3-phenyltricyclo[3.3.1.1^{3,7}]decane (171): 1-Phenyladamantane **170** was brominated by modifying a known procedure.^[194] 849.4 mg (4 mmol) 1-phenyladamantane were dissolved in 45 mL fluorobenzene. 207 mg (0.64 mmol, 16 mol-%) of tetra-n-butylammonium bromide (TBABr) were added, whereupon 14 mL of freshly prepared 50% aq. NaOH were added. The two-phase system was intensively stirred at room temperature (ca. 22 °C) for 11.5 days. The reaction mixture was

diluted with water and dichloromethane, the aqueous layer was extracted with dichloromethane and the combined organics were dried (Na_2SO_4). After filtration, the solvents were removed in vacuo using a rotary evaporator, and the residue was purified by silica gel column chromatography (3.0 x 70 cm) eluting with n-pentane, R_f (**170**) = 0.19. After evaporation of the eluent, 825.5 mg (2.83 mmol, 70.9%) of bromide **170** were isolated. The spectral data were in accordance with the literature.^[194]

1-Bromo-5-phenyl-3-acetamidotricyclo[3.3.1.1^{3,7}]decane (173): In an oven-dried two-neck 100 mL flask equipped with a thermometer, an addition funnel, and an argon inlet, 315 mg (2.7 mmol, 1.04 equivalents) of NOBF_4 were suspended in 7 mL dry acetonitrile. The reaction mixture was cooled to $-50\text{ }^\circ\text{C}$ with methanol / liquid nitrogen and a solution of 1.084 g (2.6 mmol) of phenyl-bromoiodoadamantane **172** in 20 mL dry acetonitrile was added over the course of 1 h upon stirring. The reaction mixture was then gradually warmed, and at $-15\text{ }^\circ\text{C}$ the reaction mixture became dark brown in color. The mixture was quenched with water at $-10\text{ }^\circ\text{C}$, brine and diethyl ether were added, the layers were separated and the aqueous layer was extracted with diethyl ether (3 x 100 mL). The combined organics were washed with NaHSO_3 -solution, water, and brine, and dried with Na_2SO_4 . After filtration and evaporation of the solvents, the residue was purified via silica gel column chromatography (3.0 x 60 cm) eluting with diethyl ether, R_f (**173**) = 0.30. After evaporation of the eluent, 765 mg (2.2 mmol, 84.5%) of the bromo acetamide **173** were isolated as a colorless powder, mp $150.5\text{ }^\circ\text{C}$. **$^1\text{H NMR}$** (400 MHz, CDCl_3): δ/ppm = 7.36 – 7.11 (m, 5 H, H_{Ar}); 5.25 (br. s, 1 H, NH); 2.78 – 2.55 (m, 2 H); 2.52 – 1.90 (m, 7 H); 1.89 (br. s, 4 H); 1.88 (s, 3 H, $-\text{CH}_3$). **$^{13}\text{C NMR}$** (100 MHz, CDCl_3): δ/ppm = 169.4 (C=O), 147.2 (C_q), 128.5, 126.5, 124.8, 62.4 (C-Br), 55.1, 53.3, 51.6, 47.2, 45.4, 41.9, 40.3, 39.2, 32.8, 24.5 (CH_3). **IR** (KBr): $\tilde{\nu}/\text{cm}^{-1}$ = 3271, 3068, 2937, 2914, 2861, 1653, 1637, 1558, 1371, 699. **HRMS** found, 347.0911, calc. 347.08848. **Elem. Anal.:** $\text{C}_{18}\text{H}_{22}\text{BrNO}$ (348.28): calcd. C 62.07, H 6.37, N 4.02; found C 62.23, H 6.12, N 4.17.

3-Acetamidotricyclo[3.3.1.1^{3,7}]decane-1-carboxylic acid tert. butyl ester (175a): In an oven-dried 250 mL flask under argon, 11.865 g (50 mmol) of acetamide **141** were suspended in 100 mL dry THF. 7.03 mL (50 mmol) dry triethylamine were added

and the mixture was refluxed for 45 min. After cooling to rt, 3.65 mL (50 mmol) of freshly distilled SOCl_2 were added and the mixture was refluxed another 45 min. After cooling to rt, 50 mL *tert.* butanol were added and the reaction mixture was heated another 2 h under reflux. The mixture was then cooled to rt and 150 mL water were added. Extraction with ethyl acetate (3×100 mL), washing of the combined organics with water, sat. NaHCO_3 , water and brine (100 mL each), drying (Na_2SO_4) and evaporation of the solvents under reduced pressure yielded a yellowish oil, that was purified by silica gel column chromatography eluting with *tert.* butyl methyl ether, $R_f = 0.28$. After evaporation of the eluent, 7.383 g (25.2 mmol, 50.3%) of **175a** were obtained as a colorless powder, mp 129.5 – 130.5 °C. $^1\text{H NMR}$ (400 MHz, CDCl_3): $\delta/\text{ppm} = 5.23$ (br s, 1 H, *NH*); 2.09 – 2.03 (m, 2 H); 2.02 – 1.92 (m, 4 H); 1.91 (s, 3 H, COCH_3); 1.86 – 1.73 (m, 4 H); 1.69 – 1.55 (m, 2 H); 1.42 (s, 9 H, $\text{C}(\text{CH}_3)_3$). $^{13}\text{C NMR}$ (100 MHz, CDCl_3): $\delta/\text{ppm} = 175.8$ (C=O), 169.3 (C=O), 79.9 ($\text{C}(\text{CH}_3)_3$), 52.2 (C_q), 43.1 (C_q), 42.7, 40.8, 38.0, 35.4, 29.2, 28.0 ($\text{C}(\text{CH}_3)_3$), 24.7 (COCH_3). **IR** (KBr): $\tilde{\nu}/\text{cm}^{-1} = 3277, 3207, 3085, 2955, 2918, 2863, 1723, 1648, 1561, 1269, 1242, 1172, 1139, 850$. **MS** (EI, 70 eV): $m/z = 293$ (9.6%), 237 (27.9%), 192 (100%), 150 (79.5%), 136 (30.1%), 129 (18.7%), 94 (34.5%). **HRMS** found, 293.1942, calc. 293.1991. **Elem. Anal.**: $\text{C}_{17}\text{H}_{27}\text{NO}_3$ (293.40): calcd. C 69.59, H 9.27, N 4.77; found C 69.54, H 9.43, N 4.93.

3-Acetamidotricyclo[3.3.1.1^{3,7}]decane-1-carboxylic acid methyl ester (175b): Acetamide **141** was esterified with diazomethane following a standard procedure. 12.3696 g (120 mmol, 12 eq.) N-nitroso-N-methyl urea were added to a mixture of 100 mL 40% KOH and 200 mL diethylether at 0 °C. After 10 min stirring at 0 °C, the yellow ethereal phase was separated and dried over solid KOH. This diazomethane solution was then added to a suspension of **141** in aqueous methanol at rt upon stirring until the yellow color of diazomethane continued to be visible. The mixture was stirred for another 30 min at rt. After evaporation of the solvents, the crude product was purified via silica gel column chromatography (3.0 x 30 cm) eluting with *tert.* butyl methyl ether, $R_f = 0.15$. After evaporation of the eluent, 2.510 g (99.9%) of the methyl ester **175b** were isolated as a colorless powder, mp 123.5 °C. $^1\text{H NMR}$ (400 MHz, CDCl_3): $\delta/\text{ppm} = 5.38$ (br. s, 1 H, *NH*); 3.65 (s, 3 H, CO_2CH_3); 2.28 – 2.17 (m, 2 H); 2.17 – 2.11 (m, 2 H); 2.06 – 1.88 (m, 4 H); 1.91 (s, 3 H, COCH_3); 1.88 – 1.78

(m, 4 H); 1.72 – 1.56 (m, 2 H). $^{13}\text{C NMR}$ (100 MHz, CDCl_3): δ/ppm = 176.9 (CO_2CH_3), 169.4 (NHCO), 51.9, 51.6, 42.5, 42.4, 40.6, 37.8, 35.3, 29.0 (CH), 24.5 (NHCOCH_3). **IR** (KBr): $\tilde{\nu}/\text{cm}^{-1}$ = 3280, 3085, 2948, 2915, 2856, 1736, 1649, 1633, 1559, 1245, 1222. **HRMS** found, 251.15398, calc. 251.15214. **Elem. Anal.**: $\text{C}_{14}\text{H}_{21}\text{NO}_3$ (251.32): calcd. C 66.91, H 8.42, N 5.57; found C 66.81, H 8.82, N 5.16.

3-Bromo-5-acetamidotricyclo[3.3.1.1^{3,7}]decane-1-carboxylic acid tert. butylester (176): A mixture of 586 mg (2 mmol) **175a**, 3.0 g, (9 mmol) CBr_4 , and tetra-*n*-butylammonium bromide (96 mg, 15 mol%) was dissolved in 20 mL of fluorobenzene and 10 mL NaOH (50% aq.) were added. The mixture was stirred intensively at 50 °C for 6 d in a 50 mL flask equipped with a condenser, then diluted with water and extracted with ethyl acetate. The extract was washed with water and dried (Na_2SO_4). The filtrate was concentrated under reduced pressure and the reaction was restarted with the same amounts of solvents and reagents as above and kept stirring at 50 °C for another 5 d. After workup as described above, the residue was purified by silica gel column chromatography eluting with ethyl acetate, R_f = 0.42. After evaporation of the eluent under reduced pressure, 100.5 mg (2.7 mmol, 13.5%) of **176** were collected as a colorless powder, mp 140.5 °C. $^1\text{H NMR}$ (400 MHz, CDCl_3): δ/ppm = 5.32 (br s, 1 H, *NH*); 2.65 – 2.53 (m, 2 H); 2.44 – 2.33 (m, 2 H); 2.33 – 2.28 (m, 1 H); 2.28 – 2.00 (m, 6 H); 1.93 (s, 3 H, COCH_3); 1.85 – 1.77 (m, 2 H); 1.43 (s, 9 H, $\text{C}(\text{CH}_3)_3$). $^{13}\text{C NMR}$ (100 MHz, CDCl_3): δ/ppm = 173.6 ($\text{C}=\text{O}$), 169.4 ($\text{C}=\text{O}$), 80.8 ($\text{C}(\text{CH}_3)_3$), 61.1 (C_q), 54.3 (C_q), 51.4, 48.8, 46.9, 46.1 (C_q), 41.3, 39.0, 36.4, 31.6, 28.0 ($\text{C}(\text{CH}_3)_3$), 24.4 (COCH_3). **IR** (KBr): $\tilde{\nu}/\text{cm}^{-1}$ = 3267, 3085, 2978, 2941, 2869, 1724, 1654, 1566, 1370, 1311, 1271, 1168, 849. **MS** (EI, 70 eV): m/z = 373 (0.7%), 371 (0.7%), 315 (0.8%), 300 (0.8%), 292 (22.2%), 109 (12.2%), 236 (100%), 190 (60.1%), 148 (12.3%), 133 (7.1%). **HRMS** found, 371.1105, calc. 371.1096. **Elem. Anal.**: $\text{C}_{17}\text{H}_{26}\text{BrNO}_3$ (372.30): calcd. C 54.84, H 7.04, N 3.76; found C 54.90, H 7.00, N 4.41.

12.8. Protective Group Chemistry

General procedure for Fmoc-protection: The amino acid hydrochlorides **154** – **156** and **158** were mixed with 4.5 equiv. of Na_2CO_3 and suspended in water and acetone (2 : 1). Under vigorous stirring and cooling in an ice bath, 1.1 equiv. of 9-fluorenylmethyl chloroformate in acetone were added with an addition funnel within ~ 1 h. The mixture was then stirred at rt over night, whereupon it was heated to 50 °C for

2 h to evaporate most of the acetone. The mixture was then poured over ice and carefully extracted with diethyl ether. The aqueous phase was acidified with conc. HCl (pH 5) and the yellowish precipitate was extracted with ethyl acetate. The combined organics were washed with water, dried (Na_2SO_4), and concentrated. The residue was purified by recrystallization from nitromethane. Drying in a desiccator over paraffine wax and P_2O_5 under reduced pressure over night yielded the Fmoc-protected amino acids.

3-(9-Fluorenyl)methoxycarbonylaminotricyclo[3.3.1.1^{3,7}]decane-1-carboxylic acid (**180a**): 8.347 g (36 mmol) of amino acid **154**. Yield: 10.177 g (24.4 mmol, 67.7%) of **180a** as slightly yellowish crystals, mp 185 °C. **¹H NMR** (400 MHz, d_6 -DMSO): δ /ppm = 12.23 (br s, 1 H, CO_2H); 7.88 (d, $J = 7.4$ Hz, 2 H); 7.71 (d, $J = 7.2$ Hz, 2 H); 7.41 (t, $J = 7.2$ Hz, 2 H); 7.33 (t, $J = 7.4$ Hz, 2 H); 7.11 (br s, 1 H, NH); 4.31 – 4.13 (m, 3 H); 2.21 – 1.38 (m, 14 H, adamantane). **¹³C NMR** (100 MHz, d_6 -DMSO): δ /ppm = 177.6 (C=O), 154.2 (C=O), 144.0, 140.7, 127.5, 126.9, 125.2, 120.0, 64.8 (Fmoc- CH_2), 50.1 (C_q), 46.7, 42.3, 41.5, 40.1 (C_q), 37.6, 34.9, 28.5. **IR** (KBr): $\tilde{\nu}/\text{cm}^{-1} = 3318, 3068, 2913, 2856, 1719, 1677, 1556, 1450, 1264, 1091, 733$. **MS** (EI, 70 eV): $m/z = 417$ (2.2%), 208 (3.1%), 178 (100%), 165 (9.7%), 128 (4.4%), 93 (7.9%). **HRMS** found, 417.1900, calc. 417.1900. **Elem. Anal.**: $\text{C}_{26}\text{H}_{27}\text{NO}_4$ (417.50): calcd. C 74.52, H 6.52, N 3.39; found C 74.63, H 6.57, N 3.39.

Alternative procedure using Fmoc-OSu:^[223] To minimize Fmoc-dipeptide formation upon Fmoc-protection, Fmoc-OSu was utilized to install the NH-Fmoc protection. In a 1000 mL round-bottomed flask, 6.7466 g (20 mmol) Fmoc-succinimide were dissolved in 50 mL 1,4-dioxane and cooled to 0 °C with an ice bath. To this solution was added via a dropping funnel a suspension of 5.098 g (22 mmol) of the amino acid **154**, and 4.876 g (46 mmol) Na_2CO_3 in 800 mL 1,4-dioxane / water (1 : 1) at 0 °C over the course of 2.5 h. The mixture was stirred at rt over night and diluted with water to a total volume of about 1100 mL. This solution was extracted twice with each 200 mL of a mixture of n-pentane / diethylether (4 : 1), and acidified with concentrated hydrochloric acid. The white precipitate was immediately extracted with ethyl acetate (3 x 200 mL), the combined organics were washed two times each with 100 mL of 1 N HCl, water, and brine, and dried over Na_2SO_4 . After evaporation of the solvents, the

residue was recrystallized from nitromethane to yield 6.0174 g (14.4 mmol, 72.1%) of the Fmoc-protected amino acid **180a** as slightly yellowish crystals. ^1H - and ^{13}C -NMR data are in accordance with the data given above for the Fmoc-protection using Fmoc-Cl.

This procedure is also recommended for the preparation of **180b** and **180c**.

3-(9-Fluorenyl)methoxycarbonylamino-5-methyltricyclo[3.3.1.1^{3,7}]decane-1-carboxylic acid (180b): 3.686 g (75 mmol) of amino acid **155**. Yield: 3.858 g (8.94 mmol, 59.6%) of **180b** as slightly yellowish crystals, mp 193 °C. ^1H NMR (400 MHz, d_6 -DMSO): δ /ppm = 12.01 (br s, 1 H, CO_2H); 7.88 (d, J = 7.6 Hz, 2 H); 7.72 (d, J = 6.8 Hz, 2 H); 7.41 (t, J = 7.4 Hz, 2 H); 7.31 (t, J = 7.4 Hz, 2 H); 7.14 (br s, 1 H, NH); 4.40 – 4.02 (m, 3 H); 2.23 – 2.03 (m, 1 H); 2.03 – 1.01 (m, 13 H, adamantane); 0.85 (s, 3 H, CH_3). ^{13}C NMR (100 MHz, d_6 -DMSO): δ /ppm = 177.5 (C=O), 154.2 (C=O), 143.9, 140.7, 127.5, 126.9, 125.2, 120.0, 64.7 (Fmoc- CH_2), 50.9 (C_q), 46.9, 46.7, 44.4, 42.1 (C_q), 41.9, 41.6, 39.5, 36.9, 31.3 (C_q), 29.8, 28.9. IR $\tilde{\nu}/\text{cm}^{-1}$ = 3265, 3134, 3066, 3039, 2946, 2907, 2856, 1701, 1450, 1413, 1326, 1288, 1114, 740. MS (EI, 70 eV): m/z = 431 (0.2%), 235 (2.3%), 209 (1.9%), 190 (35.1%), 178 (100%), 165 (63.5%), 134 (11.2%), 107 (10.4%). HRMS found, 431.2108 calc. 431.2097. Elem. Anal.: $\text{C}_{27}\text{H}_{29}\text{NO}_4$ (431.52): calcd. C 75.15, H 6.77, N 3.24; found C 75.41, H 6.75, N 3.55.

3-(9-Fluorenyl)methoxycarbonylamino-5,7-dimethyltricyclo[3.3.1.1^{3,7}]decane-1-carboxylic acid (180c): 520 mg (2 mmol) of amino acid **156**. Yield: 408 mg (0.92 mmol, 45.8%) of **180c** as slightly yellowish crystals, mp 176 °C. ^1H NMR (400 MHz, d_6 -DMSO): δ /ppm = 12.10 (br s, 1 H, CO_2H); 7.88 (d, J = 7.2 Hz, 2 H); 7.70 (d, J = 7.6 Hz, 2 H); 7.41 (t, J = 7.2 Hz, 2 H); 7.32 (t, J = 7.4 Hz, 2 H); 7.16 (br s, 1 H, NH); 4.31 – 4.13 (m, 3 H); 1.98 – 1.69 (m, 2 H); 1.69 – 0.45 (m, 12 H, adamantane); 0.85 (br s, 6 H, 2 \times CH_3). ^{13}C NMR (100 MHz, d_6 -DMSO): δ /ppm = 177.4 (CO_2H), 154.2 (C=O), 143.9 (C_q), 140.6 (C_q), 127.5, 126.9, 125.2, 120.0, 64.7 (Fmoc- CH_2), 51.6 (C_q), 49.1, 46.7, 46.2, 43.8, 42.7 (C_q), 41.0, 31.9 (C_q), 29.4 (2 \times CH_3). IR (KBr): $\tilde{\nu}/\text{cm}^{-1}$ = 3326, 3066, 2941, 2920, 2862, 1728, 1695, 1554, 1540, 1451, 1273, 1253, 1128, 760, 734. MS (EI, 70 eV): m/z = 445 (0.1%), 249 (1.8%), 204 (35.0%), 178 (100%), 165 (47.8%), 152 (9.5%), 122 (11.8%), 107 (6.1%). HRMS found, 445.2222, calc.

445.2253. **Elem. Anal.:** C₂₈H₃₁NO₄ (445.55): calcd. C 75.48, H 7.01, N 3.14; found C 75.53, H 7.22, N 3.28.

3-(9-Fluorenyl)methoxycarbonylamino-5-carboxymethyltricyclo[3.3.1.1^{3,7}]

decane-1-carboxylic acid (180d): 1.5748 g (5.43 mmol) of amino acid **158**. Yield: 1.8255 g (3.84 mmol, 70.6%) of **180d** as slightly yellowish powder. **¹H NMR** (400 MHz, d₆-DMSO): δ/ppm = 12.09 (br s, 2 H, 2 x CO₂H); 7.88 (d, J = 7.4 Hz, 2 H, Fmoc-CH_{Ar}); 7.72 (d, J = 7.2 Hz, 2 H, Fmoc-CH_{Ar}); 7.41 (t, J = 7.3 Hz, 2 H, Fmoc-CH_{Ar}); 7.33 (t, J = 7.4 Hz, 2 H, Fmoc-CH_{Ar}); 7.19 (br s, 1 H, NH); 4.19 (m, 3 H, Fmoc-CH and Fmoc-CH₂); 2.28 – 1.31 (m, 15 H, adamantane-CH, 6 x adamantane-CH₂, and CH₂CO₂H). **¹³C NMR** (100 MHz, d₆-DMSO): δ/ppm = 177.35 (-CO₂H), 172.17 (-CH₂CO₂H), 154.18 (Fmoc-C=O), 143.93 (C_q), 140.65 (C_q), 127.50, 126.96, 125.18, 119.99, 64.78 (Fmoc-CH₂), 50.75, 46.94, 46.67, 44.65, 42.13, 42.07, 41.91, 41.68, 39.54, 36.95, 38.72, 28.59. **Elem. Anal.:** C₂₈H₂₉NO₆ (475.53): calcd. C 70.72, H 6.15, N 2.95; found C 70.14, H 6.05, N 3.44.

General procedure for the synthesis of ^tbutyl esters 181a – 181c: The amino acids **154** – **156** (as their respective zwitterions) were refluxed with excess thionyl chloride for 2 h. After careful evaporation of the excess thionyl chloride under reduced pressure, a large excess of *tert.* butanol was added and the mixture was refluxed for another 4 h. The excess of the alcohol was again removed under reduced pressure. The residue was dissolved in diethyl ether and sat. Na₂CO₃. The aqueous phase was extracted with diethyl ether, the combined organics were dried (Na₂SO₄), filtered, and purified by silica gel column chromatography eluting with *tert.* butyl methyl ether / methanol / triethylamine (20 : 10 : 1).

3-Aminotricyclo[3.3.1.1^{3,7}]decane-1-carboxylic acid *tert.* butyl ester (181a): 1.562 g (8 mmol) of amino acid **154**, 30 mL thionyl chloride, 30 mL *tert.* butanol. Yield: 1.924 g (7.7 mmol, 95.7%) of amino ester **181a** as a slightly yellowish oil. **¹H NMR** (400 MHz, CDCl₃): δ/ppm = 2.22 – 2.05 (m, 2 H); 1.83 – 1.68 (m, 4 H); 1.66 (s, 2 H, NH₂); 1.62 – 1.50 (m, 4 H); 1.42 (s, 9 H, C(CH₃)₃); 1.33 – 1.24 (m, 2 H). **¹³C NMR** (100 MHz, CDCl₃): δ/ppm = 176.3 (CO₂^tBu), 79.6 (C(CH₃)₃), 47.7 (C_q), 47.6, 45.2, 43.5 (C_q), 37.8, 35.3, 29.6, 28.1 (C(CH₃)). **IR** (KBr): $\tilde{\nu}$ /cm⁻¹ = 3358, 2977, 2904, 2852, 1718,

1454, 1367, 1267, 1174, 1144, 853. **MS** (EI, 70 eV): m/z = 251 (37.4%), 194 (18.7%), 150 (100%), 138 (37.0%), 127 (8.6%), 108 (9.5%), 94 (67.8%). **HRMS** found, 251.1905, calc. 251.1885. **Elem. Anal.:** C₁₅H₂₅NO₂ (251.36): calcd. C 71.76, H 10.02, N 5.57; found C 71.29, H 10.26, N 5.77.

3-Amino-5-methyltricyclo[3.3.1.1^{3,7}]decane-1-carboxylic acid *tert.* butyl ester (181b): 1.046 g (5 mmol) of amino acid **155**, 12.5 mL thionyl chloride, 12.5 mL *tert.* butanol. Yield: 1.169 g (4.4 mmol, 88.1%) of amino ester **181b** as slightly yellowish oil. **¹H NMR** (400 MHz, CDCl₃): δ /ppm = 2.22 – 2.15 (m, 1 H); 1.68 – 1.64 (m, 2 H); 1.64 – 1.52 (m, 2 H); 1.51 – 1.44 (m, 2 H) 1.47 (s, 2 H, NH₂); 1.42 (s, 9 H, C(CH₃)₃); 1.39 – 1.30 (m, 2 H); 1.30 – 1.24 (m, 2 H); 1.24 – 1.16 (m, 2 H); 0.88 (s, 3 H, CH₃) **¹³C NMR** (100 MHz, CDCl₃): δ /ppm = 176.2 (CO₂^tBu), 79.7 (C(CH₃)₃), 52.4, 48.6 (C_q), 47.0, 44.8, 44.6 (C_q), 44.3, 42.5, 37.2, 32.4 (C_q), 30.09, 30.07, 28.1. **IR** (KBr): $\tilde{\nu}$ /cm⁻¹ = 3360, 2977, 2903, 2847, 1719, 1456, 1367, 1273, 1158, 852. **MS** (EI, 70 eV): m/z = 265 (13.6%), 208 (12.7%), 190 (2.7%), 164 (100%), 152 (16.2%), 138 (8.8%), 108 (52.2%). **HRMS** found, 265.2033, calc. 265.2042. **Elem. Anal.:** C₁₆H₂₇NO₂ (265.39): calcd. C 72.41, H 10.25, N 5.28; found C 72.10, H 10.30, N 4.83.

3-Amino-5,7-dimethyltricyclo[3.3.1.1^{3,7}]decane-1-carboxylic acid *tert.* butyl ester (181c): 2.233 g (10 mmol) of amino acid **156**, 25 mL thionyl chloride, 25 mL *tert.* butanol. Yield: 2.368 g (8.47 mmol, 84.7%) of amino ester **181c** as colorless solid, mp. 30 – 31 °C. **¹H NMR** (400 MHz, CDCl₃): δ /ppm = 1.54 (s, 2 H, NH₂); 1.42 (s, 9 H, C(CH₃)₃); 1.43 – 1.37 (m, 4 H); 1.28 – 1.13 (m, 4 H); 1.12 – 1.03 (m, 2 H); 0.89 (s, 6 H, 2 × CH₃). **¹³C NMR** (100 MHz, CDCl₃): δ /ppm = 176.0 (CO₂^tBu), 79.6 (C(CH₃)₃), 51.5, 49.7, 49.3 (C_q), 46.2, 44.8 (C_q), 44.0, 32.8 (C_q), 29.6 (2 × CH₃), 27.9 (C(CH₃)₃). **IR** (KBr): $\tilde{\nu}$ /cm⁻¹ = 3359, 2978, 2946, 2924, 2896, 2864, 2848, 1721, 1456, 1368, 1280, 1162, 850. **MS** (EI, 70 eV): m/z = 279 (6.0%), 208 (3.0%), 164 (3.8%), 152 (12.8%), 122 (100%), 108 (27.8%). **HRMS** found, 279.2194, calc. 279.2198. **Elem. Anal.:** C₁₇H₂₉NO₂ (279.42): calcd. C 73.07, H 10.46, N 5.01; found C 72.93, H 10.73, N 4.75.

3-(*tert.* Butoxycarbonyl)aminotricyclo[3.3.1.1^{3,7}]decane-1-carboxylic acid (182): 1.953 g (10 mmol) **154** (zwitterion) and 2.1 mL (15 mmol) triethylamine were

suspended in 40 mL water and 40 mL acetone. 2.463 g (10 mmol) 2-(*tert.*-butoxycarbonyloxyimino)-2-phenylacetonitrile ("Boc-ON") were added and the mixture was stirred at rt for 24 h. Another 2.463 g Boc-ON were added and stirring at rt was continued for 24 h. The mixture was poured over 150 g of crushed ice. 200 mg Na₂CO₃ were added and the acetone was evaporated under reduced pressure. The residual basic solution was extracted three times with diethyl ether and acidified by dropwise addition of concentrated HCl to pH 2. The precipitate was extracted with ethyl acetate, the combined organics were washed with water and dried (Na₂SO₄). The solvent was evaporated under reduced pressure and the residue was purified by dissolving it in CHCl₃ and reprecipitation through the addition of *n*-hexane. After suction filtration and drying in a desiccator over paraffine wax and P₂O₅, 1.421 g (4.81 mmol, 48.1%) of carbamate **182** were collected as colorless powder, mp 180 – 181 °C. **¹H NMR** (400 MHz, d₆-DMSO): δ/ppm = 12.06 (br s, 1 H, CO₂H); 6.46 (br s, 1 H, NH); 2.11 – 2.03 (m, 2 H); 1.95 – 1.87 (m, 2 H); 1.87 – 1.70 (m, 4 H); 1.70 – 1.61 (m, 4 H); 1.56 – 1.49 (m, 2 H); 1.37 (s, 9 H, C(CH₃)₃). **¹³C NMR** (100 MHz, d₆-DMSO): δ/ppm = 177.6 (CO₂H), 153.8 (C=O), 77.1 (C(CH₃)₃), 49.8 (C_q), 42.2, 41.5 (C_q), 40.3, 37.6, 35.0, 28.4, 28.2 (C(CH₃)₃). **IR** (KBr): $\tilde{\nu}$ /cm⁻¹ = 3359, 3263, 3130, 3003, 2970, 2949, 2916, 2856, 2643, 1690, 1480, 1541, 1392, 1365, 1284, 1245, 1168, 1071, 776. **MS** (EI, 70 eV): *m/z* = 295 (0.7%), 239 (25.5%), 195 (7.5%), 179 (15.4%), 169 (5.9%), 151 (15.2%), 138 (20.8%), 133 (8.1%), 108 (7.4%). **HRMS** found, 295.1735, calc. 295.1786. **Elem. Anal.**: C₁₆H₂₅NO₄ (295.37): calcd. C 65.06, H 8.53, N 4.74; found C 64.74, H 8.92, N 4.52.

3-(Benzyloxycarbonyl)aminotricyclo[3.3.1.1^{3,7}]decane-1-carboxylic acid (183): 463 mg (2 mmol) **5a** (hydrochloride) and 1.06 g (10 mmol) Na₂CO₃ were suspended in 10 mL water and 10 mL acetone and cooled to 0 °C in an ice bath. 512 mg (30 mmol) benzyl chloroformate were then added and the mixture was stirred 2 h at 0 °C, 1 h at rt and 2 h at 60 °C to evaporate most of the acetone. The mixture was then extracted three times with diethyl ether and acidified by dropwise addition of conc. HCl (pH 5). The precipitate was extracted with ethyl acetate, the combined organics were washed with water and dried (Na₂SO₄). The mixture was concentrated and the crude product was purified by silica gel column chromatography eluting with dichloromethane / *tert.* butylmethylether (1 : 1), R_f = 0.59. After evaporation of the eluent, 561 mg (1.65

mmol, 82.7%) of carbamate **42** were collected as a colorless powder, mp. 114 °C. **¹H NMR** (400 MHz, CDCl₃): δ /ppm = 7.38 – 7.28 (m, 5 H); 5.05 (s, 2 H, benzyl CH₂); 4.69 (br s, 1 H, NH); 2.24 – 2.15 (m, 2 H); 2.11 (br s, 2 H); 2.03 – 1.87 (m, 4 H); 1.87 – 1.79 (m, 4 H); 1.70 – 1.57 (m, 2 H). **¹³C NMR** (100 MHz, CDCl₃): δ /ppm = 182.0 (CO₂H), 154.4 (C=O), 136.7 (C_q), 128.5, 128.1, 128.07, 66.2, 51.0 (C_q), 42.52, 42.49 (C_q), 40.9, 37.7, 35.2, 29.1. **IR** (KBr): $\tilde{\nu}$ /cm⁻¹ = 3386, 3139, 3085, 3031, 2940, 2922, 2855, 1728, 1677, 1531, 1301, 1251, 1242, 1205, 1075, 694. **MS** (EI, 70 eV): m/z = 329 (1.0%), 279 (0.5%), 228 (1.7%), 221 (6.9%), 194 (8.2%), 176 (59.6%), 149 (6.5%), 133 (12.9%), 120 (17.2%), 108 (100%). **HRMS** found, 329.1612, calc. 329.1627. **Elem. Anal.**: C₁₉H₂₃NO₄ (329.39): calcd. C 69.28, H 7.03, N 4.25; found C 69.03, H 6.96, N 4.35.

12.9. Peptide Chemistry

12.9.1. Synthesis of ^AXaa peptides in solution

tert. Butyl-3[3-(9-fluorenylmethoxycarbonylamino)-tricyclo[3.3.1.1^{3,7}]dec-1-ylcarboxamido]-tricyclo[3.3.1.1^{3,7}]decane-1-carboxylate (Fmoc-^AGly-^AGly-O^tBu, **184):**

Following general procedure A, the dimer was prepared in an oven-dried 250 mL flask under argon. 3.989 g (15.9 mmol) of ^AGly-O^tBu (**181a**), 6.621 g (15.9 mmol) of Fmoc-^AGly (**180a**) and 6.015 g (15.9 mmol) O-(1-H-benzotriazol-1-yl)-*N,N,N,N*-tetramethyluronium hexafluorophosphate (HBTU) were dissolved in 150 mL dry THF. 2.05 g (15.9 mmol) Diisopropyl ethylamine (DIPEA) were added and the mixture was stirred over night at rt, then 1 h at 60 °C. After cooling to rt, 100 mL of brine were added and the mixture was extracted with CHCl₃. The combined organics were washed with 1 N HCl, 5% NaHCO₃, water and brine and dried (Na₂SO₄). The solvents were evaporated under reduced pressure and the residue was purified by silica gel column chromatography eluting with diethyl ether, R_f = 0.59. After careful evaporation of the eluent, 9.453 g (14.5 mmol, 91.6%) of the dipeptide **184** were obtained as a colorless powder, mp. 139 °C. **¹H NMR** (400 MHz, CDCl₃): δ /ppm = 7.75 (d, J = 7.5 Hz, 2 H); 7.58 (d, J = 7.4 Hz, 2 H); 7.39 (t, J = 7.3 Hz, 2 H); 7.31 (t, J = 7.4 Hz, 2 H); 5.24 (br s, 1 H, NH); 4.70 (br s, 1 H, NH); 4.45 – 4.27 (m, 2 H, Fmoc-CH₂); 4.20 (t, J = 6.5 Hz, 1 H, fluorenyl-CH_{aliph.}); 2.31 – 1.53 (m, 28 H, 2 × adamantane); 1.42 (s, 9 H, C(CH₃)₃). **¹³C NMR** (100 MHz, CDCl₃): δ /ppm = 175.8 (CO), 175.7 (C=O), 154.3 (C=O), 144.1 (C_q), 141.4 (C_q), 127.6, 127.0, 125.0, 120.0, 79.9 (C(CH₃)₃), 65.9 (Fmoc-

CH₂), 51.7 (C_q), 51.3 (C_q), 47.4, 43.2 (C_q), 43.1, 43.0 (C_q), 42.6, 40.9, 40.6, 38.3, 38.0, 35.4, 35.3, 29.3, 29.2, 28.0 (C(CH₃)₃). **IR** (KBr): $\tilde{\nu}/\text{cm}^{-1}$ = 3438, 3349, 2909, 2855, 1718, 1650, 1510, 1451, 1297, 1271, 1252, 1220, 1167, 1103, 1081, 759, 740. **MS** (ESI): m/z = 673.5 [M+Na]⁺ (calc. 673.4). **Elem. Anal.**: C₄₁H₅₀N₂O₅ (650.85): calcd. C 75.66, H 7.74, N 4.30; found C 75.92, H 7.95, N 4.14.

3[(3-amino)-tricyclo[3.3.1.1^{3,7}]dec-1-ylcarboxamido]-tricyclo[3.3.1.1^{3,7}]decane-1-carboxylic acid tert. butyl ester (H^AGly^AGly-O^tBu, 185): Following general procedure C, 1.953 g (3 mmol) of dipeptide **184** were dissolved in 40 mL of dry acetonitrile and cooled to 0 °C with an ice bath. 40 mL of diethylamine were slowly added and the mixture was stirred for 1 h at 0 °C and 24 h at rt. The solvents were evaporated under reduced pressure and the residue was purified by silica gel column chromatography eluting with tert. butyl methyl ether / methanol / triethylamine (20 : 10 : 1), R_f = 0.36. After careful evaporation of the eluent, 1.198 g (2.8 mmol, 93.1%) of the N-deprotected dipeptide **185** were obtained as colorless powder, mp 169 °C. **¹H NMR** (400 MHz, CDCl₃): δ/ppm = 5.24 (br s, 1 H, NH); 2.24 – 2.13 (m, 4 H); 2.06 – 1.83 (m, 4 H); 2.02 (s, 2 H, NH₂); 1.83 – 1.65 (m, 10 H); 1.65 – 1.50 (m, 10 H); 1.42 (s, 9 H, C(CH₃)₃). **¹³C NMR** (100 MHz, CDCl₃): δ/ppm = 176.3 (C=O), 175.9 (C=O), 79.9 (C(CH₃)₃), 51.7 (C_q), 48.1, 48.0 (C_q), 45.1, 43.4 (C_q), 43.1 (C_q), 42.7, 40.7, 38.4, 38.0, 35.4, 29.7, 29.3, 28.1 (C(CH₃)₃). **IR** (KBr): $\tilde{\nu}/\text{cm}^{-1}$ = 3320, 2977, 2908, 2853, 1719, 1635, 1534, 1276, 1252, 1171, 854. **MS** (EI, 70 eV): m/z = 428 (40.3%), 371 (10.5%), 353 (4.0%), 327 (9.9%), 279 (7.3%), 179 (8.5%), 167 (131.3%), 150 (100%), 133 (4.0%), 108 (6.2 %), 94 (35.6%). **HRMS** found, 428.3036, calc. 428.3039. **Elem. Anal.**: C₂₆H₄₀N₂O₃ (428.61): calcd. C 72.86, H 9.41, N 6.54; found C 72.85, H 9.51, N 6.52.

3[(3-amino)-tricyclo[3.3.1.1^{3,7}]dec-1-ylcarboxamido]-tricyclo[3.3.1.1^{3,7}]decane-1-carboxylic acid (Fmoc^AGly^AGly-OH, 186): Using general procedure D, 3.254 g (5 mmol) of dipeptide **184** were dissolved in 45 mL dichloromethane and cooled to 0 °C. 45 mL trifluoroacetic acid were added and the mixture was stirred 1 h at 0 °C and 24 h at rt. The solvents were carefully evaporated under reduced pressure by repeatedly adding dichloromethane. The residue was then recrystallized from nitromethane / acetone (1 : 1) to yield 2.386 g (4.0 mmol, 80.2%) of Fmoc^AGly^AGly-OH (**186**) as a

colorless powder, mp 208 °C. $^1\text{H NMR}$ (400 MHz, d_6 -DMSO): δ/ppm = 12.01 (br s, 1 H, CO_2H); 7.88 (d, J = 7.5 Hz, 2 H); 7.72 (d, J = 7.4 Hz, 2 H); 7.41 (t, J = 7.5 Hz, 2 H); 7.33 (t, J = 7.4 Hz, 2 H); 7.08 (br s, NH); 6.44 (br s, 1 H, NH); 4.31 – 4.06 (m, 3 H); 2.23 – 1.39 (m, 28 H, 2 \times adamantane). $^{13}\text{C NMR}$ (100 MHz, d_6 -DMSO): δ/ppm = 177.7 (C=O), 175.6 (C=O), 154.0 (C=O), 143.9 (C_q), 140.6 (C_q), 127.5, 126.9, 125.2, 120.0, 64.7 (Fmoc- CH_2), 50.9 (C_q), 50.5 (C_q), 46.7, 42.5 (C_q), 42.3, 42.0 (C_q), 41.5, 39.7, 39.5, 37.7, 37.5, 35.1, 34.9, 28.8, 28.5. **IR** (KBr): $\tilde{\nu}/\text{cm}^{-1}$ = 3358, 3326, 3040, 2906, 2853, 1706, 1693, 1639, 518, 1449, 1295, 1251, 1215, 1087, 737. **MS** (ESI): m/z = 594.3 [$\text{M} + \text{Na}$] $^+$. **Elem. Anal.**: $\text{C}_{37}\text{H}_{42}\text{N}_2\text{O}_5$ (594.74): calcd. C 74.72, H 7.11, N 4.71; found C 74.49, H 7.19, N 4.98.

tert. Butyl-3-{3-[3-(9-fluorenylmethoxycarbonylamino)-tricyclo[3.3.1.1^{3,7}]dec-1-yl-carboxamido]-tricyclo[3.3.1.1^{3,7}]dec-1-ylcarboxamido} tricyclo[3.3.1.1^{3,7}] decane-1-carboxylate (Fmoc-^AGly-^AGly-^AGly-^tBu, 187): This homotrimer was synthesized using general procedure C applying the DIC/HOBt activation method. 594 mg (1.42 mmol) Fmoc-^AGly (**180a**) and 192 mg (1.42 mmol) 1-Hydroxybenzotriazole (HOBt) were dissolved in 40 mL dry THF under argon. Upon cooling with an ice bath, 179 mg DIC were slowly added with a syringe. The mixture was stirred at rt for 1h. After cooling to 0 °C, 610 mg of **185** in 30 mL dry THF were slowly added via an addition funnel. The mixture was stirred at 0 °C for 1 h and at rt for 7 d. The solvent was then carefully evaporated under reduced pressure and the residue was dissolved in diethyl ether. The solution was washed 12 times with water, then with brine and dried (Na_2SO_4). Filtration and concentration under reduced pressure yielded a crude product that was purified via silica gel column chromatography eluting with diethyl ether, R_f = 0.34. After careful evaporation of the eluent, 876 mg (1.04 mmol, 73.2%) of tripeptide **187** were obtained as colorless powder, mp 191 °C. $^1\text{H NMR}$ (400 MHz, CDCl_3): δ/ppm = 7.76 (d, J = 7.5 Hz, 2 H); 7.59 (d, J = 7.4 Hz, 2 H); 7.40 (t, J = 7.4 Hz, 2 H); 7.32 (t, J = 7.4 Hz, 2 H); 5.27 (br s, 2 H, 2 \times NH); 4.67 (br s, 1 H, NH); 4.42 – 4.27 (m, 2 H, Fmoc- CH_2); 3.46 (t, J = 6.4 Hz); 2.37 – 1.48 (m, 42 H, 3 \times adamantane); 1.42 (s, 9 H, $\text{C}(\text{CH}_3)_3$). $^{13}\text{C NMR}$ (100 MHz, CDCl_3): δ/ppm = 175.88 (C=O), 175.85 (2 signals, 2 \times C=O), 154.3 (C=O), 144.4 (C_q), 141.4 (C_q), 127.7, 127.1, 125.0, 120.0, 79.9 ($\text{C}(\text{CH}_3)_3$), 66.0 (Fmoc- CH_2), 51.9 (C_q), 51.8 (C_q), 51.3 (C_q), 47.4, 43.3 (2 signals, 2 \times C_q), 43.1 (C_q), 43.0, 42.9,

42.6, 40.9, 40.7, 40.6, 38.4, 38.3, 38.0, 35.4 (2 signals), 35.3, 29.4, 29.3, 29.25, 28.0. **IR** (KBr): $\tilde{\nu}/\text{cm}^{-1}$ = 3377, 2910, 2852, 1714, 1642, 1523, 1451, 1296, 1267, 1253, 1218, 1170, 1079, 740. **MS** (ESI): m/z = 850.6 $[\text{M}+\text{Na}]^+$ (calc. 850.5). **Elem. Anal.:** $\text{C}_{52}\text{H}_{65}\text{N}_3\text{O}_6$ (828.09): calcd. C 75.42, H 7.91, N 5.07; found C 75.56, H 8.13, N 4.83.

tert. Butyl-3-[3-(3-amino-tricyclo[3.3.1.1^{3,7}]^{3,7}dec-1-yl-carboxamido)-tricyclo-[3.3.1.1^{3,7}]^{3,7}dec-1-ylcarboxamido] tricyclo[3.3.1.1^{3,7}] decane-1-carboxylate (H^AGly^AGly^AGly-O^tBu, **188):** Following general procedure C, 230 mg of **187** (0.278 mmol) were dissolved in 10 mL of dry acetonitrile and cooled to 0 °C using an ice bath. 10 mL of diethylamine were now slowly added with a syringe and the mixture was gradually warmed to rt over night upon stirring. The solvents were carefully evaporated under reduced pressure and the residue was purified by silica gel column chromatography eluting with *tert.* butyl methyl ether / methanol / triethylamine (20 : 10 : 1), R_f = 0.43. After careful evaporation of the eluent, 147 mg (0.243 mmol, 87.3%) of the N-deprotected tripeptide **188** were obtained as colorless powder, mp > 190 °C. **¹H NMR** (400 MHz, CDCl_3): δ/ppm = 5.298 (br s, 1 H, NH); 5.270 (br s, 1 H, NH); 2.23 – 2.11 (m, 6 H, 6 x adamantane-CH); 2.05 – 1.82 (m, 14 H, 6 x adamantane-CH₂ and NH₂); 1.79 – 1.66 (m, 12 H, 6 x adamantane-CH₂); 1.66 – 1.49 (m, 12 H, 6 x adamantane-CH₂); 1.43 (s, 9 H, C(CH₃)₃). **¹³C NMR** (100 MHz, CDCl_3): δ/ppm = 176.29 (C=O), 175.79 (2 signals, 2 x C=O), 79.79 (C_q, C(CH₃)₃), 51.72 (C_q), 51.66 (C_q), 48.03 (C_q), 47.76, 44.76, 43.27 (C_q), 42.99 (C_q), 42.86 (C_q), 42.80, 42.48, 40.59, 40.48, 38.28, 38.19, 37.88, 35.28, 35.26, 35.09, 29.51, 29.21, 29.10, 27.93 (C(CH₃)₃). **MS** (EI, 70 eV): m/z = 606, 549, 505, 293, 241, 149, 129, 83 (100%), 57. **HRMS** found, 605.42133, calc. 505.41926. **Elem. Anal.:** $\text{C}_{37}\text{H}_{55}\text{N}_3\text{O}_4$ (605.85): calcd. C 73.35, H 9.15, N 6.94; found C 72.13, H 9.06, N 6.78.

Fmoc^AGly^AGly^AGly^AGly-O^tBu (189) by general procedure A: In an oven-dried 250 mL flask under argon, 1.072 g (2.5 mmol) of H^AGly^AGly-O^tBu **185**, 1.487 g (2.5 mmol) of Fmoc^AGly^AGly-OH (**186**) and 1.0429 g (2.75 mmol) HBTU were dissolved in 200 mL dry acetonitrile. 354 mg (2.75 mmol) DIPEA were added and the mixture was stirred over night at rt, then 90 min at 60 °C. After cooling to rt, 100 mL of brine were added and the mixture was extracted with CHCl_3 . The combined organics were washed with 1 N HCl, 5% NaHCO_3 , water and brine and dried (Na_2SO_4). The solvents

were evaporated under reduced pressure. The crude product was dissolved in CHCl_3 and reprecipitated through slow addition of *n*-hexane. The peptide **189** was collected via suction filtration and dried *in vacuo* in a desiccator over paraffine wax and P_2O_5 . 2.345 g (2.33 mmol, 93.3%) of the tetrapeptide were obtained as a colorless powder, mp. 235 – 238 °C (decomp.). **$^1\text{H NMR}$** (400 MHz, CDCl_3): δ/ppm = 7.76 (d, J = 7.5 Hz, 2 H); 7.59 (d, J = 7.4 Hz, 2 H); 7.40 (t, J = 7.4 Hz, 2 H); 7.32 (t, J = 7.5 Hz, 2 H); 5.28 (br s, 2 H, $2 \times \text{NH}$); 5.26 (br s, 1 H, NH); 4.68 (br s, 1 H, NH); 4.46 – 4.25 (m, 2 H, Fmoc-CH_2); 4.21 (t, J = 6.4 Hz, 1 H); 2.28 – 1.53 (m, 56 H, $4 \times$ adamantane); 1.42 (s, 9 H, $\text{C}(\text{CH}_3)_3$). **$^{13}\text{C NMR}$** (100 MHz, CDCl_3): δ/ppm = 175.96 (C=O), 175.87 (C=O), 175.86 (C=O), 175.83 (C=O), 154.3 (C=O), 144.1 (C_q), 141.1 (C_q), 127.7, 127.1, 125.0, 120.0, 79.9 ($\text{C}(\text{CH}_3)_3$), 66.0 (Fmoc-CH_2), 51.92 (C_q), 51.88 (C_q), 51.77 (C_q), 51.28 (C_q), 47.4, 43.2, 43.1, 43.0 (possibly 2 signals), 42.9 (possibly 2 signals), 42.6 (possibly 2 signals), 40.9 (C_q), 40.7 (possibly 2 signals, C_q), 40.6 (C_q), 38.4 (possibly 2 signals), 38.3, 38.0, 35.4 (possibly 2 signals), 35.3 (possibly 2 signals), 29.32 (2 signals), 29.27, 29.23, 28.0. **IR** (KBr): $\tilde{\nu}/\text{cm}^{-1}$ = 3439, 3379, 2909, 2853, 1716, 1643, 1522, 1451, 1341, 1295, 1266, 1253, 1220, 1169, 740. **MS** (ESI): m/z = 1027.8 [$\text{M}+\text{Na}$] $^+$ (calc. 1027.6). **Elem. Anal.**: $\text{C}_{63}\text{H}_{80}\text{N}_4\text{O}_7$ (1005.33): calcd. C 75.27, H 8.02, N 5.57; found C 74.98, H 8.15, N 5.68.

H^AGly-^AGly-^AGly-^AGly-O^tBu (190): Following general procedure C, 2.011 g (2 mmol) of tetrapeptide **189** were dissolved in 40 mL of dry acetonitrile and cooled to 0 °C with an ice bath. 40 mL of diethylamine were slowly added and the mixture was stirred for 1 h at 0 °C and 24 h at rt. The solvents were evaporated under reduced pressure and the residue was purified by silica gel column chromatography eluting with *tert.* butyl methyl ether / methanol / triethylamine (20 : 10 : 1), R_f = 0.30. After careful evaporation of the eluent, 1.151 g (1.47 mmol, 73.5%) of H^AGly-^AGly-^AGly-^AGly-O^tBu were obtained as colorless powder, mp > 360 °C. **$^1\text{H NMR}$** (400 MHz, CDCl_3): δ/ppm = 2.28 – 2.11 (m, 8 H); 2.07 – 1.84 (m, 16 H); 2.02 (s, 2 H, NH_2); 1.83 – 1.52 (m, 32 H); 1.43 (s, 9 H, $\text{C}(\text{CH}_3)_3$). **$^{13}\text{C NMR}$** (100 MHz, CDCl_3): δ/ppm = 176.3 (C=O), 176.0 (C=O), 175.9 (2 signals, $2 \times$ C=O), 79.9 ($\text{C}(\text{CH}_3)_3$), 52.0 (C_q), 51.9 (C_q), 51.8 (C_q), 48.4 (C_q), 47.6, 44.7, 43.4 (C_q), 43.1, 43.0 (3 signals, $2 \times$ C_q), 42.97, 42.7, 40.74, 40.69, 40.67, 38.47, 38.44, 38.3, 38.0, 35.4 (3 signals), 35.2, 29.6, 29.38, 29.36, 29.26, 28.1. **IR** (KBr): $\tilde{\nu}/\text{cm}^{-1}$ = 3384, 2911, 2851, 1714, 1643, 1522, 1294,

1267, 1253, 1172. **MS** (ESI): $m/z = 783.7$ $[M+H]^+$ (calc. 783.5). **Elem. Anal.:** $C_{48}H_{70}N_4O_5$ (783.09): calcd. C 73.62, H 9.01, N 7.15; found C 73.30, H 9.15, N 7.14.

Fmoc-^AGly-^AGly-^AGly-^AGly-^AGly-^AGly-O^tBu (191): General procedure A: In an oven-dried 250 mL flask under argon, 585 mg (0.75 mmol) of H-^AGly-^AGly-^AGly-^AGly-O^tBu (**190**), 44 mg (0.75 mmol) of Fmoc-^AGly-^AGly-OH (**186**) and 312 mg (0.75 mmol) HBTU were dissolved in 75 mL dry acetonitrile. 106 mg (0.82 mmol) DIPEA were added and the mixture was stirred over night at rt, then 90 min at 60 °C. After cooling to rt, 100 mL of brine were added and the mixture was extracted with CHCl₃. The combined organics were washed with 1 N HCl, 5% NaHCO₃, water and brine and dried (Na₂SO₄). The solvents were evaporated under reduced pressure. The crude product was dissolved in CHCl₃ and reprecipitated through slow addition of diethyl ether. The peptide was collected via suction filtration and dried *in vacuo* in a desiccator over paraffine wax and P₂O₅. 2.345 g (2.33 mmol, 93.3%) of hexapeptide **191** were obtained as a slightly yellowish powder, mp. 320 – 325 °C (decomp.). **¹H NMR** (400 MHz, CDCl₃): δ /ppm = 7.76 (d, J = 7.5 Hz, 2 H); 7.58 (d, J = 7.5 Hz, 2 H); 7.40 (t, J = 7.5 Hz, 2 H); 7.31 (t, J = 7.5 Hz, 2 H); 5.28 (br s, 4 H, 4 × NH); 5.26 (br s, 1 H, NH); 4.69 (br s, 1 H, NH); 4.42 – 4.27 (m, 2 H, Fmoc-CH₂); 4.20 (t, J = 6.4 Hz, 1 H); 2.28 – 1.49 (m, 84 H, 6 × adamantane); 1.42 (s, 9 H, C(CH₃)₃). **¹³C NMR** (100 MHz, CDCl₃): Note: due to insufficient resolution of the spectrometer and low solubility of the peptide, the set of resonances is not complete. Groups of resonances are given. δ /ppm = 176.2, 176.0, 175.98, 175.89, 175.83, 175.5, 154.4, 144.1, 141.4, 127.7, 127.1, 125.0, 120.0, 79.9, 66.0, 52.1, 52.0, 51.9, 51.8, 51.3, 47.4, 43.3, 43.2, 43.0, 42.9, 42.7, 40.9, 40.7, 40.68, 40.5, 38.5, 38.4, 38.0, 35.4, 35.3, 29.4, 29.3 28.1. **IR** (KBr): $\tilde{\nu}$ /cm⁻¹ = 3378, 2928, 2910, 2852, 1719, 1642, 1521, 1450, 1293, 1267, 1255. **MS** (ESI): $m/z = 1381.9$ $[M+Na]^+$ (calc. 1381.8). **Elem. Anal.:** $C_{85}H_{110}N_6O_9$ (1359.82): calcd. C 75.08, H 8.15, N 6.18; found C 74.80, H 8.70, N 5.16.

tert. Butyl-3[3-(9-fluorenylmethoxycarbonylamino)-5-methyltricyclo[3.3.1.1^{3,7}]dec-1-ylcar-boxamido]-tricyclo[3.3.1.1^{3,7}]decane-1-carboxylate (Fmoc-^AAla-^AGly-O^tBu, 192): Following general procedure A, 502.7 mg (2 mmol) H-^AGly-O^tBu (**181a**), and 863.0 mg (2 mmol) Fmoc-^AAla-OH (**180b**) were dissolved at rt in 30 mL dry THF. 758.5 mg (2 mmol) of HBTU and 258.5 mg (2mmol) DIPEA were added and the

mixture was stirred over night at rt. 50 mL of brine were added and the mixture was extracted with CHCl_3 . The combined organics were washed with 1 N HCl, 5% NaHCO_3 , water and brine and dried (Na_2SO_4). The solvents were evaporated under reduced pressure and the residue was purified by silica gel column chromatography (2.5×50 cm) eluting with diethyl ether, $R_f = 0.55$. After evaporation of the eluent, 760 mg (1.14 mmol, 57.2%) of dipeptide **192** were isolated as colorless powder, mp. 94 – 95 °C. **$^1\text{H NMR}$** (400 MHz, CDCl_3): $\delta/\text{ppm} = 7.75$ (d, $J = 7.5$ Hz, 2 H, Fmoc- CH_{Ar}); 7.57 (d, $J = 7.4$ Hz, 2 H, Fmoc- CH_{Ar}); 7.39 (t, $J = 7.4$ Hz, 2 H, Fmoc- CH_{Ar}); 7.31 (t, $J = 7.4$ Hz, 2 H, Fmoc- CH_{Ar}); 5.25 (br s, 1 H, NH); 4.71 (br s, 1 H, NH); 4.42 – 4.24 (m, 2 H, Fmoc- CH_2); 4.20 (t, $J = 6.2$ Hz, 1 H, Fmoc-CH); 2.35 – 1.24 (m, 27 H, adamantane-CH and $-\text{CH}_2$); 1.42 (s, 9 H, $\text{C}(\text{CH}_3)_3$); 0.89 (br s, 3 H, CH_3). **$^{13}\text{C NMR}$** (100 MHz, CDCl_3): $\delta/\text{ppm} = 175.8$ (C=O), 175.5 (C=O), 154.4 (Fmoc-C=O), 144.0 (C_q), 141.3 (C_q), 127.6, 127.0, 124.9, 119.9, 79.8 (C_q , $\text{C}(\text{CH}_3)_3$), 65.9 (Fmoc- CH_2), 52.0, 51.7, 47.5, 47.3, 45.2, 43.6, 43.0, 42.6, 42.3, 40.5, 40.1, 37.9, 37.6, 35.3, 32.1, 29.8, 29.6, 29.1, 27.9 ($\text{C}(\text{CH}_3)_3$). **IR** (KBr): $\tilde{\nu}/\text{cm}^{-1} = 3357, 2856, 1719, 1651, 1510, 1451, 1268, 1254$. **MS** (ESI): $m/z = 687.4$ [$\text{M} + \text{Na}$] $^+$ (calc. 637.4). **Elem. Anal.**: $\text{C}_{42}\text{H}_{52}\text{N}_2\text{O}_5$ (664.87): calcd. C 75.87, H 7.88, N 4.21; found C 75.56, H 7.77, N 4.38.

Fmoc-^AGly-Gly-OMe (194): Following general procedure A, 126 mg (1 mmol) of glycine methyl ester hydrochloride **193**, 418 mg (1 mmol) of Fmoc-^AGly (**180a**) and 417 mg (1.1 mmol) HBTU were dissolved in 30 mL dry THF in an oven-dried 100 mL flask under argon. 259 mg (2 mmol) DIPEA were added and the mixture was stirred over night at rt, then 1 h at 60 °C. After cooling to rt, 50 mL of brine were added and the mixture was extracted with CHCl_3 . The combined organics were washed with 1 N HCl, 5% NaHCO_3 , water, and brine and were dried (Na_2SO_4). The solvents were evaporated under reduced pressure and the residue was purified by silica gel column chromatography eluting with ethyl acetate, $R_f = 0.48$. After evaporation of the eluent, 431 mg (0.88 mmol, 88.3%) of dipeptide **194** were obtained as a colorless powder, mp 128 °C. **$^1\text{H NMR}$** (400 MHz, CDCl_3): $\delta/\text{ppm} = 7.75$ (d, $J = 7.5$ Hz, 2 H); 7.58 (d, $J = 7.4$ Hz, 2 H); 7.38 (t, $J = 7.4$ Hz, 2 H); 7.32 (t, $J = 7.4$ Hz, 2 H); 6.15 (br s, 1 H, NH); 4.72 (br s, 1 H, NH); 4.44 – 4.23 (m, 2 H, Fmoc- CH_2); 4.19 (t, $J = 6.3$ Hz, 1 H); 4.00 [d, $J = 5.1$ Hz, 2 H, H_α (Gly)]; 3.74 (s, 3 H, OCH_3); 2.40 – 1.31 (m, 14 H, adamantane). **$^{13}\text{C NMR}$** (100 MHz, CDCl_3): $\delta/\text{ppm} = 176.6$ (C=O), 170.6 (C=O), 154.4 (C=O), 144.1

(C_q), 141.4 (C_q), 127.6, 127.1, 124.9, 120.0, 65.9, 52.3, 51.1 (C_q), 47.4, 43.0, 42.6, 41.2, 40.8 (C_q), 38.1, 35.2, 29.2. **IR** (KBr): $\tilde{\nu}/\text{cm}^{-1}$ = 3330, 3065, 2947, 2925, 2910, 2857, 1750, 1698, 1637, 1524, 1293, 1272, 1256, 1247, 1222, 1206, 1280, 765, 744. **MS** (ESI): m/z = 511.5 [M+Na]⁺ (calc. 511.2). **Elem. Anal.**: C₂₉H₃₂N₂O₅ (488.57): calcd. C 71.29, H 6.60, N 5.73; found C 70.99, H 6.57, N 5.62.

Fmoc^AGly-Gly-O^tBu (196): Following general method A, 167.6 mg (1 mmol) glycine *tert* butyl ester hydrochloride (**195**) and 417.5 mg (1 mmol) Fmoc^AGly (**180a**) were dissolved in 30 mL dry THF at rt. 417.2 mg (1.1 mmol) HBTU and 284.4 mg (2.2 mmol) DIPEA were added and the mixture was stirred at rt for 18 h. 70 mL of brine were added and the mixture was extracted with CHCl₃. The combined organics were washed with 1 N HCl, 5% NaHCO₃, water, and brine and were dried (Na₂SO₄). The solvents were evaporated under reduced pressure and the residue was purified by silica gel column chromatography eluting with *tert* butyl methyl ether, R_f = 0.50. After evaporation of the eluent, 456 mg (0.86 mmol, 85.9%) of dipeptide **196** were obtained as a colorless powder, mp 121.5 °C. **¹H NMR** (400 MHz, CDCl₃): δ/ppm = 7.76 (d, J = 7.5 Hz, 2 H, Fmoc-CH_{Ar}); 7.58 (d, J = 7.4 Hz, 2 H, Fmoc-CH_{Ar}); 7.39 (t, J = 7.1 Hz, Fmoc-CH_{Ar}); 7.31 (t, J = 7.4 Hz, 2 H, Fmoc-CH_{Ar}); 6.11 (br s, 1 H, NH); 4.70 (br s, 1 H, NH); 4.35 – 4.31 (m, 2 H, Fmoc-CH₂); 4.20 (t, J = 6.1 Hz, Fmoc-CH); 3.90 (d, J = 4.7 Hz, CH_α); 2.23 – 1.45 (m, 14 H, adamantane-CH and -CH₂); 1.48 (s, 9 H, C(CH₃)₃). **¹³C NMR** (100 MHz, CDCl₃): δ/ppm = 176.4 (C=O), 169.4 (C=O), 154.2 (Fmoc-C=O), 144.1 (C_q), 141.4 (C_q), 127.6, 127.1, 125.0, 120.0, 82.3 (C_q), 65.9, 51.2 (C_q), 47.4, 43.0, 42.6 (C_q), 42.0, 40.8, 38.1, 35.2, 29.2, 28.1. **MS** (ESI): m/z = 553.3 [M + Na]⁺ (calc. 553.3). **Elem. Anal.**: C₃₂H₃₈N₂O₅ (530.65): calcd. C 72.43, H 7.22, N 5.28; found C 72.44, H 7.29, N 4.96.

H^AGly-Gly-OMe (197): Following general procedure C, 977 mg (2 mmol) Fmoc^AGly-Gly-OMe **194** were dissolved in 25 mL of dry acetonitrile and cooled to 0 °C with an ice bath. 25 mL of diethylamine were slowly added and the mixture was stirred for 1 h at 0 °C and 15 h at rt. The solvents were evaporated under reduced pressure and the residue was purified by silica gel column chromatography eluting with *tert* butyl methyl ether / methanol / triethylamine (20 : 10 : 1), R_f = 0.28. After careful evaporation of the eluent, 520 mg (1.95 mmol, 97.6%) of the N-protected dipeptide **197** were obtained

as a slightly yellowish solid, mp 104.5 °C. $^1\text{H NMR}$ (400 MHz, CDCl_3): δ/ppm = 6.18 (br s, 1 H, NH); 4.03 [d, J = 5.1 Hz, 2 H, $\text{H}_\alpha(\text{Gly})$]; 3.76 (s, 3 H, OCH_3); 2.29- 2.13 (m, 2 H); 1.89 – 1.52 (m, 12 H); 1.71 (s, 2 H, NH_2). $^{13}\text{C NMR}$ (100 MHz, CDCl_3): δ/ppm = 177.1 (C=O), 170.7 (C=O), 52.4 (OCH_3), 47.9 (C_q), 47.7, 45.0, 43.1 (C_q), 41.2, 38.1, 35.2, 29.6. **IR** (KBr): $\tilde{\nu}/\text{cm}^{-1}$ = 3353, 2943, 2916, 2852, 1761, 1635, 1525, 1396, 1207, 1183, 1160, 876. **MS** (EI, 70 eV): m/z = 266 (23.4%), 252 (2.6%), 239 (6.7%), 209 (26.3%), 177 (21.3%), 150 (100%), 134 (8.9%), 120 (76.1%), 108 (27.8%), 94 (88.3%). **HRMS** found, 266.1628, calc. 266.1630. **Elem. Anal.:** $\text{C}_{14}\text{H}_{22}\text{N}_2\text{O}_3$ (266.34): calcd. C 63.13, H 8.33, N 10.52; found C 62.99, H 8.42, N 10.17.

Fmoc-Gly-^AAib-O^tBu (198): Following general procedure A, 393.2 mg (1.32 mmol) N-9-fluorenylmethoxycarbonyl glycine (**180e**) and 369.5 mg (1.32 mmol) H-^AAib-O^tBu **181c** were dissolved in 50 mL dry THF. 526.6 mg (1.39 mmol) HBTU and 181.2 mg (1.40 mmol) DIPEA were added and the mixture was stirred under argon at rt for 15 h. 75 mL of brine were added and the mixture was extracted with CHCl_3 . The combined organics were washed with 1 N HCl, 5% NaHCO_3 , water and brine and dried (Na_2SO_4). The solvents were evaporated under reduced pressure and the residue was purified by silica gel column chromatography (3 x 60 cm) eluting with n-hexane / ethyl acetate (1 : 2), R_f = 0.51. After evaporation of the eluent, 508.5 mg (0.91 mmol, 68.8%) of dipeptide **198** were obtained as a colorless powder, mp 180.5 °C. $^1\text{H NMR}$ (400 MHz, CDCl_3): δ/ppm = 7.76 (d, J = 7.4 Hz, 2 H, Fmoc- CH_{Ar}); 7.59 (d, J = 7.3 Hz, 2 H, Fmoc- CH_{Ar}); 7.40 (t, J = 7.3 Hz, 2 H, Fmoc- CH_{Ar}); 7.31 (t, J = 7.4 Hz, 2 H, Fmoc- CH_{Ar}); 5.73 (br s, 1 H, NH); 5.48 (br s, 1 H, NH); 4.41 (t, J = 6.1 Hz, 2 H, Fmoc- CH_2); 4.22 (t, J = 6.3 Hz, 1 H, Fmoc-CH); 3.77 (d, J = 5.3 Hz, 2 H, CH_α); 1.93 (br s, 2 H, adamantane- CH_2); 1.63 – 1.51 (m, 4 H, 2 x adamantane- CH_2); 1.51 – 1.33 (m, 4 H, 2 x adamantane- CH_2); 1.42 (s, 9 H, $\text{C}(\text{CH}_3)_3$); 1.19 – 1.02 (m, 2 H, adamantane- CH_2); 0.89 (s, 6 H, 2 x CH_3). $^{13}\text{C NMR}$ (100 MHz, CDCl_3): δ/ppm = 175.5 (C=O), 167.7 (C=O), 156.5 (Fmoc-C=O), 143.8 (C_q), 141.3 (C_q), 127.8, 127.1, 125.0, 120.0, 80.1 (C_q , $\text{C}(\text{CH}_3)_3$), 67.2 (Fmoc- CH_2), 54.1, 49.6, 47.1, 46.7, 45.1, 44.4, 44.1, 41.3, 32.6, 29.6, 28.0. **IR** (KBr): $\tilde{\nu}/\text{cm}^{-1}$ = 3304, 3237, 3065, 2946, 2863, 1720, 1697, 1661, 1556, 1452, 1278, 1160, 741. **MS** (ESI): m/z = 581.7 [$\text{M} + \text{Na}$]⁺; (calc. 581.3). **Elem. Anal.:** $\text{C}_{34}\text{H}_{42}\text{N}_2\text{O}_5$ (558.71): calcd. C 73.09, H 7.50, N 5.01; found C 73.17, H 7.73, N 4.74.

Fmoc-Gly-^AGly-O^tBu (199): Following general procedure A, this peptide was prepared by dissolving 2.974 g (10 mmol) **180e** and 2.51 g (10 mmol) **181a** in 150 mL dry THF. 3.7925 g (10 mmol) HBTU and 1.2925 g (10 mmol) DIPEA were added and the mixture was stirred under argon at rt over night. 100 mL brine were added and the mixture was extracted with CHCl₃. The combined organics were washed with 1 N HCl, 5% NaHCO₃, water, and brine and were dried (Na₂SO₄). The solvents were then evaporated under reduced pressure and the residue was purified via silica gel column chromatography (3.5 x 80 cm, ~ 250 g SiO₂) eluting with n-hexane / ethyl acetate (1 : 1), R_f = 0.29. After evaporation of the eluent, 2.9696 g (5.60 mmol, 56.0%) of the dipeptide **199** were isolated as a colorless powder, mp 172 °C. **¹H NMR** (400 MHz, CDCl₃): δ/ppm = 7.75 (d, J = 7.6 Hz, 2 H, Fmoc-CH_{Ar}); 7.58 (d, J = 7.4 Hz, 2 H, Fmoc-CH_{Ar}); 7.39 (t, J = 7.4 Hz, 2 H, Fmoc-CH_{Ar}); 7.28 (t, J = 7.4 Hz, 2 H, Fmoc-CH_{Ar}); 5.81 (br s, 1 H, NH); 5.59 (br s, 1 H, NH); 4.40 (d, J = 7.0 Hz, 2 H, Fmoc-CH₂); 4.21 (t, J = 7.0 Hz, 1 H, Fmoc-CH); 3.79 (d, J = 4.9 Hz, 2 H, CH_α); 2.25 – 2.11 (m, 2 H, 2 × adamantane-CH); 2.11 – 2.03 (m, 2 H, adamantane-CH₂); 2.02 – 1.81 (m, 4 H, 2 × adamantane-CH₂); 1.79 – 1.68 (m, 4 H, 2 × adamantane-CH₂); 1.65 – 1.55 (m, 2 H, adamantane-CH₂); 1.42 (s, 9 H, C(CH₃)₃). **¹³C NMR** (100 MHz, CDCl₃): δ/ppm = 175.7 (C=O), 167.6 (C=O), 156.5 (Fmoc-C=O), 143.7 (C_q), 141.3 (C_q), 127.7, 127.0, 125.0, 120.0, 79.9 (C_q, C(CH₃)₃), 67.2 (Fmoc-CH₂), 52.4, 47.0, 45.0, 43.0, 42.4, 40.6, 37.8, 35.2, 29.1 (2 × adamantane-CH), 28.0. **IR** (KBr): $\tilde{\nu}$ /cm⁻¹ = 3311, 3264, 3080, 2972, 2937, 2912, 2866, 2859, 1713, 1662, 1555, 1274, 1164. **MS** (ESI): *m/z* = 531.3 [M + H]⁺; (calc. 531.3). **Elem. Anal.:** C₃₂H₃₈N₂O₅ (530.65): calcd. C 72.43, H 7.22, N 5.28; found C 72.14, H 7.05, N 5.52.

H-Gly-^AGly-OMe (200): Following general procedure C, the Fmoc-protective group was cleaved by dissolving 1.0613 g (2 mmol) of dipeptide **199** in dry THF. The mixture was cooled to 0 °C with an ice bath under argon. 15 mL diethylamine were now slowly added via an addition funnel and the mixture was stirred over night upon warming to rt. The solvents were carefully evaporated under reduced pressure and the residue was purified by silica gel column chromatography (2.5 x 30 cm, ~ 70 g SiO₂) eluting with *tert* butyl methyl ether / methanol / triethylamine (20 : 10 : 1), R_f = 0.44 (TLC was developed with I₂). 491.4 mg (1.59 mmol, 79.7%) of dipeptide **200**

were isolated as a colorless powder, mp 98 – 99 °C. $^1\text{H NMR}$ (400 MHz, CDCl_3): δ/ppm = 7.00 (br s, 1 H, NH); 3.23 (s, 3 H, $-\text{OCH}_3$); 2.24 – 2.15 (m, 2 H, 2 \times adamantane-CH); 2.14 – 1.87 (m, 4 H, 2 \times adamantane- CH_2); 2.08 (s, 2 H, NH_2); 1.86 – 1.74 (m, 4 H, 2 \times adamantane- CH_2); 1.74 – 1.56 (m, 2 H, adamantane- CH_2); 1.56 – 1.46 (m, 2 H, adamantane- CH_2); 1.42 (s, 9 H, $\text{C}(\text{CH}_3)_3$). $^{13}\text{C NMR}$ (100 MHz, CDCl_3): δ/ppm = 175.9 (C=O), 171.7 (C=O), 79.8 (C_q , $\text{C}(\text{CH}_3)_3$), 45.3, 43.0 (C_q), 42.6, 40.6, 37.9, 35.3, 29.1, 28.0. **HRMS** found, 308.2083, calc. 308.20999. **Elem. Anal.:** $\text{C}_{17}\text{H}_{28}\text{N}_2\text{O}_3$ (308.42): calcd. C 66.20, H 9.15, N 9.08; found C 65.78, H 9.21, N 8.99.

Fmoc-^AGly-Gly-^AGly-O^tBu (201): Following general procedure A, the trimer was prepared by dissolving 308.4 mg (1 mmol) of the amino component **200** and 417.5 mg (1 mmol) **180a** in 50 mL dry THF. 142.2 mg (1.1 mmol) DIPEA and 417.2 mg (1.1 mmol) HBTU were added and the mixture was stirred at rt under over night under argon. 60 mL of brine were added and the mixture was extracted with CHCl_3 . The combined organics were washed with 1 N HCl, 5% NaHCO_3 , water, and brine and were dried (Na_2SO_4). The solvents were evaporated under reduced pressure and the residue was purified by silica gel column chromatography (2.5 x 70 cm, \sim 190 g SiO_2) eluting with ethyl acetate, R_f = 0.46. After evaporation of the eluent, 582.5 mg (0.823 mmol, 82.3%) of the trimer **201** were isolated as a colorless powder, mp 158 – 161 °C. $^1\text{H NMR}$ (400 MHz, CDCl_3): δ/ppm = 7.75 (d, J = 7.5 Hz, 2 H, Fmoc- CH_{Ar}); 7.58 (d, J = 7.4 Hz, 2 H, Fmoc- CH_{Ar}); 7.39 (t, J = 7.2 Hz, 2 H, Fmoc- CH_{Ar}); 7.31 (dt, J = 7.2 / 1.0 Hz, 2 H, Fmoc- CH_{Ar}); 6.62 (br s, 1 H, NH); 6.30 (br s, 1 H, NH); 4.82 (br s, 1 H, NH); 4.35 – 4.26 (m, 2 H, Fmoc- CH_2); 4.18 (t, J = 6.4 Hz, 1 H, Fmoc-CH); 3.84 (d, J = 5.1 Hz, 2 H, CH_α); 2.27 – 1.43 (m, 28 H, adamantane-CH and $-\text{CH}_2$); 1.41 (s, 9 H, $\text{C}(\text{CH}_3)_3$). $^{13}\text{C NMR}$ (100 MHz, CDCl_3): δ/ppm = 176.8 (C=O), 175.7 (C=O), 167.8 (C=O), 154.3 (Fmoc-C=O), 144.1 (C_q), 141.3 (C_q), 127.6, 127.0, 125.0, 119.9, 79.9 (C_q , $\text{C}(\text{CH}_3)_3$), 65.9 (Fmoc- CH_2), 60.4, 52.4, 51.1, 47.3, 43.6, 43.0, 42.9, 42.6, 42.4, 40.7, 38.1, 37.9, 35.3, 35.2, 29.2, 29.1, 28.0. **IR** (KBr): $\tilde{\nu}/\text{cm}^{-1}$ = 3408, 3291, 2975, 2910, 2858, 1741, 1717, 1676, 1649, 1543, 1525, 1449, 1365, 1274, 1243, 1227, 1167, 738. **Elem. Anal.:** $\text{C}_{43}\text{H}_{53}\text{N}_3\text{O}_6$ (707.90): calcd. C 72.96, H 7.55, N 5.94; found C 72.77, H 7.75, N 5.77.

Fmoc-Gly-^AGly-OH (202): Following general procedure D, **202** was prepared by dissolving 1.0613 g (2 mmol) of ^tBu-protected dipeptide **199** in 30 mL dichloromethane. The solution was cooled to 0 °C with an ice bath, and 10 mL of trifluoroacetic acid were added. The mixture was stirred for over night upon warming to rt. The solvents were then carefully evaporated under reduced pressure, dichloromethane was added and the mixture was again evaporated carefully (3 × 30 mL). The resulting solid was heated in 50 mL of a mixture of nitromethane and acetone (1 : 1), cooled to 0 °C with an ice bath and the colorless solid was collected via suction filtration. After drying over night under reduced pressure over paraffine wax and P₂O₅, 730 mg (1.54 mmol, 76.9%) of **202** were collected as a fluffy colorless powder that was used without further purification. **¹H NMR** (400 MHz, d₆-DMSO): δ/ppm = 12.13 (br s, 1 H, CO₂H); 7.90 (d, J = 7.5 Hz, 2 H, Fmoc-CH_{Ar}); 7.72 (d, J = 7.4 Hz, 2 H, Fmoc-CH_{Ar}); 7.42 (t, J = 7.5 Hz, 2 H, Fmoc-CH_{Ar}); 7.36 (br s, 1 H, NH); 7.33 (t, J = 7.4 Hz, 2 H, Fmoc-CH_{Ar}); 4.29 (d, J = 6.8 Hz, 2 H, Fmoc-CH₂), 4.23 (t, J = 7.0 Hz, 1 H, Fmoc-CH); 4.19 (br s, 1 H, NH); 3.54 (d, J = 6.1 Hz, 2 H, CH_α); 2.17 – 2.06 (m, 2 H, 2 × adamantane-CH); 2.06 – 1.95 (m, 2 H, adamantane-CH₂); 1.95 – 1.78 (m, 4 H, 2 × adamantane-CH₂); 1.77 – 1.64 (m, 4 H, 2 × adamantane-CH₂), 1.63 – 1.50 (m, 2 H, adamantane-CH₂). **¹³C NMR** (100 MHz, d₆-DMSO): δ/ppm = 177.6 (C=O), 168.0 (C=O), 156.4 Fmoc-C=O), 143.8 (C_q), 140.6 (C_q), 127.6, 127.0, 125.2, 120.1, 65.6 (Fmoc-CH₂), 51.0 (C_q), 46.6, 43.5, 42.1, 41.4 (C_q), 40.1, 37.6, 34.9, 28.5. **MS** (ESI): *m/z* = 497.2 [M + Na]⁺; (calc. 497.2).

Fmoc-Gly-^AGly-Gly-^AGly-OtBu (203): This tetramer was synthesized using general procedure A. 308.4 mg (1 mmol) **200** and 474.6 mg (1 mmol) **202** were suspended in 30 mL dry acetonitrile and 10 mL dry THF. 129.3 mg (1 mmol) DIPEA and 379.3 mg (1 mmol) HBTU were added and the mixture was stirred at rt. After 3 h, clear solubility could be observed. The reaction was quenched after 5.5 h by adding 50 mL of brine and extracted with CHCl₃. The combined organics were washed with 1 N HCl, 5% NaHCO₃, water, and brine and dried (Na₂SO₄). The crude product obtained after evaporation of the solvents was purified by flash column chromatography (2.5 × 60 cm, ~170 g SiO₂) eluting with ethyl acetate, R_f = 0.32. After evaporation of the eluent, 485.5 mg (0.635 mmol, 63%) of the tetramer **203** were obtained as a colorless powder, mp 125 – 127 °C.

¹H- and ¹³C-NMR Data for tetramer 203:

Entry	Residue	Position ^[a]	δ_C [ppm], mult. ^[b]	δ_H [ppm], mult. (J/Hz), Int.
1		Fmoc-C=O	156.5	-
2		Fmoc-C _{Ar}	143.7 (q)	-
3		Fmoc-C _{Ar}	141.2 (q)	-
4		Fmoc-C _{Ar}	127.7 (CH)	-
5		Fmoc-C _{Ar}	127.0 (CH)	-
6		Fmoc-C _{Ar}	125.0 (CH)	-
7		Fmoc-C _{Ar}	120.0 (CH)	-
8	Fmoc	Fmoc-CH	47.0	-
9		Fmoc-CH ₂	67.2	-
10		Fmoc-CH _{Ar}	-	7.75, d (7.6), 2 H
11		Fmoc-CH _{Ar}	-	7.57, d (7.5), 2 H
12		Fmoc-CH _{Ar}	-	7.38, t (7.4), 2 H
13		Fmoc-CH _{Ar}	-	7.28, dt (6.4, 1.0), 2 H
14		Fmoc-CH ₂	-	4.35, d (7.3), 2 H
15		Fmoc-CH	-	4.25, t (7.2), 1 H
16		NH	-	5.80, d (~5)
17	Gly ¹	α	44.7	3.90, d (4.5)
18		C=O	167.7	-
19		C=O	176.8 (q)	-
20		NH	-	6.87, br s, 1 H
21		C _{Ad} NH	52.41 (q)	-
22		C _{Ad} -CO	43.0 (q)	-
23	^A Gly ²	Ad-CH	29.2 (CH)	2.31 – 2.17, m (2 H) ^[c]
34		Ad-CH ₂	42.6 (CH ₂)	2.17 – 2.04, m (2 H) ^[c]
35		Ad-CH ₂	40.6 (CH ₂)	2.03 – 1.50, m (4 H) ^[c]
26		Ad-CH ₂	38.7 (CH ₂)	2.03 – 1.50, m (4 H) ^[c]
27		Ad-CH ₂	35.2 (CH ₂)	2.03 – 1.50, m (2 H) ^[c]
28		C=O	167.5 (q)	-
29	Gly ³	NH	-	6.77, t (~5)
30		α	43.5 (CH ₂)	3.85, d (3.8)
31		C=O	175.8 (q)	-
32		NH	-	6.69, br s (1 H)
33		C _{Ad} NH	52.36 (q)	-
34		C _{Ad} -CO	43.0 (q)	-
35	^A Gly ⁴	Ad-CH	29.2 (CH)	2.31 – 2.17, m (2 H) ^[c]
36		Ad-CH ₂	42.3 (CH ₂)	2.17 – 2.04, m (2 H) ^[c]
37		Ad-CH ₂	39.9 (CH ₂)	2.03 – 1.50, m (4 H) ^[c]
38		Ad-CH ₂	37.9 (CH ₂)	2.03 – 1.50, m (4 H) ^[c]
39		Ad-CH ₂	35.0 (CH ₂)	2.03 – 1.50, m (2 H) ^[c]
40	-O ^t Bu	C(CH ₃) ₃	79.9 (q)	-
41		C(CH ₃) ₃	28.0 (CH ₃)	1.40, s (9 H)

^[a] HMBC, HSQC, COSY, and 2D-NOESY correlations were used for the assignment. ^[b] Refers to the amplitude in a DEPT¹³⁵ spectrum. ^[c] Overlapping multiplets

12. 10. Solid Phase Peptide Synthesis of ^AGly Homooligomers

These syntheses were carried out by Dr. Chiara Cabrele, University of Regensburg, Germany. HBTU was purchased from MultiSynTech (Witten, Germany). 2-Chlorotriyl chloride resin (loading: 1.6 mmol/g) was obtained by Senn-Chemicals (Dielsdorf, Switzerland). HOBt, DIPEA, TFA, and α -cyano-4-hydroxycinnamic acid were from

Fluka (Taufkirchen, Germany). Triethylsilane (TES), acetic anhydride and methanol were obtained from Merck (Darmstadt, Germany). The peptide-synthesis-grade reagents piperidine, 1-methyl-2-pyrrolidinone (NMP), N,N-dimethylformamide (DMF), dichloromethane (DCM) and diethylether, HPLC-grade acetonitrile and TFA for UV-spectroscopy were purchased from Biosolve (Valkenswaard, the Netherlands). 2,2,2-Trifluoroethanol (TFE) was obtained from Acros (Geel, Belgium).

Plastic-syringes (2 mL and 5 mL volume) equipped with polyethylene frits (pore size: 35 μm) were purchased by Roland Vetter Laborbedarf (Ammerbuch, Germany). Analytical and preparative reverse-phase HPLC was performed on Agilent equipment (Böblingen, Germany) by using the following columns: Luna C18(2), 3 μm , 4.60 \times 150 mm, and Luna C18(2), 10 μm , 90 \AA , 21.2 \times 250 mm (Phenomenex, Aschaffenburg, Germany). The binary solvent system (A/B) was as follows: (A) 0.012 % (v/v) TFA in water, and (B) 0.01 % (v/v) TFA in acetonitrile. The flow rate was 1 mL/min and 21 mL/min for the analytical and preparative HPLC runs, respectively. The absorbance was detected at 220 nm. The molecular weights were determined by using ESI-MS (Thermoquest, Finnigan) and MALDI-TOF-MS (GSG, Bruchsal, Germany).

Solid-Phase Synthesis of the Heptamer H-(^AGly)₇-OH

Loading of the 2-Chloro-Trityl Chloride Resin with Fmoc-^AGly-OH. 108.9 mg of 2-chloro-trityl chloride resin were swollen in 1.5 mL dry DCM for 30 min. After removal of the excess solvent, 68.2 mg (0.163 mmol, 0.94 eq.) of Fmoc-^AGly-OH dissolved in 1.1 mL DCM/DMF (3:1 v/v) were added to the swollen resin, followed by 55.8 μL (0.326 mmol, 1.87 eq) DIPEA. After shaking for 3 h at rt, the resin was filtered off, washed several times with DMF, DCM, diethylether, and finally dried *in vacuo* for 4 h.

The amino acid loading was determined spectrophotometrically by measuring the absorbance at 300 nm of the fluorene-piperidine adduct obtained by treating a small portion (4 – 6 mg) of the dried resin with 20 % piperidine in DMF for 30 min. A loading of 0.89 mmol/g was calculated from the absorbance at 300 nm, using the extinction coefficient of 7800 $\text{M}^{-1} \text{cm}^{-1}$. The remaining free linker groups were capped by washing the resin five times with the mixture DCM/MeOH/DIPEA (17:2:1 v/v).

Chain Assembly. Fmoc-cleavage was performed by shaking the previously swelled resin in 800 μL of 40 % piperidine in DMF/NMP (4:1 v/v) for 5 min, and then in 800 μL of 20 % piperidine (2 \times 5 min). Single couplings were carried out for 2.5 h by using Fmoc-^AGly-OH/HOBt/HBTU/DIPEA in the ratio of 3:3:3:6 eq with respect to the resin

loading, in DMF/NMP (4:1 v/v). After each coupling a capping step was carried out with acetic anhydride/DIPEA (each 0.75 equiv. with respect to the resin loading) in DMF/NMP (5 min).

Control of the Chain Growth by HPLC. Some beads were subjected to peptide cleavage before Fmoc-deprotection of the trimer, tetramer and hexamer. The beads were shaken in 92 μ l of the mixture TFA/DCM/TES in the ratio of 25:20:1 (v/v) for 40 min. Afterwards the mixture was reduced to a minimum volume and the cleaved Fmoc-derivative was recovered by precipitation from ice-cold water and centrifugation. The residue was dissolved in MeOH and characterized by analytical HPLC and MALDI-TOF-MS.

Total Cleavage of H-(^AGly)₇-OH. The Fmoc-protected heptamer was removed from the resin by treatment with TFA/DCM/TES in the ratio of 40:10:1 (v/v) for 40 min. Afterwards the resin was filtered off and washed with TFA and DCM, the filtrate was reduced to a minimum volume and the cleaved heptamer was recovered by precipitation from ice-cold ether and centrifugation. The residue (22 mg) was insoluble in MeOH but completely soluble in TFE, where it was characterized by analytical HPLC, MALDI-TOF-MS and LC-ESI-MS.

Purification of H-(^AGly)₇-OH. The heptamer was dissolved in TFE and purified by preparative HPLC by using a C18 column and the gradient 25-85 % B in 67 min, with the elution system consisting of (A) 0.0059 % TFA in water (w/w) and of (B) acetonitrile. The fraction containing the desired compound was lyophilized, and the dry product (2 mg) was then characterized by HPLC and MALDI-TOF-MS: (M+H⁺)_{found} 1259.0 Da (MW_{calc} 1257.82 Da). HPLC gradient: 25-85 % B in 40 min, 85-95 % B in 5 min, 95 % for 10 min: t_R 18.52 min (elution at 52.78 % acetonitrile); 95.5 % purity.

Solid-Phase Synthesis of the Pentamer H-(Adg)₅-OH

Chain Assembly. 54.6 mg of Fmoc-^AGly-trityl resin (loading: 0.72 mmol/g) were swollen in DMF. Fmoc cleavage was performed by shaking the resin in 800 μ l of 40 % piperidine in DMF/NMP (4:1 v/v) for 7 min, and then in 800 μ l of 20 % piperidine (3x7 min). A single-coupling procedure was used for the attachment of the 2nd and 3rd ^AGly unit: the acylation mixture was Fmoc-^AGly-OH/HOBt/HBTU/DIPEA in the ratio of 3.7:3.7:3.7:7.4 eq with respect to the resin loading, and the reaction time was 3 h. After each coupling a capping step was carried out with acetic anhydride/DIPEA in the ratio of 1:1 (4 eq with respect to the resin loading) in DMF/NMP (10 min). For the

attachment of the 4th and 5th ^AGly unit a double-coupling procedure was applied with 4 and 5 eq of the amino acid, respectively.

Total Cleavage of H-(^AGly)₅-OH. The pentamer was removed from the resin by treatment with TFA/H₂O/TES in the ratio of 20:1:1 (v/v) for 40 min. Afterwards the resin was filtered off and washed with TFA and DCM, the filtrate was reduced to a minimum volume and the cleaved product was recovered by precipitation from ice-cold ether and centrifugation. The dried precipitate (26 mg) was then dissolved in TFE and characterized by analytical HPLC and MALDI-TOF-MS (Fig. 4). (M+H⁺)_{found} 904.2 Da (MW_{calc} 903.59 Da). HPLC gradient: 25-85 % B in 40 min, 85-95 % B in 5 min, 95 % B for 10 min: t_R 12.53 min (elution at 43.8 % acetonitrile); 87 % purity.

12.11. Solid phase synthesis of cyclization precursors **206 – 212**:

The precursors used in the cyclization study were prepared by using commercially available Wang resin preloaded with the appropriate Fmoc-amino acids and endcapped (Novabiochem, loading: Fmoc-Gly 0.8 mmol/g, Fmoc-L-Ala 0.4 mmol/g, Fmoc-L-Phe 0.74 mmol/g). The scale of the syntheses was 0.2 mmol for **206 – 210** and 0.7 mmol for **211** and **212**, respectively. Fmoc-cleavage was performed using 25% piperidine in DMF (2 × 20 min). Chain assembly steps were performed by double couplings using each 2 equivalents of the Fmoc-amino acid, HOBt and HBTU, and 4 equivalents DIPEA for 2 × 45 min. After each Fmoc cleavage and each chain elongation, the resin was washed by shaking it five times in DMF, five times in DCM, and then again five times in DMF. After the final Fmoc-deprotection, cleavage from the resin was accomplished using TFA / TIS / water (90 : 5 : 5, v/v) for 3h and with fresh cleavage cocktail for another 1 h. The peptides were precipitated by the addition of ice-cold diethyl ether, collected via suction filtration, washed with ice-cold diethyl ether and dried under reduced pressure in a desiccator over paraffine wax. After analysis with ESI-MS (vide supra), the linear precursors were used for the cyclization trials with no further purification.

12.12. Cyclization experiments: Synthesis of Cyclo-(D-Ala-^AGly-L-Ala)₂ (**213**):

In a flame-dried 250 mL flask under argon, 91.6 mg H-D-Ala-^AGly-L-Ala-D-Ala-^AGly-L-Ala-OH (**211**) and 211.4 mg (0.56 mmol, 4 eq.) HATU were dissolved in 100 mL of dry

acetonitrile. The mixture was cooled to 0 °C with an ice bath, and 244.8 mg (1.12 mmol, 8 eq.) DIPEA were added. The reaction mixture was stirred at 0 °C for 2h, until it became a clear solution, and then was stirred under argon for 14 days. The reaction was quenched with 100 mL brine and carefully extracted with 5 x 50 mL CHCl₃. The combined organics were washed with 1 N HCl, 5% NaHCO₃, water and brine and dried (Na₂SO₄). After evaporation of the solvents, the residue was purified by flash column chromatography eluting with DCM / methanol (93 : 7), R_f = 0.08. 35.1% of the cyclization product were isolated after evaporation of the eluent *in vacuo*.

Alternatively, HPLC purification of the crude product gave 19.0 mg (2.98 μ mol, 21.3 %) of **213** as a colorless powder, mp >190°C. Analytical data (¹H NMR, ¹³C NMR, ESI-MS) were identical when using both alternatives of purification. NMR spectra are, however, not analyzable due to assumed formation of aggregates and the very low solubility of the cyclopeptide. Therefore, only selected resonances are given here. Crystals suitable for X-ray structure analysis were grown by slow evaporation of a saturated solution in CHCl₃ / MeOH. ¹H NMR (400 MHz, CDCl₃ / CD₃OH): δ /ppm = 7.85 (d, J = 7 Hz, NH(Ala)); 6.72 (d, J = 5.6 Hz, NH(Ala)); 6.62 (br s, NH(^AGly)); 3.25 – 3.24 (m, 1H), 2.46 (d, J = 11.8 Hz, 1 H, Ala-H _{α}); 2.25 (d, J = 11.8 Hz, Ala-H _{α}); 2.21 – 2.02 (m, 3 H, adamantane-CH); 1.75 – 1.0 (m, adamantane-CH₂, Ala-CH₃). ¹³C NMR (400 MHz, CDCl₃ / CD₃OH): δ /ppm = 178.3 (C=O), 173.9 (C=O), 172.5 (C=O), 52.0, 50.0, 49.6, 42.2, 42.1, 39.2, 39.17, 39.0, 38.6, 37.9, 34.6, 29.1, 29.0, 16.9, 16.0. MS (ESI): m/z = 1299.5 [2 M + Na]⁺; (calc. 1299.8).

Cyclizations for linear precursors **206** – **210** and **212**, performed in the same manner as described above for precursor **211**, did not give any cyclization product as analyzed by ESI-MS.

12.13. Biological Tests

12.13.1. Anti-Influenza A

The antiviral tests were performed by Dr. Stephan Pleschka, Institute for Virology, Justus-Liebig-University / Germany. The test system is represented by repeated passaging of virus produced under selective condition and the analysis of the virus titer. Test model with both viruses were Madin-Darby canine kidney (MDCK) cells infected with *Influenza Virus A/FPV/Bratislava/79* (H7N7) and *AWSN-HK* (H1N2), respectively. Cells were grown over night at 37°C; 5% CO₂ and were infected with

virus dilution MOI = 1. Virus replication in comparison with the control substance (amantadine **19**) in the presence of substances **154** – **156** was monitored after incubation for 24h (FPV) and 48h (WSN-HK), respectively. The supernatant was harvested and diluted (1:1000) and re-infection of fresh cells was performed. Three rounds of infection were performed with the WSN virus, four with the FPV virus. The harvested supernatants were titred in dilution (10^{-1} – 10^{-8}), either by standard plaque assay or by IHC. The incubation time was 3 days for plaque assay, and 30 h for IHC-treatment. Staining and counting was performed according to standard protocols.

12.13.2. mGAT1 Uptake Experiments

The uptake experiments described here in brief were performed in the group of Prof. W. Schwarz by Dr. Stephan Krause, Max Planck Institute for Biophysics, Frankfurt / Germany. Full-grown prophase-arrested oocytes were isolated from female *X. laevis* and treated with 3 or 1.5 U/10 mL Liberase (Roche Diagnostics, Mannheim, Germany) for 2 to 4 h or overnight, respectively. mGAT1 was expressed in the oocytes by injection of 23 ng of cRNA per cell. Experiments were done after 3 days of incubation at 19°C. All experiments were conducted in climate-controlled rooms at a room temperature of 25°C. For measurements of radioactive tracer uptake, 10 to 20 oocytes were incubated in 200 μ L of the respective tracer solution for 20 min. The incubation solution utilized here contained 400 μ M GABA, of which about 1 % is labelled with ^3H , as well as 1 mM of the test substances (**141**, **142**, **154** – **156**, **185**). In stock solutions of these test substances, they were solubilized by the addition of DMSO when necessary. For GABA uptake [^3H]GABA (9.25 kBq/200 μ L) was used from GE Healthcare, Little Chalfont, Buckinghamshire, UK). After the incubation, the oocytes were washed, placed individually into counting vials, and dissolved in 0.1 mL (5%) SDS solution. The radioactivity taken up by the oocytes was then determined by liquid scintillation counting. Uptake in control oocytes, which were not injected with mGAT1 cRNA, were measured in the same manner.

12.14. AGly-based peptidic Organocatalysts incorporating His residues

Fmoc-^AGly-Phe-OMe (215): This dipeptide was prepared using general procedure A. In an oven-dried 100 mL flask under argon, 863 mg (4 mmol) of L-Phenylalanine methyl ester hydrochloride (**214**), 1.67 g (4 mmol) of Fmoc-^AGly (**180a**) and 1.517 g (4

mmol) HBTU were dissolved in 50 mL dry THF. 1.034 g (8 mmol) DIPEA were added and the mixture was stirred over night at rt, then 1 h at 60 °C. After cooling to rt, 50 mL of brine were added and the mixture was extracted with CHCl₃. The combined organics were washed with 1 N HCl, 5% NaHCO₃, water and brine and dried (Na₂SO₄). The solvents were evaporated under reduced pressure and the residue was purified by silica gel column chromatography eluting with ethyl acetate / hexane (2 : 1), R_f = 0.47. After evaporation of the eluent, 2.093 g (3.6 mmol, 90.4%) of the dipeptide were obtained as a colorless powder, mp 78 – 81 °C **¹H NMR** (400 MHz, CDCl₃): δ /ppm = 7.76 (d, J = 7.4 Hz, 2 H); 7.58 (d, J = 7.4 Hz, 2 H); 7.39 (t, J = 7.3 Hz, 2 H); 7.31 (t, J = 7.4 Hz, 2 H); 7.33 – 7.20 (m, 3 H); 7.07 (d, J = 7.1 Hz, 2 H); 6.02 (br s, 1 H, NH); 4.91 – 4.79 [m, 1 H, H _{α} (Phe)]; 4.64 (br s, 1 H, NH); 4.48 – 4.25 (m, 2 H, Fmoc-CH₂); 4.21 (t, J = 6.4 Hz, 1 H); 3.73 (s, 3 H, OCH₃); 3.22 – 3.04 [m, 2 H, H _{β} (Phe)]; 2.38 – 1.41 (m, 14 H, adamantane). **¹³C NMR** (100 MHz, CDCl₃): δ /ppm = 175.8 (C=O), 172.2 (C=O), 154.3 (C=O), 144.01 (C_q), 141.4 (C_q), 135.9 (C_q), 129.4, 128.6, 127.6, 127.2, 127.1, 125.0, 120.0, 66.0, 52.8, 52.3, 51.1 (C_q), 47.4, 43.0, 42.6 (C_q), 40.7, 38.0, 37.9, 35.2, 29.2. **MS** (ESI): m/z = 601.5 [M + Na]⁺; (calc. 601.3). **Elem. Anal.:** C₃₆H₃₈N₂O₅ (578.70): calcd. C 74.72, H 6.62, N 4.84; found C 73.53, H 6.86, N 4.58.

H^AGly-Phe-OMe (216): 2.049 g (3.54 mmol) Fmoc^AGly-Phe-OMe (**215**) were dissolved in 30 mL of dry acetonitrile according to general procedure C and cooled to 0 °C with an ice bath. 30 mL of diethylamine were slowly added and the mixture was stirred for 1 h at 0 °C and 24 h at rt. The solvents were evaporated under reduced pressure and the residue was purified by silica gel column chromatography eluting with *tert.* butyl methyl ether / methanol / triethylamine (20 : 10 : 1), R_f = 0.30. After careful evaporation of the eluent, 1.187 g (3.33 mmol, 94.1%) of the N-deprotected dipeptide **216** were obtained as a slightly yellowish solid, mp 86 °C. **¹H NMR** (200 MHz, CDCl₃): δ /ppm = 7.33 – 7.15 (m, 3 H); 7.12 – 6.99 (m, 2 H); 6.12 – 5.99 (br d, NH); 4.93 – 4.78 [m, 1 H, H _{α} (Phe)]; 3.72 (s, 3 H, OCH₃); 3.23 – 3.00 [m, 2 H, H _{β} (Phe)]; 2.26 – 2.09 (m, 2 H); 1.79 – 1.70 (m, 12 H, adamantane). **¹³C NMR** (50 MHz, CDCl₃): δ /ppm = 176.3 (C=O), 172.2 (C=O), 135.9 (C_q), 129.3, 128.5, 127.1, 52.7, 52.3, 47.8 (C_q), 47.6, 45.0, 43.0 (C_q), 38.0, 37.8, 29.5 **IR** (KBr): $\tilde{\nu}$ /cm⁻¹ = 3329, 3029, 2906, 2851, 1741, 1642, 1529, 1496, 1454, 1216, 702. **MS** (EI, 70 eV): m/z = 356

(4.8%), 299 (5.0%), 239 (3.3%), 194 (55.6%), 150 (100%), 120 (19.7%), 94 (33.4%). **HRMS** found, 356.2078, calc. 356.2030. **Elem. Anal.:** C₂₁H₂₈N₂O₃ (356.46): calcd. C 70.76, H 7.92, N 7.86; found C 70.71, H 7.84, N 7.89.

Boc-His(τ -Bn)-^AGly-Phe-OMe (218): Following general procedure A, 357 mg (1 mmol) H-^AGly-Phe-OMe (**216**), 345 mg Boc-His(τ -Bn)-OH (1 mmol, **217**) and 379 mg (1 mmol) HBTU were dissolved in 50 mL dry THF. 171 μ L (1 mmol) DIPEA were added and the mixture was stirred under argon at r.t. for 15 h. 50 mL brine and 50 mL chloroform were added, the layers were separated and the aqueous phase was extracted with chloroform (3 \times 30 mL). The combined organics were washed with 1N HCl, 5% NaHCO₃, water and brine (2 \times 30 mL each) and dried (Na₂SO₄). The crude product obtained after evaporation was purified by flash column chromatography eluting with dichloromethane / methanol (95 : 5), R_f (**218**) = 0.40. 603 mg (0.88 mmol, 88%) of tripeptide **218** were obtained as a colorless powder, mp. 97 °C. **¹H NMR** (400 MHz, CDCl₃): δ /ppm = 7.46 – 7.44 (m, 1 H); 7.38 – 7.22 (m, 6 H); 7.19 – 7.15 (m, 2 H); 7.11 – 7.06 (m, 2 H); 6.72 (br s, 1 H); 6.57 (br s, 1 H, NH); 6.20 (br s, 1 H, NH); 6.04 (d, J = 7.4 Hz, 1 H); 5.04 (s, 2 H, CH₂Ph); 4.89 – 4.82 (m, 1 H, H _{α} (Phe)); 4.29 (br s, 1 H, H _{α} (His)); 3.73 (s, 3 H, OCH₃); 3.20 – 3.05 (M, 3 H, H _{β} (Phe) and H _{β} (His)); 2.88 – 2.80 (m, 1 H, H _{β} (His)); 2.22 – 1.50 (m, 14 H, adamantane); 1.46 (s, 9 H, C(CH₃)₃). **¹³C NMR** (100 MHz, CDCl₃): δ /ppm = 176.0 (C=O), 172.2 (C=O), 170.8 (C=O), 138.6 (C_q), 136.5, 136.0 (C_q), 135.9 (C_q), 129.3, 129.0, 128.6, 128.3, 127.5, 127.1, 117.3, 79.7 (C_q), 52.8, 52.3, 51.8, 50.9, 42.5, 42.4, 40.3, 40.1, 38.1, 38.0, 37.8, 35.2, 30.7, 29.1, 28.4. **IR** (KBr): $\tilde{\nu}$ /cm⁻¹ = 3337, 2976, 2911, 2856, 1741, 1701, 1654, 1507, 1455, 1365, 1249, 1169. **MS** (ESI): m/z = 684.3 [M + H]⁺; (calc. 684.4). **Elem. Anal.:** C₃₉H₄₉N₅O₆ (683.84): calcd. C 68.50, H 7.22, N 10.24; found C 68.01, H 7.21, N 10.03.

Boc-His(π -Me)-^AGly-Phe-OMe (220): Following general procedure A, 178.2 mg (0.5 mmol) H-^AGly-Phe-OMe (**216**), 134.7 mg (0.5 mmol) Boc-His(π -Me)-OH (**219**) and 189.6 mg (0.5 mmol) HBTU were dissolved in 30 mL dry THF. 86 μ L (0.5 mmol) DIPEA were added and the mixture was stirred under argon at r.t. for 16 h. 30 mL brine and 30 mL chloroform were added, the layers were separated and the aqueous layer was extracted with chloroform (3 \times 20 mL). The combined organics were

washed with 1 N HCl, 5% NaHCO₃, water and brine (2 × 20 mL each) and dried (Na₂SO₄). The crude product obtained after evaporation of the solvents was purified by flash column chromatography eluting with dichloromethane / methanol (9:1), R_f (**220**) = 0.21. 199.5 mg (0.33 mmol, 66%) of tripeptide **220** were isolated as a colorless powder, mp. 71 °C. ¹H NMR (400 MHz, CDCl₃): δ /ppm = 7.39 (br s, 1 H); 7.33 – 7.22 (m, 3 H, H_{Ar}); 7.09 – 7.05 (m, 2 H, H_{Ar}); 6.85 (s, 1 H); 6.04 (d, J = 7.6 Hz, NH(Phe)); 5.71 (s, 1 H, NH(^AGly)); 5.17 (br s, 1 H, NH(His)); 4.88 – 4.81 (m, 1 H, H _{α} (Phe)); 4.21 – 4.08 (m, 1 H, H _{α} (His)); 3.73 (s, 3 H, O-CH₃); 3.58 (s, 3 H, N-CH₃); 3.20 – 2.91 (m, 4 H, H _{β} (Phe) and H _{β} (His)); 2.21 – 1.51 (m, 14 H, adamantane); 1.44 (s, 9 H, C(CH₃)₃). ¹³C NMR (100 MHz, CDCl₃): δ /ppm = 175.7 (C=O), 172.2 (C=O), 169.5 (C=O), 155.3 (C=O_{Boc}); 138.2, 135.8 (C_q), 129.2, 128.5, 128.2, 127.1, 80.4 (C_q), 52.7, 52.3, 52.2, 42.4, 42.1, 40.24, 40.20, 38.0, 37.9, 37.7, 35.0, 31.4, 29.0, 28.2, 26.7. IR (KBr): $\tilde{\nu}$ /cm⁻¹ = 3434, 2913, 1740, 1701, 1659, 1509, 1366, 1169. MS (ESI): m/z = 608.3 [M + H]⁺; (calc. 608.3). Elem. Anal.: C₃₃H₄₅N₅O₆ (607.74): calcd. C 65.22, H 7.46, N 11.52; found C 64.78, H 7.49, N 11.44.

Boc-His-^AGly-Phe-OMe (222): General procedure A was used. In an oven-dried 100 mL flask under argon, 357 mg (1 mmol) H-^AGly-Phe-OMe (**216**), 255 mg (1 mmol) Boc-His-OH (**221**) and 129.3 mg DIPEA (1 mmol) were dissolved in 30 mL dry acetonitrile and cooled to -20 °C. 379 mg (1 mmol) HBTU were added and the mixture was stirred upon warming to rt for 18 h. To complete the reaction, the mixture was stirred 1 h at 60 °C. 50 mL of brine were added, the mixture was extracted with chloroform and the combined organics were washed with water, 5% NaHCO₃, water and brine. After drying (Na₂SO₄) and evaporation of the solvents, the crude product was purified by flash column chromatography eluting with *tert.* butyl methyl ether / methanol / triethylamine (9 : 2 : 1), R_f = 0.39. After careful evaporation of the eluent, 455 mg (0.77 mmol, 76.7%) of the tripeptide **222** were obtained as a colorless powder, mp 119 °C. ¹H NMR (400 MHz, CDCl₃): δ /ppm = 7.62 (s, 1 H); 7.36 – 7.23 [m, 3 H, H_{Ar} (Phe)]; 7.10 – 7.05 [m, 2 H, H_{Ar} (Phe)]; 6.66 (br s, 1 H, NH); 6.05 (d, J = 7.6 Hz, 1 H); 6.00 (br s, 1 H, NH); 4.91 – 4.78 [m, 1 H, H _{α} (His)]; 4.43 – 4.20 [m, 1 H, H _{α} (Phe)]; 3.76 (s, 3 H, OCH₃); 3.22 – 2.86 [m, 4 H, H _{β} (Phe) + H _{β} (His)]; 2.20 – 1.55 (m, 14 H, adamantane); 1.44 [s, 9 H, C(CH₃)₃]. ¹³C NMR (100 MHz, CDCl₃): δ /ppm = 176.1 (C=O), 172.6 (C=O), 171.0 (C=O), 155.7 (C=O), 135.9 (C_q), 134.7, 129.39, 129.36,

128.7, 127.3, 117.8 (C_q), 80.1 ($C(CH_3)_3$), 52.9 (C_q), 52.8 (C_q), 52.5, 52.0 (OCH_3), 42.5, 41.8, 40.7 (C_q), 38.0, 37.8, 35.2, 29.0, 28.4 ($C(CH_3)_3$). **IR** (KBr): $\tilde{\nu}/cm^{-1} = 3366, 3029, 2976, 2912, 2856, 1741, 1662, 1518, 1455, 1366, 1250, 1171$. **MS** (ESI): $m/z = 616.4 [M+Na]^+$ (calc. 616.3). **Elem. Anal.:** $C_{32}H_{43}N_5O_6$ calc. C 64.74, H 7.30, N 11.80, found C 64.32, H 7.63, N 11.36.

Fmoc-^AGly-^AGly-Phe-OMe (223): Following general procedure A, this trimer was synthesized by dissolving 356.5 mg (1 mmol) of dipeptide **216**, 417.5 mg (1 mmol) Fmoc-^AGly-OH **180a** and 379.3 mg (1 mmol) HBTU in 30 mL dry acetonitrile at 0 °C. 129.3 mg (1 mmol) DIPEA were added and the mixture was stirred over night upon warming to rt. The mixture was heated to 60 °C for 1h. After cooling to rt, the reaction was quenched by adding 60 mL brine. The mixture was extracted with $CHCl_3$, the combined organics were washed with 1 N HCl, 5% $NaHCO_3$, water and brine and dried (Na_2SO_4). The crude product obtained after evaporation of the solvents was purified by flash column chromatography (2.5 × 35 cm, ~ 100 g SiO_2) eluting with n-hexane / ethyl acetate (1 : 4), $R_f = 0.42$. After evaporation of the eluent, 455 mg (0.602 mmol, 60.2%) of trimer **223** were isolated as colorless powder, mp 168 °C. **¹H NMR** (400 MHz, $CDCl_3$): $\delta/ppm = 7.76$ (d, J = 7.5 Hz, Fmoc); 7.59 (d, J = 7.7 Hz, 2 H); 7.40 (t, J = 7.4 Hz, 2 H); 7.35 – 7.21 (m, 5 H); 7.11 – 7.05 (m, 2 H); 6.04 (d, J = 7.6 Hz, NH); 5.26 (br s, 1 H, NH); 4.85 (dd, J = 6.7 / 1.5 Hz, 1 H); 4.70 (br s, 1 H, NH); 4.38 – 4.28 (m, 2 H, Fmoc- CH_2); 4.21 (t, J = 6.5 Hz, 1 H, Fmoc- CH); 3.72 (s, 3 H, OCH_3); 3.19 – 3.03 (m, 2 H, Phe- H_β); 2.80 (s, impurity of N,N,N',N'-tetramethylurea); 2.31 – 2.12 (m, 4 H, 4 × adamantane- CH); 2.08 – 1.80 (m, 12 H, 6 × adamantane- CH_2); 1.80 – 1.49 (m, 12 H, 6 × adamantane- CH_2). **¹³C NMR** (100 MHz, $CDCl_3$): $\delta/ppm = 176.0$ (C=O), 175.8 (C=O), 172.2 (C=O), 154.3 (Fmoc-C=O), 144.1 (C_q), 141.3 (C_q), 135.9 (C_q), 129.3, 128.6, 127.7, 127.1, 127.0, 125.0, 120.0, 66.0, 52.8, 52.3, 51.7, 51.3, 47.3, 43.2, 43.0, 42.6, 40.8, 40.4, 38.6, 38.24, 38.15, 38.10, 37.8, 35.3, 35.2, 29.22, 29.18. **MS** (ESI): $m/z = 756.3 [M+H]^+$ (calc. 756.4). **Elem. Anal.:** $C_{47}H_{53}N_3O_6$ calc. C 74.68, H 7.07, N 5.56, found C 74.39, H 7.14, N 5.92.

H-^AGly-^AGly-Phe-OMe (224): The Fmoc group of trimer **223** was cleaved following general procedure C. 305 mg (0.4 mmol) of **223** were suspended in 10 mL dry acetonitrile and cooled to 0 °C with an ice bath. 10 mL diethylamine were added, and

the mixture was stirred over night upon warming to rt. The solvents were carefully evaporated under reduced pressure, and the residue was purified by flash column chromatography (2.5 × 30 cm, ~ 80 g SiO₂) eluting with *tert* butyl methyl ether / methanol / triethylamine (60 : 30 : 1), R_f = 0.30. After evaporation of the eluent, 166 mg (0.311 mmol, 77.2%) **224** were isolated as a colorless powder that was used with no further purifications. ¹H NMR (400 MHz, CDCl₃): δ /ppm = 7.32 – 7.20 (m, 3 H); 7.12 – 7.05 (m, 2 H), 6.09 (d, J = 7.6 Hz, NH); 5.31 (br s, 1 H, NH); 4.84 (dd, J = 6.7 / 1.5 Hz, 1 H); 3.72 (s, 3 H, OCH₃); 3.18 – 3.04 (m, 2 H, Phe-H _{β); 2.29 – 2.13 (m, 4 H, 4 × adamantane-CH); 2.04 – 1.86 (m, 4 H, 2 × adamantane-CH₂); 2.00 (br s, 2 H, NH₂); 1.79 – 1.51 (m, 20 H, 10 × adamantane-CH₂). ¹³C NMR (100 MHz, CDCl₃): δ /ppm = 176.1 (C=O), 176.0 (C=O), 172.2 (C=O), 136.0 (C_q), 129.3, 128.5, 127.1, 52.9, 52.3, 51.7, 49.2, 43.58, 43.55, 43.2, 42.6, 40.47, 40.40, 38.18, 38.12, 37.8, 35.3, 35.0, 29.4, 29.2.}

Boc-His(π -Me)-^AGly-^AGly-Phe-OMe (225): The tetramer was prepared according to general procedure A. 166 mg (0.311 mmol) H-^AGly-^AGly-Phe-OMe (**224**), 107.4 mg (0.311 mmol) Boc-His(π -Me)-OH (**219**) and 118 mg (0.311 mmol) HBTU were dissolved in 25 mL dry acetonitrile and cooled to 0 °C with an ice bath. 40.2 mg (0.311 mmol) DIPEA were added and the mixture was stirred over night upon warming to rt. The reaction was quenched by adding 50 mL brine. The mixture was carefully extracted with CHCl₃ (4 × 50 mL), and the combined organics were washed with 1 N HCl, 5% NaHCO₃, water, and brine. After drying (Na₂SO₄) and evaporation of the solvents under reduced pressure, the residue was purified by flash chromatography (2.5 × 30 cm, ~ 80 g SiO₂) eluting with dichloromethane / methanol (90 : 10), R_f = 0.30. After evaporation of the eluent, 155.5 mg (0.198 mmol, 63.7%) of the tetramer **225** were isolated as a colorless powder, mp 130 °C. ¹H NMR (400 MHz, CDCl₃): δ /ppm = 7.33 (s, 1 H, His-imidazol); 7.27 – 7.14 (m, 3 H); 7.05 – 6.99 (m, 2 H); 6.78 (s, 1 H, His-imidazol); 6.01 (d, J = 7.6 Hz, Phe-NH); 5.69 (br s, 1 H, ^AGly-NH); 5.19 (br s, 1 H, ^AGly-NH); 5.09 (d, J = 5.2 Hz, His-NH); 4.77 (dd, J = 6.4 / 1.5 Hz, 1 H, Phe-H _{α); 4.16-4.03 (m, 1 H, His-H _{α); 3.65 (s, 3 H, OCH₃); 3.54 (s, 3 H, NCH₃); 3.12 – 2.97 (m, 2 H, Phe-H _{β); 2.93 (d, J = 6.9 Hz, 2 H, His-H _{β); 2.18 – 2.08 (m, 4 H, 4 × adamantane-CH); 1.99 – 1.48 (m, 24 H, 12 × adamantane-CH₂); 1.37 (s, 9 H, C(CH₃)₃). ¹³C NMR (100 MHz, CDCl₃): δ /ppm = 176.0 (C=O), 175.7 (C=O), 172.2 (C=O), 169.7 (C=O),}}}}

155.4 (Boc-C=O), 138.3 (His-imidazol), 135.9, 129.3, 128.5, 128.3, 127.2, 127.1, 80.5 (C_q, C(CH₃)₃), 52.8, 52.5 (C_q), 52.3, 51.7 (C_q), 42.9 (C_q), 42.60, 42.55, 40.47, 40.45, 40.43, 40.37, 38.27, 38.24, 38.18, 38.11, 37.83, 35.25, 35.21, 31.5, 29.7, 29.2, 28.3 (His-C_β). **IR** (KBr): $\tilde{\nu}/\text{cm}^{-1}$ = 3338, 3030, 2910, 2856, 1741, 1714, 1662, 1507, 1456, 1365, 1290, 1251, 1216, 1170. **MS** (ESI): m/z = 807.3 [M+Na]⁺ (calc. 807.4). **Elem. Anal.**: C₄₄H₆₀N₆O₇ calc. C 67.32, H 7.70, N 10.71, found C 66.67, H 10.72, N 10.06.

Solid-Phase synthesis of the organocatalysts 226 – 228:

The peptides were synthesized on solid support using commercially available Wang polystyrene resin endcapped and preloaded with Fmoc-protected L-phenylalanine (Novabiochem). Fmoc cleavage was performed by shaking the resin twice for 20 min in 25% piperidine in DMF (v / v). The resin was washed 5 times each with DMF, dichloromethane and DMF. Chain elongation with Fmoc-^AGly-OH was performed by a double coupling procedure using Fmoc-^AGly-OH, HBTU, and DIPEA (two times 2 : 2: 4 equiv., 1 h). Chain elongation with the α amino acids was performed in the same manner. After washing (5 times each with DMF, dichloromethane and diethylether), the peptides were cleaved from the resin as their respective methyl esters by shaking 5 days with methanol / triethylamine / THF (9 : 1 : 1, v / v). The resin was filtered off and washed several times with THF. The collected solutions were concentrated and the residue was purified by flash chromatography eluting with dichloromethane / methanol (95 : 5). The peptides was characterized by ESI-MS and NMR.

Boc-His(τ -Bn)-^AGly-^AGly-Phe-OMe (226): Mp 103.5 °C. **¹H NMR** (400 MHz, CDCl₃): δ/ppm = 7.47 (s, 1 H, His-imidazol); 7.38 – 7.21 (m, 6 H, Phe- and τ -Bn-CH_{Ar}); 7.19 – 7.14 (m, 2 H, τ -Bn-CH_{Ar}); 7.10 – 7.05 (m, 2 H, Phe-CH_{Ar}); 6.72 (s, 1 H, His-imidazol); 6.64 (br s, 1 H, Phe-NH); 6.20 (br s, 1 H, His-NH); 6.01 (d, J = 7.6 Hz, 1 H, ^AGly-NH); 5.24 (br s, 1 H, ^AGly-NH); 5.05 (s, 2 H, τ -Bn-CH₂); 4.84 (dd, J = 6.6 / 1.5 Hz, 1 H, Phe-H_α); 3.72 (s, 3 H, OCH₃); 3.18 – 3.03 (m, 3 H, 2 × Phe-H_β and 1 × His-H_β); 2.89 – 2.80 (m, 1 H, His-H_β); 2.25 – 2.11 (m, 4 H, 4 × adamantane-CH); 2.04 – 1.54 (m, 24 H, 12 × adamantane-CH₂); 1.44 (s, 9 H, C(CH₃)₃). **¹³C NMR** (100 MHz, CDCl₃): δ/ppm = 176.0 (C=O), 175.9 (C=O), 172.18 (C=O), 172.16 (C=O), 155.6 (Boc-C=O), 137.4, 135.9, 135.8, 135.1, 129.3, 129.2, 128.7, 128.6, 127.7, 127.1, 117.5, 79.7, 52.8, 52.3, 52.2, 51.4, 42.8, 42.6, 42.4, 40.47, 40.45, 40.37, 40.34, 38.3, 38.3, 38.1, 37.8, 35.29,

35.27, 29.2 (2 signals), 28.3. **MS** (ESI): $m/z = 883.4$ $[M+Na]^+$ (calc. 883.5). **Elem. Anal.:** $C_{50}H_{64}N_6O_7$ calc. C 69.74, H 7.49, N 10.33, found C 69.73, H 7.61, N 10.33.

Boc-His(τ -Bn)-Aib- α Gly-Phe-OMe (227): Mp 108 – 110 °C. **1H NMR** (400 MHz, $CDCl_3$): $\delta/ppm = 7.50$ (br s, 1 H, His-imidazol); 7.40 – 7.12 (m, 9 H, Phe- CH_{Ar} and His- τ -Bn- CH_{Ar} and His-imidazol); 7.10 – 7.05 (m, 2 H, Phe- CH_{Ar}); 6.80 – 6.59 (m, 2 H, His- τ -Bn- CH_{Ar}); 6.34 (br s, 1 H, NH); 6.18 (br s, 1 H, NH); 6.03 (d, J = 7.6 Hz, Phe-NH); 5.05 (s, 2 H, τ -Bn- CH_2); 5.04 (br s, 1 H, NH); 4.82 (dd, J = 6.5 / 1.6 Hz, 1 H, Phe- H_α); 4.19 (q, J = 5.7 Hz, 1 H, His- H_α); 3.69 (s, 3 H, OCH_3); 3.18 – 3.01 (m, 3 H, 2 \times Phe- H_β and 1 \times His- H_β); 2.93 – 2.81 (m, 1 H, His- H_β); 2.20 – 1.50 (m, 14 H, adamantane); 1.48 (br s, 6 H, 2 \times Aib- CH_3); 1.44 (s, 9 H, $C(CH_3)_3$). **^{13}C NMR** (100 MHz, $CDCl_3$): $\delta/ppm = 176.2$ (C=O), 176.0 (C=O), 173.3 (C=O), 172.1 (C=O), 155.8 (Boc-CO), 136.6, 135.9, 129.3, 129.1, 129.0, 128.55, 128.53, 127.6, 127.13, 127.07, 117.42, 79.9 (C_q), 64.4, 55.5, 52.8, 51.8, 51.1, 42.5, 40.0, 38.2, 38.1, 37.9, 35.3, 29.1, 28.3, 25.4. Note: Some signals are not visible due to the poor signal-to-noise ratio of the available spectrum. **MS** (ESI): $m/z = 791.4$ $[M+Na]^+$ (calc. 791.4). **Elem. Anal.:** $C_{43}H_{56}N_6O_7$ calc. C 67.17, H 7.34, N 10.93, found C 66.25, H 7.10, N 10.09.

Boc-His(τ -Bn)- α Gly-Aib-Phe-OMe (228): Mp 114 – 117 °C. **1H NMR** (400 MHz, $CDCl_3$): $\delta/ppm = 7.48$ (br s, 1 H, His-imidazol); 7.43 – 7.00 (m, 11 H, Phe- CH_{Ar} and τ -Bn- CH_{Ar} and His-imidazol); 6.84 – 6.60 (m, 2 H, τ -Bn- CH_{Ar}); 6.15 (br s, 1 H, NH); 5.05 (br s, 1 H, NH); 4.88 – 4.73 (m, 1 H, Phe- H_α); 4.27 (br s, 1 H, NH); 4.28 – 4.12 (m, 1 H, His- H_α); 3.71 (s, 3 H, OCH_3); 3.20 – 2.96 (m, 3 H, 2 \times Phe- H_β and 1 \times His- H_β); 2.95 – 2.78 (m, 1 H, His- H_β); 2.22 – 1.51 (m, 14 H, adamantane); 1.48 (br s, 6 H, 2 \times Aib- CH_3); 1.44 (s, 9 H, $C(CH_3)_3$). **^{13}C NMR** (100 MHz, $CDCl_3$): $\delta/ppm = 176.4$ (C=O), 174.2 (C=O), 171.9 (C=O), 170.7 (C=O), 155.7 (Boc-C=O), 135.9, 129.3, 129.1, 129.0, 128.5, 128.4, 128.3, 127.5, 127.1, 117.4, 79.8 (C_q), 64.4, 56.8, 53.4, 52.3, 51.9, 51.0, 42.8, 42.1, 40.2, 38.1, 37.8, 35.2, 30.6, 29.1, 28.3, 25.4. **MS** (ESI): $m/z = 791.4$ $[M + Na]^+$ (calc. 791.4). **Elem. Anal.:** $C_{43}H_{56}N_6O_7$ calc. C 67.17, H 7.34, N 10.93, found C 63.40, H 6.96, N 10.48.

12.15. Synthesis of peptidic thiourea organocatalysts incorporating AGly

***N*-[3,5-bis(trifluoromethyl)phenyl]-*N'*-3{[carboxy(glycine methyl ester)amido]tricyclo [3.3.1.1^{3,7}]dec-1-yl}thiourea (TU-^AGly-Gly-OMe, **239a**)** In an oven-dried 100 mL flask under argon, 1.019 g (3.82 mmol) H-^AGly-Gly-OMe **197** were dissolved in 20 mL dry THF and 493 mg (3.82 mmol) DIPEA were added. The mixture was cooled to 0 °C with an ice bath and 1.037 g (3.82 mmol) 3,5-bis(trifluoromethyl)phenyl isothiocyanate in 20 mL dry THF were added with an addition funnel. The mixture was stirred upon warming to rt for 24 h. After careful evaporation of the solvents *in vacuo*, the crude product was dissolved in CHCl₃ and reprecipitated by the addition of *n*-hexane. The product was collected via suction filtration and dried in a desiccator under vacuum over P₂O₅ and paraffine wax. 1.672 g (3.11 mmol, 81.3%) of the thiourea derivative were isolated as a colorless solid, mp 189 °C. ¹H NMR (400 MHz, d₆-DMSO): δ/ppm = 9.89 (s, 1 H); 8.22 (s, 2 H); 77.95 [t, J = 5.7 Hz, NH (Gly)]; 7.89 (s, 1 H); 7.71 (s, 1 H); 3.79 [d, J = 5.7 Hz, H_α (Gly)]; 3.62 (s, 3 H, OCH₃); 2.54 – 2.49 (m, 2 H); 2.33 – 2.14 (m, 6 H); 1.84 – 1.68 (m, 4 H); 1.68 – 1.53 (m, 2 H). ¹³C NMR (100 MHz, d₆-DMSO): δ/ppm = 178.6 (C=S), 176.5 (C=O), 170.4 (C=O), 141.8 (C_q), 130.0 (q, ²J_{C-F} = -33 Hz, 2 × C-CF₃), 123.2 (q, ¹J_{C-F} = -273 Hz, 2 × CF₃), 122.1, 115.9, 54.3 (C_q), 51.5 (OCH₃), 41.8, 40.7, 39.6, 37.6, 34.9, 28.8. One quarternary ¹³C signal lies under DMSO signal. IR (KBr): $\tilde{\nu}/\text{cm}^{-1}$ = 3326, 3213, 3044, 2909, 2857, 1721, 1640, 1531, 1387, 1277, 1175, 1138. MS (EI, 70 eV): *m/z* = 537 (0.3%), 466 (0.7%), 387 (0.4%), 309 (0.3%), 271 (100%), 250 (20.4%), 213 (21.2%), 150 (60.6%), 120 (32.1%). HRMS found, 537.1470, calc. 537.1521. Elem. Anal.: C₂₃H₂₅F₆N₃O₃S (537.52): calcd. C 51.39, H 4.69, N 7.82; found C 51.42, H 4.27, N 8.07.

***N*-[3,5-bis(trifluoromethyl)phenyl]-*N'*-3{[carboxy(phenylalanine methyl ester)amido]tricyclo [3.3.1.1^{3,7}]dec-1-yl}thiourea (TU-^AGly-Phe-OMe, **239b**):** In an oven-dried 100 mL flask under argon, 1.167 g (3.27 mmol) H-^AGly-Phe-OMe **197** were dissolved in 15 mL dry THF and 423 mg (3.27 mmol) DIPEA were added. The mixture was cooled to 0 °C with an ice bath and 888 mg (3.27 mmol) 3,5-bis(trifluoromethyl)phenyl isocyanate in 30 mL dry THF were added with an addition funnel. The mixture was stirred upon warming to rt for 24 h. After careful evaporation of the solvents *in vacuo*, the crude product was purified by silica gel column chromatography eluting with ethyl acetate / hexane (2 : 1), R_f (**239b**) = 0.50. After

evaporation of the eluent, 1.859 g (2.96 mmol, 90.6%) of the thiourea were isolated as a colorless powder, mp 96 – 97 °C. **¹H NMR** (400 MHz, CDCl₃): δ /ppm = 8.63 (s, 1 H); 7.89 (s, 2 H); 7.62 (s, 1 H); 7.33 – 7.18 (m, 3 H); 7.08 – 6.97 (m, 2 H); 6.56 (br s, 1 H, NH); 6.25 (d, J = 7.5 Hz, NH); 4.73 [t, J = 6.6 Hz, 1 H, H _{α} (Phe)]; 3.71 (s, 3 H, OCH₃); 3.16 – 3.01 [s, 2 H, H _{β} (Phe)]; 2.42 – 1.56 (m, 14 H, adamantane). **¹³C NMR** (100 MHz, CDCl₃): δ /ppm = 179.5 (C=S), 176.9 (C=O), 171.8 (C=O), 140.1 (C_q), 135.2 (C_q), 132.0 (q, ²J_{C-F} = -34 Hz, 2 × C- CF₃), 129.1, 128.7, 127.4, 123.0 (q, ¹J_{C-F} = -273 Hz, 2 × CF₃), 124.0, 118.2, 54.9, 53.0 (C_q), 52.5 (OCH₃), 42.8 (C_q), 42.7, 40.0, 37.9, 37.5, 35.0, 29.2. **IR** (KBr): $\tilde{\nu}$ /cm⁻¹ = 3434, 3331, 3089, 3032, 2914, 2858, 1747, 1640, 1532, 1386, 1278, 1176, 1132, 701, 682. **MS** (ESI): *m/z* = 650.4 [M+Na]⁺ (calc. 650.2). **Elem. Anal.**: C₃₀H₃₁F₆N₃O₃S (627.64): calcd. C 57.41, H 4.98, N 6.69; found C 57.38, H 4.90, N 6.70.

Fmoc-^AGly-Trp-OMe (242): This dimer was synthesized following general procedure A. 1.0336 g (4 mmol) Trp-OMe · HCl (**241**), 1.67 g (4 mmol) Fmoc-^AGly-OH (**180a**) and 1.517 g HBTU (4 mmol) were suspended in 100 mL dry acetonitrile and cooled to 0 °C with an ice bath. 517 mg (4 mmol) DIPEA were added and the mixture was stirred for 28 h upon warming to rt. The reaction was quenched with 100 mL brine, the mixture was extracted with CHCl₃, and the combined organics were washed with 1 N HCl, 5% NaHCO₃, brine, and were dried (Na₂SO₄). After evaporation of the solvents under reduced pressure, the crude product was purified by flash column chromatography (2.5 × 70 cm, ~ 200 g SiO₂) eluting with ethyl acetate / n-hexane (1 : 1) R_f = 0.19. After evaporation of the solvents, 2.1492 g (3.48 mmol, 87.0%) of dimer 242 were isolated as a colorless powder, mp 130 – 131 °C. **¹H NMR** (400 MHz, CDCl₃): δ /ppm = 8.08 (br s, 1 H, indol-NH); 7.76 (d, J = 7.0 Hz, 2 H, Fmoc-CH_{Ar}); 7.59 (d, J = 7.0 Hz, 2 H, Fmoc-CH_{Ar}); 7.57 – 7.26 (m, 6 H, Fmoc-CH_{Ar} and indol-CH_{Ar}); 7.21 – 7.05 (m, 2 H, CH_{Ar}); 6.96 (d, J = 2.3 Hz, 1 H, indol-CH_{Ar}); 6.09 (d, J = 7.7 Hz, 1 H, Trp-NH); 4.91 (dd, J = 6.2 / 2.2 Hz, 1 H, Trp-H _{α}); 4.58 (br s, 1 H, NH); 4.49 – 4.27 (m, 2 H, Fmoc-CH₂); 4.21 (t, J = 6.4 Hz, 1 H, Fmoc-CH); 3.70 (s, 3 H, OCH₃); 3.31 (d, J = 5.4 Hz, 2 H, Trp-H _{β}); 2.29 – 1.44 (m, 14 H, adamantane). **¹³C NMR** (100 MHz, CDCl₃): δ /ppm = 176.0 (C=O), 172.5 (C=O), 154.3 (Fmoc-C=O), 144.0, 141.3, 136.1, 127.6, 127.0, 125.0, 124.9, 122.8, 122.3, 120.0, 119.6, 118.7, 111.3, 110.1, 65.9, 53.4, 52.7, 52.3, 51.0, 47.3, 42.5, 40.6, 37.9 / 37.8 (diastereotopic); 35.0, 29.09 /

29.06 (diastereotopic), 27.5. **IR** (KBr): $\tilde{\nu}/\text{cm}^{-1} = 3424, 3324, 3061, 2911, 2855, 1727, 1709, 1648, 1450, 1242, 1215, 1081, 741$. **MS** (ESI): $m/z = 640.3$ $[\text{M}+\text{Na}]^+$ (calc. 640.3). **Elem. Anal.**: $\text{C}_{38}\text{H}_{39}\text{N}_3\text{O}_5$ (617.73): calcd. C 73.88, H 6.36, N 6.80; found C 73.78, H 46.61, N 6.84.

H-^AGly-Trp-OMe (243): The Fmoc-group in **242** was cleaved following general procedure C. 1.2227 g (1.98 mmol) Fmoc-^AGly-Trp-OMe (**242**) were dissolved in 20 mL dry acetonitrile and cooled to 0 °C with an ice bath. 20 mL diethylamine were slowly added and the mixture was stirred for 5.5 h upon warming to rt. The solvents were carefully evaporated under reduced pressure and the residue was purified by silica gel column chromatography (2.5 × 35 cm, ~ 80 g SiO₂) eluting with *tert* butyl methyl ether / methanol / triethylamine (60 : 30 : 1), $R_f = 0.28$. After evaporation of the eluent, 734.5 mg (1.86 mmol, 93.8%) of the amine **243** were isolated as a slightly yellowish oil that crystallized upon standing for several days, mp 140 – 143 °C. **¹H NMR** (400 MHz, CDCl₃): $\delta/\text{ppm} = 8.75$ (br s, 1 H, indol-NH); 7.51 (d, $J = 7.8$ Hz, 1 H, indol-CH_{Ar}); 7.36 (d, $J = 8.1$ Hz, 1 H, indol-CH_{Ar}); 7.17 (dt, $J = 7.6 / 1.1$ Hz, 1 H, indol-CH_{Ar}); 7.10 (dt, $J = 7.5 / 0.9$ Hz, 1 H, indol-CH_{Ar}); 6.98 (br s, 1 H, indol-CH_{Ar}); 6.16 (d, $J = 7.8$ Hz, 1 H, indol-CH_{Ar}); 4.89 (dd, $J = 6.4 / 2.1$ Hz, 1 H, Trp-H_α); 3.80 (br s, 2 H, NH₂); 3.70 (s, 3 H, OCH₃); 3.39 – 3.23 (m, 2 H, Trp-H_β); 2.23 – 2.07 (m, 2 H, adamantane-CH); 1.81 – 1.55 (m, 10 H, 5 × adamantane-CH₂); 1.55 – 1.47 (m, 2 H, adamantane-CH₂). **¹³C NMR** (100 MHz, CDCl₃): $\delta/\text{ppm} = 176.3$ (C=O), 172.6 (C=O), 136.2 (C_q), 127.7 (C_q), 123.1, 122.1, 119.5, 118.6, 111.5, 109.7 (C_q); 52.7, 52.4, 49.4, 45.8, 43.33 / 43.30 (diastereotopic), 42.8, 37.7 / 37.6 (diastereotopic), 34.9, 29.3, 27.5. **IR** (KBr): $\tilde{\nu}/\text{cm}^{-1} = 3424, 3332, 3276, 2909, 2850, 1741, 1646, 1512, 1456, 1440, 1366, 1343, 1213, 743$. **MS** (ESI): $m/z = 396.2$ $[\text{M}+\text{H}]^+$ (calc. 396.2).

N-[3,5-bis(trifluoromethyl)phenyl]-N'-3{[carboxy(tryptophane methyl ester)amido]tricyclo [3.3.1.1^{3,7}]dec-1-yl}thiourea (TU-^AGly-Trp-OMe, 239c): In an oven-dried 100 mL flask under argon, 237.3 mg (0.6 mmol) H-^AGly-Trp-OMe **243** were dissolved in 10 mL dry THF and 77.6 mg (0.6 mmol) DIPEA were added. The mixture was cooled to 0 °C with an ice bath and 162.7 mg (0.6 mmol) 3,5-bis(trifluoromethyl)phenyl isocyanate in 15 mL dry THF were added with an addition funnel. The mixture was stirred upon warming to rt for 24 h. After careful evaporation of the solvents *in vacuo*,

the crude product was purified by silica gel column chromatography eluting with *tert* butyl methyl ether, R_f (**239c**) = 0.35. After evaporation of the eluent, 322.2 mg (0.483 mmol, 80.5%) of the thiourea were isolated as a colorless powder, mp 127 – 131 °C. **$^1\text{H NMR}$** (400 MHz, CDCl_3): δ/ppm = 8.61 (br s, 1 H, NH); 8.27 (br s, 1 H, NH); 7.82 (s, 2 H, thiourea- CH_{Ar}); 7.53 (s, 1 H, thiourea- CH_{Ar}); 7.39 (d, J = 7.8 Hz, 1 H, indol- CH_{Ar}); 7.23 (d, J = 8.0 Hz, 1 H, indol- CH_{Ar}); 7.09 (dt, J = 7.5 / 0.9 Hz, 1 H, indol- CH_{Ar}); 7.03 (dt, J = 7.5 / 1.0 Hz, 1 H, indol- CH_{Ar}); 6.89 (d, J = 2.3 Hz, 1 H, Indol- CH_{Ar}); 6.54 (br s, 1 H, NH); 4.68 (q, J = 6.2 Hz, 1 H, Trp- H_{α}); 3.58 (s, 3 H, OCH_3); 3.21 (d, J = 5.5 Hz, 2 H, Trp- H_{β}); 2.30 – 2.00 (m, 8 H, adamantane); 1.71 – 1.38 (m, 6 H, adamantane). **$^{13}\text{C NMR}$** (100 MHz, CDCl_3): δ/ppm = 179.4 (C=S), 177.2 (C=O), 172.2 (C=O), 140.3 (C_q), 136.1, 131.8 (q, $^2J_{\text{C-F}}$ = -3.3 Hz, C- CF_3); 127.2, 123.9, 123.1 (q, $^1J_{\text{C-F}}$ = -272 Hz, CF_3); 123.0, 122.4, 119.7, 118.2, 118.1, 111.4, 109.2, 65.8, 54.8, 52.8, 52.5, 42.7, 42.6, 40.0, 37.8 / 37.7 (diastereotopic), 34.9, 29.1. **MS** (ESI): m/z = 689.3 $[\text{M}+\text{Na}]^+$ (calc. 689.2). **Elem. Anal.:** $\text{C}_{32}\text{H}_{32}\text{F}_6\text{N}_4\text{O}_3\text{S}$ (666.68): calcd. C 57.65, H 4.84, N 8.40; found C 57.68, H 5.39, N 7.96.

Fmoc- A Gly-Tyr-OMe (245): The dimer was synthesized following general procedure A. 780.9 mg (4 mmol) H-Tyr-OMe · HCl (**244**), 1.67 g (4 mmol) Fmoc- A Gly (**180c**) and 1.517 g (4 mmol) HBTU were dissolved in 50 mL dry acetonitrile and cooled to 0 °C with an ice bath. 1.034 g (8 mmol) DIPEA were added and the mixture was stirred for 28 h upon slowly warming up to rt. 100 mL brine were added, the mixture was extracted with CHCl_3 , and the combined organics were washed with 1 N HCl, 5 % NaHCO_3 , water and brine. After drying (Na_2SO_4) and evaporation of the solvents, the crude product was purified by flash chromatography (2.5 × 70 cm, ~ 200 g SiO_2) eluting with dichloromethane / methanol (97 : 3), R_f = 0.35. After evaporation of the eluent, 1.475 g (2.48 mmol, 62.0%) of the dimer were obtained as a colorless powder, mp 96 °C. **$^1\text{H NMR}$** (200 MHz, CDCl_3): δ/ppm = 7.75 (d, J = 7.0 Hz, 2 H, Fmoc- CH_{Ar}); 7.58 (d, J = 7.1 Hz, 2 H, Fmoc- CH_{Ar}); 7.45 – 7.26 (m, 4 H, Fmoc- CH_{Ar}); 6.91 (d, J = 8.4 Hz, 2 H, Tyr- CH_{Ar}); 6.73 (d, J = 5.5 Hz, 2 H, Tyr- CH_{Ar}); 6.07 (br s, 1 H, Tyr-NH); 4.88 – 4.74 (m, 1 H, Tyr- H_{α}); 4.69 (br s, 1 H, A Gly-NH); 4.44 – 4.25 (m, 2 H, Fmoc- CH_2); 4.19 (t, J = 6.4 Hz, Fmoc-CH); 3.72 (s, 3 H, OCH_3); 3.15 – 2.88 (m, 2 H, Tyr- H_{β}); 2.29 – 1.32 (m, 14 H, adamantane). **$^{13}\text{C NMR}$** (50 MHz, CDCl_3): δ/ppm = 176.6 (C=O), 172.3 (C=O), 155.5 (C_q), 154.4 (Fmoc-C=O); 143.8 (C_q), 141.2 (C_q), 130.3,

127.6, 127.0, 126.9, 124.9, 119.9, 115.6, 66.0, 53.0, 52.3, 51.0, 47.2, 42.7, 42.5, 40.5, 37.7, 37.0, 34.9, 29.0. **MS** (ESI): $m/z = 617.3$ $[M+Na]^+$ (calc. 617.3). **Elem. Anal.:** $C_{36}H_{38}N_2O_6$ (594.70): calcd. C 72.71, H 6.44, N 4.71; found C 72.98, H 6.63, N 4.63.

H^AGly-Tyr-OMe (246): Following general procedure C, 594.7 mg (1 mmol) Fmoc-^AGly-Tyr-OMe (**245**) were dissolved in 6 mL dry acetonitrile and cooled to 0 °C with an ice bath. 6 mL diethylamine were slowly added and the mixture was stirred over night upon warming to rt. The solvents were evaporated under reduced pressure and the residue was purified by flash column chromatography (2.5 × 30 cm, ~ 80 g SiO₂) eluting with *tert* butyl methyl ether / methanol / triethylamine (9 : 2 : 1), $R_f = 0.12$. After evaporation of the eluent, 331.9 mg (0.891 mmol, 89.1 %) of the amino peptide **246** were isolated as a colorless powder, mp = 155 °C. **¹H NMR** (400 MHz, CDCl₃): $\delta/ppm = 6.91$ (d, J = 8.5 Hz, 2 H, Tyr-CH_{Ar}); 6.74 (d, J = 8.5 Hz, 2 H, Tyr-CH_{Ar}); 6.04 (d, J = 7.8 Hz, Tyr-NH); 4.82 (dd, J = 6.4 / 1.9 Hz, 1 H, Tyr-H_α); 3.75 (s, 3 H, OCH₃); 3.57 (br s, 2 H, NH₂); 3.13 – 2.93 (m, 2 H, Tyr-H_β); 2.23 – 2.15 (m, 2 H, adamantane-CH); 1.85 – 1.52 (m, 12 H, 6 × adamantane-CH₂). **¹³C NMR** (100 MHz, CDCl₃): $\delta/ppm = 176.3$ (C=O), 172.4 (C=O), 155.9 (C_q), 130.4, 126.7, 115.8, 52.8, 52.4, 48.4, 46.8, 44.55, 44.49, 42.9, 37.79 / 37.75 (diastereotopic), 37.0, 35.0, 29.40 / 29.38 (diastereotopic). **MS** (ESI): $m/z = 373.1$ $[M+H]^+$ (calc. 373.2). **Elem. Anal.:** $C_{21}H_{28}N_2O_4$ (372.46): calcd. C 67.72, H 7.58, N 7.52; found C 65.20, H 8.07, N 7.27.

N-[3,5-bis(trifluoromethyl)phenyl]-N'-3{[carboxy(tyrosine methyl ester)amido]-tricyclo [3.3.1.1^{3,7}]dec-1-yl}thiourea (TU-^AGly-Tyr-OH, **239d):** In an oven-dried 50 mL flask under argon, 256 mg (0.687 mmol) H-^AGly-Tyr-OMe **245** were dissolved in 10 mL dry THF and 88.4 mg (0.687 mmol) DIPEA were added. The mixture was cooled to 0 °C with an ice bath and 186.4 mg (0.687 mmol) 3,5-bis(trifluoromethyl)phenyl isocyanate in 15 mL dry THF were added with an addition funnel. The mixture was stirred upon warming to rt for 24 h. After careful evaporation of the solvents *in vacuo*, the crude product was purified by flash chromatography (2.5 × 60 cm, ~ 170 g SiO₂) eluting with n-hexane / ethyl acetate, R_f (**239d**) = 0.55. After evaporation of the eluent, 402.6 mg (0.626 mmol, 91.0%) of the thiourea were isolated as a colorless powder, mp 121 – 123 °C. **¹H NMR** (400 MHz, CDCl₃): $\delta/ppm = 8.41$ (br s, 1 H, NH); 7.83 (s, 2 H, thiourea-CH_{Ar}); 7.62 (s, 1 H, thiourea-CH_{Ar}); 6.91 (d, J =

8.5 Hz, 2 H, tyrosine- CH_{Ar}); 6.74 (d, $J = 8.5$ Hz, 2 H, tyrosine- CH_{Ar}); 6.38 (br s, 1 H, NH); 6.25 (d, $J = 7.9$ Hz, Tyr- NH); 4.75 (t, $J = 6.6$ Hz, 1 H, Tyr- H_{α}); 3.72 (s, 3 H, OCH_3); 2.12 – 2.89 (m, 2 H, Tyr- H_{β}); 2.30 – 1.51 (m, 14 H, adamantane). ^{13}C NMR (100 MHz, $CDCl_3$): $\delta/ppm = 179.3$ (C=S), 177.0 (C=O), 172.2 (C=O), 155.3, 140.0, 132.2 (q, $^2J_{C-F} = -33$ Hz, C- CF_3), 130.3, 126.9, 124.0, 123.0 (q, $^1J_{C-F} = -273$ Hz, CF_3), 115.8, 73.1, 55.0, 53.2, 52.6, 42.8, 42.4, 40.3 / 40.2 (diastereotopic), 37.84 / 37.77 (diastereotopic), 37.0, 35.0, 29.1. IR (KBr): $\tilde{\nu}/cm^{-1} = 3329, 2915, 2866, 1639, 1516, 1473, 1453, 1385, 1279, 1175, 1133$. MS (ESI): $m/z = 666.4$ [$M+Na$] $^+$ (calc. 666.2). **Elem. Anal.:** $C_{30}H_{31}F_6N_3O_4S$ (643.64): calcd. C 55.98, H 4.85, N 6.53; found C 56.34, H 4.80, N 6.14.

Fmoc- A Gly-His(π -Me)-OMe (248): Following general procedure A, 3.34 g (8 mmol) Fmoc- A Gly-OH (**180a**), 2.049 g (8 mmol) His(π -Me)-OMe \cdot 2 HCl **247** (8 mmol) and 3.034 g (8 mmol) HBTU were dissolved in 100 mL dry acetonitrile and 10 mL dry methanol and cooled to 0 °C with an ice bath. 3.102 g (24 mmol) DIPEA were added and the mixture was stirred upon warming to rt for 3.5 h (TLC-control, DCM / methanol 9 : 1). The reaction was quenched with 150 mL brine and extracted with $CHCl_3$. The combined organics were washed with water, 5% $NaHCO_3$ and brine and were dried (Na_2SO_4). The crude product obtained after evaporation of the solvents was purified by flash chromatography (3.0 \times 80 cm, \sim 250 g SiO_2) eluting with dichloromethane / methanol (90 : 10), $R_f = 0.41$. After evaporation of the solvents, 3.8157 g (6.55 mmol, 81.9%) of the dimer **248** were obtained as a colorless powder that was used with no further purifications. 1H NMR (400 MHz, $CDCl_3$): $\delta/ppm = 7.75$ (d, $J = 7.5$ Hz, 2 H, Fmoc- CH_{Ar}); 7.58 (d, $J = 7.3$ Hz, 2 H, Fmoc- CH_{Ar}); 7.42 (s, 1 H, imidazol- CH_{Ar}); 7.39 (t, $J = 7.4$ Hz, 2 H, Fmoc- CH_{Ar}); 7.31 (t, $J = 7.4$ Hz, 2 H, Fmoc- CH_{Ar}); 6.76 (s, 1 H, imidazol- CH_{Ar}); 6.24 (br s, 1 H, NH); 4.78 (t, $J = 6.6$ Hz, 1 H, His- H_{α}); 4.72 (br s, 1 H, NH); 4.42 – 4.24 (m, 2 H, Fmoc- CH_2); 4.19 (t, $J = 6.4$ Hz, 1 H, Fmoc- CH); 3.74 (s, 3 H, OCH_3); 3.58 (s, 3 H, NCH_3); 3.17 – 3.00 (m, 2 H, His- H_{β}); 2.29 – 1.48 (m, 14 H, adamantane). MS (ESI): $m/z = 583.3$ [$M+H$] $^+$ (calc. 583.3).

H- A Gly-His(π -Me)-OMe (249): Following general procedure C, Fmoc-cleavage was accomplished by dissolving 1.1654 g (2 mmol) Fmoc- A Gly-His(π -Me)-OMe (**248**) in 20 mL dry acetonitrile. At 0 °C, 20 mL diethylamine were slowly added and the mixture

was stirred upon warming to rt for 2 h. The solvents were then evaporated under reduced pressure, and the residue was purified by flash chromatography (2.5 × 30 cm, ~ 80 g SiO₂) eluting with TBME / methanol / triethylamine (60 : 30 : 1), R_f = 0.08. After evaporation of the eluent, 666.9 mg (1.85 mmol, 92.5%) of aminopeptide **249** were obtained as a slightly yellowish oil that crystallizes upon standing for several weeks. **¹H NMR** (400 MHz, CDCl₃): δ/ppm = 7.39 (s, 1 H, imidazol-CH_{Ar}); 6.76 (s, 1 H, imidazol-CH_{Ar}); 6.31 (d, J = 7.2 Hz, 1 H, His-NH); 4.80 (t, J = 6.6 Hz, His-H_α); 3.75 (s, 3 H, OCH₃); 3.59 (s, 3 H, N-CH₃); 3.20 – 3.02 (m, 2 H, His-H_β); 2.30 – 2.16 (m, 2 H, adamantane-CH); 1.93 – 1.51 (m, 12 H, adamantane-CH₂); 1.85 (br s, 2 H, NH₂). **¹³C NMR** (100 MHz, CDCl₃): δ/ppm = 176.7 (C=O), 171.8 (C=O), 138.3 (imidazol-C), 128.3 (imidazol-C), 126.2 (imidazol-C), 52.6, 51.0, 47.8, 47.4, 44.7, 42.9, 37.9, 35.0, 31.3, 29.3, 26.5. **IR** (KBr): $\tilde{\nu}$ /cm⁻¹ = 3340, 2910, 2853, 1741, 1646, 1533, 1510, 1452, 1440, 1290, 1242, 1219, 1202. **MS** (ESI): *m/z* = 361.2 [M+H]⁺ (calc. 361.2).

***N*-[3,5-bis(trifluoromethyl)phenyl]-*N'*-3-[[carboxy(histidine(3-methyl)methyl ester)amido]-tricyclo [3.3.1.1^{3,7}]dec-1-yl]thiourea (TH-^AGly-His(π -Me)-OMe, **239e**):** In an oven-dried 50 mL flask under argon, 440 mg (1.22 mmol) H-^AGly-His(π -Me)-OMe **249** were dissolved in 20 mL dry THF. The mixture was cooled to 0 °C with an ice bath and 331 mg (1.22 mmol) 3,5-bis(trifluoromethyl)phenyl isocyanate in 15 mL dry THF were added with an addition funnel. The mixture was stirred upon warming to rt for 12 h. After careful evaporation of the solvents *in vacuo*, the crude product was purified by flash chromatography (2.5 × 70 cm, ~ 200 g SiO₂) eluting with DCM / methanol (85 : 15), R_f (**239e**) = 0.54. After evaporation of the eluent, 730.8 mg (0.116 mmol, 94.8%) of the thiourea were isolated as a slightly yellowish foam, mp 121 – 131 °C. **¹H NMR** (400 MHz, CDCl₃): δ/ppm = 9.23 (br s, 1 H, thiourea-NH); 7.87 (s, 2 H, thiourea-CH_{Ar}); 7.57 (s, 1 H, thiourea-CH_{Ar}); 7.47 (s, 1 H, imidazol-CH_{Ar}); 6.79 (s, 2 H, thiourea-NH and imidazol-CH_{Ar}); 6.43 (d, J = 8.1 Hz, 1 H, His-NH); 4.87 (dd, J = 8.1 / 1.0 Hz, 1 H, His-H_α); 3.76 (s, 3 H, OCH₃); 3.61 (s, 3 H, NCH₃); 3.42 – 2.82 (m, 2 H, His-H_β); 2.50 – 1.52 (m, 14 H, adamantane). **¹³C NMR** (100 MHz, CDCl₃): δ/ppm = 179.6 (C=S), 176.6 (C=O), 171.6 (C=O), 140.4 (C_q), 138.3, 131.8 (q, ²J_{C-F} = -34 Hz, C-CF₃); 127.8, 126.9, 123.3, 123.1 (q, ¹J_{C-F} = -273 Hz, CF₃); 117.7, 54.8, 52.8, 50.9, 42.7, 42.5, 40.5 / 40.1 (diastereotopic), 38.0 / 37.8 (diastereotopic), 35.1, 31.6, 29.2 / 29.1 (diastereotopic), 26.5. **IR** (KBr): $\tilde{\nu}$ /cm⁻¹ = 3428, 3336, 3056, 2913, 2856, 1746, 1652,

1538, 1511, 1474, 1456, 1386, 1359, 1338, 1278, 1173, 1131, 1108. **MS** (ESI): $m/z = 632.2$ $[M+H]^+$ (calc. 632.2). **Elem. Anal.**: $C_{28}H_{31}F_6N_5O_3S$ (631.63): calcd. C 53.24, H 4.95, N 11.09, found C 53.60, H 4.46, N 10.86.

Fmoc-^AGly-His(τ -Bn)-OMe (251): Following general procedure A, 1.3283 g (4 mmol) Boc-His(τ -Bn)-OH, 1.67 g (4 mmol) Fmoc-^AGly-OH (**180a**) and 1.517 g (4 mmol) HBTU were dissolved in 50 mL dry acetonitrile and cooled to 0 °C with an ice bath. 1.551 g (12 mmol) DIPEA were added and the mixture was stirred over night upon warming to rt. 100 mL brine were added and the mixture was extracted with $CHCl_3$. The combined organics were washed with water, 5% $NaHCO_3$, water and brine and dried (Na_2SO_4). The crude compound obtained after evaporation of the solvents was purified by flash chromatography (2.5 × 70 cm, ~ 200 g SiO_2) eluting with DCM / methanol (93 : 7), $R_f = 0.38$. After evaporation of the eluent, 2.1378 g (3.25 mmol, 81.1%) of the dimer were obtained as a slightly yellowish foam that was used for further conversions without additional purification. **¹H NMR** (400 MHz, $CDCl_3$): $\delta/ppm = 7.68$ d, $J = 7.5$ Hz, 2 H, Fmoc- CH_{Ar} ; 7.51 (d, $J = 7.4$ Hz, 2 H, Fmoc- CH_{Ar}); 7.40 (br s, 1 H, His-NH); 7.38 (s, 1 H, imidazol); 7.32 (t, $J = 7.4$ Hz, 2 H, Fmoc- CH_{Ar}); 7.28 – 7.21 (m, 5 H, Fmoc- CH_{Ar} and τ -Bn- CH_{Ar}); 7.06 – 6.99 (m, 2 H, τ -Bn- CH_{Ar}); 6.56 (s, 1 H, imidazol); 4.94 (s, 2 H, τ -Bn- CH_2); 4.79 – 4.56 (m, 2 H, NH and His- H_α); 4.34 – 4.16 (m, 2 H, Fmoc- CH_2); 4.13 (t, $J = 6.6$ Hz, Fmoc-CH); 3.55 (s, 3 H, OCH_3); 3.06 – 2.85 (m, 2 H, His- H_β); 2.73 (s, impurity of N,N,N',N'-tetramethylurea); 2.27 – 1.38 (m, 14 H, adamantane). **¹³C NMR** (100 MHz, $CDCl_3$): $\delta/ppm = 176.6$ (C=O), 172.0 (C=O), 154.2 (Fmoc-C=O), 144.1 (C_q), 141.3 (C_q); 138.0, 137.1, 135.9, 127.6, 127.2, 127.0, 125.0, 119.9, 65.9, 52.8, 52.1, 51.2, 50.8, 47.3, 43.1, 42.5, 40.6, 38.6, 37.9, 35.2, 29.6, 29.4, 29.2. **MS** (ESI): $m/z = 659.4$ $[M+H]^+$ (calc. 659.3).

H-^AGly-His(τ -Bn)-OMe (252): Following general procedure C, 2.0948 g (3.18 mmol) of the Fmoc-protected dipeptide **251** obtained as described above were dissolved in 20 mL dry acetonitrile and cooled to 0 °C. 10 mL diethylamine were slowly added and the mixture was stirred for 2 h upon warming to rt. The solvents were carefully evaporated and the residue was purified by flash chromatography (2.5 × 80 cm, ~ 100 g SiO_2) eluting with TBME / methanol / triethylamine (60 : 30 : 1), $R_f = 0.16$. After evaporation of the eluent, 1.1655 g (2.67 mmol, 84.0%) of the aminopeptide were

obtained as a slightly yellowish oil that crystallized upon standing for several days. $^1\text{H NMR}$ (400 MHz, CDCl_3): δ/ppm = 7.68 (d, J = 7.4 Hz, 1 H, His-NH); 7.47 (s, 1 H, imidazol); 7.38 – 7.27 (m, 3 H, $\tau\text{-Bn-CH}_{\text{Ar}}$); 7.15 – 7.06 (m, 2 H, $\tau\text{-Bn-CH}_{\text{Ar}}$); 6.63 (s, 1 H, imidazol); 5.04 (s, 2 H, $\tau\text{-Bn-CH}_2$); 4.78 – 4.70 (m, 1 H, His- H_α); 3.61 (s, 3 H, OCH_3); 3.11 – 2.93 (m, 2 H, His- H_β); 2.21 – 2.15 (m, 2 H, 2 \times adamantane-CH); 1.87 – 1.50 (m, 14 H, 6 \times adamantane- CH_2 and NH_2). $^{13}\text{C NMR}$ (100 MHz, CDCl_3): δ/ppm = 177.1 (C=O), 172.1 (C=O), 138.2, 137.2, 136.1, 129.0, 128.3, 127.2, 116.9, 52.2, 52.1, 50.8, 48.0, 47.6, 44.9, 44.8, 42.9, 37.94 / 37.89 (diastereotopic), 35.2, 29.6 / 29.5 (diastereotopic). **IR** (KBr): $\tilde{\nu}/\text{cm}^{-1}$ = 3344, 3064, 3032, 2910, 2861, 1744, 1653, 1500, 1455, 1359, 1301, 1212, 1174, 717. **MS** (ESI): m/z = 437.3 $[\text{M}+\text{H}]^+$ (calc. 437.5).

***N*-[3,5-bis(trifluoromethyl)phenyl]-*N'*-3{[carboxy(histidine(1-benzyl)methyl ester) amido]-tricyclo [3.3.1.1^{3,7}]dec-1-yl}thiourea (TU-^AGly-His(τ -Bn)-OMe, **239f**):** In an oven-dried 50 mL flask under argon, 290.5 mg (0.66 mmol) H-^AGly-His(τ -Bn)-OMe **252** were dissolved in 10 mL dry THF. The mixture was cooled to 0 °C with an ice bath and 180.3 mg (0.665 mmol) 3,5-bis(trifluoromethyl)phenyl isocyanate in 15 mL dry THF were added with an addition funnel. The mixture was stirred upon warming to rt over night. After careful evaporation of the solvents *in vacuo*, the crude product was purified by flash chromatography (2.5 x 30 cm, ~ 80 g SiO_2) eluting with DCM / methanol (93 : 7), R_f (**239f**) = 0.42. After evaporation of the eluent, 359 mg (0.51 mmol, 76.2 %) of the thiourea were isolated as a slightly yellowish foam, mp 94 - 96 °C. $^1\text{H NMR}$ (400 MHz, CDCl_3): δ/ppm = 9.12 (br s, 1 H, NH); 8.06 (d, J = 6.9 Hz, His-NH); 7.92 (s, 2 H, thiourea- CH_{Ar}); 7.49 (s, 1 H, thiourea- CH_{Ar}); 7.42 (d, J = 1.1 Hz, imidazol); 7.35 – 7.20 (m, 3 H, $\tau\text{-Bn-CH}_{\text{Ar}}$); 7.10 – 7.00 (m, 2 H, $\tau\text{-Bn-CH}_{\text{Ar}}$); 6.92 (br s, 1 H, NH); 6.56 (s, 1 H, imidazol); 4.97 (s, 2 H, $\tau\text{-Bn-CH}_2$); 4.52 – 4.42 (m, 1 H, His- H_α); 3.42 (s, 3 H, OCH_3); 3.00 – 2.80 (m, 2 H, His- H_β); 2.80 – 2.70 (m, 2 H, adamantane- CH_2); 2.28 – 2.15 (m, 2 H, 2 \times adamantane-CH); 2.15 – 2.03 (m, 2 H, adamantane- CH_2); 2.05 – 1.45 (m, 8 H, 4 \times adamantane- CH_2). $^{13}\text{C NMR}$ (100 MHz, CDCl_3): δ/ppm = 179.8 (C=S), 178.0 (C=O), 171.3 (C=O), 140.9, 137.6, 137.4, 135.8, 131.9, 131.6, 131.2, 130.9, 129.0, 128.4, 127.3, 124.6, 124.0, 121.9, 117.5, 117.0, 54.9, 52.7, 52.2, 50.9, 43.8, 42.8, 39.6 / 39.5 (diastereotopic), 38.2 / 37.9 (diastereotopic), 34.9, 29.3, 29.0. **IR** (KBr): $\tilde{\nu}/\text{cm}^{-1}$ = 3433, 3335, 3092, 3067, 2913, 2857, 1745, 1637, 1540,

1501, 1474, 1457, 1386, 1278, 1175, 1132, 681. **MS** (ESI): $m/z = 708.2$ $[M+H]^+$ (calc. 708.2). **Elem. Anal.**: $C_{34}H_{35}F_6N_5O_3S$ (707.73): calcd. C 57.70, H 4.98, N 9.90, found C 57.38, H 4.60, N 9.69.

Fmoc-^AGly-His(τ -Trt)-OMe (254): 1.7918 g (4 mmol) H-His(τ -Trt)-OMe \cdot HCl (**253**), 1.67 g (4 mmol) Fmoc-^AGly-OH (**180a**) and 1.517 g (4 mmol) HBTU were dissolved in 50 mL dry acetonitrile following general procedure A. The mixture was cooled to 0 °C with an ice bath and 1.034 g (8 mmol) DIPEA were added. The reaction was stirred for 8 h upon warming to rt. 100 mL brine were added and the mixture was extracted with $CHCl_3$. The combined organics were washed with water, 5% $NaHCO_3$, water and brine, and were dried (Na_2SO_4). The crude product obtained after evaporation of the solvents was subjected to flash chromatography (2.5 \times 30 cm, 80 g SiO_2) eluting with DCM / methanol (90 : 10). Fractions containing the product were collected, the eluent was evaporated and the product **254** was used for further conversions with no additional purifications performed. **¹H NMR** (200 MHz, $CDCl_3$): $\delta/ppm = 7.76$ (d, J = 7.5 Hz, 2 H, Fmoc- CH_{Ar}); 7.61 (br s, 1H, His-NH); 7.57 (d, J = 7.6 Hz, 2 H, Fmoc- CH_{Ar}); 7.44 – 7.24 (m, 14 H); 7.16 – 7.00 (m, 6 H, τ -Trt); 6.53 (s, 1 H, imidazol); 4.83 – 4.69 (m, 1 H, His- H_α); 4.66 (br s, 1 H, NH); 4.39 – 4.21 (m, 2 H, Fmoc- CH_2); 4.18 (t, J = 6.4 Hz, 1 H, Fmoc- CH); 3.59 (s, 3 H, OCH_3); 3.18 – 2.86 (m, 2 H, His- H_β); 2.79 (s, N,N,N',N'-tetramethylurea); 2.33 – 1.50 (m, 14 H, adamantane). **¹³C NMR** (50 MHz, $CDCl_3$): $\delta/ppm = 176.6$ (C=O), 171.9 (C=O), 154.0 (Fmoc-C=O), 144.1 (C_q), 142.2, 141.3 (C_q), 138.7, 136.6, 129.7, 128.1, 127.9, 127.6, 127.0, 125.0, 119.9, 119.5, 75.3 (C_q), 65.9, 52.3, 52.0, 51.2, 47.3, 43.2, 42.6, 40.6, 38.6, 38.0, 35.1, 29.6, 29.3.

H-^AGly-His(τ -Trt)-OMe (255): Fmoc-cleavage was performed according to general procedure C. Fmoc-His(τ -Trt)-OMe (**254**), obtained as described above, was dissolved in 20 mL dry acetonitrile, cooled to 0 °C with an ice bath, and 20 mL diethylamine were added. The mixture was then stirred over night upon warming to rt. After evaporation of the solvents, the crude product was purified by silica gel column chromatography (2.5 \times 30 cm, ~ 80 g SiO_2) eluting with TBME / methanol / triethylamine (60 : 30 : 1), $R_f = 0.28$. After evaporation of the eluent, 1.7874 g (3.04 mmol, 75.9% over two steps) of the aminopeptide **255** were isolated as a slightly yellowish powder, mp 119 – 122 °C. **¹H NMR** (400 MHz, $CDCl_3$): $\delta/ppm = 7.60$ (d, J

= 7.7 Hz, 1 H, His-NH); 7.37 (s, 1 H, imidazol); 7.36 – 7.28 (m, 9 H, Trt-CH_{Ar}); 7.14 – 7.04 (m, 6 H, Trt-CH_{Ar}); 6.53 (s, 1 H, imidazol); 4.81 – 4.70 (m, 1 H, His-H_α); 3.57 (s, 3 H, OCH₃); 3.10 – 2.87 (m, 2 H, His-H_β); 2.23 – 2.11 (m, 2 H, 2 × adamantane-CH); 1.86 (br s, 2 H, NH₂); 1.82 – 1.43 (m, 12 H, 6 × adamantane-CH₂). ¹³C NMR (100 MHz, CDCl₃): δ/ppm = 177.0 (C=O), 171.9 (C=O), 142.2, 138.7, 136.6, 129.7, 128.04, 128.0, 119.5, 75.2, 52.5, 52.0, 48.0, 47.4, 44.63, 44.59, 42.9, 37.86 / 37.81 (diastereotopic), 35.1, 29.6 / 29.5 (diastereotopic). **MS** (ESI): *m/z* = 589.9 [M + H]⁺ (calc. 588.3).

***N*-[3,5-bis(trifluoromethyl)phenyl]-*N'*-3-[[carboxy(histidine(1-trityl)methyl ester) amido]-tricyclo [3.3.1.1^{3,7}]dec-1-yl]thiourea (TU-^AGly-His(τ-Trt)-OMe, **239g**):** In an oven-dried 50 mL flask under argon, 588.7 mg (1 mmol) H-^AGly-His(τ-Trt)-OMe **255** were dissolved in 15 mL dry THF. The mixture was cooled to 0 °C with an ice bath and 271.2 mg (1 mmol) 3,5-bis(trifluoromethyl)phenyl isocyanate in 15 mL dry THF were added with an addition funnel. The mixture was stirred upon warming to rt over night. After careful evaporation of the solvents *in vacuo*, the crude product was purified by flash chromatography (2.5 × 60 cm, ~ 170 g SiO₂) eluting with DCM / methanol (95 : 5), R_f (**239g**) = 0.34. After evaporation of the eluent, 249.5 mg (0.29 mmol, 29.0 %) of the thiourea were isolated as a slightly yellowish foam, mp 122 – 125 °C. ¹H NMR (400 MHz, CDCl₃): δ/ppm = 9.13 (br s, 1 H, thiourea-NH); 8.20 (d, J = 7.2 Hz, His-NH); 7.92 (s, 2 H, thiourea-CH_{Ar}); 7.48 (s, 1 H, thiourea-CH_{Ar}); 7.34 (s, 1 H, imidazol); 7.33 – 7.12 (m, 9 H, τ-Trt-CH_{Ar}); 7.05 (s, 1 H, thiourea-NH); 7.03 – 6.98 (m, 6 H, τ-Trt-CH_{Ar}); 6.45 (s, 1 H, imidazol); 4.51 – 4.45 (m, 1 H, His-H_α); 3.32 (s, 3 H, OCH₃); 3.05 – 2.83 (m, 2 H, adamantane-CH₂); 2.98 – 2.77 (m, 2 H, His-H_β); 2.30 – 2.12 (m, 2 H, 2 x adamantane-CH); 2.12 – 1.96 (m, 2 H, adamantane-CH₂); 1.94 – 1.77 (m, 4 H, 2 x adamantane-CH₂); 1.76 – 1.49 (m, 2 H, adamantane-CH₂). ¹³C NMR (100 MHz, CDCl₃): δ/ppm = 179.9 (C=S), 178.2 (C=O), 170.8 (C=O), 142.1, 140.9, 138.8, 136.1, 131.3 (q, ²J_{C-F} = -33 Hz, C-CF₃), 129.7, 128.12, 128.1, 124.22, 124.19, 123.3 (q, ¹J_{C-F} = -274 Hz, CF₃), 119.7, 119.2, 117.4, 75.4, 54.8, 52.7, 52.0, 44.3, 42.9, 39.3 / 39.2 (diastereotopic), 38.2, 38.0 (diastereotopic), 34.8, 29.3, 29.0 **IR** (KBr): $\tilde{\nu}$ /cm⁻¹ = 3432, 3336, 3062, 2913, 2856, 1745, 1637, 1534, 1495, 1474, 1451, 1386, 1278, 1176, 1133, 701. **MS** (ESI): *m/z* = 860.1 [M+H]⁺ (calc. 860.3). **Elem.**

Anal.: C₄₆H₄₃F₆N₅O₃S (859.92): calcd. C 63.25, H 5.04, N 8.14, found C 63.72, H 3.61, N 7.65.

12.15. Morita-Baylis-Hillman test reaction: Synthesis of **258**

For the test reactions, 0.5 mmol freshly distilled benzaldehyde, 0.6 mmol distilled cyclohexenone (1.2 equivalents) and 0.125 mmol (25 mol%) DABCO and 0.1 mmol (20 mol%) of the catalyst were stirred at rt under argon for 24 h. The reactions were then stopped by the addition of saturated NH₄Cl, the mixture was extracted thoroughly with ethyl acetate, the combined organics were washed with water and dried. After evaporation of the solvent, the crude products were purified by silica gel column chromatography (1.3 × 50 cm, ~ 45 g SiO₂) eluting with n-hexane / ethyl acetate (1 : 1), R_f (**258**) = 0.28. A blind reaction without the catalyst under otherwise identical conditions did not give any Baylis-Hillman adduct.

258: ¹H NMR (400 MHz, CDCl₃): δ /ppm = 7.44 – 7.16 (m, 6 H); 6.74 (t, J = 4.2 Hz, 1 H); 5.56 (s, 1 H); 2.52 – 2.28 (m, 4 H); 2.08 – 1.86 (m, 2 H). ¹³C NMR (100 MHz, CDCl₃): δ /ppm = 200.4 (C=O), 147.3, 141.6, 128.3, 127.4, 126.4, 72.4, 38.5, 25.7, 22.4. Product fractions were > 95% homogenous as analyzed by GC-MS.

12.16. Catalyst screening of peptidic thioureas in the Morita-Baylis-Hillman reaction.

The test reactions were run in 0.5 mmol scale using 4 equivalents of cyclohexenone and 20 mol% of the catalysts and, if used, the co-catalysts. The reactions were run in parallel under ar at rt for 86 h, they were quenched with saturated NH₄Cl. After extraction with ethyl acetate, washing and drying as described above, the crude reaction mixtures were analyzed by TLC and GC-MS. Experiments that gave conversion to the adduct were purified by flash chromatography (1.5 × 40 cm, ~45 g SiO₂) eluting with n-hexane / ethyl acetate (3 : 1), R_f (**260**) = 0.13. A second flash chromatography eluting with TBME gave product fractions of sufficient purities (> 95% as analyzed by GC-MS). The enantiomeric ratio of the product fractions was analyzed by chiral stationary phase GC, using a Macherey-Nagel Hydrodex[®] β -6 TBDM column. Hydrogen was used as the carrier gas, the temperature program was 100 °C to 250 °C with 5 °C / min, then 35 min at 250 °C.

12.17. Solid phase peptide synthesis of model peptides 261 – 265.

These peptides were synthesized in 0.65 mmole scale using commercially available Wang resin preloaded with Fmoc-Gly and endcapped (Novabiochem). Fmoc-cleavage was performed with 25% piperidine in DMF for 2 × 30 min (to minimize diketopiperazine-formation, di- α -peptides were cleaved with 50% piperidine in DMF for 5 minutes). Chain elongation was accomplished by double couplings (2 × 1 h) with the respective Fmoc-amino acid, HOBt, HBTU and DIPEA in DMF in 2 : 2 : 2 : 4 stoichiometry. After each synthetic operation, the resin was washed five times for 1 minute each with DMF, dichloromethane, and then again 5 times with DMF. After the attachment of the N-terminal amino acid and Fmoc-cleavage, the peptides were acetylated with 10 equivalents of acetic anhydride and 20 equivalents of DIPEA in DMF for 3 h. After washing, cleavage from the resin was achieved by shaking the beads for 5 days with a mixture of methanol, THF and triethylamine (9 : 1 : 1), whereupon the peptides are obtained as the respective methyl esters. The beads were washed several times with THF, the solvents were evaporated under reduced pressure and the peptides were purified as described below.

Ac-Gly-^AGly-Gly-OMe (261): Purification by two twofold flash chromatography (2 × 45 cm, ~ 55 g SiO₂) eluting with DCM / methanol (85 : 15), R_f (**261**) = 0.52. ¹H NMR (400 MHz, CDCl₃): δ /ppm = 6.53 (t, 1 H, J ~ 5 Hz, Gly³-NH); 6.26 (t, 1 H, J ~ 5 Hz, Gly¹-NH); 6.16 (br s, 1 H, ^AGly²-NH); 4.00 (d, J = 5.2 Hz, 2 H, Gly¹-H _{α}); 3.82 (d, J = 5.2 Hz, 2 H, Gly³-H _{α}); 3.75 (s, 3 H, OCH₃); 2.30 – 1.58 (m, 14 H, adamantane). ¹³C NMR (100 MHz, CDCl₃): δ /ppm = 176.7 (^AGly²-C=O), 170.63 (Gly¹-C=O), 170.60 (acetyl-C=O), 167.97 (Gly³-C=O), 52.40 (adamantane-N-C_q), 52.35 (O-CH₃), 43.9 (Gly³-C _{α}), 42.5 (adamantane), 41.2 (C _{α} Gly¹), 40.5 (adamantane), 38.1 (adamantane), 35.2 (adamantane), 29.1 (2 × adamantane-CH), 23.0 (acetyl-CH₃). MS (ESI): m/z = 388.3 [M + Na]⁺ (calc. 388.3).

Ac-Gly¹-^AGly²-^AGly³-Gly⁴-OMe (262): Purification by twofold flash chromatography (2 × 45 cm, ~ 55 g SiO₂) eluting with DCM / methanol (85 : 15), R_f (**262**) = 0.49. ¹H NMR (400 MHz, CDCl₃): δ /ppm = 6.52 (t, J ~ 5 Hz, 1 H, Gly¹-NH); 6.30 (t, J ~ 5 Hz, 1 H, Gly⁴-NH); 6.02 (br s, 1 H, ^AGly²-NH); 5.37 (br s, 1 H, ^AGly³-NH); 4.01 (d, J = 5.2 Hz,

2 H, Gly⁴-H _{α}); 3.82 (d, J = 5.2 Hz, 2 H, Gly¹-H _{α}); 3.75 (s, 3 H, OCH₃); 2.30 – 1.53 (m, 28 H, adamantane); 2.03 (s, 3 H, acetyl-CH₃). ¹³C NMR (100 MHz, CDCl₃): δ /ppm = 176.8 (^AGly²-C=O), 175.9 (^AGly³-C=O), 170.64 (acetyl-C=O), 170.56 (Gly⁴-C=O), 168.0 (Gly¹-C=O), 52.5 (adamantane-N-C_q), 52.3 (OCH₃), 51.8 (adamantane-N-C_q), 43.92 (Gly¹-C _{α}), 42.88 (adamantane-CH₂), 42.8 (adamantane-C_q), 42.6 (adamantane-CH₂), 42.5 (adamantane-C_q), 41.1 (Gly⁴-C _{α}), 40.6 (adamantane-CH₂), 40.5 (adamantane-CH₂), 38.22 (adamantane-CH₂), 38.17 (adamantane-CH₂), 35.3 (adamantane-CH₂), 35.2 (adamantane-CH₂), 29.19 (adamantane-CH), 29.15 (adamantane-CH₂), 23.0 (acetyl-CH₃). **MS** (ESI): m/z = 1107.3 [2M + Na]⁺ (calc. 1107.6).

Ac-Gly¹-^AGly²-Gly³-Gly⁴-OMe (263): Purification by twofold flash chromatography (2 × 45 cm, ~ 55 g SiO₂) eluting with DCM / methanol (85 : 15), R_f (**263**) = 0.26. ¹H NMR (400 MHz, CDCl₃): δ /ppm = 7.31 (t, 1 H, J ~ 5 Hz, Gly⁴-NH); 6.71 (t, 1 H, J ~ 5 Hz, Gly³-NH); 6.63 (s, 1 H, ^AGly²-NH); 6.59 (t, J ~ 5 Hz, 1 H, Gly¹-NH); 4.05 (d, J = 5.4 Hz, 2 H, Gly⁴-H _{α}); 4.00 (d, J = 4.8 Hz, 2 H, Gly³-H _{α}); 3.88 (d, J = 4.8 Hz, 2 H, Gly¹-H _{α}); 3.76 (s, 3 H, OCH₃); 2.35 – 2.14 (m, 4 H, 2 × adamantane-CH and adamantane-CH₂); 2.14 – 1.99 (m, 2 H, adamantane-CH₂); 2.03 (s, 3 H, acetyl-CH₃); 1.95 – 1.74 (m, 6 H, 3 × adamantane-CH₂); 1.74 – 1.58 (m, 2 H, adamantane-CH₂). ¹³C NMR (100 MHz, CDCl₃): δ /ppm = 177.3 (^AGly³-C=O), 170.6 (Gly⁴-C=O), 169.4 (Gly³-C=O), 167.9 (Gly¹-C=O), 52.4 (adamantane-N-C_q), 52.36 (OCH₃), 44.0 (Gly¹-C _{α}), 43.1 (Gly³-C _{α}), 42.8 (adamantane-C_q), 42.6 (adamantane-CH₂), 41.2 (Gly⁴-CH _{α}), 40.2 (adamantane-CH₂), 38.4 (adamantane-CH₂), 35.1 (adamantane-CH₂), 29.2 (adamantane-CH), 23.0 (acetyl-CH₃). **MS** (ESI): m/z = 445.5 [M + Na]⁺ (calc. 445.2).

Ac-Gly¹-Gly²-^AGly³-Gly⁴-OMe (264): Purification by twofold flash chromatography (2 × 45 cm, ~ 55 g SiO₂) eluting with DCM / methanol (85 : 15), R_f (**264**) = 0.21. The compound was further purified by preparative HPLC using a diol-phase eluting with TBME / methanol (80 : 20), 2 mL / min, detecting at 220 nm. ¹H NMR (400 MHz, CDCl₃): δ /ppm = 6.89 (t, J ~ 5 Hz, 1 H, Gly¹-NH); 6.48 (t, J ~ 5 Hz, 1 H, Gly²-NH); 6.35 (t, J ~ 5 Hz, 1 H, Gly⁴-NH); 5.93 (br s, 1 H, ^AGly³-NH); 4.01 (d, J = 5.2 Hz, 2 H, Gly⁴H _{α}); 3.96 (d, J = 5.2 Hz, 2 H, Gly²-H _{α}); 3.85 (d, J = 5.2 Hz, 2 H, Gly¹-H _{α}); 3.76 (s, 3 H, OCH₃), 2.30 – 2.20 (m, 2 × adamantane-CH); 2.15 – 2.08 (m, 2 H, adamantane-

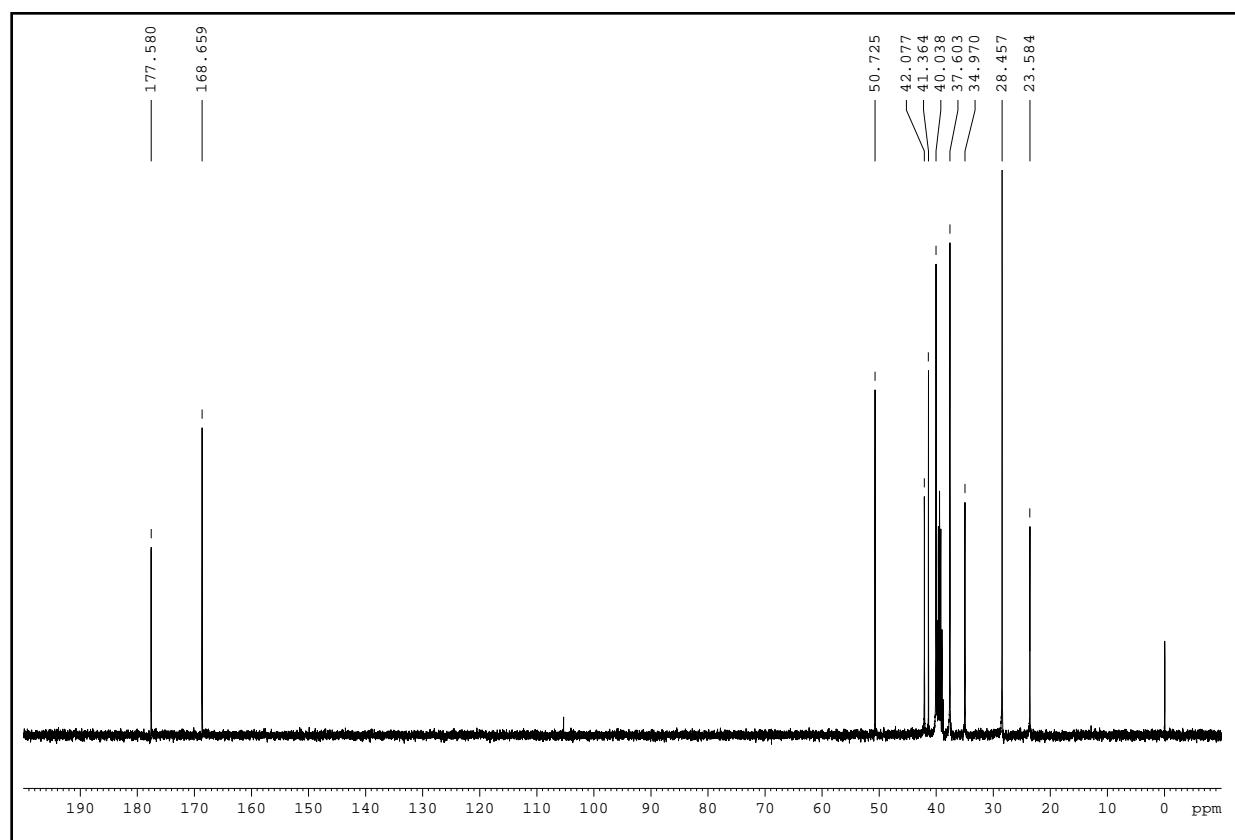
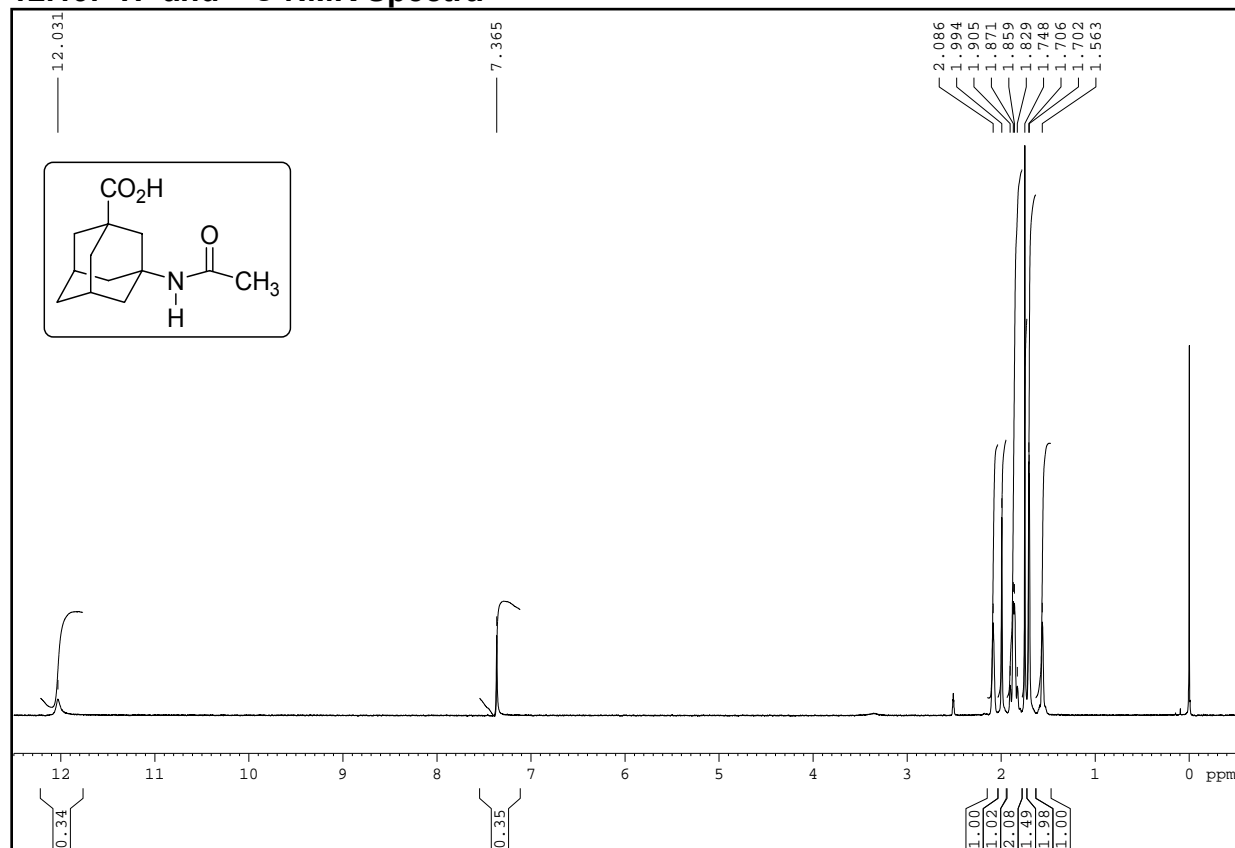
CH_2); 2.06 (s, 3 H, acetyl- CH_3); 2.05 – 1.88 (m, 4 H, 2 × adamantane- CH_2); 1.85 – 1.79 (m, 4 H, 2 × adamantane- CH_2); 1.75 – 1.59 (m, 2 H, adamantane- CH_2). ^{13}C NMR (100 MHz, $CDCl_3$): δ/ppm = 177.1 ($^AGly^3-C=O$), 171.2 ($Gly^4-C=O$), 170.8 (acetyl- $C=O$), 169.7 ($Gly^1-C=O$), 167.9 ($Gly^2-C=O$), 52.4 (adamantane- $N-C_q$), 52.3 (OCH_3), 43.5 (Gly^2-C_α), 43.2 (Gly^1-C_α), 42.5 (adamantane- CH_2), 42.3 (adamantane- C_q), 41.2 (Gly^4-C_α), 40.4 (adamantane- CH_2), 38.1 (adamantane- CH_2), 35.2 (adamantane- CH_2), 29.1 (2 × adamantane- CH), 23.0 (acetyl- CH_3). MS (ESI): m/z = 445.5 [$2M + Na$] $^+$ (calc. 445.2). Mp = 181 – 183 °C.

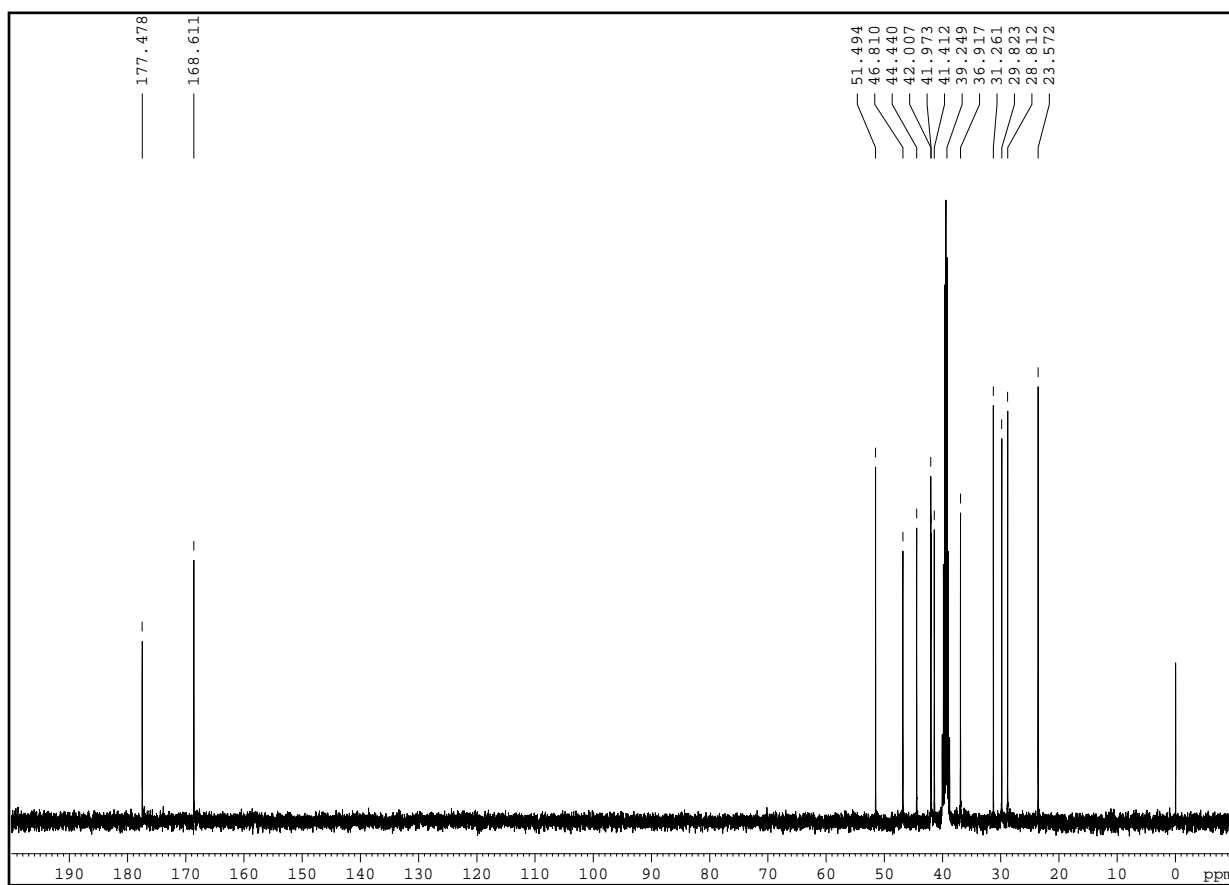
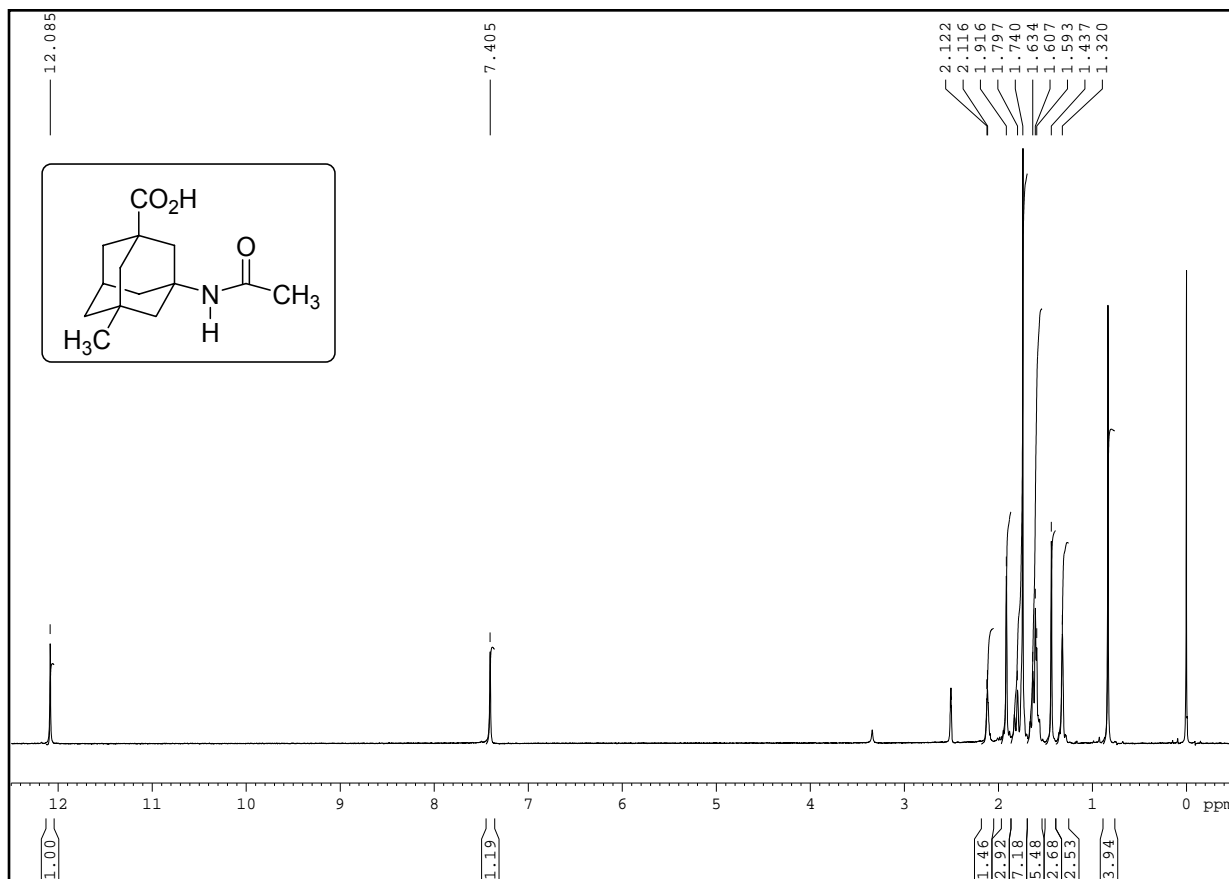
Ac-Gly¹-Gly²-^AGly³-Gly⁴-Gly⁵-OMe (265): Purification by twofold flash chromatography (2 × 45 cm, ~ 55 g SiO_2) eluting with DCM / methanol (85 : 15), R_f (265) = 0.12. The compound was further purified by preparative HPLC using a diol-phase eluting with TBME / methanol (80 : 20), 2 mL / min, detecting at 220 nm. 1H NMR (400 MHz, $CDCl_3$): δ/ppm = 7.47 (t, $J \sim 5$ Hz, 1 H, Gly^5-NH); 7.31 (t, $J \sim 5$ Hz, 1 H, Gly^4-NH); 6.97 (t, $J \sim 5$ Hz, 1 H, Gly^1-NH); 6.95 (t, $J \sim 5$ Hz, 1 H, Gly^2-NH); 6.76 (br s, 1 H, $^AGly^3-NH$), 4.06 (d, $J = 5.2$ Hz, 2 H, Gly^5-H_α); 3.99 (d, $J \sim 5$ Hz, 2 H, Gly^1-H_α); 3.98 (d, $J \sim 5$ Hz, 2 H, Gly^2-H_α); 3.85 (d, $J = 5.2$ Hz, 2 H, Gly^4-H_α); 3.76 (s, 3 H, OCH_3); 2.30 – 2.20 (m, 2 H, 2 × adamantane- CH); 2.20 – 2.10 (m, 2 H, adamantane- CH_2); 2.05 (s, 3 H, acetyl- CH_3); 2.08 – 1.99 (m, 2 H, adamantane- CH_2); 1.93 – 1.75 (m, 6 H, 3 × adamantane- CH_2); 1.71 – 1.54 (m, 2 H, adamantane- CH_2). ^{13}C NMR (100 MHz, $CDCl_3$): δ/ppm = 177.5 ($^AGly^3-C=O$), 171.0 (acetyl- $C=O$), 170.4 ($Gly^5-C=O$), 169.58 ($Gly^1-C=O$), 169.55 ($Gly^4-C=O$), 167.7 ($Gly^2-C=O$), 52.5 (adamantane- $N-C_q$), 52.4 (OCH_3), 43.6 (Gly^4-C_α), 43.12 (adamantane- C_q), 43.08 (Gly^2-C_α), 42.64 (Gly^1-C_α), 42.56 (adamantane- CH_2), 41.3 (Gly^5-C_α), 40.1 (adamantane- CH_2), 38.3 (adamantane- CH_2), 35.1 (adamantane- CH_2), 29.1 (2 × adamantane- CH), 22.9 (acetyl- CH_3). MS (ESI): m/z = 502.4 [$M + Na$] $^+$ (calc. 502.2). Mp = 128 - 131 °C.

12.18. Miscellaneous: Synthesis of compound 266

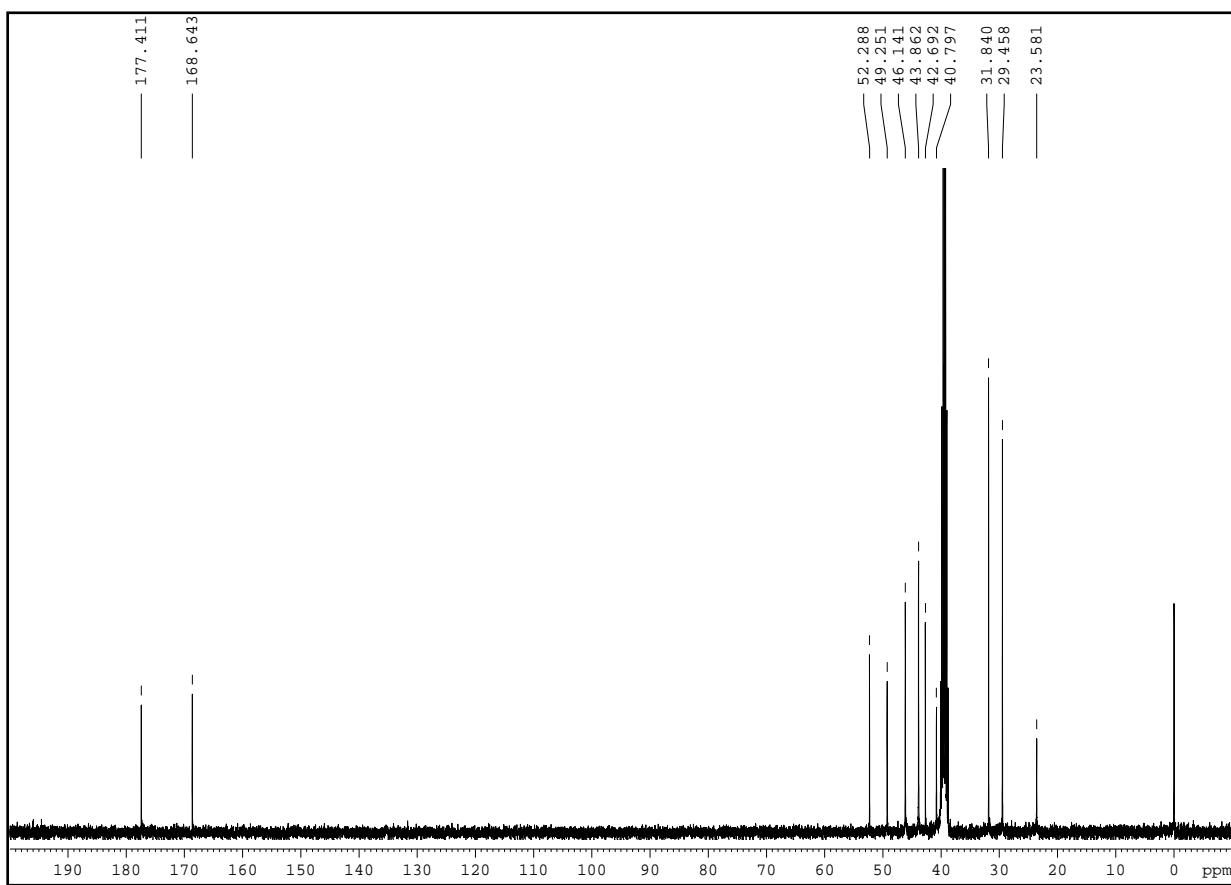
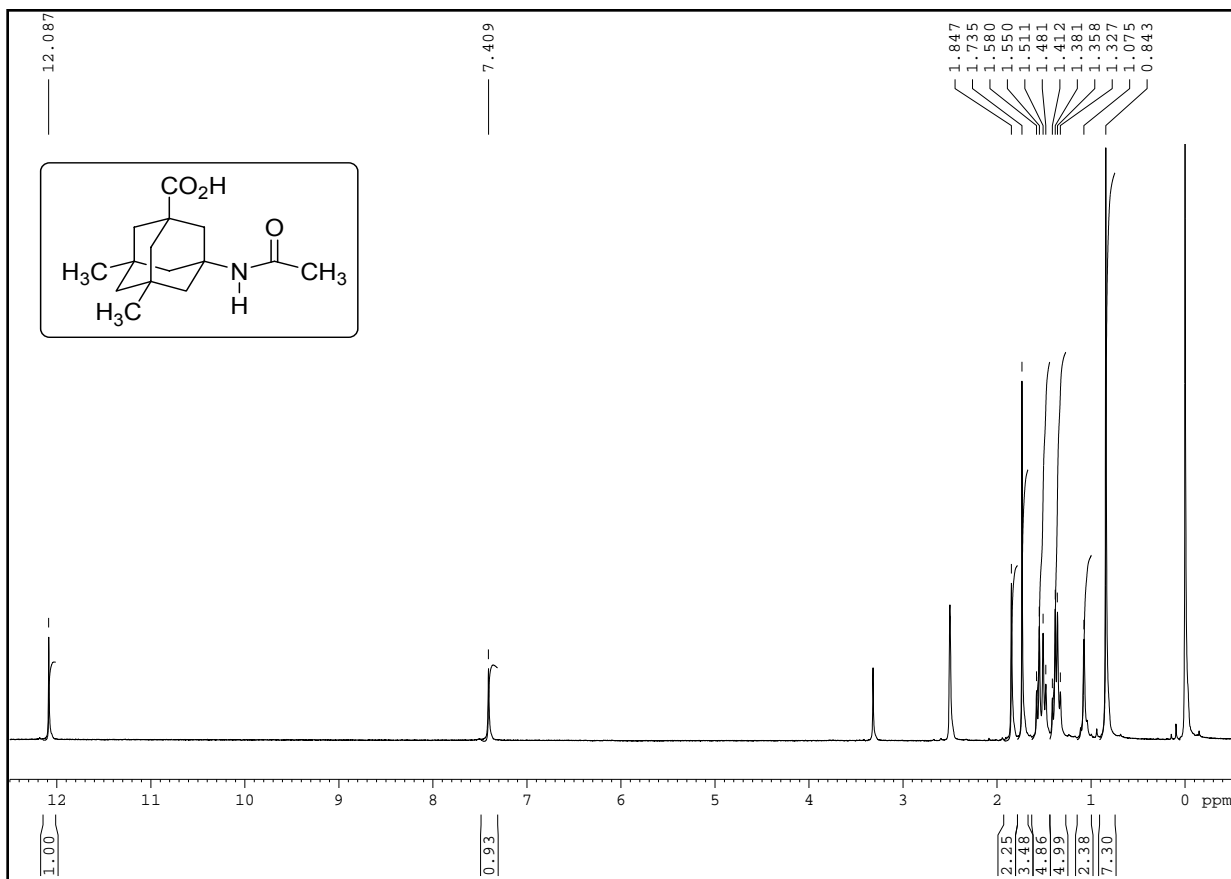
N-[3,5-bis(trifluoromethyl)phenyl]-N'-3(tert. butylcarboxy)tricyclo [3.3.1.1^{3,7}]dec-1-yl}thiourea (TU-^AGly-O^tBu, 266): In an oven-dried 50 mL flask under argon, 1.2568 (5 mmol) H-^AGly-O^tBu **181a** were dissolved in 15 mL dry THF. 646.3 mg (5 mmol) DIPEA were added and the mixture was cooled to 0 °C with an ice bath. 1.3559 g (5 mmol) 3,5-bis(trifluoromethyl)phenyl isocyanate in 15 mL dry THF were

then slowly added with an addition funnel. The mixture was stirred upon warming to rt over night. After careful evaporation of the solvents *in vacuo*, the crude product was dissolved in CHCl_3 and re-precipitated by the addition of n-hexane. The precipitate was collected via suction filtration and dried in a desiccator over night under reduced pressure over paraffine wax and P_2O_5 . 1.6668 g (3.190 mmol, 63.8%) of the thiourea were isolated as a colorless powder, mp 147.5 °C. **^1H NMR** (400 MHz, CDCl_3): δ/ppm = 8.11 (br s, 1 H, NH); 7.77 (s, 2 H, thiourea- CH_{Ar}); 7.68 (s, 1 H, thiourea- CH_{Ar}); 6.16 (br s, 1 H, NH); 2.32 – 2.20 (m, 6 H, adamantane); 2.18 – 2.08 (m, 2 H, adamantane); 1.88 – 1.57 (m, 6 H, adamantane); 1.42 (s, 9 H, $\text{C}(\text{CH}_3)_3$). **^{13}C NMR** (100 MHz, CDCl_3): δ/ppm = 178.8 (C=S), 175.5 (C=O), 139.1 (C_q), 132.6 (q, $^2J_{\text{C-F}}$ = -33 Hz, C- CF_3), 123.8, 122.6 (q, $^1J_{\text{C-F}}$ = -273 Hz, CF_3), 118.9, 118.6, 80.3 (C_q), 55.4, 43.1, 42.4, 40.4, 37.6, 34.8, 29.0, 27.7. **IR** (KBr): $\tilde{\nu}/\text{cm}^{-1}$ = 3285, 3048, 2981, 2915, 2861, 1723, 1538, 1472, 1458, 1388, 1370, 1339, 1282, 1246, 1179, 1127, 1107, 683. **MS** (ESI): m/z = 545.2 $[\text{M} + \text{Na}]^+$ (calc. 545.2). **Elem. Anal.**: $\text{C}_{24}\text{H}_{28}\text{F}_6\text{N}_2\text{O}_2\text{S}$ (522.55): calcd. C 55.16 H 5.40, N 5.36, found C 54.83, H 5.56, N 4.96.

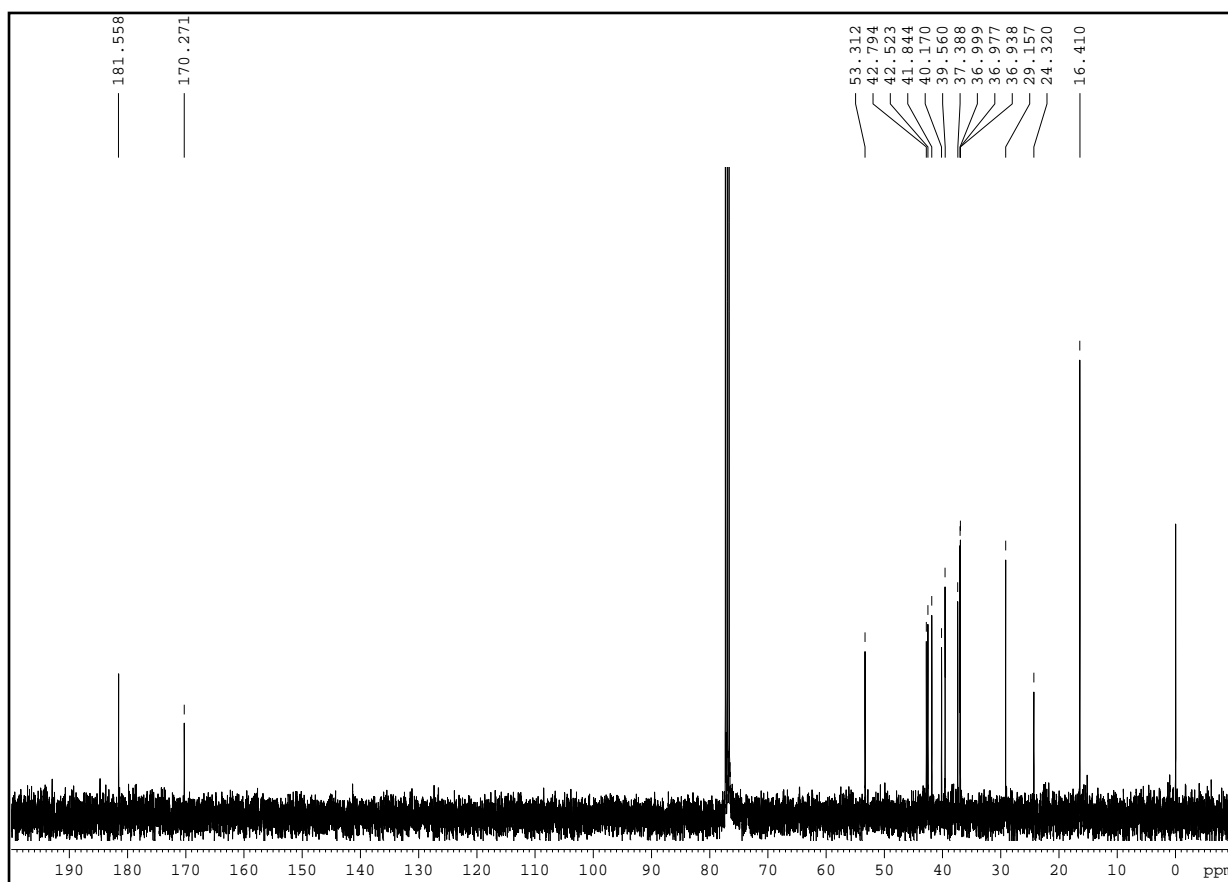
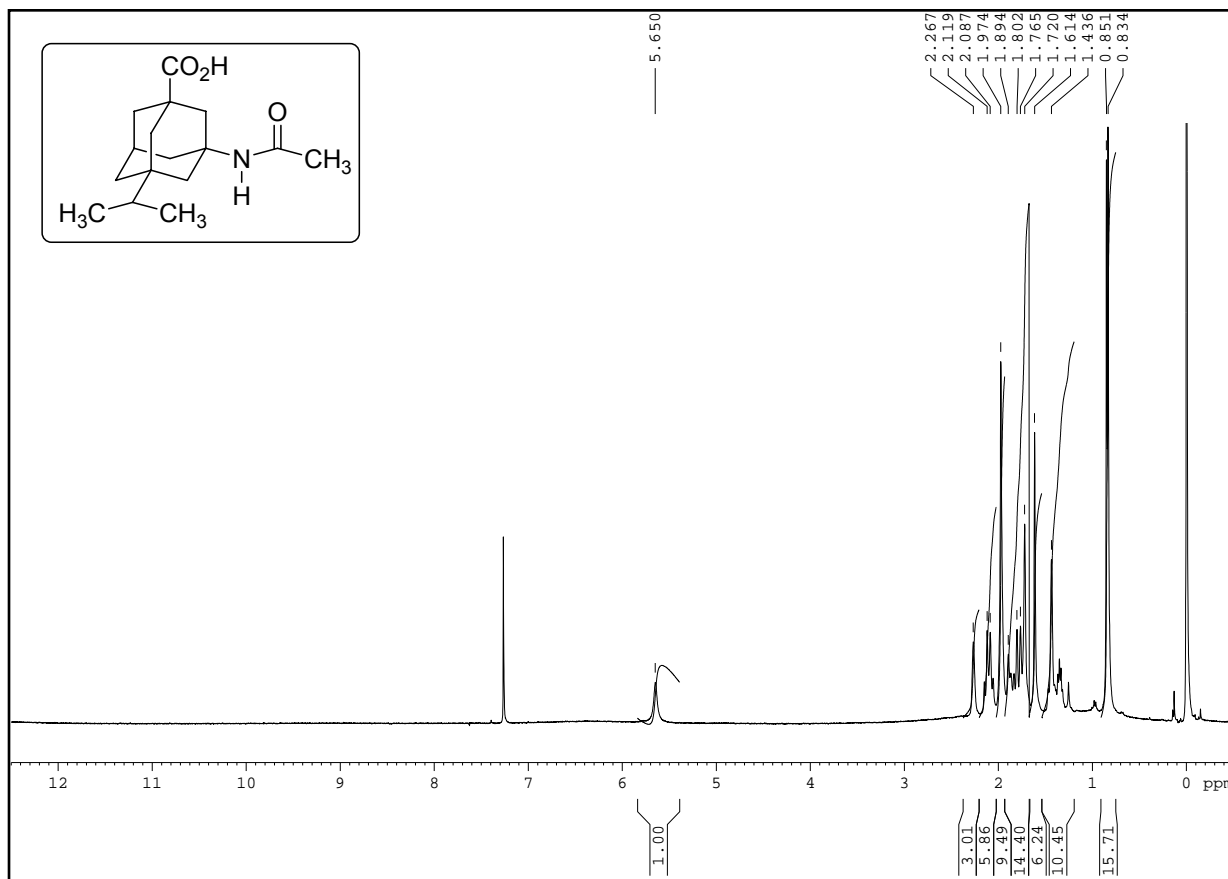
12.19. ^1H - and ^{13}C NMR Spectra3-Acetamidotricyclo[3.3.1.1^{3,7}]decane-1-carboxylic acid (**141**)



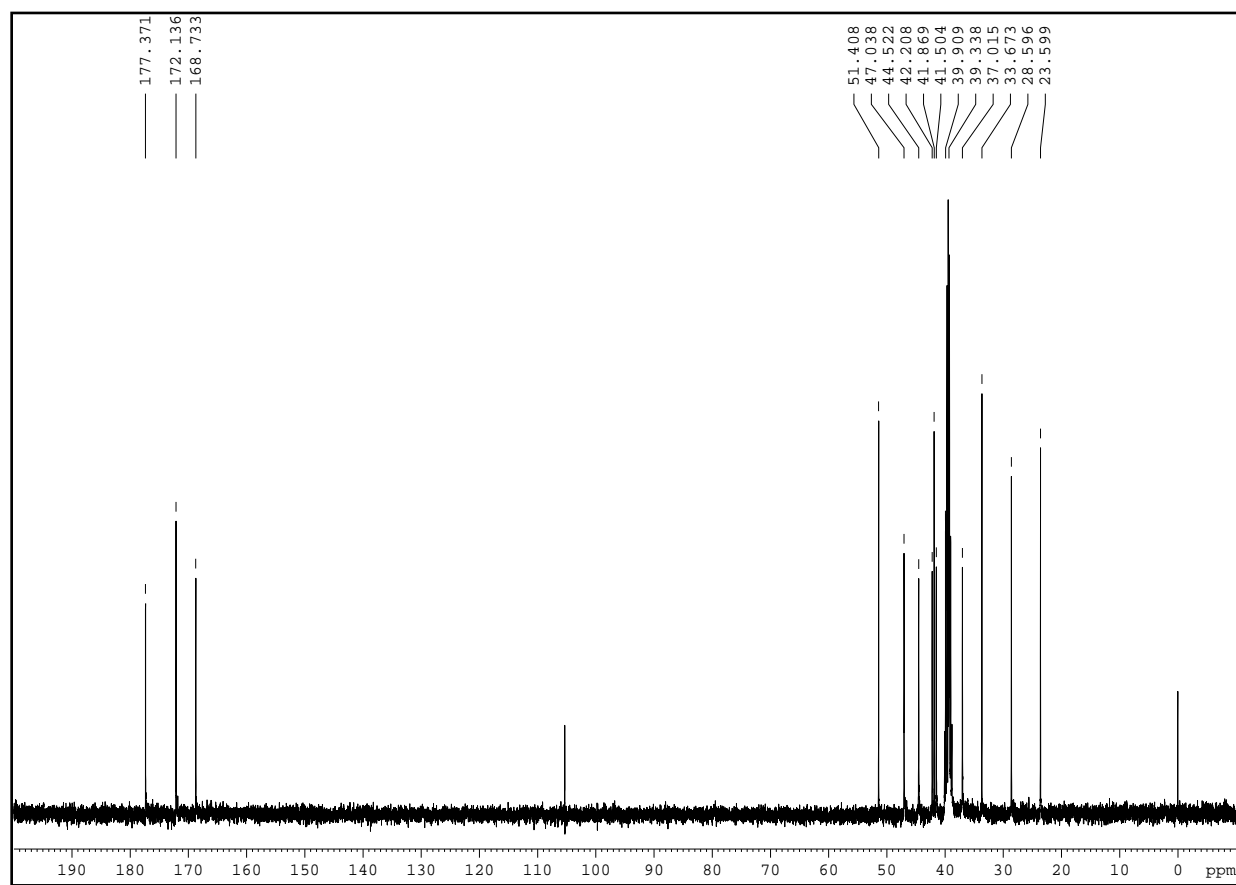
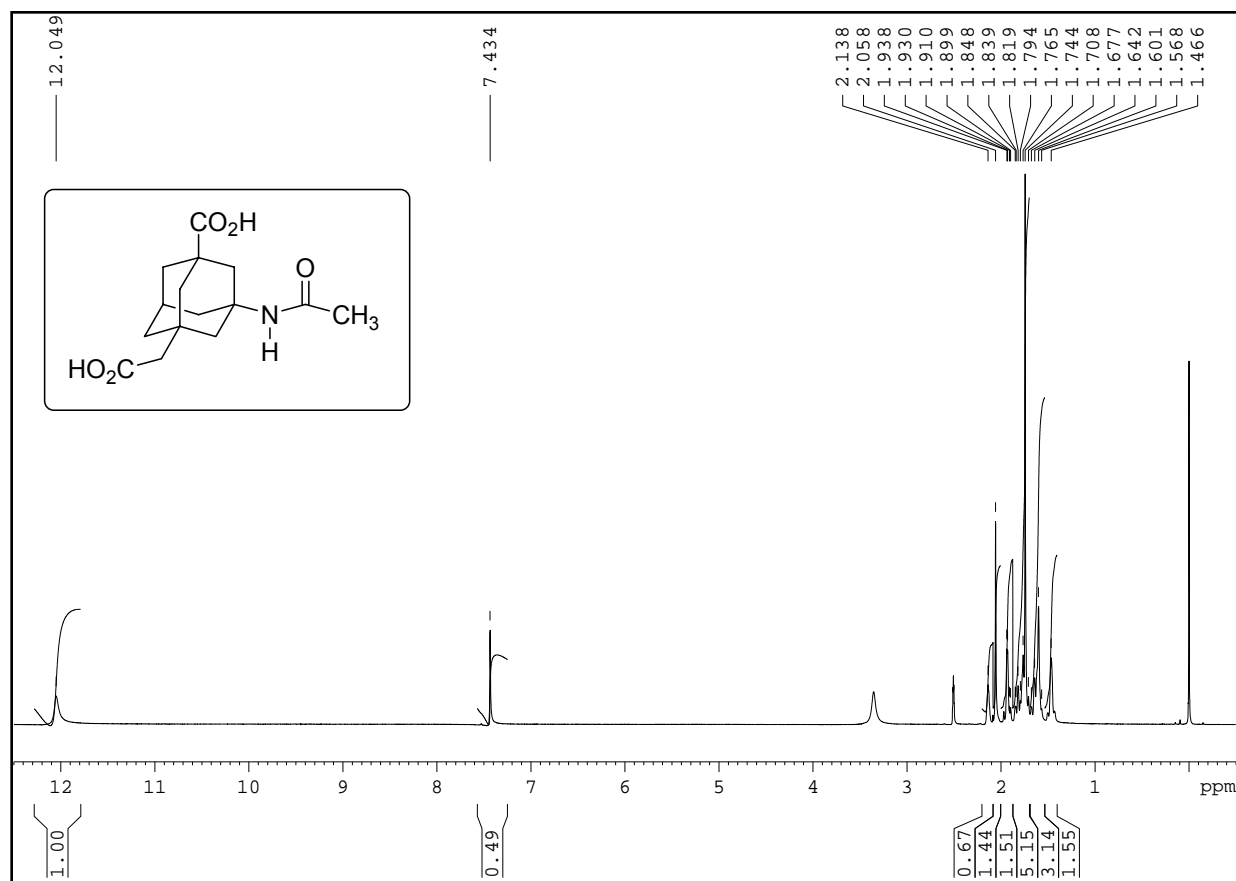
3-Acetamido-5-methyltricyclo[3.3.1.1^{3,7}]decane-1-carboxylic acid (142)



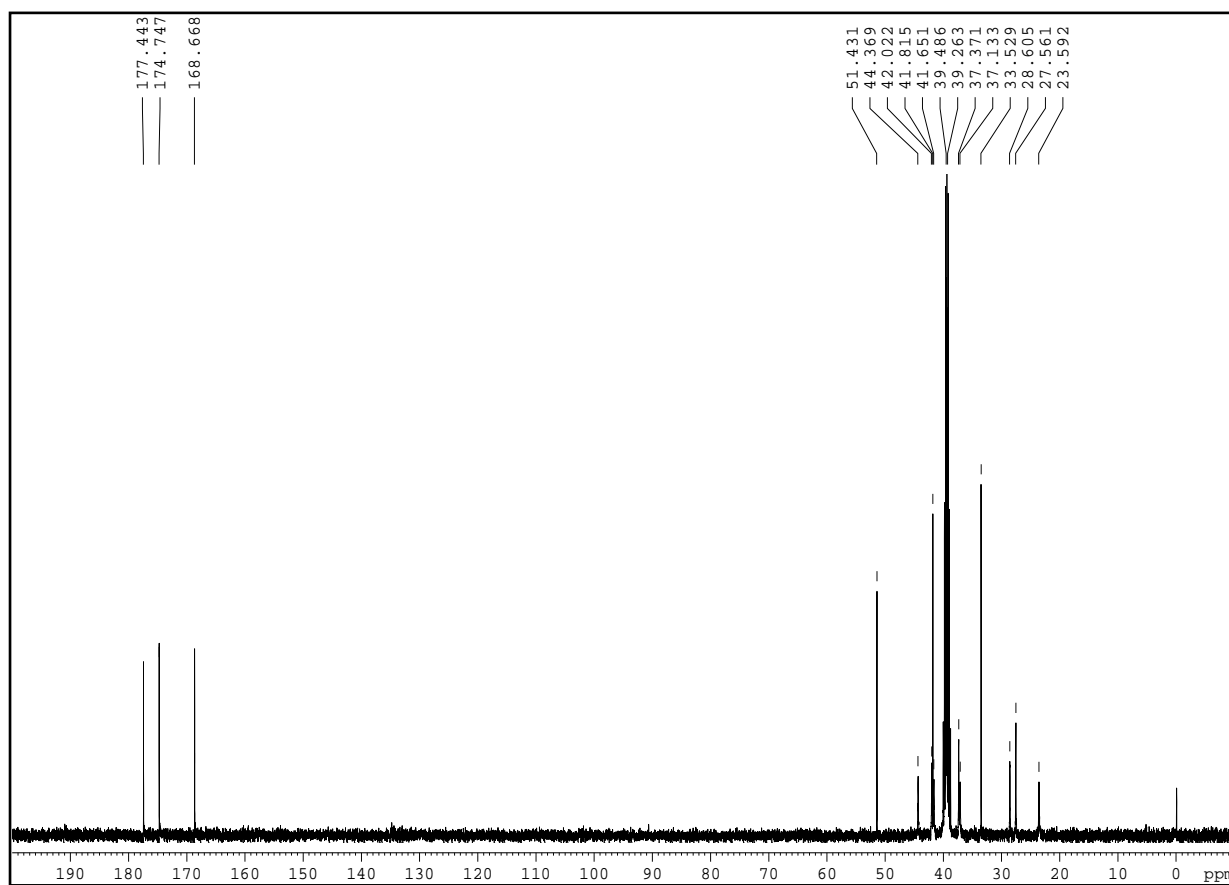
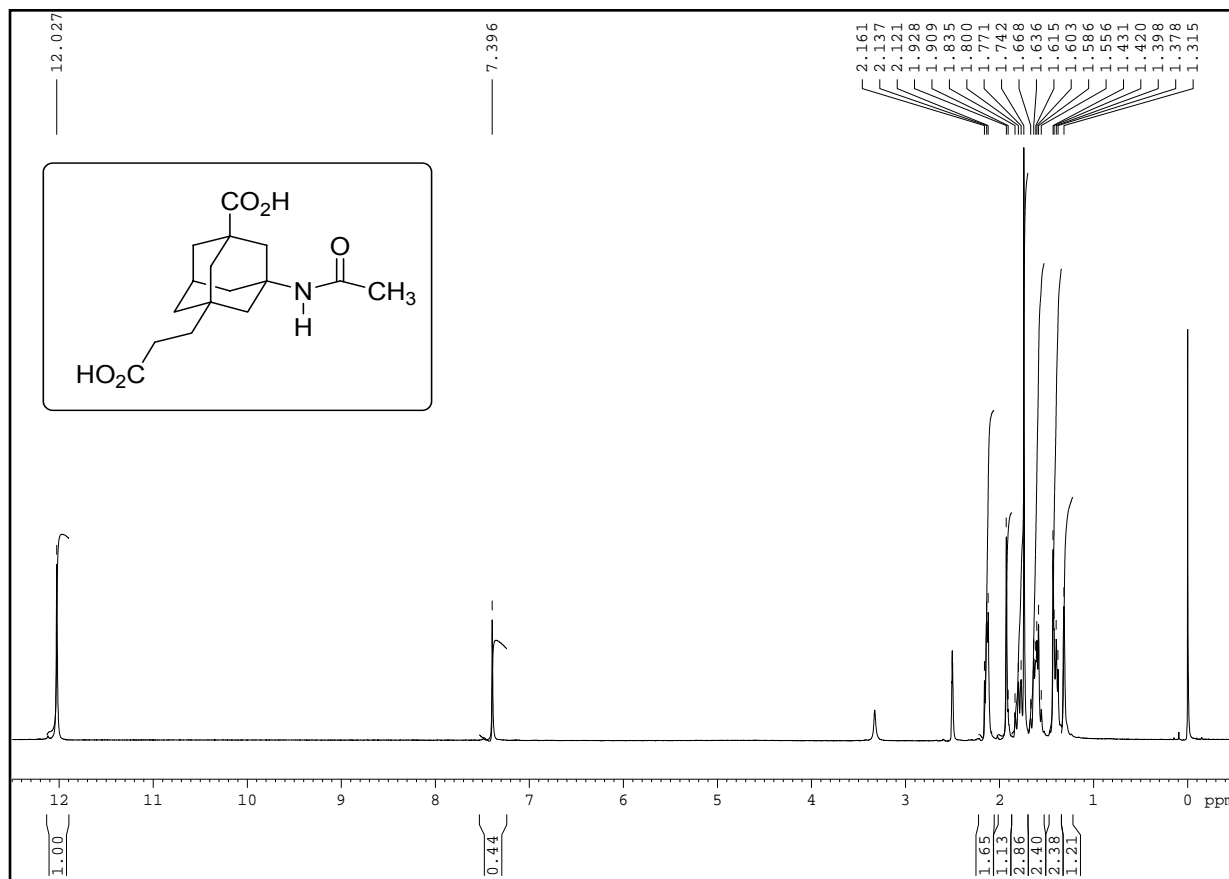
3-Acetamido-5,7-dimethyltricyclo[3.3.1.1^{3,7}]decane-1-carboxylic acid (143)



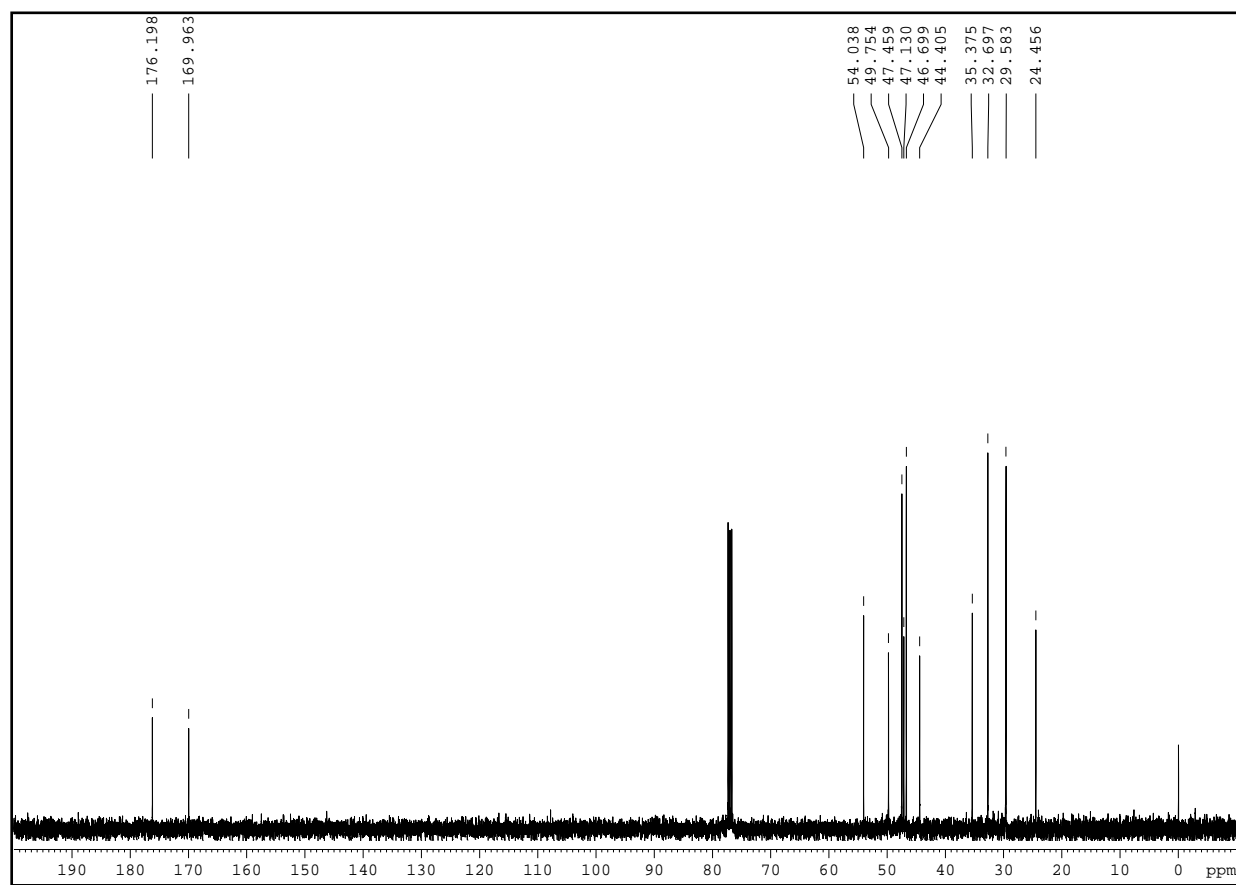
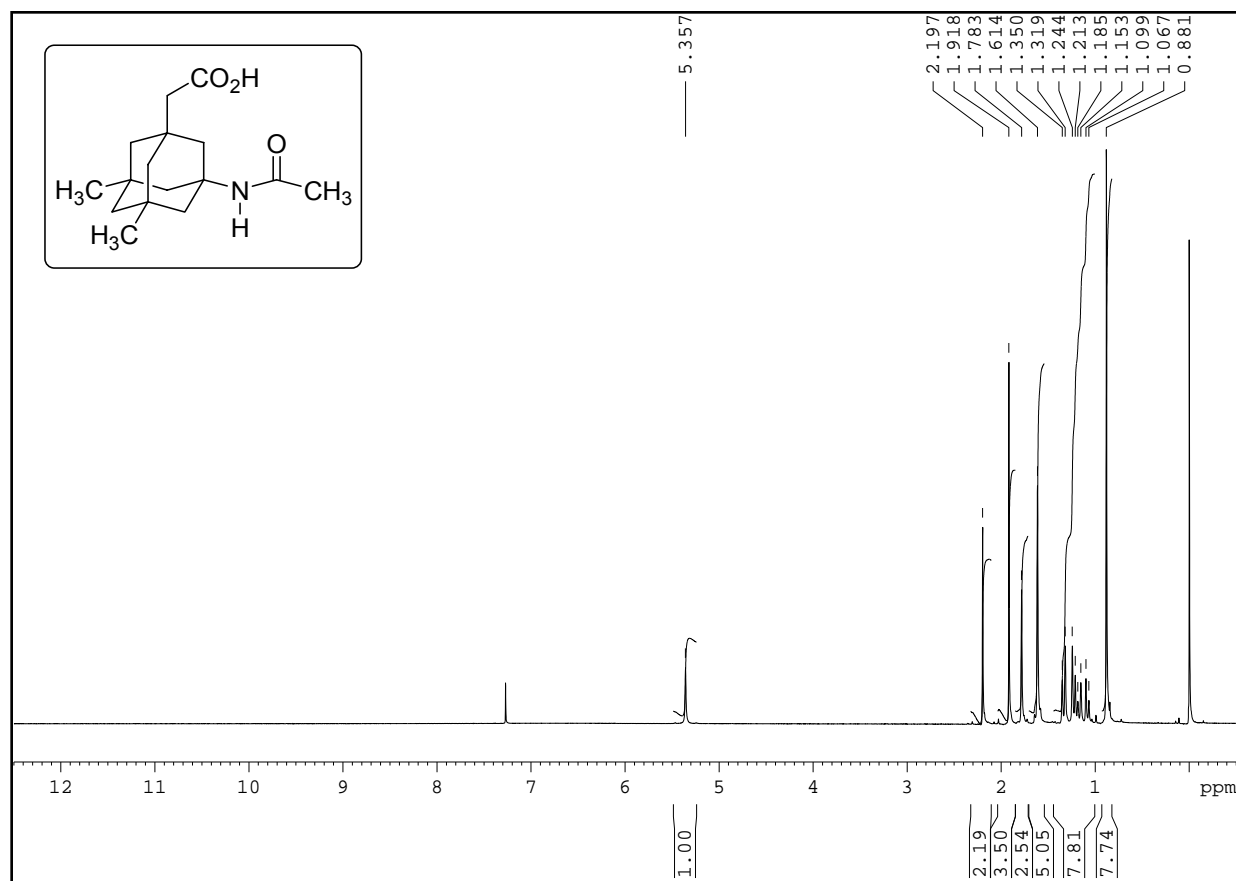
3-Acetamido-5-isopropyltricyclo[3.3.1.1^{3,7}]decane-1-carboxylic acid (144)



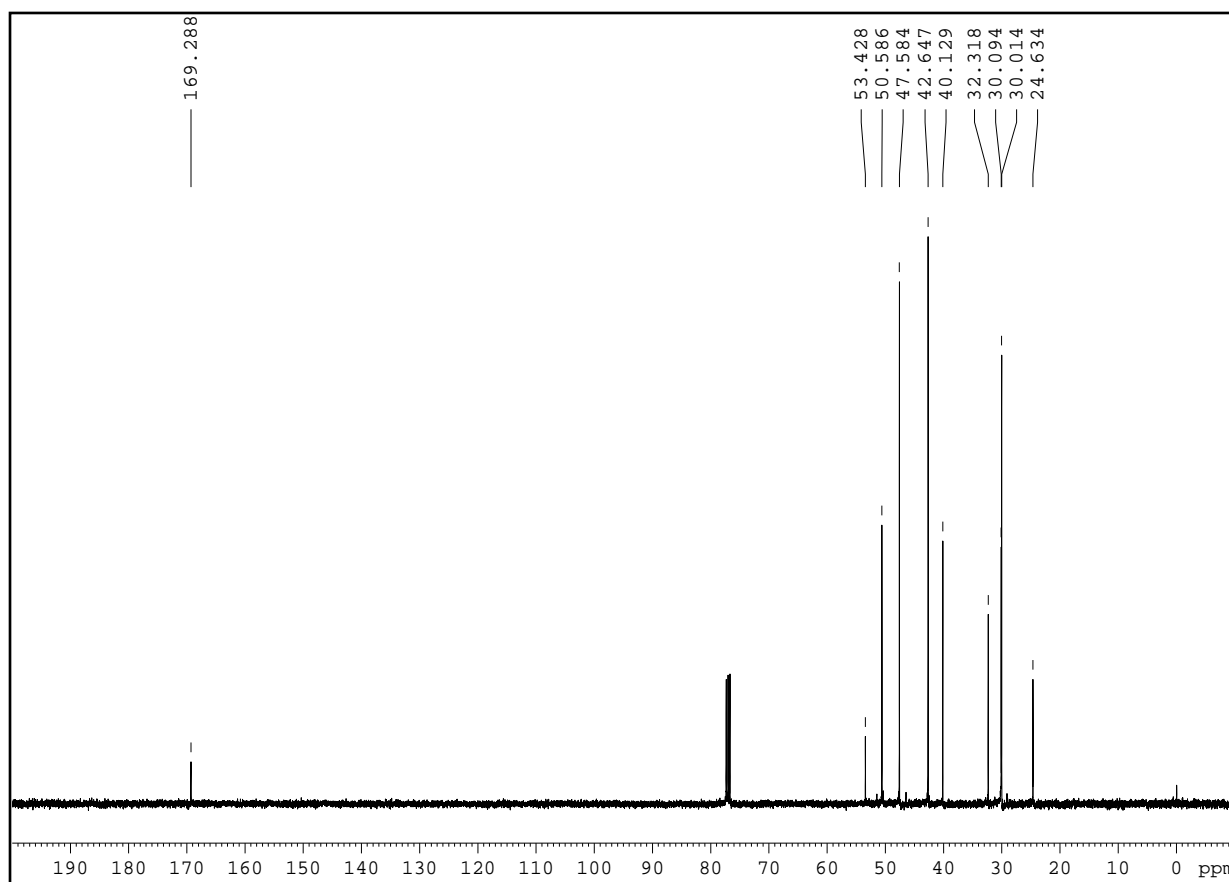
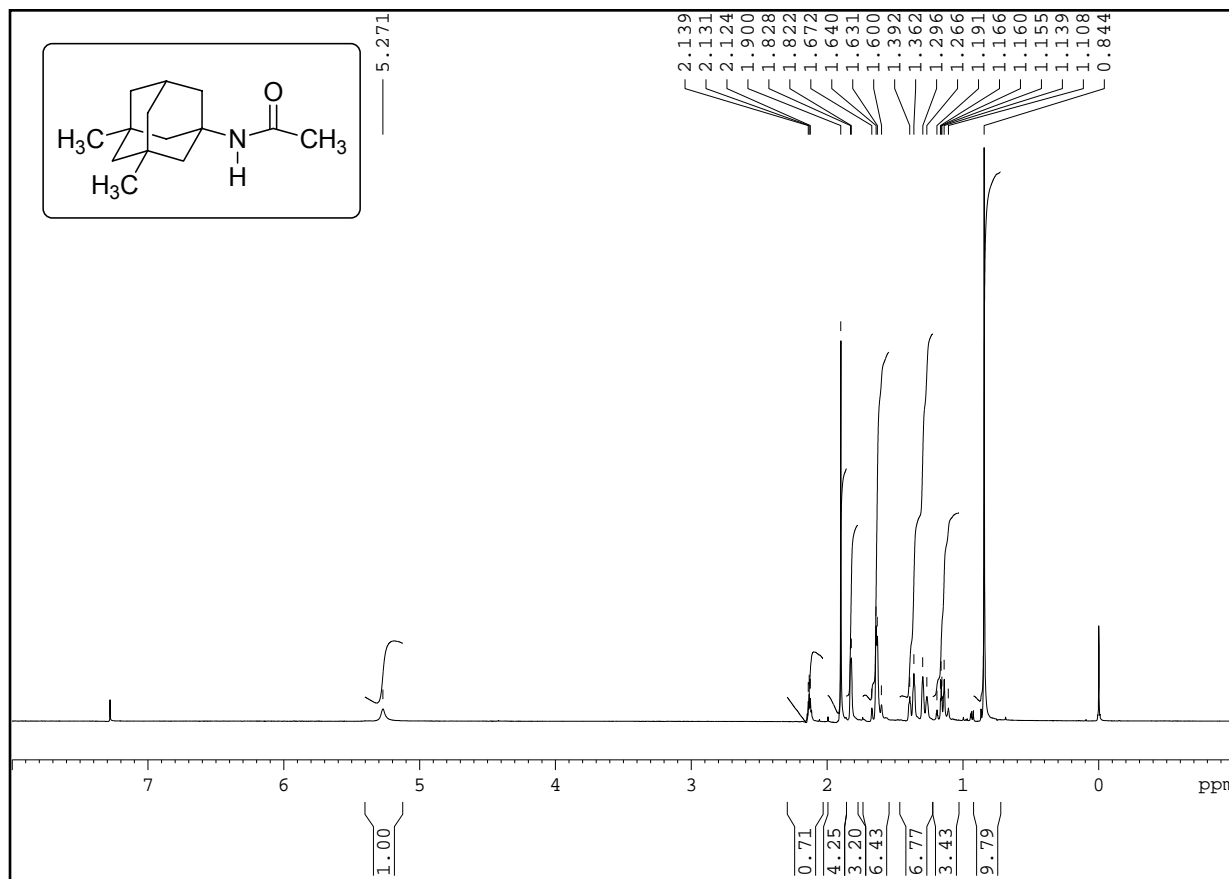
3-Acetamido-5-carboxymethyltricyclo[3.3.1.1^{3,7}]decane-1-carboxylic acid (145)



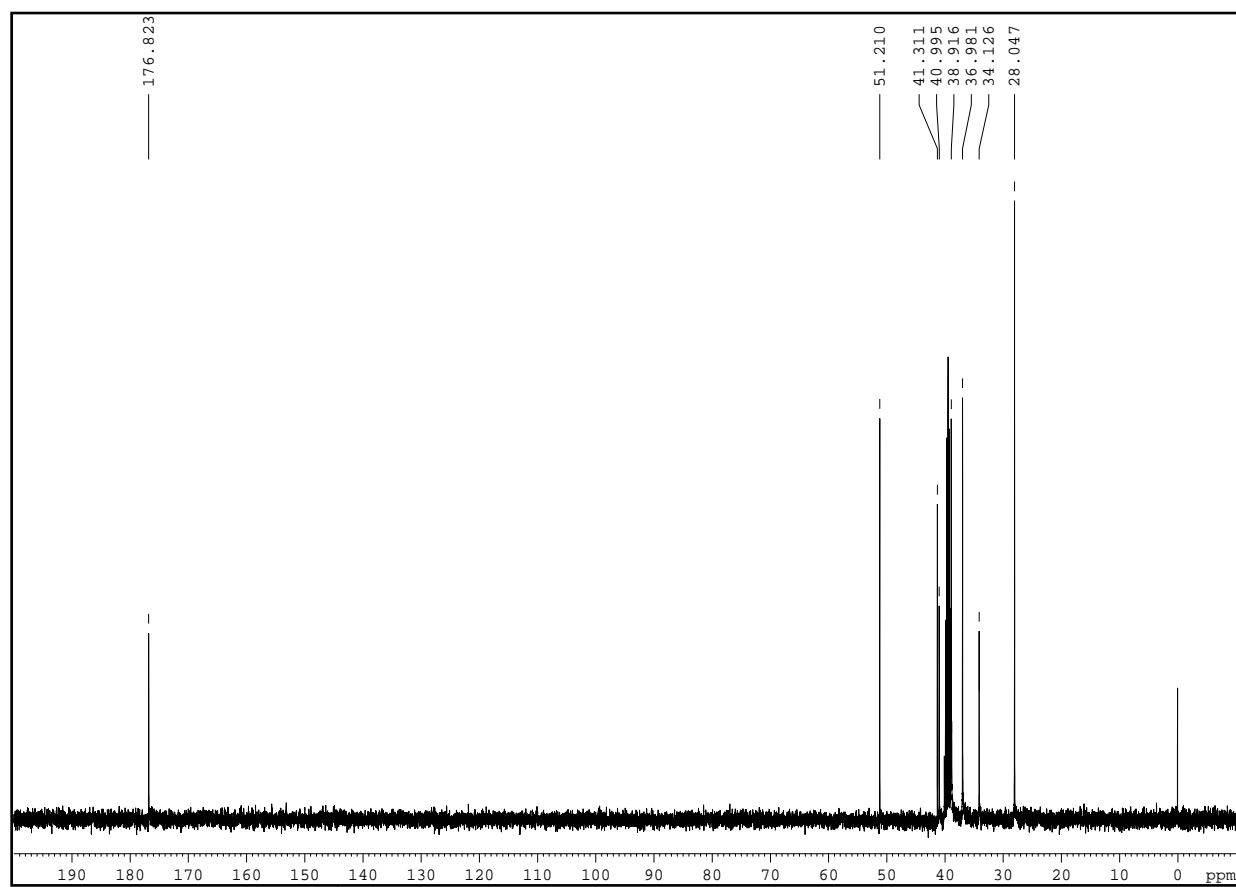
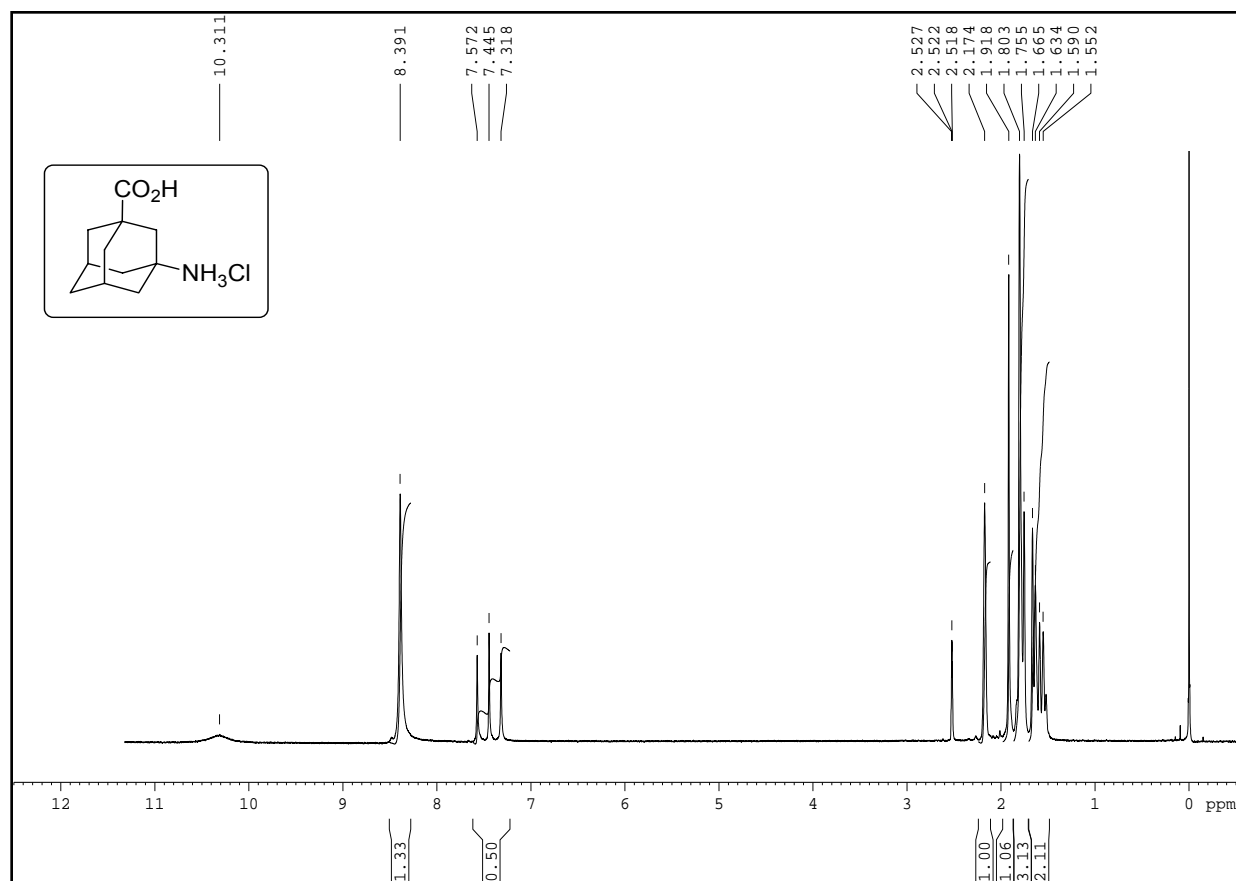
3-(3-Acetamido-5-carboxy-1-tricyclo[3.3.1.1^{3,7}]decane) propanoic acid (146)



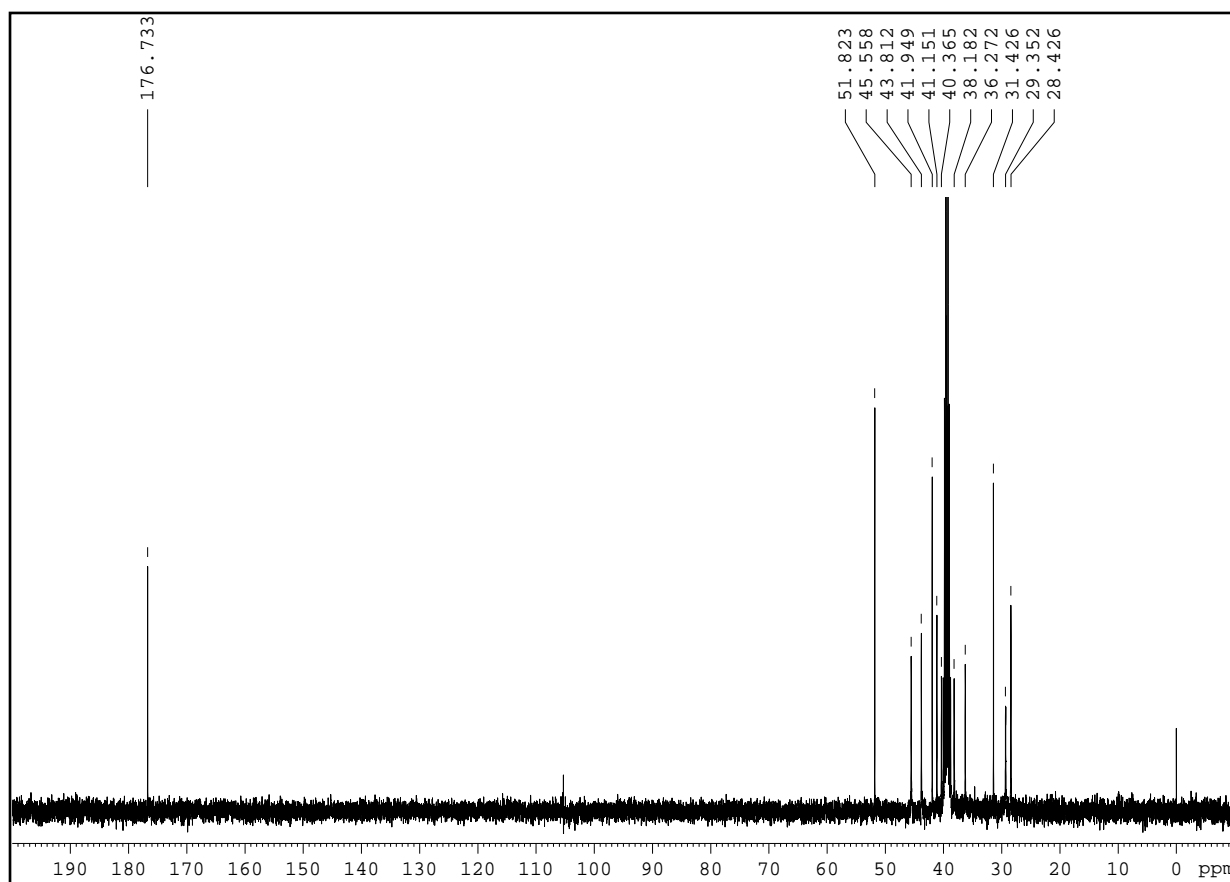
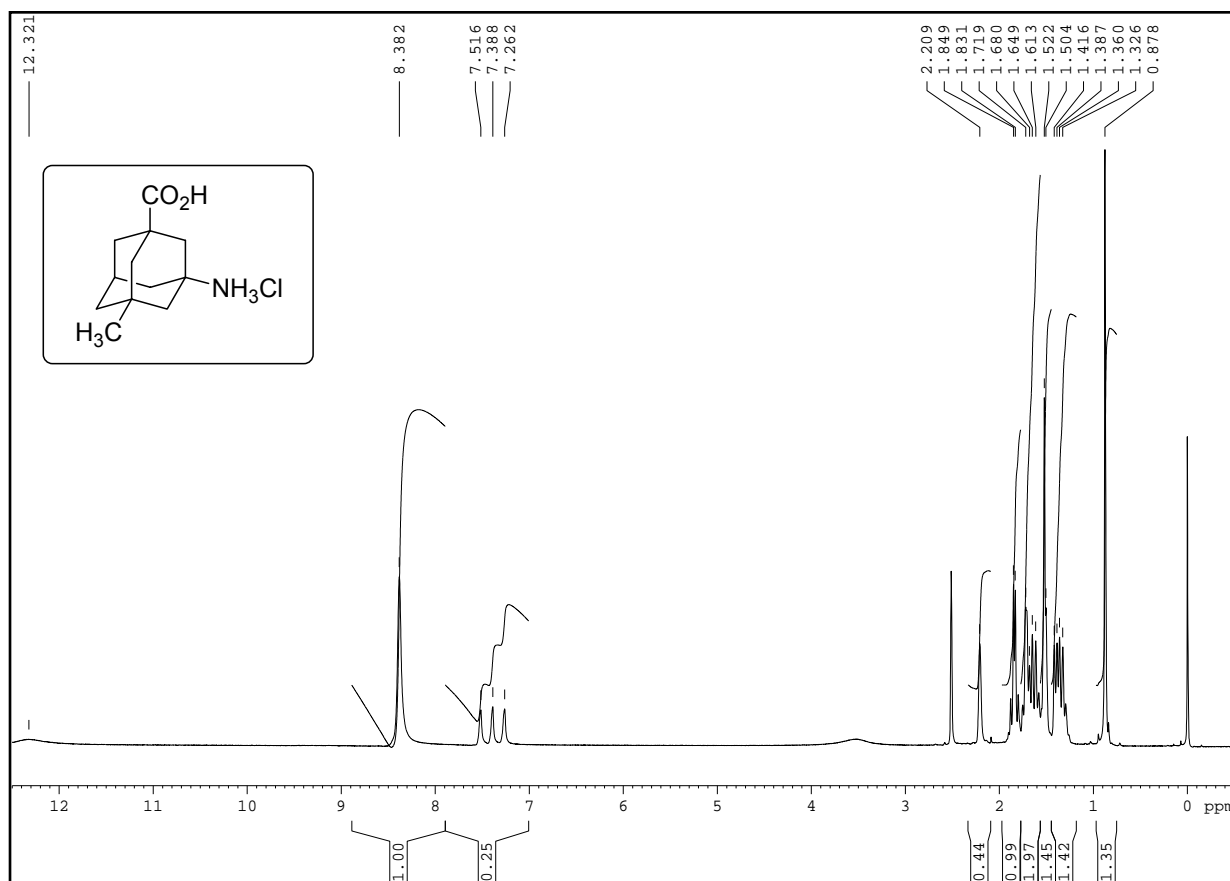
2-(3-Acetamido-3,5-dimethyltricyclo[3.3.1.1^{3,7}]dec-1-yl) acetic acid (147)



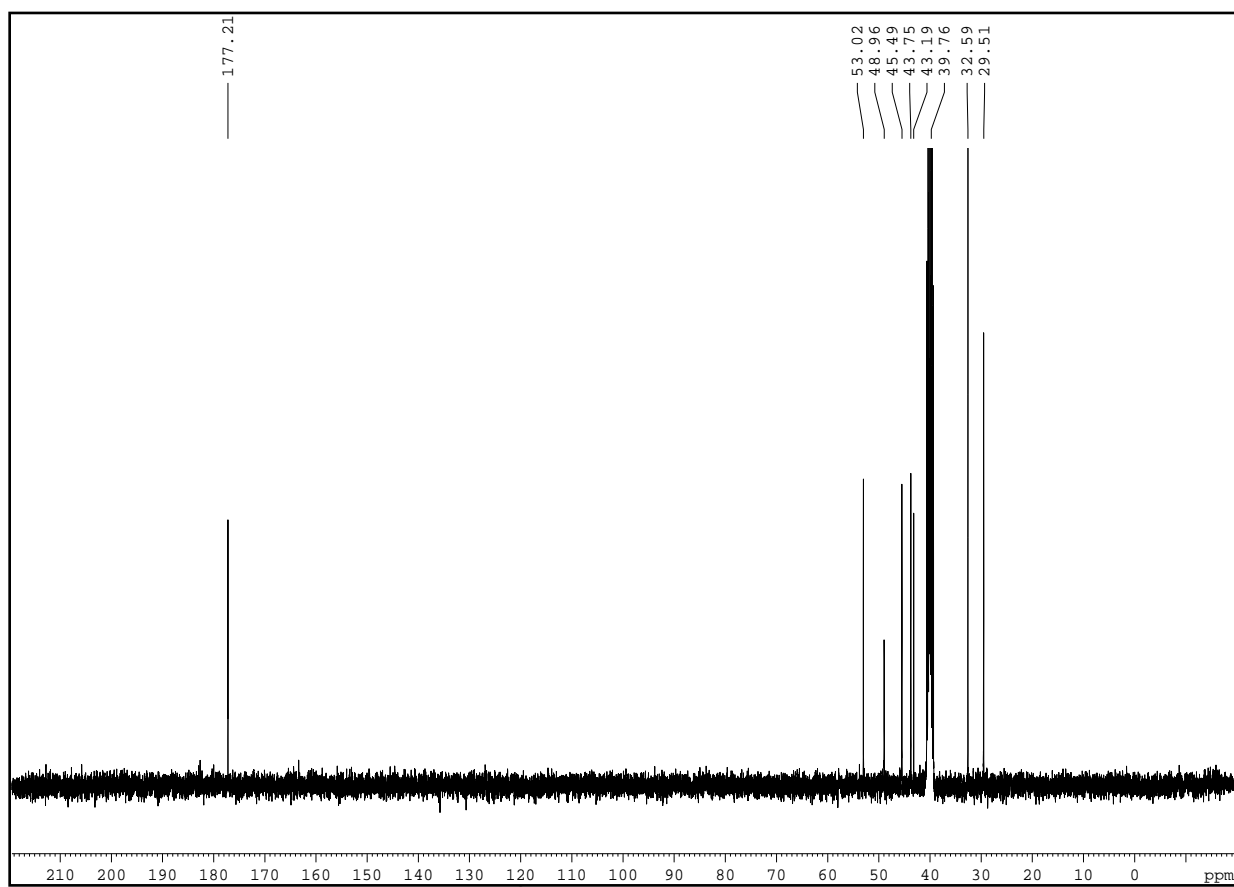
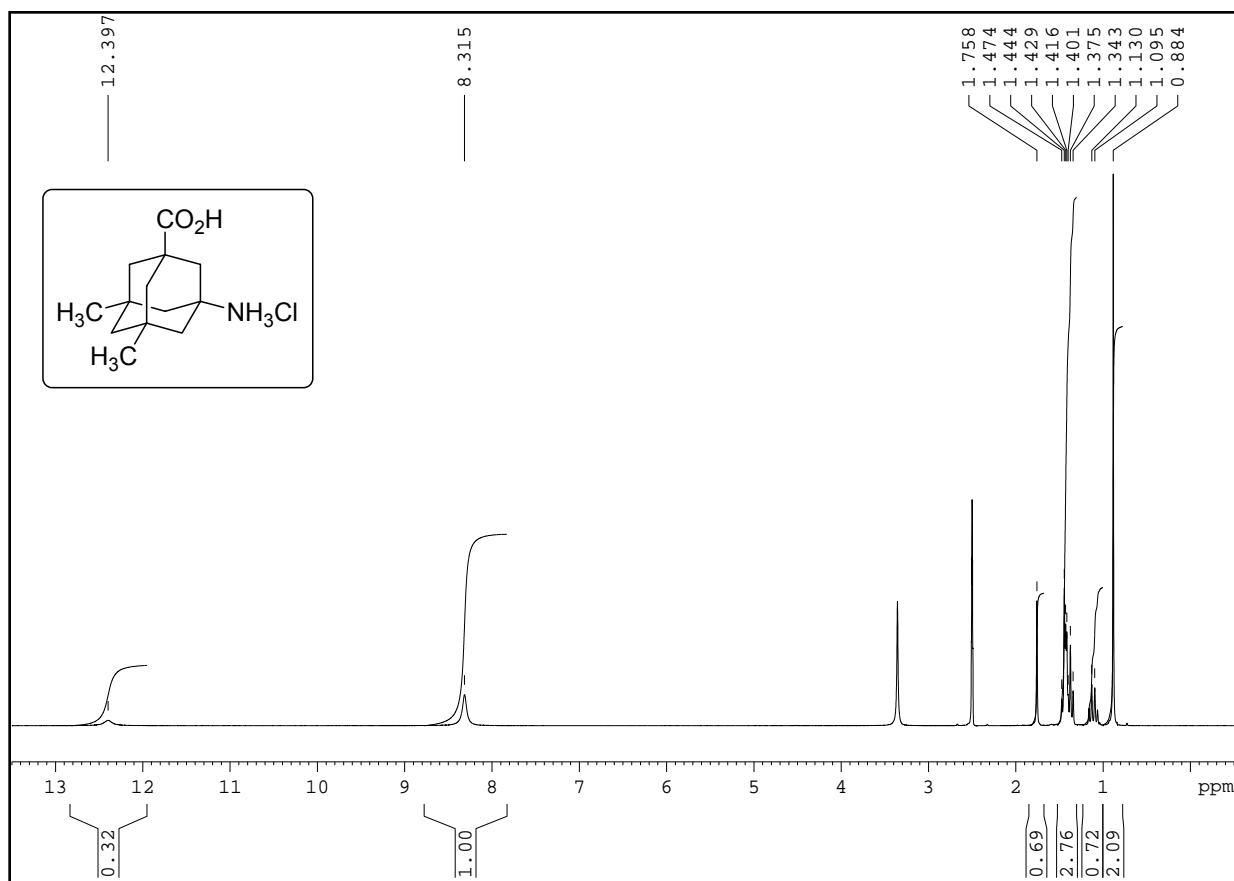
1-Acetamido-3,5-dimethyltricyclo[3.3.1.1^{3,7}]decane (148)



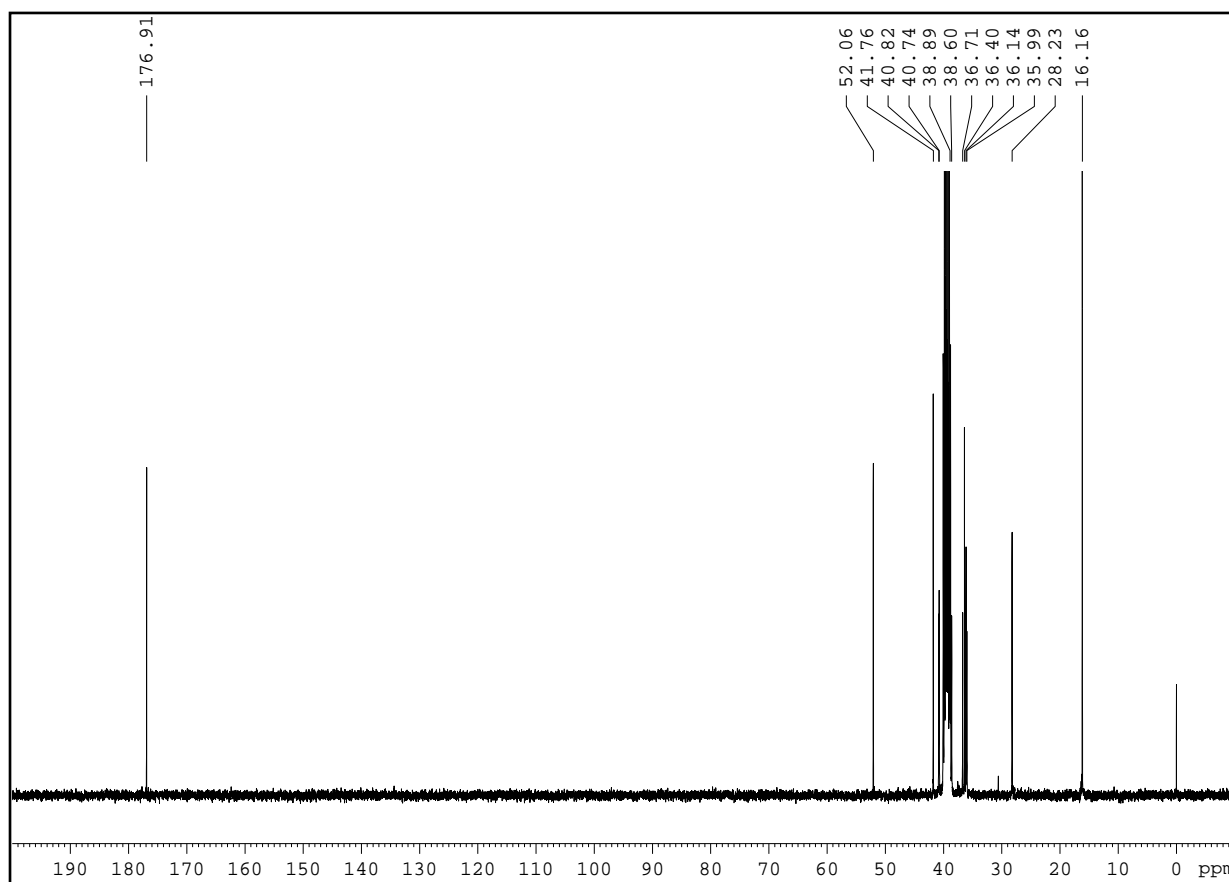
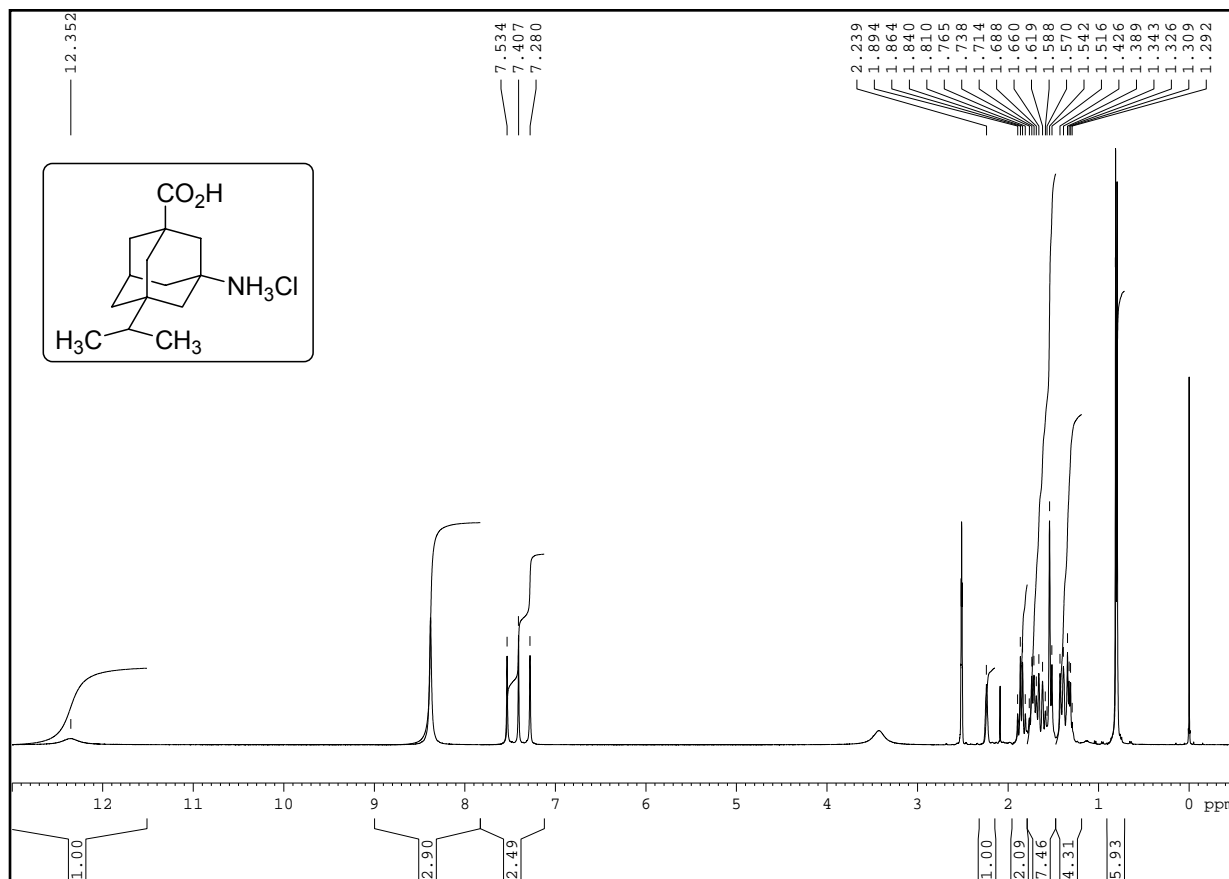
3-aminotricyclo[3.3.1.1^{3,7}]decane-1-carboxylic acid hydrochloride (154)



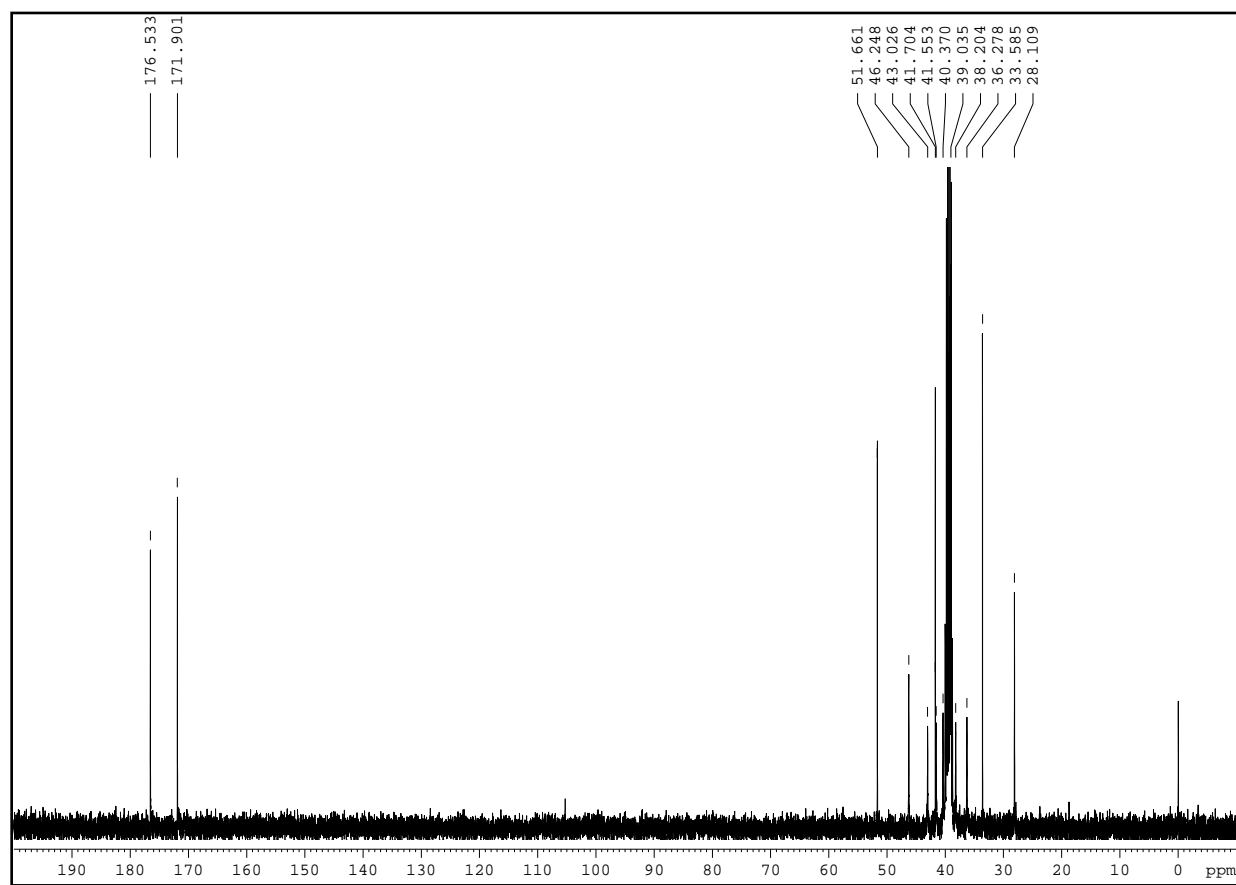
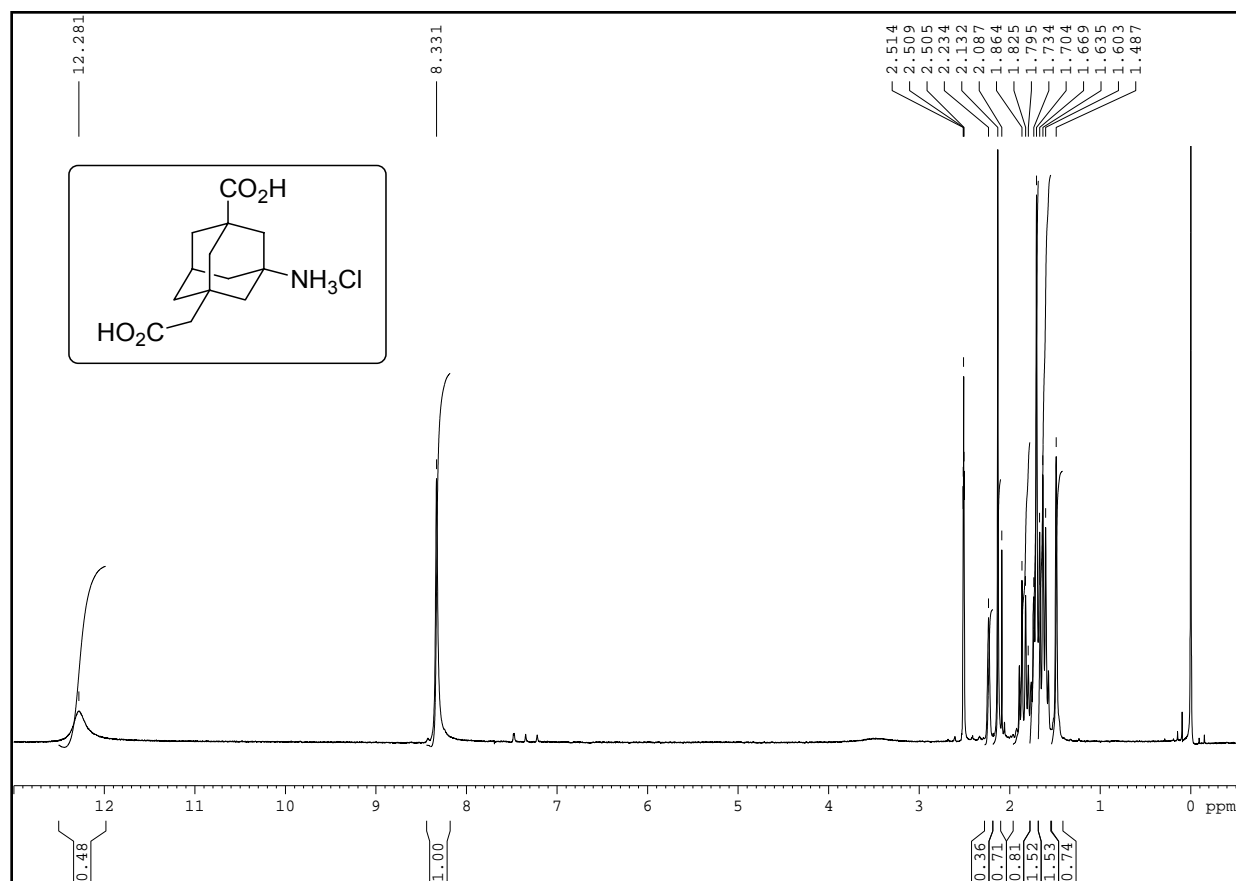
3-amino-5-methyltricyclo[3.3.1.1^{3,7}]decane-1-carboxylic acid hydrochloride (155)



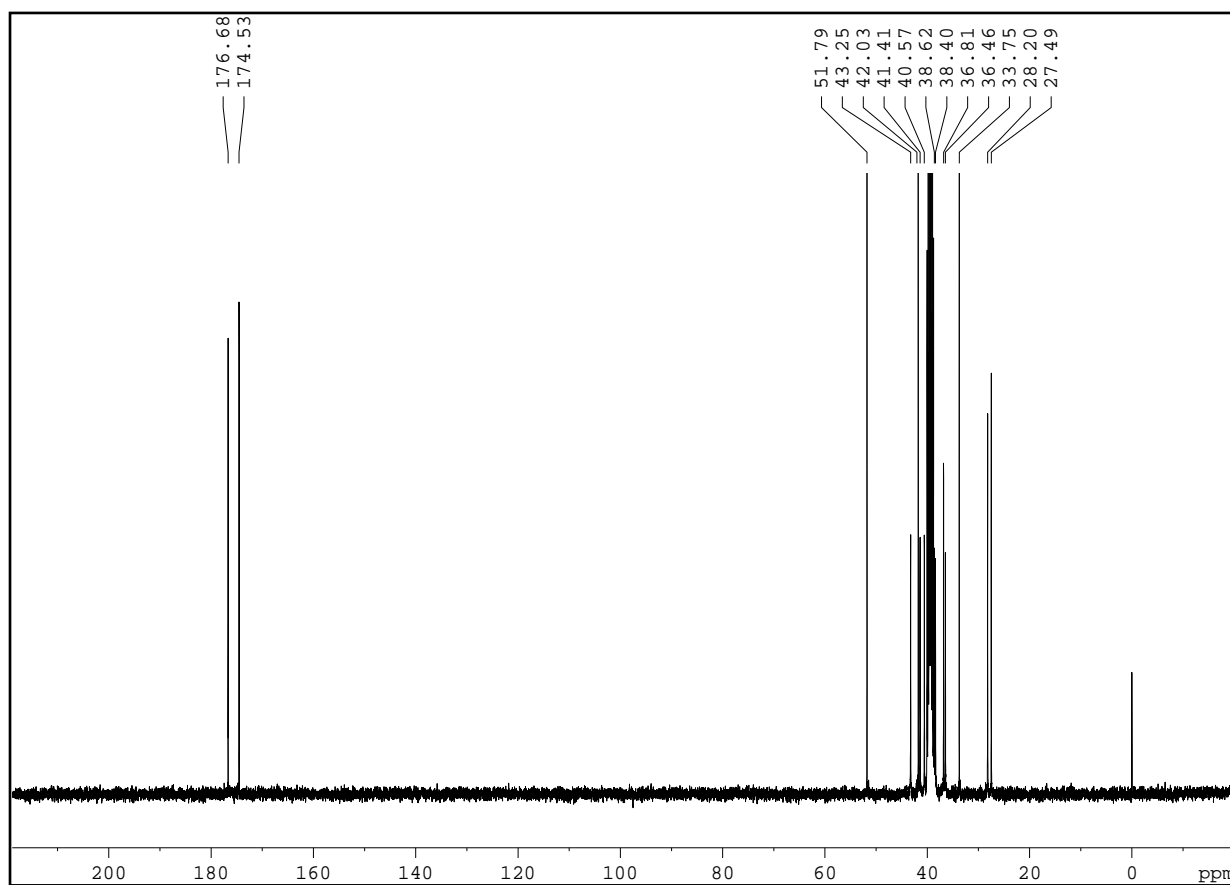
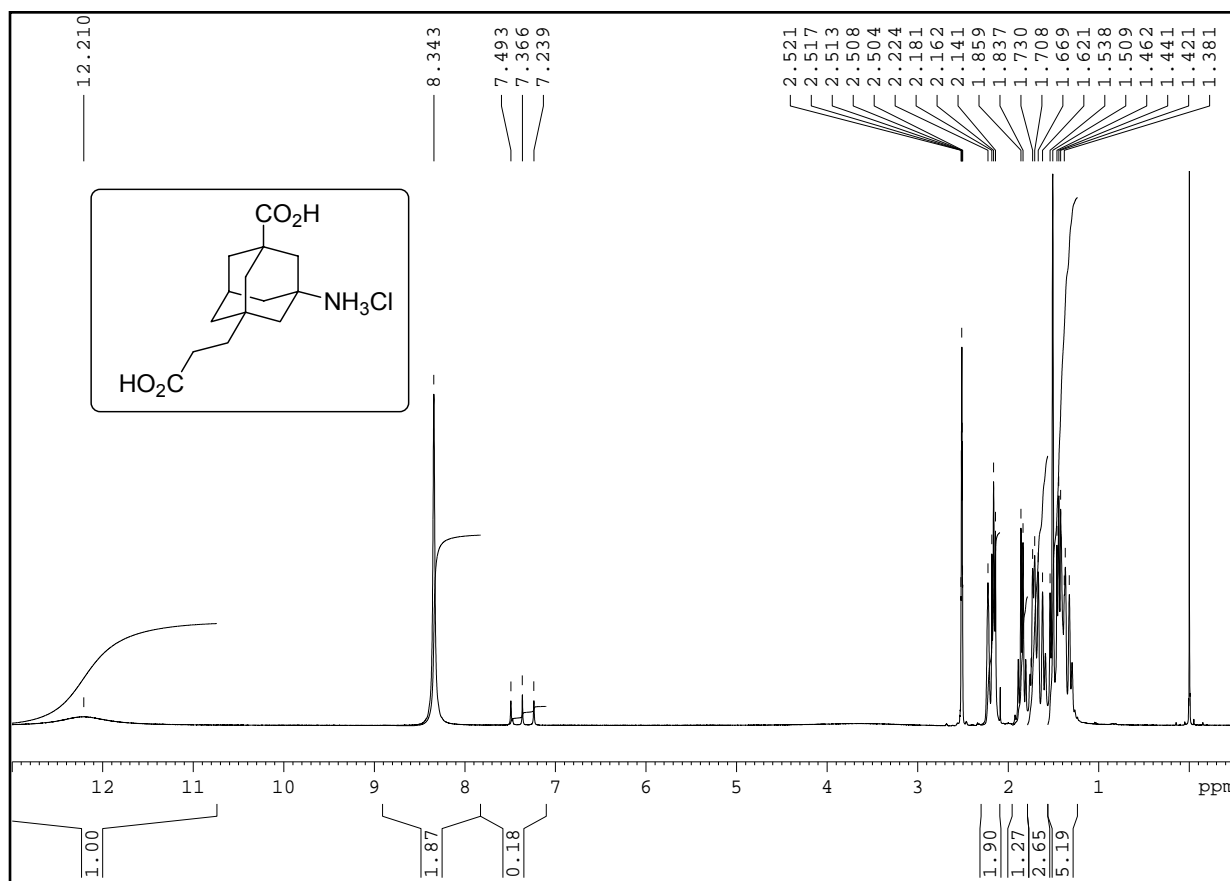
3-amino-5,7-dimethyltricyclo[3.3.1.1^{3,7}]decane-1-carboxylic acid hydrochloride (156)



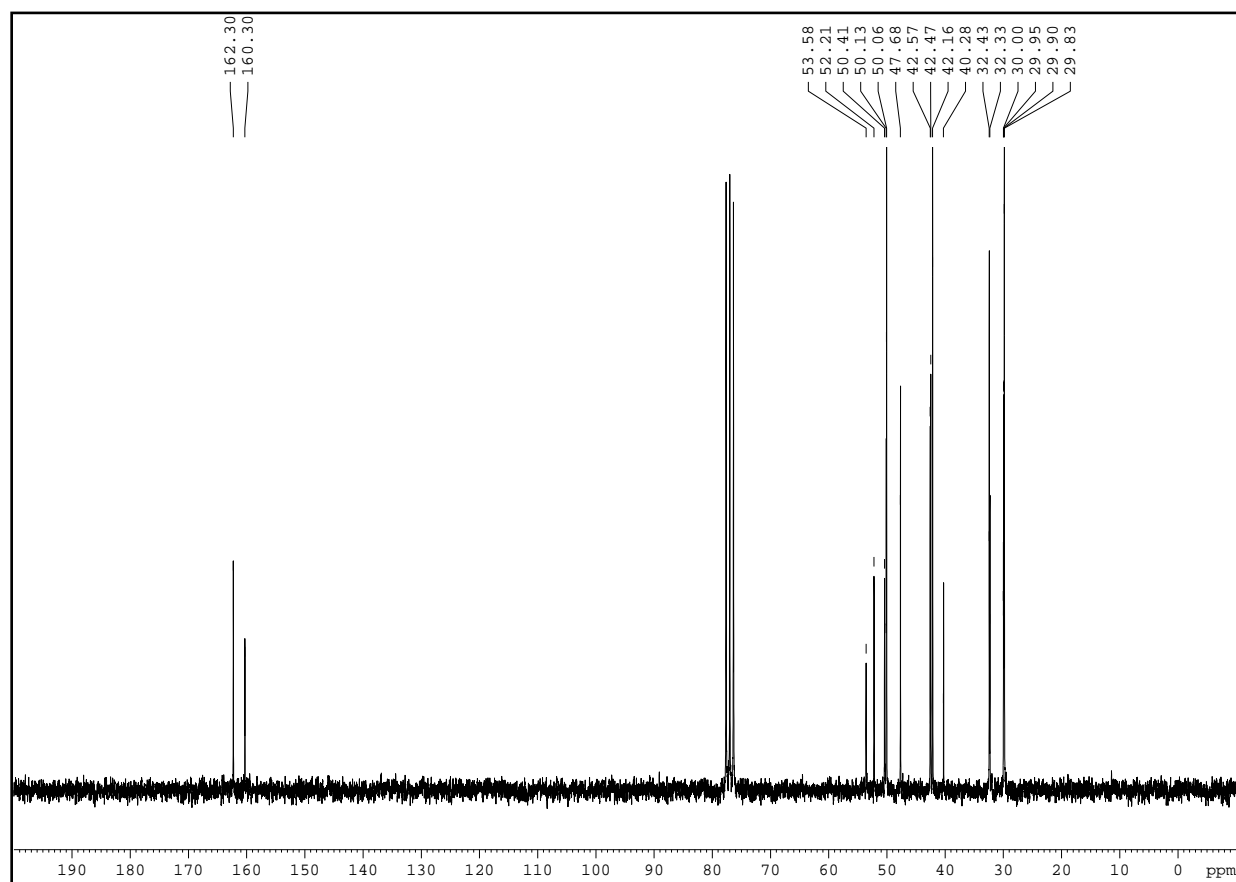
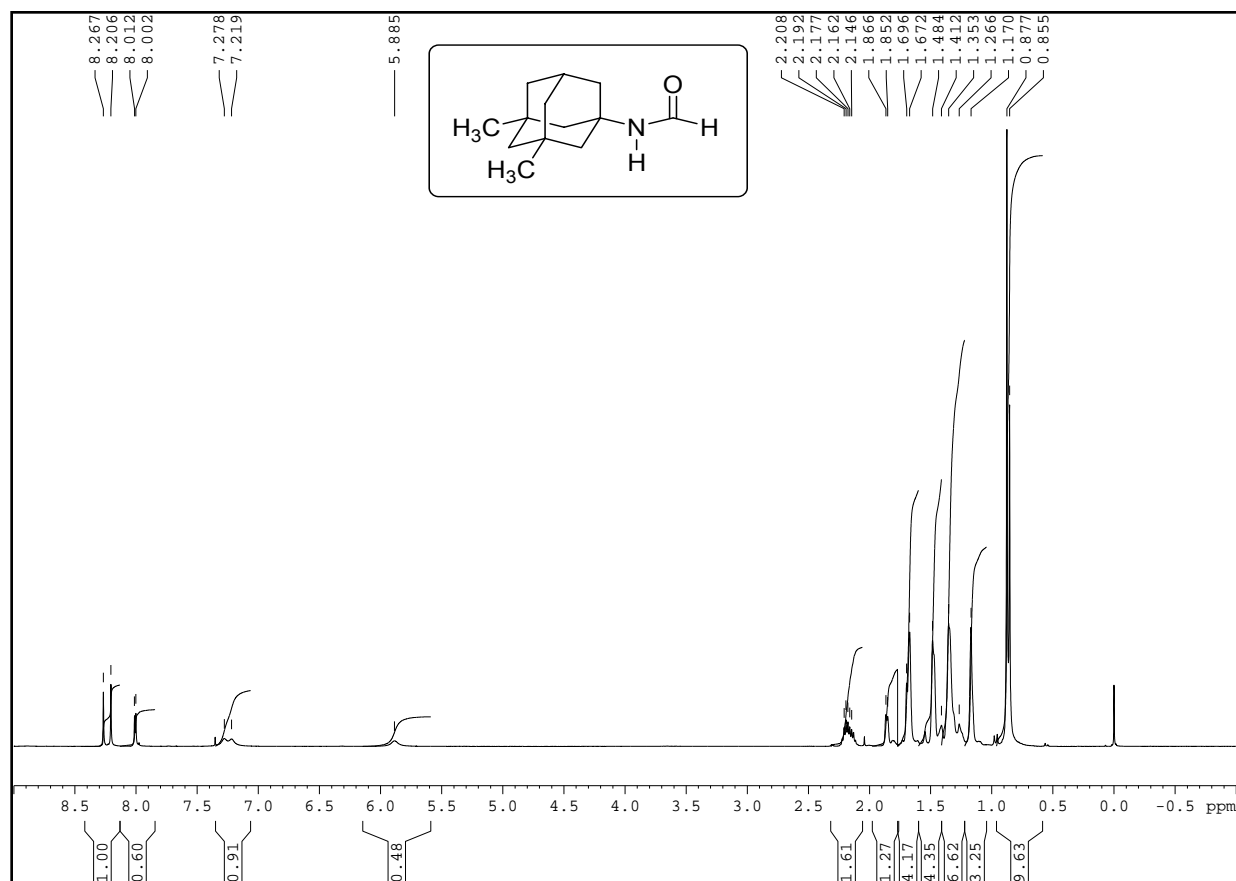
3-amino-5-(2-propyl)tricyclo[3.3.1.1^{3,7}]decane carboxylic acid hydrochloride (157)



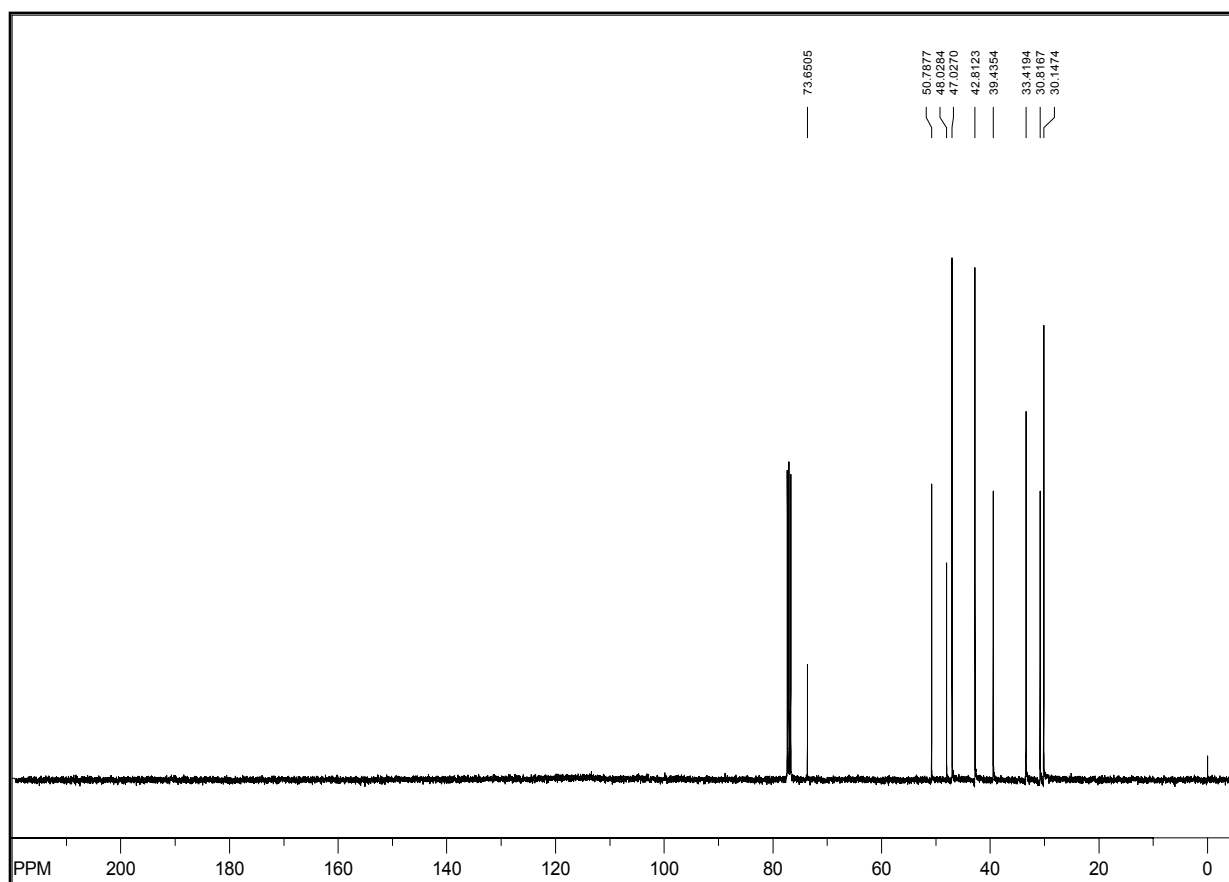
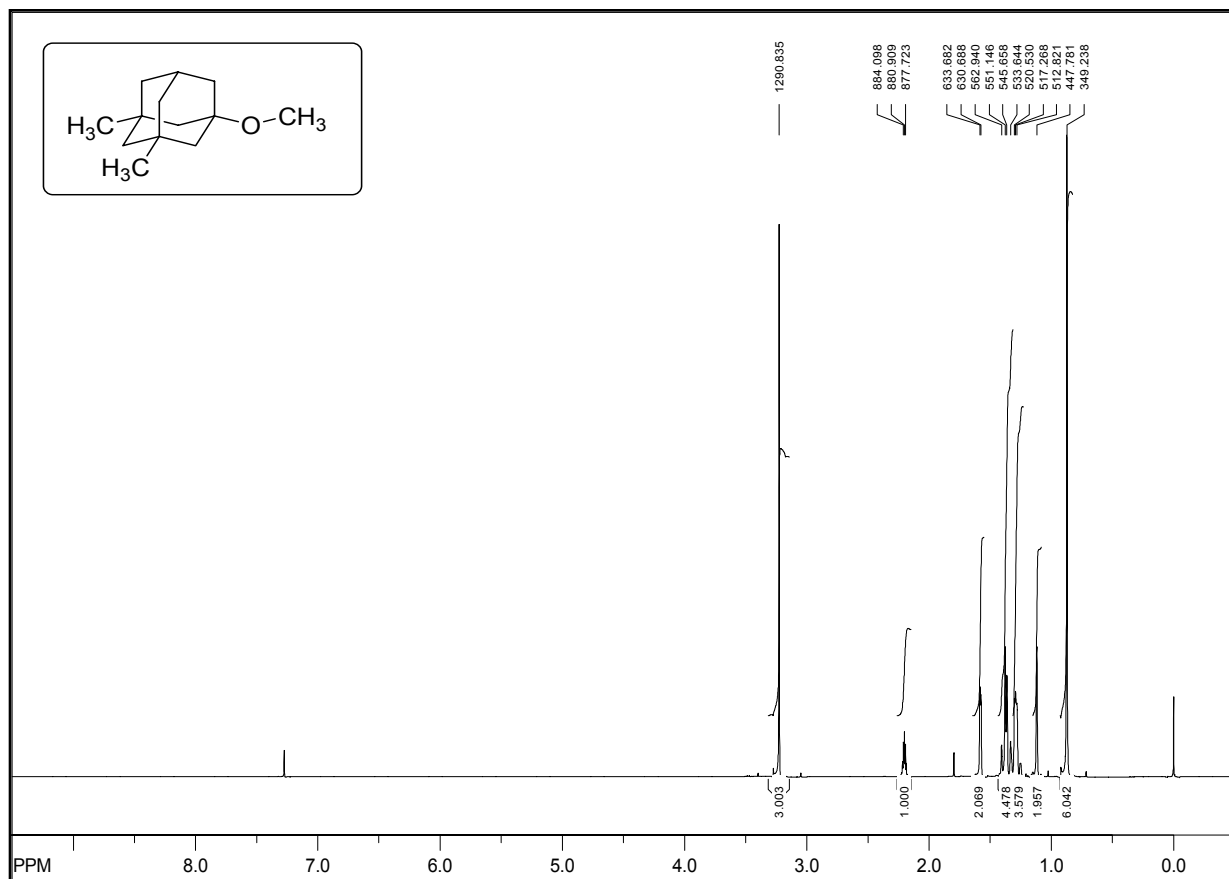
3-amino-5-carboxymethyltricyclo[3.3.1.1^{3,7}]decane-1-carboxylic acid hydrochloride (**158**)



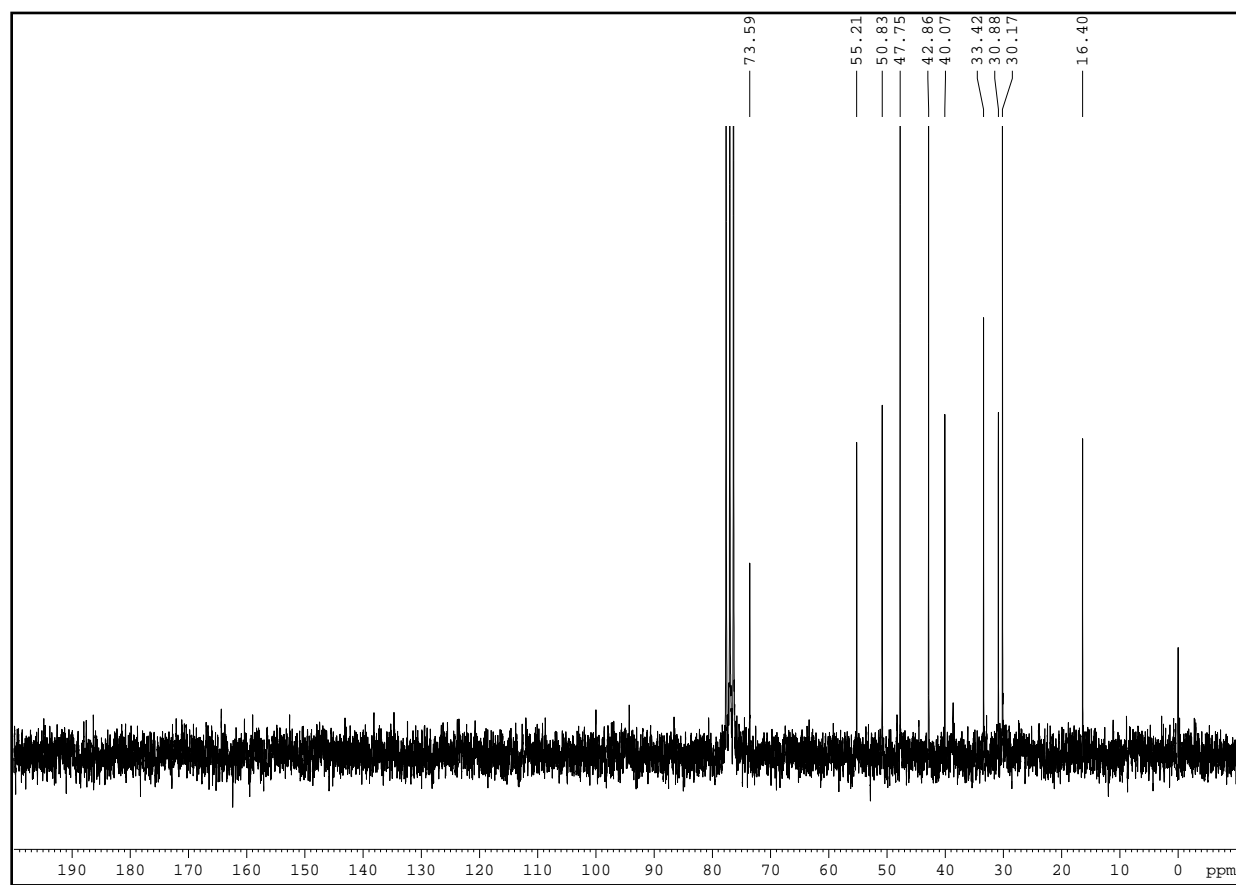
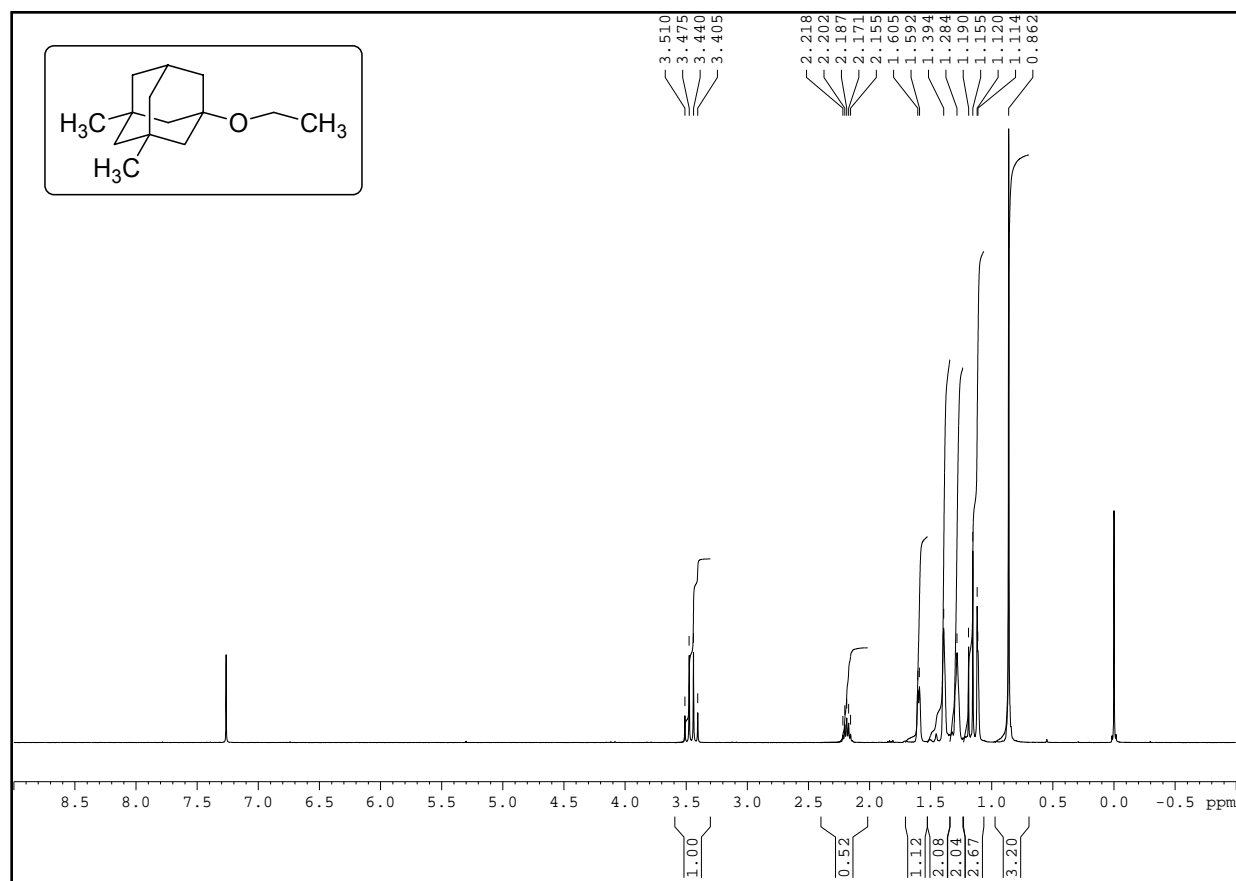
3-amino-5-carboxytricyclo[3.3.1.1^{3,7}]decane-1-propanoic acid hydrochloride (159)

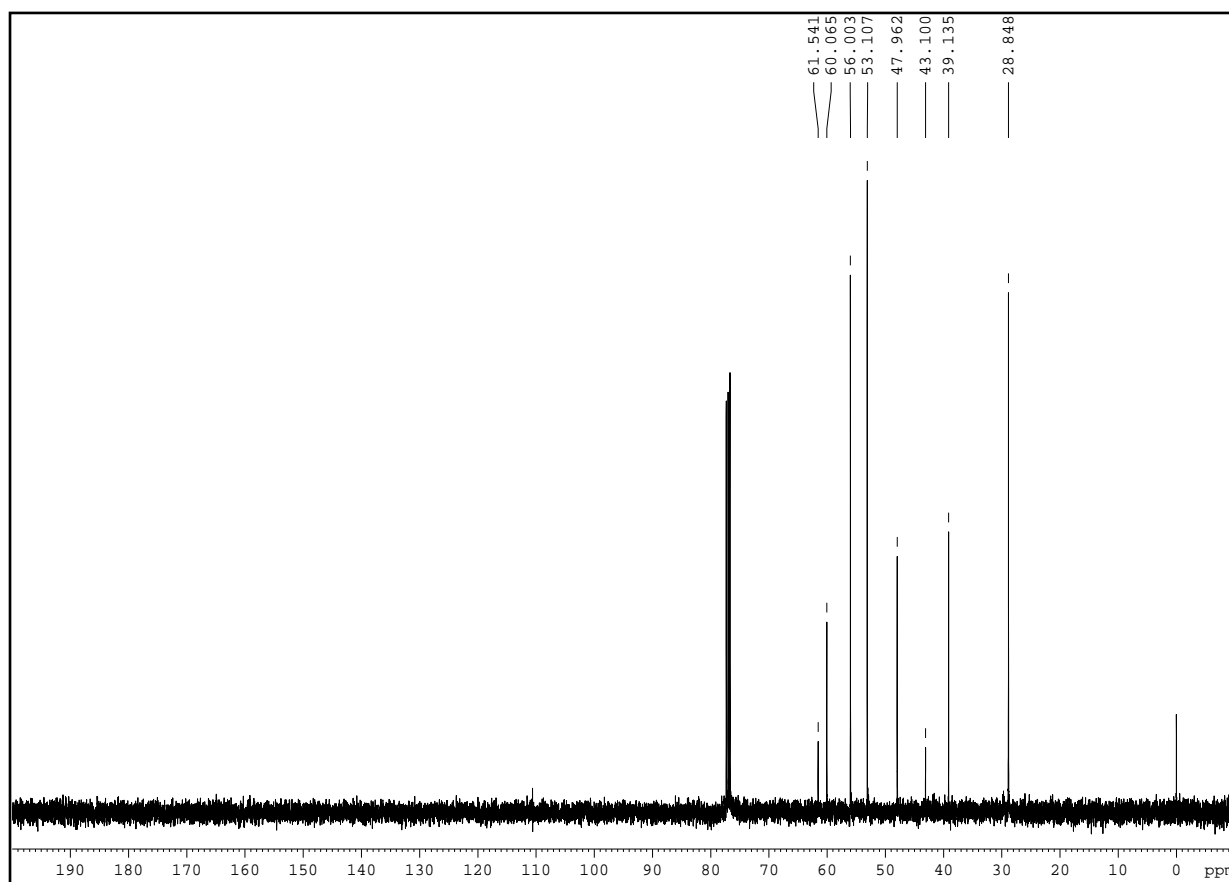
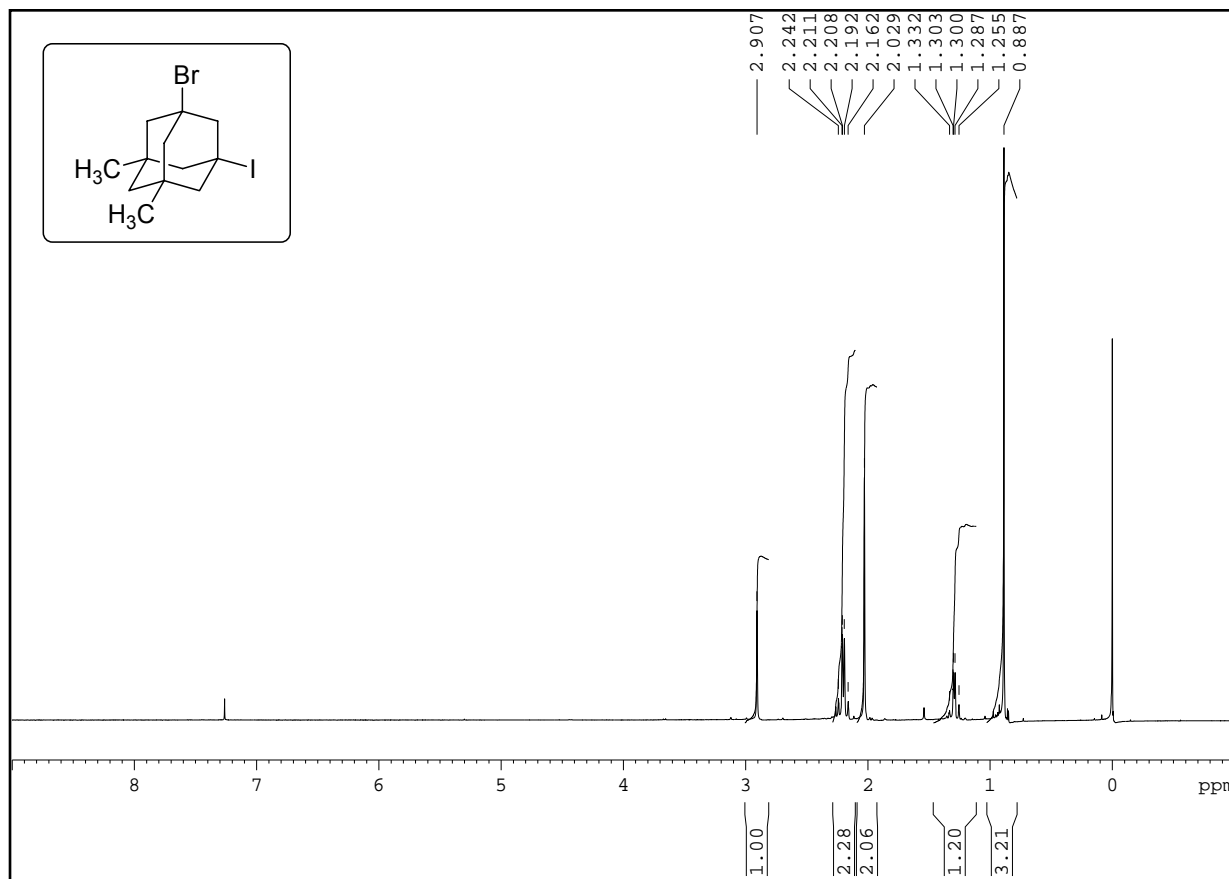


1-Formamido-3,5-dimethyltricyclo[3.3.1.1^{3,7}]decane (160)

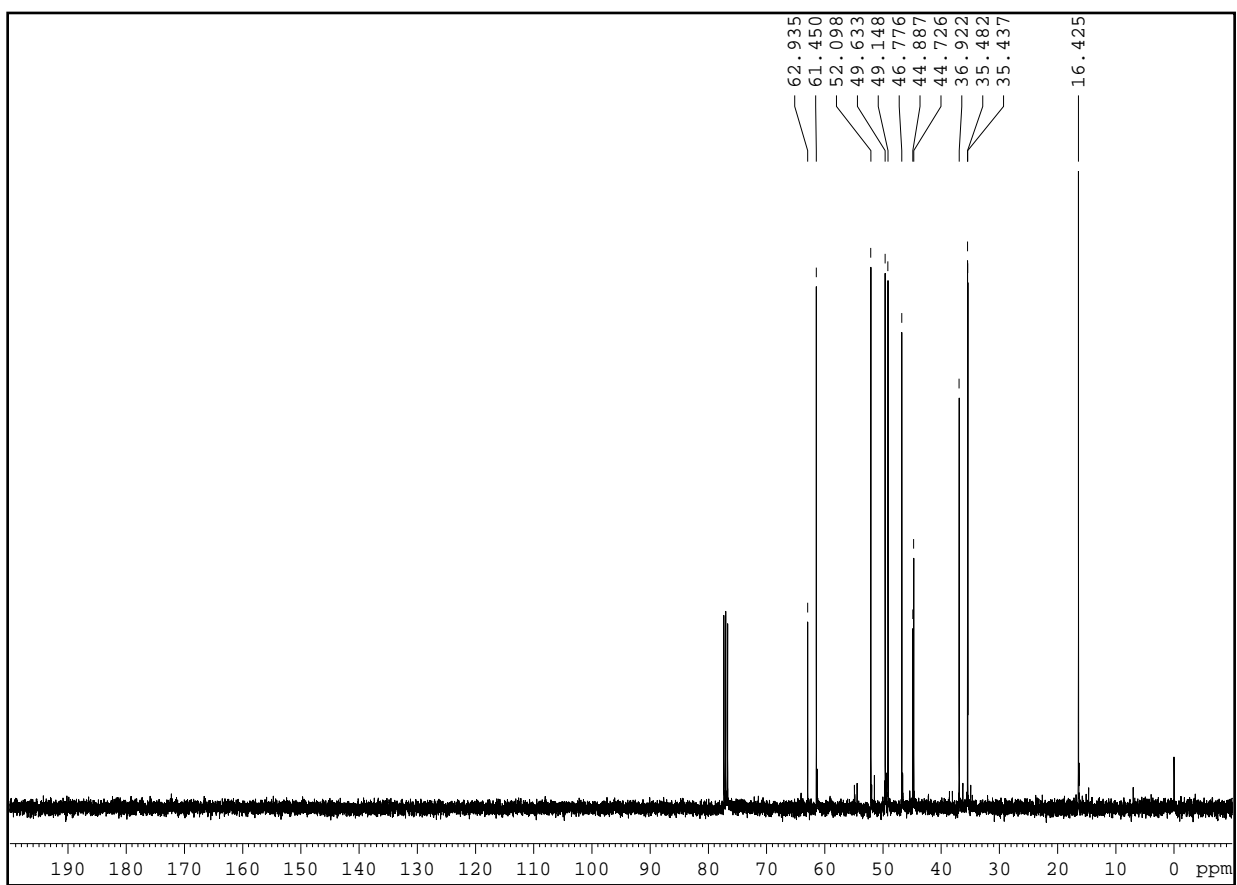
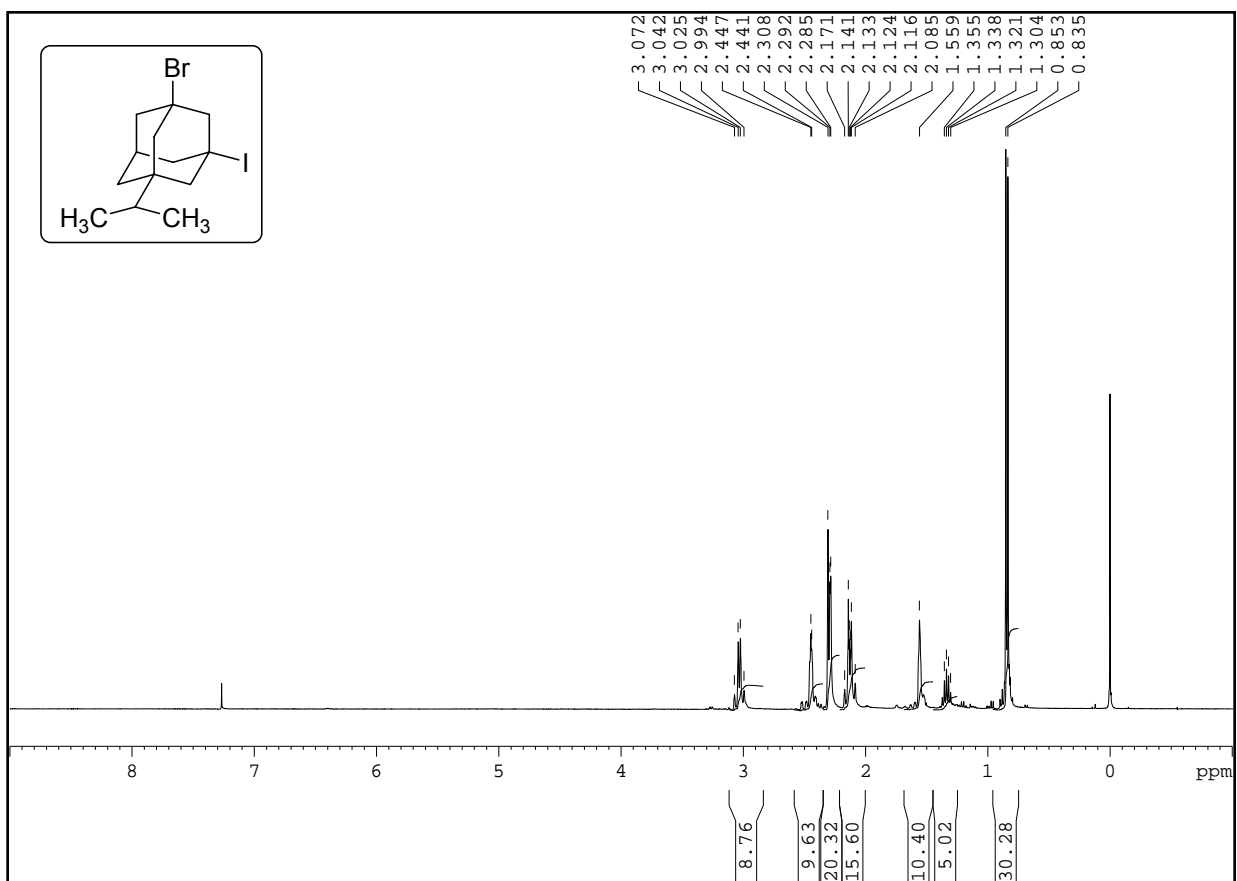


3,5-dimethyltricyclo[3.3.1.1^{3,7}]decane-1-yl-methyl ether (**165**)

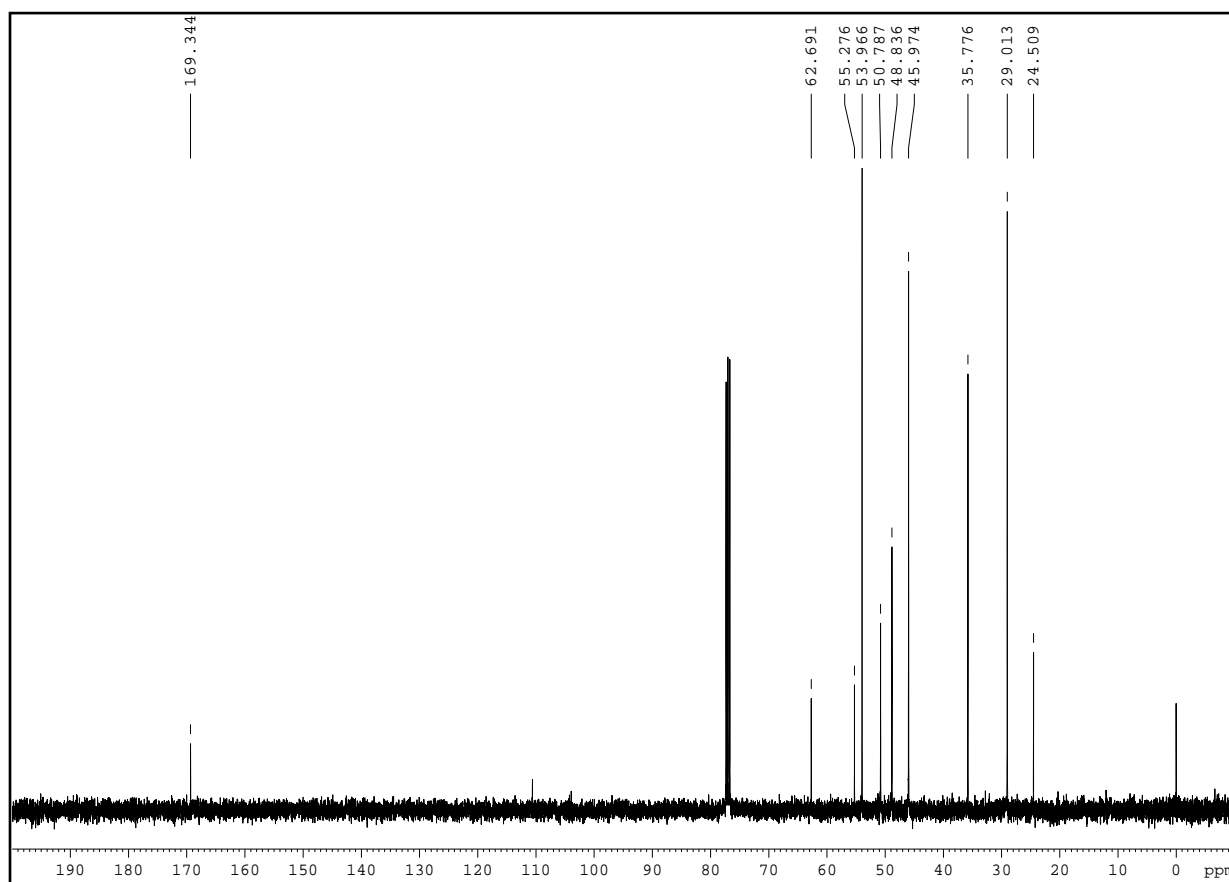
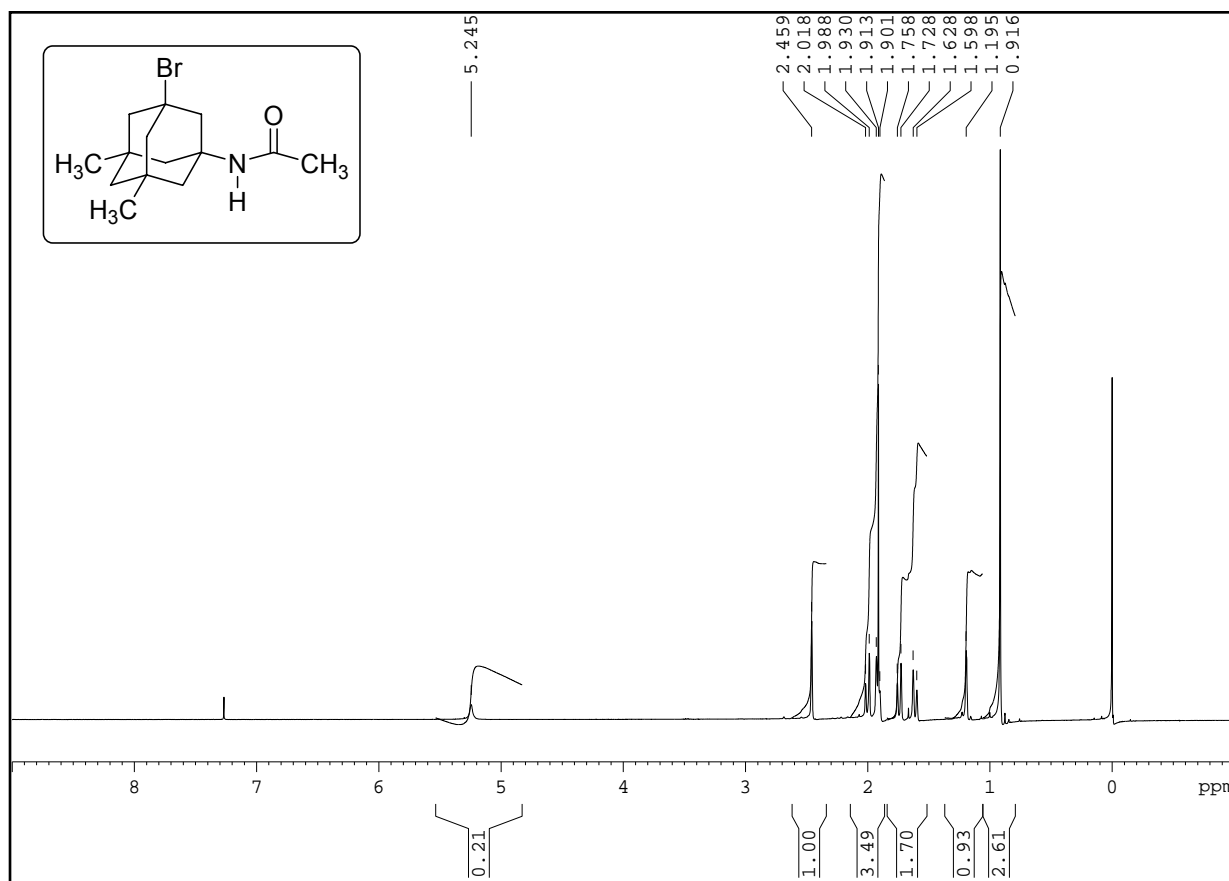
3,5-dimethyltricyclo[3.3.1.1^{3,7}]decane-1-yl-ethyl ether (166)



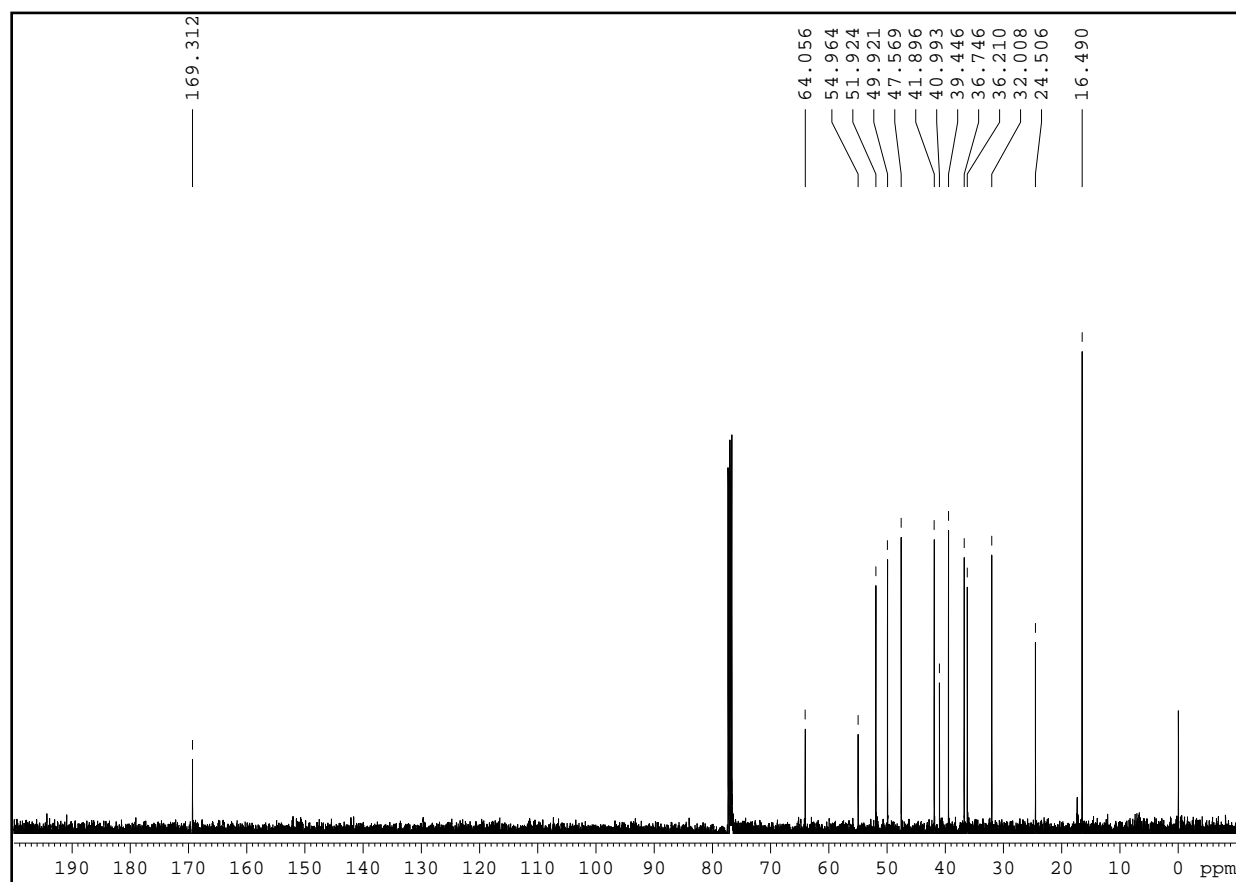
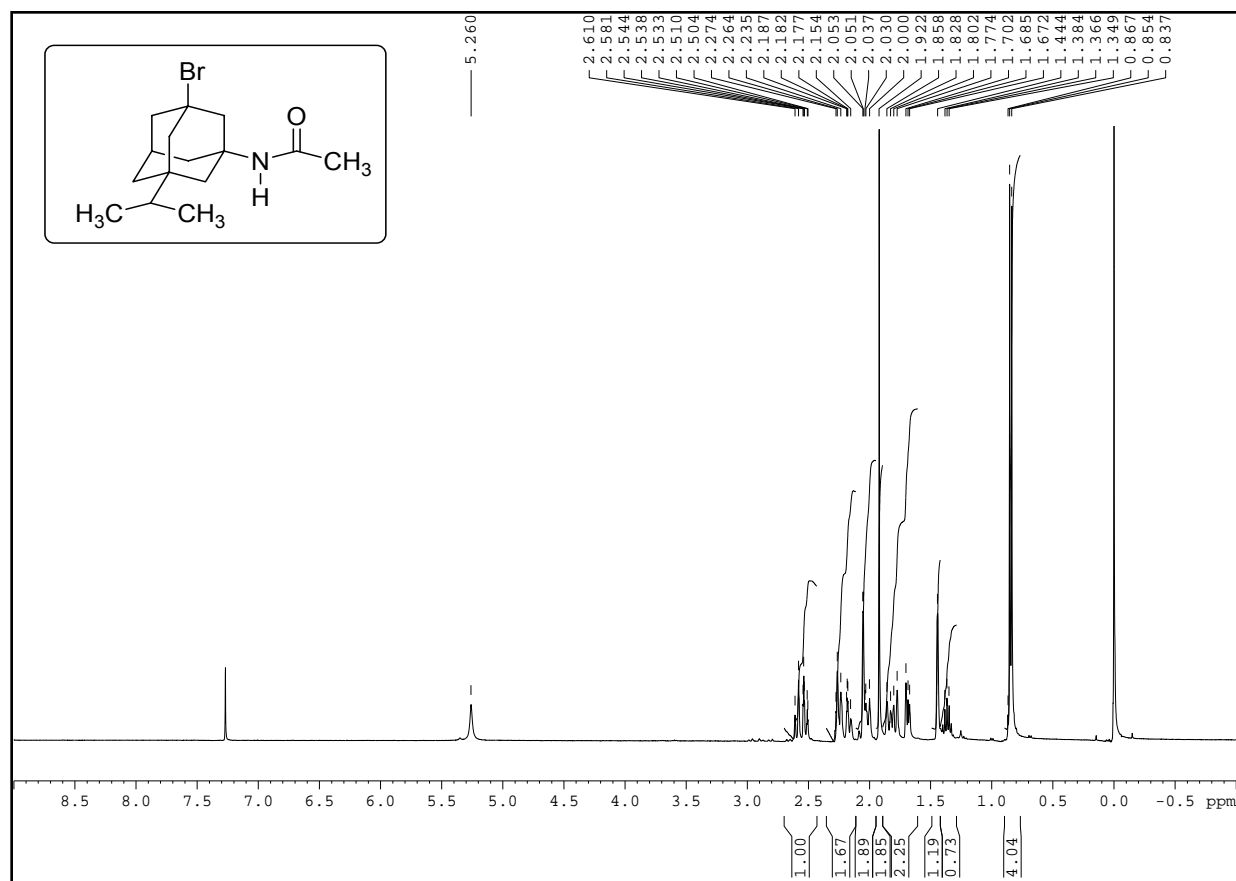
1-iodo-3-bromo-5,7-dimethyltricyclo[3.3.1.1^{3,7}]decane (168a)



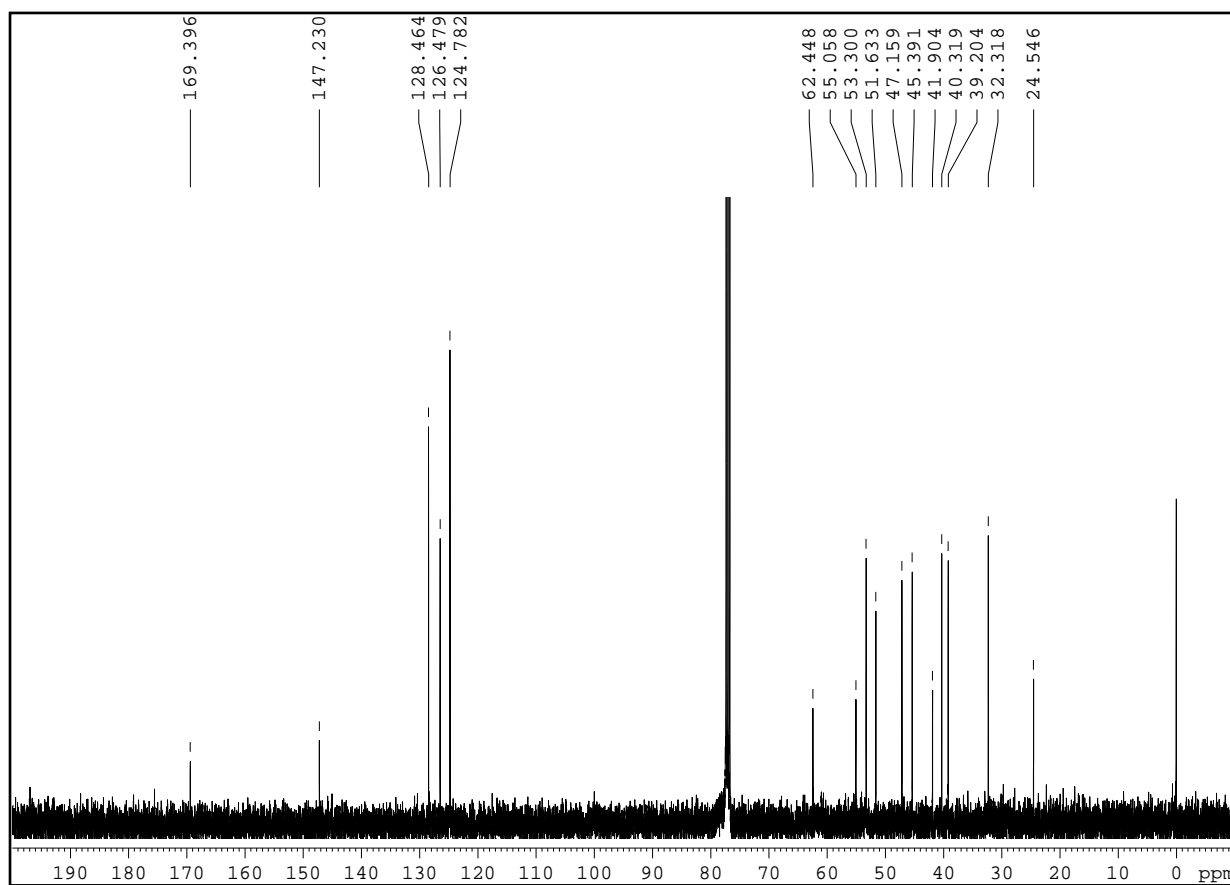
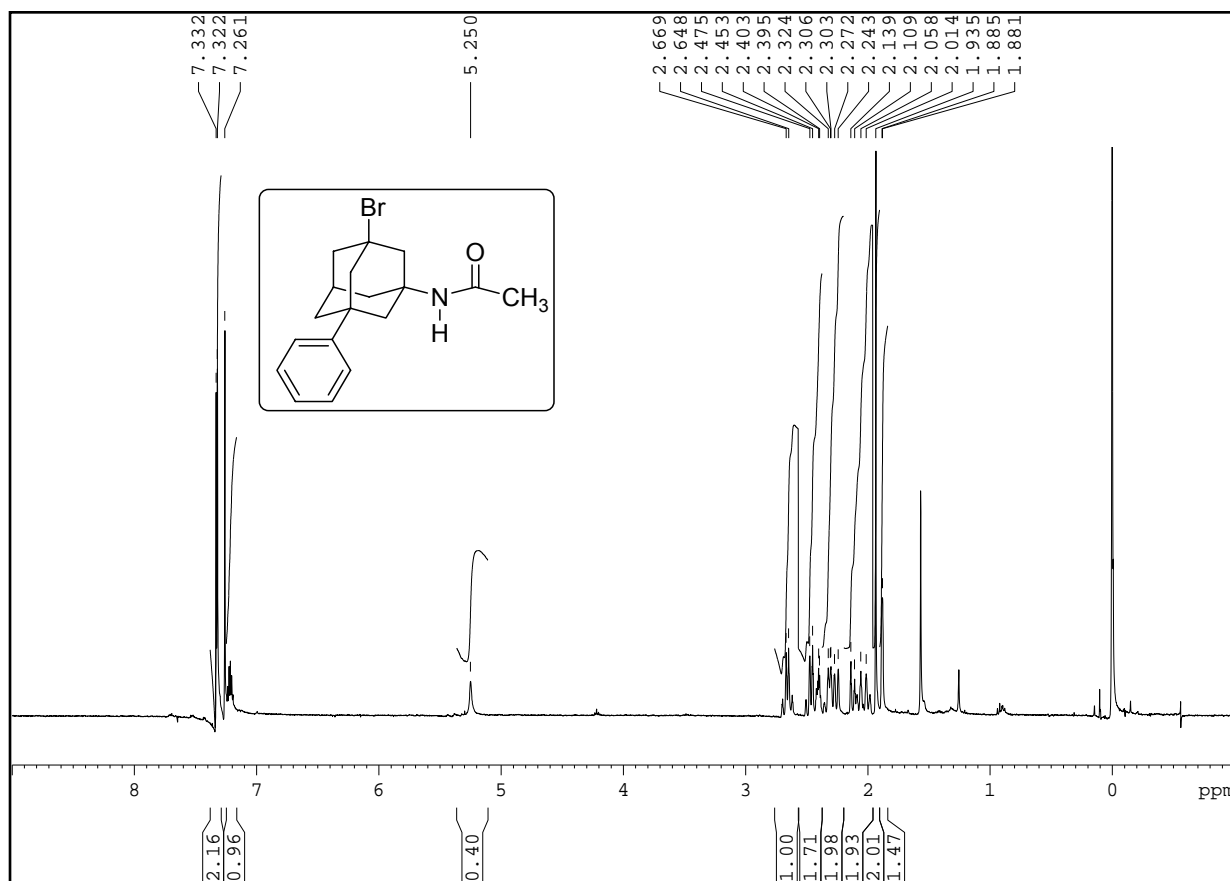
1-iodo-3-bromo-5-(1'-methyl)ethyltricyclo[3.3.1.1^{3,7}]decane (**168b**)



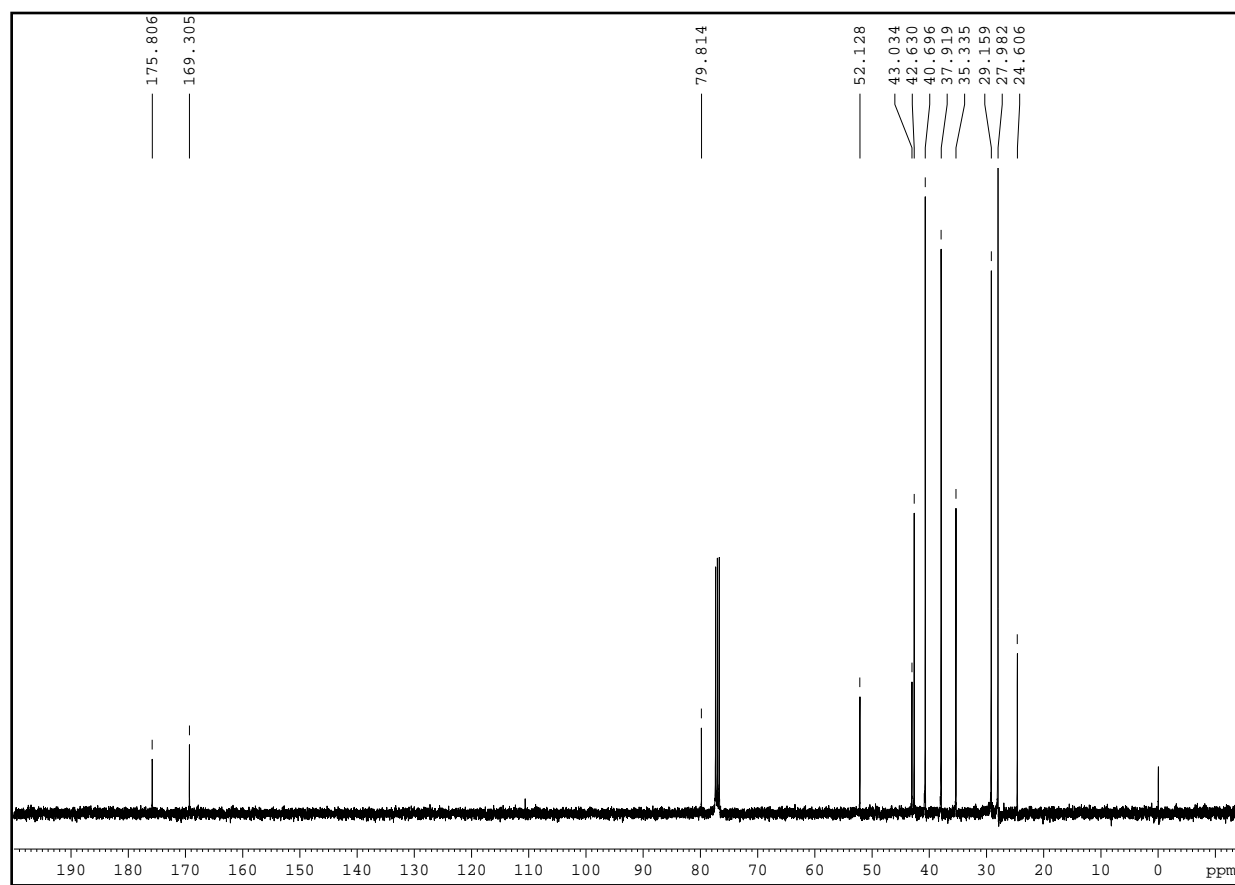
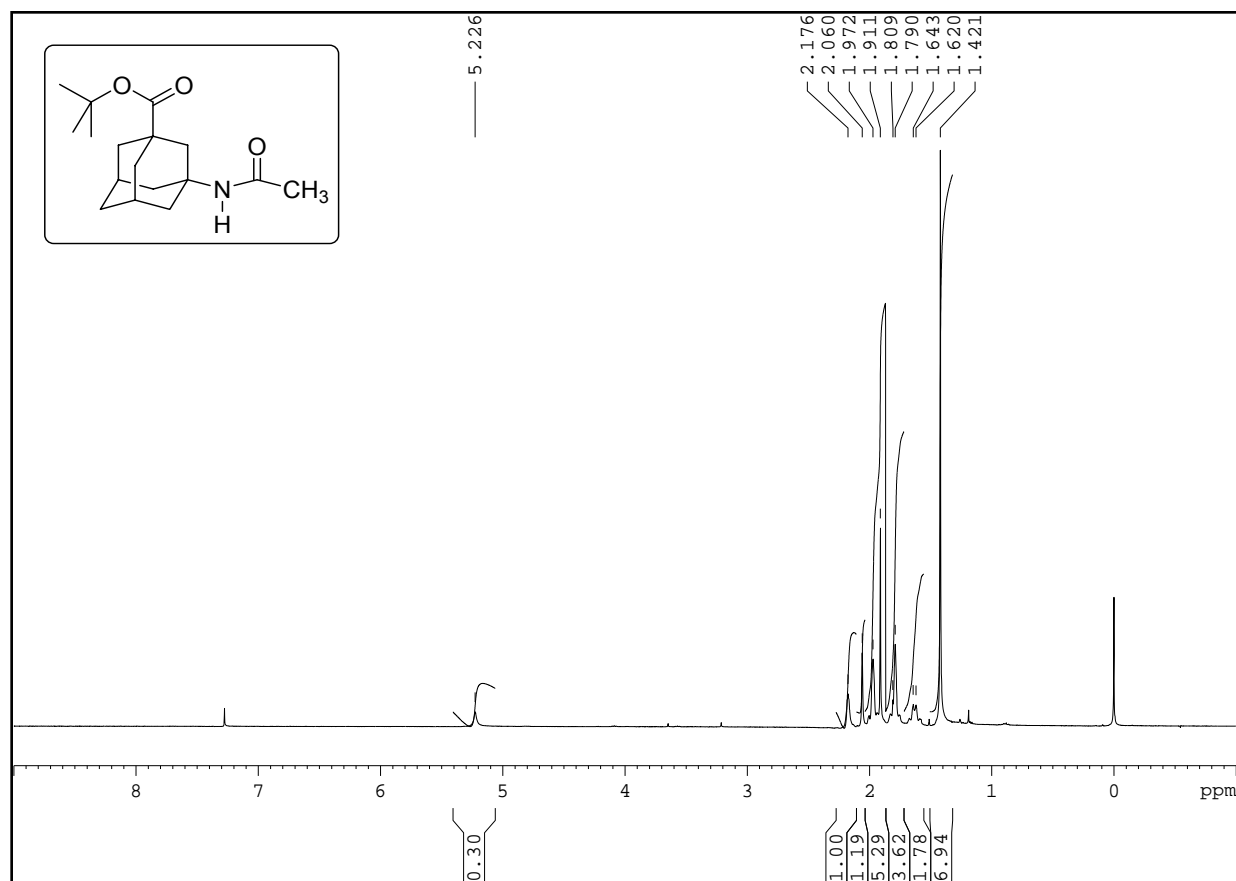
1-Bromo-3-acetamido-5,7-dimethyltricyclo[3.3.1.1^{3,7}]decane (169a)



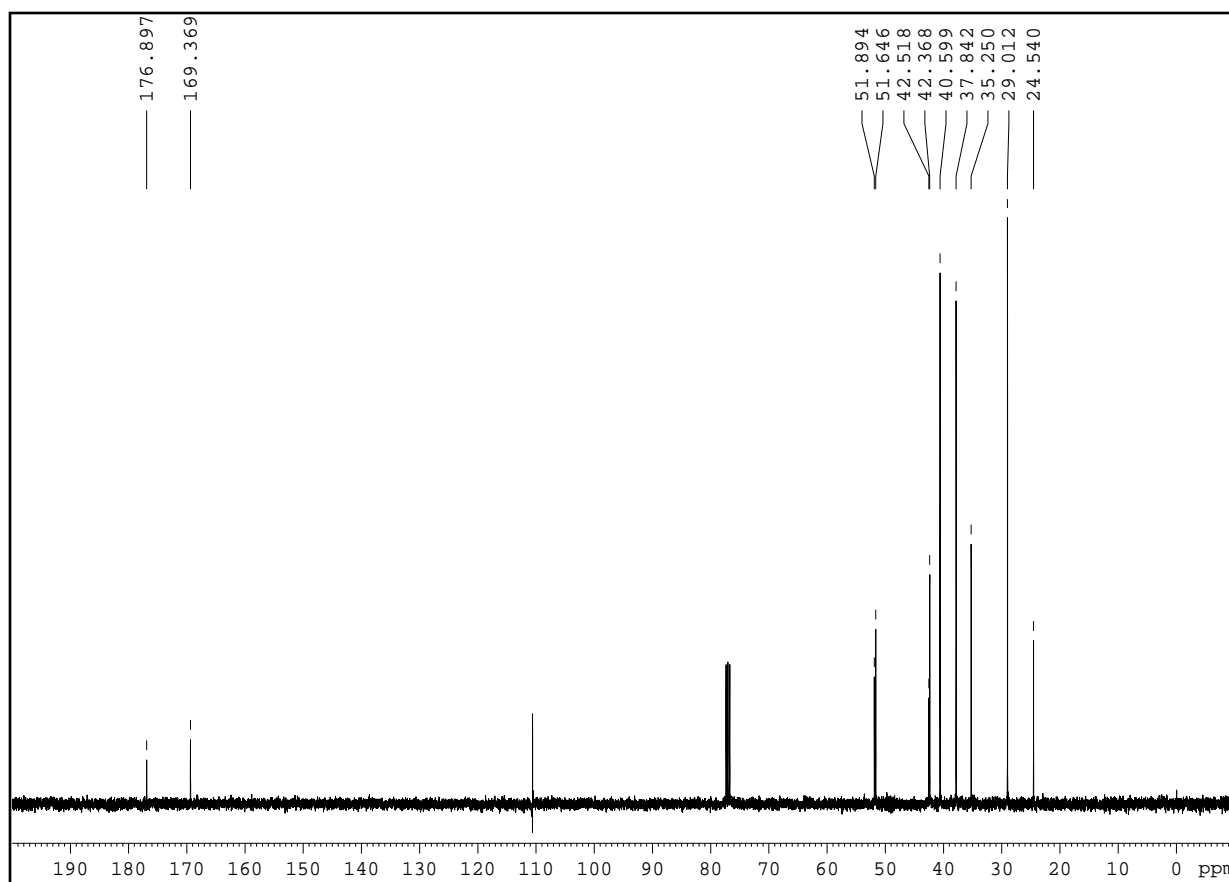
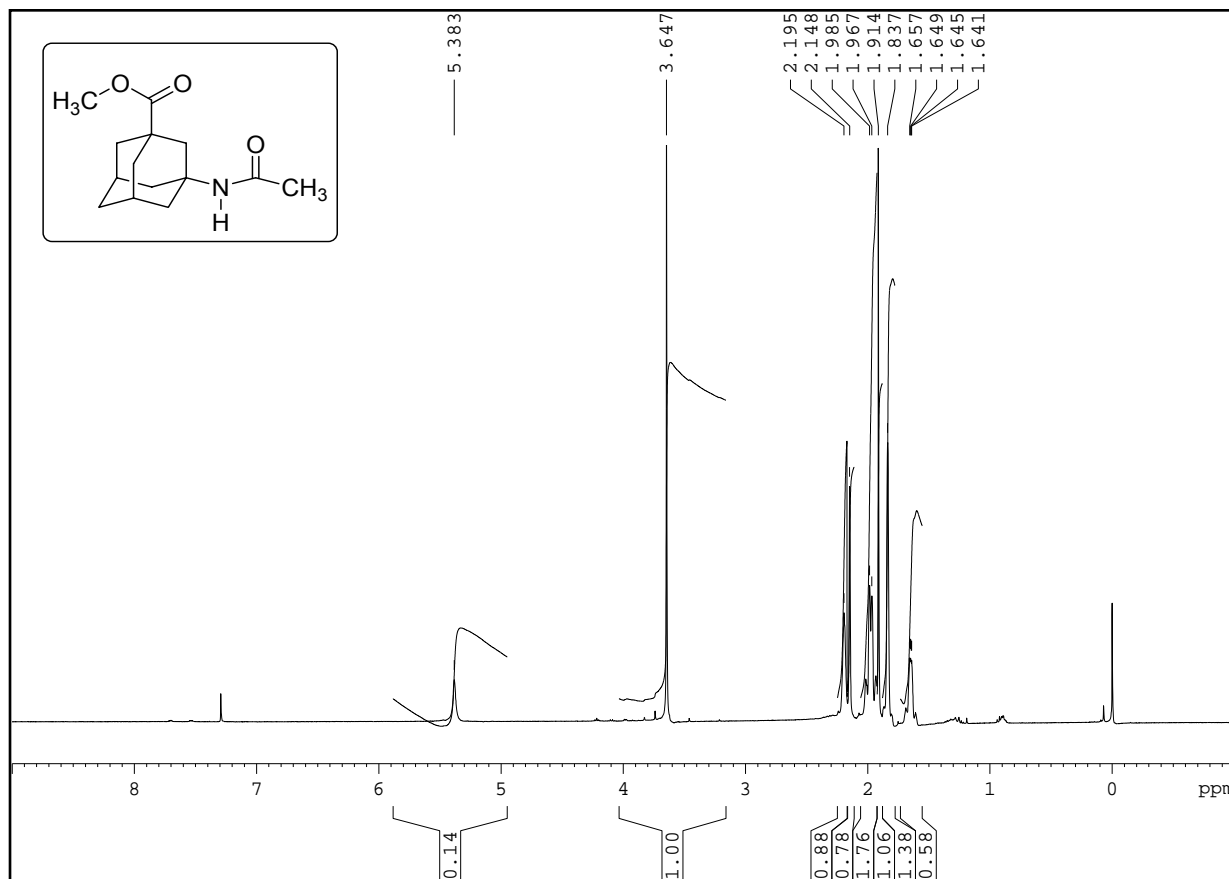
1-Bromo-3-acetamido-5-(1-methyl)ethyltricyclo[3.3.1.1^{3,7}]decane (**169b**)



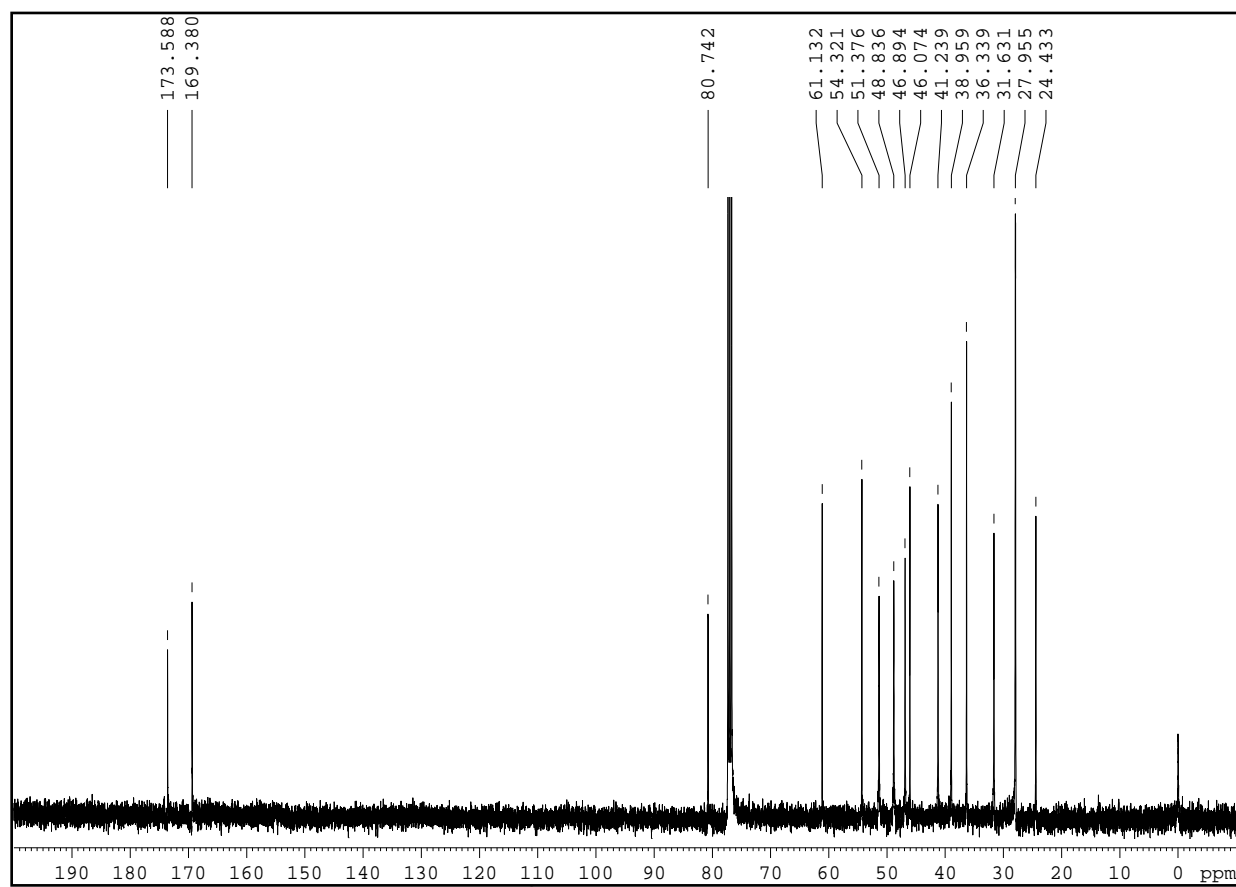
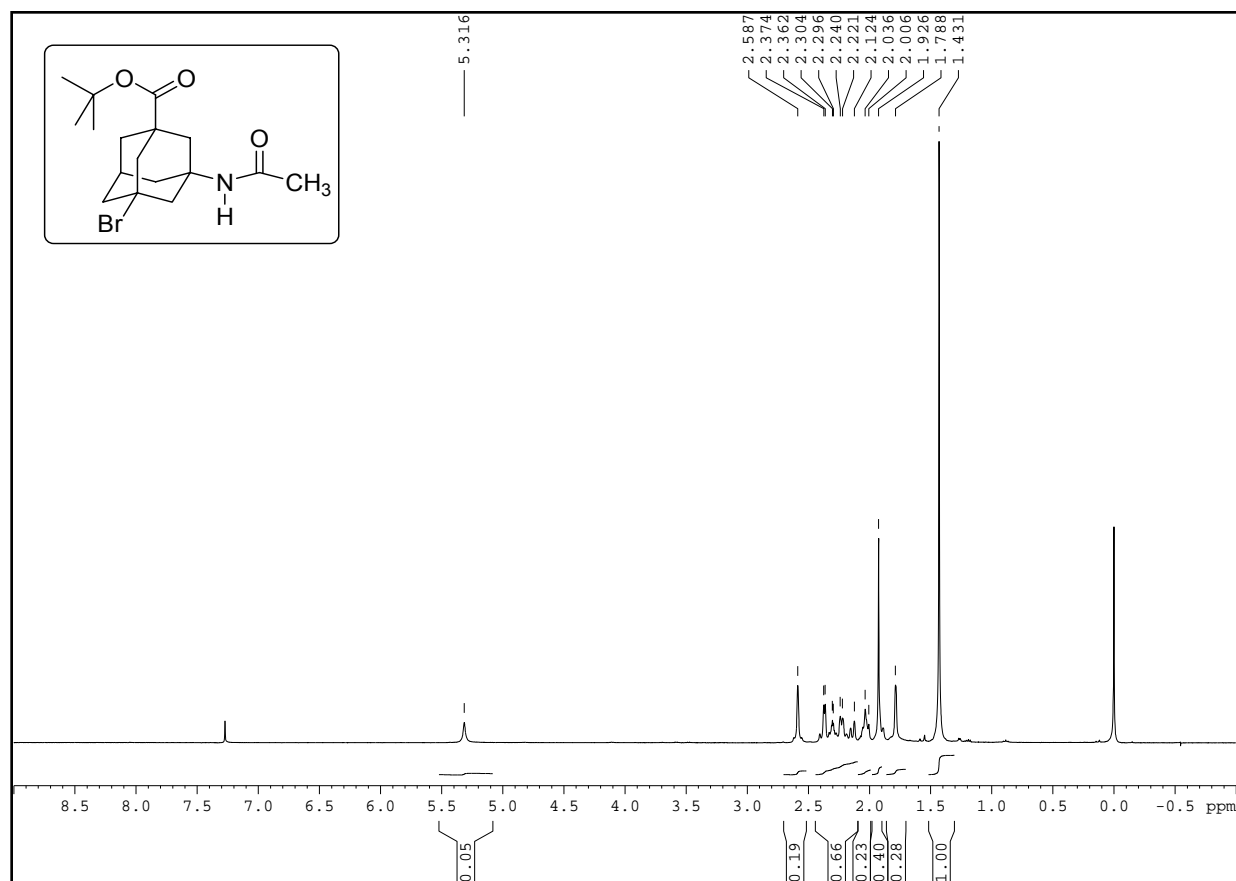
1-Bromo-5-phenyl-3-acetamidotricyclo[3.3.1.1^{3,7}]decane (173)



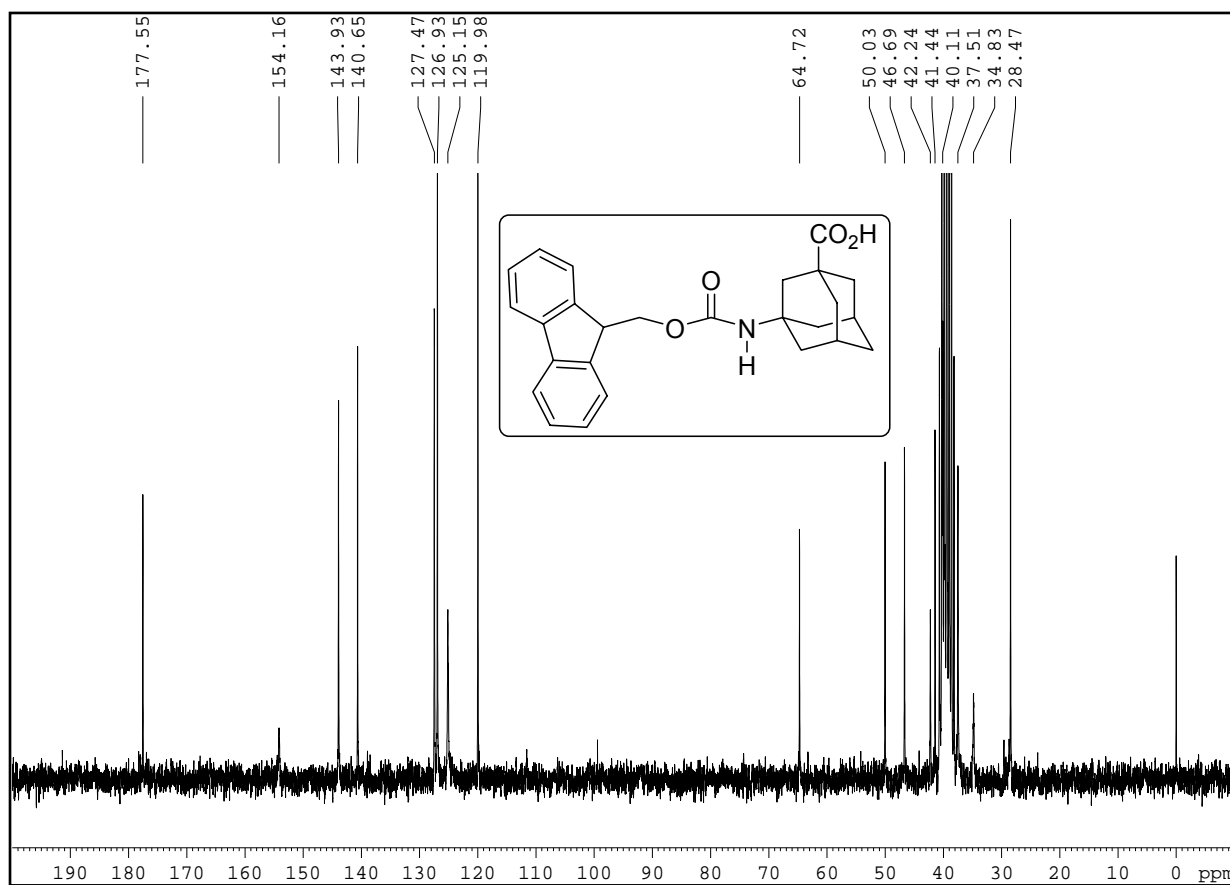
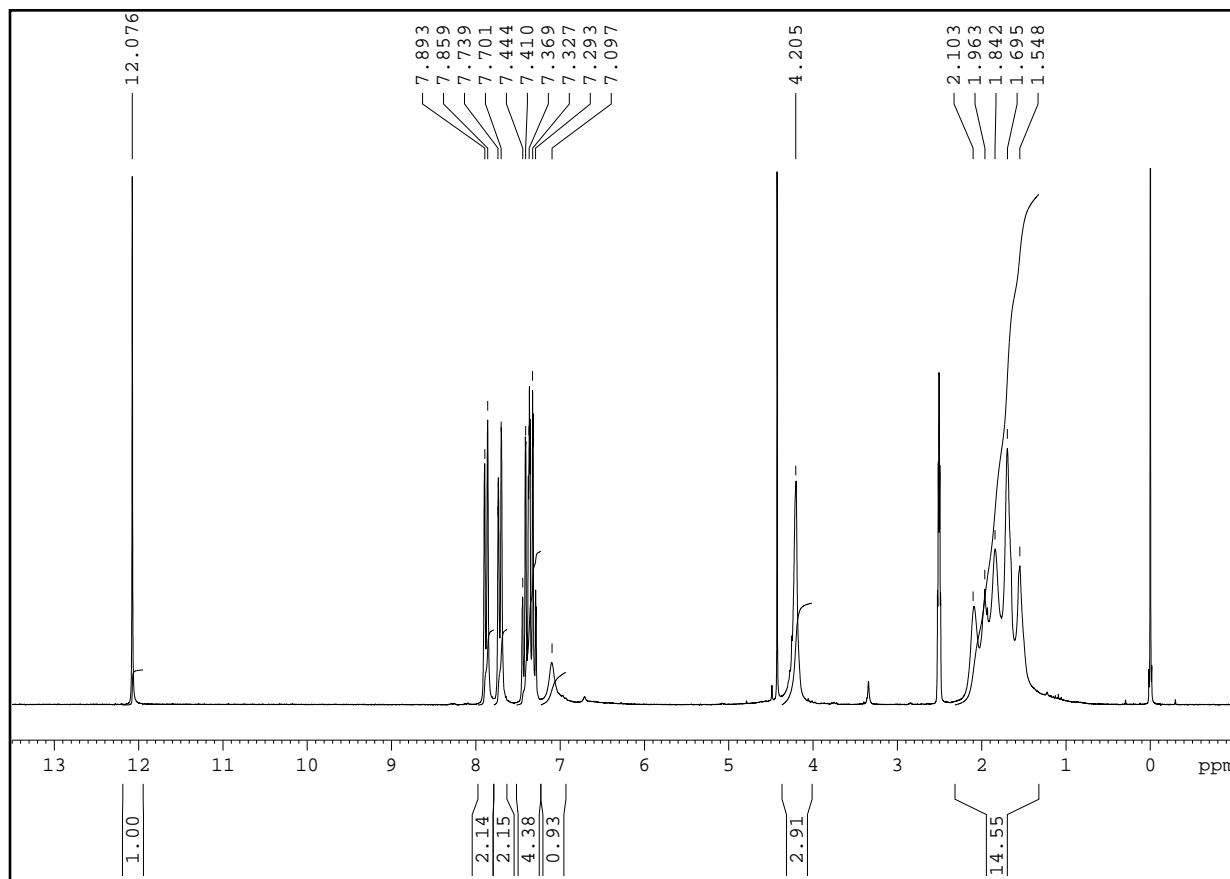
3-Acetamidotricyclo[3.3.1.1^{3,7}]decane-1-carboxylic acid *tert.* butyl ester (175a)



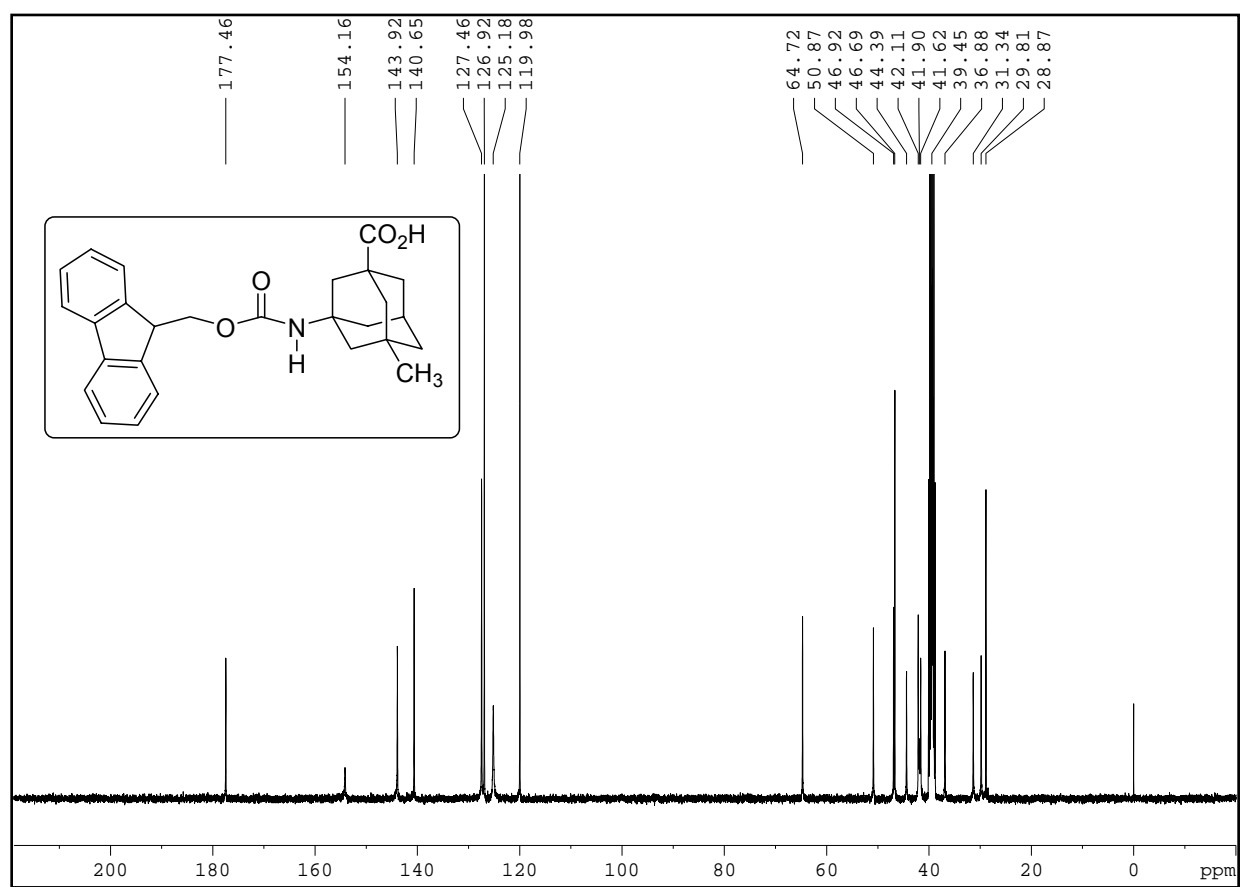
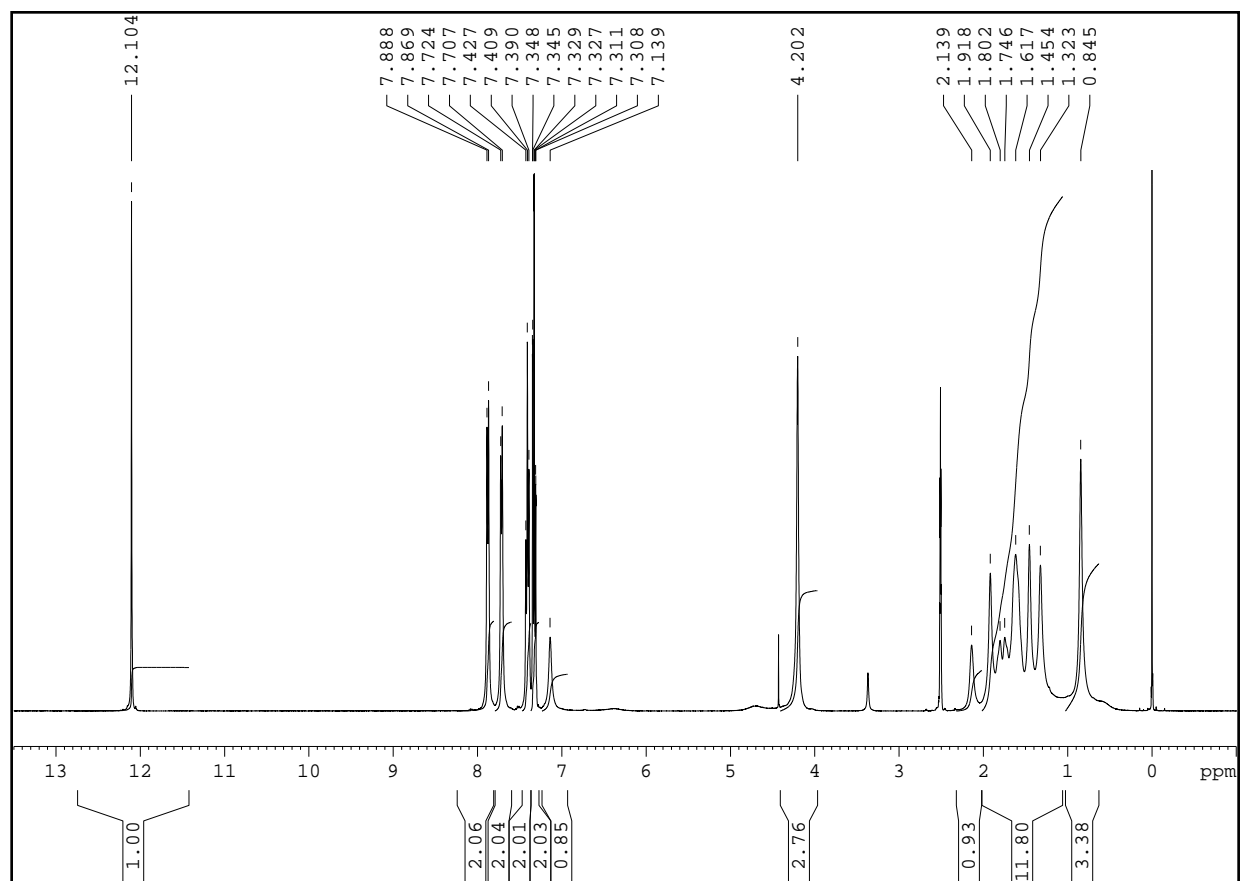
3-Acetamidotricyclo[3.3.1.1^{3,7}]decane-1-carboxylic acid methyl ester (175b)



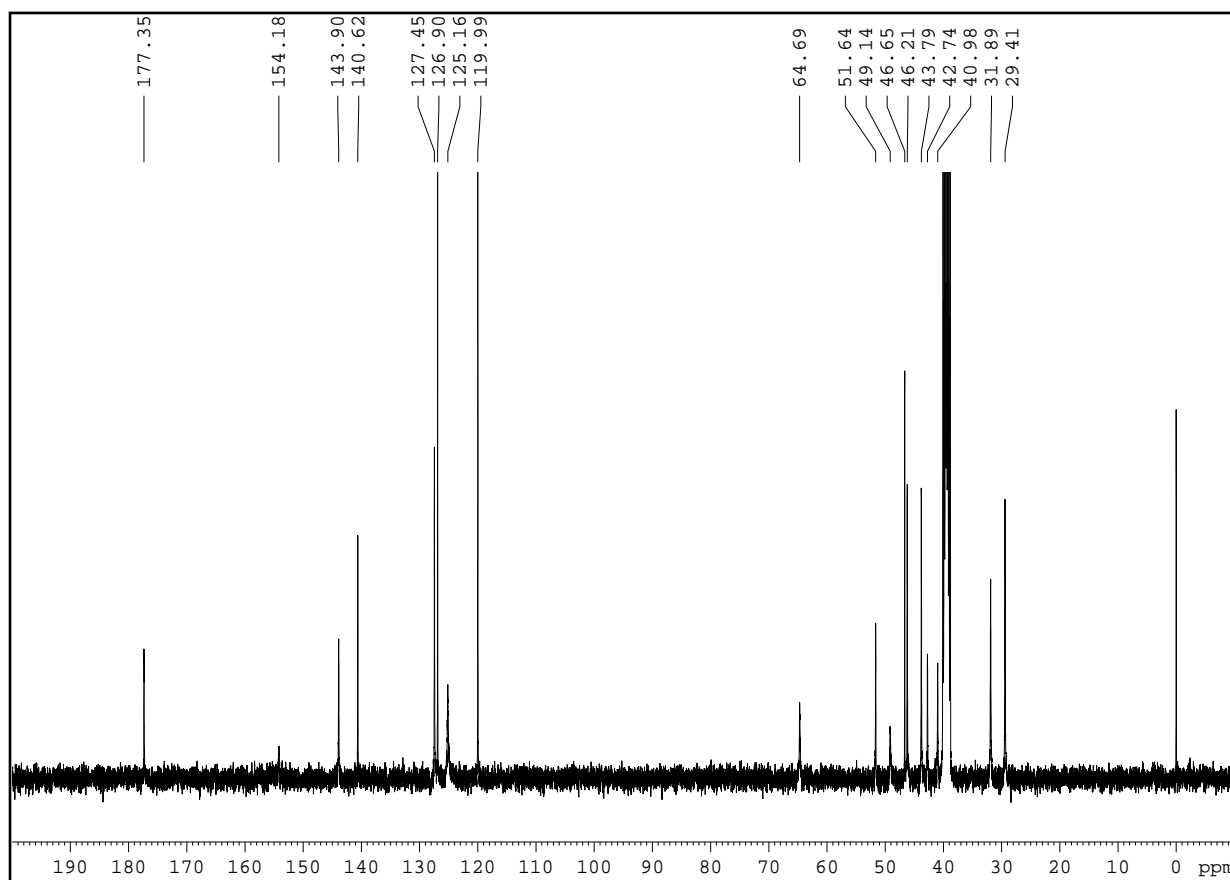
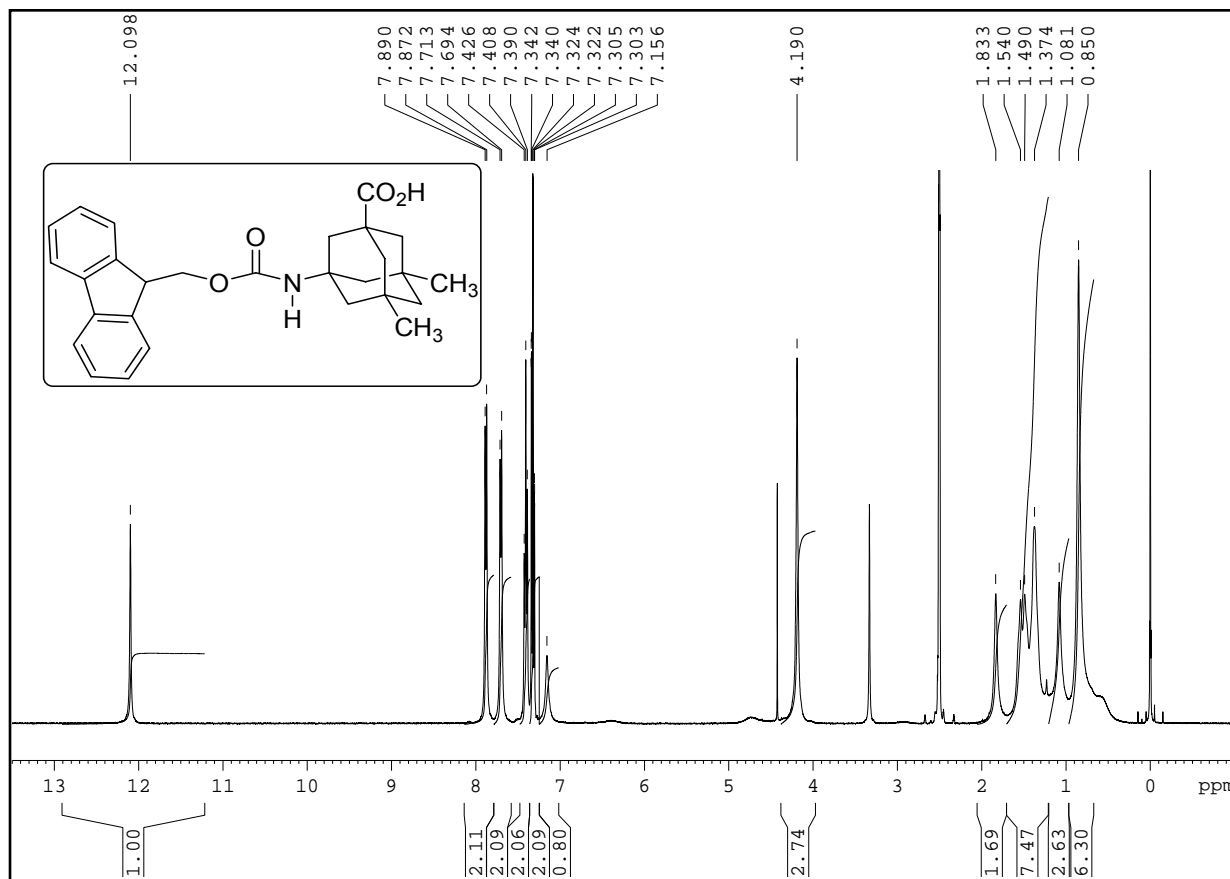
3-Bromo-5-acetamidotricyclo[3.3.1.1^{3,7}]decane-1-carboxylic acid *tert.* butylester (176)



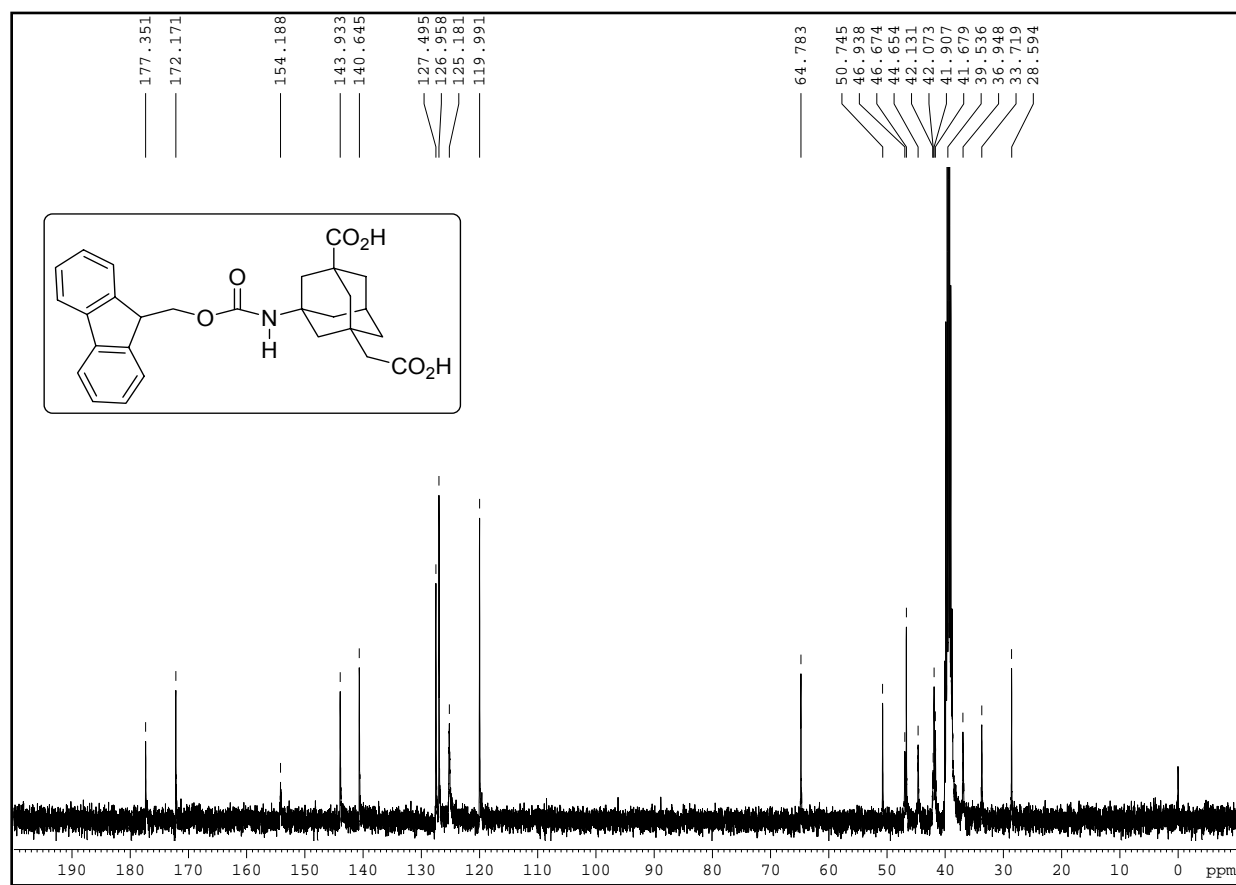
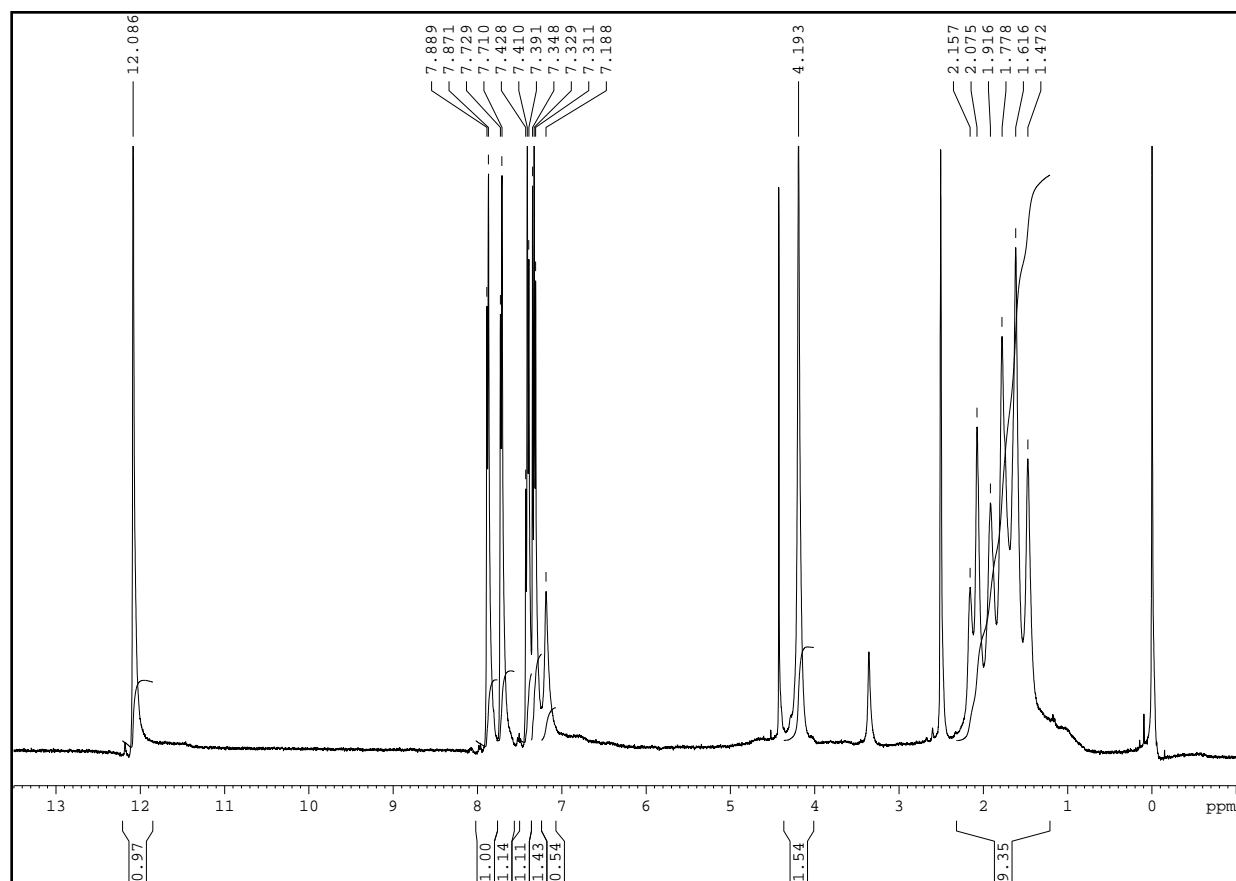
3-(9-Fluorenyl)methoxycarbonylamino-tricyclo[3.3.1.1^{3,7}]decane-1-carboxylic acid (**180a**)

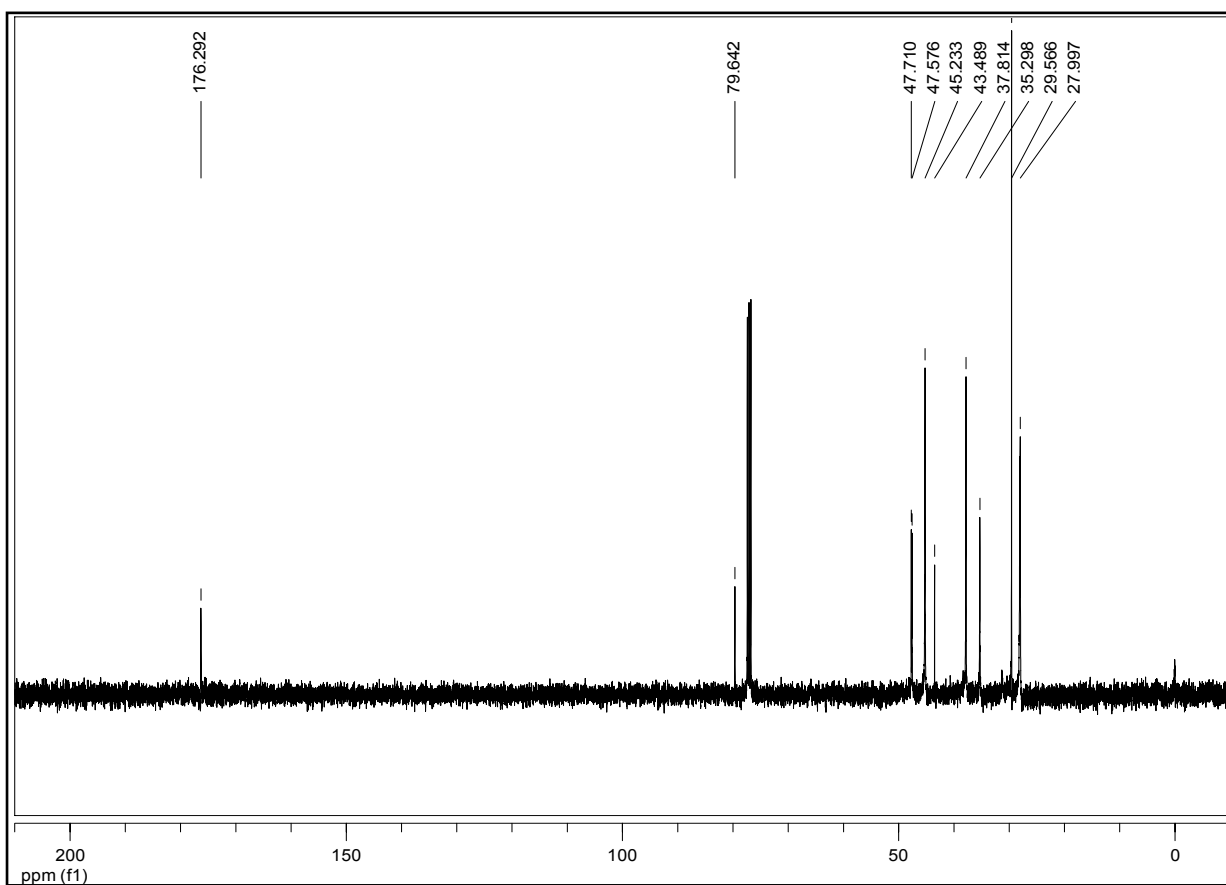
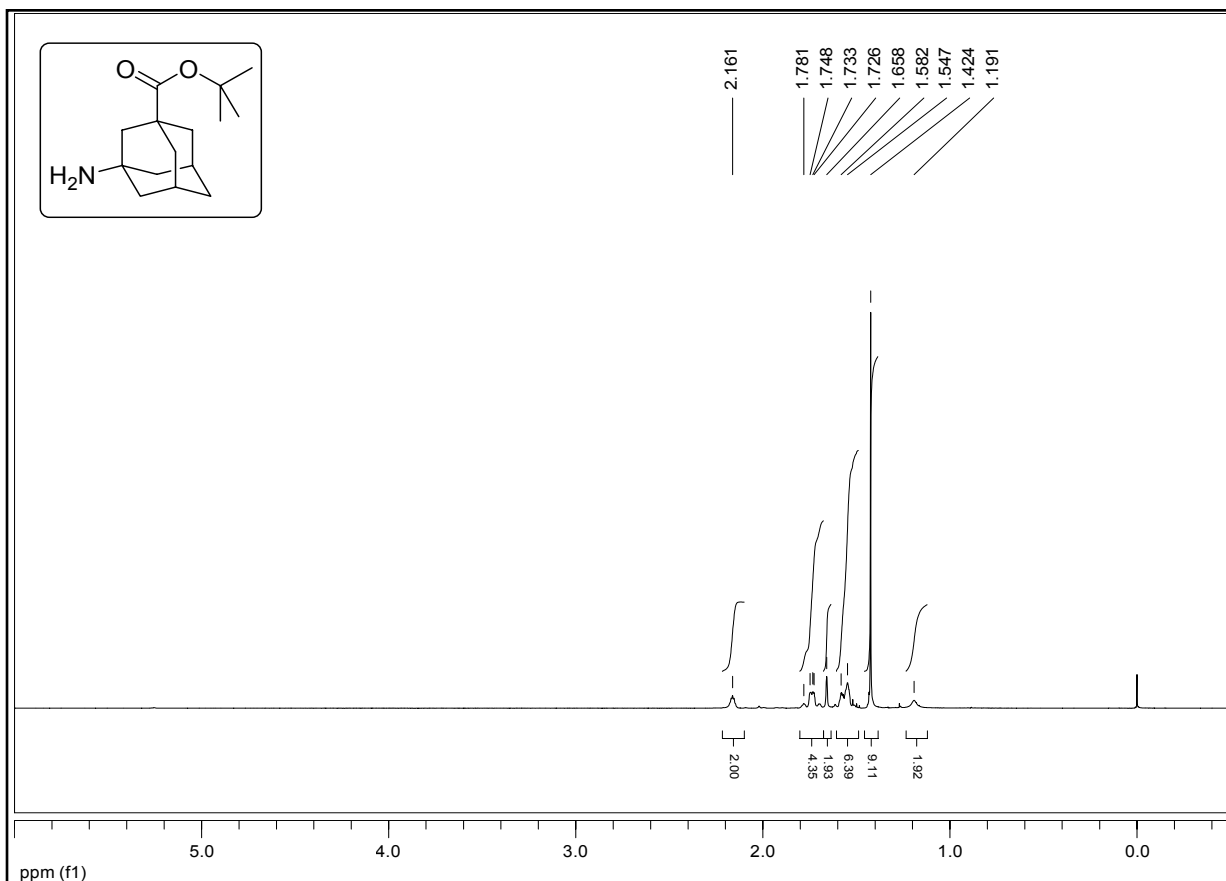


Fmoc-Ala-OH (180b)

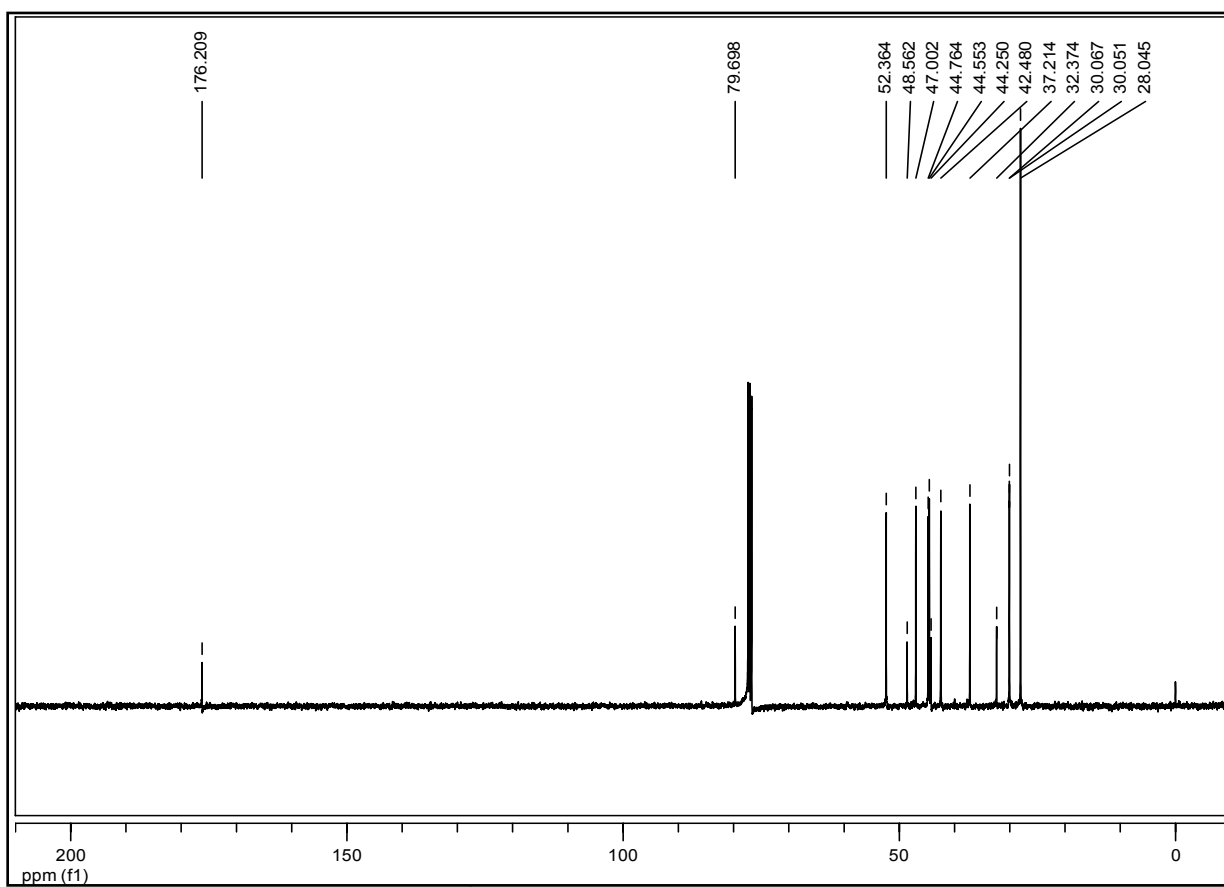
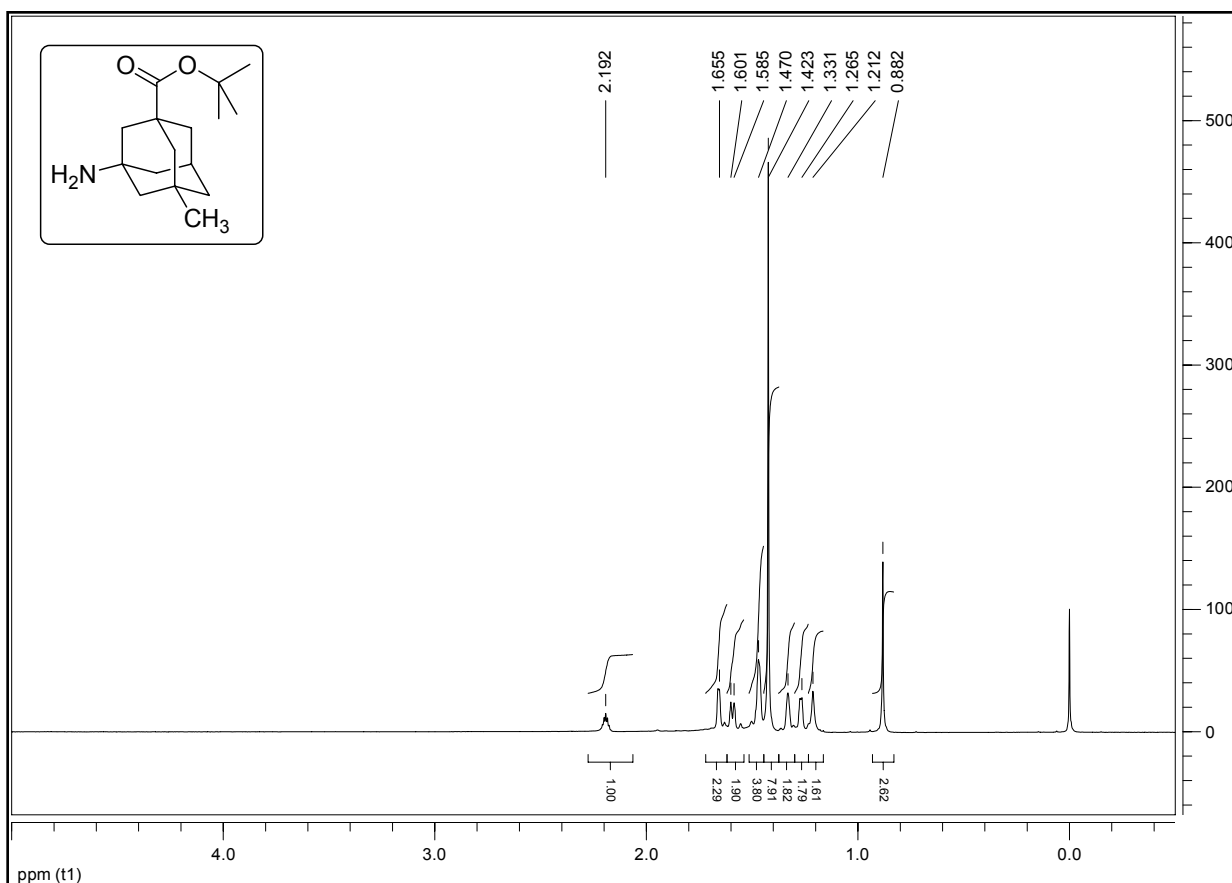


Fmoc-Aib-OH (180c)

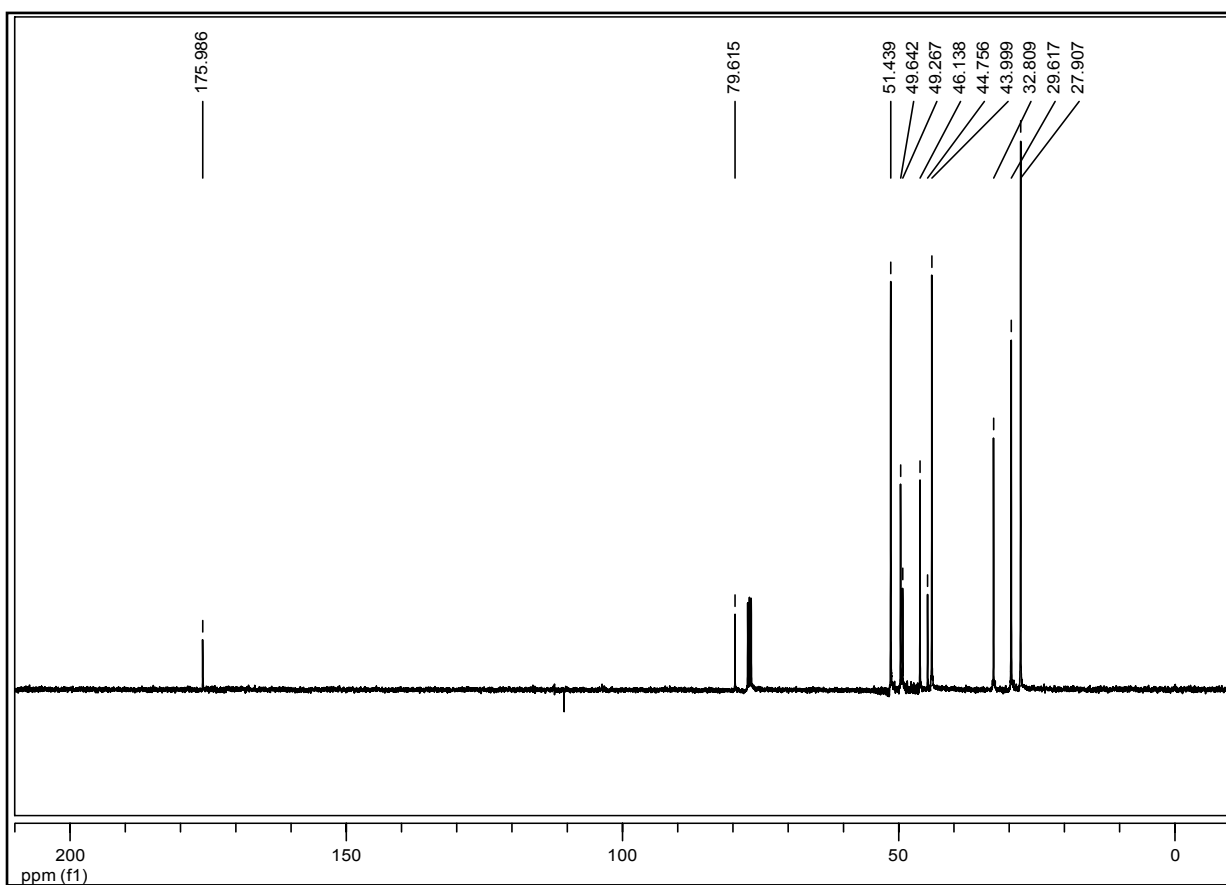
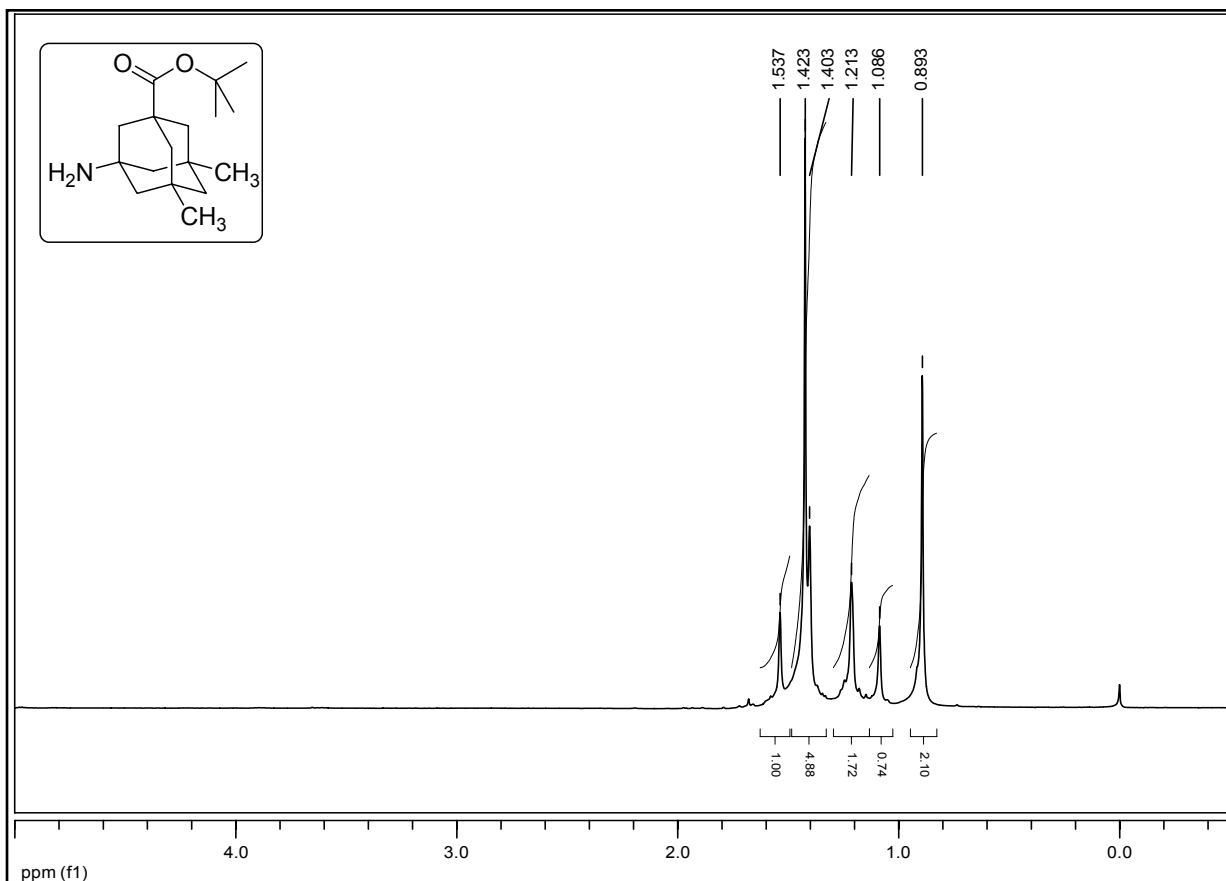
Fmoc-^AAsp-OH (180d)



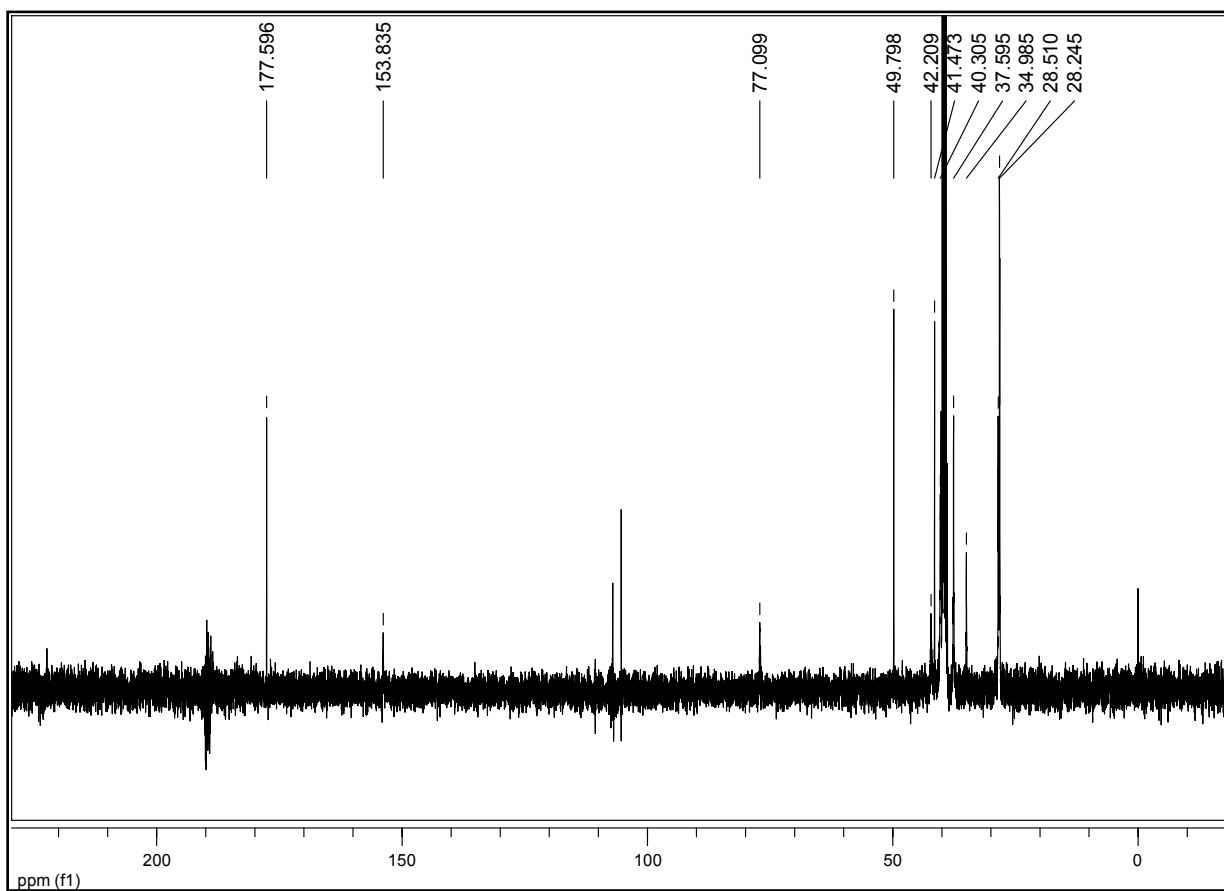
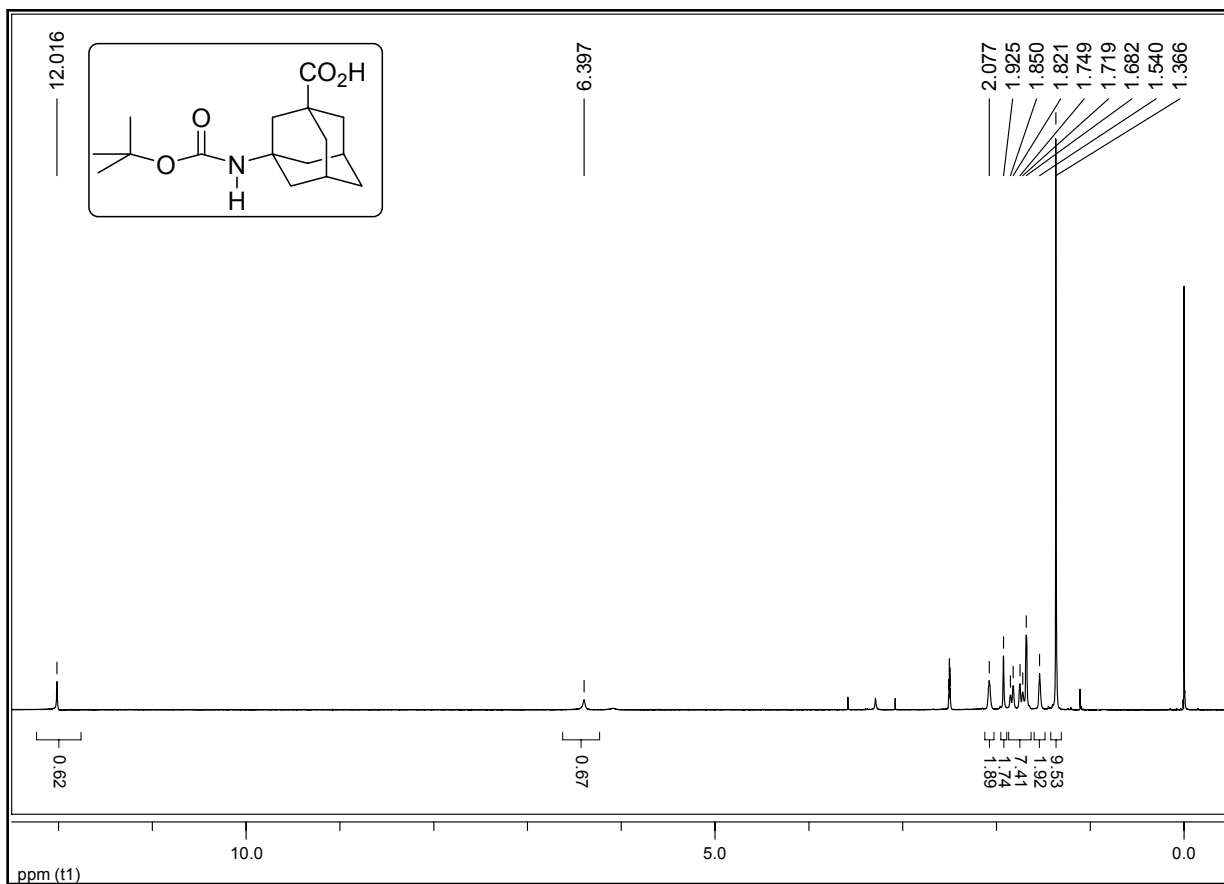
3-Aminotricyclo[3.3.1.1^{3,7}]decane-1-carboxylic acid *tert.* butyl ester (181a)



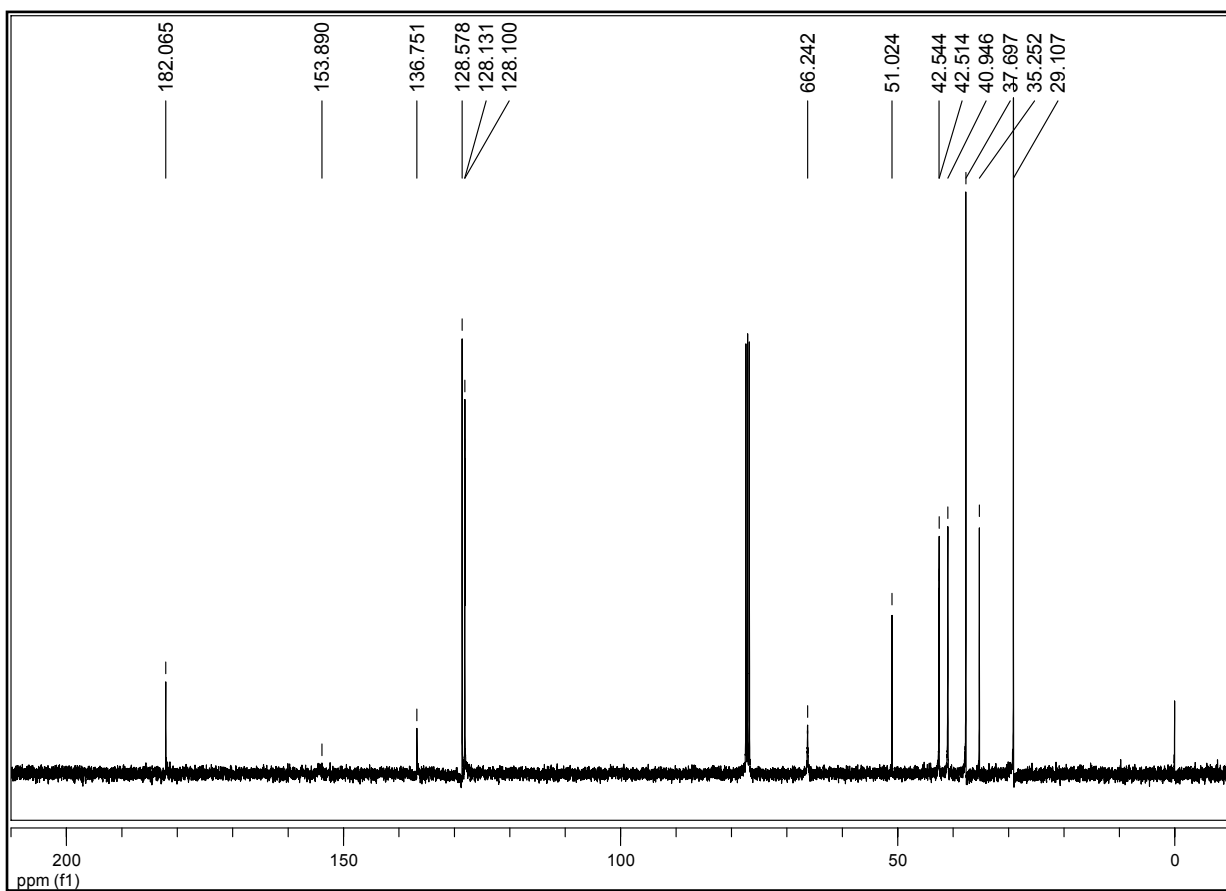
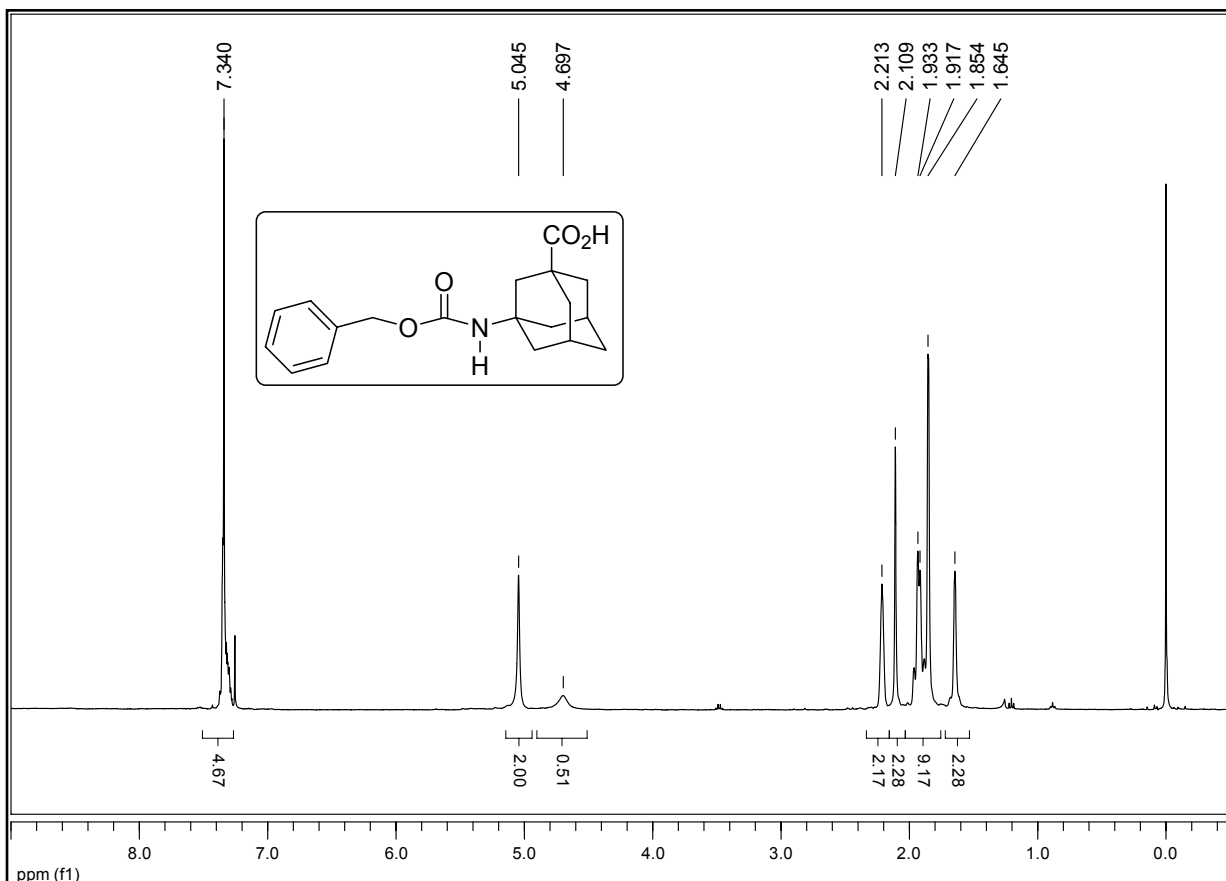
3-Amino-5-methyltricyclo[3.3.1.1^{3,7}]decane-1-carboxylic acid *tert.* butyl ester (**181b**)



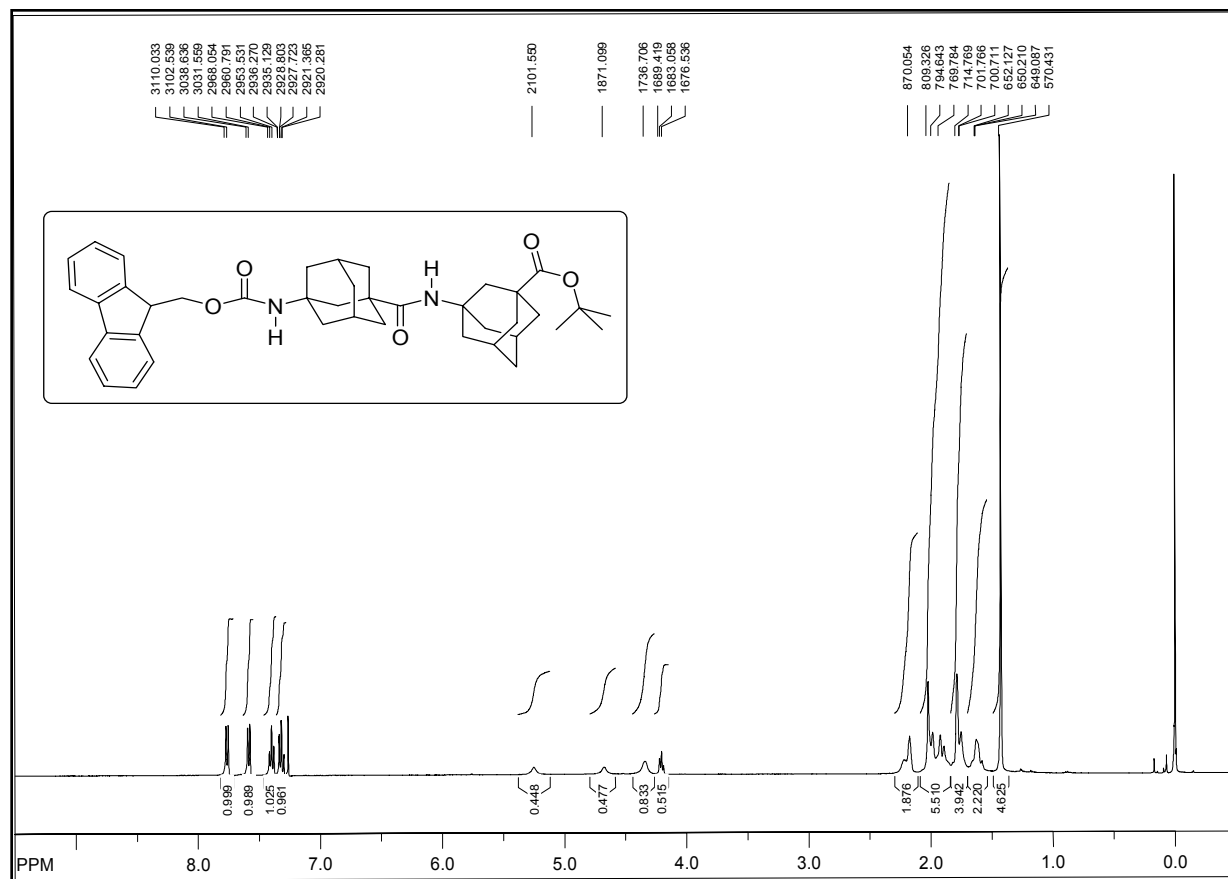
3-Amino-5,7-dimethyltricyclo[3.3.1.1^{3,7}]decane-1-carboxylic acid *tert.* butyl ester (**181c**)

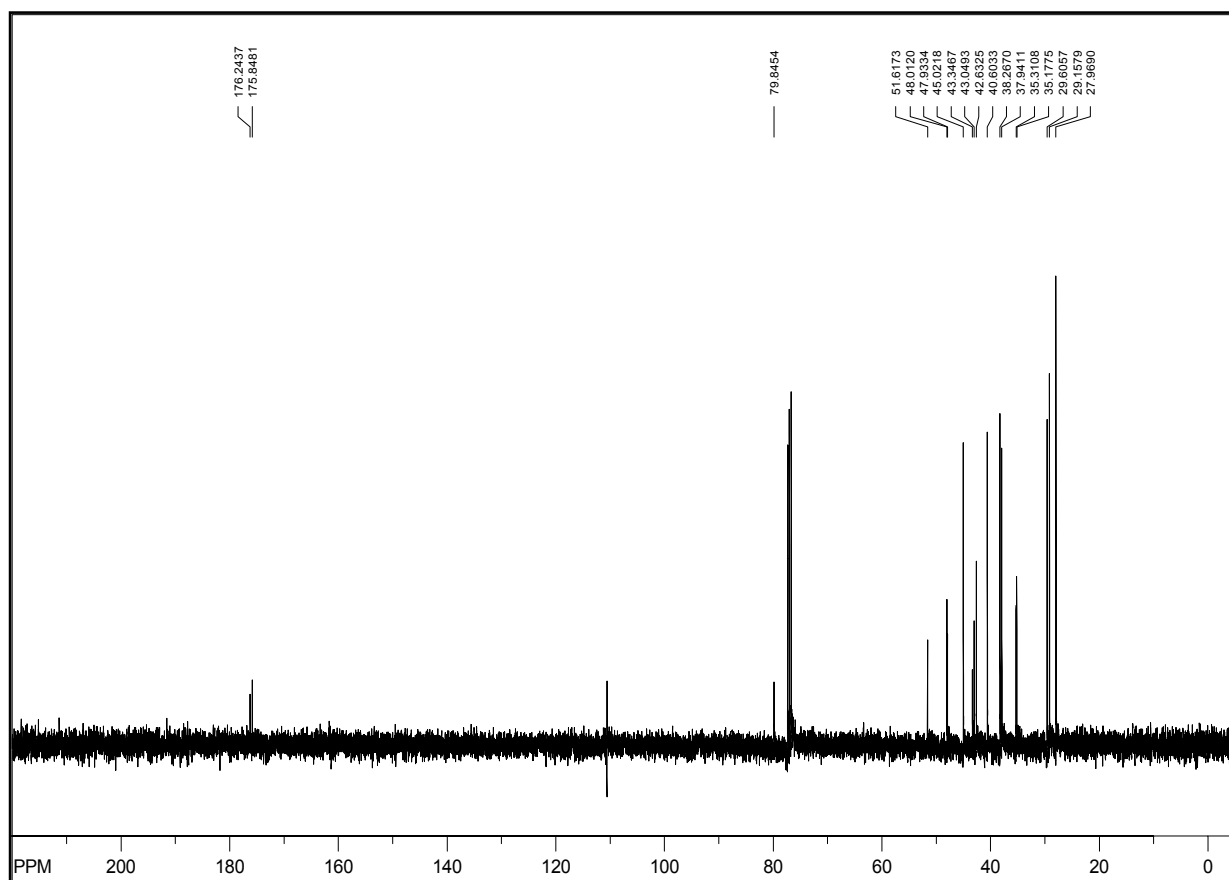
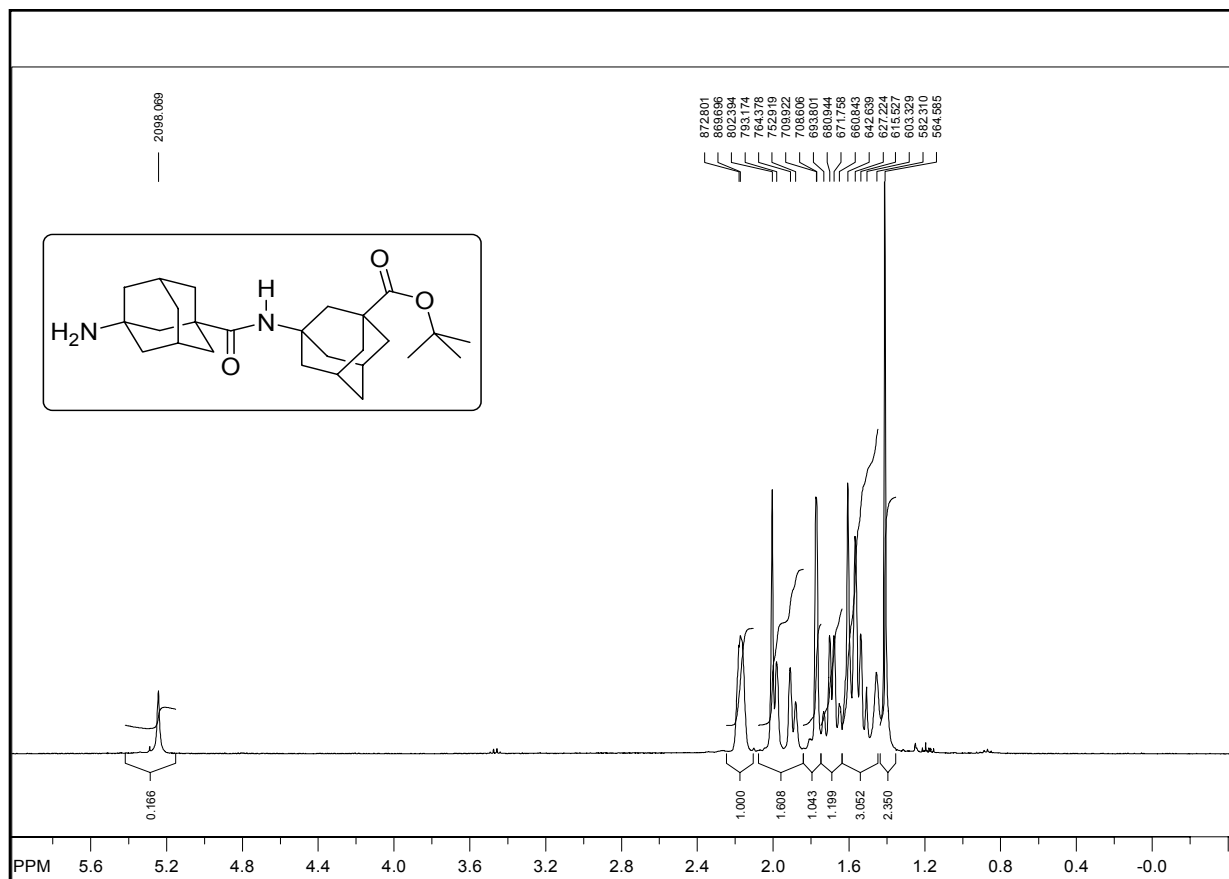


3-(*tert.* Butoxycarbonyl)aminotricyclo[3.3.1.1^{3,7}]decane-1-carboxylic acid (**182**)

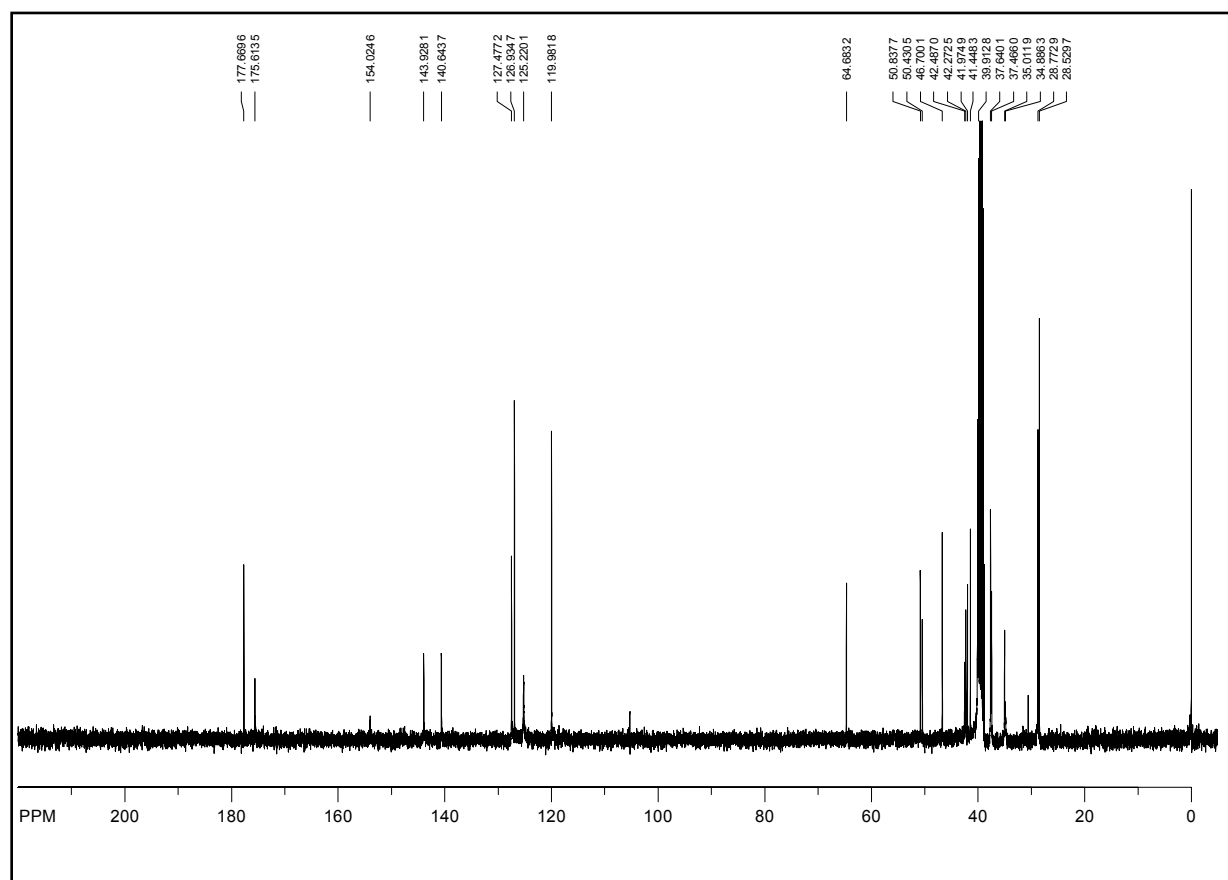
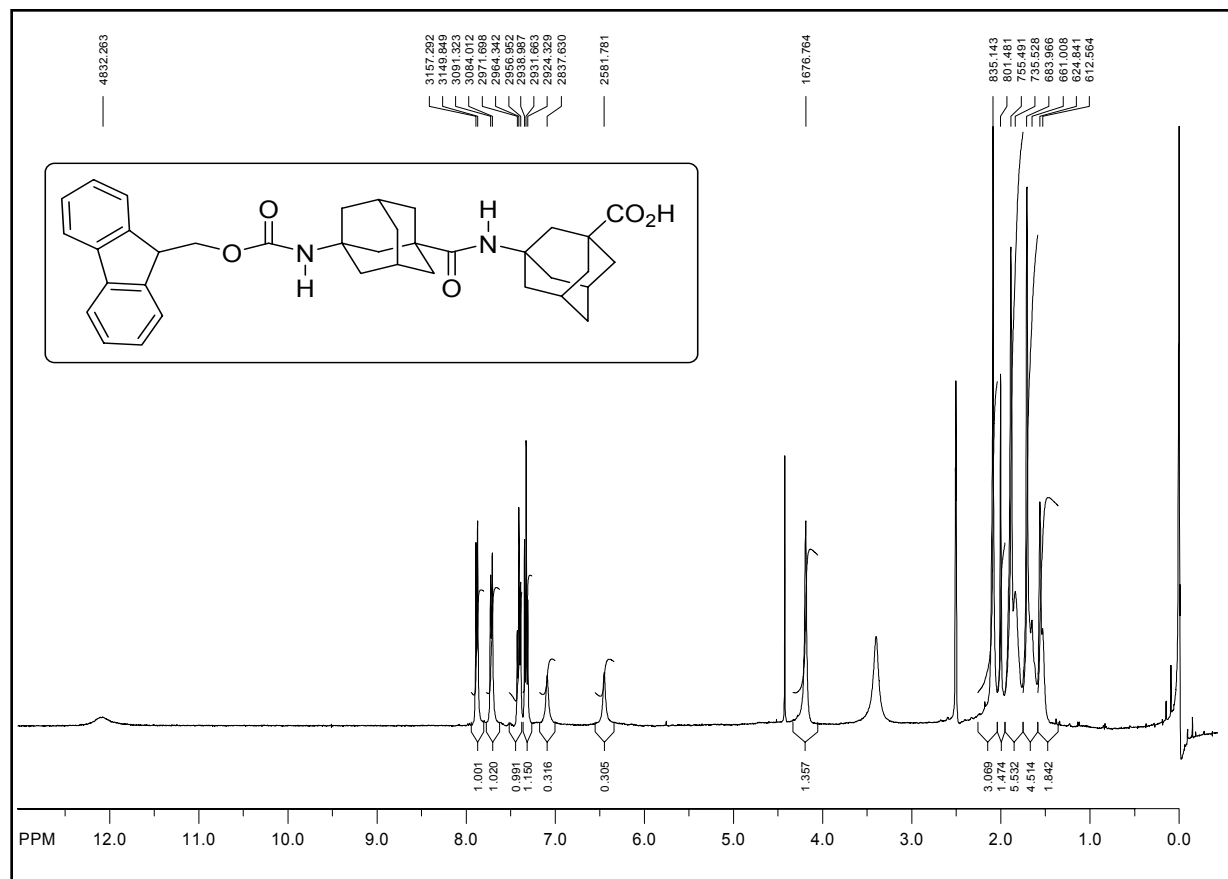


3-(Benzyloxycarbonyl)aminotricyclo[3.3.1.1^{3,7}]decane-1-carboxylic acid (**183**)

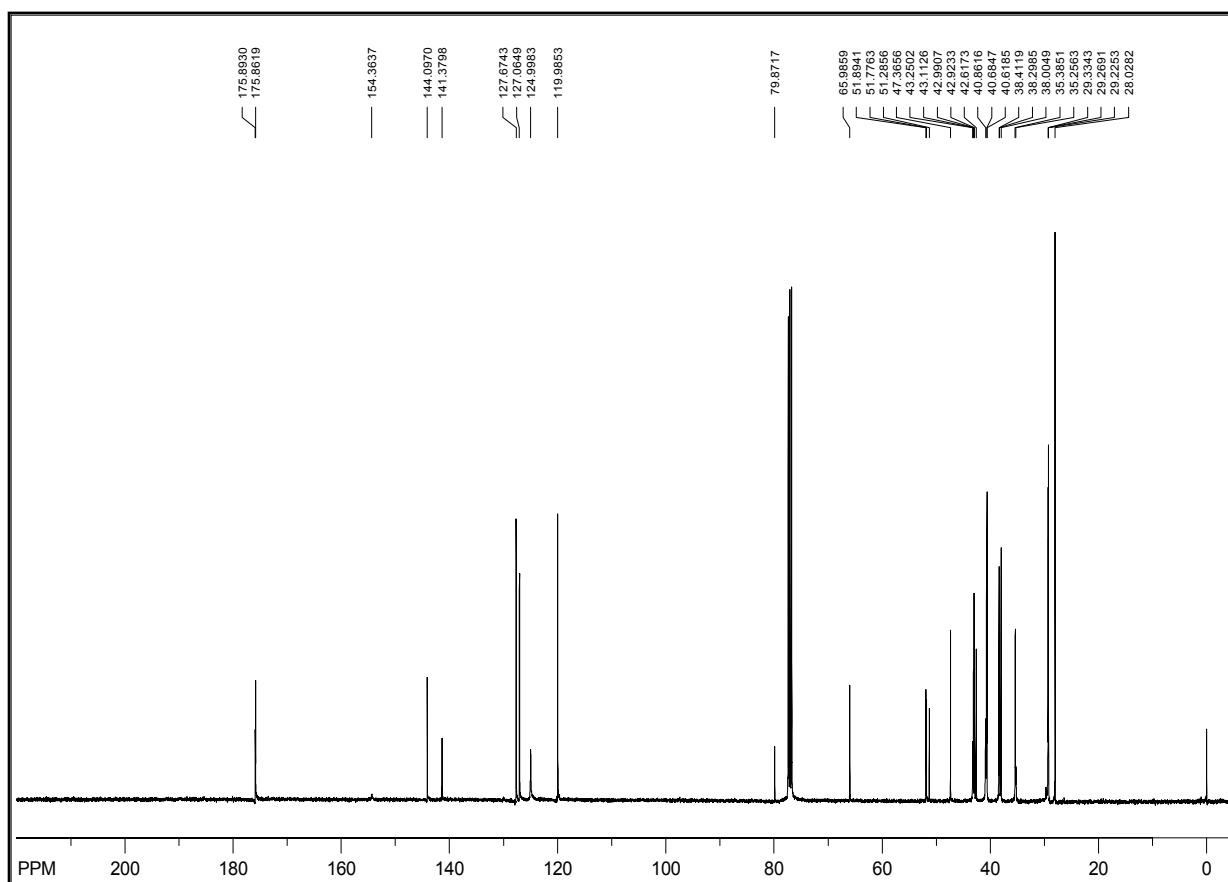
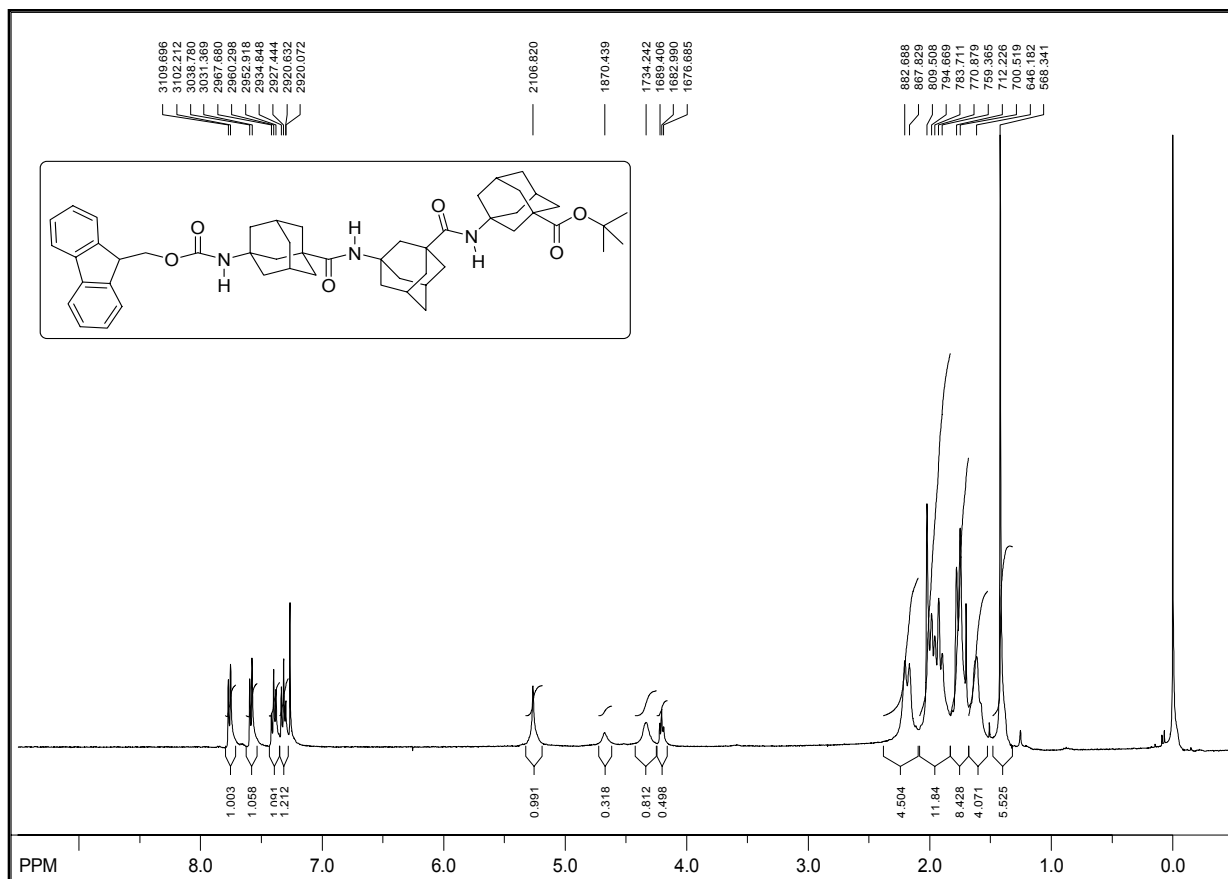




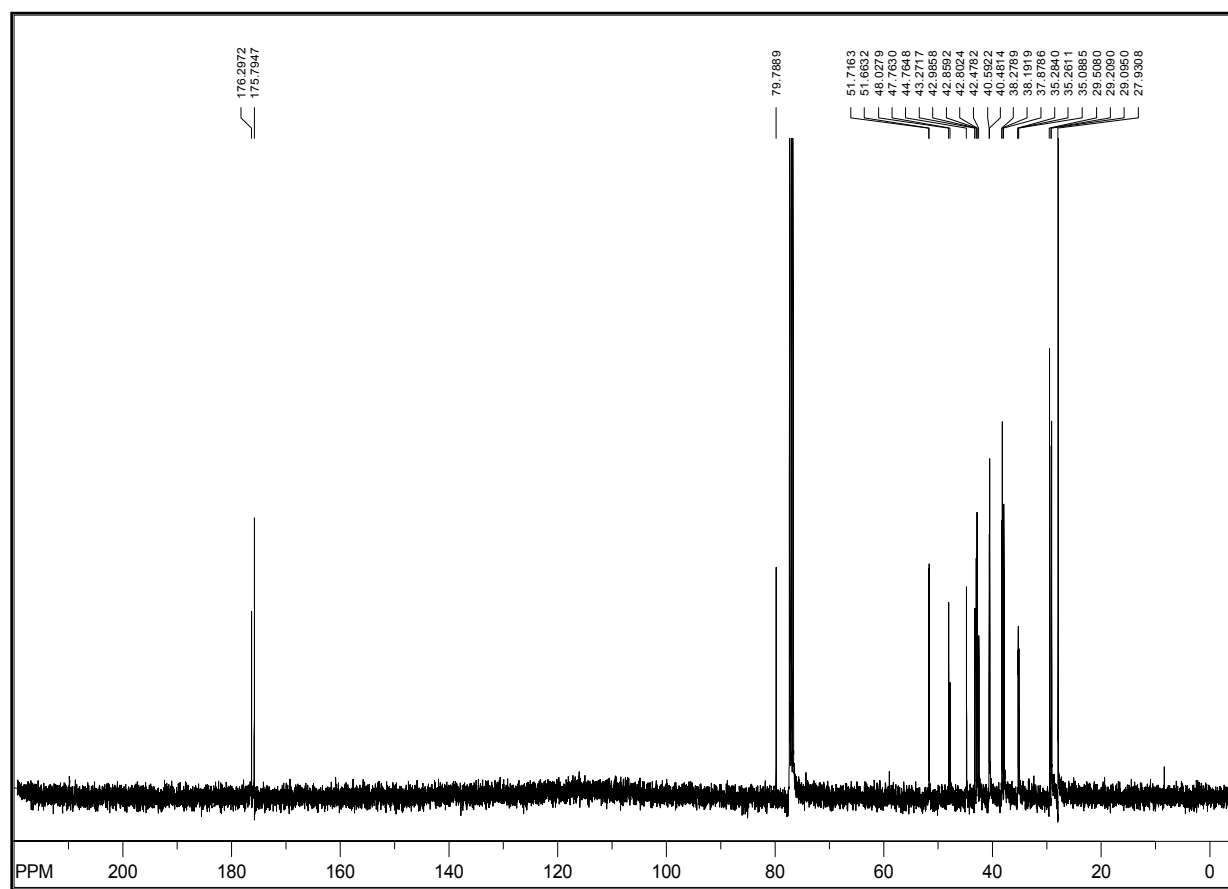
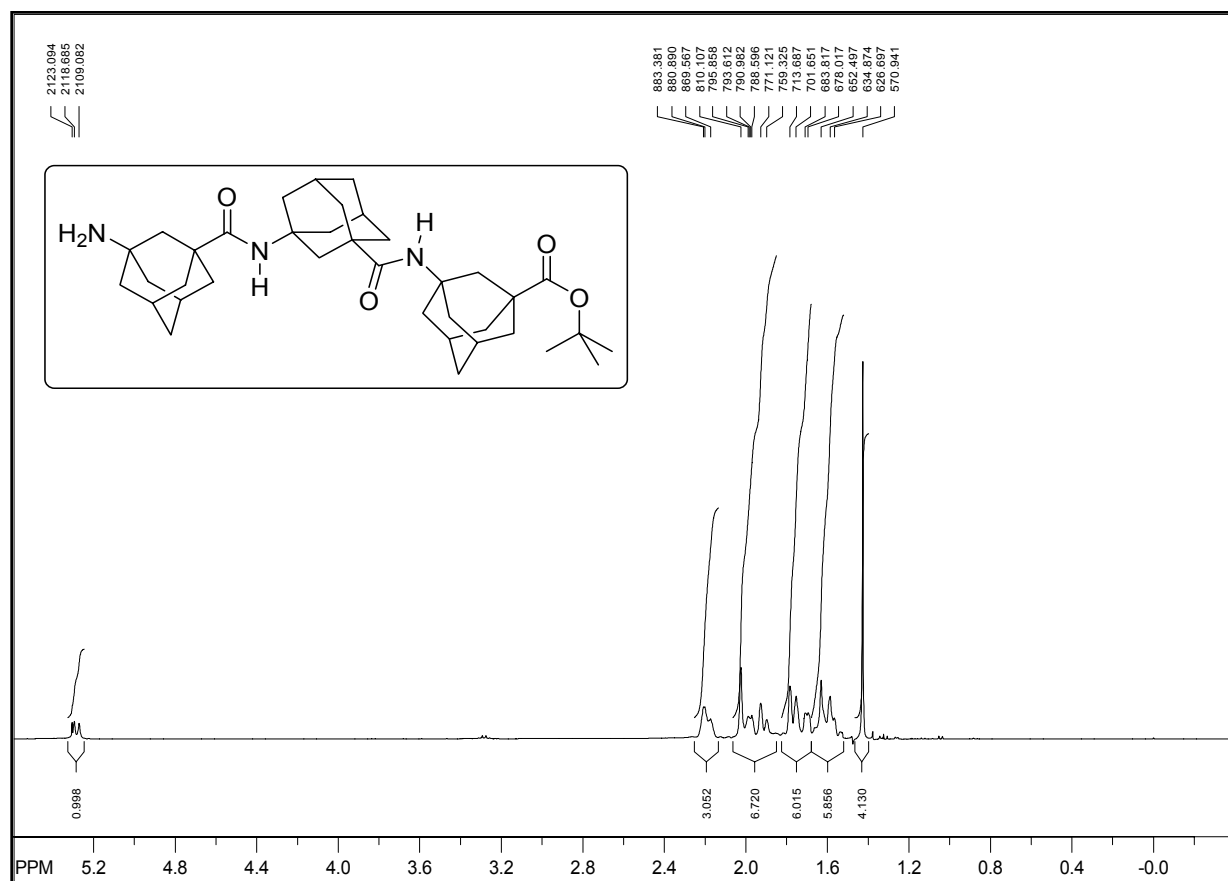
H-^AGly-A-^AGly-O^tBu (185)



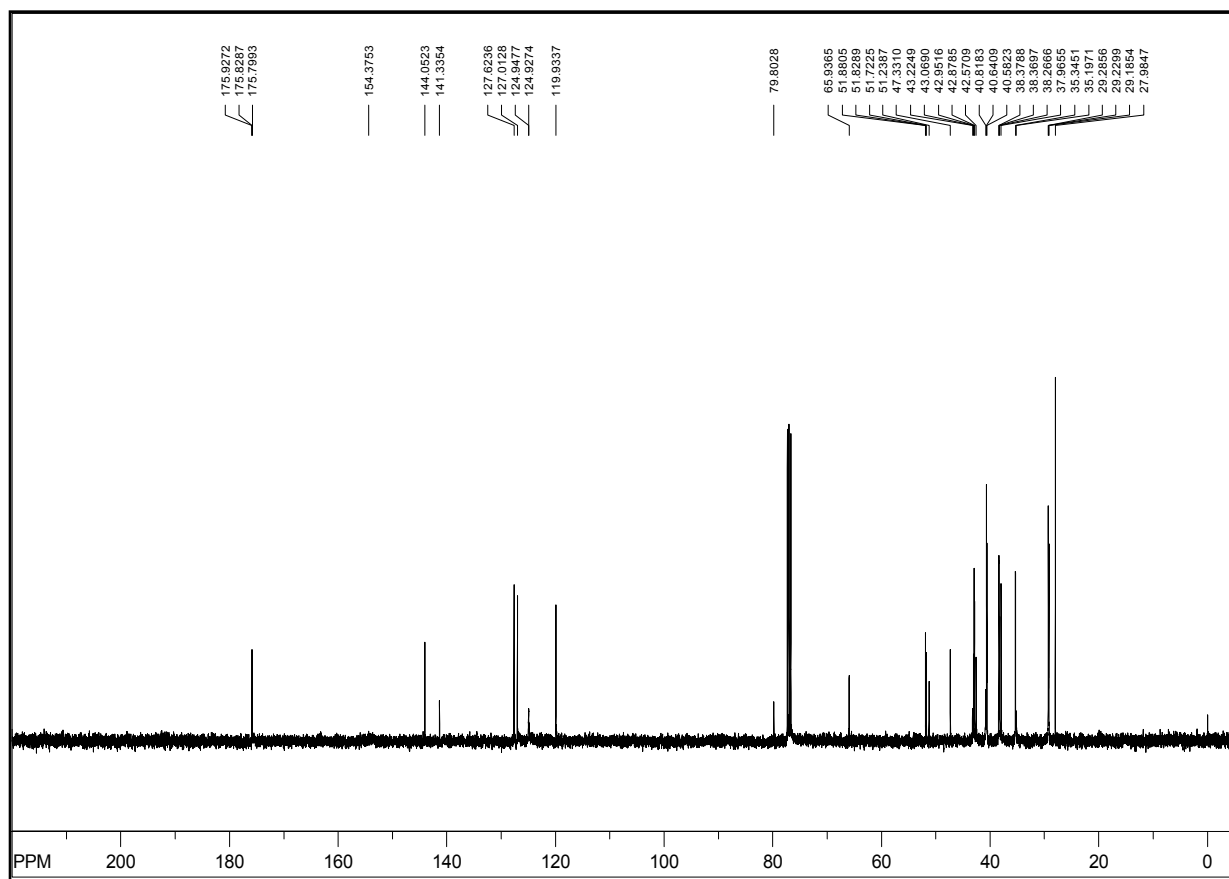
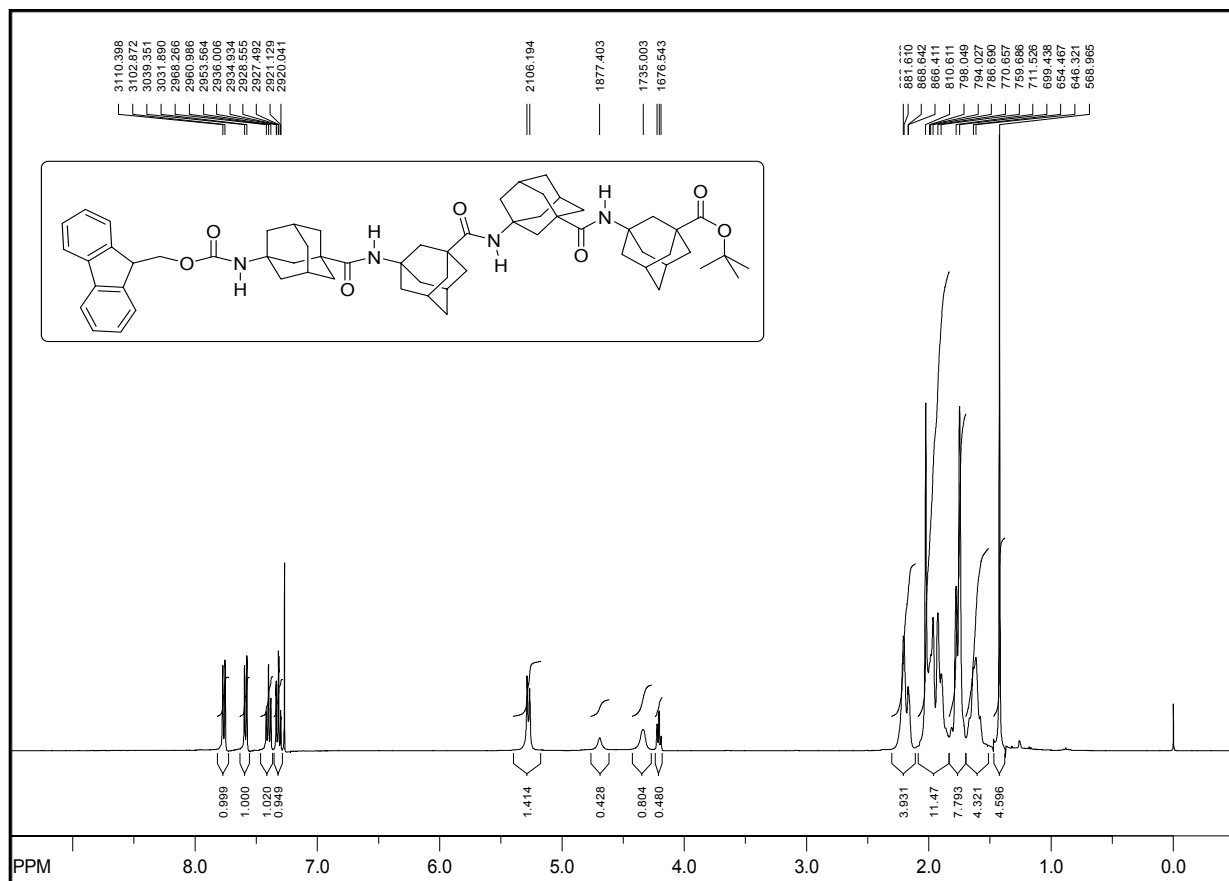
Fmoc-Gly-Gly-OH (186)



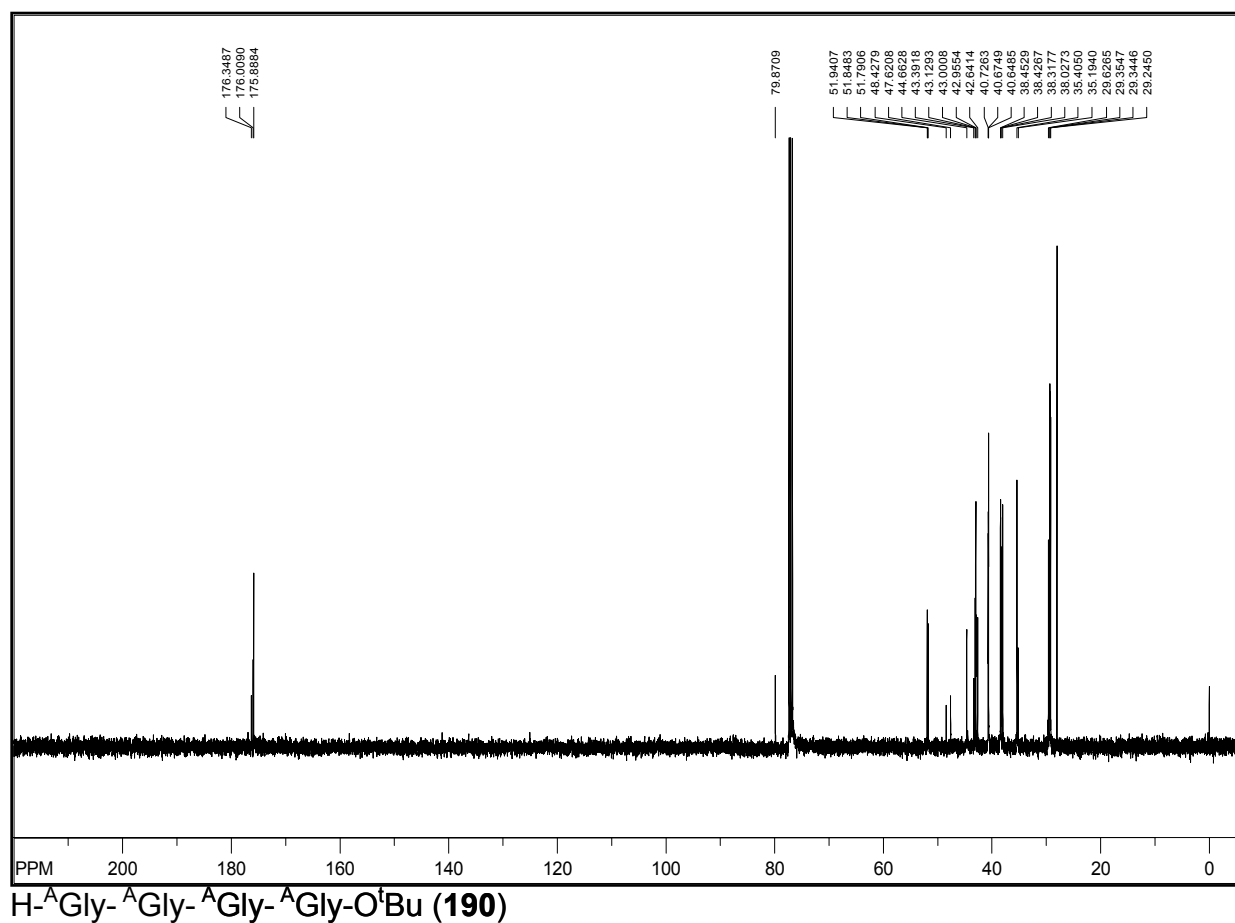
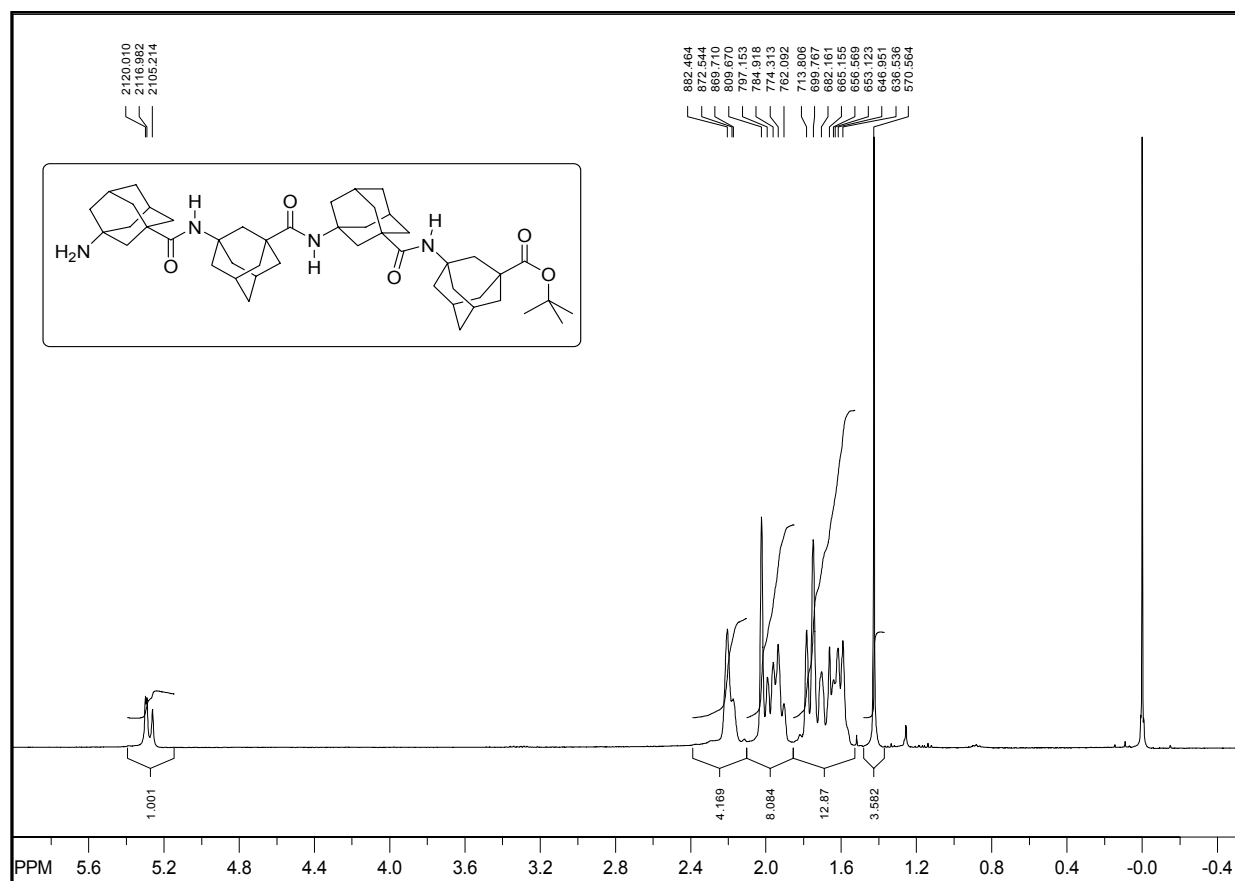
Fmoc-^AGly-^AGly-^AGly-O^tBu (187)



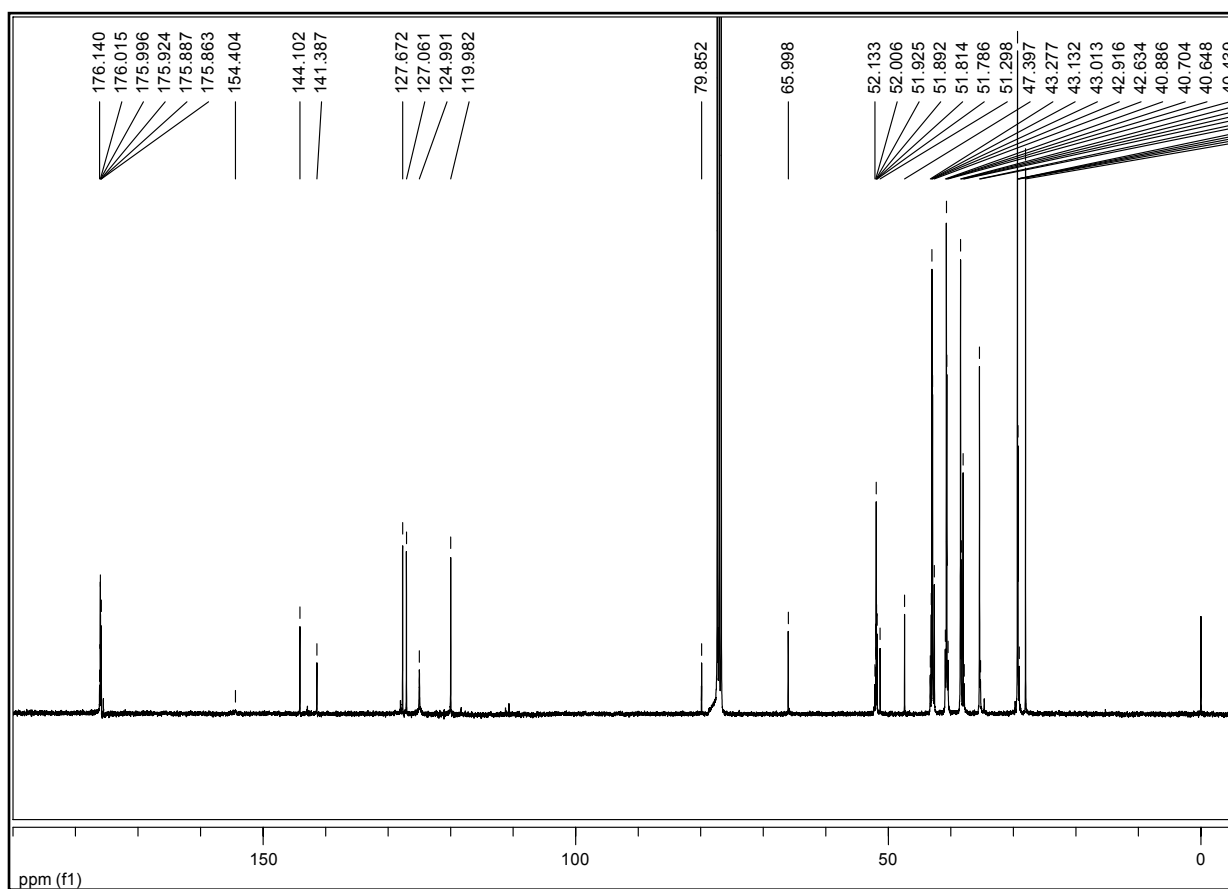
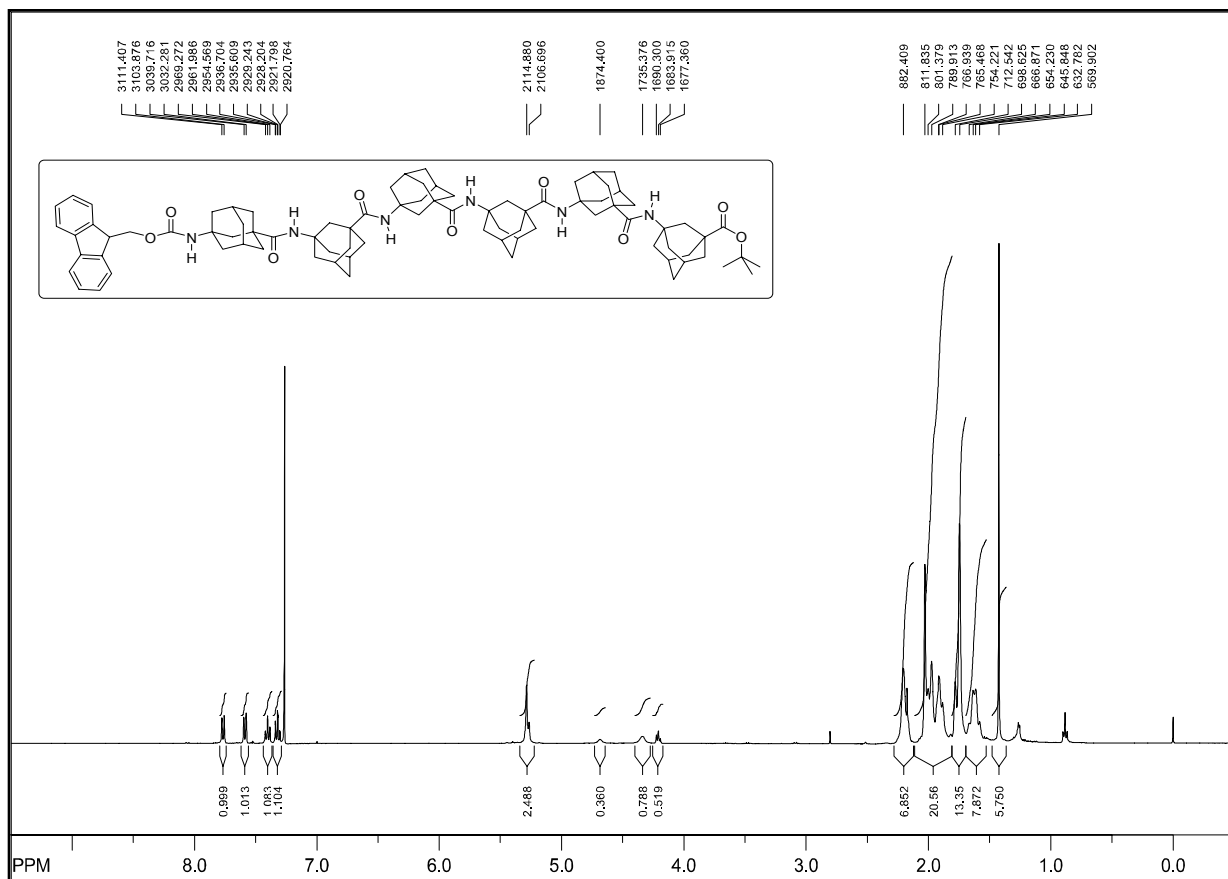
$\text{H-Gly-Gly-Gly-O}^t\text{Bu}$ (188)



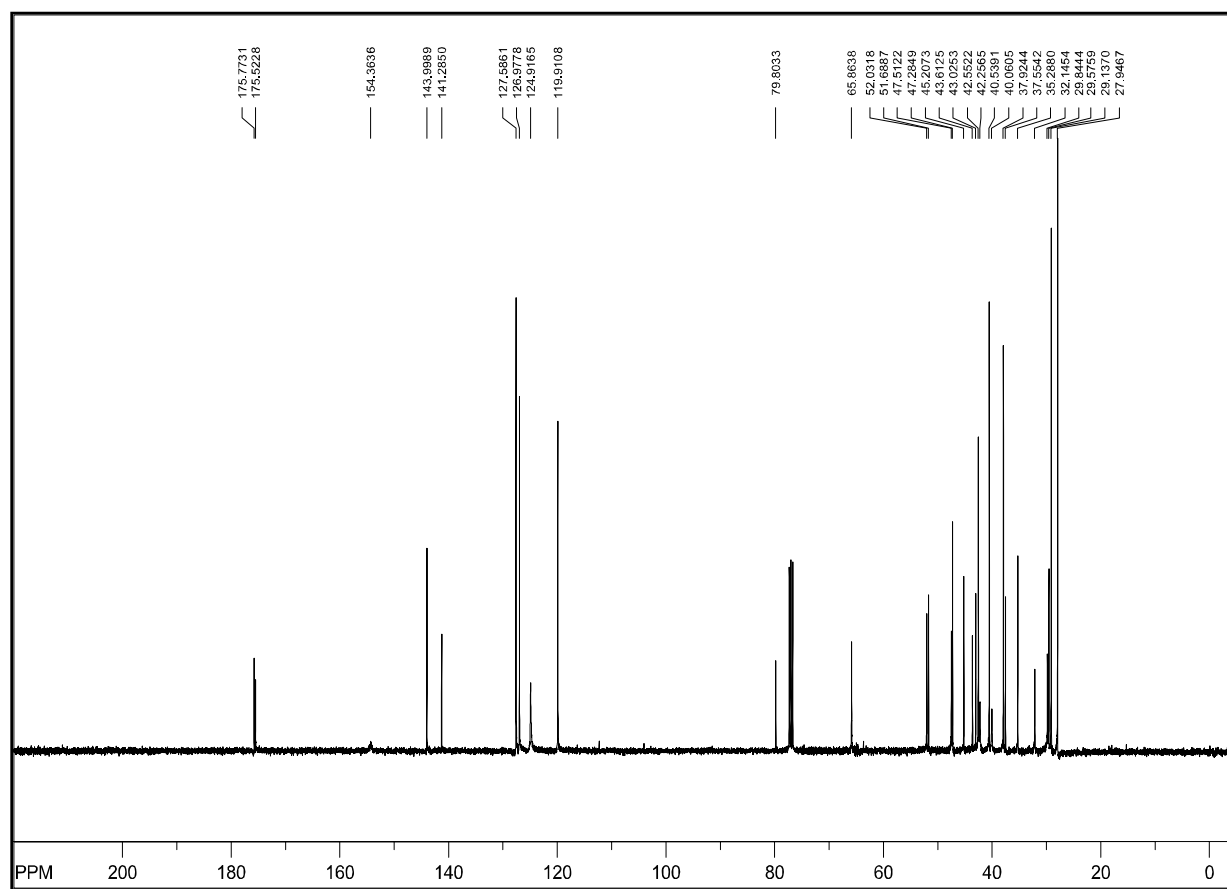
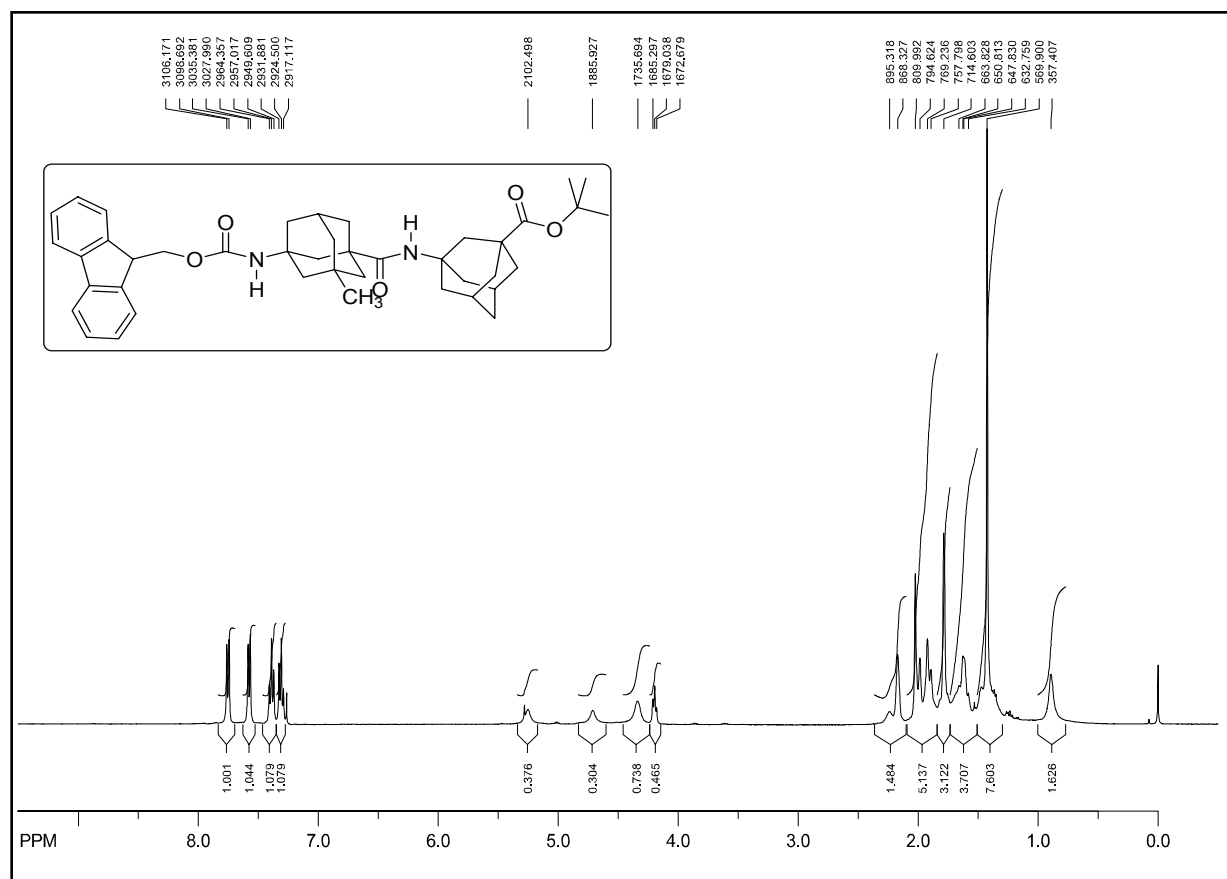
Fmoc- γ -Gly- γ -Gly- γ -Gly- γ -Gly-O^tBu (189)

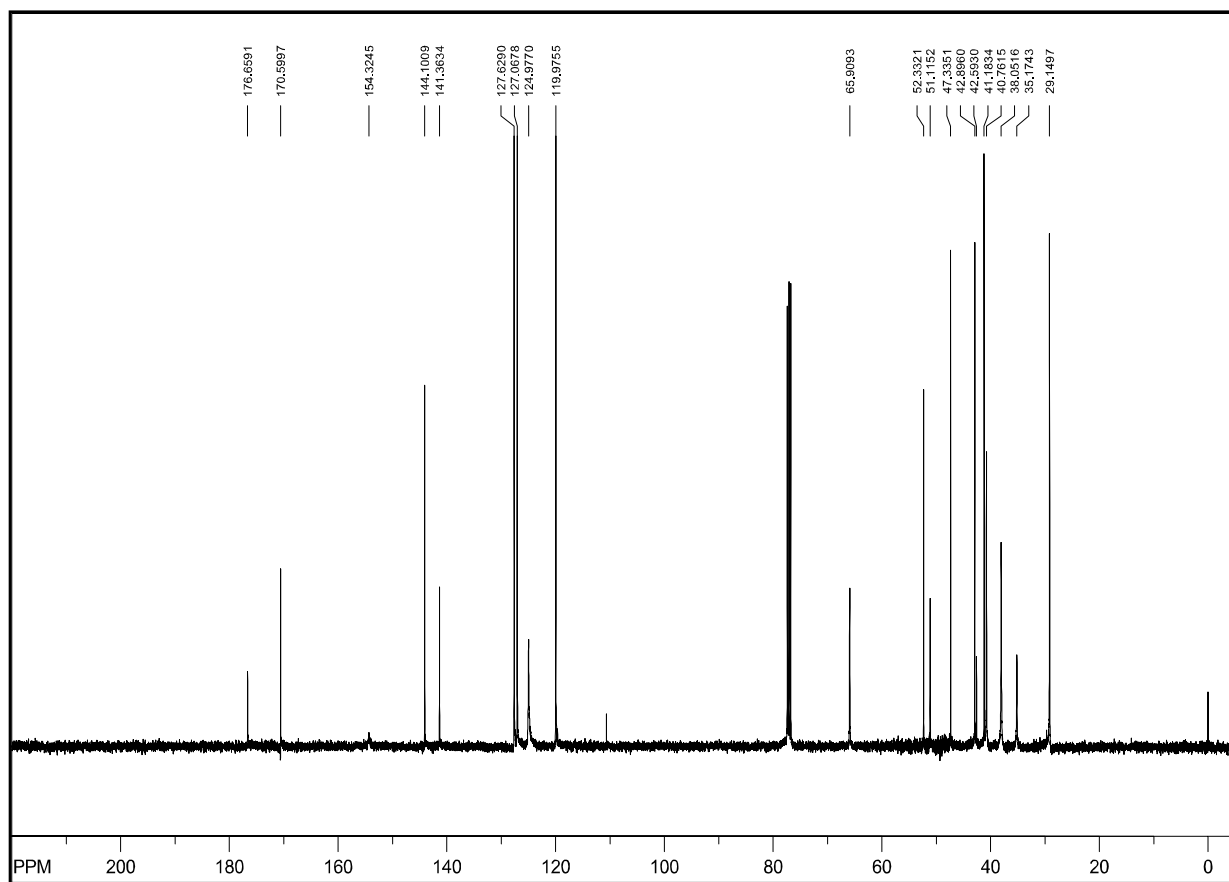
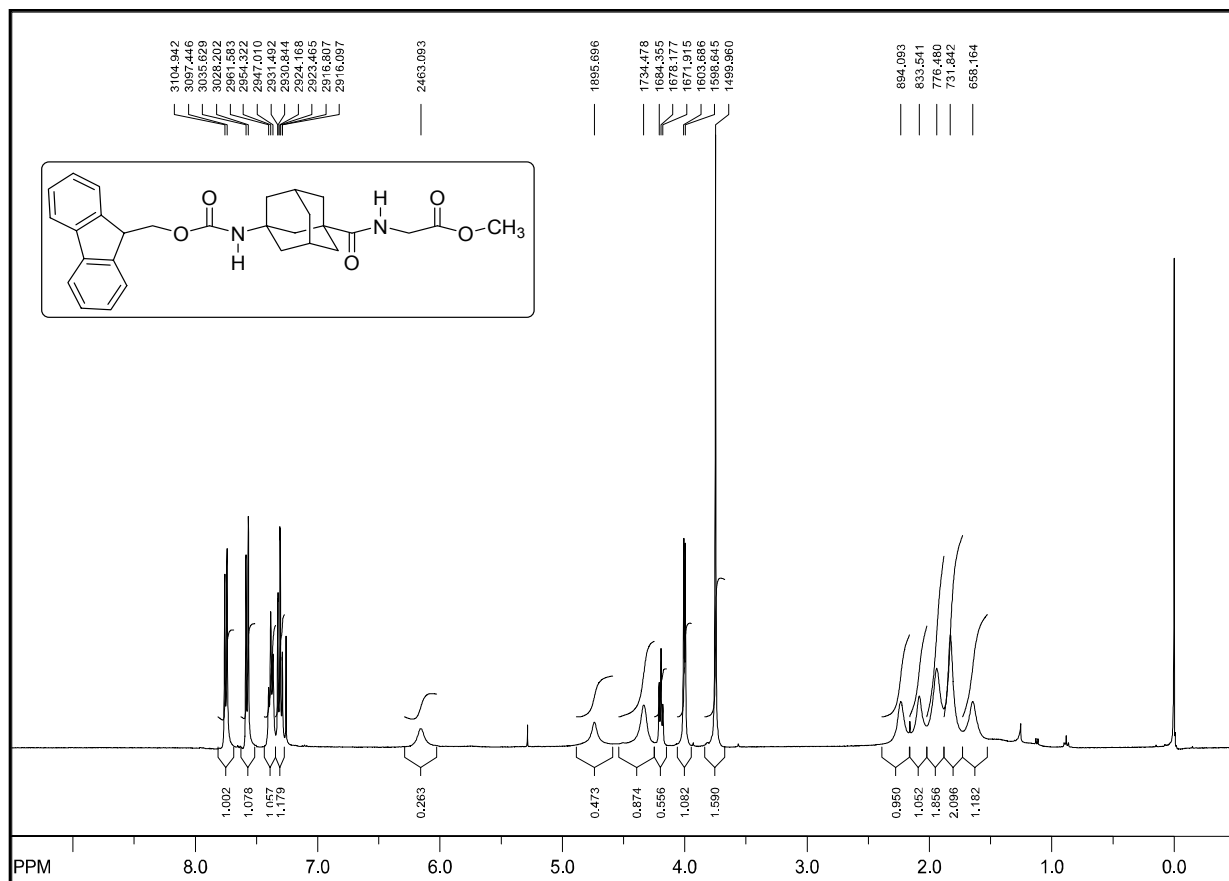


H^AGly-^AGly-^AGly-^AGly-O^tBu (**190**)

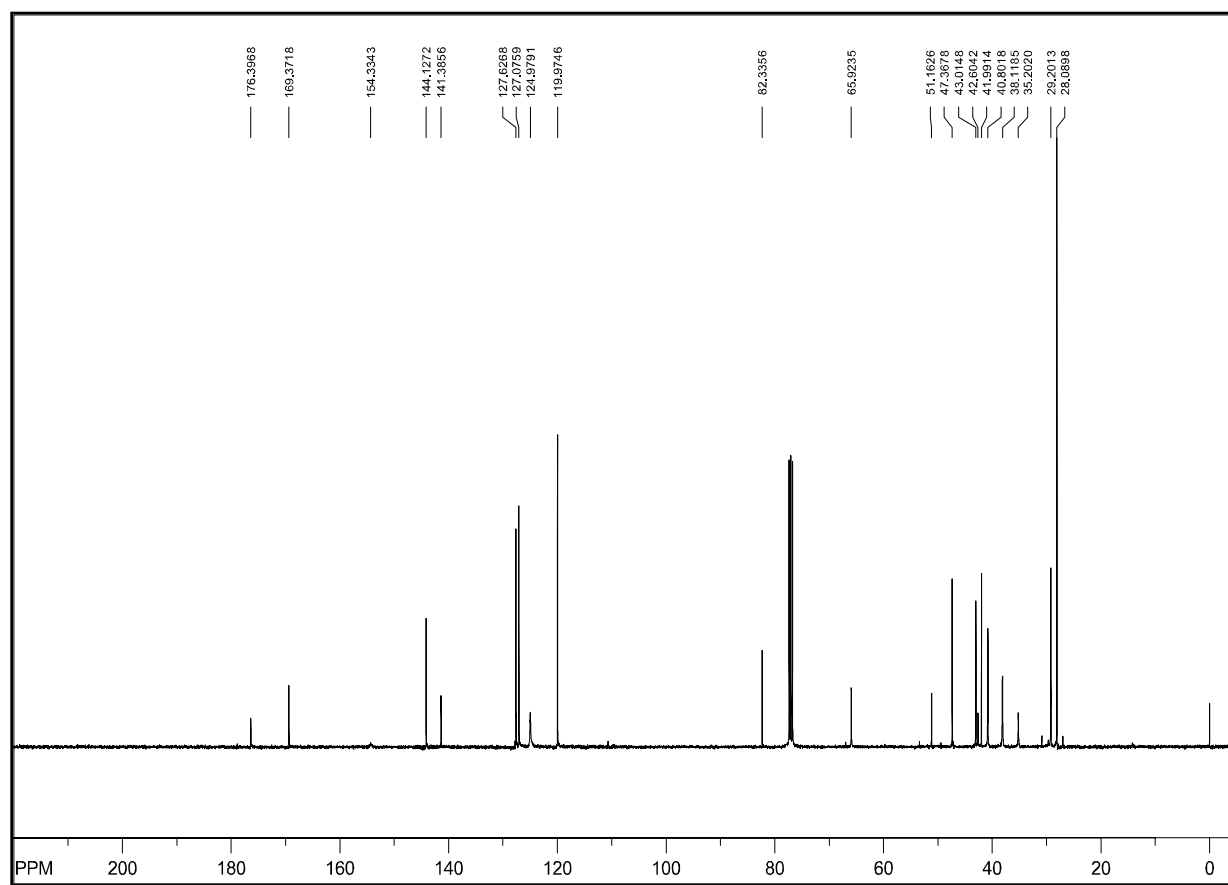
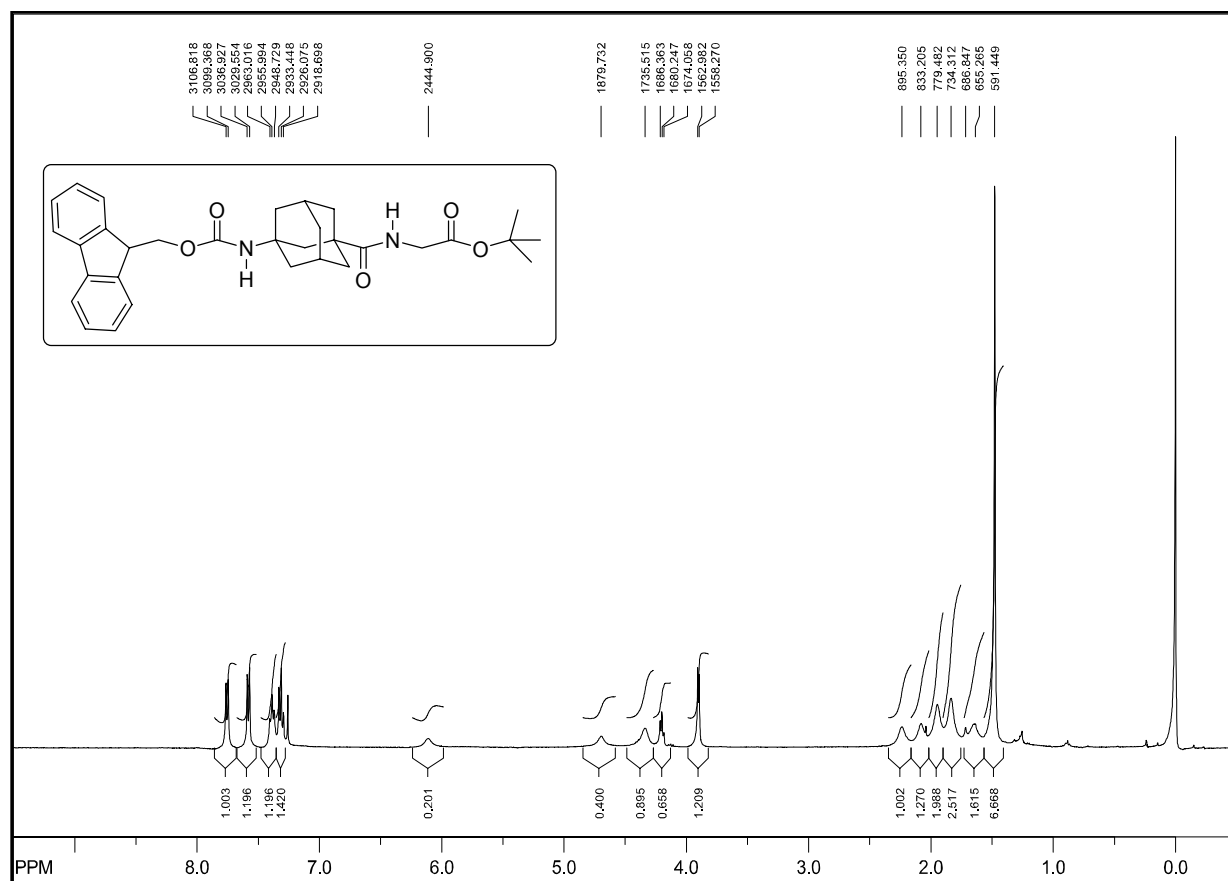


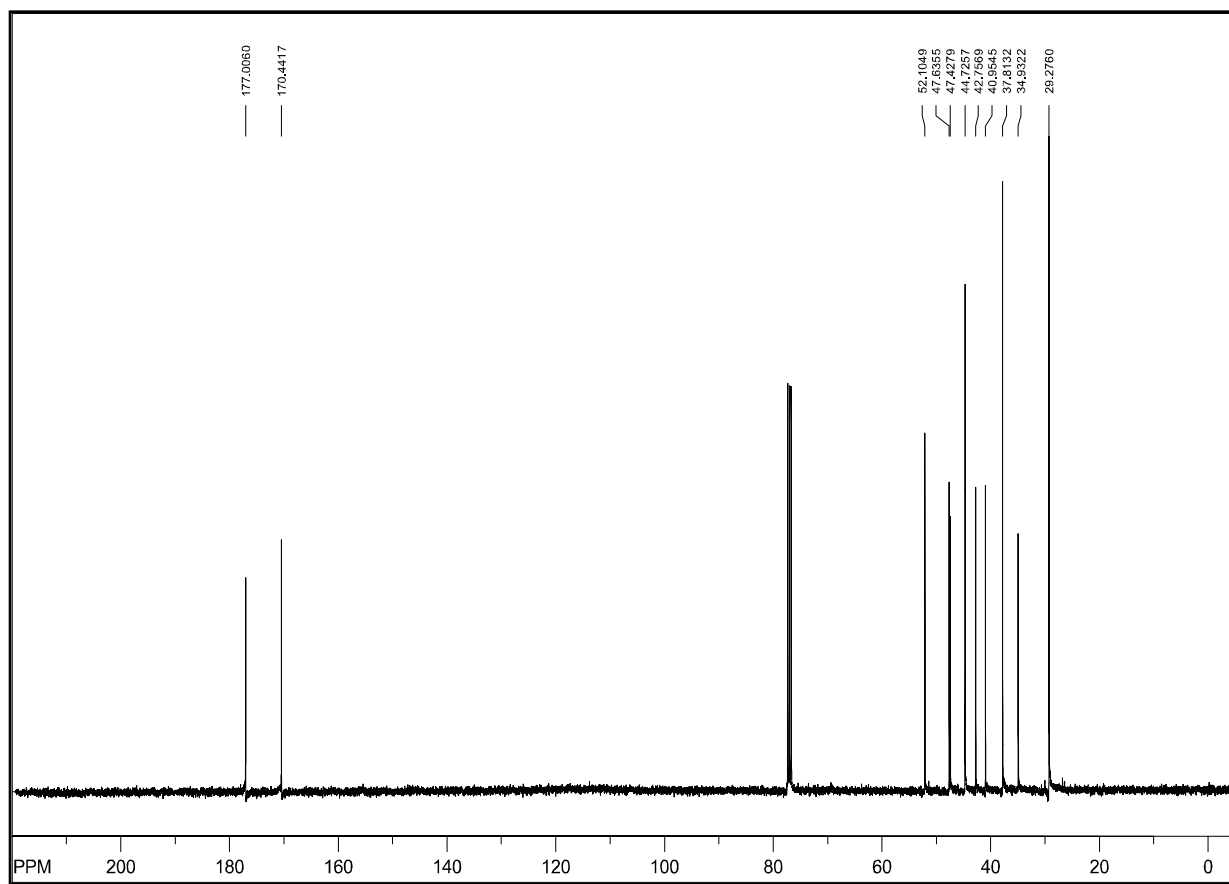
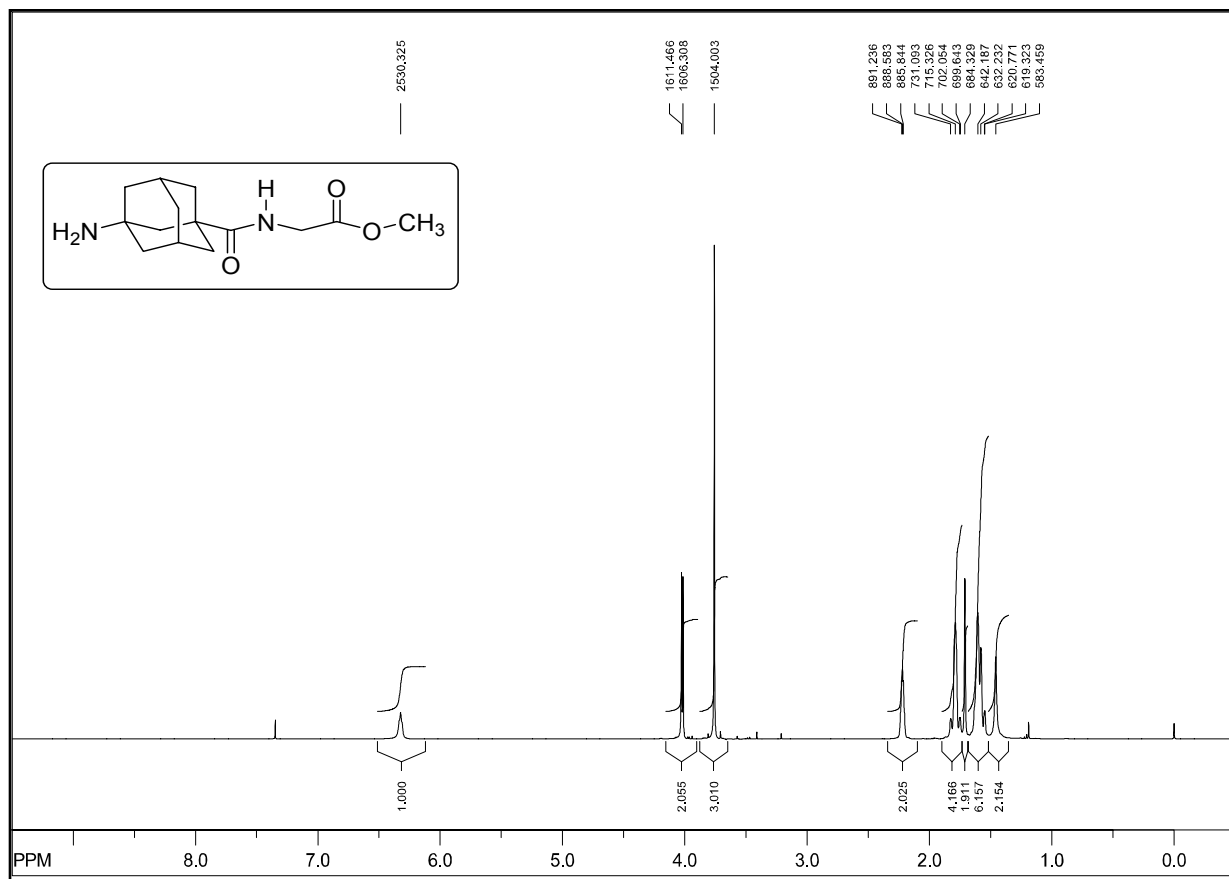
Fmoc-Gly-Gly-Gly-Gly-Gly-Gly-OBu (191)

Fmoc-^AAla-^AGly-O^tBu (192)

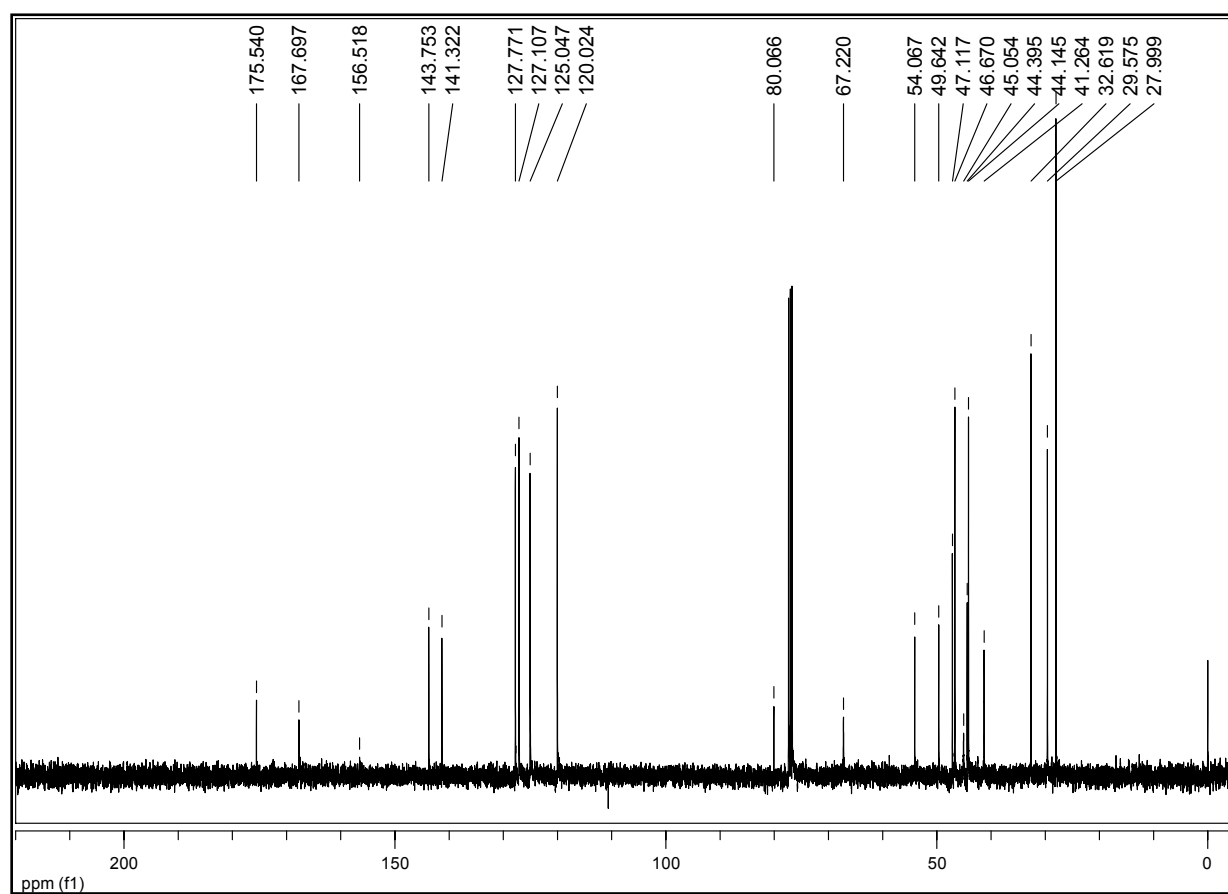
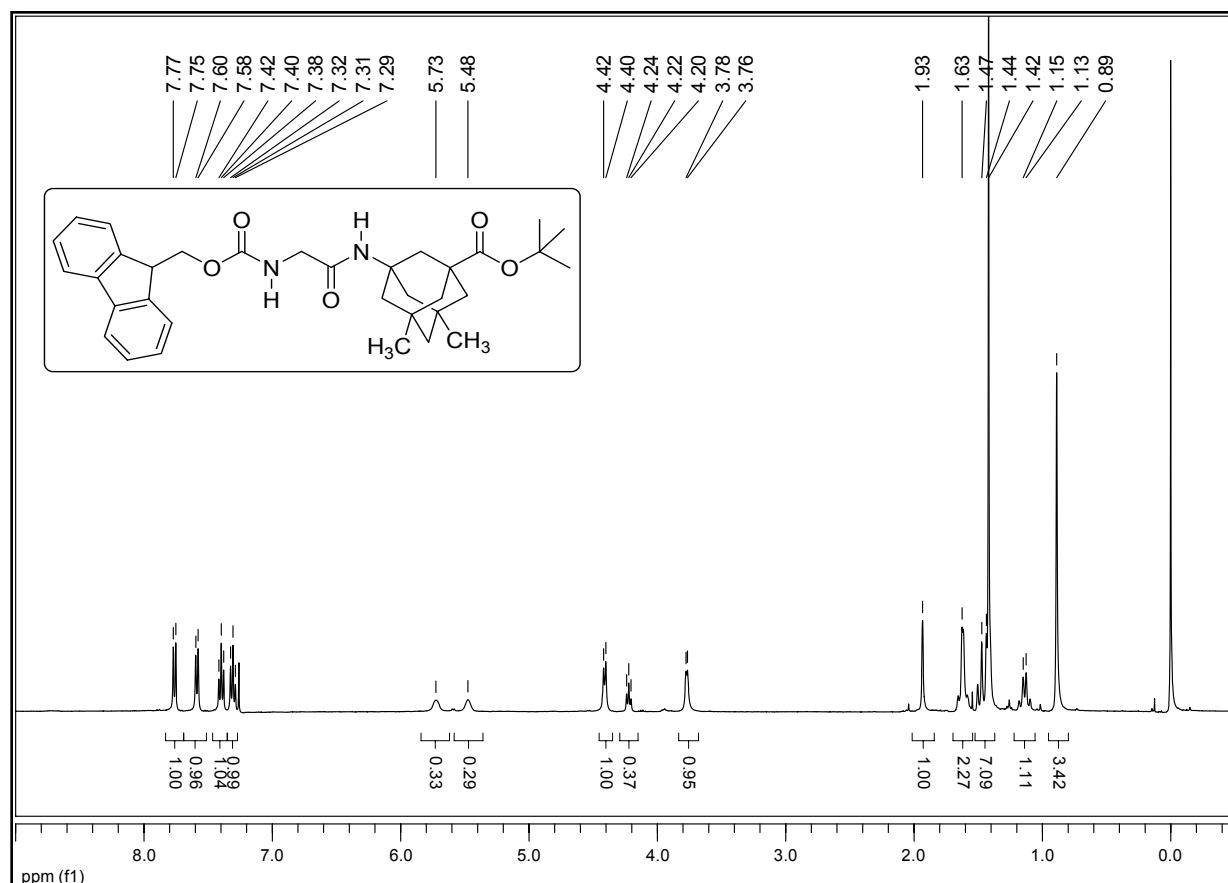


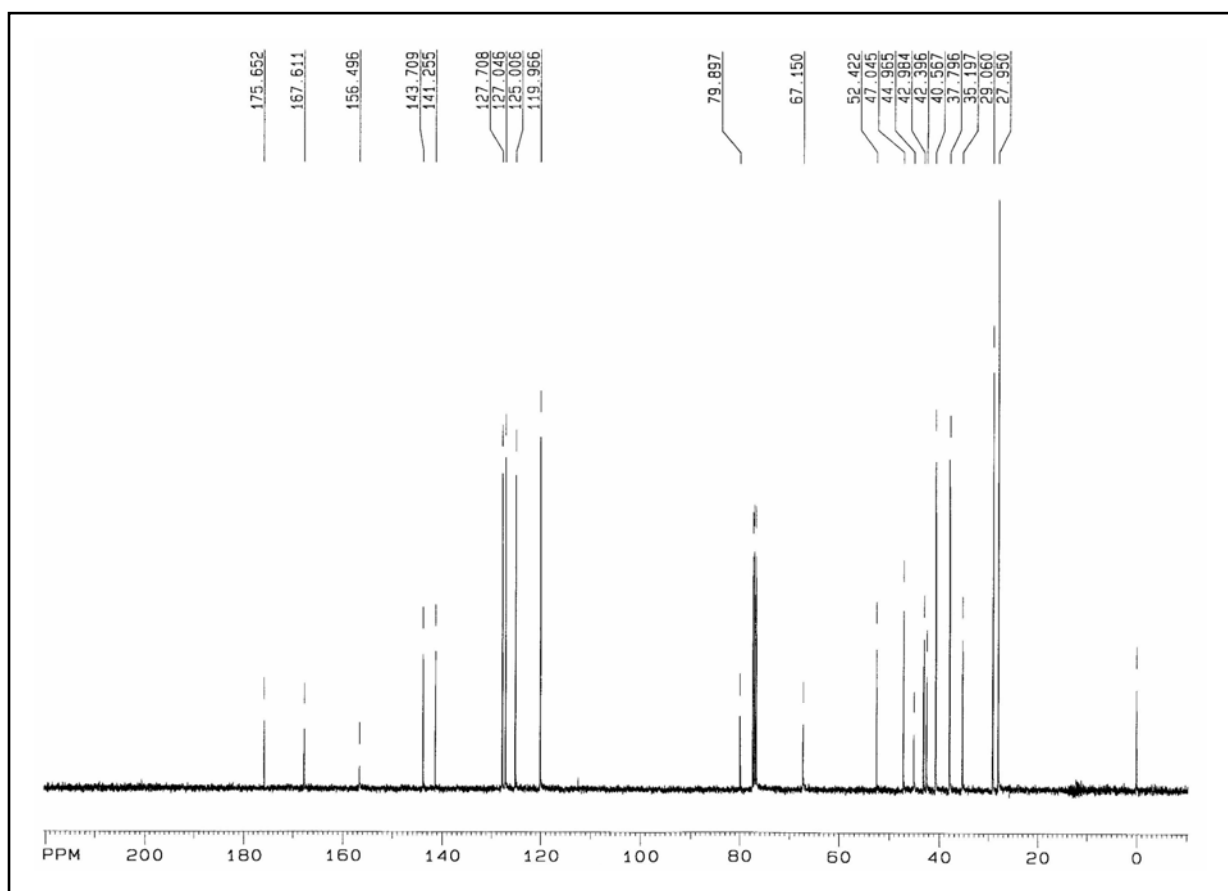
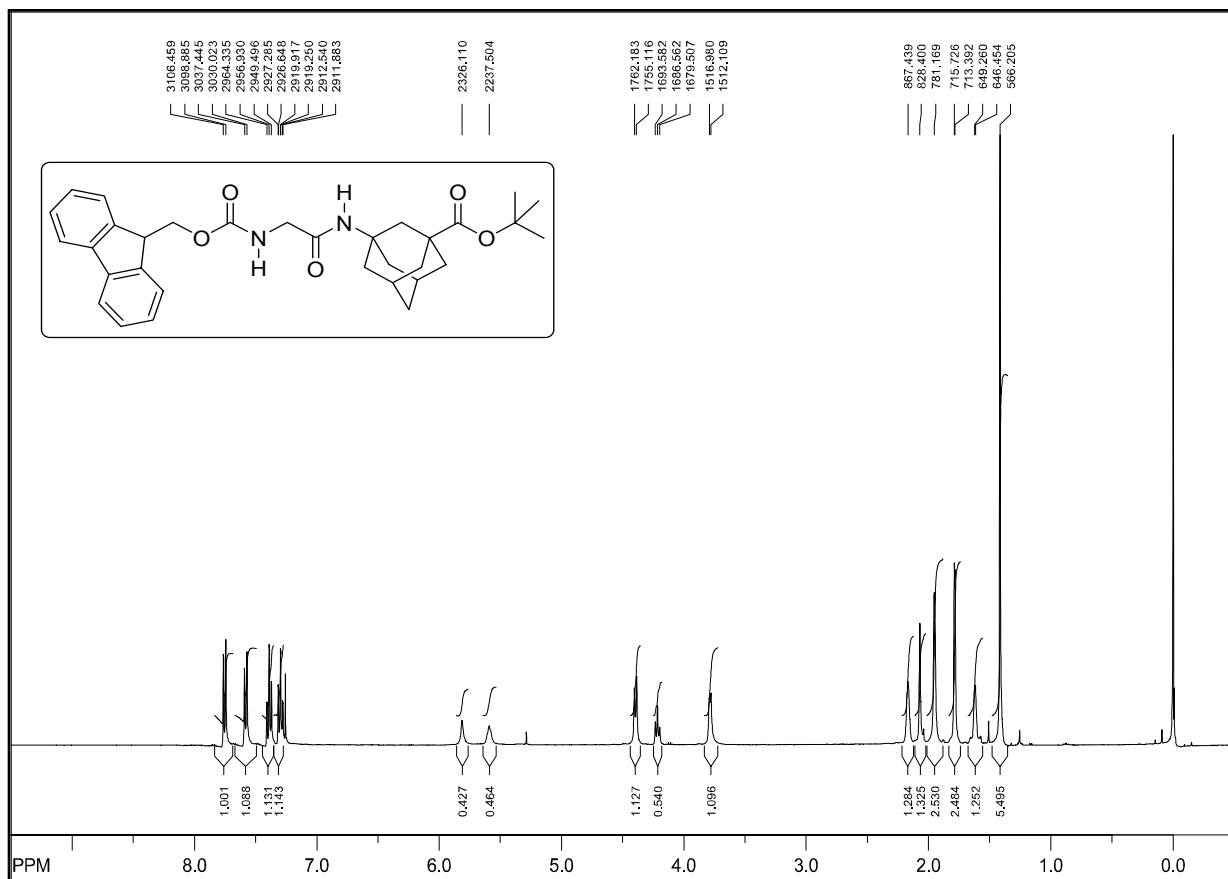
Fmoc-A-Gly-Gly-OMe (194)

Fmoc-Gly-Gly-O^tBu (196)

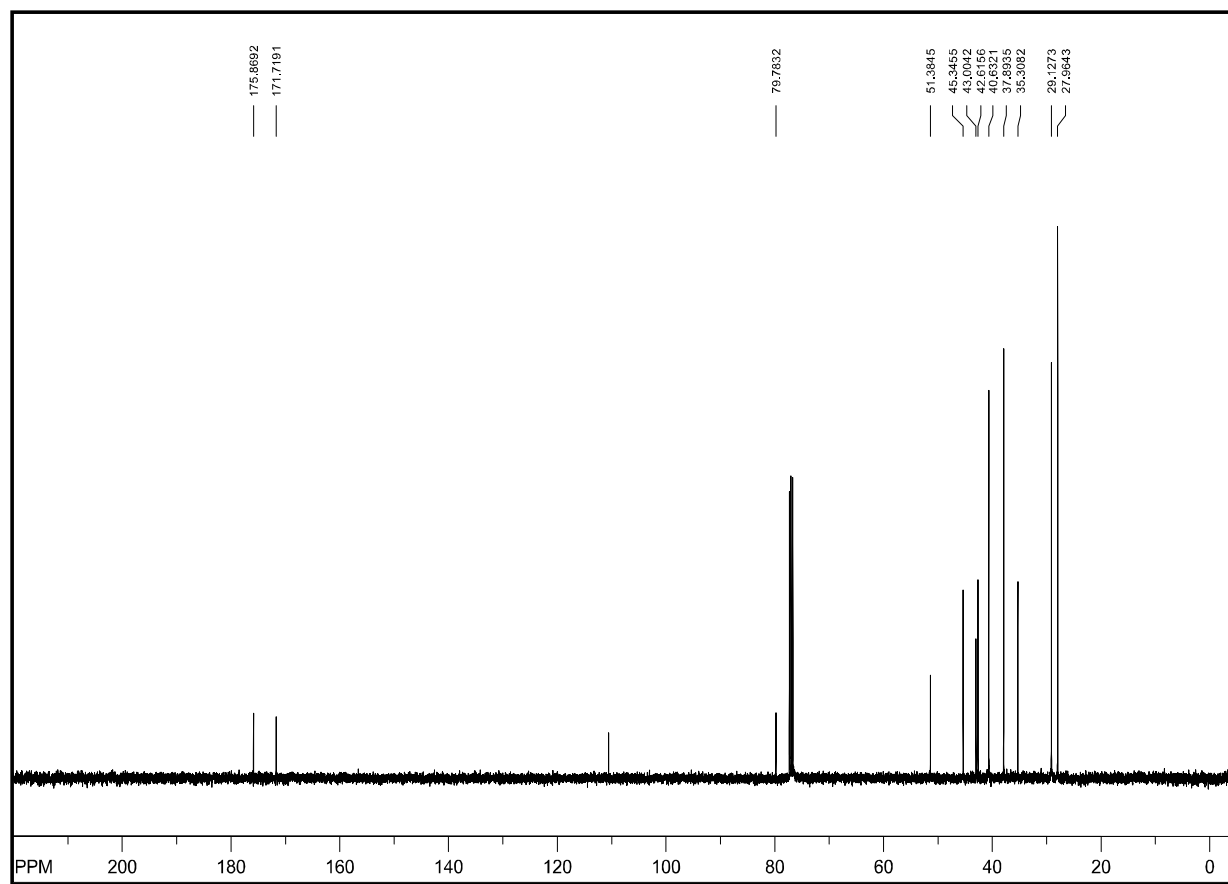
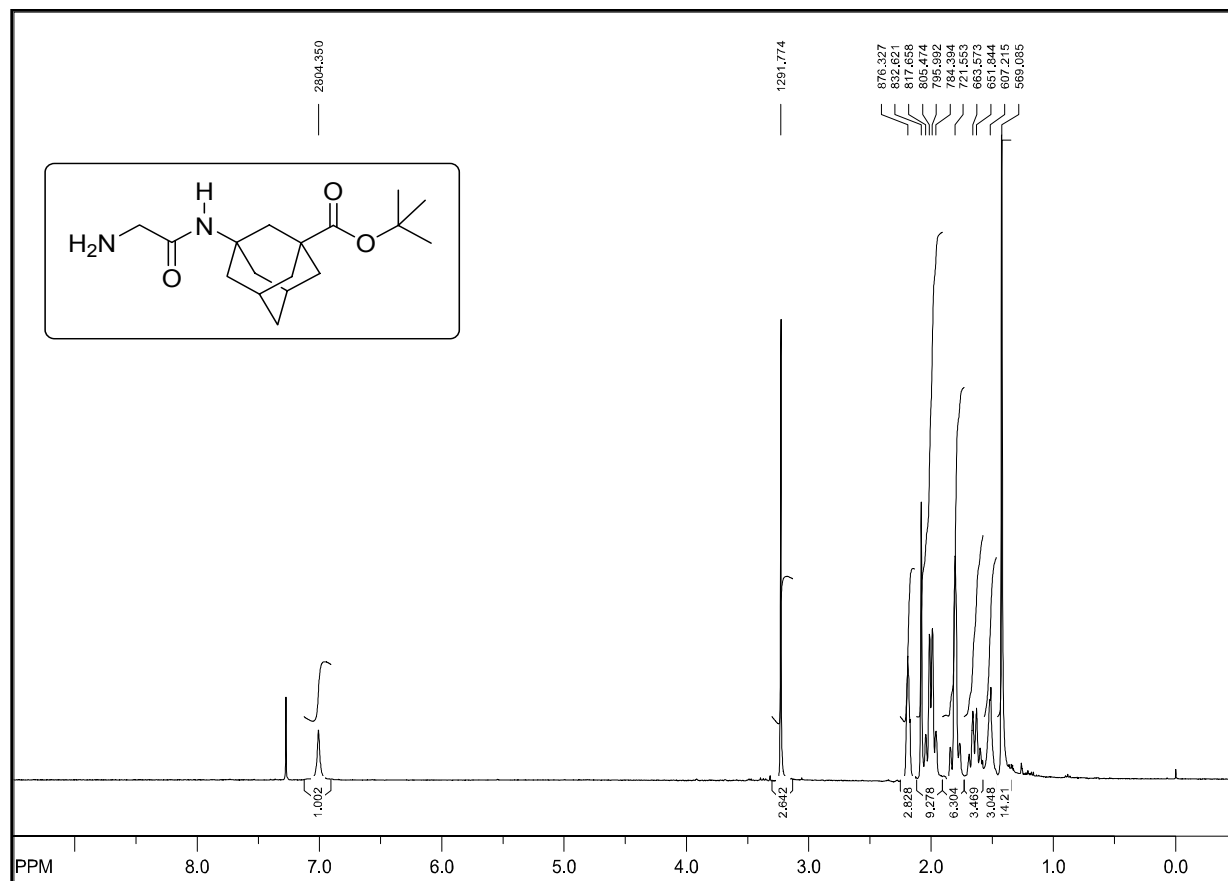


^1H - A Gly-Gly-OMe (197)

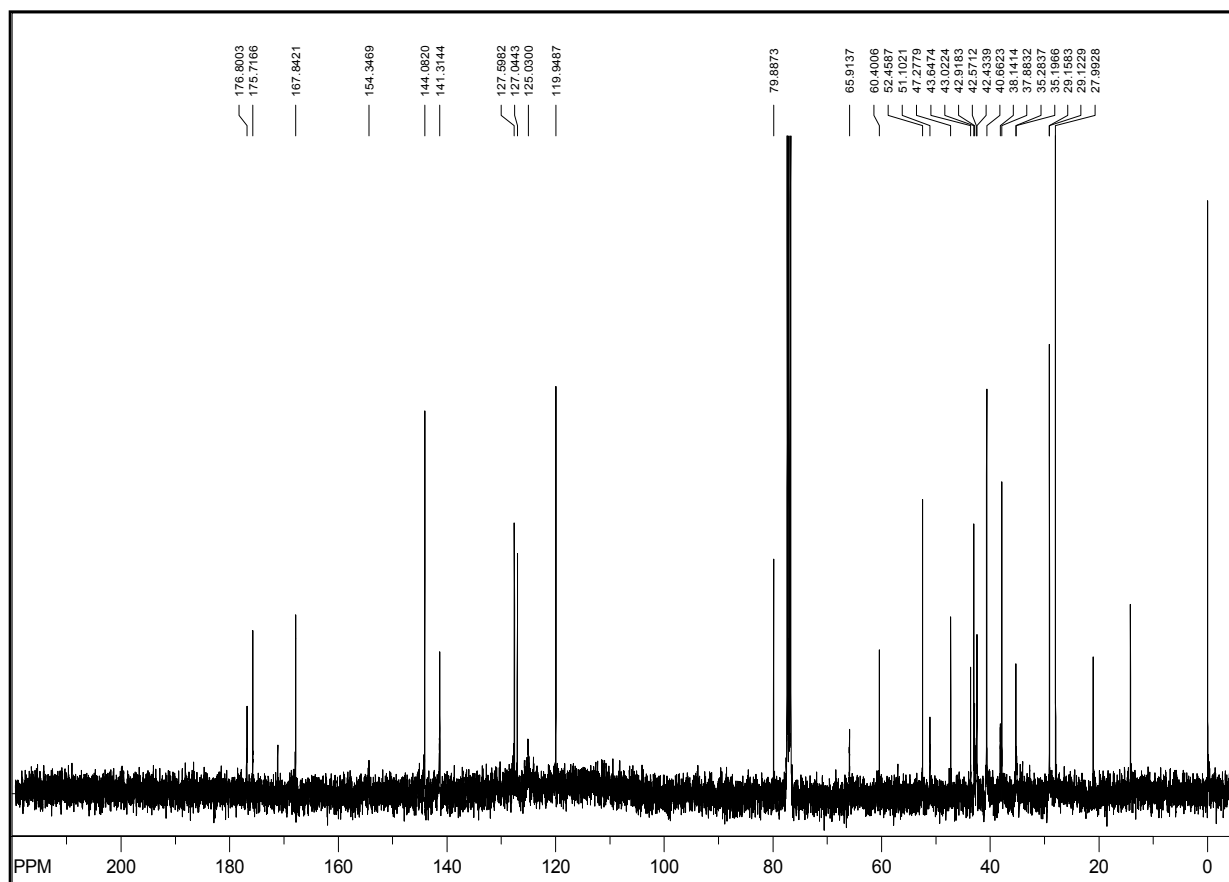
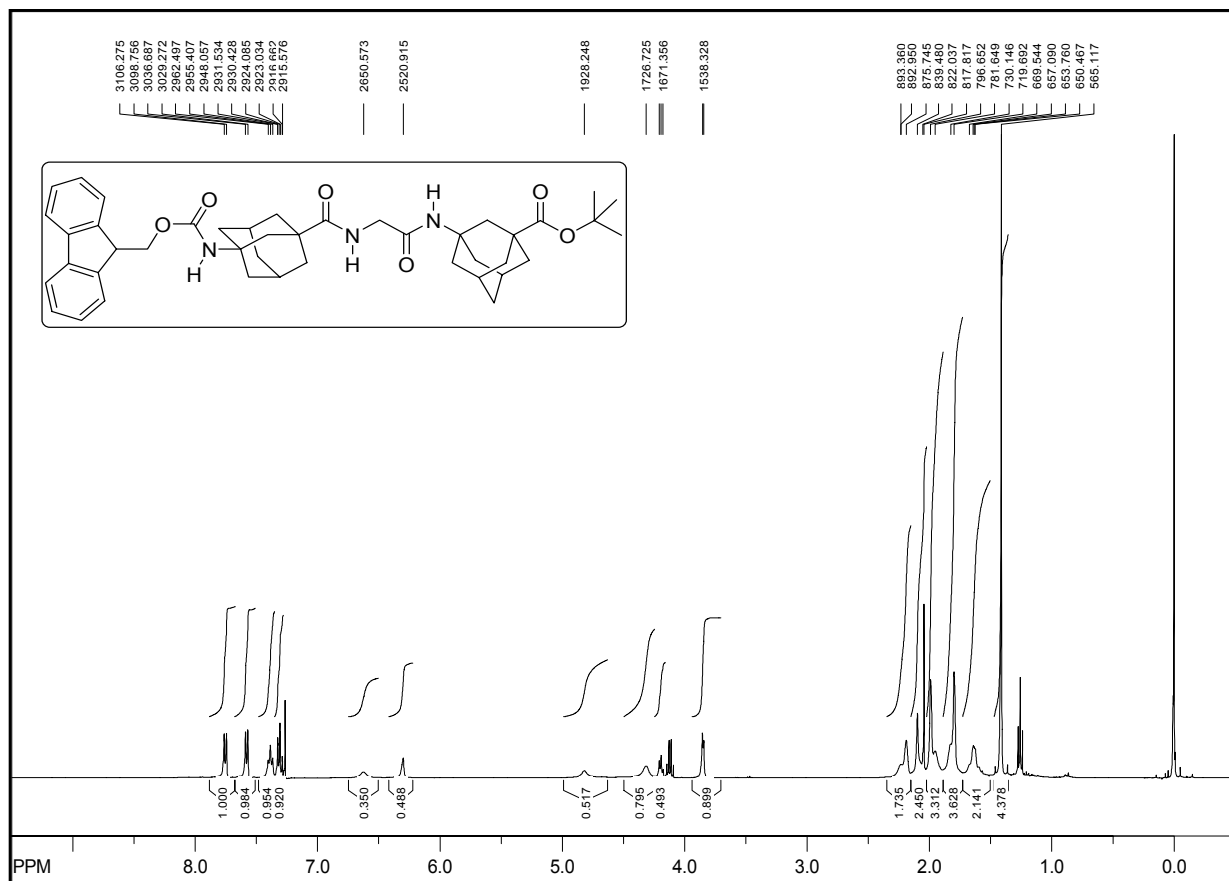
Fmoc-Gly-Aib-O^tBu (198)



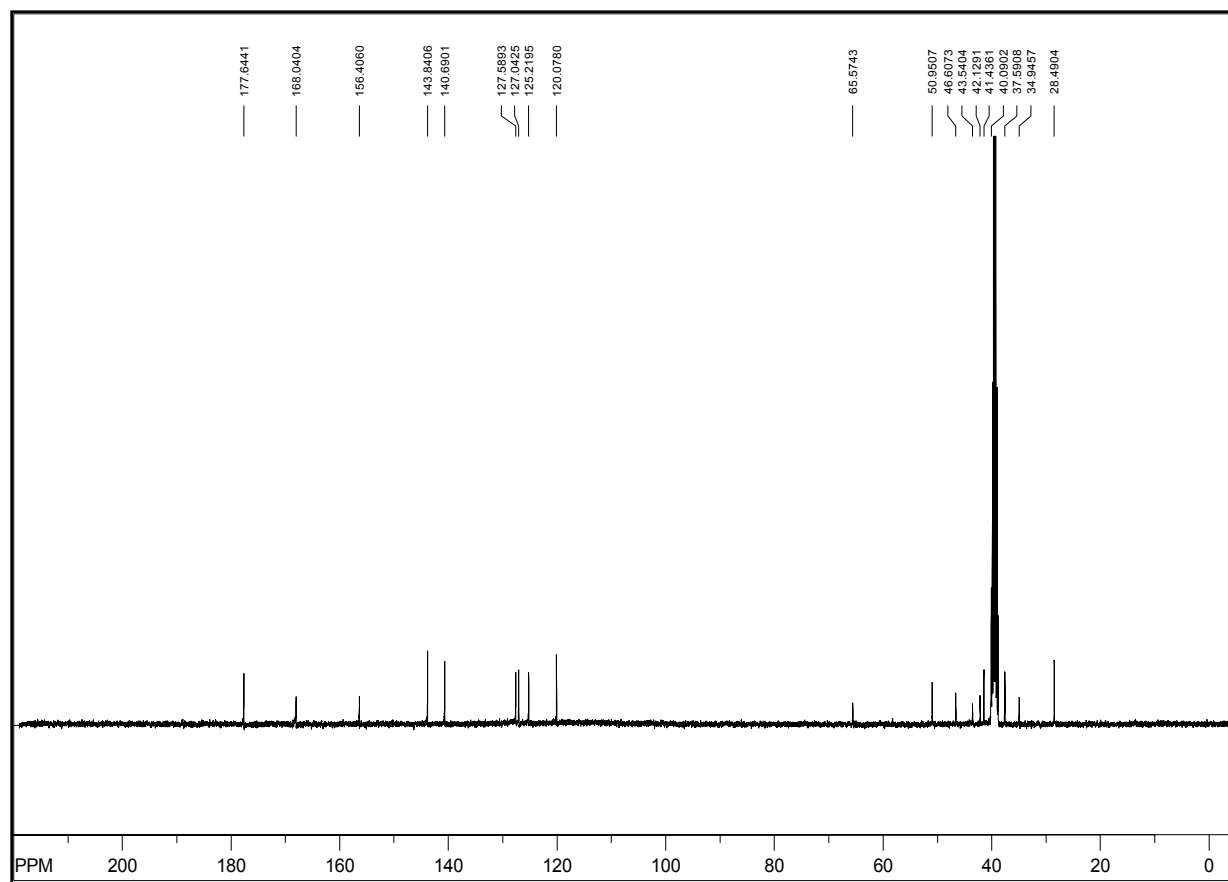
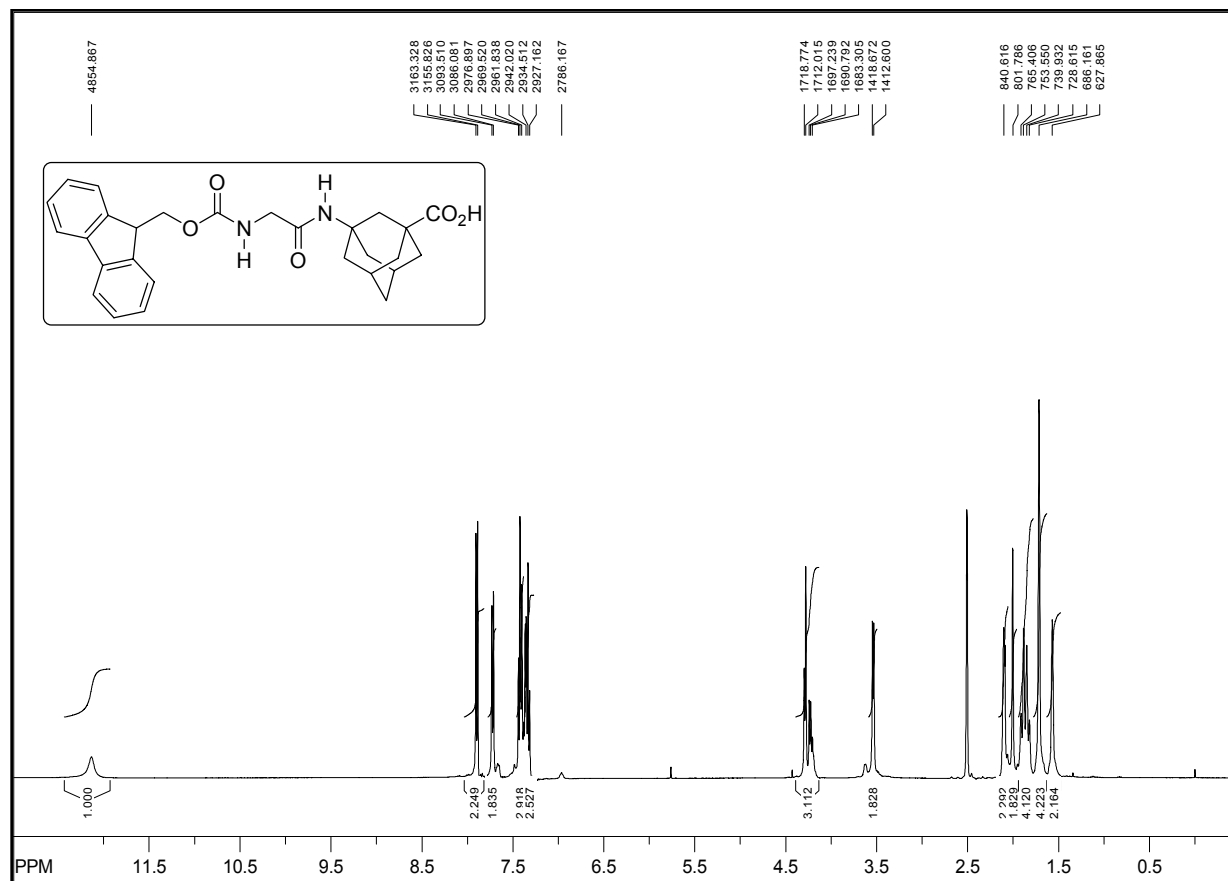
Fmoc-Gly-^AGly-O^tBu (199)



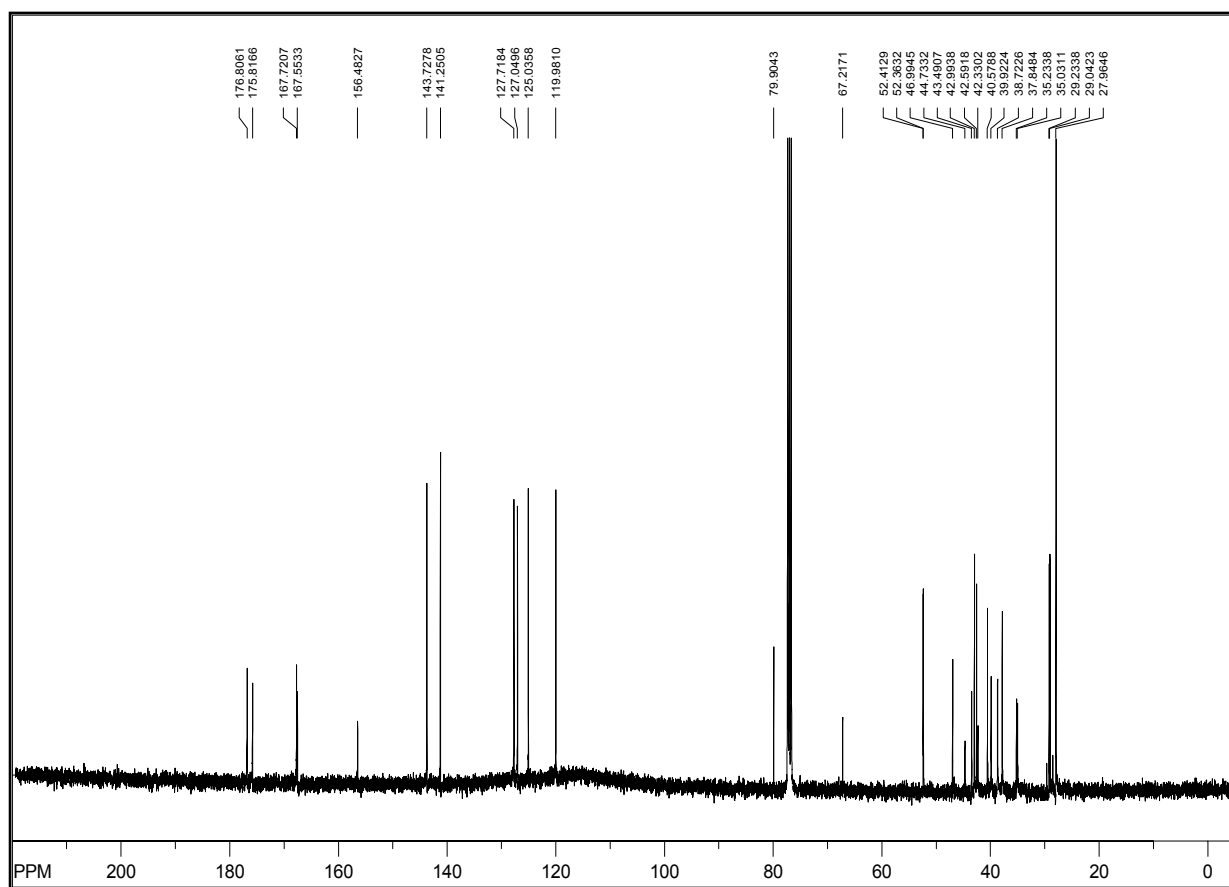
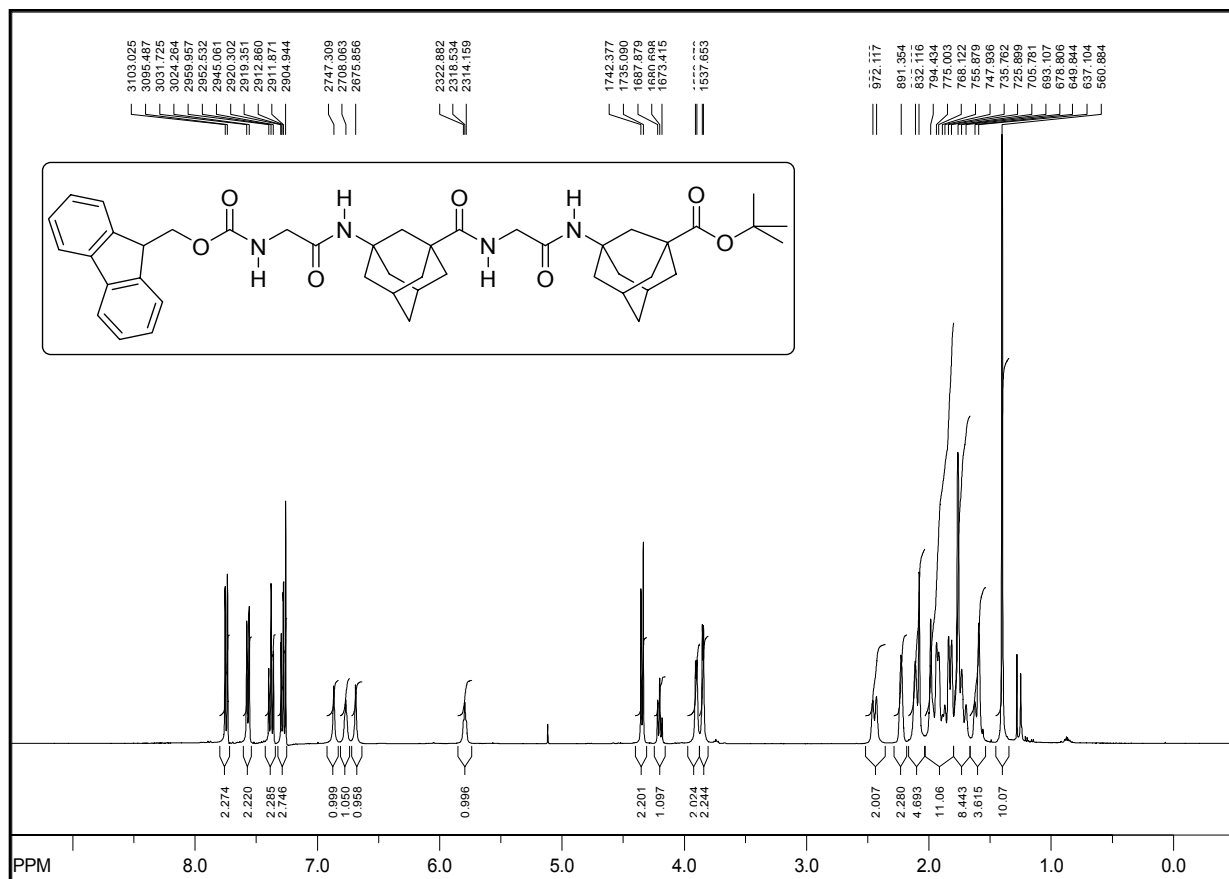
H-Gly-A-Gly-OMe (200)



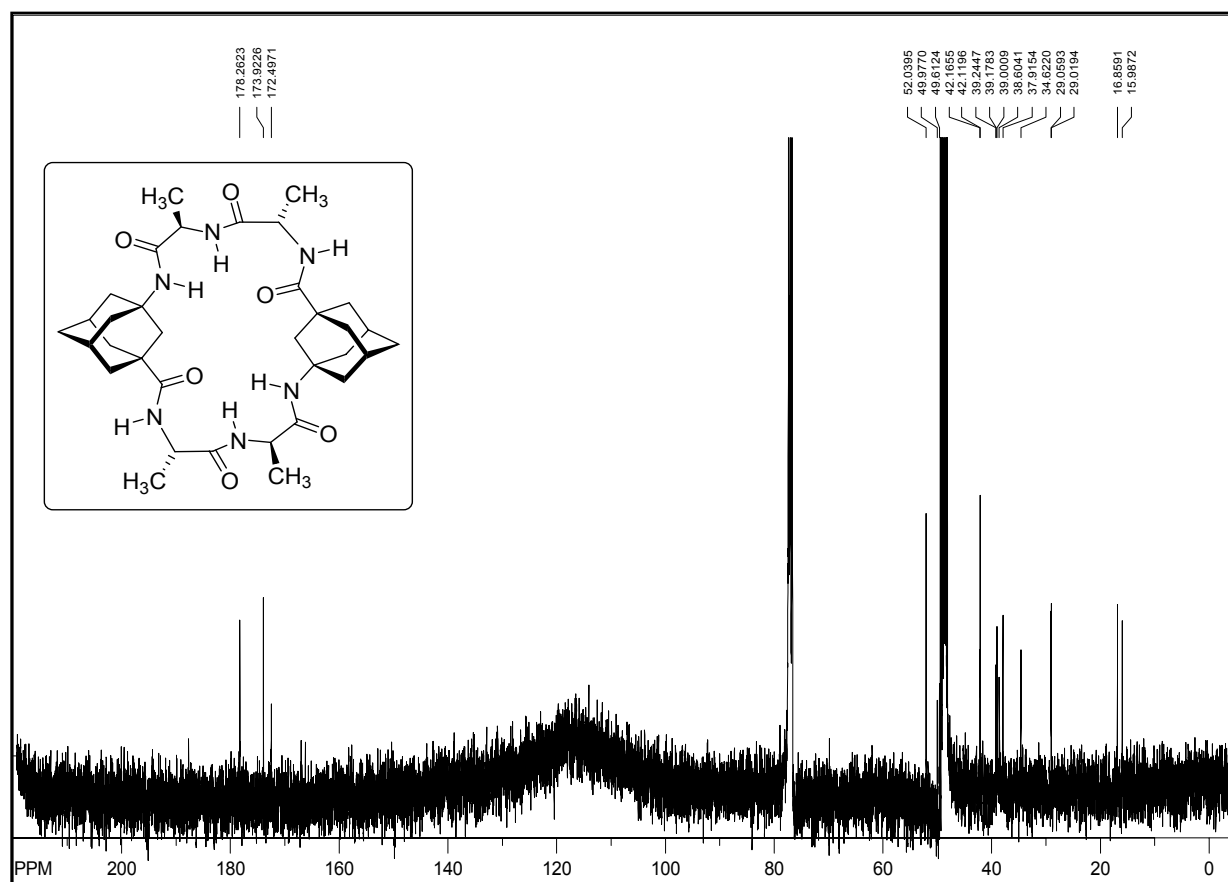
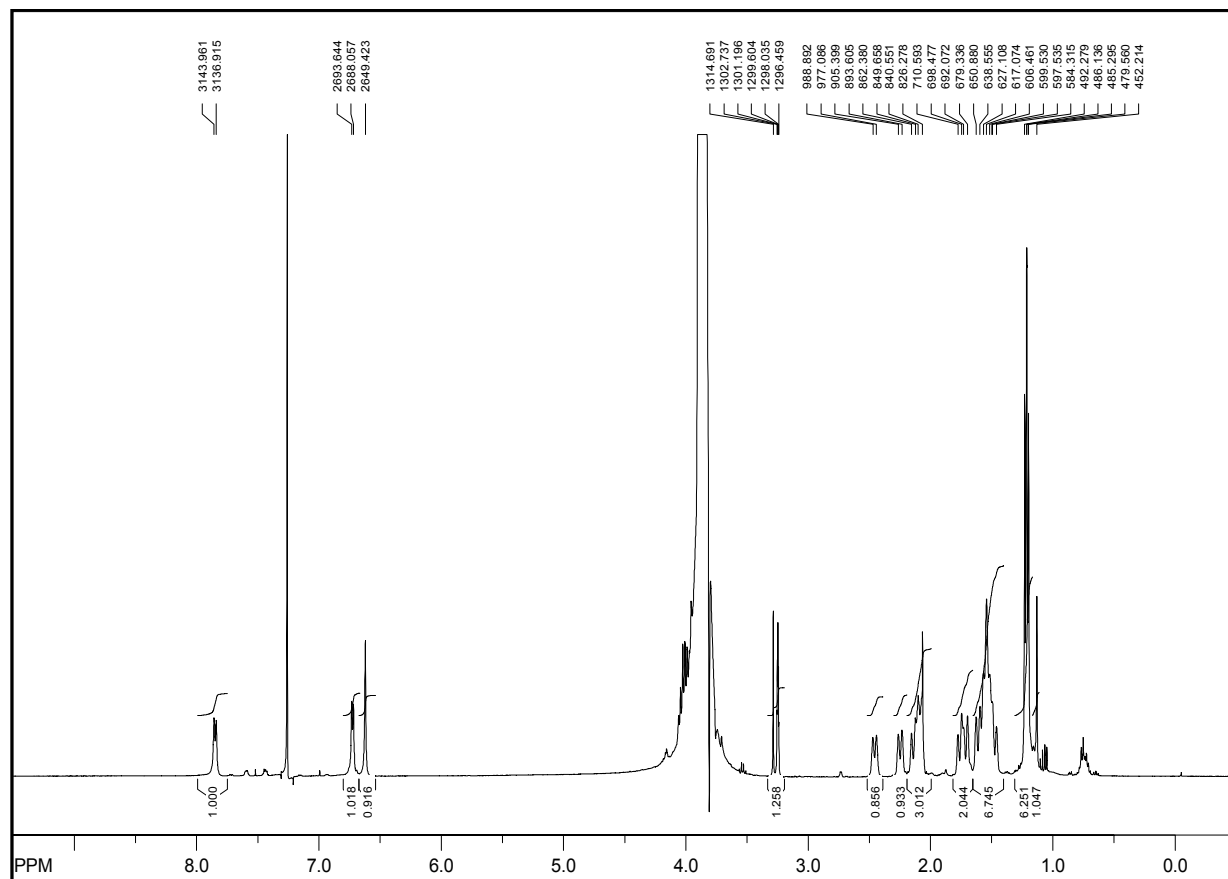
Fmoc-^AGly-Gly-^AGly-O^tBu (201)

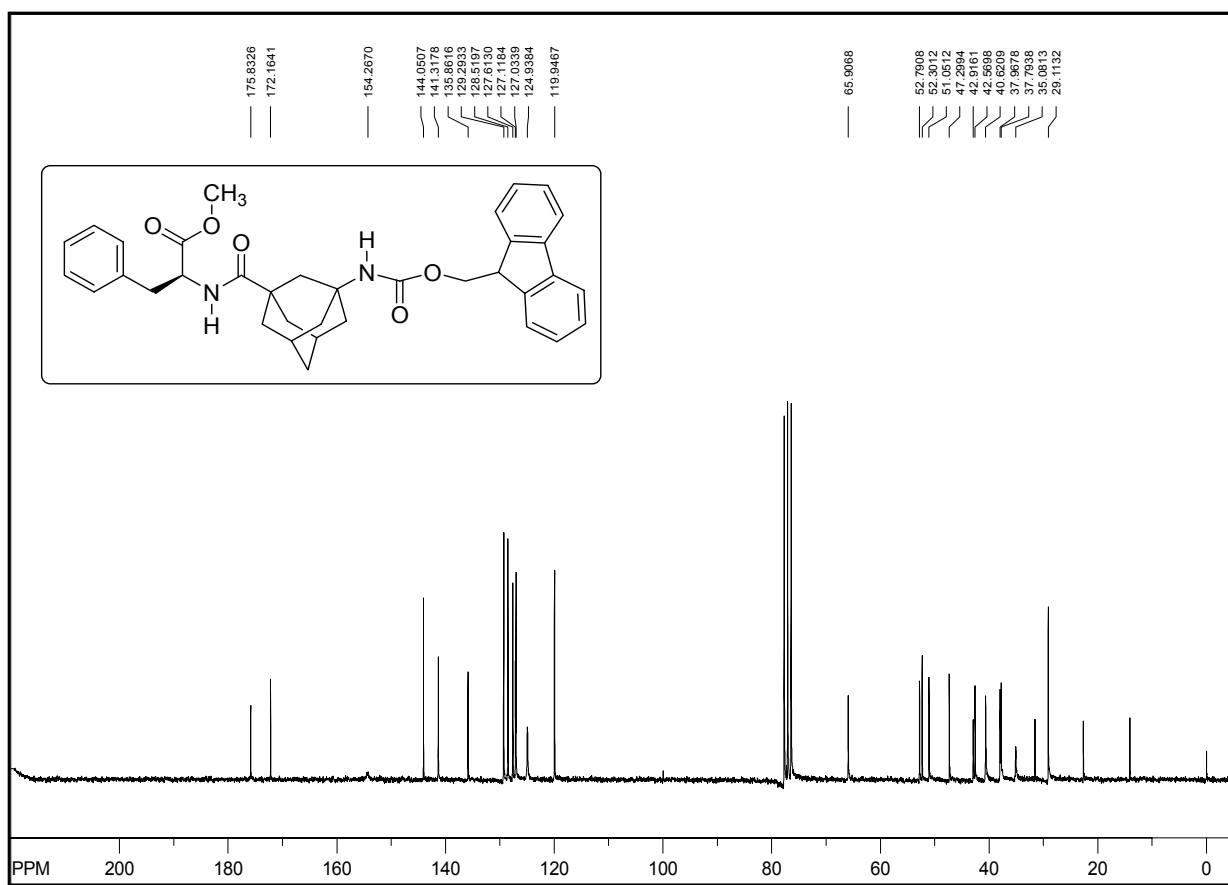
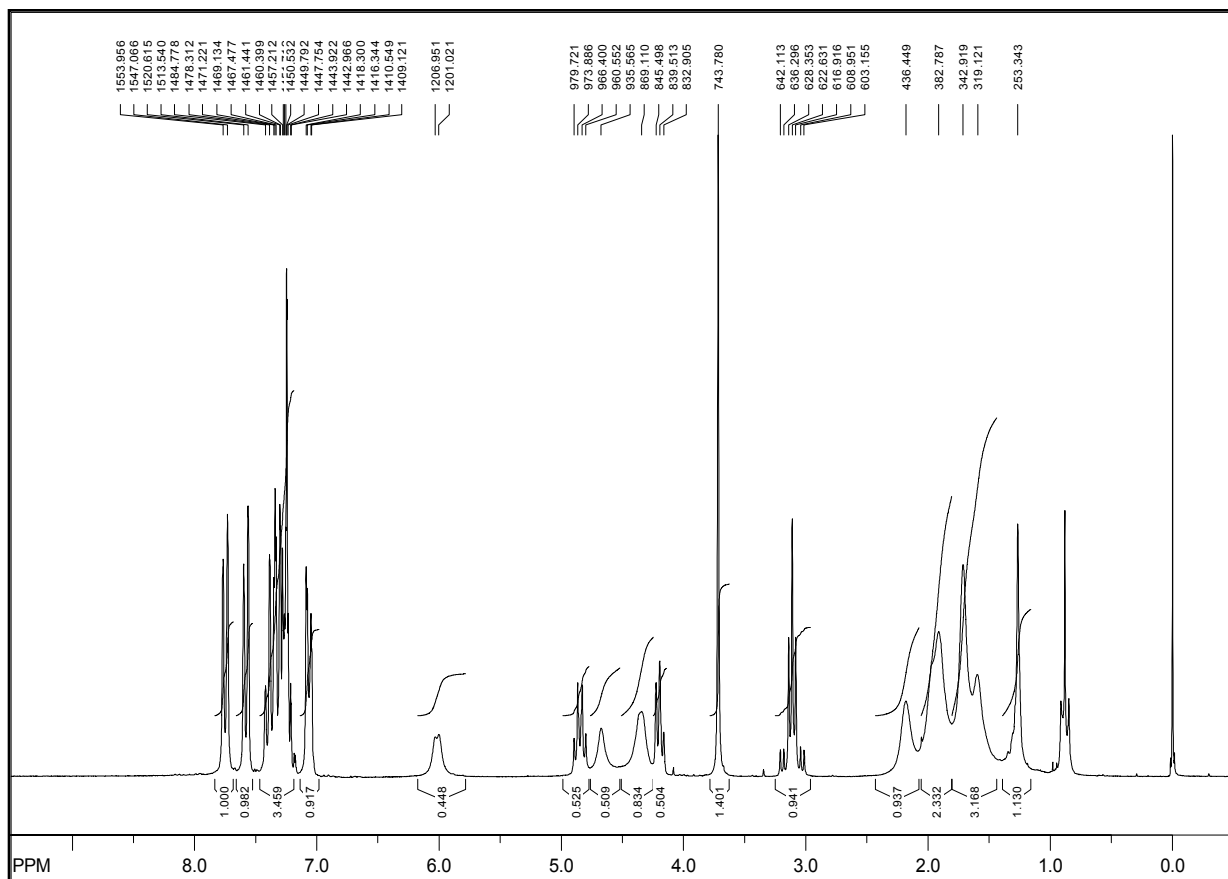


Fmoc-Gly-A-Gly-OH (202)

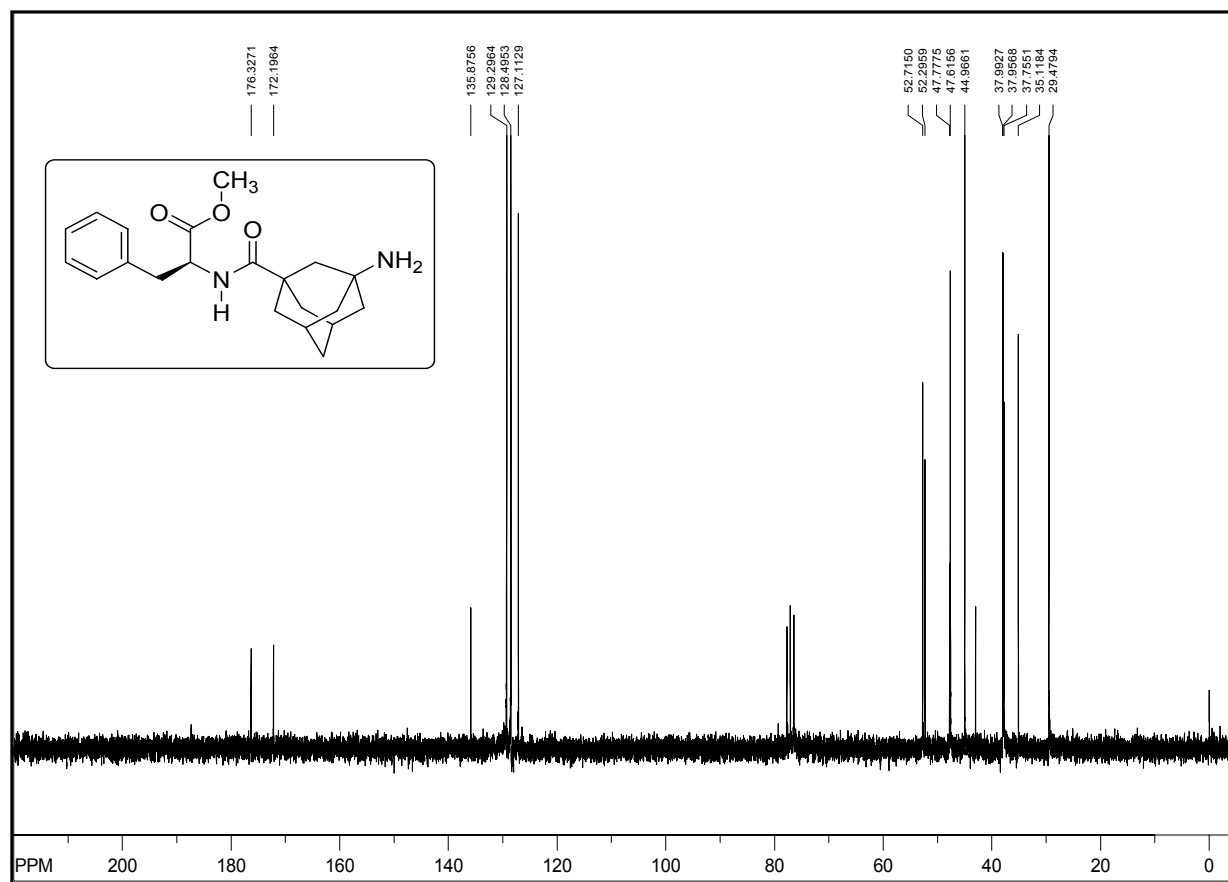
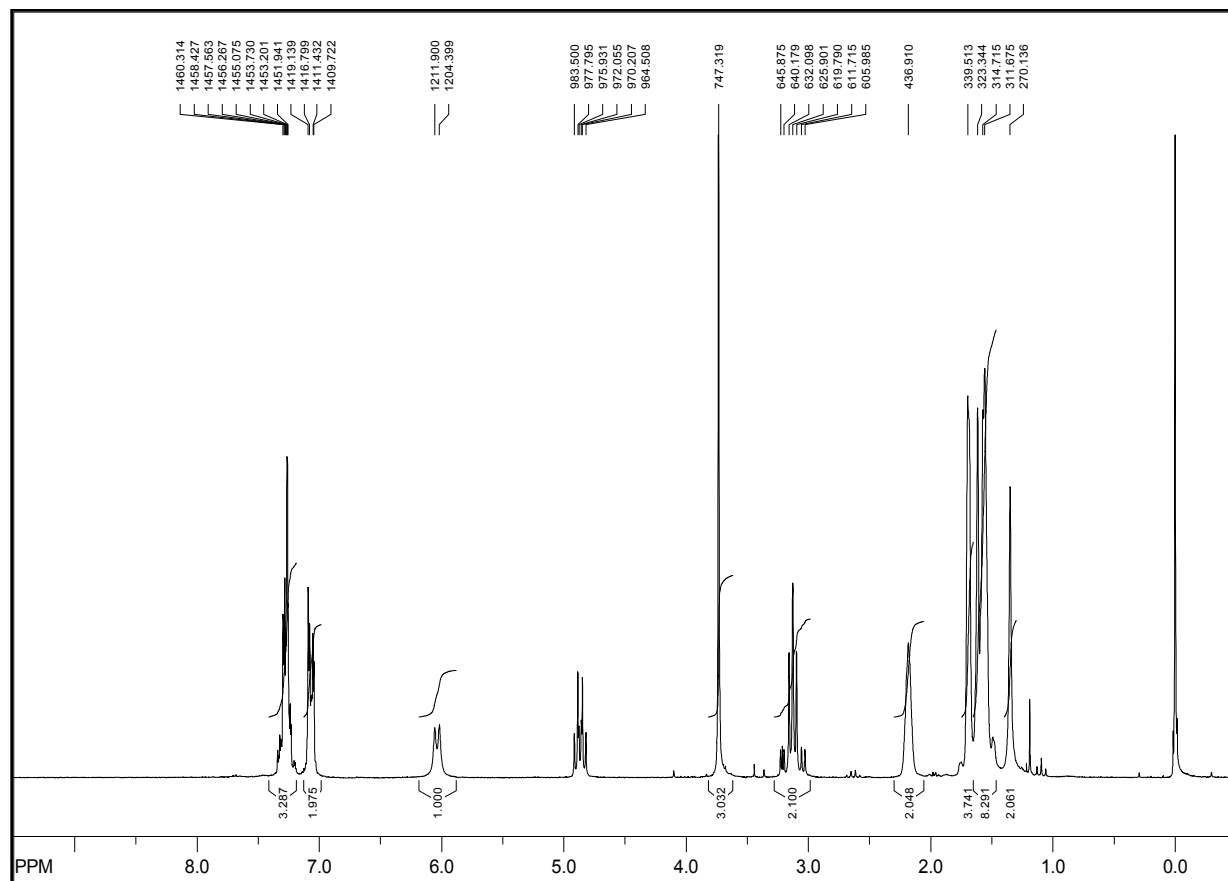


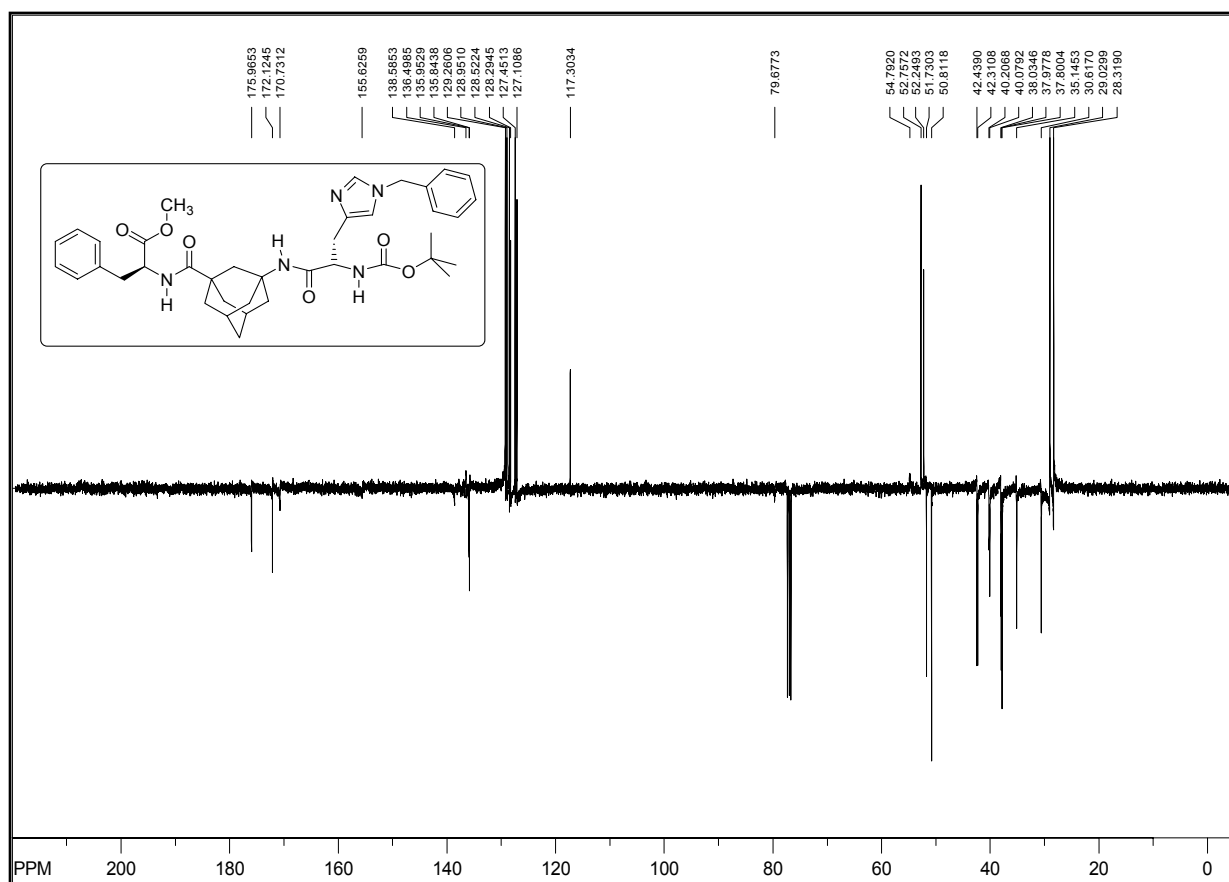
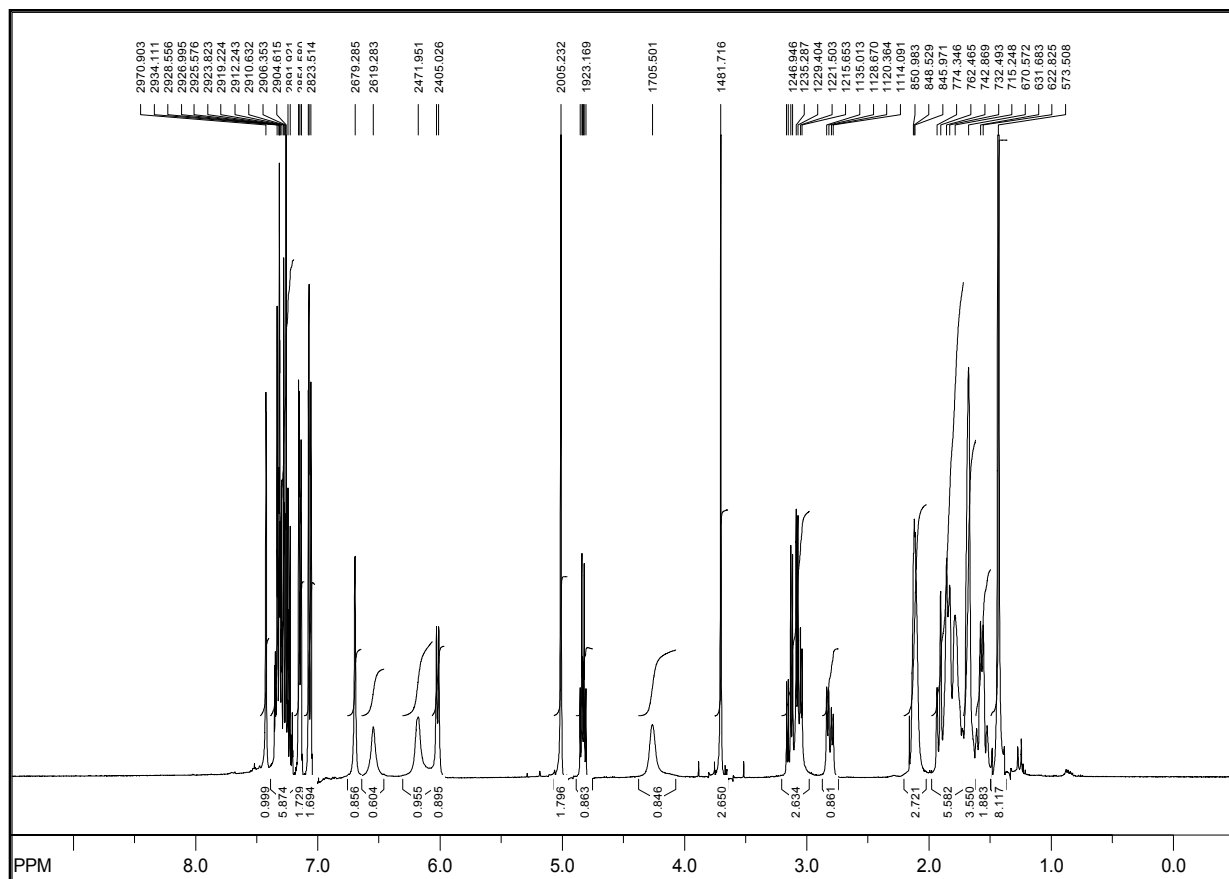
Fmoc-Gly-^AGly-Gly-^AGly-OtBu (**203**)

Cyclo-(D-Ala-AGly-L-Ala)₂ (213)

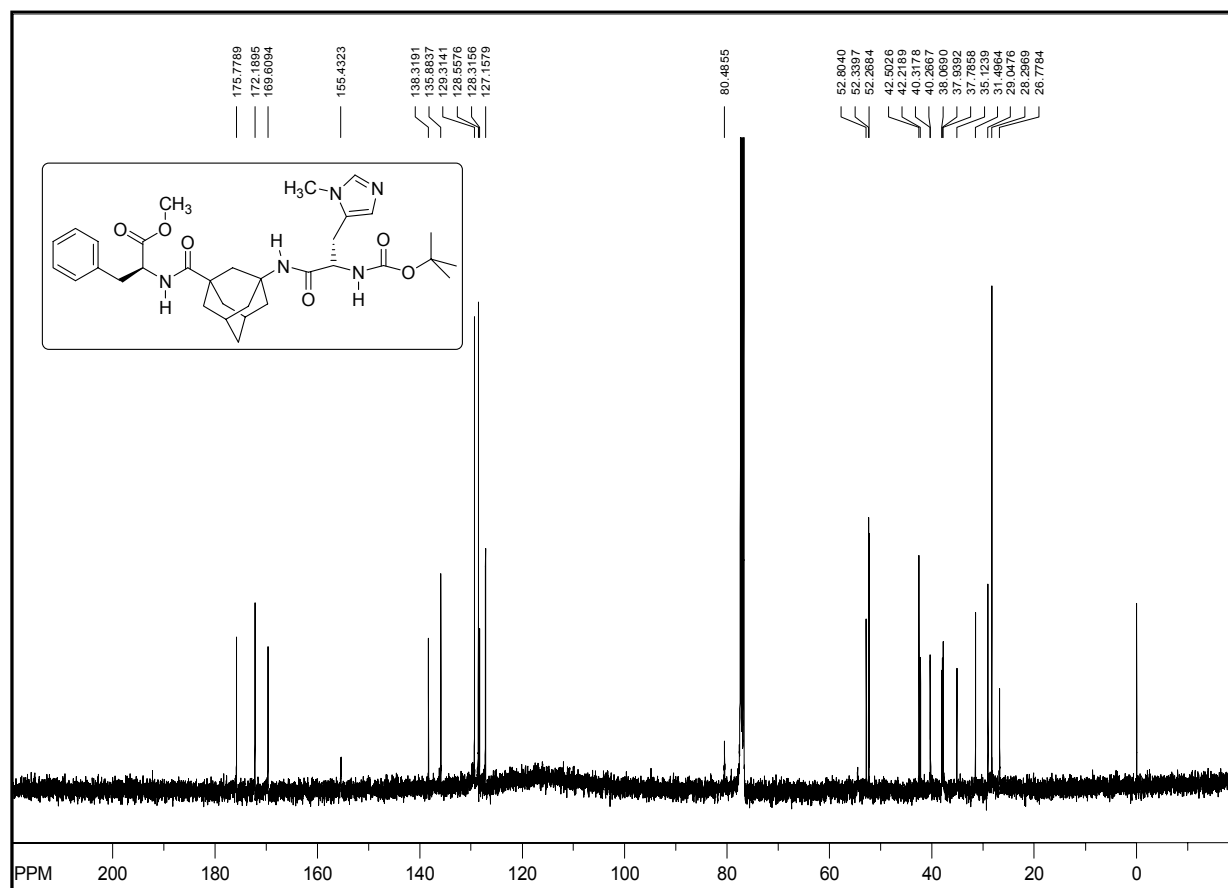
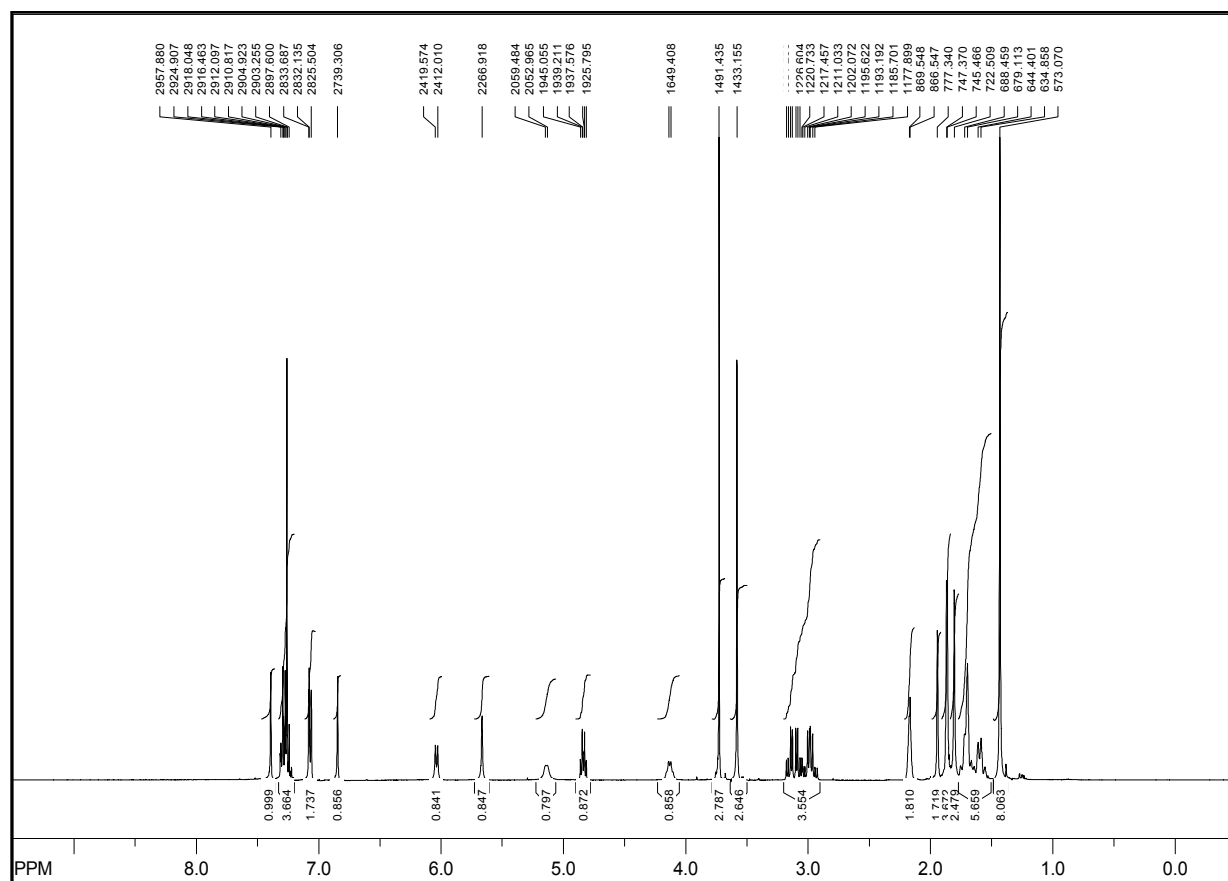


Fmoc-A¹Gly-Phe-OMe (215)

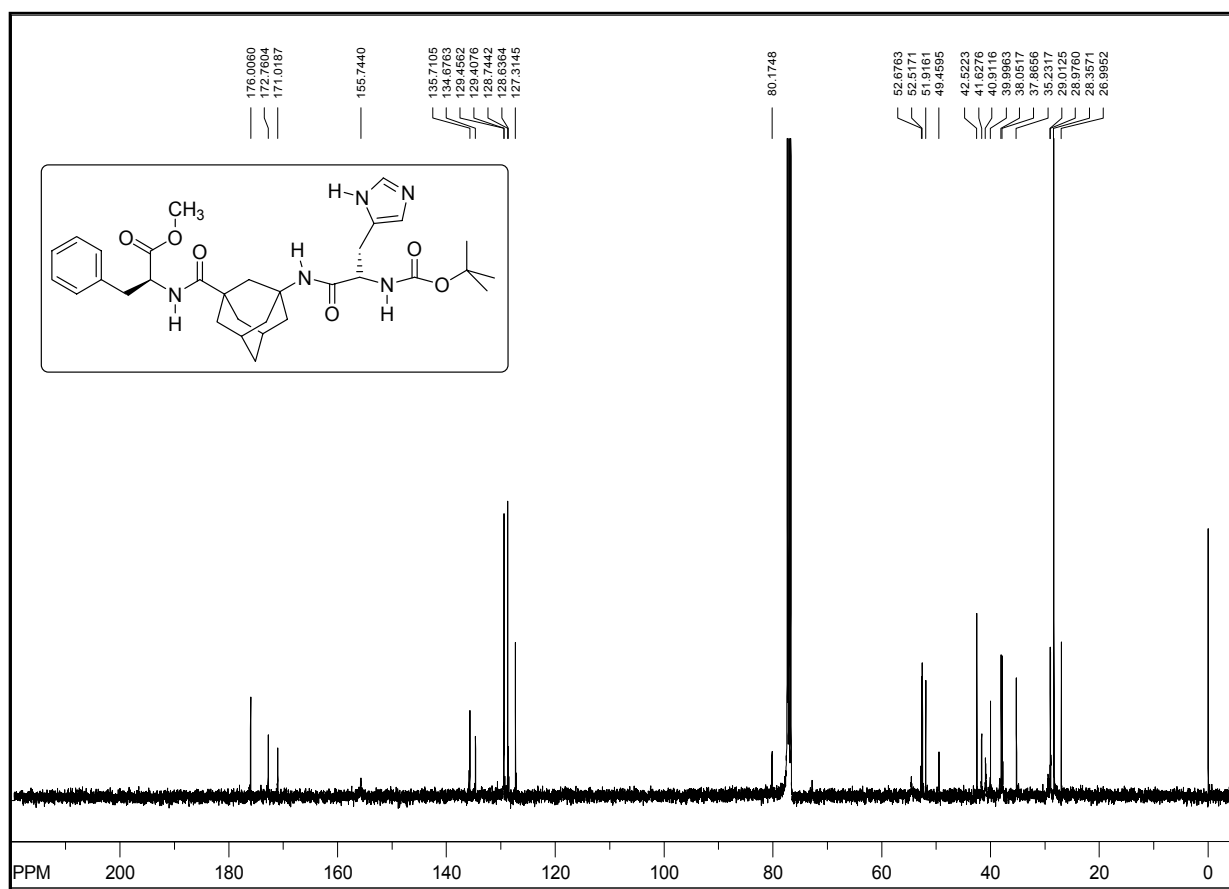
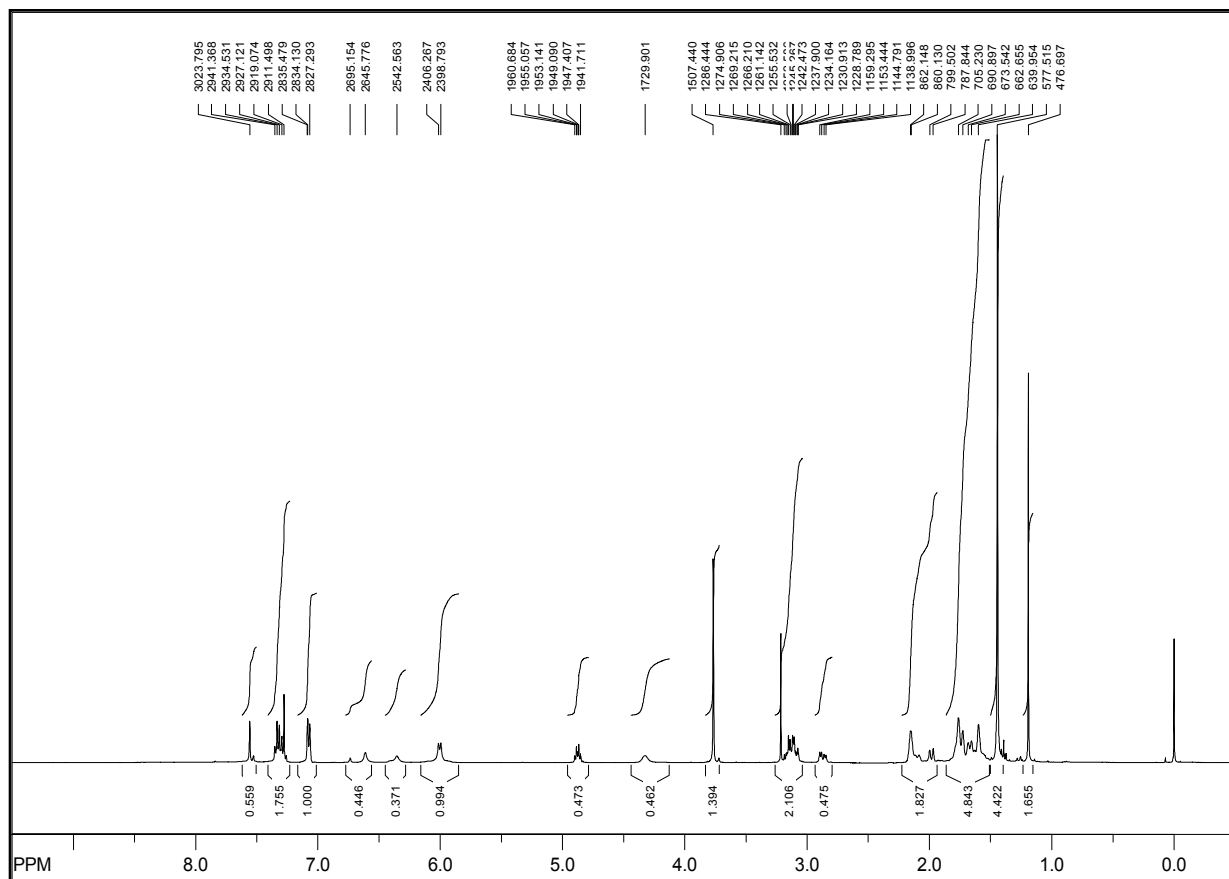
H^A-Gly-Phe-OMe (216)



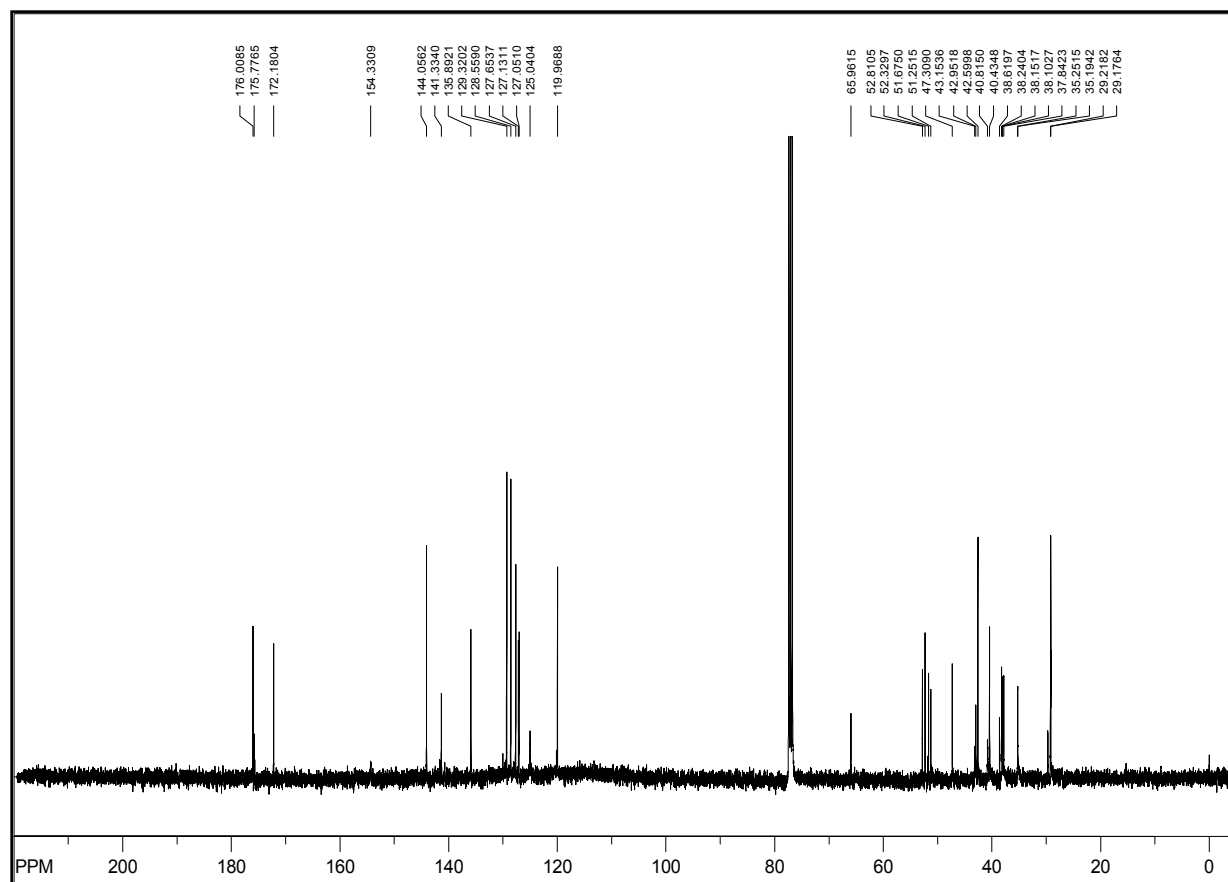
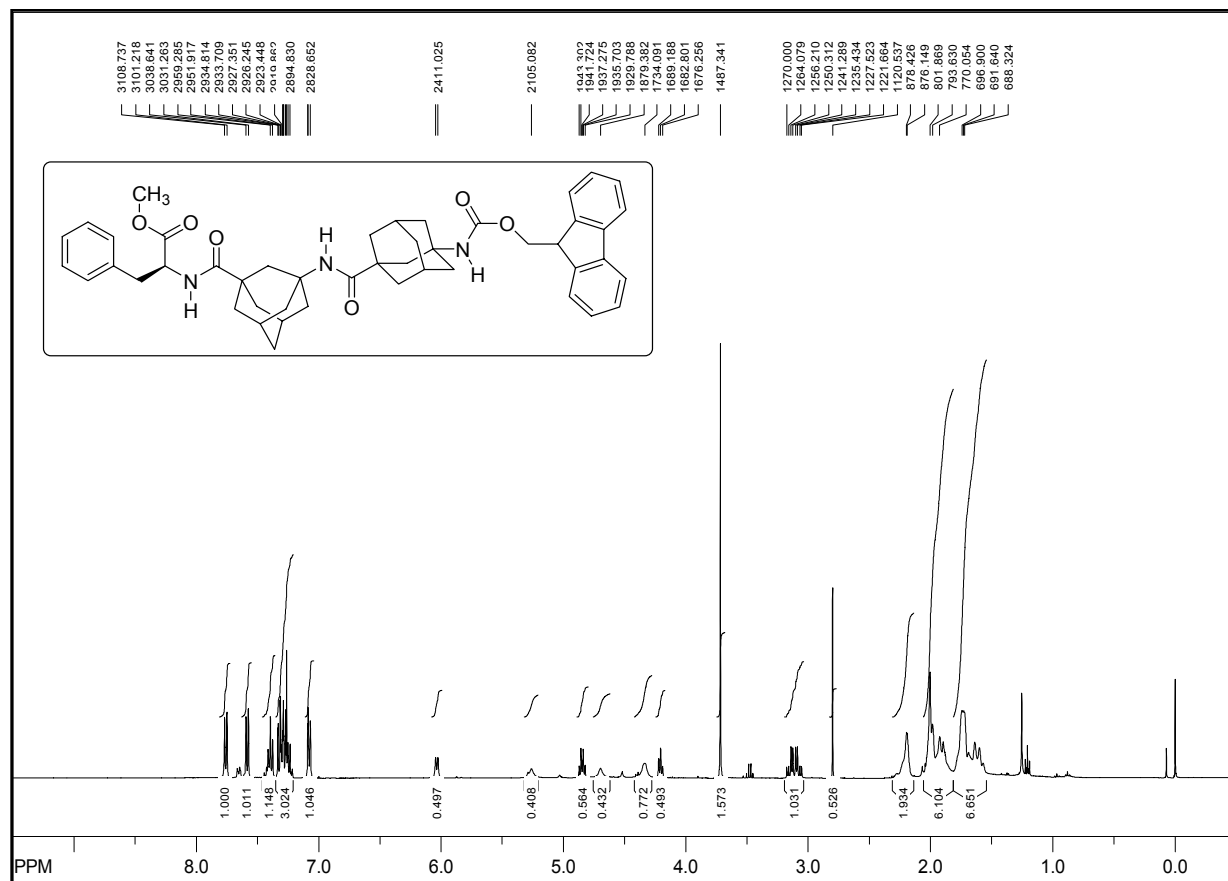
Boc-His(τ -Bn)-A-Gly-Phe-OMe (218)



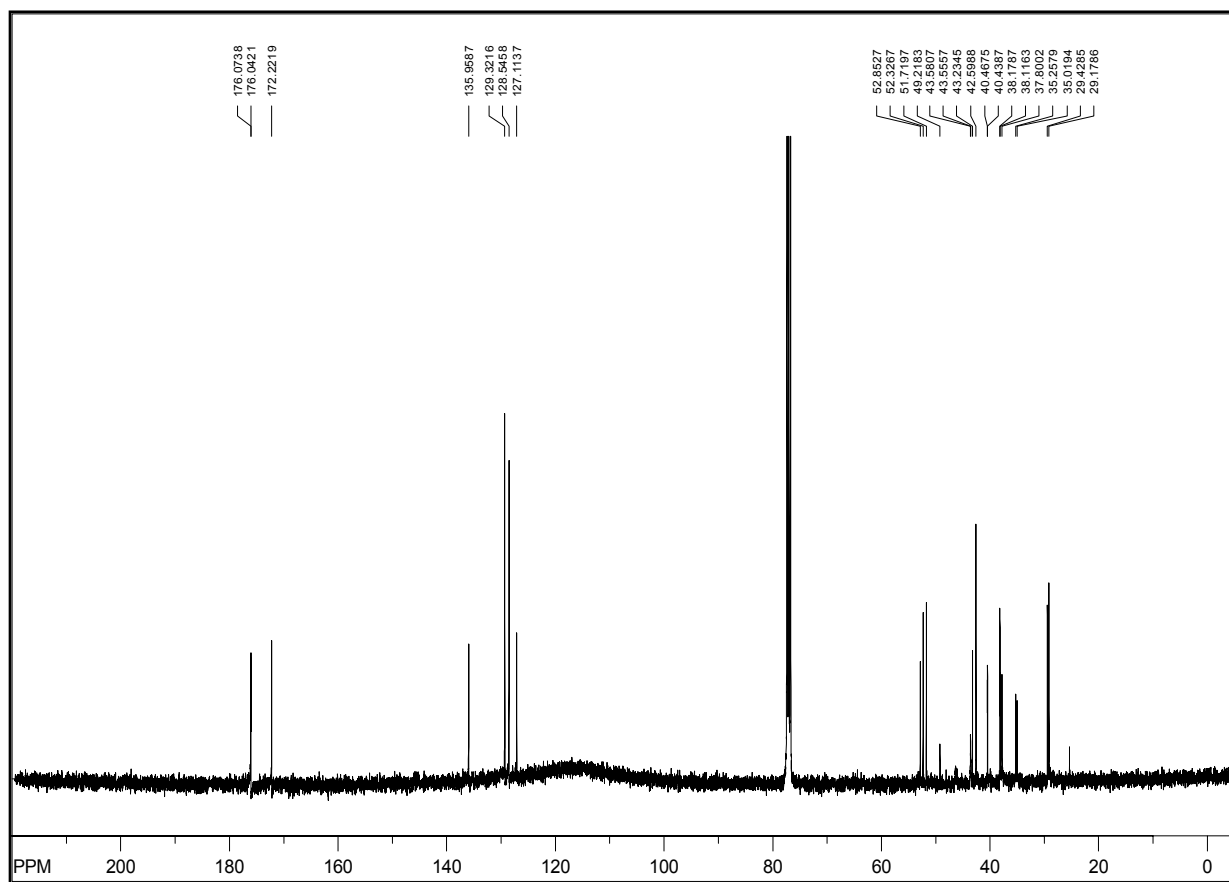
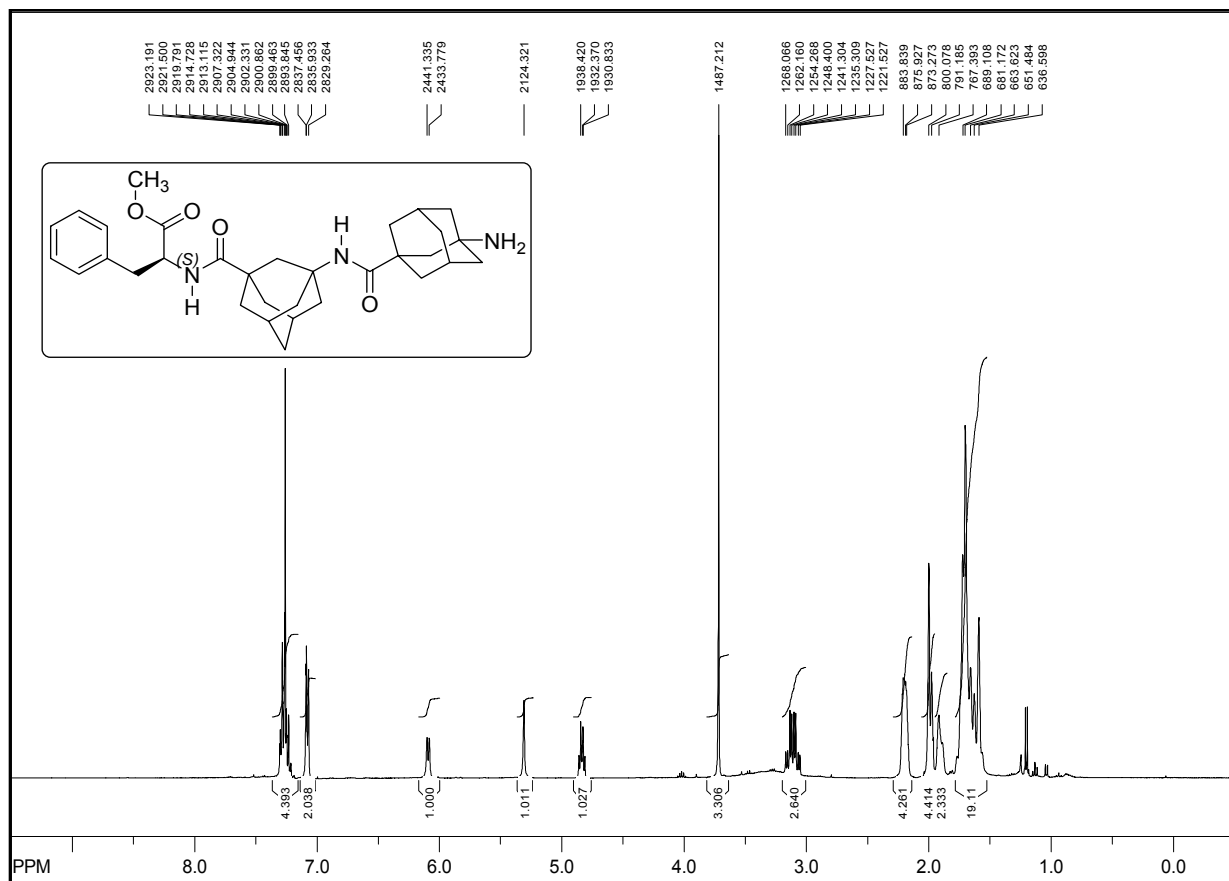
Boc-His(π -Me)-A-Gly-Phe-OMe (220)



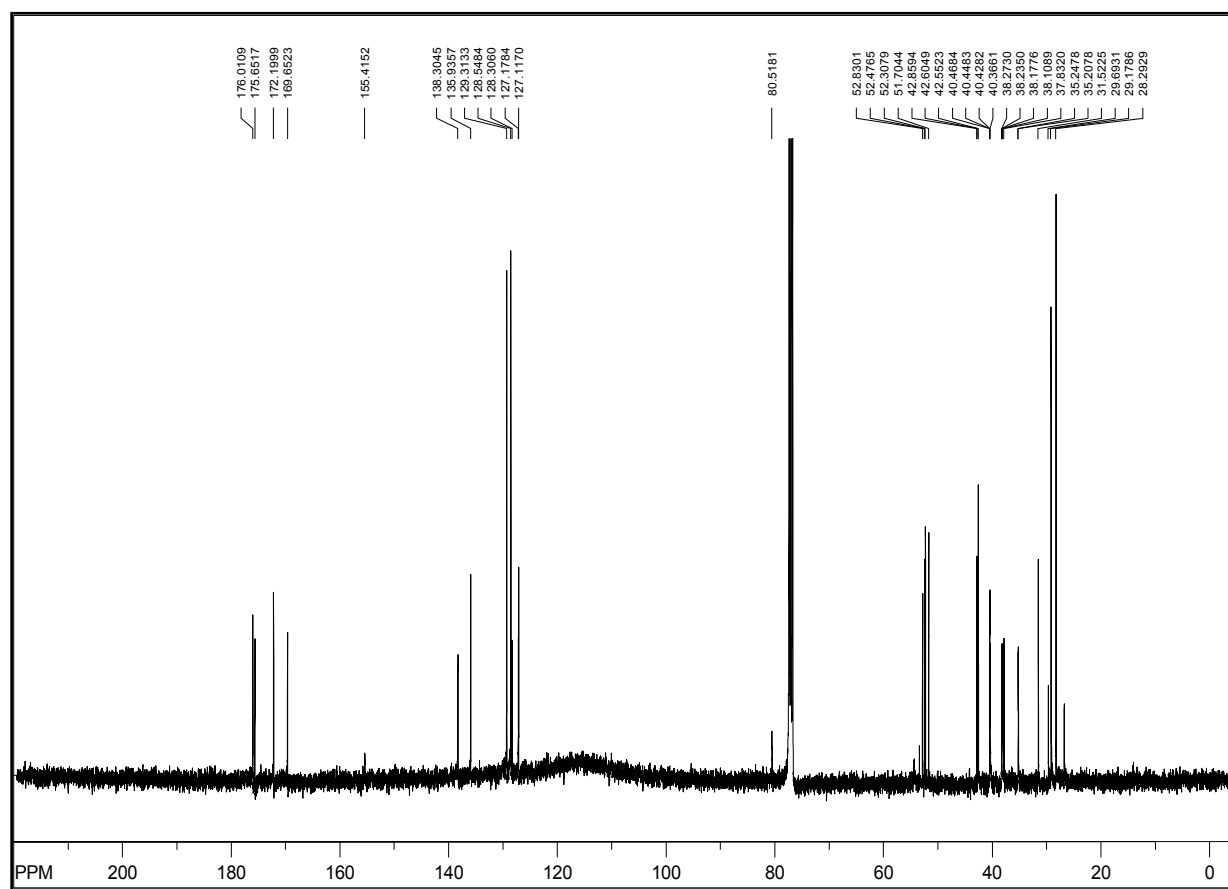
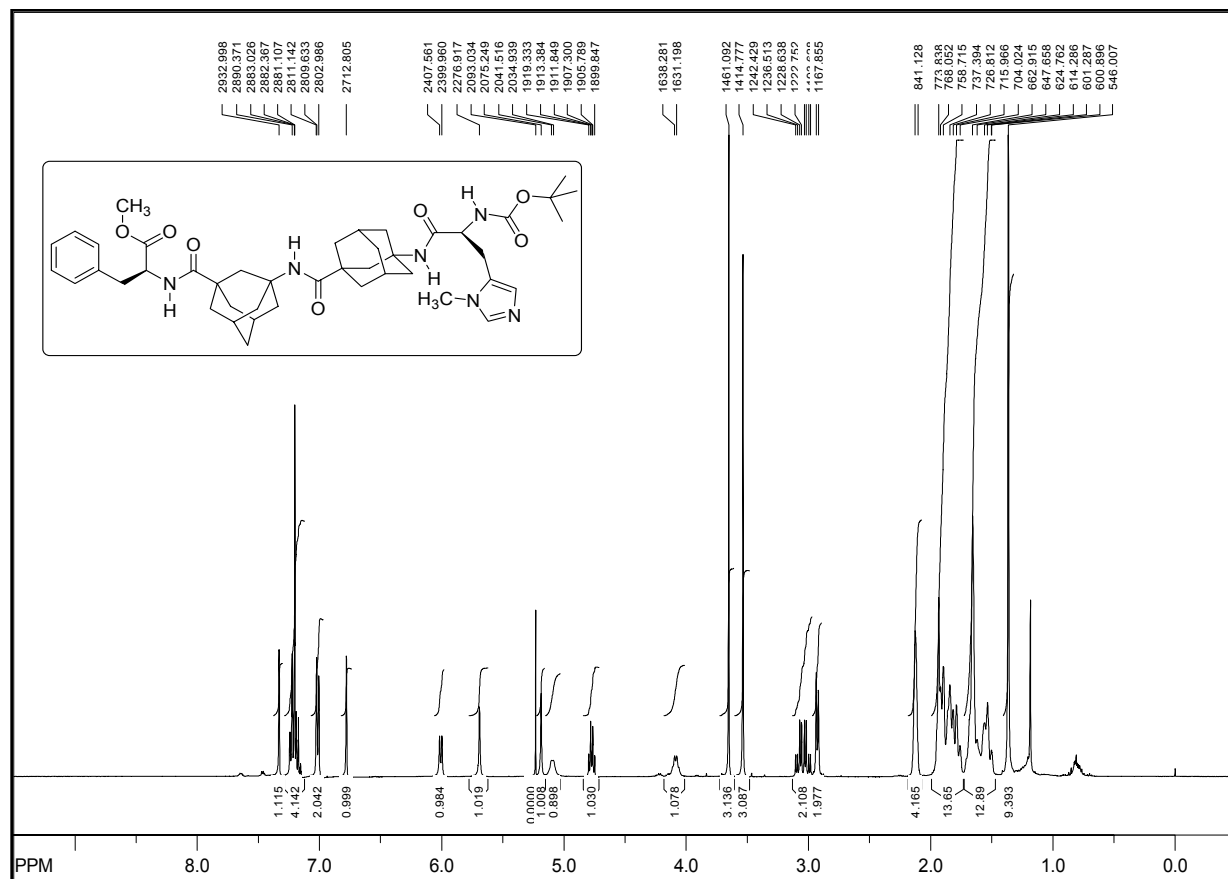
Boc-His-A-Gly-Phe-OMe (222)



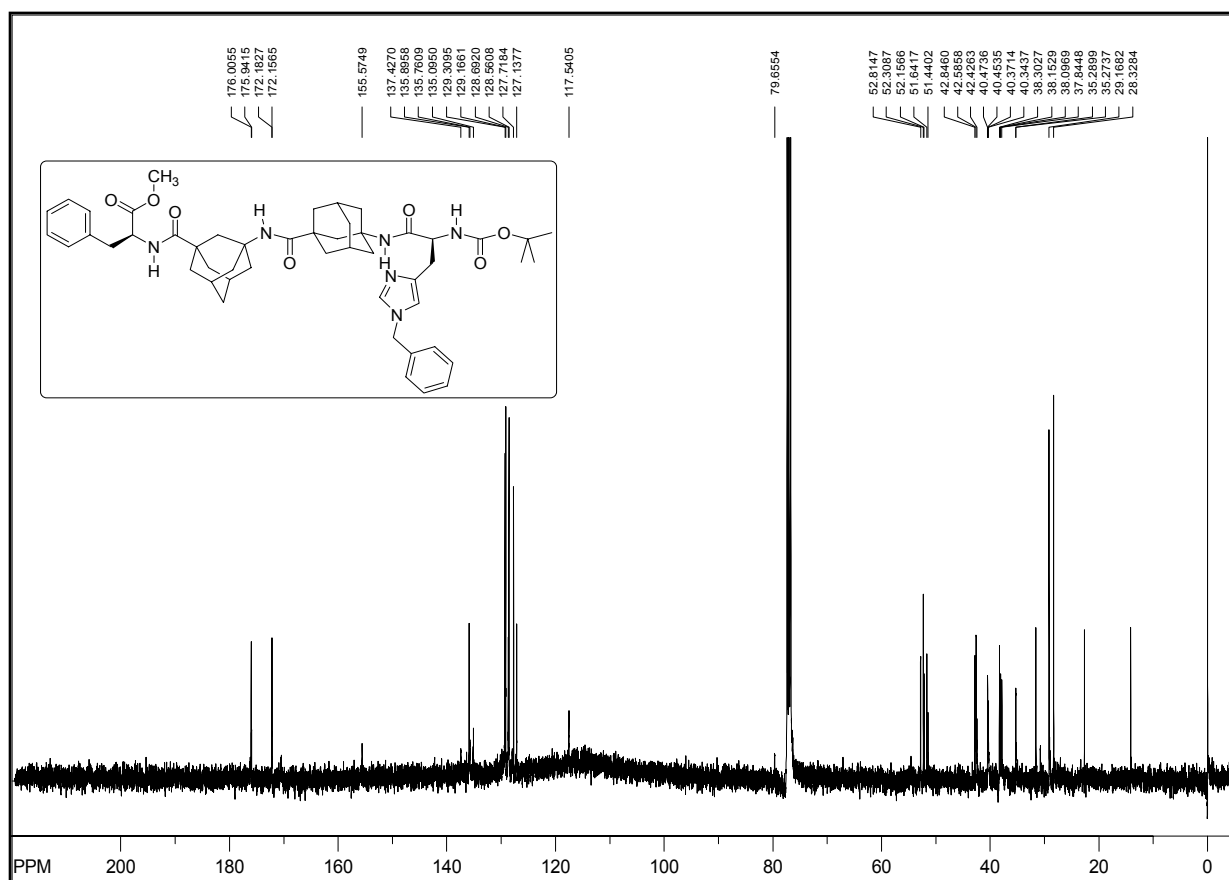
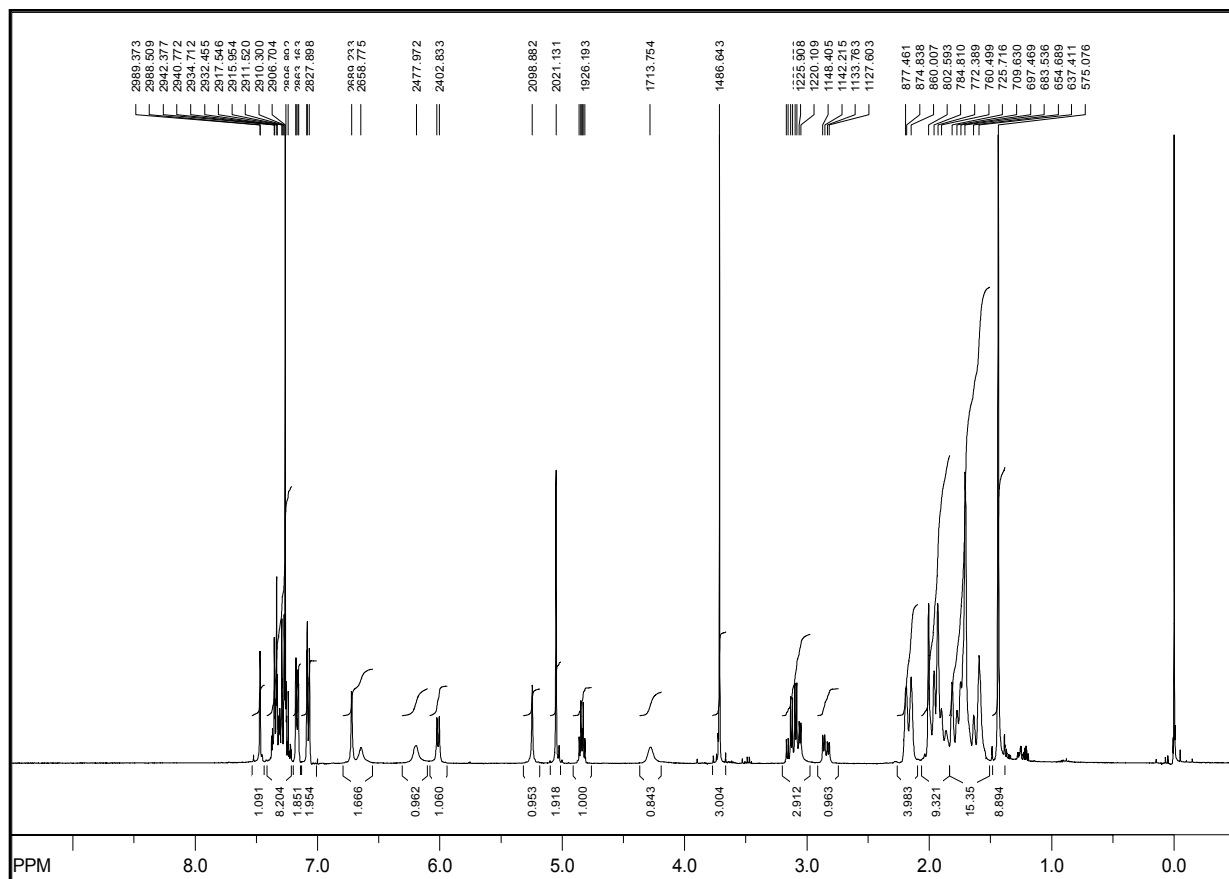
Fmoc-Gly-Gly-Phe-OMe (223)



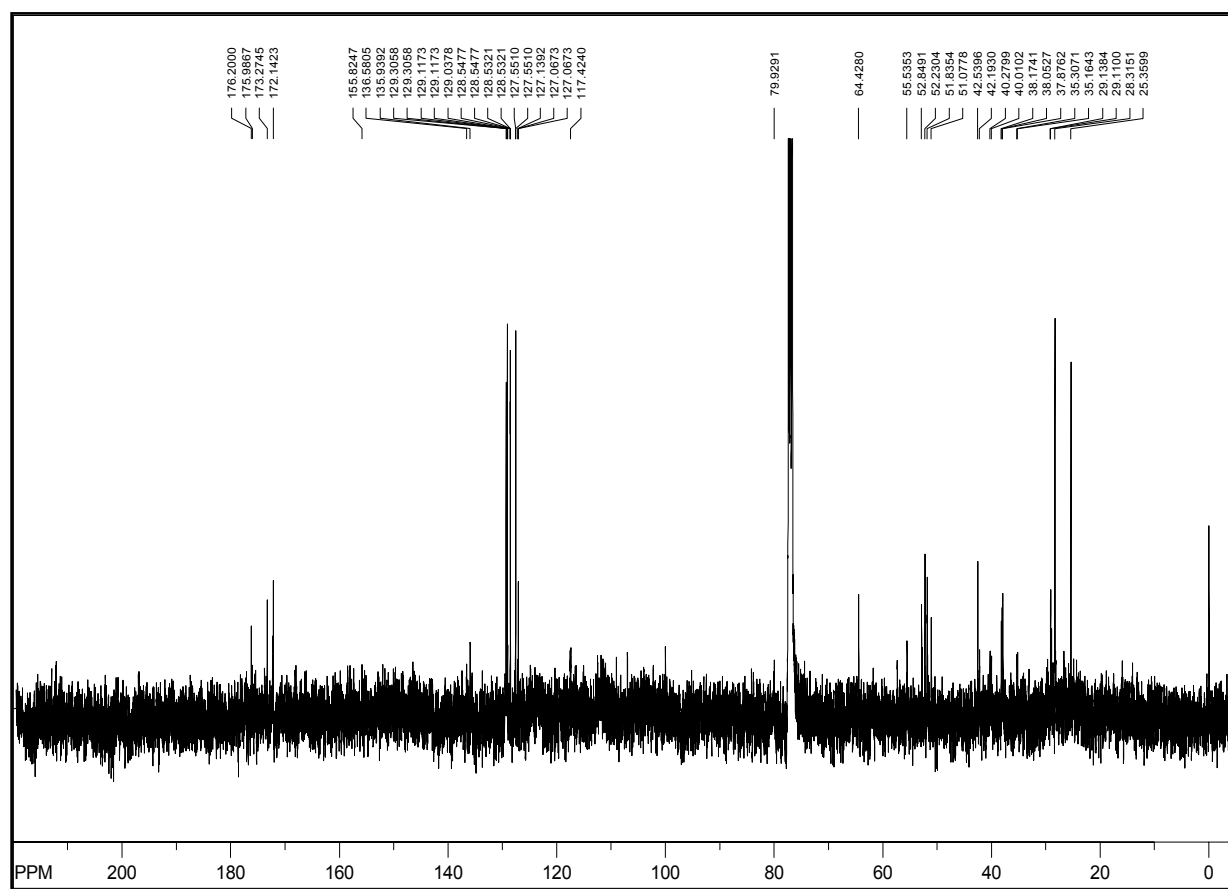
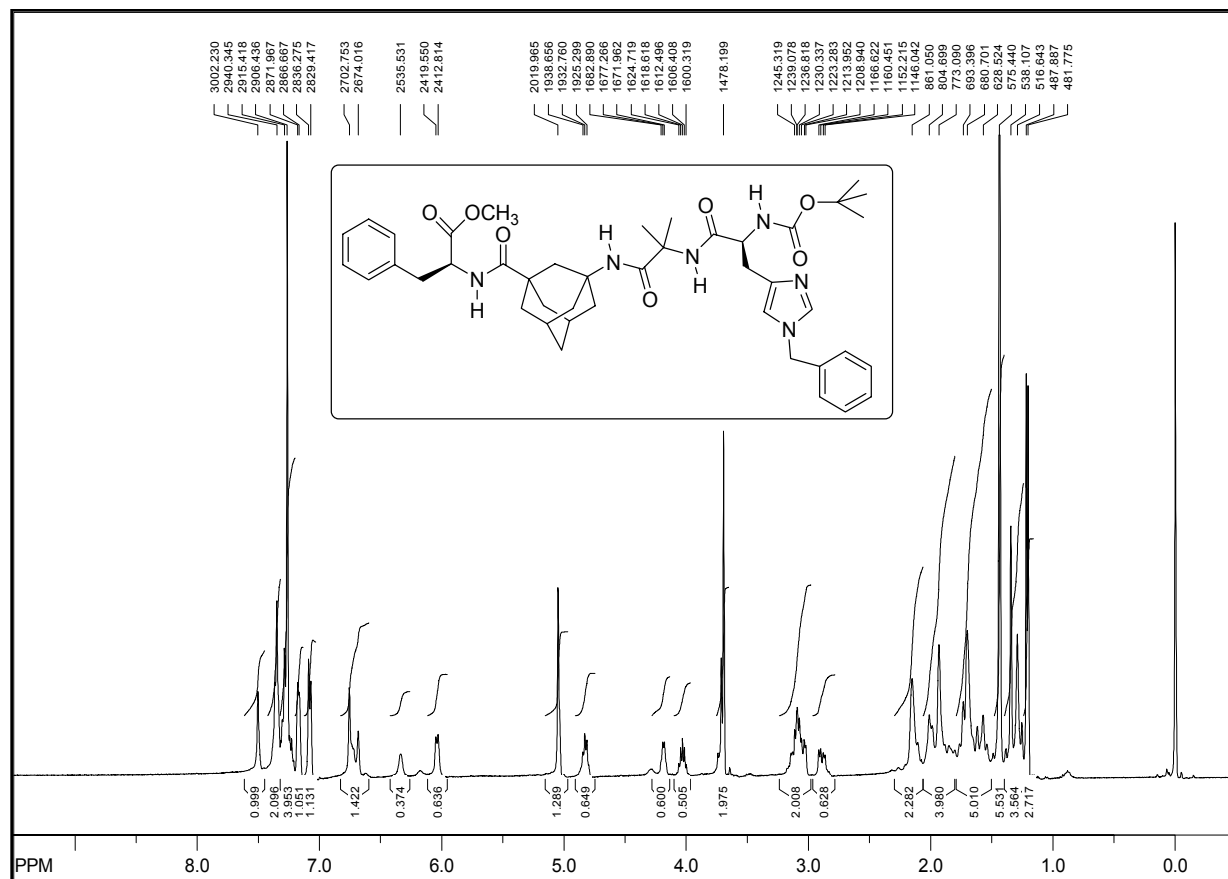
¹H-¹³C Gly-¹³C Gly-Phe-OMe (224)

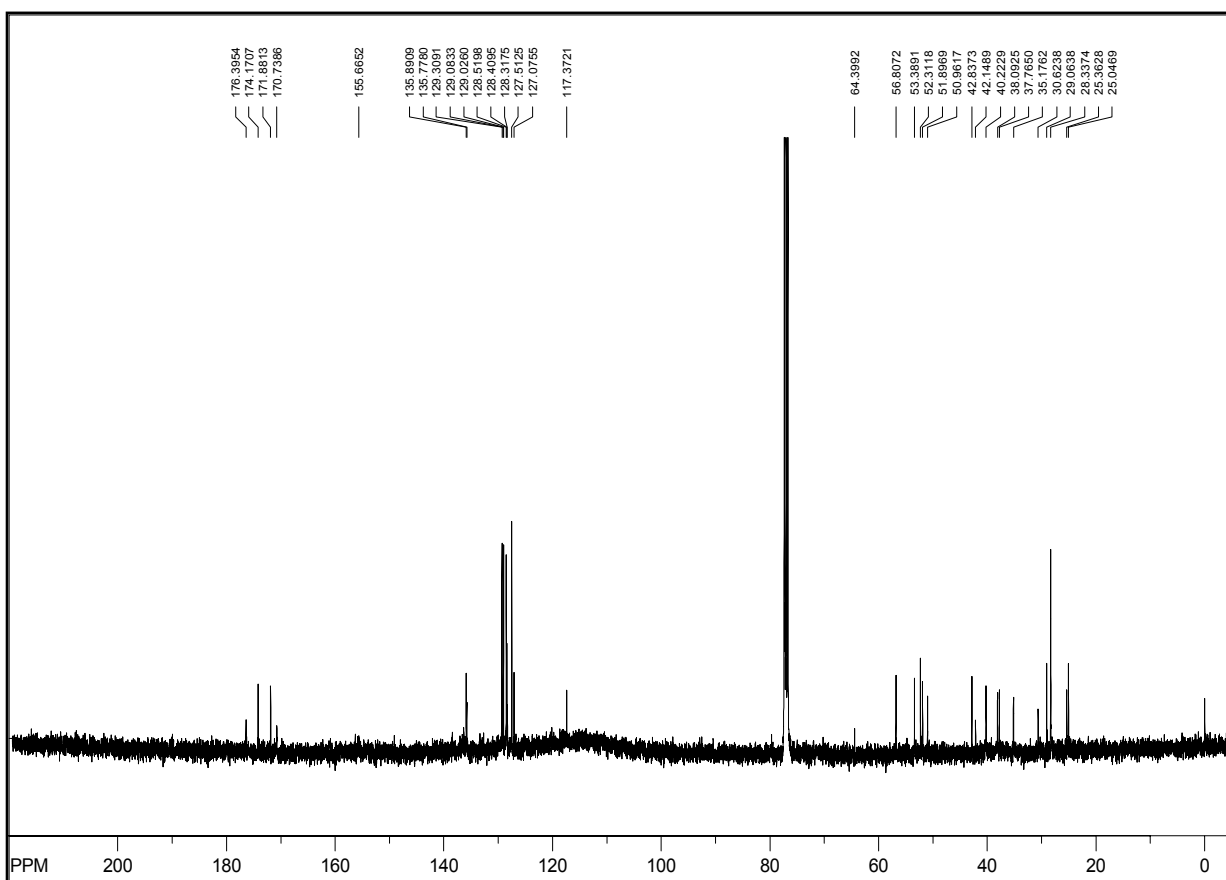
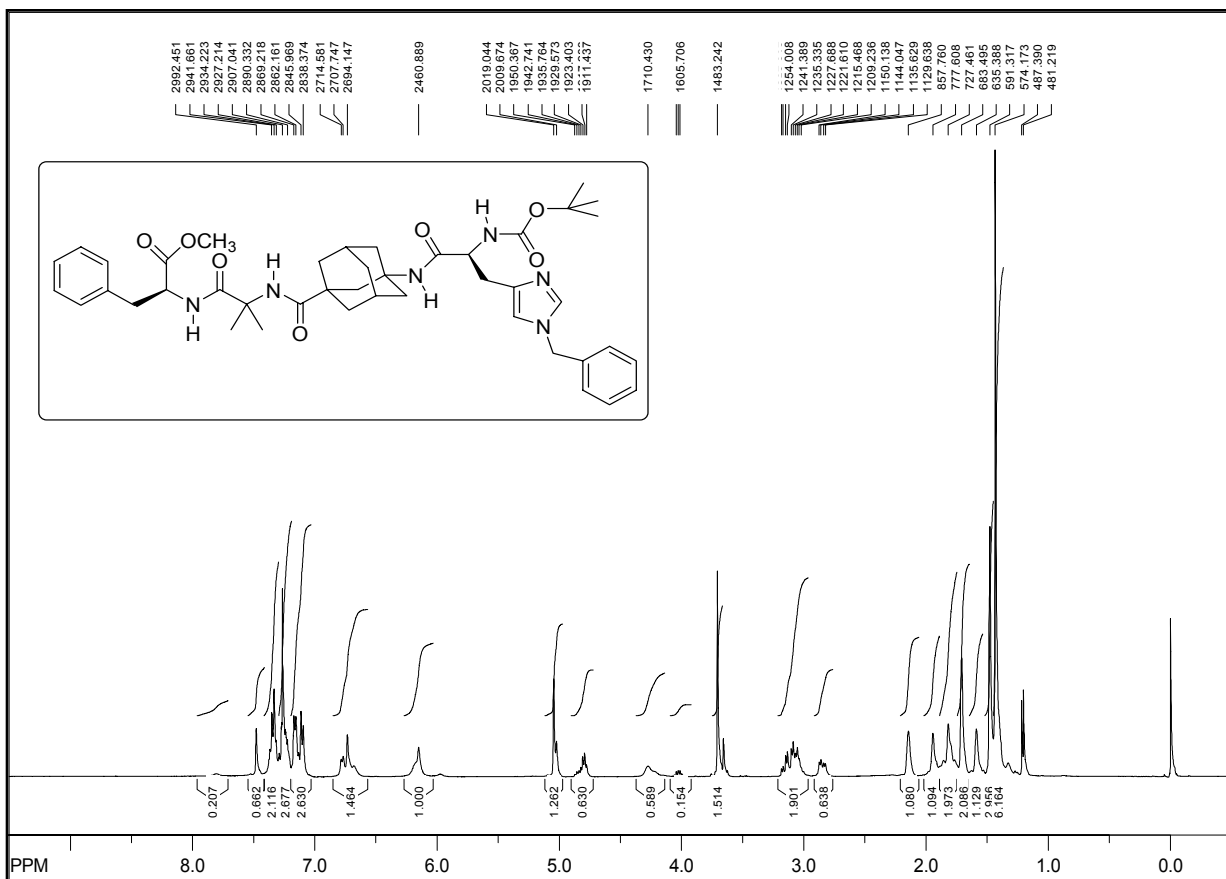


Boc-His(π-Me)-A-Gly-A-Gly-Phe-OMe (225)

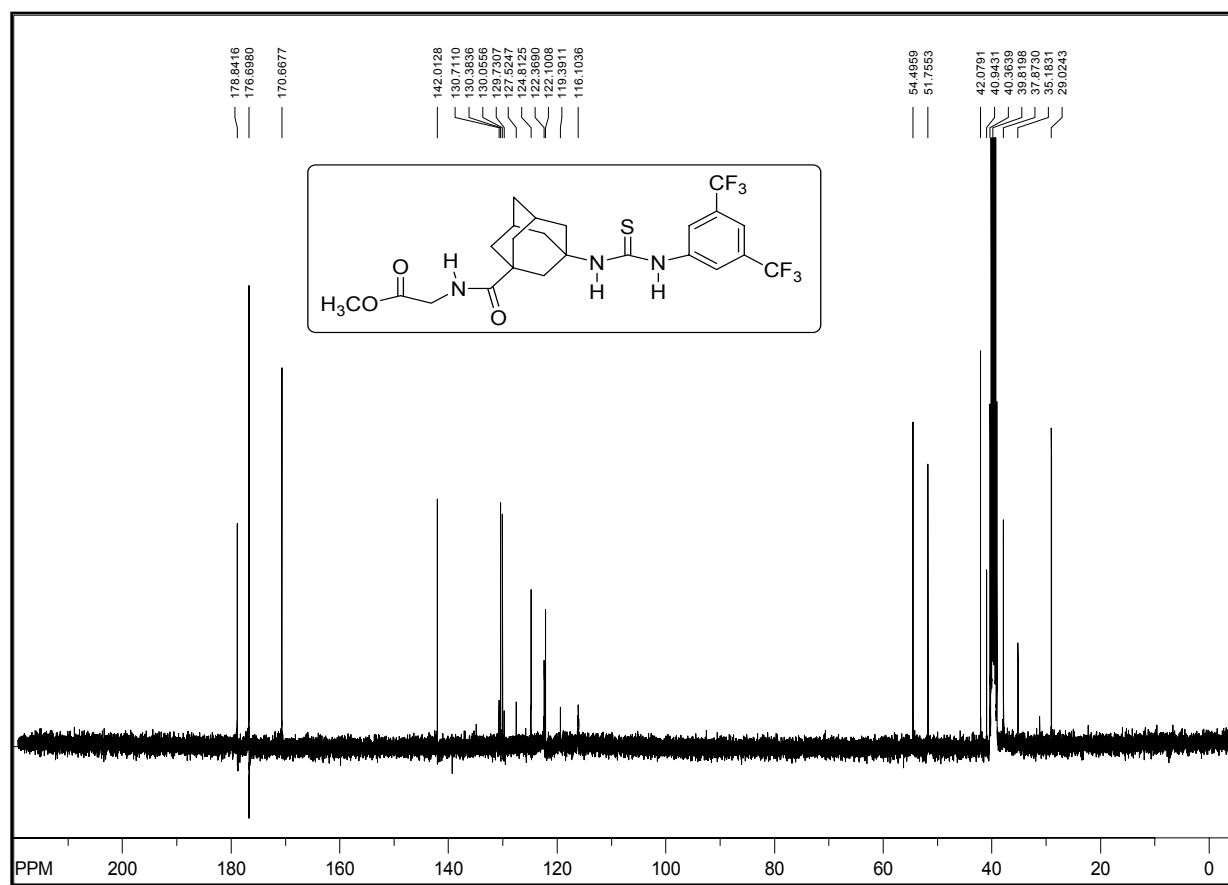
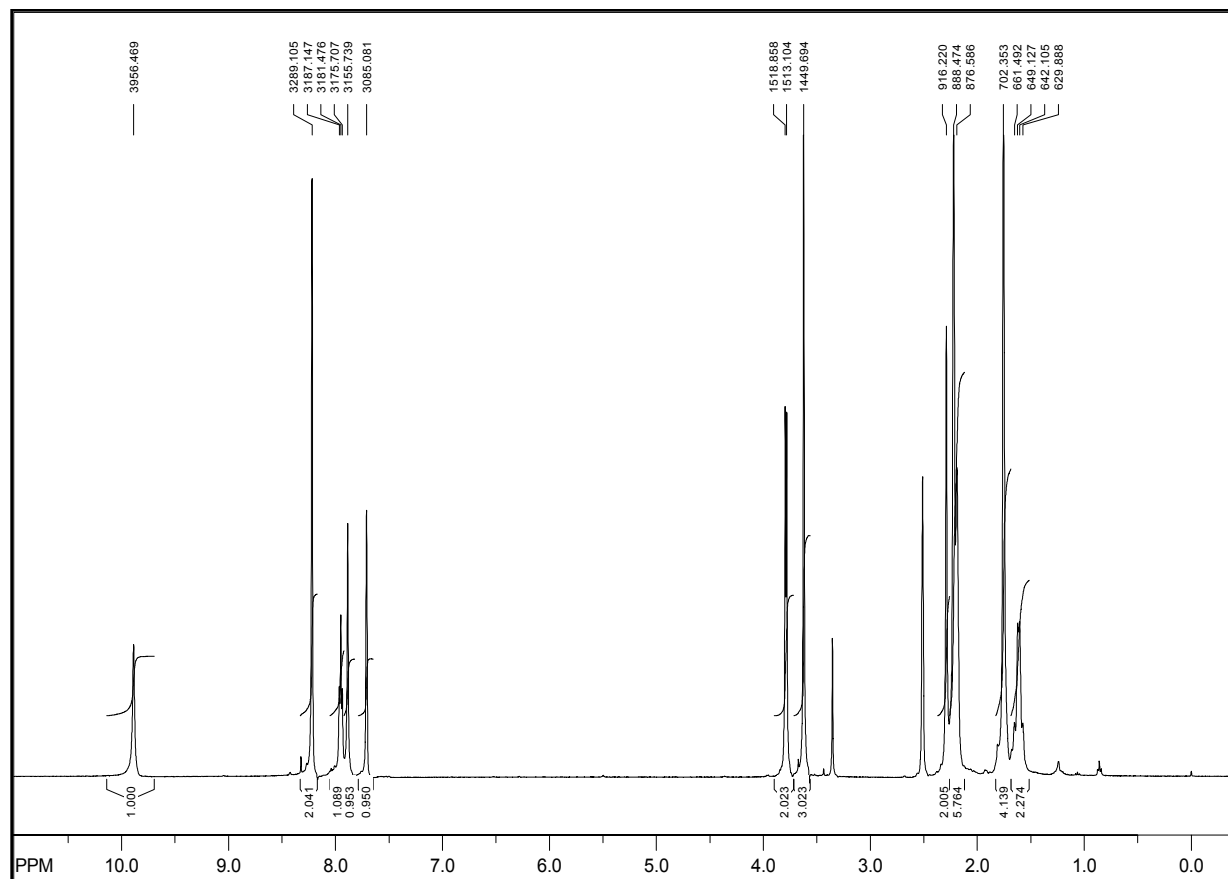


Boc-His(τ -Bn)-^AGly-^AGly-Phe-OMe (226)

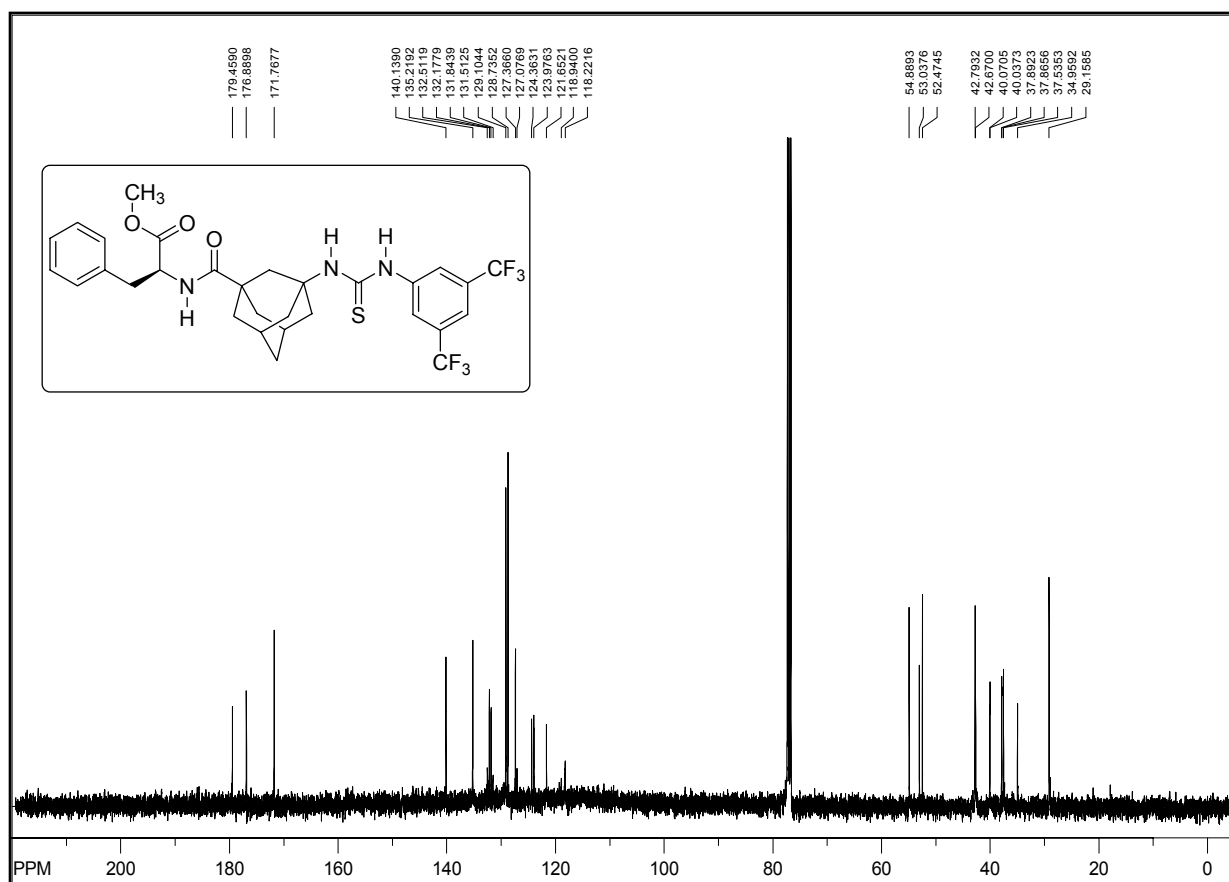
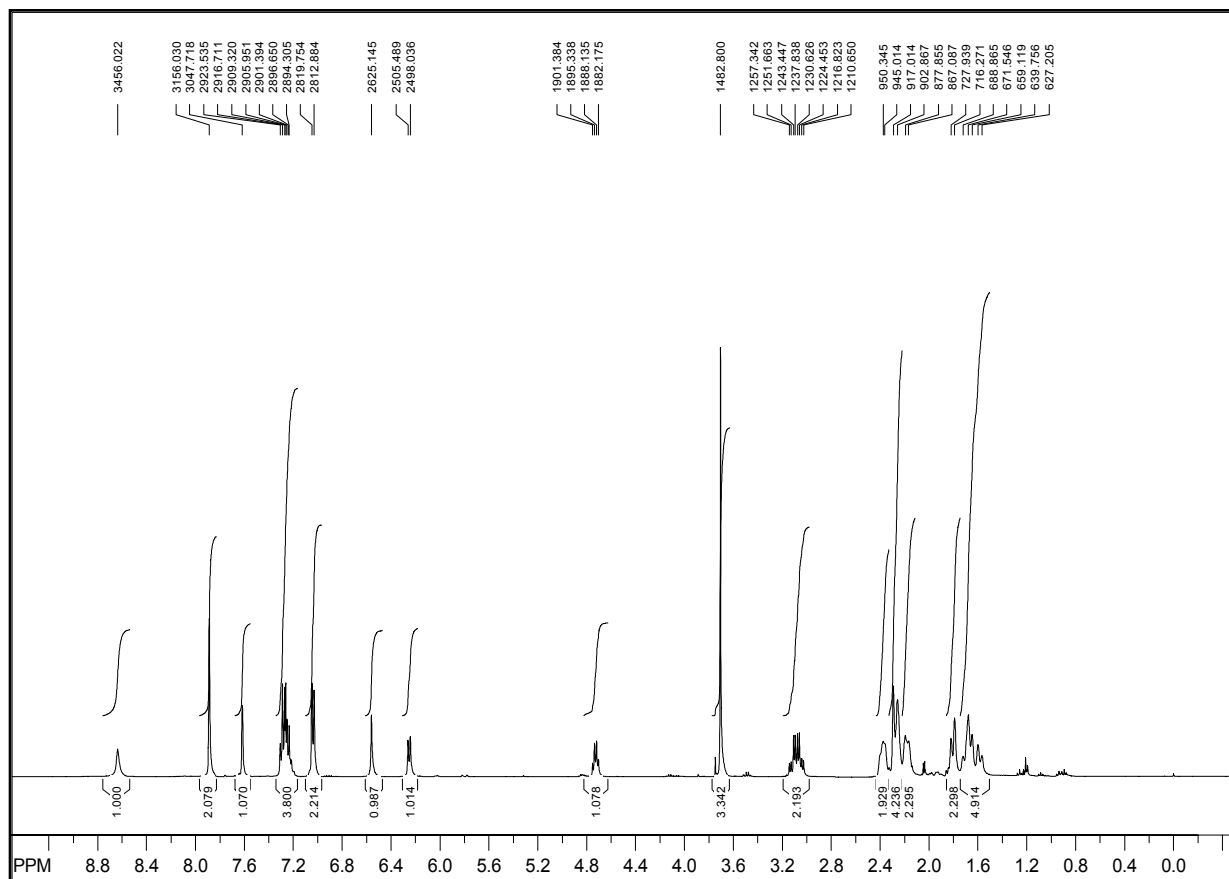
Boc-His(τ -Bn)-Aib-^AGly-Phe-OME (227)



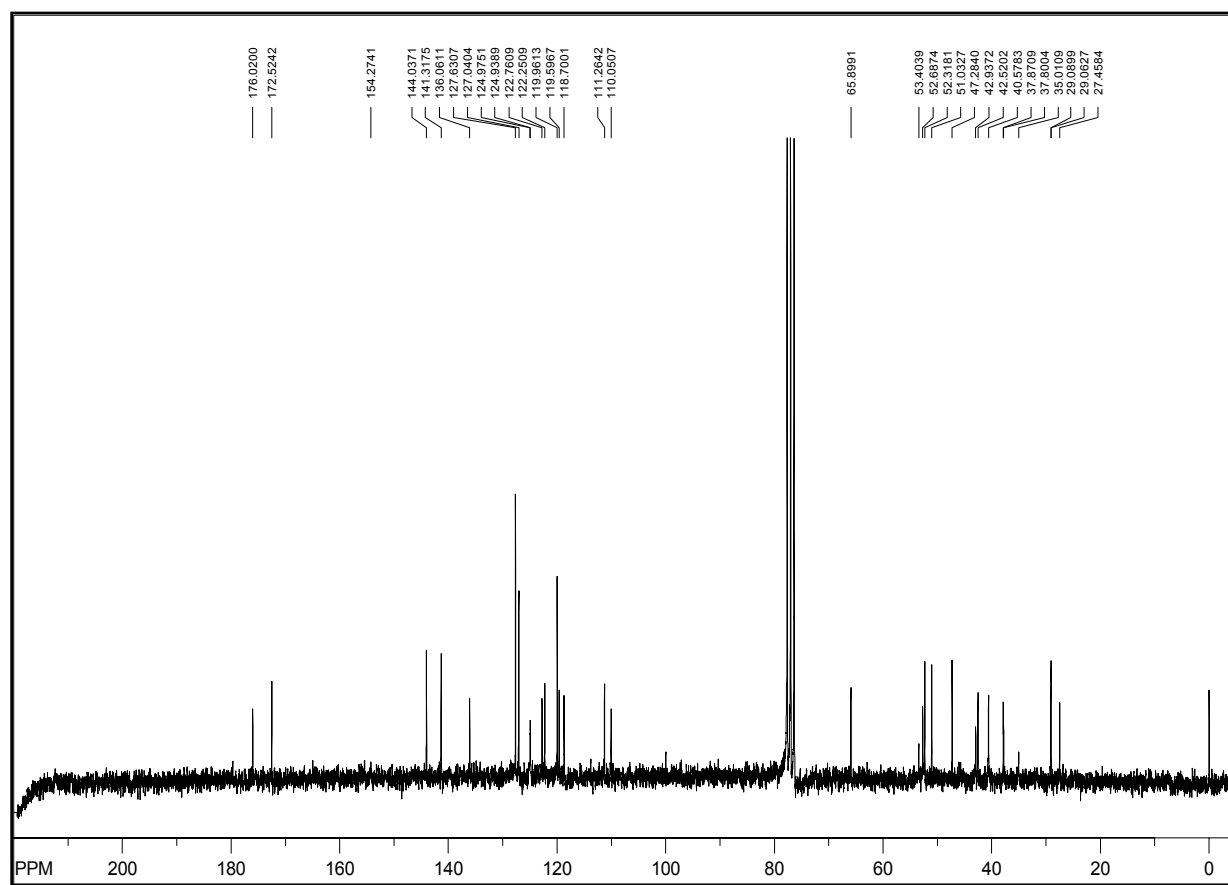
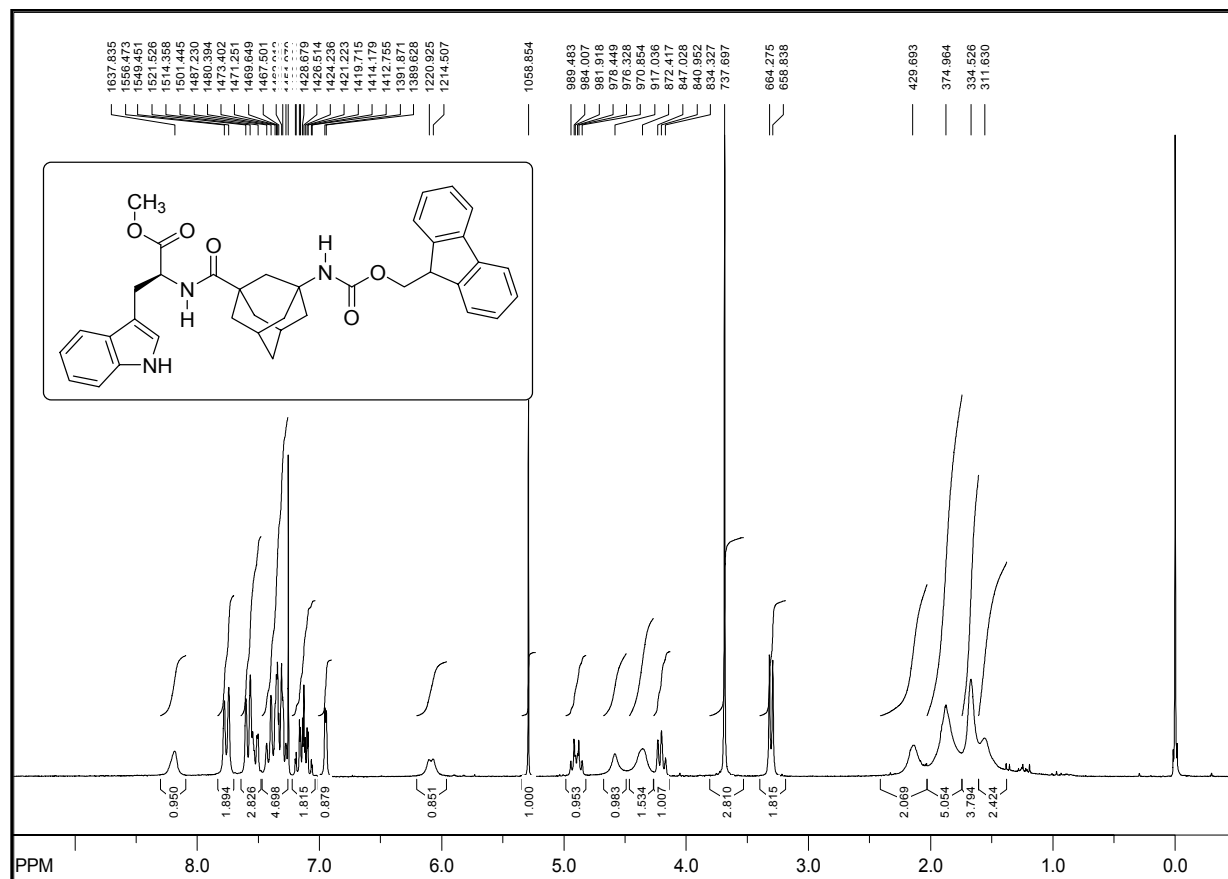
Boc-His(τ -Bn)-^AGly-Aib-Phe-OMe (228)



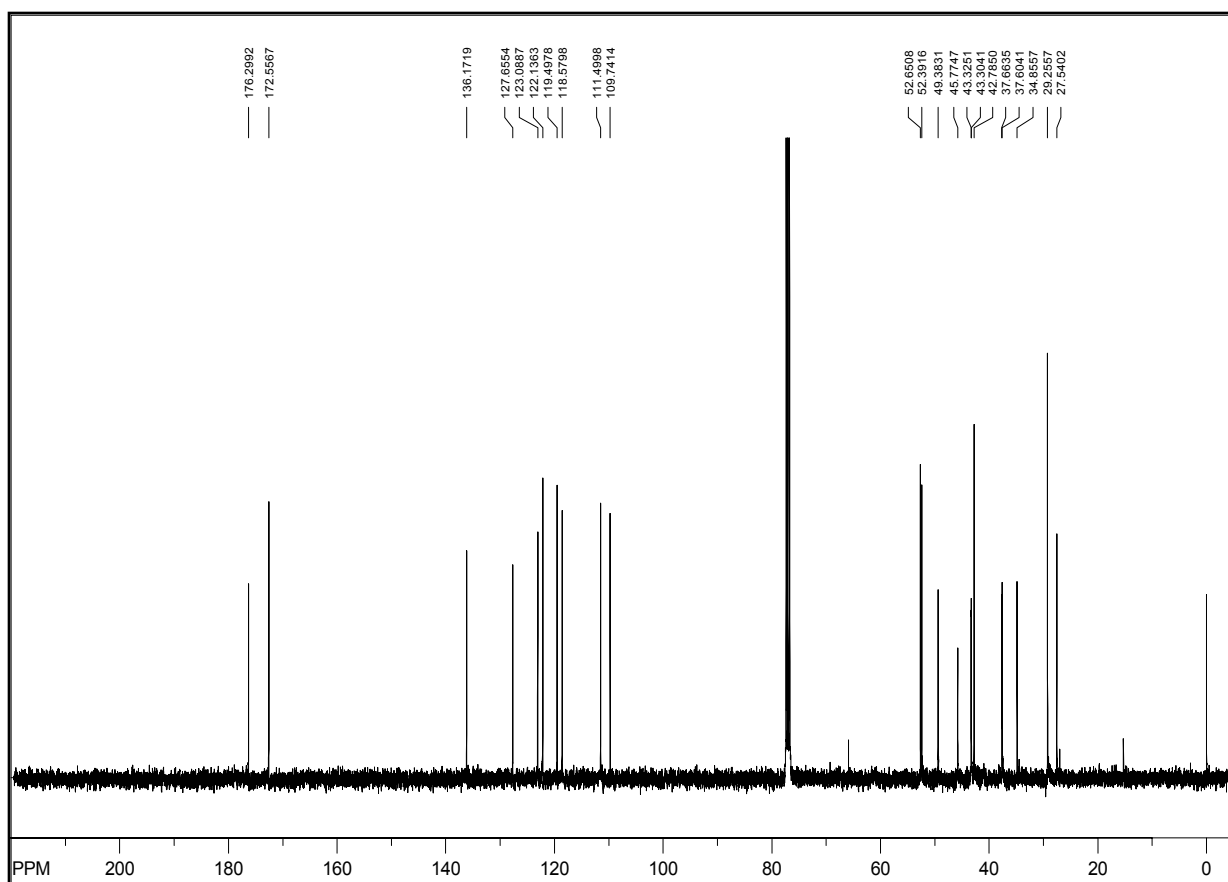
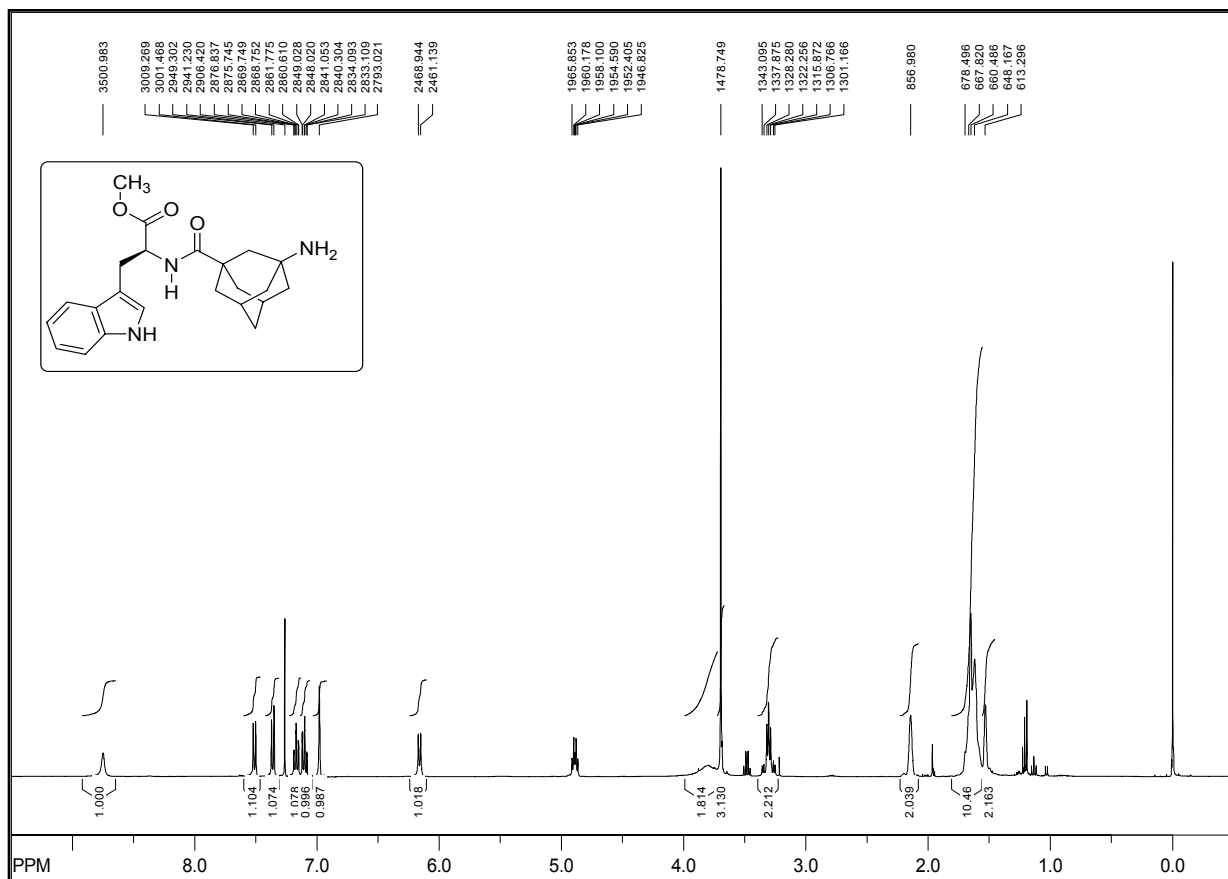
TU-A Gly-Gly-OMe (239a)



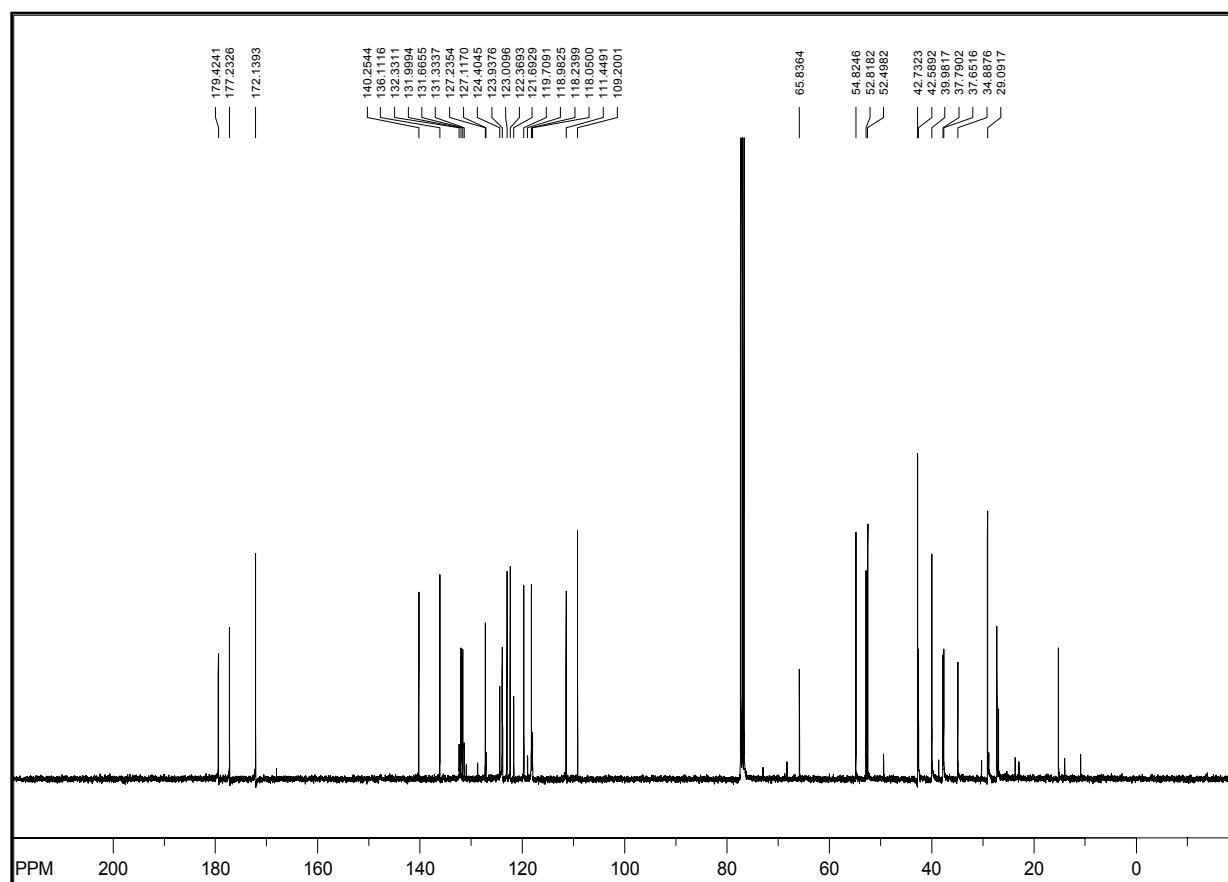
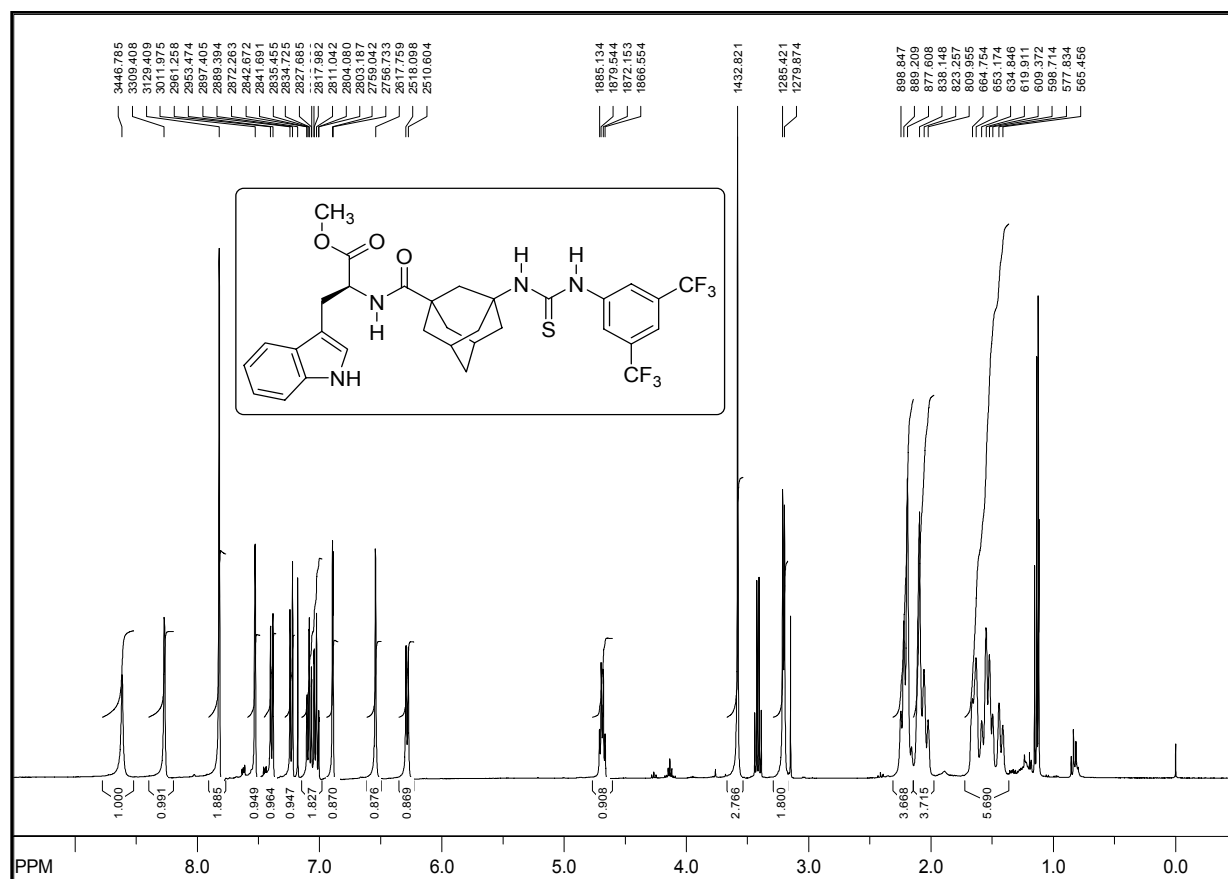
TU-A Gly-Phe-OMe (239b)



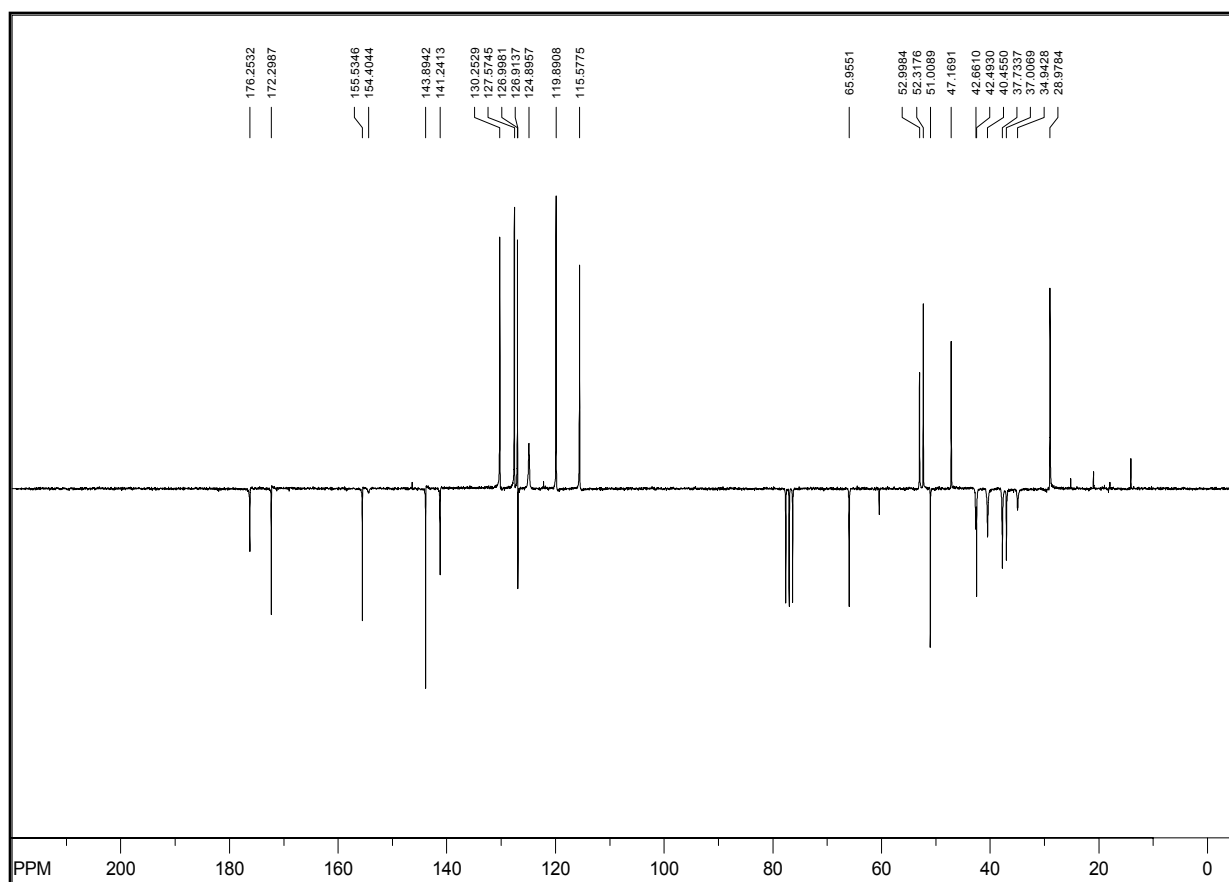
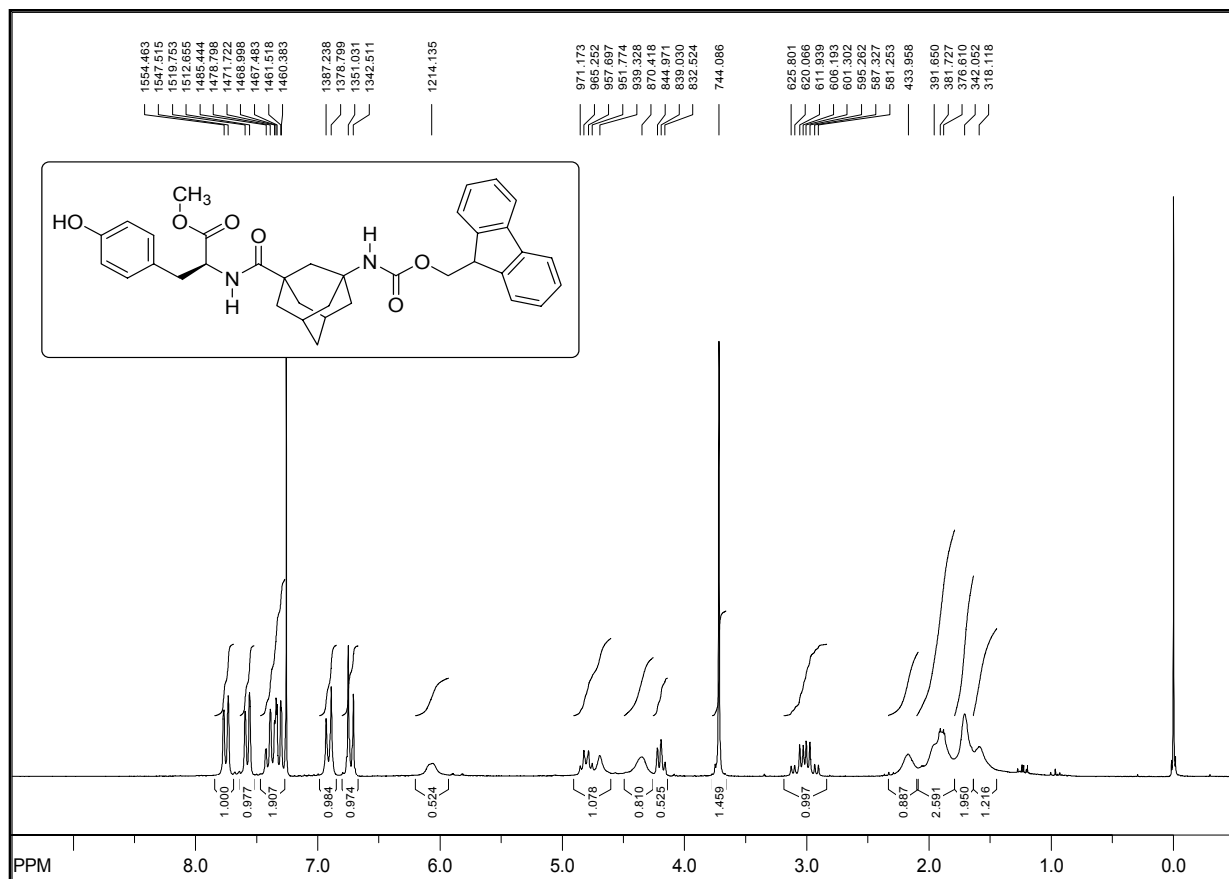
Fmoc-A-Gly-Trp-OMe (242)



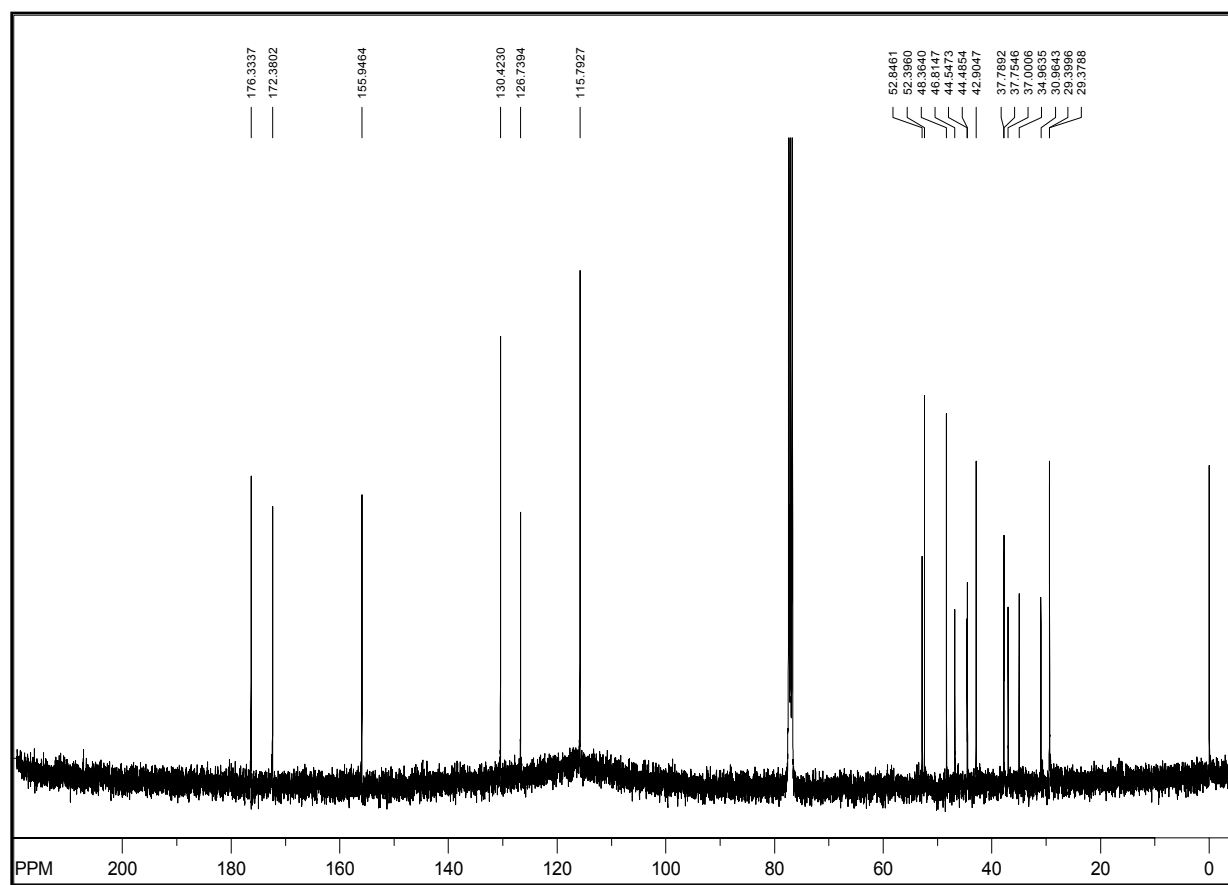
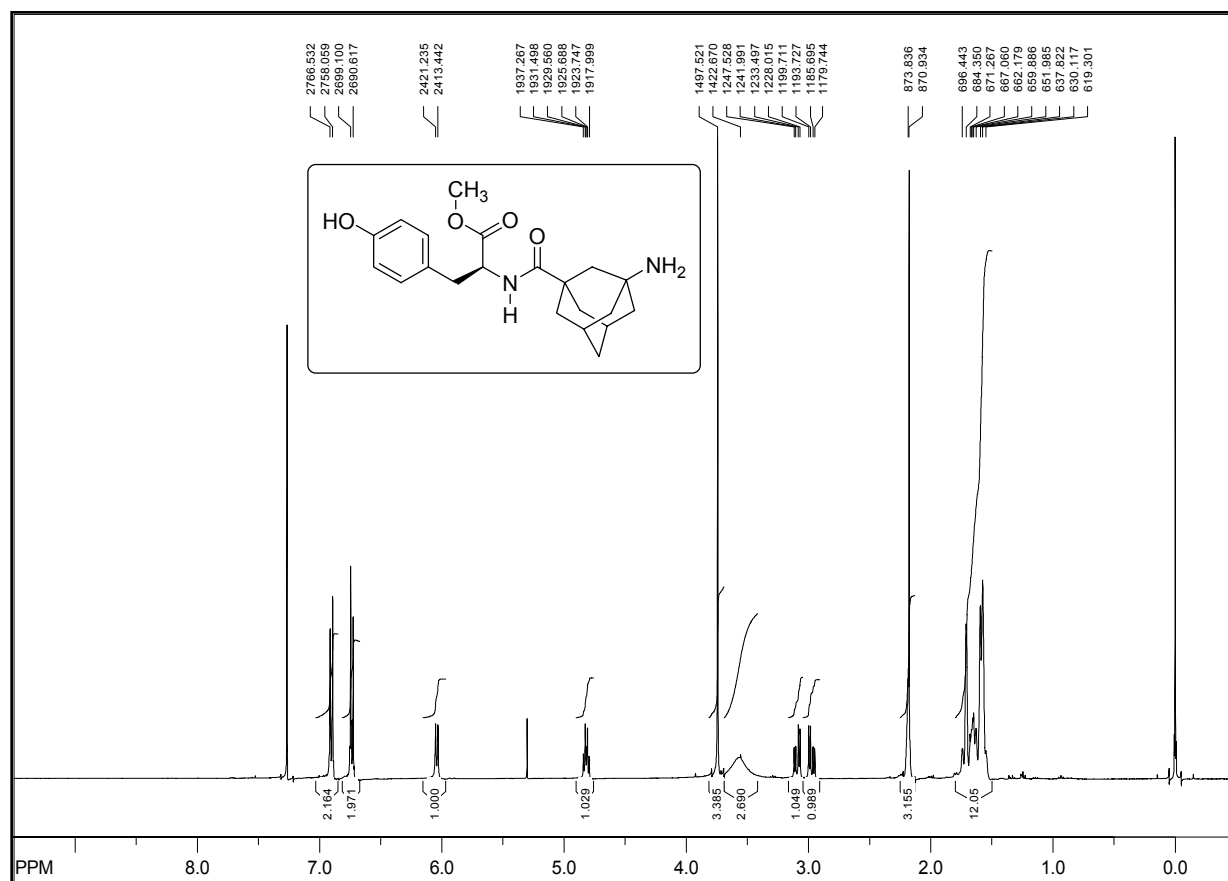
^1H - ^1H Gly-Trp-OMe (243)



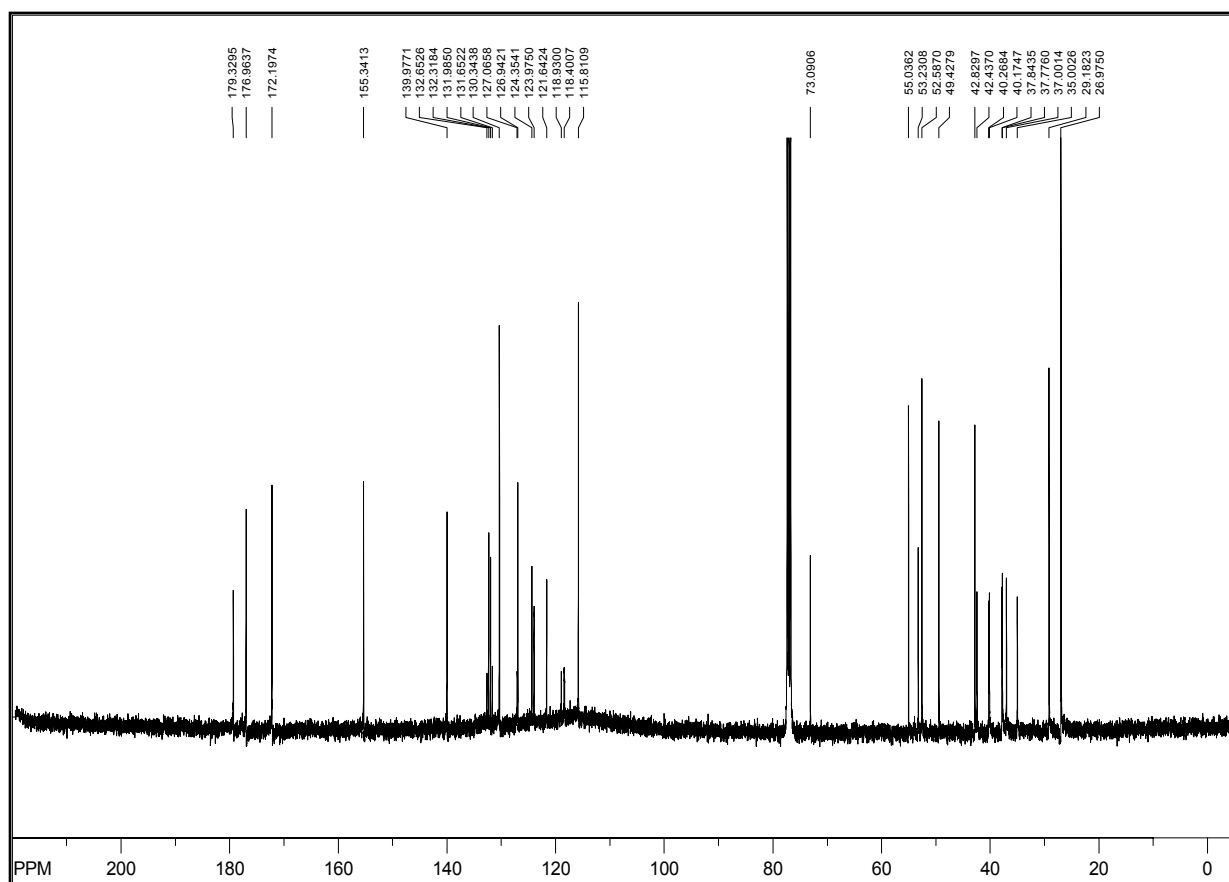
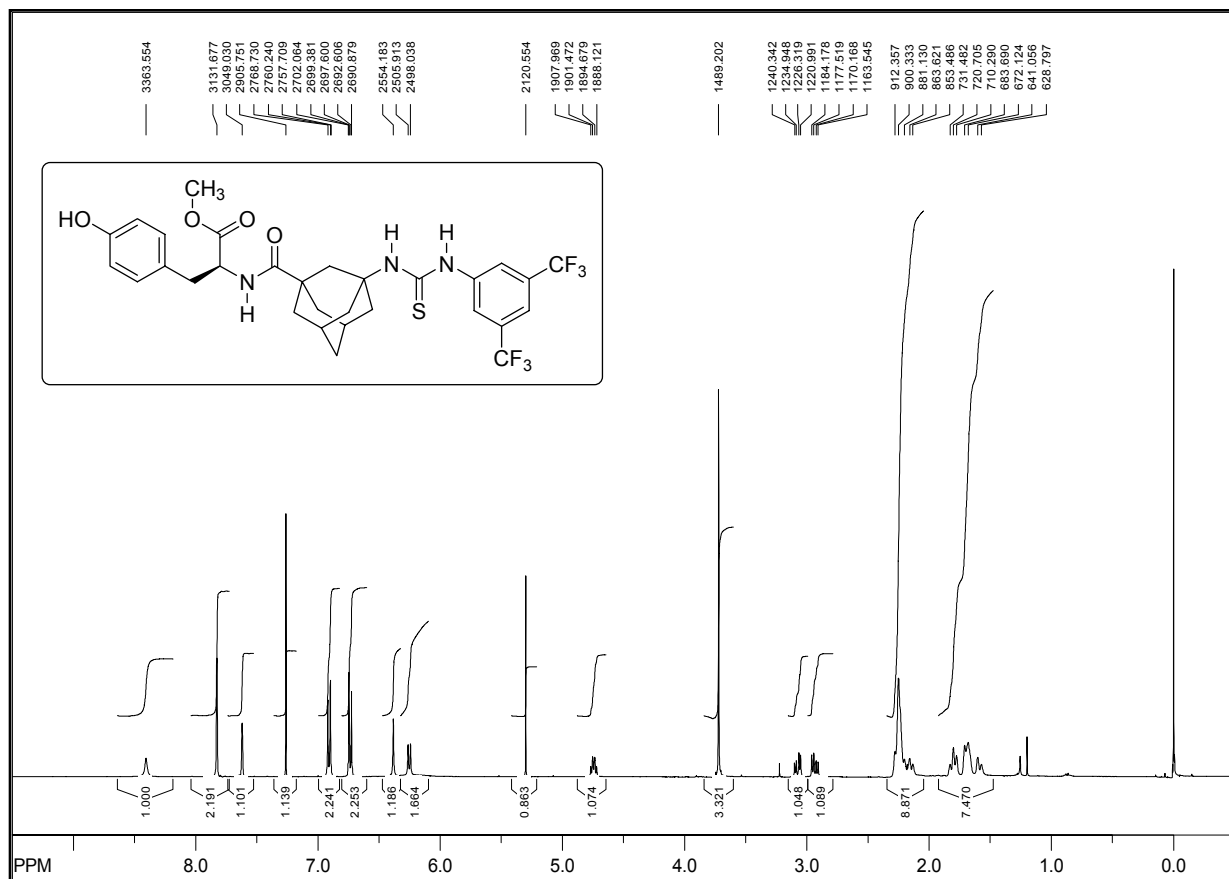
TU-A Gly-Trp-OMe (239c)



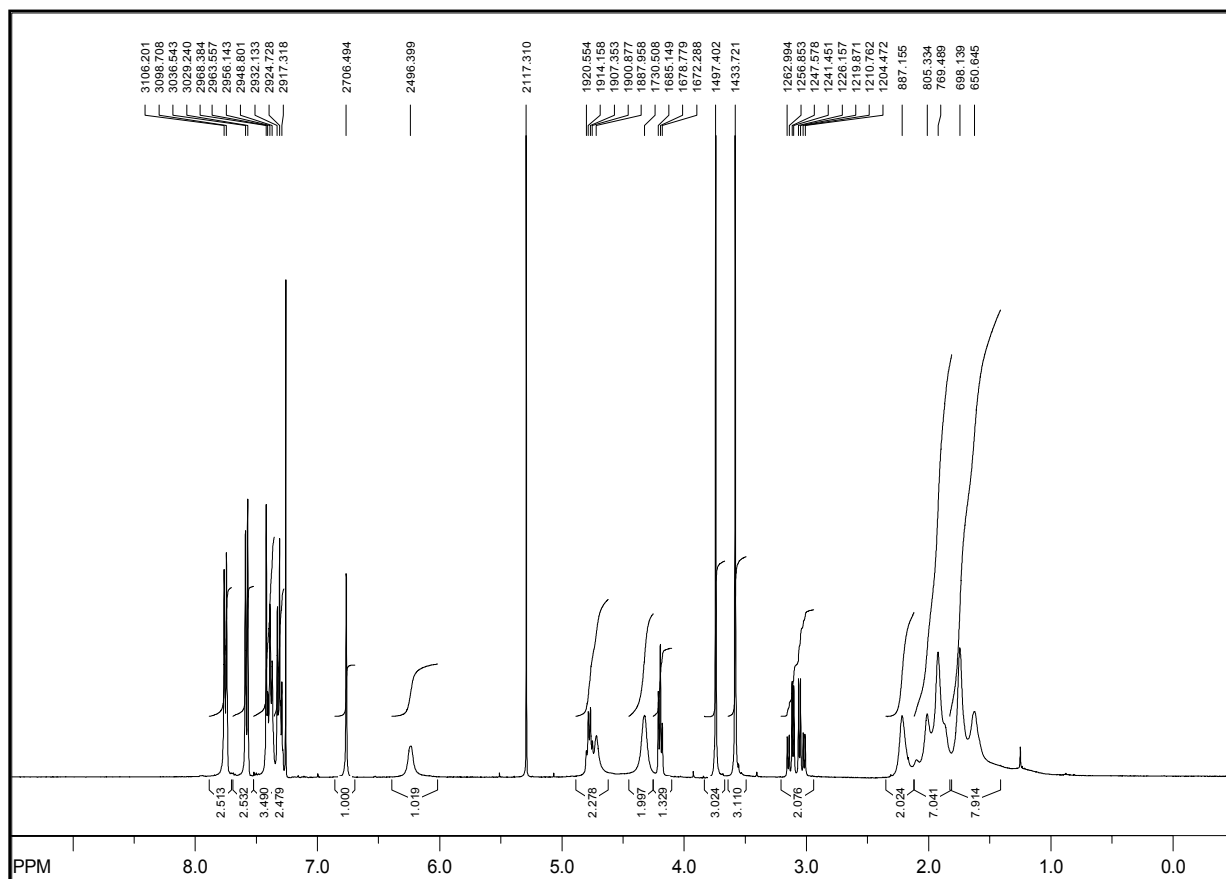
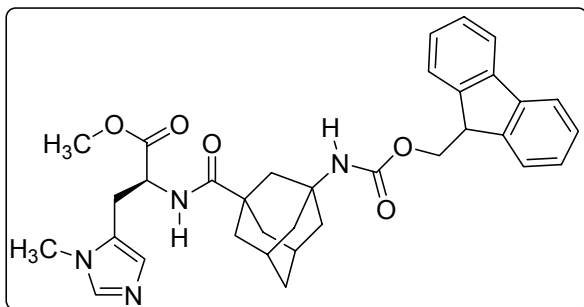
Fmoc-A-Gly-Tyr-OMe (245)



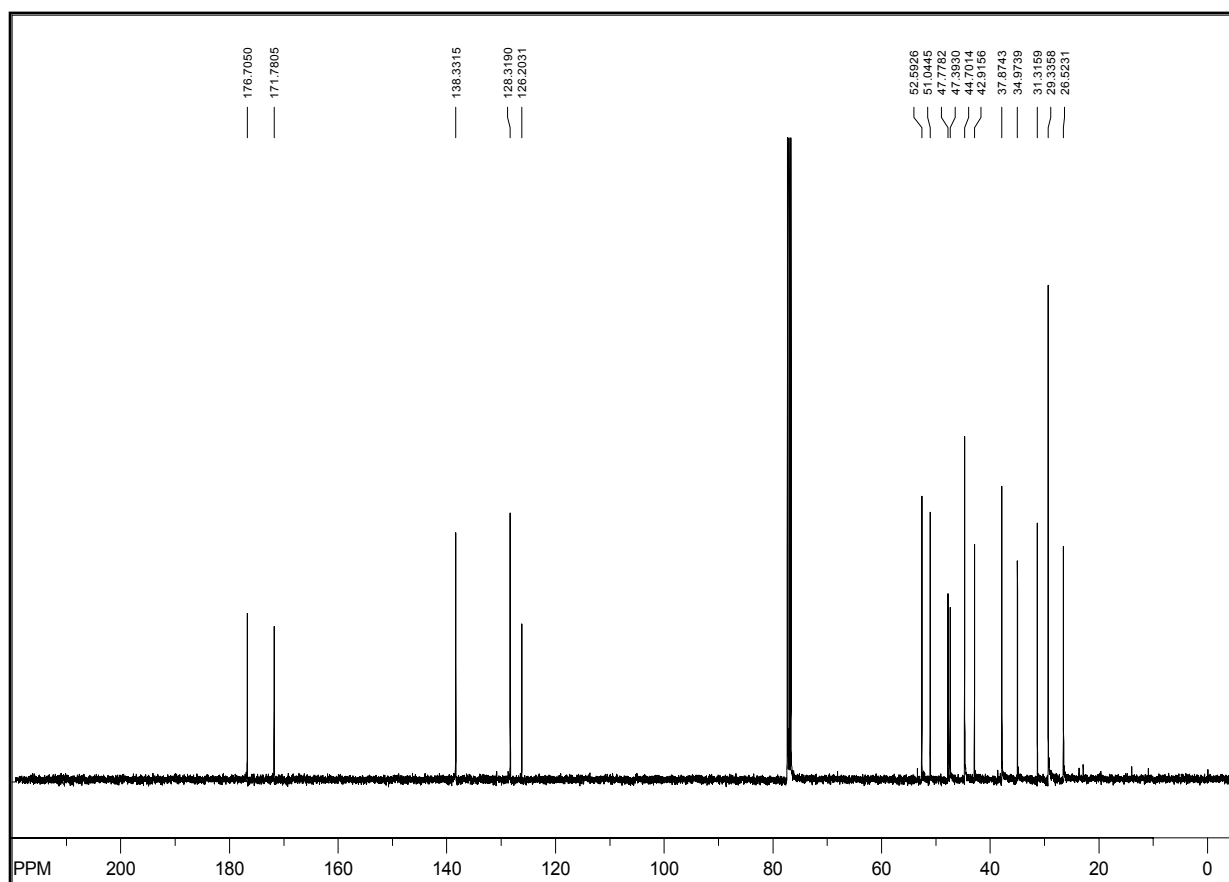
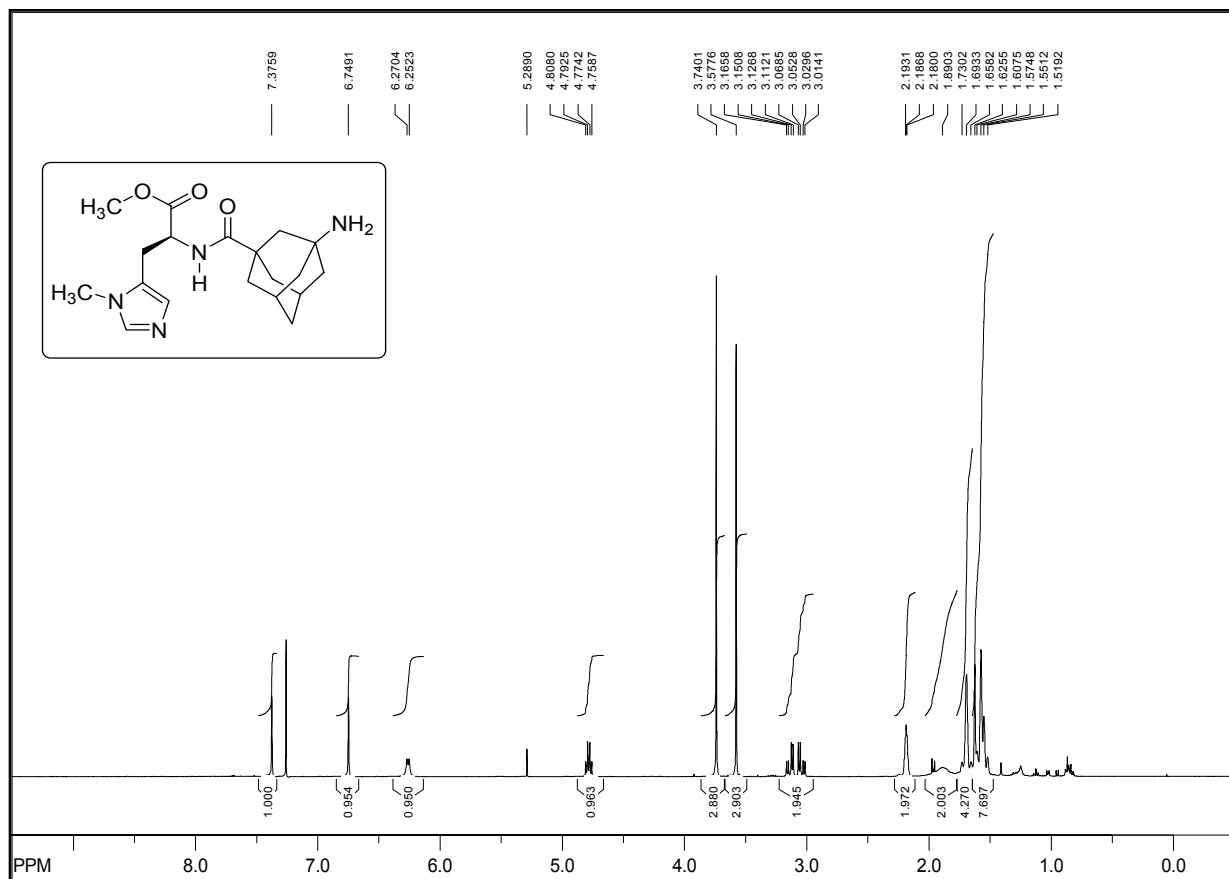
H-A-Gly-Tyr-OMe (246)



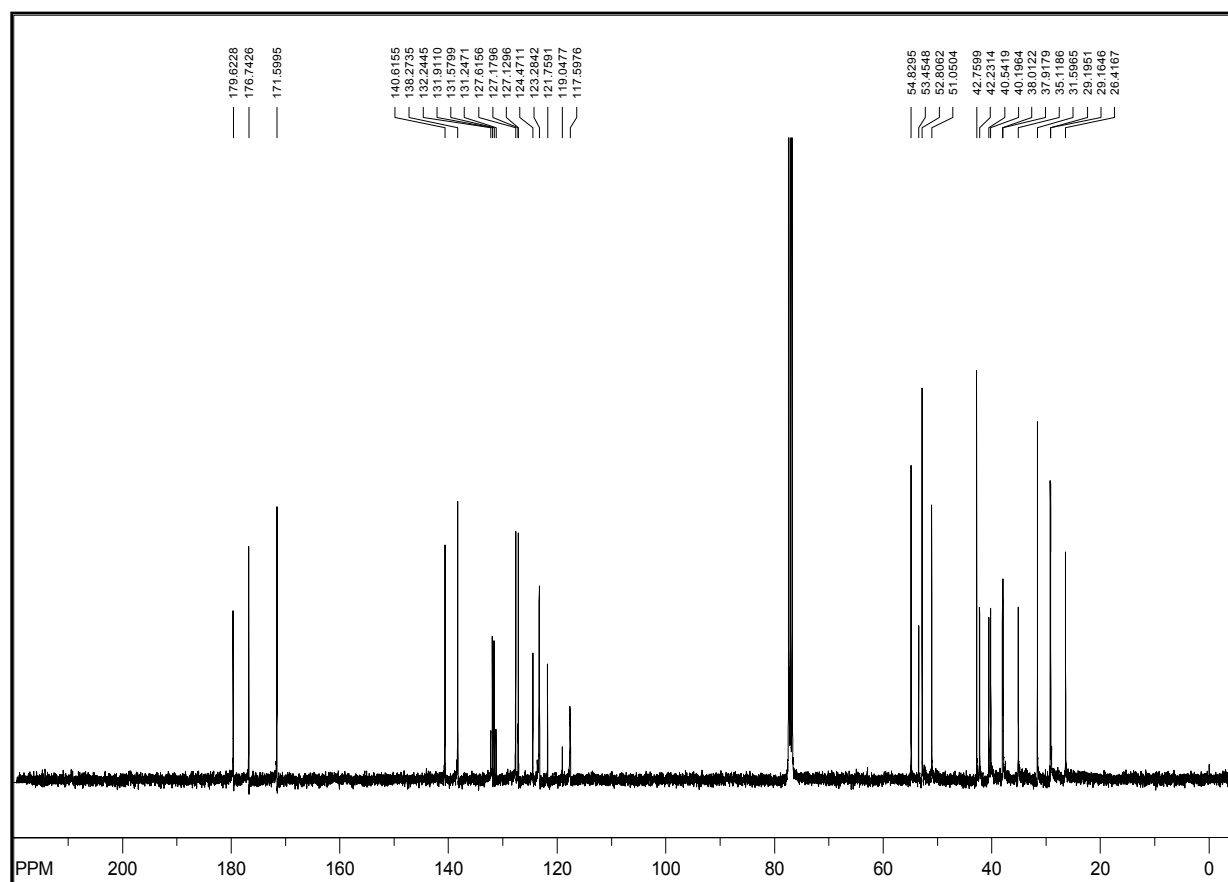
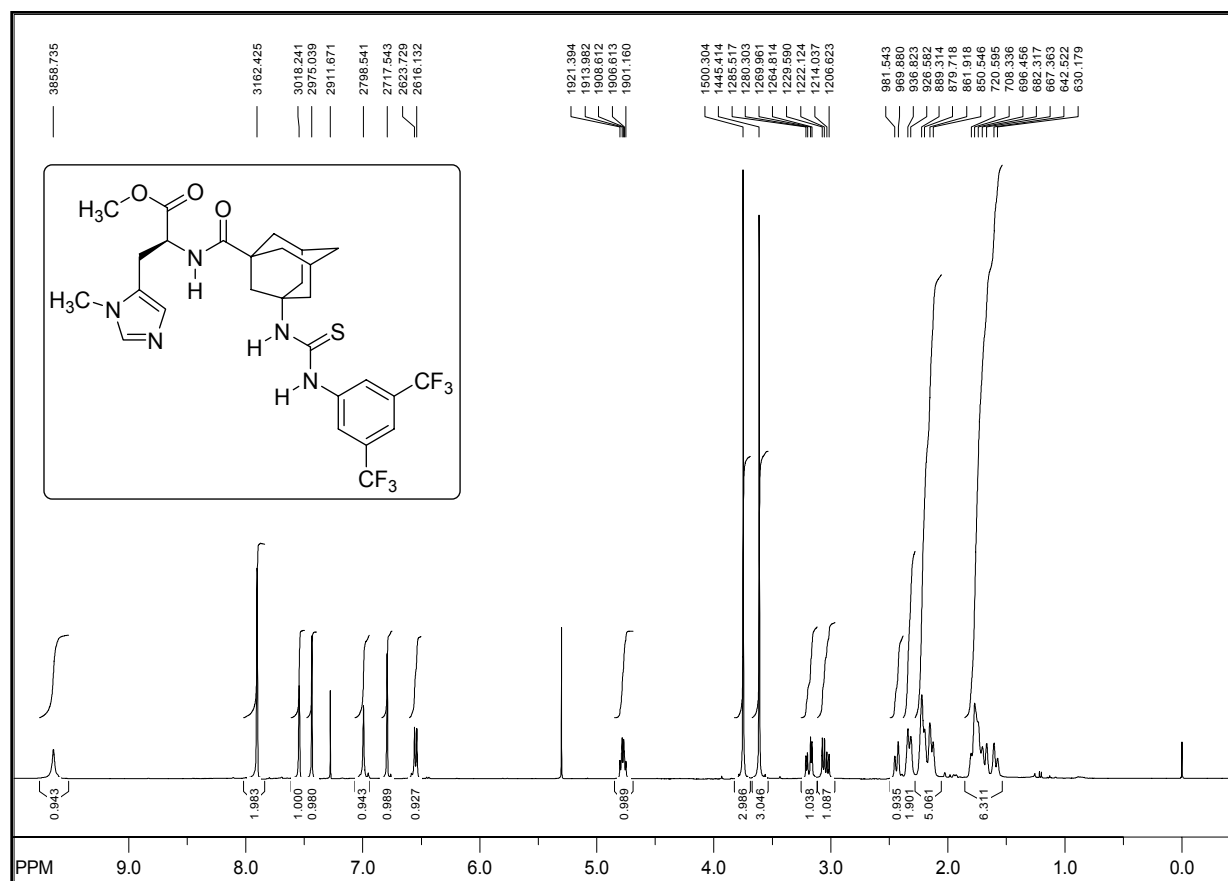
TU-A Gly-Tyr-OH (239d)

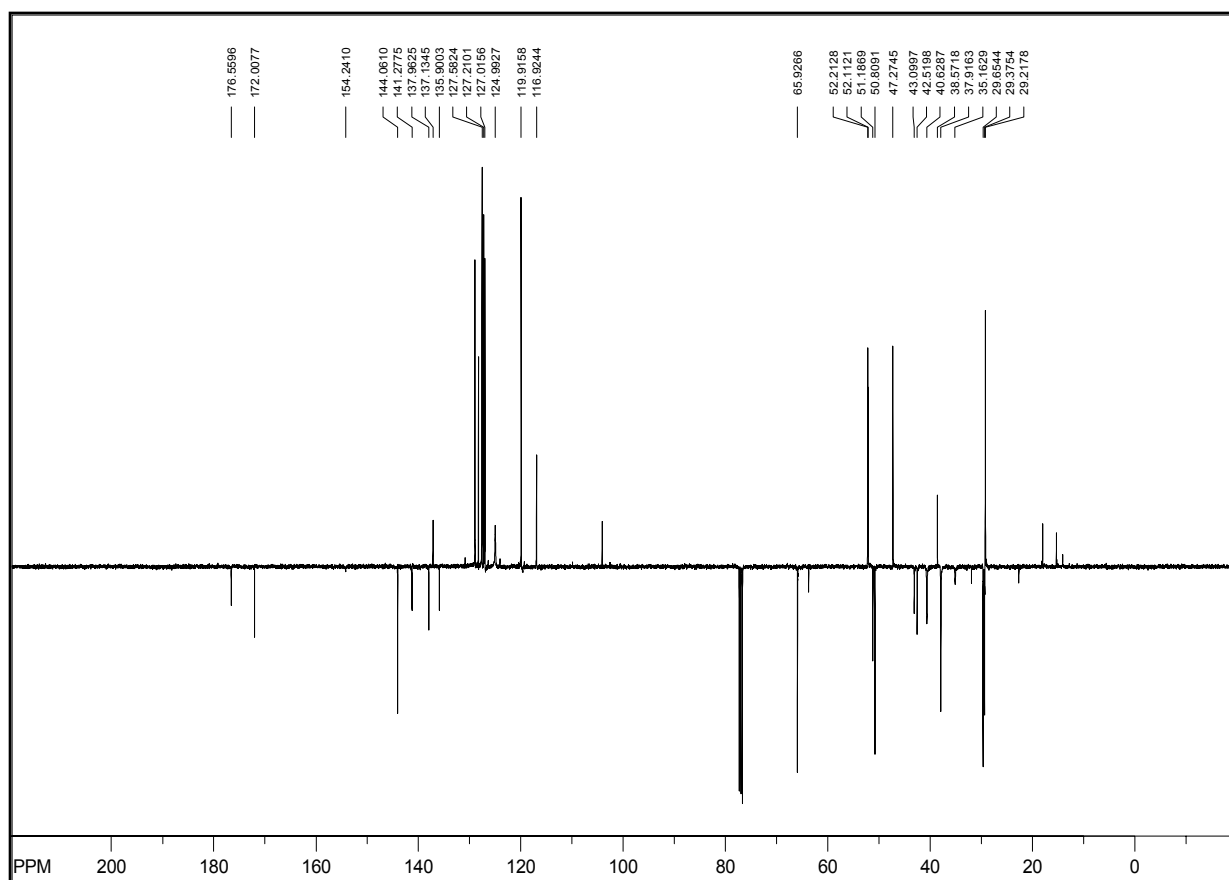
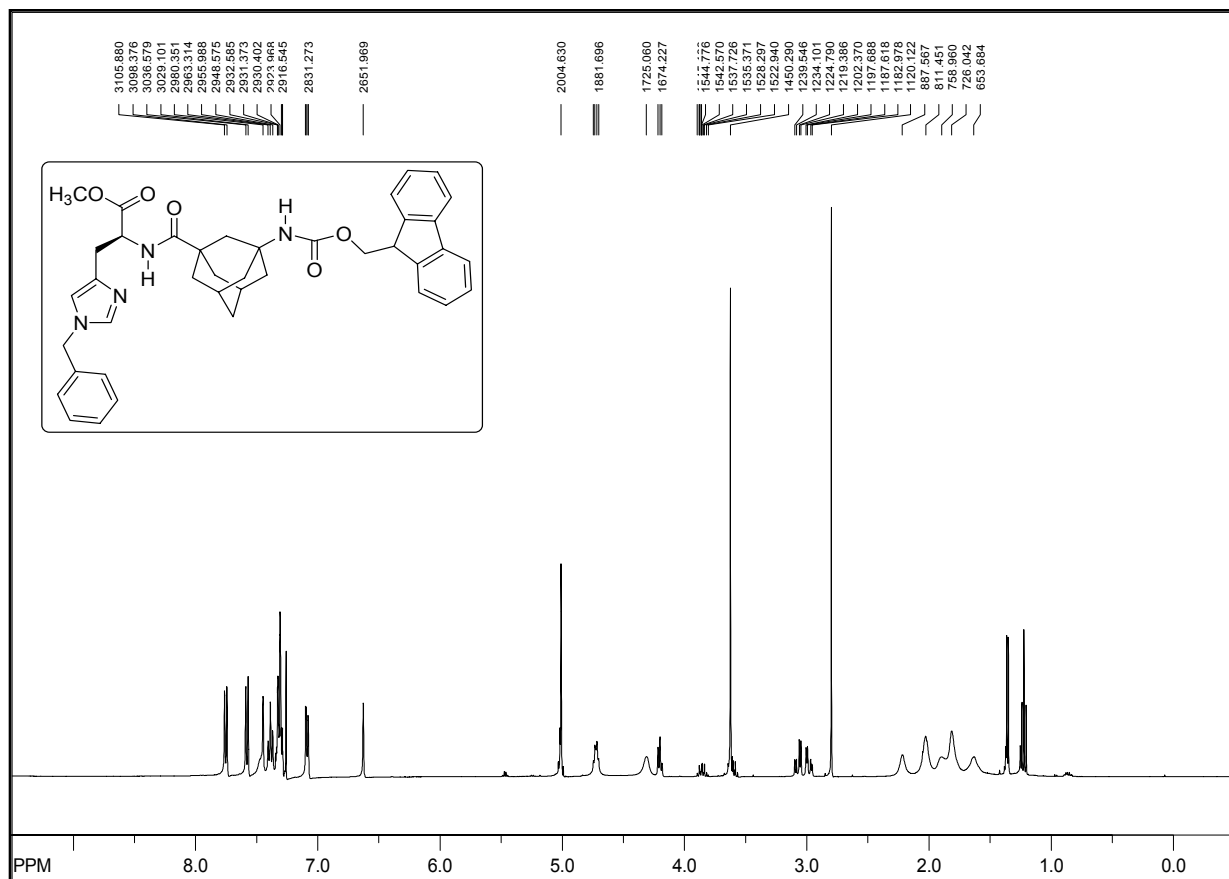


Fmoc-^AGly-His(π -Me)-OMe (**248**)

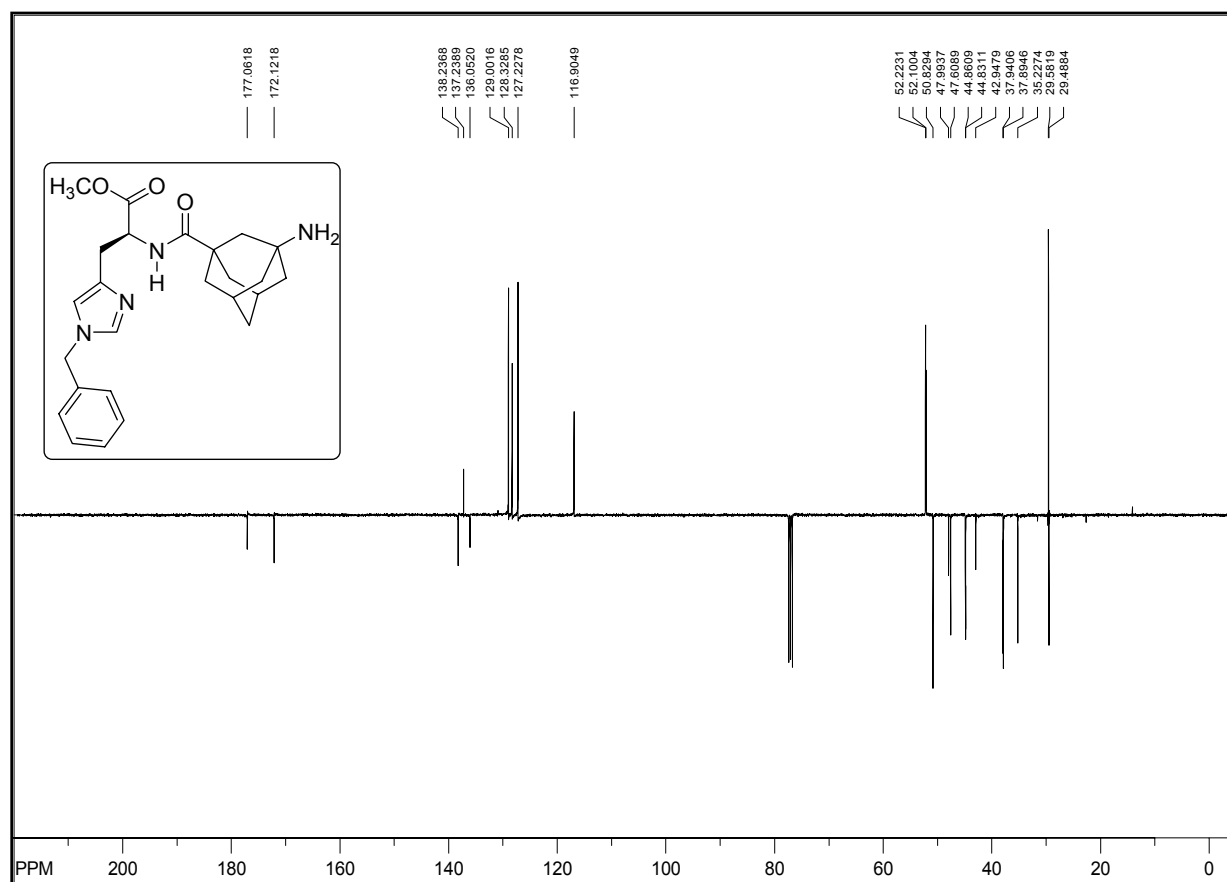
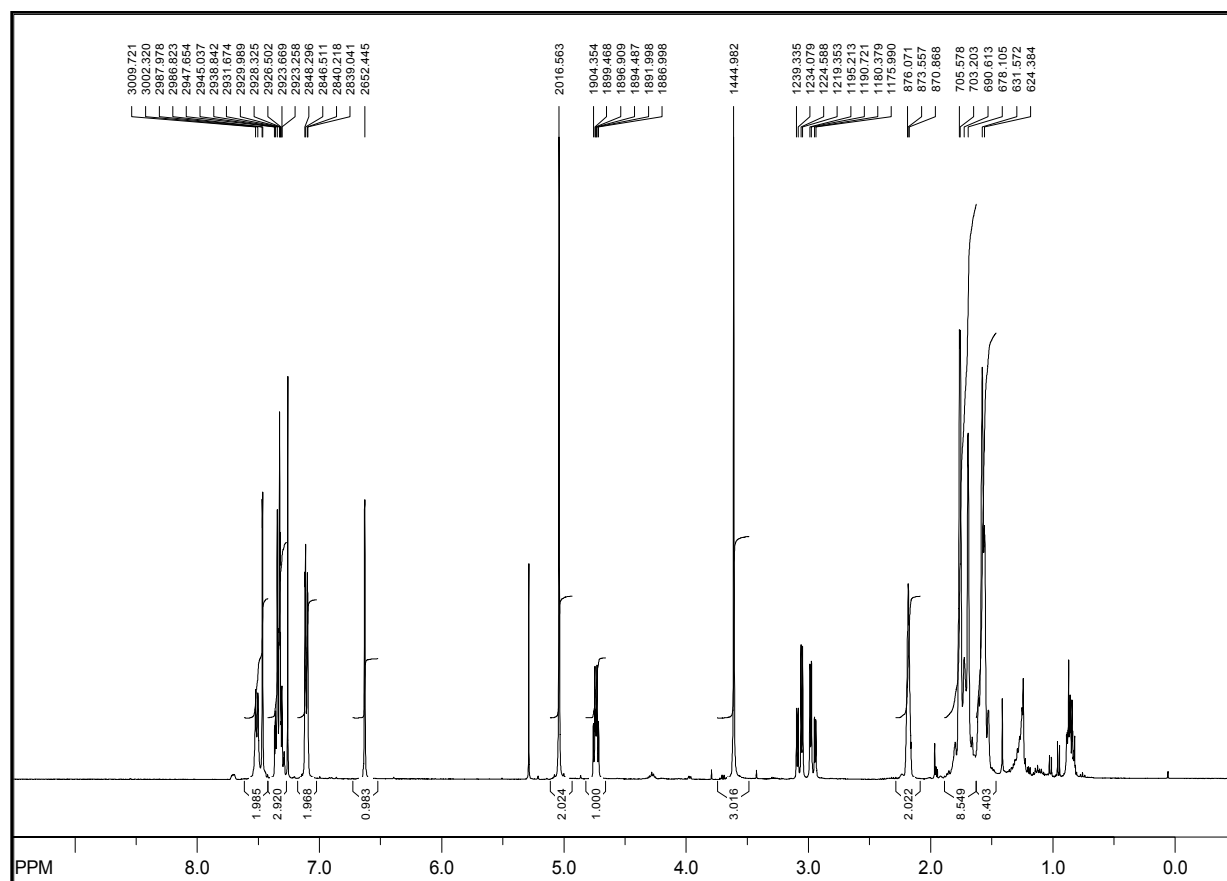


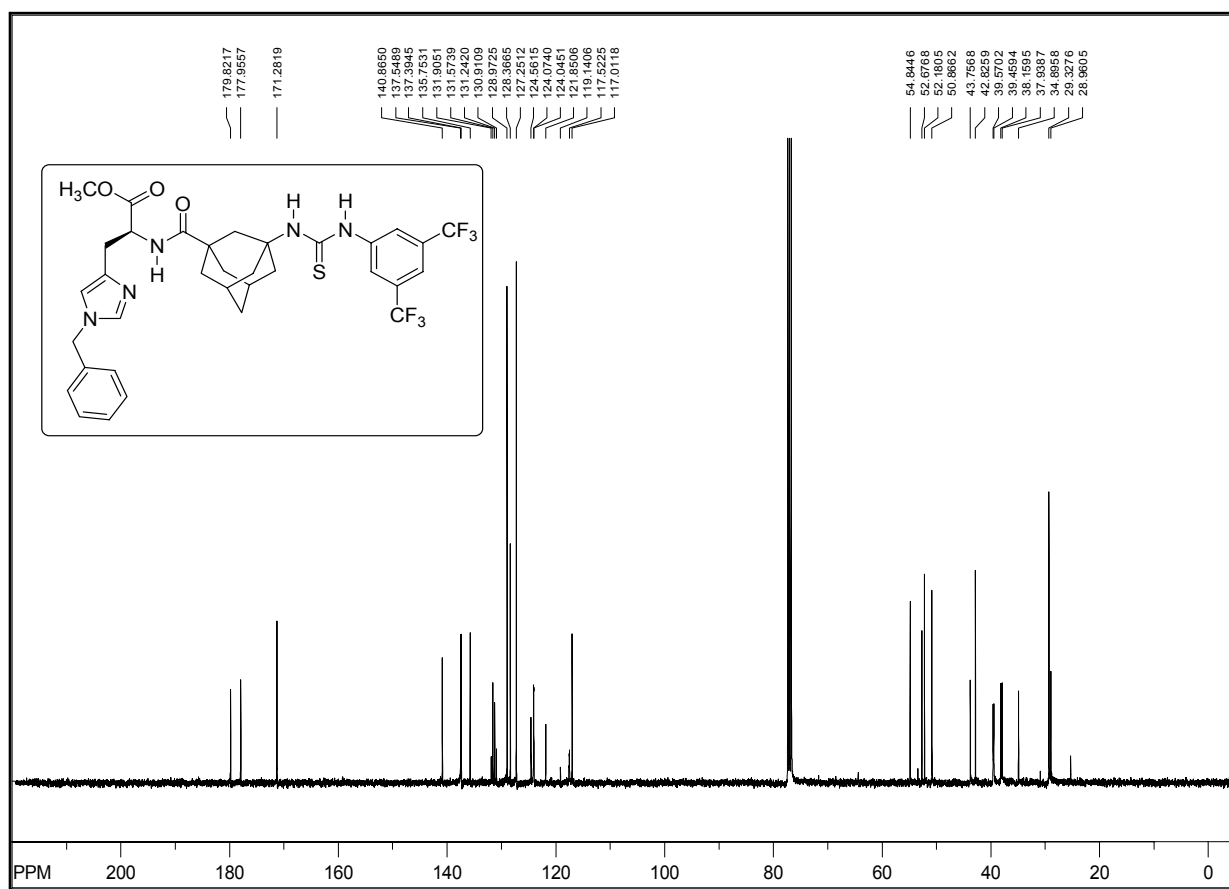
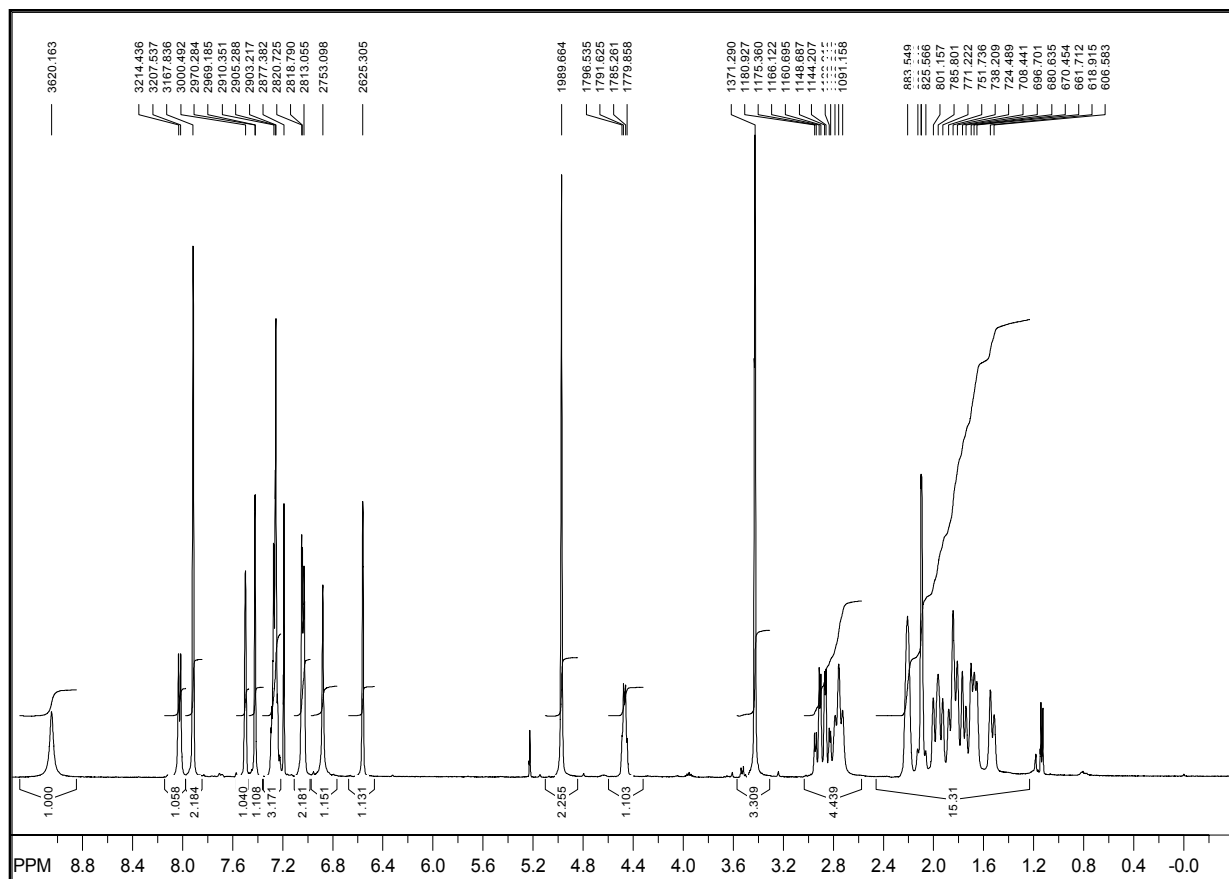
H^{A} -Gly-His(π -Me)-OMe (249)

TH^AGly-His(π -Me)-OMe (239e)

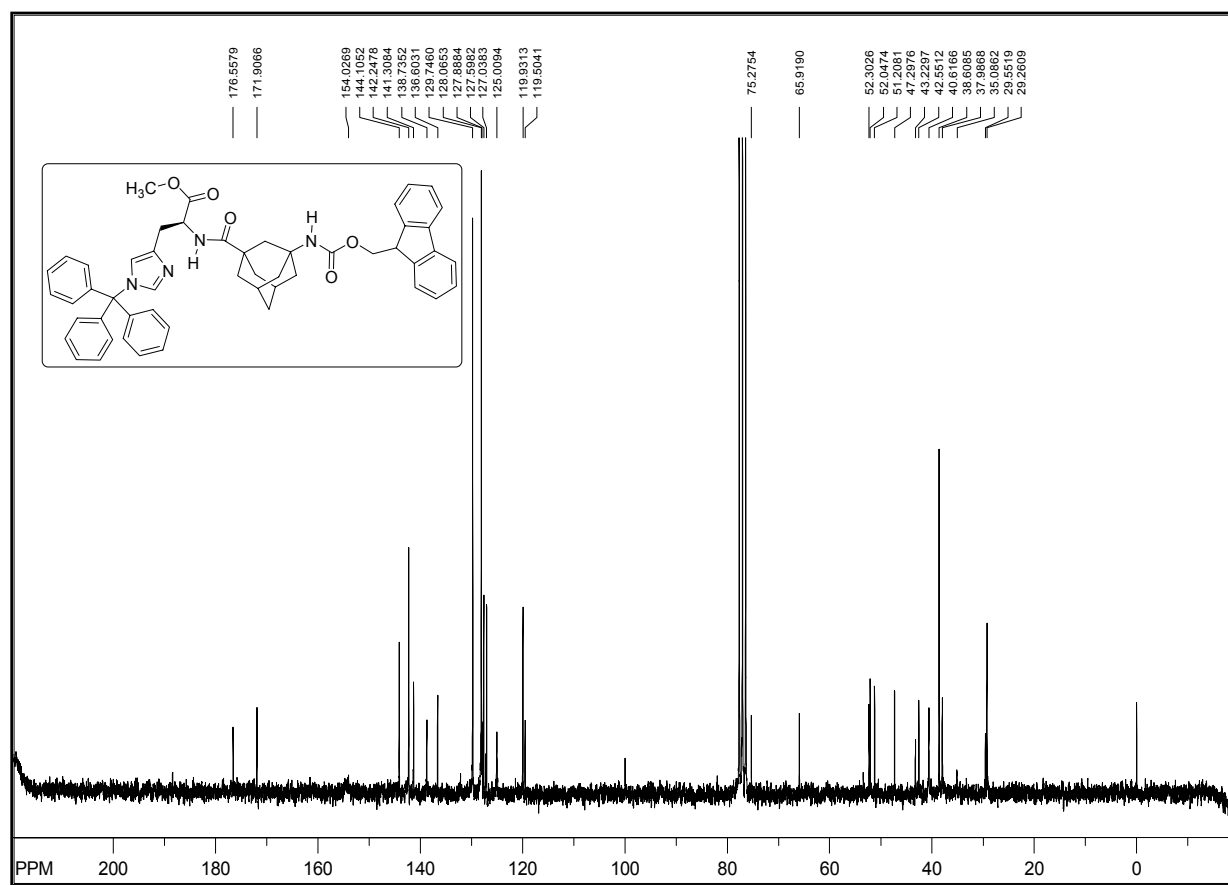
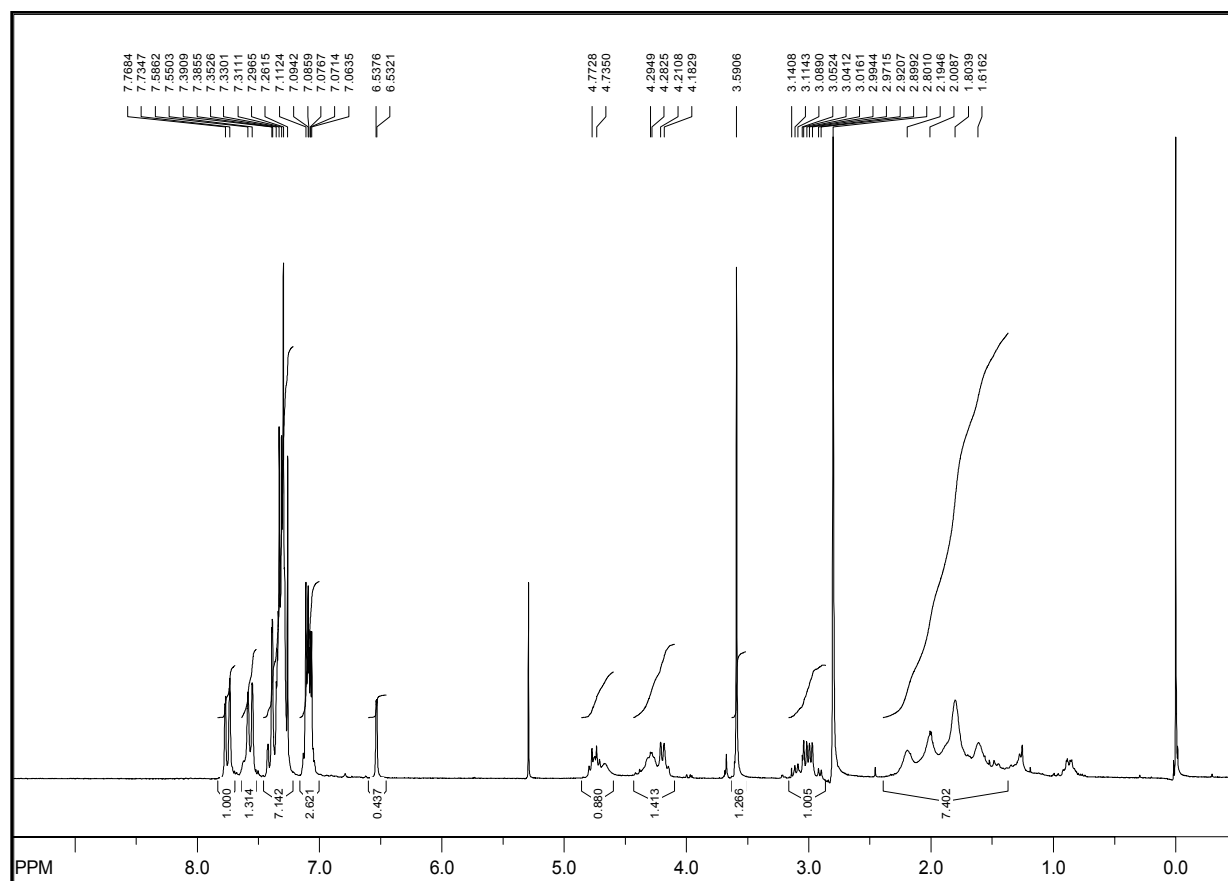


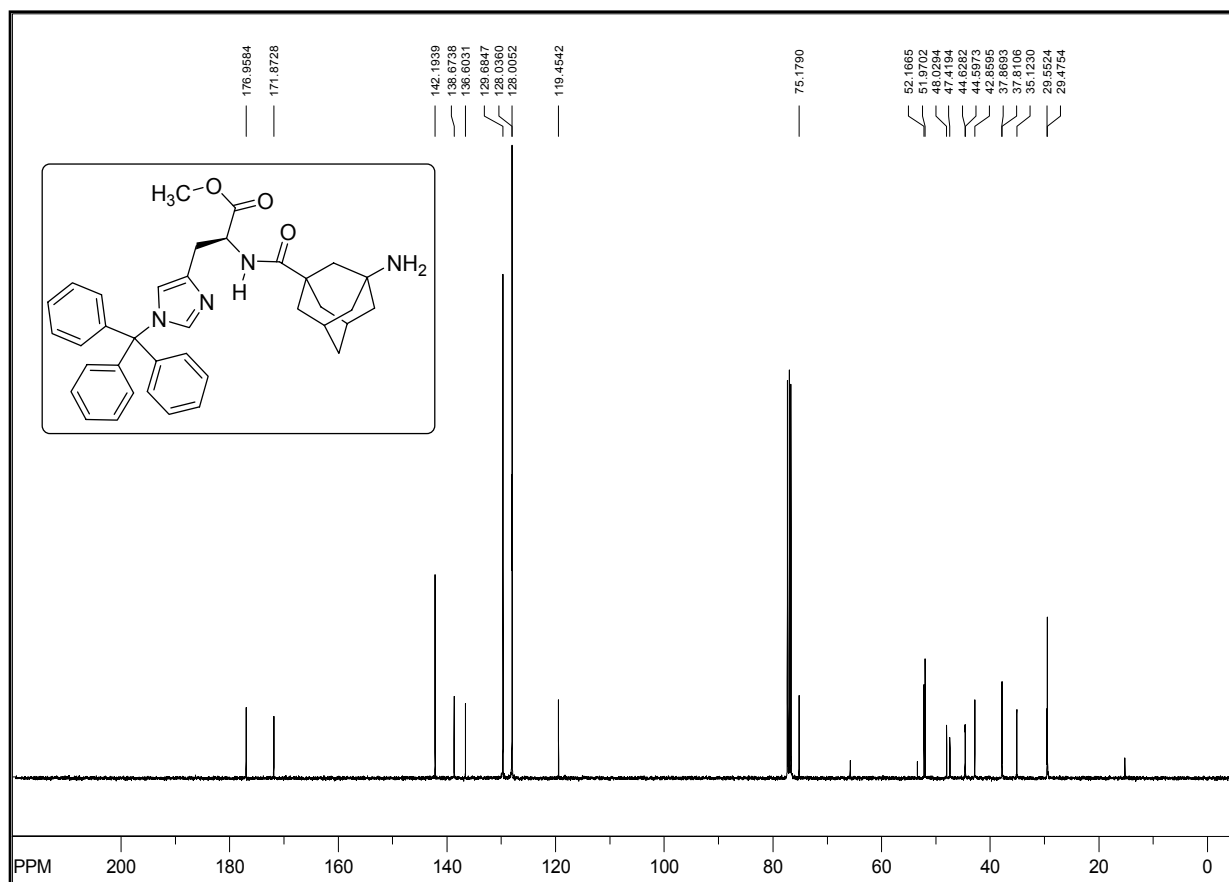
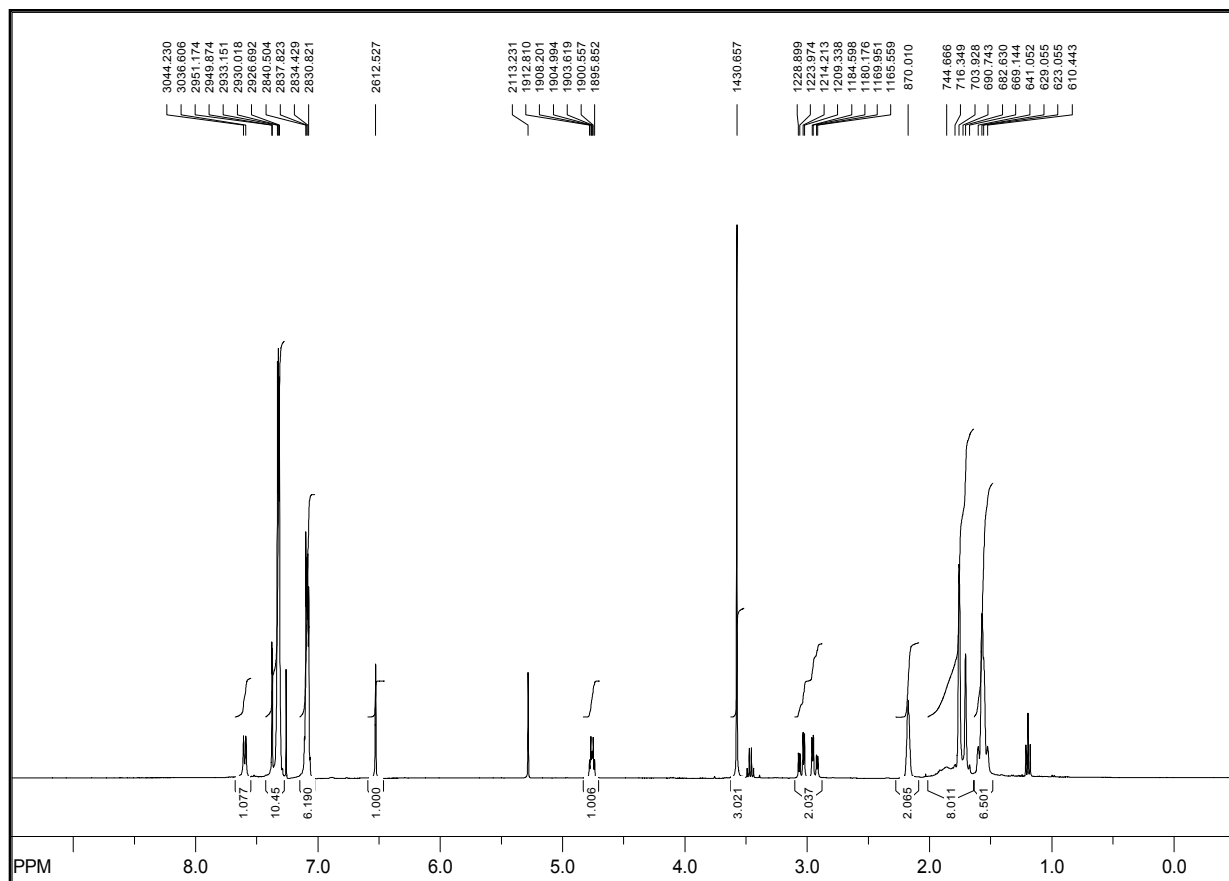
Fmoc-^AGly-His(τ -Bn)-OMe (251)

H-A Gly-His(τ -Bn)-OMe (252)

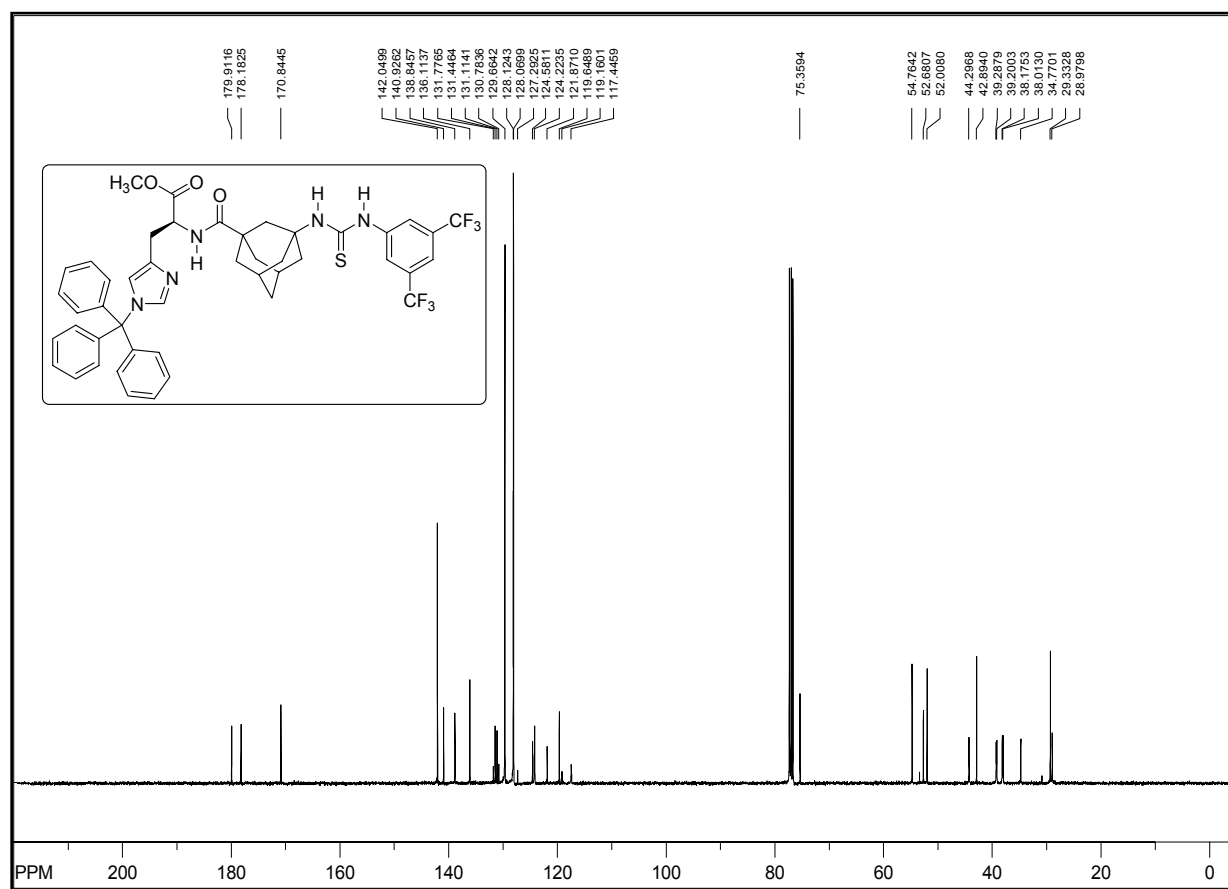
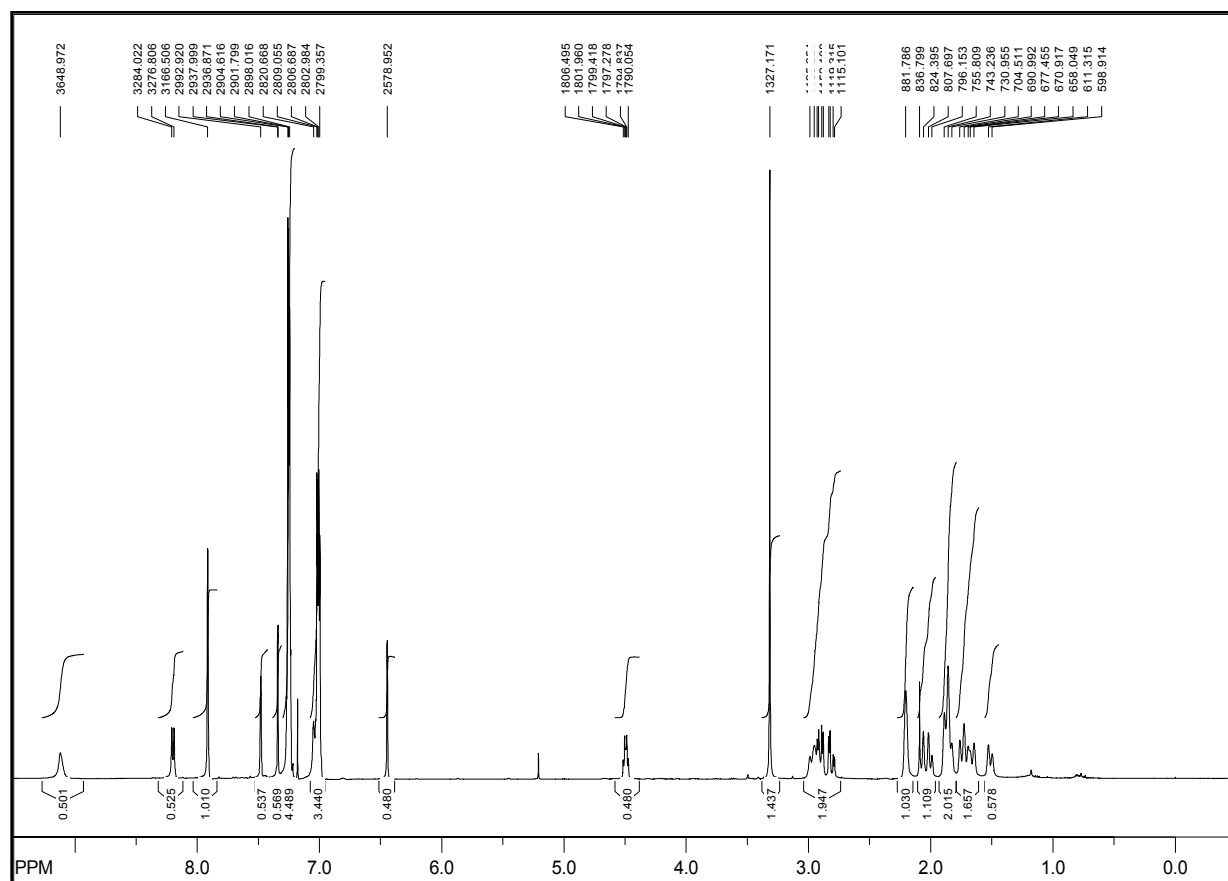


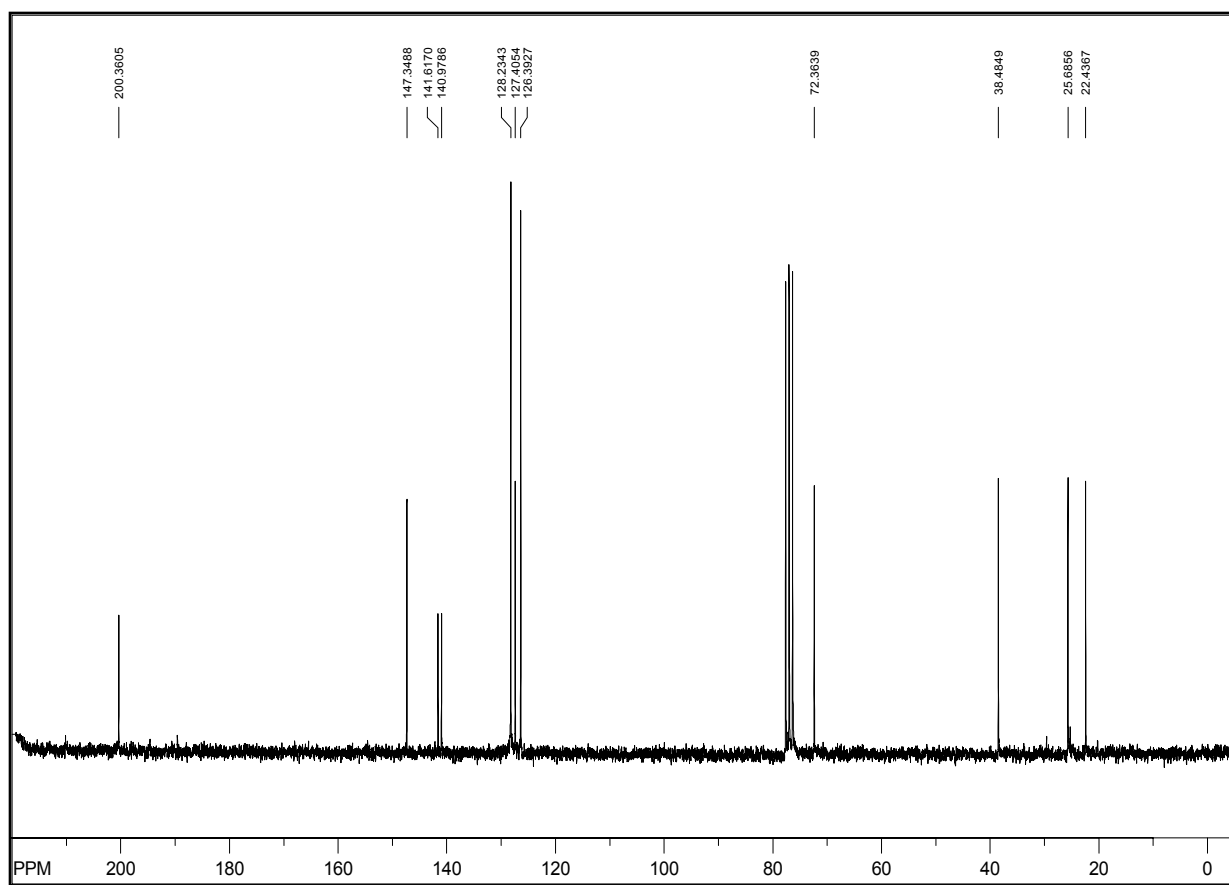
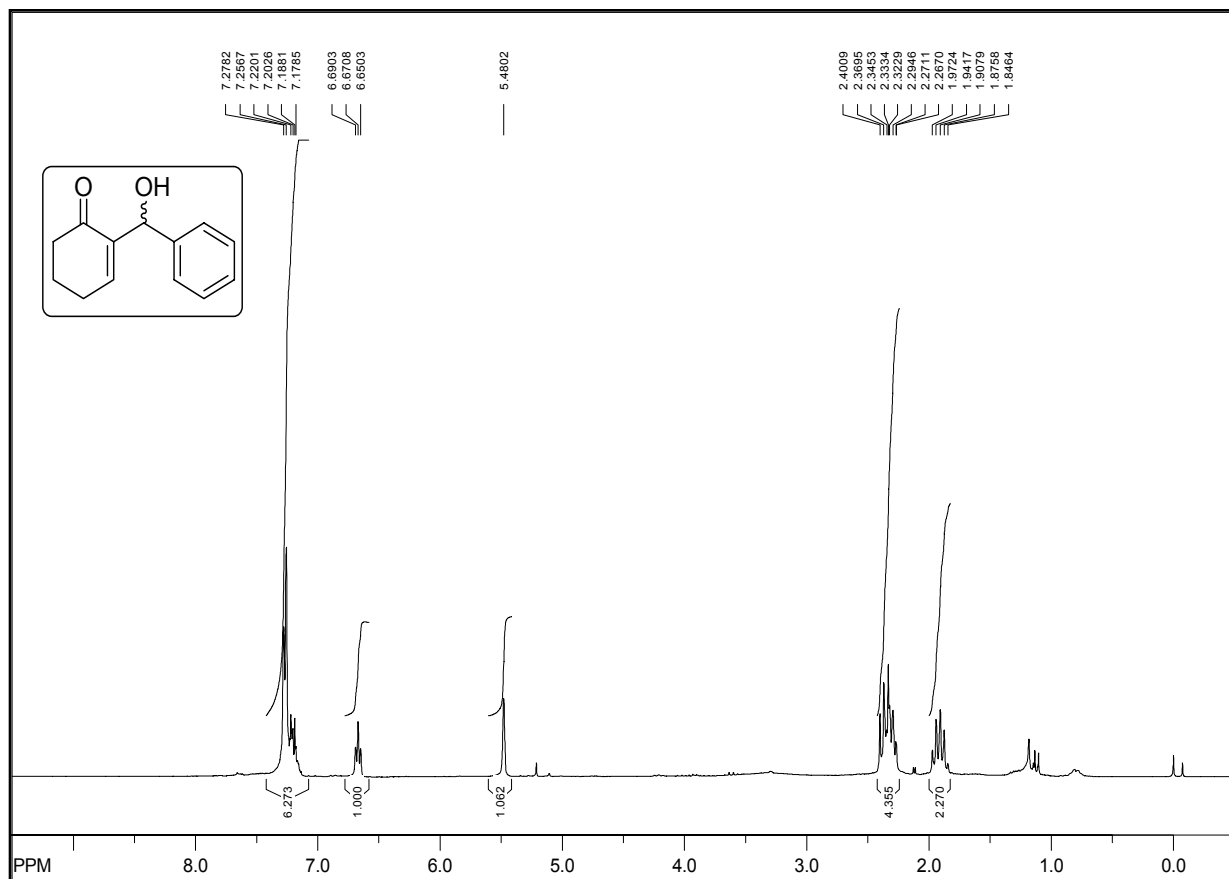
TU-^AGly-His(τ -Bn)-OMe (239f)

Fmoc-^AGly-His(τ-Trt)-OME (254)

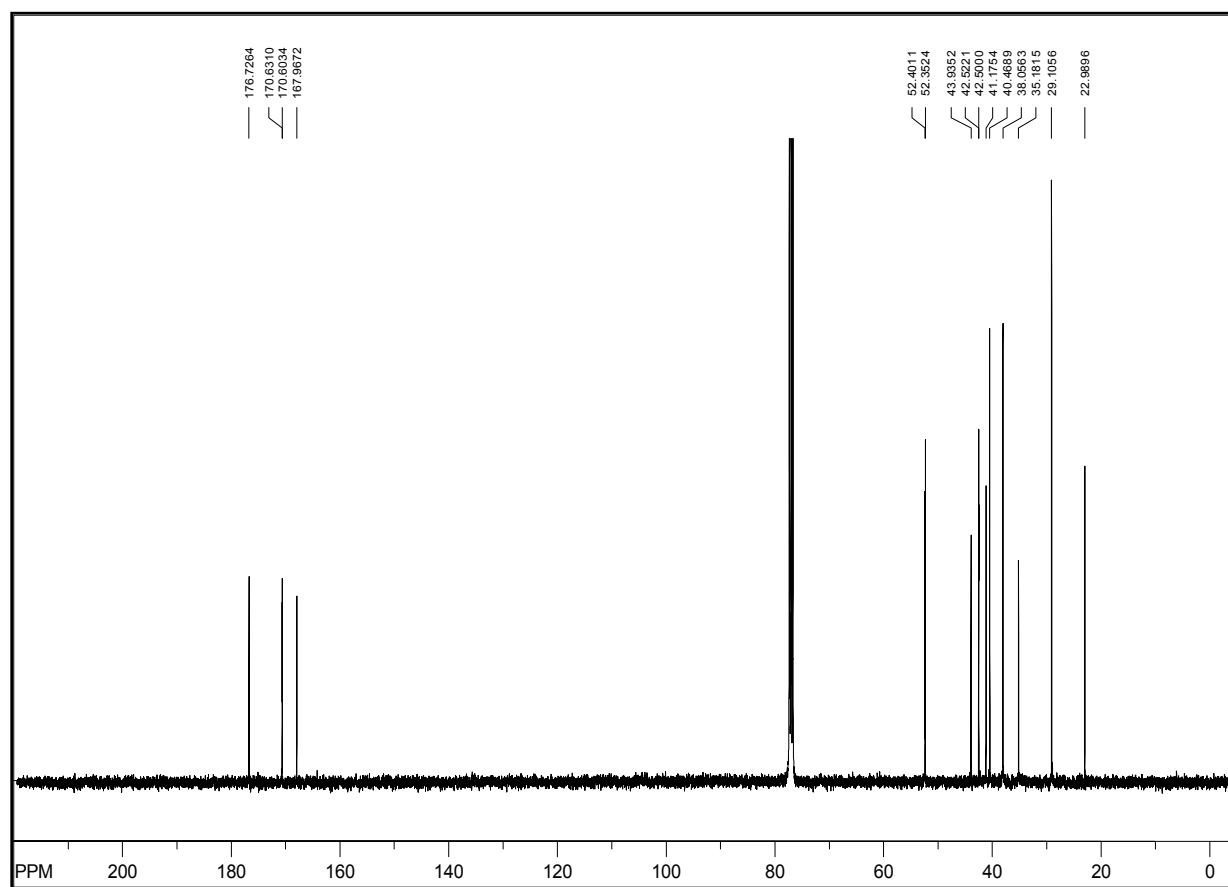
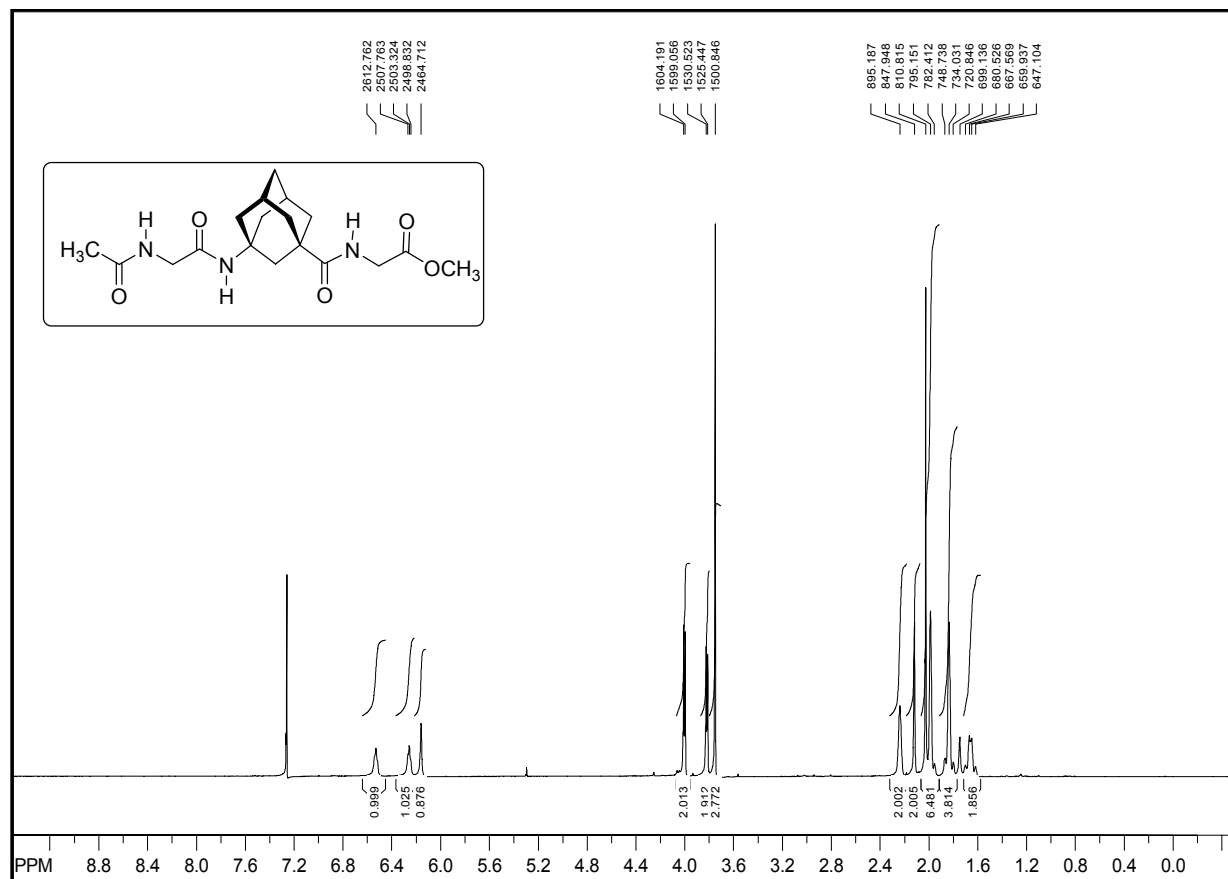


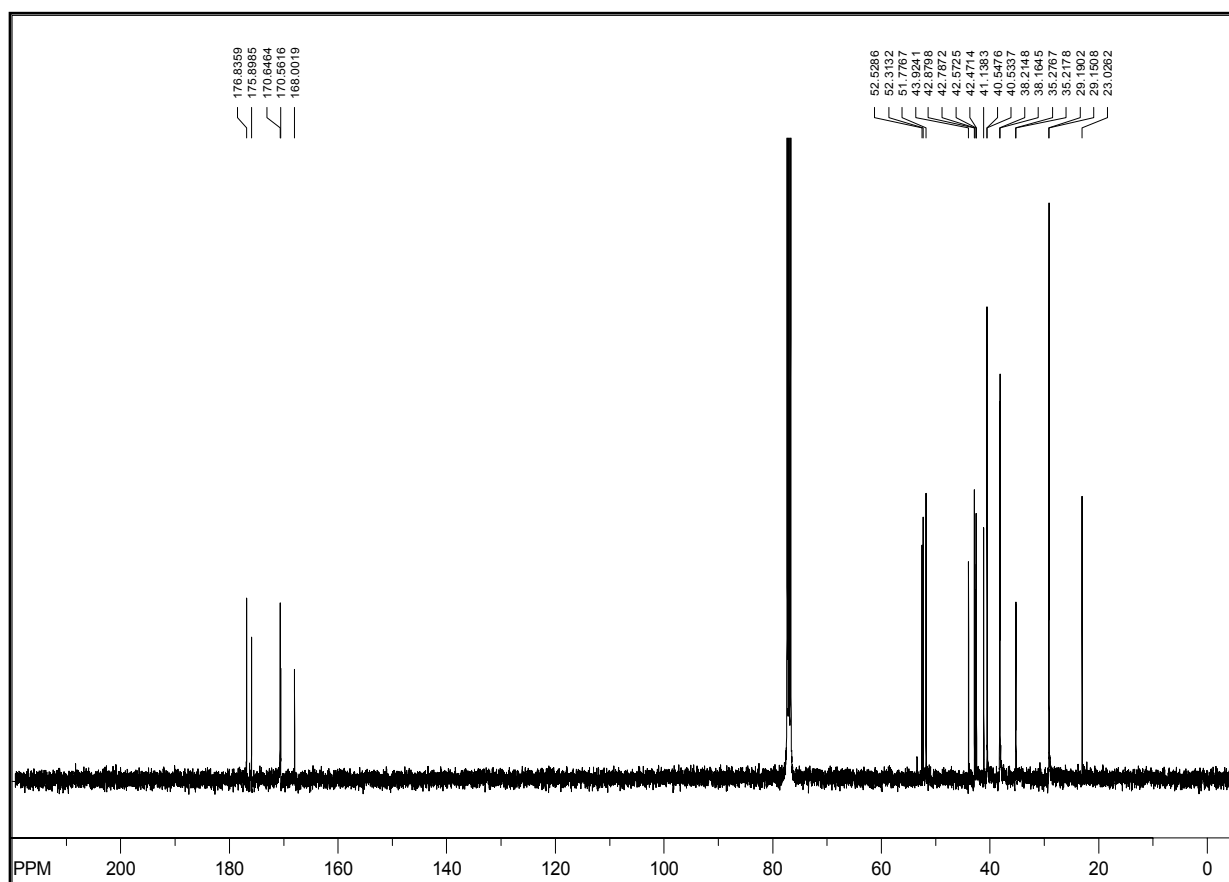
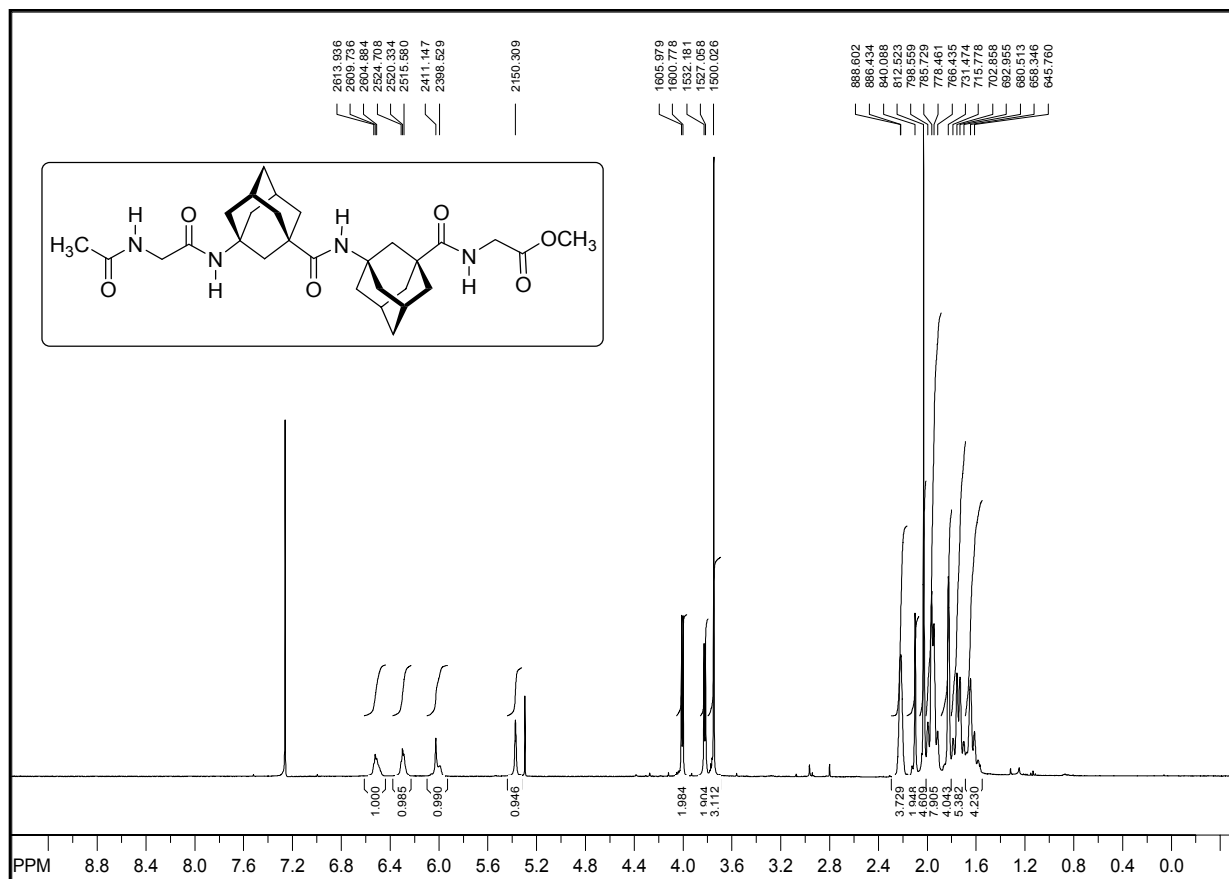
H^AGly-His(τ -Trt)-OME (255)

TU^AGly-His(τ-Trt)-OME (239g)

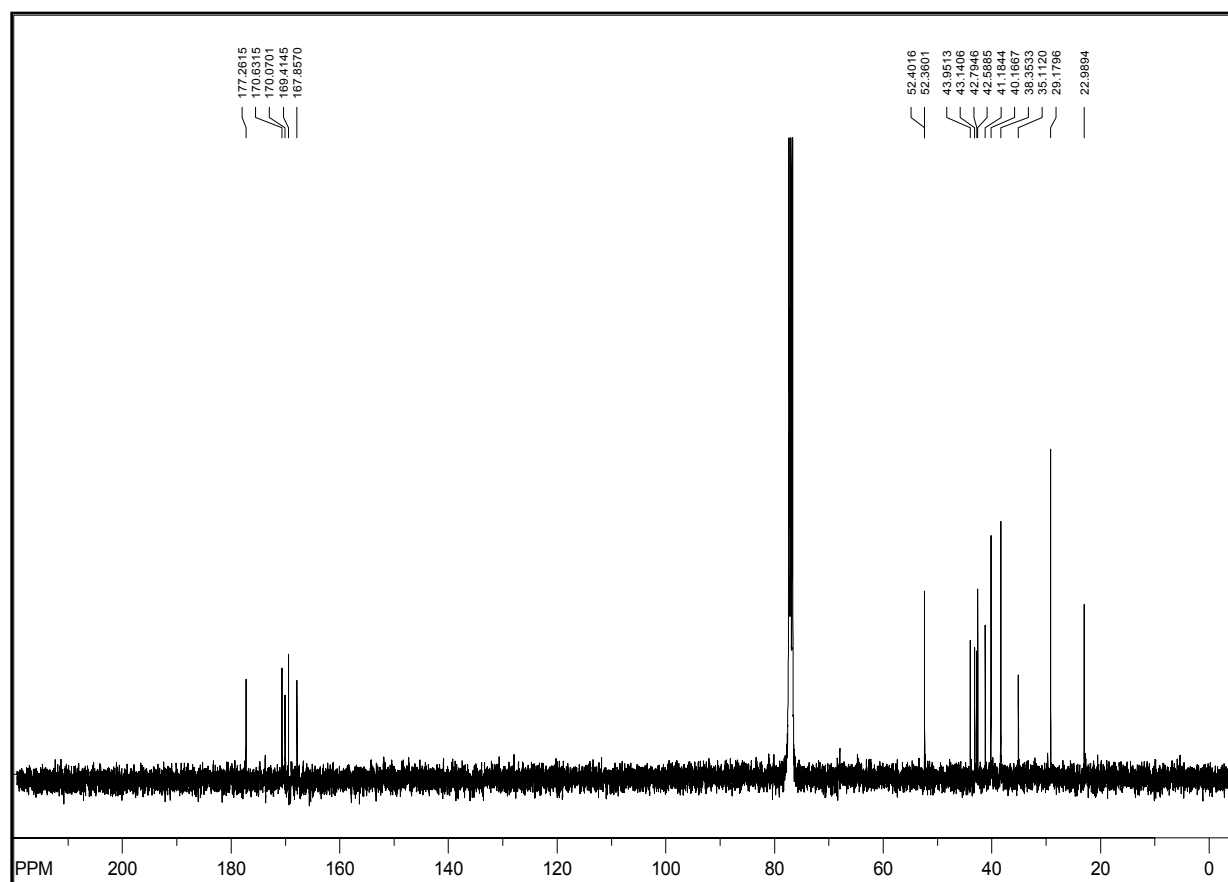
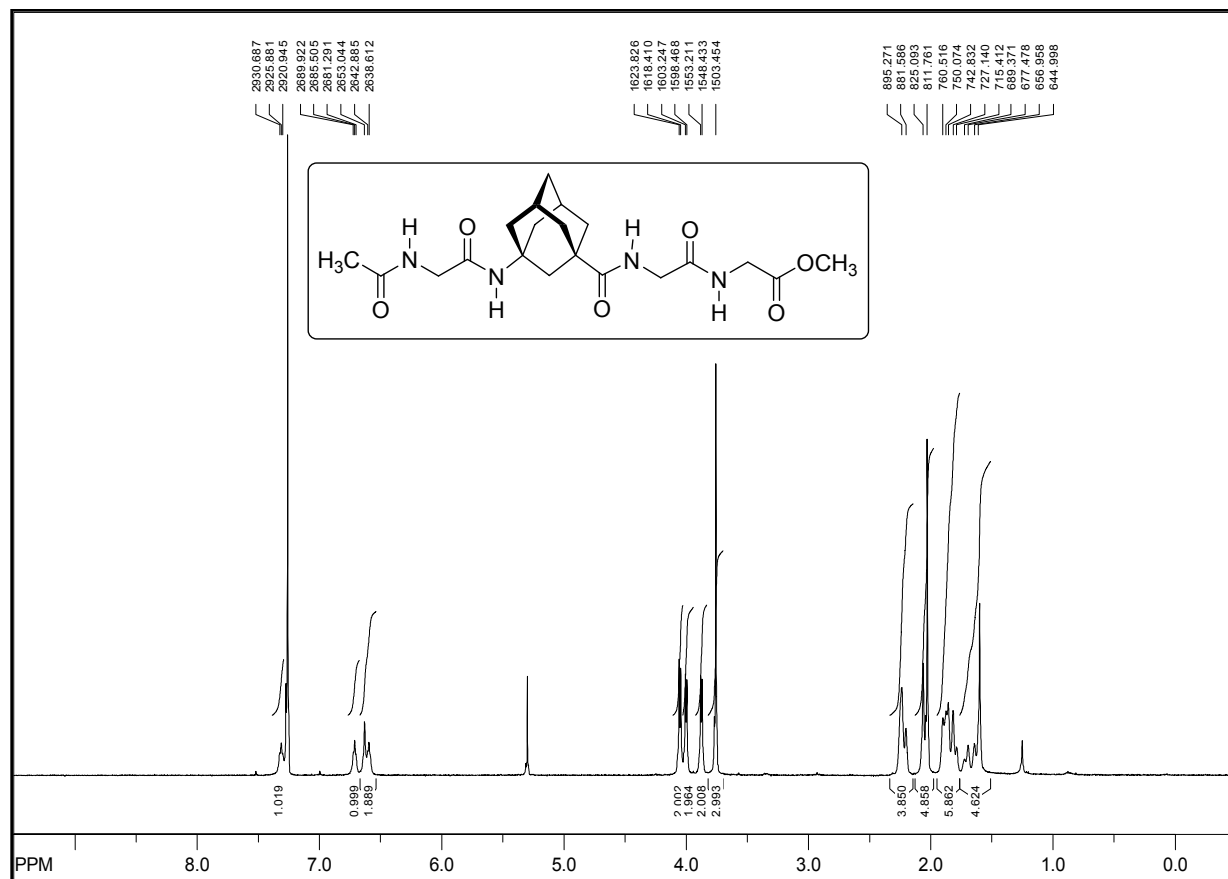


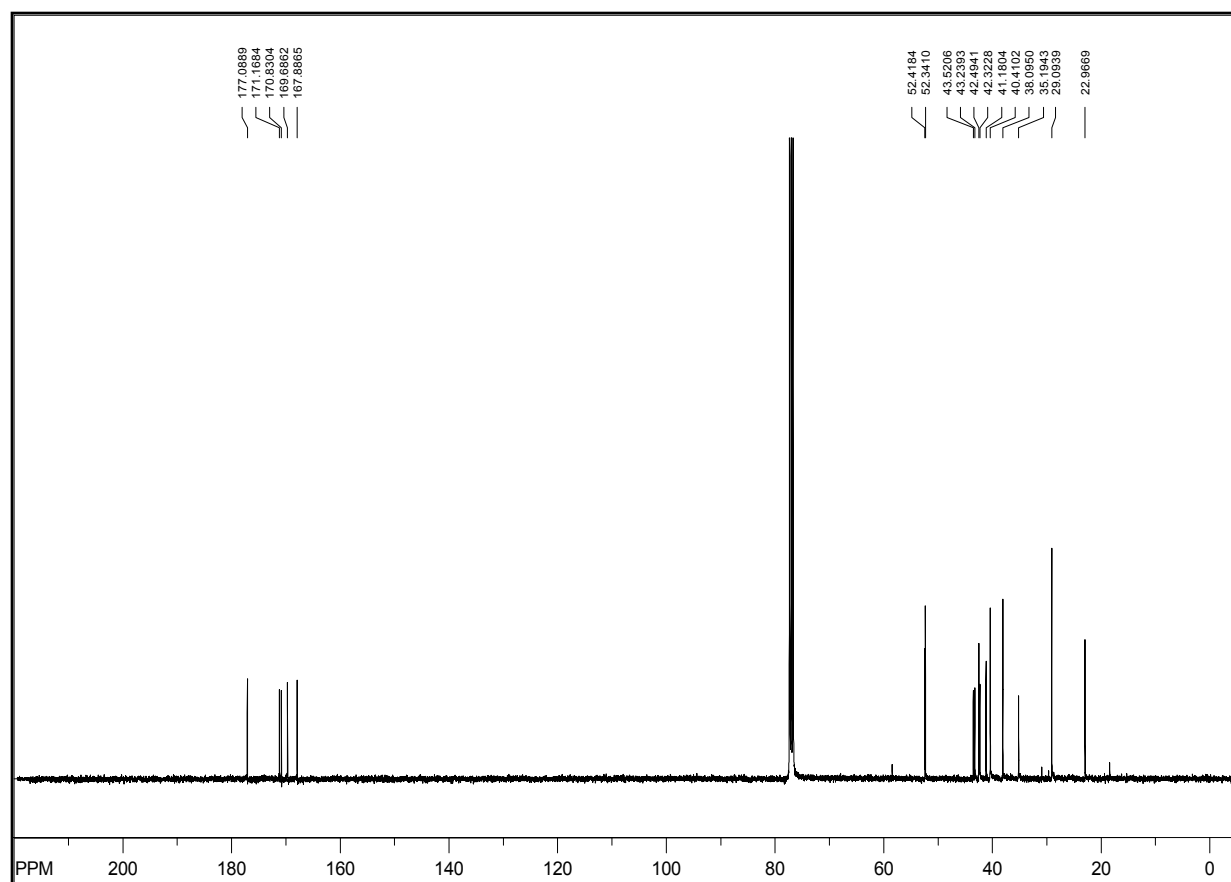
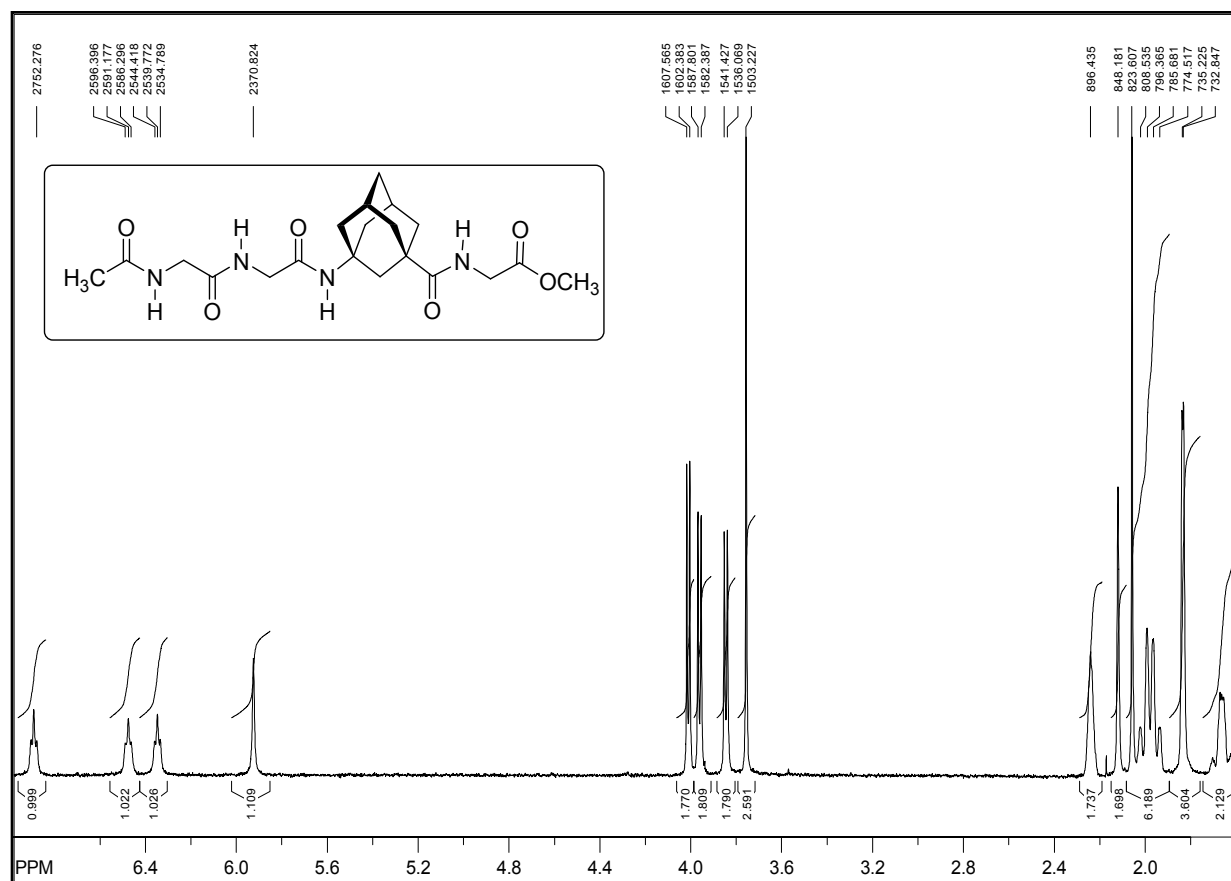
MBH adduct from the test reaction (**260**)

Ac-Gly- α -Gly-Gly-OMe (261)

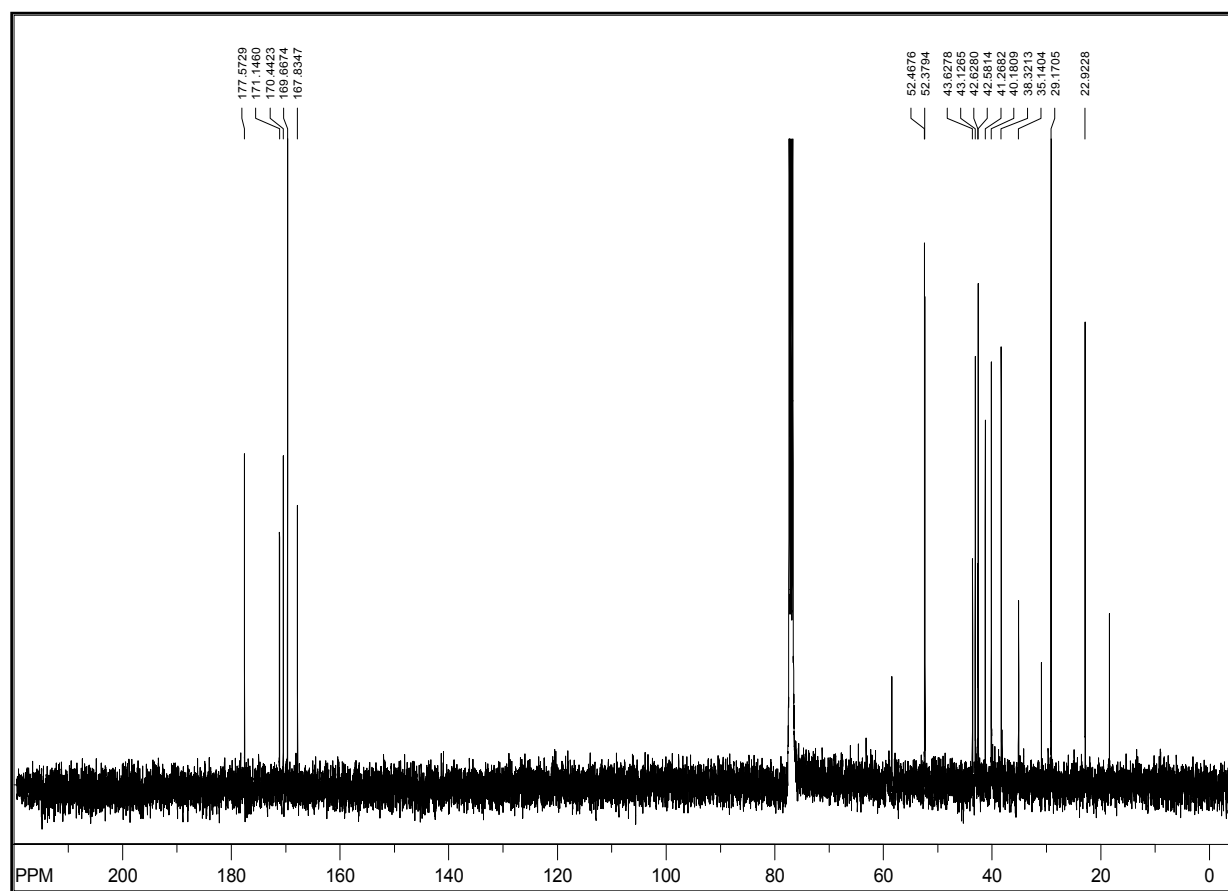
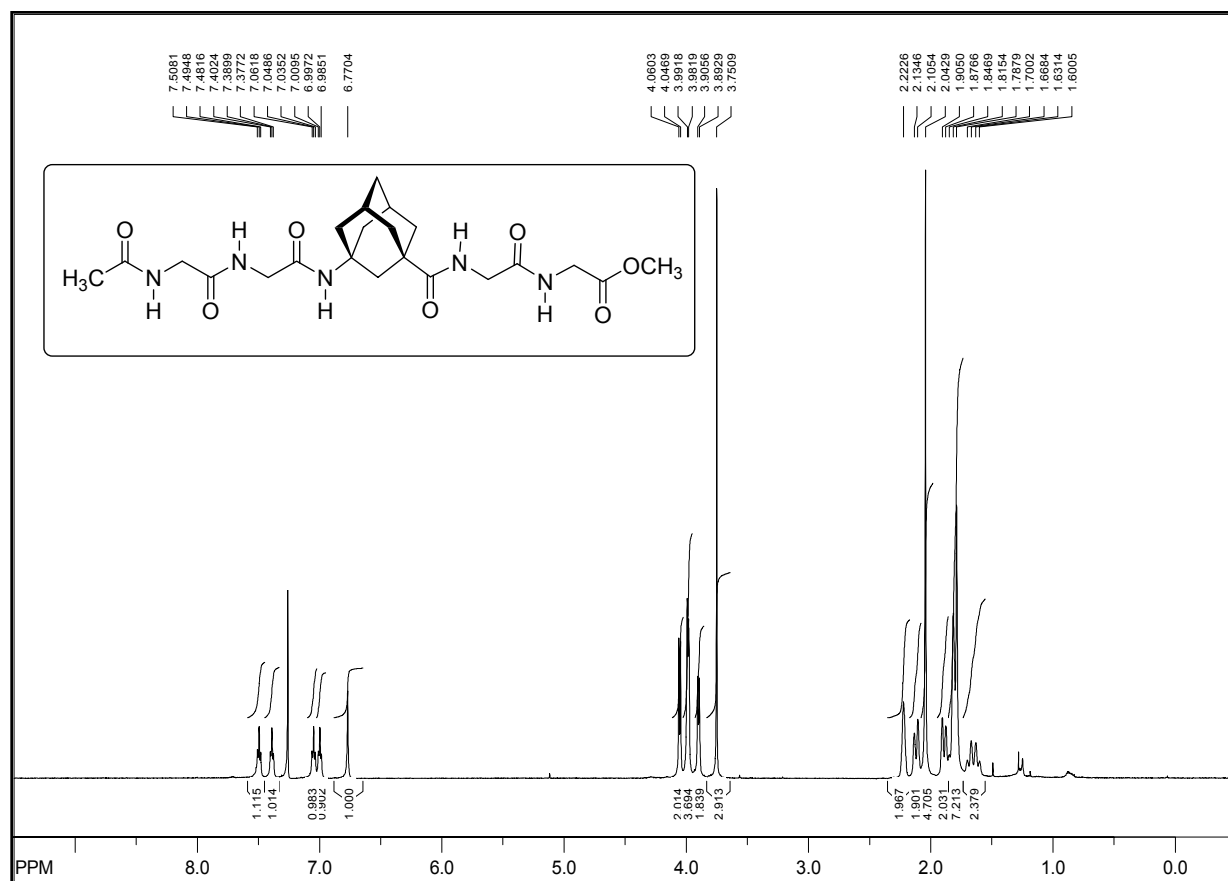


Ac-Gly¹-A-Gly²-A-Gly³-Gly⁴-OMe (262)

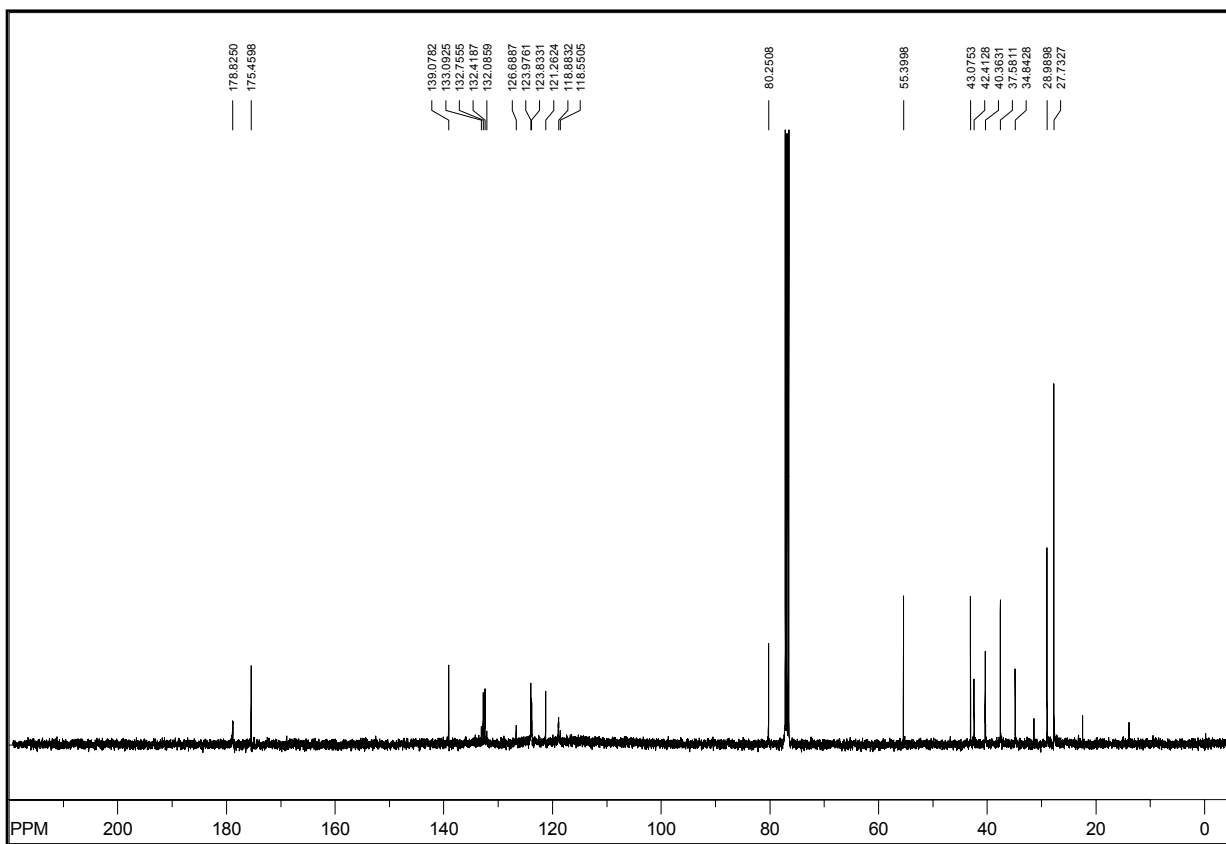
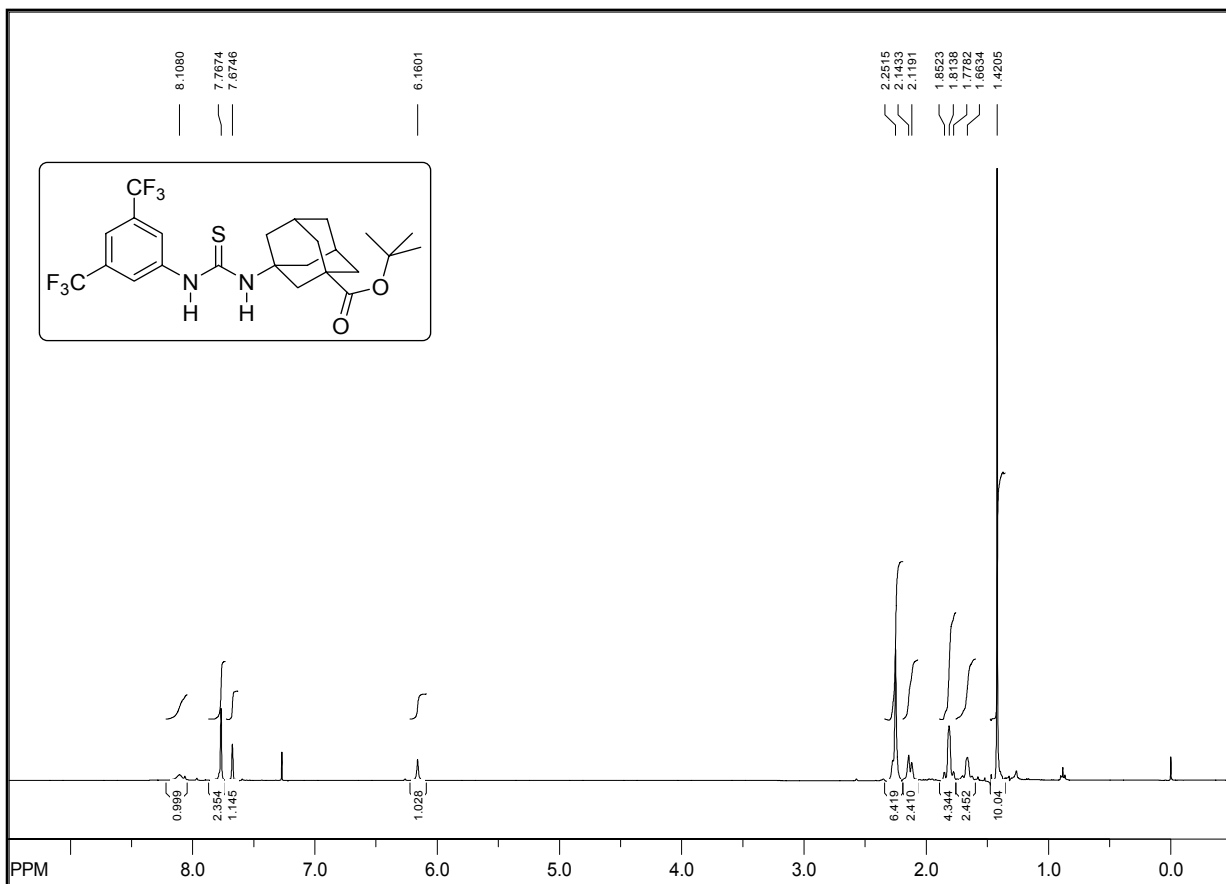
Ac-Gly¹-Gly²-Gly³-Gly⁴-OMe (**263**)



Ac-Gly¹-Gly²-A-Gly³-Gly⁴-OMe (264)



Ac-Gly¹-Gly²-A-Gly³-Gly⁴-Gly⁵-OMe (265)



TU-A Gly-O^tBu (266)

13. Abbreviations

μM	micromole per liter	CNS	Central nervous system
2-Adoc	(2-Adamantyl-oxo)carbonyl	COSY	Correlation spectroscopy.
^AAib	5,7-Dimethyl-3-aminoadamantane-1-carboxylic acid	Da	Dalton
^AAla	5-Methyl-3-aminoadamantane-1-carboxylic acid	DEPT¹³⁵	Distortionless enhancement via polarization transfer. 135° pulse angle
^AAsp	5-Carboxymethyl-3-aminoadamantane-1-carboxylic acid	DFT	Density functional theory. A computational chemistry approach.
AD	Alzheimer's disease	DIC	N,N' diisopropyl carbodiimide
^AGlu	5-(2-Carboxy)ethyl-3-aminoadamantane-1-carboxylic acid	DIPEA	N-Ethyl-N,N-Diisopropylamine
^AGly	3-Aminoadamantane-1-carboxylic acid	DMSO	Dimethyl sulfoxide.
Aib	Aminoisobutyric acid		2',6'-dimethyl-L-tyrosine. Unnatural amino acid used in combination with the Tic moiety in specific opioid receptor antagonists.
Ala	Alanine	Dmt	Dipeptidyl peptidase IV. An indiscriminate enzyme playing a major role in glucose metabolism.
AM1	Austin model 1. A semi-empirical model.	DPP-IV	
AMPA	α-amino-3-hydroxy-5-methyl-4-isoxazolepropionate. A ligand used to distinguish glutamate receptor subtypes.	e.r.	Enantiomeric ratio
APT	Attached proton test. NMR method to distinguish signals of carbons with 1 / 3 or 2 / 0 hydrogen atoms attached to it.	EC₅₀	Half maximal effective concentration: The concentration of a drug to induce 50% of the maximum response.
Asp	Aspartate	EMA	European Medicines Agency. An EU regulatory agency for the evaluation of medicinal products
ATP	Adenosine triphosphate	eq.	Equation
^AVal	5-Isopropyl-3-aminoadamantane-1-carboxylic acid	ER	Estrogen receptor
^AXaa	An arbitrary γ-aminoadamantane-1-carboxylic acid residue	ESI	Electrospray ionisation
α-Xaa	An arbitrary alpha amino acid residue	FDA	Food and Drug Administration
B3LYP	Becke-3-Lee-Yang-Parr. A density functional theory method with three empirical parameters.	Fmoc-	9-Fluorenylmethoxycarbonyl-. Standard, base-labile amino protective group in SPPS.
BBB	Blood-brain-barrier	FPV	Fowl Plague virus. An <i>Influenza A</i> subtype.
Bn	Benzyl-	GABA	γ-Amino butyric acid. The major inhibitory neurotransmitter in human CNS.
Boc	<i>tert.</i> -Butoxycarbonyl-	GC	Gas chromatography
BSSE	Basis set superimposition error	GC-MS	Gas chromatography coupled with a mass spectrometer
		Glu	Glutamate

Gly	Glycine	MeCN	Acetonitrile
HA	Haemagglutinin	mGAT-1	Murine GABA transporter
HATU	{N-[(dimethylamino)-1H-1,2,3-triazolo[4,5-b]pyridin-1-yl-methylene]-N-methylmethanaminium hexafluorophosphate N-oxide}	mGluR	Metabotropic glutamate receptor
HBTU	O-(1-Benzotriazolyl)-N,N,N',N'-tetramethyluronium hexafluorophosphate	MIC	Minimum inhibitory concentration
HCV	<i>Hepatitis C</i> virus	MM	Molecular mechanics
HF	Hartree-Fock	mM	Millimolar
His	Histidine	MM3	Molecular mechanics 3. A force field developed by Allinger et al.
HIV	Human Immunodeficiency Virus	MMFF-94	Merck molecular force field 1994
HMBC	Heteronuclear multiple quantum coherence. An experiment frequently used in NMR spectroscopy to detect $^2J(\text{C-H})$ and $^3J(\text{C-H})$ correlations.	MW	Molecular weight
HOBt	Hydroxybenzotriazol	nM	Nanomol per liter
HPLC	High Performance Liquid Chromatography	NMDA	N-Methyl D-aspartate. A ligand used to distinguish glutamate receptors.
HSQC	Heteronuclear Single Quantum Coherence. An experiment frequently used in NMR spectroscopy to detect correlations $^1J(\text{C-H})$.	NMR	Nuclear magnetic resonance
HSV	Herpes Simplex Virus	NOE	Nuclear Overhauser effect
I₂^{PP2A}	Inhibitor 2 of Protein Phosphatase 2A	NOESY	Nuclear Overhauser effect spectroscopy. NMR method utilizing through-space-interactions of protons to detect spatial proximity.
IC₅₀	Inhibitory Concentration (50%) or the half maximal inhibitory concentration. Concentration of an inhibitor that is required for 50% inhibition.	PCP	Phencyclidine, a NMDA receptor antagonist.
iPr	isopropyl-	PD	Parkinson's disease
IR	Infrared	PES	Potential energy surface
LCAO	Linear Combination of Atomic Orbitals	Phe	Phenylalanine
Leu	Leucine	Phg	Phenylglycine
M_{abs.}	Absolute molecular mass	PP-2A	Protein phosphatase 2A
MALDI-TOF	Matrix-Assisted Laser Desorption Ionisation-Time of Flight.	Pro	Proline
MBH	Morita-Baylis-Hillman	PT	Phase transfer
MDCK	Madin Darby Canine Kidney cell line	PTC	Phase transfer catalysis
Me	Methyl	PTK	Phasentransferkatalyse

r.t.	Room temperature	TFA	2,2,2-Trifluoroacetic acid
Rf	Retention factor	THF	Tetrahydrofuran
ROS	Reactive oxygen species	Tic	L-1,2,3,4-Tetrahydroisoquinoline-3-carboxylate. A subunit of the Dmt-Tic pharmacophor used as an opioid receptor antagonist.
RP-HPLC	Reversed-phase high performance liquid chromatography	TLC	Thin layer chromatography
SAR	Structure activity relationship	TOCSY	Total correlation spectroscopy
SARS	Severe acute respiratory syndrome	t_R	Retention time
sEH	Soluble epoxide hydrolase	Val	Valine
SET	Single electron transfer	VANBA	Vanillinbananin, a trioxadamantane (1-(4-hydroxy-3-methoxyphenyl)-2,8,9-trioxadamantane-3,5,7-triol).
SPPS	Solid phase peptide synthesis	vDNA	Viral desoxyribonucleic acid
STO	Slater type orbitals	WSN	An <i>Influenza A</i> virus subtype
TAT	Trioxadamantane triol	ZNS	Zentrales nervensystem
TBABr	tetra n-butyl ammonium bromide. A phase-transfer catalyst.		

14. References

- [1] A. Hinman, J. Du Bois, *J. Am. Chem. Soc.* **2003**, *125*, 11510-11511.
- [2] U. Koert, *Angew. Chem. Int. Ed.* **2004**, *43*, 5572-5576.
- [3] K. Sato, S. Akai, N. Sugita, T. Ohsawa, T. Kogure, H. Shoji, J. Yoshimura, *J. Org. Chem.* **2005**, *70*, 7496-7504.
- [4] D. Urabe, T. Nishikawa, M. Isobe, *Chem. Asian J.* **2006**, *1*, 125-135.
- [5] F. Hucho, *Angew. Chem. Int. Ed.* **1995**, *34*, 39-50.
- [6] D. M. Roll, J. E. Biskupiak, C. L. Mayne, C. M. Ireland, *J. Am. Chem. Soc.* **1986**, *108*, 6680-6682.
- [7] R. W. Hoffman, G. Dahmann, *Tetrahedron Lett.* **1993**, *34*, 1115-1118.
- [8] J. T. Blanchfield, D. J. Brecknell, I. M. Brereton, M. J. Garson, D. D. Jones, *Aust. J. Chem.* **1994**, *47*, 2255-2269.
- [9] L.-H. Hu, K.-Y. Sim, *Tetrahedron Lett.* **1998**, *39*, 7999-8002.
- [10] L.-H. Hu, K.-Y. Sim, *Tetrahedron Lett.* **1999**, *40*, 759-762.
- [11] Y.-L. Lin, Y.-S. Wu, *Helv. Chim. Acta* **2003**, *86*, 2156-2163.
- [12] L. H. Hu, K. Y. Sim, *Org. Lett.* **1999**, *1*, 879-882.
- [13] D. G. J. Young, D. Zeng, *J. Org. Chem.* **2002**, *67*, 3134-3137.
- [14] L.-H. Hu, K.-Y. Sim, *Tetrahedron* **2000**, *56*, 1379-1386.
- [15] S. Landa, V. Machacek, *Collect. Czech. Chem. C.* **1933**, *5*, 1-5.
- [16] J. E. Dahl, S. G. Liu, R. M. K. Carlson, *Science* **2003**, *299*, 96-99.
- [17] P. R. Schreiner, N. A. Fokina, B. A. Tkachenko, H. Hausmann, M. Serafin, J. E. P. Dahl, S. Liu, R. M. K. Carlson, A. A. Fokin, *J. Org. Chem.* **2006**, *71*, 6709-6720.
- [18] W. C. Webber, P. A. Harthoorn, *Chlorinated and brominated polycyclic hydrocarbons*, GB 819240, **1959**.
- [19] P. v. R. Schleyer, *J. Am. Chem. Soc.* **1957**, *79*, 3292.
- [20] K. Gerzon, E. V. Krumalns, R. L. Brindle, F. J. Marshall, M. A. Root, *J. Med. Chem.* **1963**, *6*, 760-763.
- [21] R. T. Rapala, R. J. Kraay, K. Gerzon, *J. Med. Chem.* **1965**, *8*, 580-583.
- [22] K. Gerzon, D. Kau, *J. Med. Chem.* **1967**, *10*, 189-199.
- [23] L. F. Fieser, M. Z. Nazer, S. Archer, D. A. Berberian, R. G. Slighter, *J. Med. Chem.* **1967**, *10*, 517-521.
- [24] K. Gerzon, D. J. Tobias, R. E. Holmes, R. E. Rathbun, R. W. Kattau, *J. Med. Chem.* **1967**, *10*, 603-606.
- [25] W. L. Davies, R. R. Grunert, R. F. Haff, J. W. McGahen, E. M. Neumayer, M. Paulshock, J. C. Watts, T. R. Wood, E. C. Hermann, C. E. Hoffmann, *Science* **1964**, *144*, 862-863.
- [26] H. W. Geluk, J. Schut, J. L. M. A. Schlatmann, *J. Med. Chem.* **1969**, *12*, 712-715.
- [27] J. G. Whitney, W. A. Gregory, J. C. Kauer, J. R. Roland, J. A. Snyder, R. E. Benson, E. C. Hermann, *J. Med. Chem.* **1970**, *13*, 254-260.
- [28] P. E. Aldrich, E. C. Hermann, W. E. Meier, M. Paulshock, W. W. Prichard, J. A. Synder, J. C. Watts, *J. Med. Chem.* **1971**, *14*, 535-543.
- [29] A. Tsunoda, H. F. Maassab, K. W. Cochran, W. C. Eveland, *Antimicrob. Agents Chemother.* **1965**, 553-560.

- [30] K. Lundahl, J. Schut, J. L. M. A. Schlatmann, G. B. Paerels, A. Peters, *J. Med. Chem.* **1972**, *15*, 129-132.
- [31] R. Van Hes, A. Smit, T. Kralt, A. Peters, *J. Med. Chem.* **1972**, *15*, 132-136.
- [32] A. Kreuzberger, H. H. Schroeders, *Tetrahedron Lett.* **1969**, 5101-5104.
- [33] A. Kreuzberger, A. Tantawy, *Arzneimittel-Forsch.* **1983**, *33*, 512-514.
- [34] J. W. Tilley, P. Levitan, M. J. Kramer, *J. Med. Chem.* **1979**, *22*, 1009-1010.
- [35] R. Pellicciari, M. C. Fioretti, P. Cogolli, M. Tiecco, *Arzneimittel-Forsch.* **1980**, *30*, 2103-2105.
- [36] P. S. Manchand, R. L. Cerruti, J. A. Martin, C. H. Hill, J. H. Merrett, E. Keech, R. B. Belshe, E. V. Connell, I. S. Sim, *J. Med. Chem.* **1990**, *33*, 1992-1995.
- [37] B. Vranesic, J. Tomasic, D. Kantoci, S. Smerdel, G. Sava, I. Hrsak, *21st Proc. Eur. Pept. Symp.* **1991**, 885-886.
- [38] N. Kolocouris, G. B. Foscolos, A. Kolocouris, P. Marakos, N. Pouli, G. Fytas, S. Ikeda, E. De Clercq, *J. Med. Chem.* **1994**, *37*, 2896-2902.
- [39] N. Kolocouris, A. Kolocouris, G. B. Foscolos, G. Fytas, J. Neyts, E. Padalko, J. Balzarini, R. Snoeck, G. Andrei, E. De Clercq, *J. Med. Chem.* **1996**, *39*, 3307-3318.
- [40] A. Kolocouris, D. Tataridis, G. Fytas, T. Mavromoustakos, G. B. Foscolos, N. Kolocouris, E. De Clercq, *Bioorg. Med. Chem. Lett.* **1999**, *9*, 3465-3470.
- [41] G. Stamatiou, A. Kolocouris, N. Kolocouris, G. Fytas, G. B. Foscolos, J. Neyts, E. De Clercq, *Bioorg. Med. Chem. Lett.* **2001**, *11*, 2137-2142.
- [42] G. Stamatiou, G. B. Foscolos, G. Fytas, A. Kolocouris, N. Kolocouris, C. Pannecouque, M. Witvrouw, E. Padalko, J. Neyts, E. De Clercq, *Bioorgan. Med. Chem.* **2003**, *11*, 5485-5492.
- [43] I. Stylianakis, A. Kolocouris, N. Kolocouris, G. Fytas, G. B. Foscolos, E. Padalko, J. Neyts, E. De Clercq, *Bioorg. Med. Chem. Lett.* **2003**, *13*, 1699-1703.
- [44] A. S. Monto, S. E. Ohmit, K. Hornbuckle, C. L. Pearce, *Antimicrob. Agents Chemother.* **1995**, *39*, 2224-2228.
- [45] C. Scholtissek, R. G. Webster, *Antivir. Res.* **1998**, *38*, 213-215.
- [46] V. Farina, J. D. Brown, *Angew. Chem. Int. Ed.* **2006**, *45*, 7330-7334.
- [47] C. Scholtissek, G. Quack, H. D. Klenk, R. G. Webster, *Antivir. Res.* **1998**, *37*, 83-95.
- [48] A. C. Hurt, P. Selleck, N. Komadina, R. Shaw, L. Brown, I. G. Barr, *Antivir. Res.* **2007**, *73*, 228-231.
- [49] R. B. Belshe, M. H. Smith, C. B. Hall, R. Betts, A. J. Hay, *J. Virol.* **1988**, *62*, 1508-1512.
- [50] L. H. Pinto, L. J. Holsinger, R. A. Lamb, *Cell* **1992**, *69*, 517-528.
- [51] S. Grambas, A. J. Hay, *Virology* **1992**, *190*, 11-18.
- [52] T.-I. Lin, H. Heider, C. Schroeder, *J. Gen. Virol.* **1997**, *78*, 767-774.
- [53] C. S. Gandhi, K. Shuck, J. D. Lear, G. R. Dieckmann, W. F. DeGrado, R. A. Lamb, L. H. Pinto, *J. Biol. Chem.* **1999**, *274*, 5474-5482.
- [54] K. Nishimura, S. Kim, L. Zhang, T. A. Cross, *Biochemistry* **2002**, *41*, 13170-13177.
- [55] K. Keppeler, G. Kiefer, E. De Clercq, *Arch. Pharm.* **1984**, *317*, 867-873.
- [56] M. F. Powell, A. Magill, N. Chu, K. Hama, C. I. Mau, L. Foster, R. Bergstrom, *Pharm. Res.* **1991**, *8*, 1418-1423.
- [57] A. Scherm, D. Peteri, *Antiviral 1-(aminoethoxyacetylamino)adamantanes*, DE 69-19412181941218, **1971**.

- [58] D. E. Ickes, T. M. Venetta, Y. Phonphok, K. S. Rosenthal, *Antivir. Res.* **1990**, *14*, 75-85.
- [59] T. Berg, B. Kronenberger, H. Hinrichsen, T. Gerlach, P. Buggisch, E. Herrmann, U. Spengler, T. Goeser, S. Nasser, K. Wursthorn, G. R. Pape, U. Hopf, S. Zeuzem, *Hepatology* **2003**, *37*, 1359-1367.
- [60] R. Sarbach, J. Mizoule, C. Ricci, D. Yavordios, *Cholagogically-active adamantanecarboxylic acids of pyridoxines, pyridoxamines, or pyridoxals*, DE 69-19206731920673, **1971**.
- [61] C. R. Kinsolving, V. S. Georgiev, *Esters of 2-adamantanone oxime*, US 83-5244844486601, **1984**.
- [62] N. Tsuzuki, T. Hama, M. Kawada, A. Hasui, R. Konishi, S. Shiwa, Y. Ochi, S. Futaki, K. Kitagawa, *J. Pharm. Sci.* **1994**, *83*, 481-484.
- [63] G. Fytas, G. Stamatiou, G. B. Foscolos, A. Kolocouris, N. Kolocouris, M. Witvrouw, C. Pannecouque, E. De Clercq, *Bioorg. Med. Chem. Lett.* **1997**, *7*, 1887-1890.
- [64] R. Mahfoud, M. Mylvaganam, C. A. Lingwood, J. Fantini, *J. Lipid Res.* **2002**, *43*, 1670-1679.
- [65] J. Balzarini, C. Pannecouque, E. De Clercq, A. Y. Pavlov, S. S. Printsevskaya, O. V. Miroshnikova, M. I. Reznikova, M. N. Preobrazhenskaya, *J. Med. Chem.* **2003**, *46*, 2755-2764.
- [66] S. S. Printsevskaya, S. E. Solovieva, E. N. Olsufyeva, E. P. Mirchink, E. B. Isakova, E. De Clercq, J. Balzarini, M. N. Preobrazhenskaya, *J. Med. Chem.* **2005**, *48*, 3885-3890.
- [67] A. A. El-Emam, O. A. Al-Deeb, M. Al-Omar, J. Lehmann, *Bioorgan. Med. Chem.* **2004**, *12*, 5107-5113.
- [68] G. M. Bertot, P. D. Becker, C. A. Guzman, S. Grinstein, *J. Infect. Dis.* **2004**, *189*, 1304-1312.
- [69] K. N. Masihi, K. Masek, *Int. J. Immunother.* **1993**, *9*, 143-150.
- [70] A. J. Kesel, *Curr. Med. Chem.* **2005**, *12*, 2095-2162.
- [71] R. S. Schwab, A. C. England, Jr., D. C. Poskanzer, R. R. Young, *J. Amer. Med. Ass.* **1969**, *208*, 1168-1170.
- [72] J. K. Chakrabarti, M. J. Foulis, T. M. Hotten, S. S. Szinai, A. Todd, *J. Med. Chem.* **1974**, *17*, 602-609.
- [73] J. K. Chakrabarti, T. M. Hotten, S. Sutton, D. E. Tupper, *J. Med. Chem.* **1976**, *19*, 967-969.
- [74] P. A. Swift, M. L. Stagnito, G. B. Mullen, G. C. Palmer, V. S. Georgiev, *Eur. J. Med. Chem.* **1988**, *23*, 465-471.
- [75] A. Scherm, D. Peteri, *3,5-Dialkyl-1-aminoadamantanes for the treatment of parkinsonism*, DE 73-23184612318461, **1974**.
- [76] J. G. Henkel, Hane, J. T., *J. Med. Chem.* **1982**, *25*, 51-56.
- [77] J. M. Rabey, P. Nissipeanu, A. D. Korczyn, *J. Neural Transm-Park.* **1992**, *4*, 277-282.
- [78] J. Kornhuber, K. Schoppmeyer, P. Riederer, *Neurosci. Lett.* **1993**, *163*, 129-131.
- [79] M. Weller, F. Finiels-Marlier, S. M. Paul, *Brain Res.* **1993**, *613*, 143-148.
- [80] R. Spanagel, B. Eilbacher, R. Wilke, *Eur. J. Pharmacol.* **1994**, *262*, 21-26.
- [81] G. Page, M. Peeters, J. M. Maloteaux, E. Hermans, *Eur. J. Pharmacol.* **2000**, *403*, 75-80.
- [82] J. W. Keabian, D. R. Britton, M. P. DeNinno, R. Perner, L. Smith, P. Jenner, R. Schoenleber, M. Williams, *Eur. J. Pharmacol.* **1992**, *229*, 203-209.

- [83] L. A. Smith, M. J. Jackson, G. Al-Barghouthy, P. Jenner, *J. Neural Transm.* **2002**, *109*, 123-140.
- [84] J. Skolimowski, A. Kochman, L. Gebicka, D. Metodiewa, *Bioorgan. Med. Chem.* **2003**, *11*, 3529-3539.
- [85] M. Nakazono, S. Hasegawa, T. Yamamoto, K. Zaitso, *Bioorg. Med. Chem. Lett.* **2004**, *14*, 5619-5621.
- [86] K. D. Meisheri, S. J. Humphrey, S. A. Khan, L. A. Cipkus-Dubray, M. P. Smith, A. W. Jones, *J. Pharmacol. Exp. Ther.* **1993**, *266*, 655-665.
- [87] E. Guillemare, E. Honore, J. De Weille, M. Fosset, M. Lazdunski, K. Meisheri, *Mol. Pharmacol.* **1994**, *46*, 139-145.
- [88] D. B. Tikhonov, B. S. Zhorov, L. G. Magazanik, *Biophys. J.* **1999**, *77*, 1914-1926.
- [89] H. Lavreysen, C. Janssen, F. Bischoff, X. Langlois, J. E. Leysen, A. S. J. Lesage, *Mol. Pharmacol.* **2003**, *63*, 1082-1093.
- [90] H. Lavreysen, S. N. Pereira, J. E. Leysen, X. Langlois, A. S. J. Lesage, *Neuropharmacology* **2004**, *46*, 609-619.
- [91] L. G. Magazanik, S. L. Buldakova, M. V. Samoilo, V. E. Gmiro, I. R. Mellor, P. N. R. Usherwood, *J. Physiol.* **1997**, *505*, 655-663.
- [92] K. V. Bolshakov, D. B. Tikhonov, V. E. Gmiro, L. G. Magazanik, *Neurosci. Lett.* **2000**, *291*, 101-104.
- [93] M. Chebib, G. A. R. Johnston, *J. Med. Chem.* **2000**, *43*, 1427-1447.
- [94] G. A. R. Johnston, *Curr. Pharm. Des.* **2005**, *11*, 1867-1885.
- [95] P. Krosgaard-Larsen, B. Frolund, K. Frydenvang, *Curr. Pharm. Des.* **2000**, *6*, 1193-1209.
- [96] G. Satzinger, *Arzneimittel-Forsch.* **1994**, *44*, 261-266.
- [97] C. P. Taylor, *Neurology* **1994**, *44*, S10-16; discussion S31-12.
- [98] M. J. Field, Z. Li, J. B. Schwarz, *J. Med. Chem.* **2007**, *50*, 2569-2575.
- [99] G. Zoidis, I. Papanastasiou, I. Dotsikas, A. Sandoval, R. G. Dos Santos, Z. Papadopoulou-Daifoti, A. Vamvakides, N. Kolocouris, R. Felix, *Bioorgan. Med. Chem.* **2005**, *13*, 2791-2798.
- [100] J. S. Bryans, N. Davies, N. S. Gee, V. U. K. Dissanayake, G. S. Ratcliffe, D. C. Horwell, C. O. Kneen, A. I. Morrell, R. J. Oles, J. C. O'Toole, G. M. Perkins, L. Singh, *J. Med. Chem.* **1998**, *41*, 1838-1845.
- [101] M. Pallas, A. Camins, *Curr. Pharm. Des.* **2006**, *12*, 4389-4408.
- [102] S. Gilead, E. Gazit, *Angew. Chem. Int. Ed.* **2004**, *43*, 4041-4044.
- [103] C. Schmuck, P. Frey, M. Heil, *ChemBioChem* **2005**, *6*, 628-631.
- [104] G. M. Bores, F. P. Huger, W. Petko, A. E. Mutlib, F. Camacho, D. K. Rush, D. E. Selk, V. Wolf, R. W. Kosley, Jr., et al., *J. Pharmacol. Exp. Ther.* **1996**, *277*, 728-738.
- [105] J. Bormann, M. R. Gold, W. Schatton, *Use of adamantane derivatives in the prevention and treatment of cerebral ischemia*, EP 89-106657392059, **1990**.
- [106] H. S. V. Chen, J. W. Pellegrini, S. K. Aggarwal, S. Z. Lei, S. Warach, F. E. Jensen, S. A. Lipton, *J. Neurosci.* **1992**, *12*, 4427-4436.
- [107] R. J. Bergeron, W. R. Weimar, Q. Wu, J. K. Austin, Jr., J. S. McManis, *J. Med. Chem.* **1995**, *38*, 425-428.
- [108] S. Samnick, S. Ametamey, M. R. Gold, P. A. Schubiger, *J. Labelled Compd. Rad.* **1997**, *39*, 241-250.
- [109] M. A. Rogawski, *Amino Acids* **2000**, *19*, 133-149.
- [110] W. Danysz, C. G. Parsons, G. Quack, *Amino Acids* **2000**, *19*, 167-172.
- [111] S. K. Sonkusare, C. L. Kaul, P. Ramarao, *Pharmacol. Res.* **2005**, *51*, 1-17.

- [112] S. A. Lipton, *Nat. Rev. Drug Discovery* **2006**, *5*, 160-170.
- [113] K. V. Bolshakov, V. E. Gmiro, D. B. Tikhonov, L. G. Magazanik, *J. Neurochem.* **2003**, *87*, 56-65.
- [114] K. V. Bolshakov, K. H. Kim, N. N. Potapjeva, V. E. Gmiro, D. B. Tikhonov, P. N. R. Usherwood, I. R. Mellor, L. G. Magazanik, *Neuropharmacology* **2005**, *49*, 144-155.
- [115] A. M. Gerber, M. L. Vallano, *Mini-Reviews in Medicinal Chemistry* **2006**, *6*, 805-815.
- [116] A. Jirgensons, V. Kauss, A. F. Mishnev, I. Kalvinsh, *J. Chem. Soc. Perk. T 1* **1999**, 3527-3530.
- [117] A. Jirgensons, V. Kauss, I. Kalvinsh, M. R. Gold, W. Danysz, C. G. Parsons, G. Quack, *Eur. J. Med. Chem.* **2000**, *35*, 555-565.
- [118] A. G. S. Blommaert, J. H. Weng, A. Dorville, I. McCort, B. Ducos, C. Durieux, B. P. Roques, *J. Med. Chem.* **1993**, *36*, 2868-2877.
- [119] B. Bellier, I. McCort-Tranchepain, B. Ducos, S. Danascimento, H. Meudal, F. Noble, C. Garbay, B. P. Roques, *J. Med. Chem.* **1997**, *40*, 3947-3956.
- [120] I. V. Ekhatov, Y. Huang, *J. Labelled Compd. Rad.* **1997**, *39*, 1019-1038.
- [121] B. K. Trivedi, J. K. Padia, A. Holmes, S. Rose, D. S. Wright, J. P. Hinton, M. C. Pritchard, J. M. Eden, C. Kneen, L. Webdale, N. Suman-Chauhan, P. Boden, L. Singh, M. J. Field, D. Hill, *J. Med. Chem.* **1998**, *41*, 38-45.
- [122] M. Kajbaf, P. Rossato, J. R. Barnaby, M. Pellegatti, *Xenobiotica* **1998**, *28*, 167-178.
- [123] E. A. Harper, N. P. Shankley, J. W. Black, *Brit. J. Pharmacol.* **1999**, *126*, 1504-1512.
- [124] P. Munoz-Ruiz, M. T. Garcia-Lopez, E. Cenarruzabeitia, J. Del Rio, M. Dufresne, M. Foucaud, D. Fourmy, R. Herranz, *J. Med. Chem.* **2004**, *47*, 5318-5329.
- [125] T. E. Christos, A. Arvanitis, G. A. Cain, A. L. Johnson, R. S. Potorf, S. W. Tam, W. K. Schmidt, *Bioorg. Med. Chem. Lett.* **1993**, *3*, 1035-1040.
- [126] D. Gully, B. Labeeuw, R. Biogegrain, F. Oury-Donat, A. Bachy, M. Poncelet, R. Steinberg, M. F. Suaud-Chagny, V. Santucci, N. Vita, F. Pecceu, C. Labbe-Jullie, P. Kitabgi, P. Soubrie, G. Le Fur, J. P. Maffrand, *J. Pharmacol. Exp. Ther.* **1997**, *280*, 802-812.
- [127] C. Betancur, M. Canton, A. Burgos, B. Labeeuw, D. Gully, W. Rostene, D. Pelaprat, *Eur. J. Pharmacol.* **1998**, *343*, 67-77.
- [128] E. B. Binder, B. Kinkead, M. J. Owens, C. D. Kilts, C. B. Nemeroff, *J. Neurosci.* **2001**, *21*, 601-608.
- [129] S. Barroso, F. Richard, D. Nicolas-Etheve, J.-L. Reversat, J.-M. Bernassau, P. Kitabgi, C. Labbe-Jullie, *J. Biol. Chem.* **2000**, *275*, 328-336.
- [130] F. G. Costa, R. Frussa-Filho, L. F. Felicio, *Eur. J. Pharmacol.* **2001**, *428*, 97-103.
- [131] B. Lammek, Y. X. Wang, I. Gavras, H. Gavras, *J. Pharm. Pharmacol.* **1991**, *43*, 887-888.
- [132] J. W. Dear, K. Wirth, G. K. Scadding, J. C. Foreman, *Brit. J. Pharmacol.* **1996**, *119*, 1054-1062.
- [133] W. D. Ehringer, M. J. Edwards, R. D. Gray, F. N. Miller, *Inflammation* **1997**, *21*, 279-298.
- [134] H. Matsuda, K. Hayashi, S. Wakino, E. Kubota, M. Honda, H. Tokuyama, I. Takamatsu, S. Tatematsu, T. Saruta, *Hypertension* **2004**, *43*, 603-609.

- [135] S. Tanabe, Y. Shishido, Y. Nakayama, M. Furushiro, S. Hashimoto, T. Terasaki, G. Tsujimoto, T. Yokokura, *Pharmacol. Biochem. Be.* **1999**, *63*, 549-553.
- [136] T. Zenteno-Savin, I. Sada-Ovalle, G. Ceballos, R. Rubio, *Eur. J. Pharmacol.* **2000**, *410*, 15-23.
- [137] G. Flouret, T. Majewski, L. Balaspiri, W. Brieher, K. Mahan, O. Chaloin, L. Wilson, Jr., J. Slaninova, *J. Pept. Sci.* **2002**, *8*, 314-326.
- [138] J. Hughes, T. W. Smith, H. W. Kosterlitz, L. A. Fothergill, B. A. Morgan, H. R. Morris, *Nature* **1975**, *258*, 577-579.
- [139] R. H. Mazur, *N-Adamantane-substituted tetrapeptidamide and its pharmacologically compatible salts*, DE 80-30447933044793, **1981**.
- [140] M. Comb, P. H. Seeburg, J. Adelman, L. Eiden, E. Herbert, *Nature* **1982**, *295*, 663-667.
- [141] D. Kim Quang, R. Schwyzer, *Helv. Chim. Acta* **1981**, *64*, 2084-2089.
- [142] N. Tsuzuki, T. Hama, T. Hibi, R. Konishi, S. Futaki, K. Kitagawa, *Biochem. Pharmacol.* **1991**, *41*, R5-R8.
- [143] S. Horvat, K. Mlinaric-Majerski, L. Glavas-Obrovac, A. Jakas, J. Veljkovic, S. Marczi, G. Kragol, M. Roscic, M. Matkovic, A. Milostic-Srb, *J. Med. Chem.* **2006**, *49*, 3136-3142.
- [144] M. A. Abou-Gharbia, W. E. Childers, Jr., H. Fletcher, G. McGaughey, U. Patel, M. B. Webb, J. Yardley, T. Andree, C. Boast, R. J. Kucharik, K. Marquis, H. Morris, R. Scerni, J. A. Moyer, *J. Med. Chem.* **1999**, *42*, 5077-5094.
- [145] P. Zajdel, G. Subra, A. J. Bojarski, B. Duszynska, M. Pawlowski, J. Martinez, *J. Comb. Chem.* **2004**, *6*, 761-767.
- [146] F. E. Murdoch, J. Gorski, *Mol. Cell. Endocrinol.* **1991**, *78*, C103-C108.
- [147] Y. Yamakoshi, Y. Otani, S. Fujii, Y. Endo, *Biol. Pharm. Bull.* **2000**, *23*, 259-261.
- [148] R. Liu, S.-H. Yang, E. Perez, K. D. Yi, S. S. Wu, K. Eberst, L. Prokai, K. Prokai-Tatrai, Z. Y. Cai, D. F. Covey, A. L. Day, J. W. Simpkins, *Stroke* **2002**, *33*, 2485-2491.
- [149] D. M. Kumar, E. Perez, Z. Yun Cai, P. Aoun, A.-M. Brun-Zinkernagel, D. F. Covey, J. W. Simpkins, N. Agarwal, *Free Radical Bio. Med.* **2005**, *38*, 1152-1163.
- [150] E. Perez, R. Liu, S.-H. Yang, Z. Y. Cai, D. F. Covey, J. W. Simpkins, *Brain Res.* **2005**, *1038*, 216-222.
- [151] R. S. Muthyala, S. Sheng, K. E. Carlson, B. S. Katzenellenbogen, J. A. Katzenellenbogen, *J. Med. Chem.* **2003**, *46*, 1589-1602.
- [152] Y. Fujita, Y. Tsuda, T. Li, T. Motoyama, M. Takahashi, Y. Shimizu, T. Yokoi, Y. Sasaki, A. Ambo, A. Kita, Y. Jinsmaa, S. D. Bryant, L. H. Lazarus, Y. Okada, *J. Med. Chem.* **2004**, *47*, 3591-3599.
- [153] S. D. Bryant, C. George, J. L. Flippen-Anderson, J. R. Deschamps, S. Salvadori, G. Balboni, R. Guerrini, L. H. Lazarus, *J. Med. Chem.* **2002**, *45*, 5506-5513.
- [154] A. A. Wilson, R. F. Dannals, H. T. Ravert, M. S. Sonders, E. Weber, H. N. Wagner, Jr., *J. Med. Chem.* **1991**, *34*, 1867-1870.
- [155] A. S. Kimes, A. A. Wilson, U. Scheffel, B. G. Campbell, E. D. London, *J. Med. Chem.* **1992**, *35*, 4683-4689.
- [156] G. Ronsisvalle, A. Marrazzo, O. Prezzavento, L. Pasquinucci, B. Falcucci, R. Di Toro, S. Spampinato, *Bioorgan. Med. Chem.* **2000**, *8*, 1503-1513.
- [157] A. Marrazzo, O. Prezzavento, L. Pasquinucci, F. Vittorio, G. Ronsisvalle, *Farmaco* **2001**, *56*, 181-189.

- [158] B. Bourrie, E. Bribes, N. De Nys, M. Esclangon, L. Garcia, S. Galiegue, P. Lair, R. Paul, C. Thomas, J.-C. Vernieres, P. Casellas, *Eur. J. Pharmacol.* **2002**, *456*, 123-131.
- [159] F. Oesch, *Xenobiotica* **1973**, *3*, 305-340.
- [160] C. Morisseau, M. H. Goodrow, D. Dowdy, J. Zheng, J. F. Greene, J. R. Sanborn, B. D. Hammock, *P. Natl. Acad. Sci. USA* **1999**, *96*, 8849-8854.
- [161] I.-H. Kim, C. Morisseau, T. Watanabe, B. D. Hammock, *J. Med. Chem.* **2004**, *47*, 2110-2122.
- [162] I.-H. Kim, F. R. Heitzler, C. Morisseau, K. Nishi, H.-J. Tsai, B. D. Hammock, *J. Med. Chem.* **2005**, *48*, 3621-3629.
- [163] K. R. Smith, K. E. Pinkerton, T. Watanabe, T. L. Pedersen, S. J. Ma, B. D. Hammock, *P. Natl. Acad. Sci. USA* **2005**, *102*, 2186-2191.
- [164] S. H. Hwang, C. Morisseau, Z. Do, B. D. Hammock, *Bioorg. Med. Chem. Lett.* **2006**, *16*, 5773-5777.
- [165] A. Yaron, F. Naider, *Crit. Rev. Biochem. Mol.* **1993**, *28*, 31-81.
- [166] B. D. Green, P. R. Flatt, C. J. Bailey, *Expert Opin. Em. Drugs* **2006**, *11*, 525-539.
- [167] E. B. Villhauer, J. A. Brinkman, G. B. Naderi, B. F. Burkey, B. E. Dunning, K. Prasad, B. L. Mangold, M. E. Russell, T. E. Hughes, *J. Med. Chem.* **2003**, *46*, 2774-2789.
- [168] D. Green Brian, R. Flatt Peter, J. Bailey Clifford, *Diab. Vasc. Dis. Res.* **2006**, *3*, 159-165.
- [169] D. J. Augeri, J. A. Robl, D. A. Betebenner, D. R. Magnin, A. Khanna, J. G. Robertson, A. Wang, L. M. Simpkins, P. Taunk, Q. Huang, S.-P. Han, B. Abboa-Offei, M. Cap, L. Xin, L. Tao, E. Tozzo, G. E. Welzel, D. M. Egan, J. Marcinkeviciene, S. Y. Chang, S. A. Biller, M. S. Kirby, R. A. Parker, L. G. Hamann, *J. Med. Chem.* **2005**, *48*, 5025-5037.
- [170] L. Li, A. Sengupta, N. Haque, I. Grundke-Iqbal, K. Iqbal, *FEBS Lett.* **2004**, *566*, 261-269.
- [171] H. Tanimukai, I. Grundke-Iqbal, K. Iqbal, *Am. J. Pathol.* **2005**, *166*, 1761-1771.
- [172] K. Iqbal, A. Del C. Alonso, S. Chen, M. O. Chohan, E. El-Akkad, C.-X. Gong, S. Khatoon, B. Li, F. Liu, A. Rahman, H. Tanimukai, I. Grundke-Iqbal, *Biochim. Biophys. Acta* **2005**, *1739*, 198-210.
- [173] M. O. Chohan, S. Khatoon, I.-G. Iqbal, K. Iqbal, *FEBS Lett.* **2006**, *580*, 3973-3979.
- [174] L. R. Kelland, F. J. Barnard, I. G. Evans, B. A. Murrer, B. R. C. Theobald, S. B. Wyer, P. M. Goddard, M. Jones, M. Valenti, et al., *J. Med. Chem.* **1995**, *38*, 3016-3024.
- [175] F. Zak, J. Turanek, A. Kroutil, P. Sova, A. Mistr, A. Poulouva, P. Mikolin, Z. Zak, A. Kasna, D. Zaluska, J. Neca, L. Sindlerova, A. Kozubik, *J. Med. Chem.* **2004**, *47*, 761-763.
- [176] W. Lasek, T. Switaj, J. Sienko, M. Kasprzycka, G. Basak, P. Miklaszewicz, M. Maj, D. Nowis, T. Grzela, J. Golab, I. Mlynarczuk, A. Jalili, B. Kaminska, M. Dziembowska, K. Czajkowski, M. Nowaczyk, A. Gorska, Z. Kazmierczuk, *Cancer. Chemother. Pharmacol.* **2002**, *50*, 213-222.
- [177] B. Charpentier, J.-M. Bernardon, J. Eustache, C. Millois, B. Martin, S. Michel, B. Shroot, *J. Med. Chem.* **1995**, *38*, 4993-5006.
- [178] R. Lotan, *J. Biol. Reg. Homeos. AG* **2003**, *17*, 13-28.
- [179] H. T. Nagaswa, J. A. Elberling, F. N. Shirota, *J. Med. Chem.* **1973**, *16*, 823-826.

- [180] H. T. Nagasawa, J. A. Elberling, F. N. Shiota, *J. Med. Chem.* **1975**, *18*, 826-830.
- [181] A. Zask, G. Birnberg, K. Cheung, J. Kaplan, C. Niu, E. Norton, R. Suayan, A. Yamashita, D. Cole, Z. Tang, G. Krishnamurthy, R. Williamson, G. Khafizova, S. Musto, R. Hernandez, T. Annable, X. Yang, C. Discafani, C. Beyer, L. M. Greenberger, F. Loganzo, S. Ayral-Kaloustian, *J. Med. Chem.* **2004**, *47*, 4774-4786.
- [182] W. Maison, J. V. Frangioni, N. Pannier, *Org. Lett.* **2004**, *6*, 4567-4569.
- [183] I. S. Morozov, N. N. Klelmenova, *Eksp. Klin. Farm.* **1998**, *61*, 51-53.
- [184] G. I. Wadler, *Performance-Enhancing Substances in Sport and Exercise* **2002**, 305-321.
- [185] A. Baxter, J. Bent, K. Bowers, M. Braddock, S. Brough, M. Fagura, M. Lawson, T. McNally, M. Mortimore, M. Robertson, R. Weaver, P. Webborn, *Bioorg. Med. Chem. Lett.* **2003**, *13*, 4047-4050.
- [186] V. S. C. Yeh, R. Kurukulasuriya, F. A. Kerdesky, *Org. Lett.* **2006**, *8*, 3963-3966.
- [187] V. S. C. Yeh, R. Kurukulasuriya, S. Fung, K. Monzon, W. Chiou, J. Wang, D. Stolarik, H. Imade, R. Shapiro, V. Knourek-Segel, E. Bush, D. Wilcox, P. T. Nguyen, M. Brune, P. Jacobson, J. T. Link, *Bioorg. Med. Chem. Lett.* **2006**, *16*, 5555-5560.
- [188] V. S. C. Yeh, R. Kurukulasuriya, D. Madar, J. R. Patel, S. Fung, K. Monzon, W. Chiou, J. Wang, P. Jacobson, H. L. Sham, J. T. Link, *Bioorg. Med. Chem. Lett.* **2006**, *16*, 5408-5413.
- [189] V. S. C. Yeh, J. R. Patel, H. Yong, R. Kurukulasuriya, S. Fung, K. Monzon, W. Chiou, J. Wang, D. Stolarik, H. Imade, D. Beno, M. Brune, P. Jacobson, H. Sham, J. T. Link, *Bioorg. Med. Chem. Lett.* **2006**, *16*, 5414-5419.
- [190] F. N. Stepanov, Srebrodolskii, Y. I., *Zh. Org. Khim.* **1966**, *2*, 1612-1615.
- [191] P. R. Schreiner, O. Lauenstein, I. V. Kolomitsyn, S. Nadi, A. A. Fokin, *Angew. Chem. Int. Ed.* **1998**, *37*, 1895-1897.
- [192] P. R. Schreiner, O. Lauenstein, E. D. Butova, P. A. Gunchenko, I. V. Kolomitsin, A. Wittkopp, G. Feder, A. A. Fokin, *Chem. Eur. J.* **2001**, *7*, 4996-5003.
- [193] P. R. Schreiner, A. A. Fokin, *Chem. Rec.* **2004**, *3*, 247-257.
- [194] O. Lauenstein, *Univ. Göttingen* **2001**.
- [195] S. S. Novikov, Khardin, A. P., Butenko, L. N., Kulev, I. A., Novakov, I. A., Radchenko, S. S., Burdenko, S. S., *Zh. Org. Khim.* **1980**, *16*, 1433-1435.
- [196] V. V. Pershin, L. N. Butenko, I. A. Novakov, *Method for the preparation of 1-acetamidoadamantane*, SU 88-46068071643528, **1991**.
- [197] P. R. Schreiner, L. Wanka, *Preparation of aminoadamantanes as antivirals, artificial ion channels, and for treatment of diseases related to defects of the GABA system*, PCT 2005-DE13042006010362, **2006**.
- [198] J. J. Ritter, P. P. Minieri, *J. Am. Chem. Soc.* **1948**, *70*, 4045-4048.
- [199] H. Koch, W. Haaf, *Angew. Chem.* **1958**, *70*, 311.
- [200] H. Koch, W. Haaf, *Ann.* **1958**, *618*, 251-266.
- [201] H. Stetter, M. Schwarz, A. Hirschhorn, *Chem. Ber.* **1959**, *92*, 1629-1635.
- [202] H. Koch, W. Haaf, *Angew. Chem.* **1960**, *72*, 628.
- [203] A. A. Fokin, P. R. Schreiner, *Chem. Rev.* **2002**, *102*, 1551-1593.
- [204] A. A. Fokin, T. E. Shubina, P. A. Gunchenko, S. D. Isaev, A. G. Yurchenko, P. R. Schreiner, *J. Am. Chem. Soc.* **2002**, *124*, 10718-10727.
- [205] R. E. Delimarskii, V. N. Rodionov, A. G. Yurchenko, *Ukr. Khim. Zh.* **1988**, *54*, 437-438.

- [206] W. Haaf, *Chem. Ber.* **1963**, 96, 3359-3369.
- [207] S. R. Jones, J. M. Mellor, *Synthesis* **1976**, 32-33.
- [208] G. A. Olah, B. G. B. Gupta, S. C. Narang, *Synthesis* **1979**, 274-276.
- [209] E. Shokova, T. Mousoulou, Y. Luzikov, V. Kovalev, *Synthesis* **1997**, 1034-1040.
- [210] R. D. Bach, J. W. Holubka, R. C. Badger, S. J. Rajan, *J. Am. Chem. Soc.* **1979**, 101, 4416-4417.
- [211] W. Haaf, *Angew. Chem.* **1961**, 73, 144.
- [212] O. Onomura, Y. Yamamoto, N. Moriyama, F. Iwasaki, Y. Matsumura, *Synlett.* **2006**, 2415-2418.
- [213] G. L. Anderson, W. A. Burks, I. I. Harruna, *Synth. Commun.* **1988**, 18, 1967-1974.
- [214] V. F. Baklan, A. N. Khil'chevskii, V. P. Kukhar, *Zh. Org. Khim.* **1987**, 23, 2381-2384.
- [215] P. R. Schreiner, L. Wanka, A. A. Fokin, D. M. Wolfe, *Amidoadamantanes and Methods for the Preparation Thereof*, DE 10 2006 009 278.3, **2006**.
- [216] P. R. Schreiner, L. Wanka, A. A. Fokin, D. M. Wolfe, *Method for the Preparation of 1-Formamido-3,5-dimethyladamantane*, DE 10 2006 009 279.1, **2006**.
- [217] J. R. Alford, B. D. Cuddy, D. Grant, M. A. McKervey, *J. Chem. Soc. Perk. T 1* **1972**, 2707-2713.
- [218] T. Kimura, M. Fujita, H. Sohmiya, T. Ando, *Ultrason. Sonochem.* **2002**, 9, 205-207.
- [219] T. Sasaki, A. Usuki, M. Ohno, *J. Org. Chem.* **1980**, 45, 3559-3564.
- [220] T. Sasaki, A. Nakanishi, M. Ohno, *J. Org. Chem.* **1981**, 46, 5445-5447.
- [221] J. Applequist, Rivers, P., Applequist, D. E., *J. Am. Chem. Soc.* **1969**, 91, 5705-5711.
- [222] L. A. Carpino, G. Y. Han, *J. Org. Chem.* **1972**, 37, 3404-3409.
- [223] G. F. Sigler, W. D. Fuller, N. C. Chaturvedi, M. Goodman, M. Verlander, *Biopolymers* **1983**, 22, 2157-2162.
- [224] V. Dourtoglou, J. C. Ziegler, B. Gross, *Tetrahedron Lett.* **1978**, 1269-1272.
- [225] F. Albericio, J. M. Bofill, A. El-Faham, S. A. Kates, *J. Org. Chem.* **1998**, 63, 9678-9683.
- [226] G. R. Pettit, S. R. Taylor, *J. Org. Chem.* **1996**, 61, 2322-2325.
- [227] R. B. Merrifield, *J. Am. Chem. Soc.* **1963**, 85, 2149-2154.
- [228] N. Sewald, H.-D. Jakubke, *Peptides: Chemistry and Biology*, Wiley-VCH, Weinheim, **2003**.
- [229] G. A. Grant, *Synthetic Peptides: A User's Guide*, Oxford University Press, Oxford / New York, **2002**.
- [230] D. C. Gournelis, G. G. Laskaris, R. Verpoorte, *Nat. Prod. Rep.* **1997**, 14, 75-82.
- [231] P. Wipf, *Chem. Rev.* **1995**, 95, 2115-2134.
- [232] S. Fernandez-Lopez, H. S. Kim, E. C. Choi, M. Delgado, J. R. Granja, A. Khasanov, K. Kraehenbuehl, G. Long, D. A. Weinberger, K. M. Wilcoxon, M. R. Ghadiri, *Nature* **2001**, 412, 452-455.
- [233] J. S. Davies, *J. Pept. Sci.* **2003**, 9, 471-501.
- [234] N. R. Clement, J. M. Gould, *Biochemistry* **1981**, 20, 1539-1543.
- [235] M. R. Ghadiri, J. R. Granja, R. A. Milligan, D. E. McRee, N. Khazanovich, *Nature* **1994**, 372, 709-709.
- [236] T. D. Clark, M. R. Ghadiri, *J. Am. Chem. Soc.* **1995**, 117, 12364-12365.
- [237] M. Engels, D. Bashford, M. R. Ghadiri, *J. Am. Chem. Soc.* **1995**, 117, 9151-9158.

- [238] M. R. Ghadiri, K. Kobayashi, J. R. Granja, R. K. Chadha, D. E. McRee, *Angew. Chem. Int. Ed.* **1995**, *34*, 93-95.
- [239] W. S. Horne, C. D. Stout, M. R. Ghadiri, *J. Am. Chem. Soc.* **2003**, *125*, 9372-9376.
- [240] J. Sanchez-Ouesada, M. P. Isler, M. R. Ghadiri, *J. Am. Chem. Soc.* **2002**, *124*, 10004-10005.
- [241] D. Ranganathan, V. Haridas, K. P. Madhusudanan, R. Roy, R. Nagaraj, G. B. John, M. B. Sukhaswami, *Angew. Chem. Int. Ed.* **1996**, *35*, 1105-1107.
- [242] D. Ranganathan, V. Haridas, R. Nagaraj, I. L. Karle, *J. Org. Chem.* **2000**, *65*, 4415-4422.
- [243] D. Ranganathan, *Acc. Chem. Res.* **2001**, *34*, 919-930.
- [244] S. E. Gibson, C. Lecci, *Angew. Chem. Int. Ed.* **2006**, *45*, 1364-1377.
- [245] D. Ranganathan, V. Haridas, K. P. Madhusudanan, R. Roy, R. Nagaraj, G. B. John, *J. Am. Chem. Soc.* **1997**, *119*, 11578-11584.
- [246] D. Skropeta, K. A. Jolliffe, P. Turner, *J. Org. Chem.* **2004**, *69*, 8804-8809.
- [247] L. A. Carpino, H. Imazumi, A. El-Faham, F. J. Ferrer, C. Zhang, Y. Lee, B. M. Foxman, P. Henklein, C. Hanay, C. Mugge, H. Wenschuh, J. Klose, M. Beyermann, M. Bienert, *Angew. Chem. Int. Ed.* **2002**, *41*, 441-445.
- [248] S. Krause, W. Schwarz, *Mol. Pharmacol.* **2005**, *68*, 1728-1735.
- [249] J. Frackenhohl, P. I. Arvidsson, J. V. Schreiber, D. Seebach, *ChemBioChem* **2001**, *2*, 445-455.
- [250] A. Berkessel, H. Gröger, *Asymmetric Organocatalysis: From Biomimetic Concepts to Applications in Asymmetric Synthesis*, Wiley-VCH, Weinheim / New York, **2005**.
- [251] S. J. Miller, *Acc. Chem. Res.* **2004**, *37*, 601-610.
- [252] E. R. Jarvo, S. J. Miller, *Tetrahedron* **2002**, *58*, 2481-2495.
- [253] G. T. Copeland, E. R. Jarvo, S. J. Miller, *J. Org. Chem.* **1998**, *63*, 6784-6785.
- [254] D. J. Guerin, T. E. Horstmann, S. J. Miller, *Org. Lett.* **1999**, *1*, 1107-1109.
- [255] T. E. Horstmann, D. J. Guerin, S. J. Miller, *Angew. Chem. Int. Ed.* **2000**, *39*, 3635-3638.
- [256] D. J. Guerin, S. J. Miller, *J. Am. Chem. Soc.* **2002**, *124*, 2134-2136.
- [257] B. R. Sculimbrene, S. J. Miller, *J. Am. Chem. Soc.* **2001**, *123*, 10125-10126.
- [258] B. R. Sculimbrene, A. J. Morgan, S. J. Miller, *Chem. Commun.* **2003**, 1781-1785.
- [259] B. R. Sculimbrene, Y. Xu, S. J. Miller, *J. Am. Chem. Soc.* **2004**, *126*, 13182-13183.
- [260] J. E. Imbriglio, M. M. Vasbinder, S. J. Miller, *Org. Lett.* **2003**, *5*, 3741-3743.
- [261] C. E. Aroyan, S. J. Miller, *J. Am. Chem. Soc.* **2007**, *129*, 256-257.
- [262] A. J. Morgan, S. Komiya, Y. Xu, S. J. Miller, *J. Org. Chem.* **2006**, *71*, 6923-6931.
- [263] F. Formaggio, A. Barazza, A. Bertocco, C. Toniolo, Q. B. Broxterman, B. Kaptein, E. Brasola, P. Pengo, L. Pasquato, P. Scrimin, *J. Org. Chem.* **2004**, *69*, 3849-3856.
- [264] C. A. Lewis, A. Chiu, M. Kubryk, J. Balsells, D. Pollard, C. K. Esser, J. Murry, R. A. Reamer, K. B. Hansen, S. J. Miller, *J. Am. Chem. Soc.* **2006**, *128*, 16454-16455.
- [265] C. E. Müller, L. Wanka, P. R. Schreiner, *Chem. Commun.* **Submitted**.
- [266] D. A. Annis, O. Helluin, E. N. Jacobsen, *Angew. Chem. Int. Ed.* **1998**, *37*, 1907-1909.

- [267] E. R. Jarvo, G. T. Copeland, N. Papaioannou, P. J. Bonitatebus, Jr., S. J. Miller, *J. Am. Chem. Soc.* **1999**, *121*, 11638-11643.
- [268] A. Wittkopp, P. R. Schreiner, *Chem. Eur. J.* **2003**, *9*, 407-414.
- [269] P. R. Schreiner, *Chem. Soc. Rev.* **2003**, *32*, 289-296.
- [270] P. M. Pihko, *Angew. Chem. Int. Ed.* **2004**, *43*, 2062-2064.
- [271] Y. Takemoto, *Org. Biomol. Chem.* **2005**, *3*, 4299-4306.
- [272] M. S. Taylor, E. N. Jacobsen, *Angew. Chem. Int. Ed.* **2006**, *45*, 1520-1543.
- [273] S. J. Connon, *Chem. Eur. J.* **2006**, *12*, 5419-5427.
- [274] M. Kotke, P. R. Schreiner, *Tetrahedron* **2005**, *62*, 434-439.
- [275] M. Kotke, P. R. Schreiner, *Synthesis* **2007**, 779-790.
- [276] A. B. Baylis, M. E. D. Hillman, *Acrylic compounds*, DE 71-21551132155113, **1972**.
- [277] P. Langer, *Angew. Chem. Int. Ed.* **2000**, *39*, 3049-3052.
- [278] K. Morita, Z. Suzuki, H. Hirose, *B. Chem. Soc. Jpn.* **1968**, *41*, 2815.
- [279] L. Kürti, B. Czako, *Strategic Applications of Named Reactions in Organic Synthesis*, Elsevier Academic Press, Burlington, San Diego, London, **2005**.
- [280] C. E. Aroyan, M. M. Vasbinder, S. J. Miller, *Org. Lett.* **2005**, *7*, 3849-3851.
- [281] J. Wang, H. Li, X. Yu, L. Zu, W. Wang, *Org. Lett.* **2005**, *7*, 4293-4296.
- [282] I. T. Raheem, E. N. Jacobsen, *Adv. Synth. Catal.* **2005**, *347*, 1701-1708.
- [283] Y. Sohtome, A. Tanatani, Y. Hashimoto, K. Nagasawa, *Tetrahedron Lett.* **2004**, *45*, 5589-5592.
- [284] A. Berkessel, K. Roland, J. M. Neudoerfl, *Org. Lett.* **2006**, *8*, 4195-4198.
- [285] P. Edman, *Arch. Biochem. Biophys.* **1949**, *22*, 475-476.
- [286] H. D. Niall, *Method. Enzymol.* **1973**, *27*, 942-1010.
- [287] SPARTAN '02 for Windows, Wavefunction Inc., Irvine, California, **2002**.
- [288] Gaussian 03, Revision D.02, M. J. Frisch, G. W. Trucks, H. B. Schlegel, G. E. Scuseria, M. A. Robb, J. R. Cheeseman, J. A. Montgomery, T. V. Jr., K. N. Kudin, J. C. Burant, J. M. Millam, S. S. Iyengar, J. Tomasi, V. Barone, B. Mennucci, M. Cossi, G. Scalmani, N. Rega, G. A. Petersson, H. Nakatsuji, M. Hada, M. Ehara, K. Toyota, R. Fukuda, J. Hasegawa, M. Ishida, T. Nakajima, Y. Honda, O. Kitao, H. Nakai, M. Klene, X. Li, J. E. Knox, H. P. Hratchian, J. B. Cross, V. Bakken, C. Adamo, J. Jaramillo, R. Gomperts, R. E. Stratmann, O. Yazyev, A. J. Austin, R. Cammi, C. Pomelli, J. W. Ochterski, P. Y. Ayala, K. Morokuma, G. A. Voth, P. Salvador, J. J. Dannenberg, V. G. Zakrzewski, S. Dapprich, A. D. Daniels, M. C. Strain, O. Farkas, D. K. Malick, A. D. Rabuck, K. Raghavachari, J. B. Foresman, J. V. Ortiz, Q. Cui, A. G. Baboul, S. Clifford, J. Cioslowski, B. B. Stefanov, G. Liu, A. Liashenko, P. Piskorz, I. Komaromi, R. L. Martin, D. J. Fox, T. Keith, M. A. Al-Laham, C. Y. Peng, A. Nanayakkara, M. Challacombe, P. M. W. Gill, B. Johnson, W. Chen, M. W. Wong, C. Gonzalez, J. A. Pople, Gaussian, Inc., Wallingford, CT, **2004**.
- [289] C. J. Cramer, *Essentials of Computational Chemistry. Theories and Models*, John Wiley & Sons, Chichester, **2002**.
- [290] T. A. Halgren, *J. Comput. Chem.* **1996**, *17*, 490-519.
- [291] T. A. Halgren, *J. Comput. Chem.* **1996**, *17*, 520-552.
- [292] T. A. Halgren, *J. Comput. Chem.* **1996**, *17*, 553-586.
- [293] T. A. Halgren, R. B. Nachbar, *J. Comput. Chem.* **1996**, *17*, 587-615.
- [294] T. A. Halgren, *J. Comput. Chem.* **1996**, *17*, 616-641.
- [295] R. G. Parr, W. Yang, *Annual Review of Physical Chemistry* **1995**, *46*, 701-728.
- [296] W. Kohn, L. J. Sham, Univ. of California, La Jolla, CA, USA., **1965**, p. 21 pp.
- [297] A. D. Becke, *Phys. Rev. A* **1988**, *38*, 3098-3100.

- [298] A. D. Becke, *J. Chem. Phys.* **1993**, *98*, 5648-5652.
- [299] R. McWeeny, G. Diercksens, *J. Chem. Phys.* **1968**, *49*, 4852-4856.
- [300] B. Miehlich, A. Savin, H. Stoll, H. Preuss, *Chem. Phys. Lett.* **1989**, *157*, 200-206.
- [301] E. R. Davidson, D. Feller, *Chem. Rev.* **1986**, *86*, 681-696.
- [302] W. J. Hehre, R. F. Stewart, J. A. Pople, *J. Chem. Phys.* **1969**, *51*, 2657-2664.
- [303] S. H. Gellman, G. P. Dado, G. B. Liang, B. R. Adams, *J. Am. Chem. Soc.* **1991**, *113*, 1164-1173.
- [304] G. P. Dado, S. H. Gellman, *J. Am. Chem. Soc.* **1994**, *116*, 1054-1062.
- [305] J. Yang, L. A. Christianson, S. H. Gellman, *Org. Lett.* **1999**, *1*, 11-13.
- [306] J. S. Nowick, M. Abdi, K. A. Bellamo, J. A. Love, E. J. Martinez, G. Noronha, E. M. Smith, J. W. Ziller, *J. Am. Chem. Soc.* **1995**, *117*, 89-99.
- [307] B. W. Gung, Z. Zhu, *J. Org. Chem.* **1996**, *61*, 6482-6483.
- [308] W. Koch, M. C. Holthausen, *A Chemist's Guide to Density Functional Theory. Second Edition*, Wiley-VCH, Weinheim, **2001**.
- [309] P. R. Schreiner, *Angew. Chemie* **2007**, *119*, 4295-4297.
- [310] D. H. Appella, L. A. Christianson, I. L. Karle, D. R. Powell, S. H. Gellman, *J. Am. Chem. Soc.* **1996**, *118*, 13071-13072.
- [311] G. V. M. Sharma, P. Jayaprakash, K. Narsimulu, A. R. Sankar, K. R. Reddy, P. R. Krishna, A. C. Kunwar, *Angew. Chem. Int. Ed.* **2006**, *45*, 2944-2947.
- [312] P. G. Vasudev, N. Shamala, K. Ananda, P. Balaram, *Angew. Chem. Int. Ed.* **2005**, *44*, 4972-4975.
- [313] D. J. Hill, M. J. Mio, R. B. Prince, T. S. Hughes, J. S. Moore, *Chem. Rev.* **2001**, *101*, 3893-4011.
- [314] C. E. Dempsey, *Progr. Nucl. Mag. Res. Sp.* **2001**, *39*, 135-170.
- [315] C. L. Perrin, C. P. Lollo, *J. Am. Chem. Soc.* **1984**, *106*, 2754-2757.
- [316] R. S. Molday, S. W. Englander, R. G. Kallen, *Biochemistry* **1972**, *11*, 150-158.
- [317] C.-T. Chen, J.-H. Kuo, V. D. Pawar, Y. S. Munot, S.-S. Weng, C.-H. Ku, C.-Y. Liu, *J. Org. Chem.* **2005**, *70*, 1188-1197.
- [318] J. T. Blank, S. J. Miller, *Biopolymers* **2006**, *84*, 38-47.
- [319] T. P. Yoon, E. N. Jacobsen, *Science* **2003**, *299*, 1691-1693.
- [320] A. Berkessel, B. Koch, C. Toniolo, M. Rainaldi, B. Broxterman Quirinus, B. Kaptein, *Biopolymers* **2006**, *84*, 90-96.
- [321] G. Molle, J. E. Dubois, P. Bauer, *Can. J. Chem.* **1987**, *65*, 2428-2433.
- [322] C. A. Grob, W. Schwarz, H. P. Fischer, *Helv. Chim. Acta* **1964**, *47*, 1385-1401.
- [323] G. I. Danilenko, G. K. Palii, N. A. Mokhort, V. F. Baklan, *Fiziologicheskii Aktivnye Veshchestva* **1975**, *7*, 144-147.
- [324] K. Bott, *Chem. Ber.* **1968**, *101*, 564-573.
- [325] V. M. Plakhotnik, V. Y. Kovtun, V. G. Yashunskii, *Zh. Org. Khim.* **1982**, *18*, 1001-1005.
- [326] Geigy, *3-Amino-1-adamantanecarboxylic acid*, NL 6600715, **1966**.
- [327] X. Zhang, *Preparation of a substituted symmetry adamantane amine derivatives*, CN 2003-1483451566075, **2005**.
- [328] M. Minozzi, D. Nanni, J. C. Walton, *Org. Lett.* **2003**, *5*, 901-904.
- [329] S. Landa, J. Vais, J. Burkhard, *Z. Chem.* **1967**, *7*, 233.
- [330] S. Kato, T. Iwahama, S. Sakaguchi, Y. Ishii, *J. Org. Chem.* **1998**, *63*, 222-223.
- [331] A. E. Sorochinsky, A. A. Petrenko, V. A. Soloshonok, G. Resnati, *Tetrahedron* **1997**, *53*, 5995-6000.

15. Bibliography

Parts of this thesis have been published:

1. P. R. Schreiner, L. Wanka, ***Preparation of aminoadamantanes as antivirals, artificial ion channels, and for treatment of diseases related to defects of the GABA system***, International Patent Application PCT 2005-DE13042006010362, **2006**.
2. P. R. Schreiner, L. Wanka, A. A. Fokin, D. M. Wolfe, ***Amidoadamantanes and Methods for the Preparation Thereof***, German Patent Application DE 10 2006 009 278.3, **2006**.
3. P. R. Schreiner, L. Wanka, A. A. Fokin, D. M. Wolfe, ***Method for the Preparation of 1-Formamido-3,5-dimethyladamantane***, German Patent Application DE 10 2006 009 279.1, **2006**.
4. L. Wanka, C. Cabrele, M. Vanejews, P. R. Schreiner, ***γ -Aminoadamantanecarboxylic acids through direct C-H bond amidations***, *Eur. J. Org. Chem.* **2007**, 1474-1490.

The following publication, which will contain parts of this thesis, is in preparation:

C. E. Müller, L. Wanka, P. R. Schreiner, ***Oligopeptides Incorporating γ -Aminoadamantane Carboxylic Acids: A New Organocatalytic Platform for Enantioselective Acylations***, *Chem. Commun.* **2007**, Submitted.

Parts of this thesis have been presented as a talk:

Direct Carboxylation and Amidation Reactions of Adamantane

Program of emphasis "Oxidative C–H activation" of the DFG, Regensburg, April, **2004**

Parts of this thesis have been presented as posters:

L. Wanka, Peter R. Schreiner

 γ -Aminoadamantane Carboxylic Acids: α -Amino Acids in Disguise

Postgraduate Winter School on Organic Reactivity – WISOR XII, Bressanone / Italy,
January, **2003**

L. Wanka, C. Cabrele, Peter R. Schreiner

Peptidic Foldamers Incorporating Novel γ -Aminoadamantane Carboxylic Acids

Summer School Medicinal Chemistry, Shanghai / China
September, **2005**

L. Wanka, C. Cabrele, Peter R. Schreiner

 γ -Aminoadamantane Carboxylic Acids: Orientating Tether for Peptides

ORCHEM Bad Nauheim / Germany
September, **2006**

C. E. Müller, L. Wanka, Peter R. Schreiner

Novel Peptides Incorporating Adamantyl Amino Acids

ORCHEM Bad Nauheim / Germany
September, **2006**

Es ist nicht genug, zu wissen,
man muß auch anwenden.
Es ist nicht genug, zu wollen,
man muß auch tun.

J.W.G.